



**Acute arterial hypoxaemia and its impact on drug  
pharmacokinetics in humans;  
clinical and in-vitro investigation.**

**Acute arterial hypoxaemia and its impact on drug  
pharmacokinetics in humans;  
clinical and in-vitro investigation.**

A thesis submitted in accordance with the conditions  
governing candidates for the degree

of

*Philosophiae Doctor in Cardiff University*

by

**Dalal Alablani**

August 2023

Cardiff School of Pharmacy and Pharmaceutical Sciences  
Cardiff University

## Abstract

Arterial hypoxaemia ultimately leads to the formation of systemic and localised free radicals, activating pathways of oxidative-inflammatory-nitrosative stress. The physiological adjustments, encompassing redox and haemodynamic responses, have the potential to influence the pharmacokinetics (PK) and pharmacodynamics (PD) of both acutely and chronically administered medications. Sildenafil, a drug that acts through phosphodiesterase-5 inhibition and is clinically used for pulmonary hypertension, also serves as a short-term treatment to prevent or mitigate altitude-induced pulmonary vasoconstriction, a key factor in the development of high-altitude pulmonary oedema (HAPE). This thesis aims to simulate the PK/PD outcomes of sildenafil under acute hypoxaemia and identify the underlying mechanistic pathway that drives PK/PD alterations under hypoxia.

The PK/PD profile of a single oral 100 mg sildenafil oral tablet was simulated using R V.3.6.3 with the IQRtools package. A Monte Carlo method was employed, involving 1000 subjects, with a one-compartment first-order elimination and absorption model. The HepaRG cell line served as an in-vitro model to predict the intrinsic clearance ( $Cl_{int}$ ) of sildenafil under hypoxia (1%  $O_2$ ). This was accomplished by evaluating CYP3A4 and CYP2C9 turnover activities and investigating the associated mechanistic pathway.

Hypoxia resulted in a significant decrease in the turnover activity of both CYP3A4 and CYP2C9, leading to a 29% reduction in  $Cl_{int}$  compared to the normoxic control. Monte Carlo simulations revealed that acute hypoxia increased the maximum concentration ( $C_{max}$ ), half-life ( $t_{1/2}$ ), area under the curve ( $AUC_{0-\infty}$ ), as well as AUC above the inhibitory concentration 50% ( $IC_{50}$ ). Hypoxia stimulated stressors such as cytokine and superoxide production, had exerting a negative regulatory effect on CYP3A4/2C9. The preservation of CYP3A4/2C9 activity under hypoxia was achieved by employing reactive oxygen species (ROS) scavengers like Tiron. Furthermore, hypoxia may regulate CYP3A4/2C9 through the modulation of the pregnane x receptor (PXR). The MAPK/ERK signalling pathway appears to be the target pathway for this regulation.

In conclusion, hypoxia has the capacity to alter the PK/PD profile of drugs, warranting dosage regimen adjustments, particularly for drugs with narrow therapeutic indices. Further mechanistic studies focusing on the PXR pathway are necessary to fully comprehend the mechanisms underlying hypoxia-induced alterations.

## **Acknowledgements**

First and foremost, I would like to express my sincere gratitude to my supervisor Prof Mark Gumbleton for giving me the opportunity to work on this project, providing valuable guidance and feedback, and challenging me to grow as a scientist. Thank you for being a great supervisor; without you, none of this work would have been possible.

I would also like to extend my thanks to Prof Damian Bailey and Prof James Coulson for their support, invaluable advice and ideas that were vital for the achievement of this work.

I want to give my deepest appreciation to Ghaith aljyoussi for his time, help and advice in the simulation work. I am also grateful to my colleagues for sharing the knowledge and creating a good work environment.

Words will never suffice to express my deepest love and gratitude to my dear family, who unceasingly supported me at all times during my study.

Finally, this project would not have been possible without the funding provided by Prince Sattam Bin Abdulaziz University. Thank you.

## List of abbreviations

<b>ATP</b>	Adenosine triphosphate
<b>A-a</b>	Alveolar to arterial oxygen gradient
<b>Ahr</b>	Aryl hydrocarbon receptors
<b>AMS</b>	Acute mountain sickness
<b>AUC</b>	Area under the curve
<b>ADH</b>	Antidiuretic hormone
<b>ABC</b>	ATP-binding cassette
<b>BBB</b>	Blood-brain barrier
<b>BCRP</b>	Breast cancer resistance protein
<b>CL</b>	Total body clearance
<b>CL<sub>R</sub></b>	Renal clearance
<b>Cl<sub>int</sub></b>	Intrinsic clearance
<b>CL<sub>h</sub></b>	Hepatic clearance
<b>CYP450</b>	Cytochrome P450
<b>C<sub>max</sub></b>	Maximal or peak concentration
<b>CVBF</b>	Cerebral blood flow
<b>cGMP</b>	Cyclic guanosine monophosphate
<b>Caco2</b>	Human colorectal adenocarcinoma cells
<b>COPD</b>	Chronic obstructive pulmonary disease
<b>CAR</b>	Constitutive androstane receptor
<b>CK19</b>	Cytokeratin 19
<b>CI</b>	95% confidence intervals
<b>DMSO</b>	Dimethylsulfoxide
<b>DCF-DA</b>	Dichlorofluorescein diacetate
<b>EPT</b>	Erythropoietin

<b>EC<sub>50</sub></b>	Half maximal effective concentration
<b>ER</b>	Endoplasmic reticulum
<b>E<sub>H</sub></b>	Hepatic extraction ratio
<b>ERK1/2</b>	Extracellular signal-regulated kinases ½
<b>FiO<sub>2</sub></b>	Fraction of inspired oxygen
<b>F</b>	Bioavailability
<b>F<sub>u</sub></b>	Fraction unbound in plasma
<b>F<sub>u<sub>b</sub></sub></b>	Fraction unbound in blood
<b>FMO</b>	Flavine-containing monooxygenases
<b>FMN</b>	Flavin mononucleotide
<b>FDN</b>	Flavin dinucleotide
<b>F<sub>lumen</sub></b>	Fraction of drug bioavailable in GI trac
<b>F<sub>hepatic</sub></b>	Fraction of drug bioavailable after first pass metabolism in the liver
<b>F<sub>total</sub></b>	Total of drug bioavailable including both F <sub>lumen</sub> and F <sub>hepatic</sub>
<b>GFR</b>	Glomerular filtration rate
<b>GST</b>	Glutathione s-transferases
<b>GC</b>	Guanylate cyclase
<b>HepG2</b>	Human hepatocellular carcinoma cells
<b>HepaRG</b>	Human bipotent progenitor cell line
<b>HPV</b>	Hypoxic pulmonary vasoconstriction
<b>HAPE</b>	High-altitude pulmonary oedema
<b>HACE</b>	High-altitude cerebral oedema
<b>Hct</b>	Hematocrit
<b>HIFs</b>	Hypoxia-inducible factors
<b>HREs</b>	Hypoxia-responsive elements
<b>HPV</b>	Hepatic portal vein
<b>IL-6</b>	Interleukin-6
<b>IC<sub>50</sub></b>	Half maximal inhibitory concentration

<b>IFN-<math>\gamma</math></b>	Interferon gamma
<b>K<sub>abs</sub></b>	Absorption rate constant
<b>K</b>	Elimination rate constant
<b>MRT</b>	Mean residence time of the drug
<b>MRP2</b>	Multidrug-resistance-associated protein-2
<b>MAPKs</b>	Mitogen-activated protein kinases
<b>MEK1/2</b>	Mitogen-activated protein kinase ½
<b>NAC</b>	N-acetylcysteine
<b>NF-<math>\kappa\beta</math></b>	Nuclear factor kappa light chain enhancer of activated $\beta$ cells
<b>NAT</b>	N-acetyltransferases
<b>OI</b>	Oxygenation index
<b>PK</b>	Pharmacokinetics
<b>PD</b>	Pharmacodynamics
<b>PAO<sub>2</sub></b>	Alveolar oxygen levels
<b>PaO<sub>2</sub></b>	Arterial oxygen tension / partial pressure of arterial oxygen
<b>PO<sub>2</sub></b>	Partial pressure of oxygen
<b>PDE-5</b>	Phosphodiesterase-5 inhibitors
<b>PCO<sub>2</sub></b>	Partial pressure of carbon dioxide
<b>PHD2</b>	Prolyl hydroxylase enzyme domain
<b>PKC</b>	Protein kinase C
<b>PHH</b>	Primary human hepatocyte
<b>PXR</b>	Pregnane X receptor
<b>PPAR</b>	peroxisome proliferator-activated receptor
<b>P-gp</b>	Phosphoglycoprotein
<b>Q<sub>hepatic</sub></b>	Blood flow in the liver
<b>RNS</b>	Reactive nitrogen species
<b>ROS</b>	Reactive oxygenase species
<b>ROO<math>\cdot</math></b>	Peroxyl radicals

<b>ROOH</b>	Hydroperoxide
<b>RXR</b>	Retinoid X receptor
<b>RIF</b>	Rifampicin
<b>ROI</b>	Reactive oxygen intermediates
<b>SaO<sub>2</sub></b>	Arterial oxygen saturation
<b>SpO<sub>2</sub></b>	Peripheral oxygen saturation
<b>sIL-6R</b>	Soluble interleukin-6 receptor
<b>sGC</b>	Soluble intracellular GC
<b>SURE</b>	Specialist Unit for Review Evidence
<b>SMD</b>	Standardised mean difference
<b>SULT</b>	Sulfurotrnsferase
<b>SOD</b>	Superoxide dismutase
<b>SRC-1</b>	Steroid receptor coactivator 1
<b>t<sub>1/2</sub><sub>abs</sub></b>	Absorption half-life
<b>t<sub>1/2</sub></b>	Elimination half-life
<b>T<sub>max</sub></b>	Time to peak concentration
<b>TNF-<math>\alpha</math></b>	Tumour necrosis factor-alpha
<b>3D</b>	Three dimensional
<b>2D</b>	Two dimensional
<b>UGT</b>	Uridine Glucuronide Transferase
<b>V/Q</b>	Ventilation /Perfusion
<b>Vd</b>	Volume of distribution
<b>VHL</b>	Von Hippel -Lindau protein



# Table of contents

<b>Abstract</b> .....	<b>I</b>
<b>Acknowledgements</b> .....	<b>II</b>
<b>List of abbreviations</b> .....	<b>III</b>
<b>Index of Figures</b> .....	<b>XV</b>
<b>Index of Tables</b> .....	<b>XX</b>

## Chapter 1: Introduction

1.1 Arterial hypoxaemia .....	1
1.2 Pathophysiology of hypoxaemia .....	2
1.2.1 Ventilation /perfusion (V/Q) mismatch.....	2
1.2.2 Right-to-left shunt .....	5
1.2.3 Diffusion impairment .....	5
1.2.4 Hypoventilation.....	5
1.2.5 Low Fraction of inspired oxygen (FiO <sub>2</sub> ) .....	6
1.3 Measures of oxygenation .....	6
1.3.1 Arterial oxygen saturation (SpO <sub>2</sub> and SaO <sub>2</sub> ) .....	7
1.3.2 Arterial oxygen tension (PaO <sub>2</sub> ).....	7
1.3.3 Alveolar to arterial (A-a) oxygen gradient .....	7
1.3.4 PaO <sub>2</sub> /FiO <sub>2</sub> ratio .....	7
1.3.5 Arterial to alveolar (a-A) oxygen ratio.....	8
1.3.6 Oxygenation index (OI).....	8
1.4 High altitude arterial hypoxaemia: complications and management.....	8
1.5 Hypoxia and physiological change that may be relevant to altered drug pharmacokinetics .....	9
1.5.1 Hypoxia and physiological systems .....	10
1.5.1.1 Gastrointestinal system .....	10
1.5.1.2 Respiratory and cardiovascular systems .....	10

1.5.1.3 Haematological system .....	12
1.5.1.4 Renal system.....	13
1.5.1.5 Cerebrovascular system .....	14
1.5.1.6 Cytochrome P450 .....	15
1.5.2 Human studies exploring the impact of hypobaric hypoxia upon drug pharmacokinetics. ....	20
1.6 Hypoxia and inflammatory mediators .....	23
1.7 Hypoxia and Reactive Oxygen Species (ROS) .....	23
1.8 Hypoxia and Hypoxia-inducible factors (HIFs).....	25
1.9 Sildenafil .....	28
1.9.1 Pharmacology of sildenafil .....	28
1.9.2 Structure and physiochemical properties of sildenafil .....	28
1.9.3 Metabolism of sildenafil.....	29
1.9.4 Pharmacokinetics of sildenafil.....	30
1.10 Project aim, hypothesis, and experimental objectives .....	31
<b>Chapter 2: General Laboratory Material and Method for In-Vitro Work</b>	
2.1 Cell culture .....	34
2.1.1 HepG2 cells (Hepatocyte model).....	34
2.1.2 HepaRG cells (Hepatocyte model).....	34
2.1.3 Caco2 cells.....	34
2.1.4 3-Dimensional (3D) HepaRG cultures .....	35
2.2 Cell staining and immunofluorescence.....	36
2.2.1 Live/ dead staining .....	36
2.2.2 Immunofluorescent staining and microscopy .....	36
2.3 General assays .....	37
2.3.1 CYP450 enzymes activity measurement using P450-Glo™ assay .....	37
2.3.2 CellTiter-Glo luminescent cell viability assay.....	38

2.3.3 Rhodamine 6G and Hoechst 33342 accumulation assay in HEPG2 and Caco2 cells	38
2.4 Molecular assessment for genes of interest	39
2.4.1 RNA extraction	39
2.4.2 Reverse transcription (cDNA synthesis)	40
2.4.3 Primer design	40
2.4.4 TaqMan gene expression assay	41
2.4.5 Quantitative Polymerase Chain Reaction (qRT-PCR)	41
2.5 Western blot	43
2.5.1 Protein lysis and concentration determination	43
2.5.2 Sample preparation and gel electrophoresis	43
2.5.3 Transfer of protein from gel to membrane	43
2.5.4 Immunodetection	44

**Chapter 3: The Impact of Hypoxaemia on Drug Pharmacokinetics in Adults:  
A Rapid Systematic Review and Meta-Analysis**

3.1 Introduction	46
3.1.1 Aim and objectives	46
3.2 Methods	47
3.2.1 Database and search strategy	47
3.2.2 Selection and quality assessment	47
3.2.3 Data management	48
3.2.4 Data extraction	49
3.2.5 Statistical analysis	50
3.3 Results	50
3.3.1 Study identification	50
3.3.2 Risk of bias	51
3.3.3 General characteristics of the included studies	52
3.3.4 Systematic review	58

3.3.4.1 $C_{max}$ , $T_{max}$ , Area Under the Curve.....	58
3.3.4.2 Half-life ( $t_{1/2}$ ) and elimination rate constant (K).....	58
3.3.4.3 Mean residence time (MRT) .....	58
3.3.4.4 Plasma Clearance (CL) .....	59
3.3.4.5 Volume of Distribution ( $V_d$ ).....	59
3.3.4.6 Bioavailability (F).....	60
3.3.5 Meta-analysis .....	67
3.3.6 Analysis of publication bias.....	80
3.4 Discussion and conclusions.....	81
 <b>Chapter 4: Development of an in-vitro hepatocyte model to test the effect of hypoxia on CYP3A4 and CYP2C9</b>	
4.1 Introduction .....	86
4.1.1 General overview of the liver .....	86
4.1.2 In-vitro metabolism models .....	88
4.1.2.1 Organ-/tissue-level models.....	89
4.1.2.2 Primary cell cultures, cell lines and iPSCs.....	89
4.1.2.3 Subcellular fractions .....	93
4.1.2.4 Isolated Enzymes .....	94
4.1.3 Aim and Objectives.....	94
4.2 Material and Methods .....	95
4.2.1 Cell culture.....	95
4.2.1.1 Two-dimensional (2D) monolayer.....	95
4.2.1.2 Three-dimensional (3D) cultures and cell treatments.....	96
4.2.2 Live/dead staining and viability assay .....	96
4.2.3 CYP3A4 and CYP2C9 expression.....	97
4.2.4 Isolation of RNA and quantitative real-time reverse transcription PCR (qRT-PCR) .....	97
4.2.5 Protein extraction and Western blot .....	98

4.2.6 Rhodamine 6G and Hoechst 33342 accumulation assay .....	98
4.2.7 Statistics .....	98
4.3 Results and Discussion .....	99
4.3.1 HepG2 cells as an in-vitro hepatocyte model: Studies under normoxia .....	99
4.3.2 HepaRG cells as an in-vitro hepatocyte model: Studies under normoxia .....	101
4.3.2.1 HepaRG cells cultured in 2D monolayer format .....	101
4.3.2.2 HepaRG cells cultured in 3D format as spheroids.....	106
4.3.2.3 HepaRG cells: CYP3A4 and CYP2C9 functional expression in 2D monolayer vs 3D spheroid model.....	111
4.3.3 HepaRG cells as an in-vitro hepatocyte model: Studies under hypoxia .....	114
4.3.3.1 HepaRG cells: Effect of hypoxia (1 % O <sub>2</sub> ) on CYP3A4 and CYP2C9 in 2D cell monolayer format .....	114
4.3.3.2 HepaRG cells: Effect of hypoxia (1% O <sub>2</sub> ) on CYP3A4 and CYP2C9 in 3D cell spheroid format .....	118
4.3.4 Effect of acute hypoxia on ABC transporters .....	122
4.4 Conclusions .....	125
<b>Chapter 5: Mechanism of REDOX regulation and CYP450 alteration under hypoxia</b>	
5.1 Introduction .....	127
5.1.1 Reactive Oxygen Species (ROS) .....	127
5.1.2 Regulation of CYP450 by ROS .....	129
5.1.3 Hypoxia, inflammation, nuclear receptors and CYP450s .....	130
5.1.4 MAPK/ ERK and the regulation of PXR nuclear receptor and CYP450 .....	134
5.1.5 Aim and Objectives.....	136
5.2 Methods.....	137
5.2.1 Cell culture and treatments .....	137
5.2.2 Primer design and Quantitative Real-Time Reverse Transcription PCR (qRT-PCR) .....	137

5.2.3 Western blot.....	138
5.2.4 Cell viability.....	138
5.2.5 H <sub>2</sub> O <sub>2</sub> measurement assay (ROS-Glo H <sub>2</sub> O <sub>2</sub> assay) .....	139
5.2.6 Total ROS detection (Total ROS detection Kit) .....	139
5.2.7 Mitochondrial superoxide measurement (MitoSOX assay). .....	140
5.2.8 Statistics.....	141
5.3 Results and Discussion .....	142
5.3.1 Effect of acute hypoxia on REDOX generation.....	142
5.3.2 Impact of menadione, NAC and Tiron on ROS generation in HepaRG Cells .....	149
5.3.3 Impact of ROS on CYP3A4 and CYP2C9 expression in HepaRG Cells.....	157
5.3.4 Hypoxia induces transcription of proinflammatory-related cytokines by HepaRG cells .....	164
5.3.5 Impact of pro-inflammatory cytokines on CYP3A4 and CYP2C9 expression in HepaRG cells under normoxia conditions.....	166
5.3.6 PXR regulates CYP3A4 and CYP2C9 and is downregulated by hypoxia and pro-inflammatory cytokines treatment .....	171
5.3.7 MAPK/ERK, PXR and hypoxia.....	174
5.3.7.1 ERK 1/2 phosphorylation under hypoxia.....	175
5.3.7.2 PD98059 inhibits ERK 1/2 activation in HepaRG cells .....	175
5.3.7.3 PD98059 enhances PXR expression.....	177
5.3.7.4 PD98059 enhances CYP450 expression .....	179
5.4 Conclusions .....	185
<b>Chapter 6: Acute arterial hypoxaemia and its impact on drug pharmacokinetics in humans; a pharmacokinetic-pharmacodynamic Monte Carlo simulation study</b>	
6.1 Introduction .....	187
6.1.1 Aim and Objectives.....	188
6.2 Method .....	190

6.2.1 Literature search.....	190
6.2.1.1 Pharmacokinetic parameters for sildenafil.....	190
6.2.1.2 IC <sub>50</sub> of sildenafil .....	192
6.2.1.3 Renal blood flow changes under acute hypoxia .....	192
6.2.1.4 Hepatic blood flow changes under hypoxia .....	193
6.2.2 In-vitro CYP3A4 and CYP2C9 functional activity assay .....	193
6.2.3 Determination of CL-based parameters for simulation .....	193
6.2.4 Determination of extent of oral bioavailability parameters for simulation .....	197
6.2.5 Monte Carlo simulation.....	200
6.3 Results and Discussion .....	205
6.3.1 In-vitro CYP3A4 CYP2C9 functional activity measurements toward setting intrinsic Clearance parameters for simulation.....	205
6.3.2 Monte Carlo simulation SET 1: .....	207
6.3.2.1 SET 1 Scenario A - the maximal effect of hypoxia on hepatic metabolism is already present before the start of the 24-h PK-PD simulation .....	207
6.3.2.2 SET 1 Scenario B - the maximal effect of hypoxia on hepatic metabolism is developed in a progressive linear manner between time 0 h and 4 h of the PK-PD simulation.....	211
6.3.2.3 SET 1 Scenario C - the maximal effects of hypoxia on hepatic metabolism occur abruptly in a ‘step-function’ at 4 h into the PK-PD simulation. ....	211
6.3.3 Monte Carlo simulation SET 2: .....	217
6.3.3.1 SET 2 Scenario A - the maximal effect of hypoxia is established prior to the 24- h PK-PD simulation with, in addition to the hypoxia-induced a maximal decrease in hepatic intrinsic clearance (as in SET 1 Scenario A), there is now also a hypoxia-induced increase in Q <sub>h</sub> by 40% .....	217
6.4 Conclusions .....	227
<b>Chapter 7: Summary Discussion and Future Work</b>	
<b>References: .....</b>	<b>240</b>
<b>Appendices .....</b>	<b>276</b>

Appendix 1- clinical trial protocol and all required documents for MHRA approval. ....	277
Appendix 2- Western blot experiment data .....	384
Appendix 3.....	403
Appendix 3.1- optimisation of the 3D spheroid HepaRG model .....	403
Appendix 3.2 -Effect of ROS manipulation on CYP3A4/2C9 in HepaRG under normoxia .....	404
Appendix 4- Search strategy, data extraction tables, and quality appraisal of systematic review and meta-analysis study.....	408



# Index of Figures

## Chapter 1

Figure 1.1 Normal partial pressure of the gases in the blood.....	1
Figure 1.2-Types of ventilation /perfusions (V/Q) mismatch. ....	4
Figure 1.3 Various mechanisms in hypoxaemia and associated medical conditions. ....	6
Figure 1.4 Respiratory acclimatisation to hypoxia. Improved tissue oxygenation occurs through increased pulmonary ventilation and diffusion capacity.....	11
Figure 1.5 Cardiovascular adaptation to hypoxia.....	12
Figure 1.6 Haematological response to hypoxia.....	13
Figure 1.7 Mechanism of hypoxic diuretic response leading to decreased plasma volume ...	14
Figure 1.8 Abundances of cytochrome P450 enzymes in the liver and small intestine.....	16
Figure 1.9 ROS formation pathway and its physiological balance.....	25
Figure 1.10 The oxygen-dependent regulation of the transcription factor HIF-1 $\alpha$ . ....	26
Figure 1.11 signal transduction pathways activated by hypoxia result in upregulation of the genes responsible for cells survival and down-regulation of CYP1A1 /1A2 due to the reduction of aryl-hydrocarbon receptor nuclear translocator (ARNT) availability. ....	27
Figure 1.12 Chemical structure of Sildenafil.....	29
Figure 1.13 Metabolic pathways and metabolites of sildenafil. ....	30

## Chapter 2

Figure 2.1 Schematic protocol for HepaRG differentiation and spheroid formation. ....	35
Figure 2.2 Chemical structures of substrate used in P450-Glo™ assay. ....	38

## Chapter 3

Figure 3.1 Flow chart of article searches and selection strategies.....	51
Figure 3.2 A pooled meta-analysis of drug pharmacokinetics in patients with respiratory diseases and hypoxaemia.....	68
Figure 3.3 Pooled meta-analysis of drug pharmacokinetics in healthy volunteers with hypoxaemia.....	70
Figure 3.4 Forest plot of bioavailability (F).....	71
Figure 3.5 Forest plot of maximum concentration ( $C_{max}$ ).....	72
Figure 3.6 Forest plot of time to maximum concentration ( $T_{max}$ ).....	73
Figure 3.7 Forest plot of area under the curve (AUC) at high-altitude.....	74

Figure 3.8 Forest plot of elimination constant (K) at high-altitude .....	75
Figure 3.9 Forest plot of elimination half-life ( $t_{1/2}$ ).....	76
Figure 3.10 Forest plot of clearance (Cl) .....	77
Figure 3.11 Forest plot of volume of distribution ( $V_d$ ) .....	78
Figure 3.12 Forest plot of mean residence time (MRT) at high-altitude. ....	79
Figure 3.13 Begg’s funnel plot for the assessment of publication bias .....	80

## Chapter4

Figure 4.1 Blood flow and structural organisation of the liver.....	87
Figure 4.2 Simple in vitro to more complex in- vivo models to study drug metabolism. ....	88
Figure 4.3 Metabolic enzymes in subcellular S9 fraction .....	93
Figure 4.4 Schematic protocol for HepaRG differentiation and spheroid formation .....	96
Figure 4.5 HepG2 cell morphology .....	99
Figure 4.6 Induction of CYP3A4 and CYP2C9 in HepG2 cells after 48 h treatment with CYP450 inducer rifampicin (RIF) at 0 to 100 $\mu$ M concentrations.. .....	101
Figure 4.7 Morphology of HepaRG cells.....	103
Figure 4.8 Expression of hepatocyte and biliary cells specific marker on HepaRG cells ....	104
Figure 4.9 Comparison between HepG2 and HepaRG CYP3A4 and CYP2C9 mRNA and protein expression .....	105
Figure 4.10 Formation of 3D HepaRG spheroid .....	106
Figure 4.11 Representative images of a developing ‘necrotic core’ in HepaRG cells with increases in ULA plate cell seeding densities .....	108
Figure 4.12 Measurement of HepaRG 3D spheroid diameter after 10 days in ULA plate culture. ....	109
Figure 4.13 Cell arrangement within HepaRG 3D culture.....	110
Figure 4.14 Viability assay of rifampicin and ketoconazole treatment in HepaRG monolayer .....	111
Figure 4.15 CYP3A4 and CYP2C9 mRNA transcript gene expression in HepaRG cultured in 2D monolayer and 3D spheroid formats .....	112
Figure 4.16 CYP3A4 and CYP2C9 activity in HepaRG cultured as monolayer (2D) and in spheroid formats (3D). ....	113
Figure 4.17 Effect of hypoxia (1% $O_2$ ) on HepaRG cell viability in 2D cell format. HepaRG cultured as 2D monolayer.....	114

Figure 4.18 Effect of hypoxia (1% O <sub>2</sub> ) on CYP3A4 and CYP2C9 expression in HepaRG cells grown in 2D monolayer format. ....	115
Figure 4.19 Immunofluorescent microscopy of 2D monolayer HepaRG cells and the effect of hypoxia on CYP3A4. ....	116
Figure 4.20 Immunofluorescent microscopy of 2D monolayer HepaRG cells and the effect of hypoxia on CYP2C9 ....	116
Figure 4.21 Effect of hypoxia (1% O <sub>2</sub> for 4, 6 or 24 h) on CYP3A4 and CYP2C9 activity in HepaRG 2D monolayer. ....	117
Figure 4.22 Representative images of HepaRG 3D spheroid viability at 1% O <sub>2</sub> over a 72 h exposure period. ....	119
Figure 4.23 Effect of hypoxia (1% O <sub>2</sub> for 24 h) on CYP3A4 and CYP2C9 activity and transcript expression in HepaRG 3D spheroids. ....	120
Figure 4.24 Effect of hypoxia on ABC transporter expression and functional activity. ....	123

## Chapter 5

Figure 5.1 ROS formation pathway .....	127
Figure 5.2 Possible signal transduction pathways mediated by ROS that regulate CYP450 isoforms under hypoxia .....	130
Figure 5.3 Summary of different assays used to measure ROS. ....	141
Figure 5.4 Impact of hypoxia upon H <sub>2</sub> O <sub>2</sub> generation. ....	143
Figure 5.5 Impact of hypoxia upon ROS production in HepaRG cells .....	144
Figure 5.6 Impact of hypoxia on mitochondrial superoxide radical generation in HepaRG cells .....	147
Figure 5.7 Effect of menadione treatment on HepaRG viability .....	151
Figure 5.8 Effect of menadione on H <sub>2</sub> O <sub>2</sub> and superoxide radical generation .....	152
Figure 5.9 Effects of NAC and Tiron treatment on HepaRG cell viability .....	153
Figure 5.10 Effect of NAC on ROS scavenger under normoxia and hypoxia .....	154
Figure 5.11 Effect of Tiron on ROS scavenger under normoxia and hypoxia using MitoSox assay .....	156
Figure 5.12 The effect of ROS induction and suppression on CYP3A4 in HepaRG cells ...	159
Figure 5.13 The effect of ROS induction and suppression on CYP2C9 in HepaRG cells ...	163
Figure 5.14 Gene expression of proinflammatory-related mediators in HepaRG cultured at normoxic (21% O <sub>2</sub> ) or hypoxic (1% O <sub>2</sub> for 6, 24 or 72 h) conditions .....	166
Figure 5.15 Cell viability of HepaRG cells upon IL-6 treatment .....	167

Figure 5.16 The effect of IL-6 treatment on CYP3A4 and CYP2C9 mRNA and protein expression in HepaRG cells.....	168
Figure 5.17 Cell viability of HepaRG cells upon TNF- $\alpha$ treatment .....	169
Figure 5.18 The effect of TNF- $\alpha$ on CYP3A4 and CYP2C9 mRNA expression and protein level in HepaRG cells.....	170
Figure 5.20 Regulation of CYP3A4 and CYP2C9 expression by PXR ligand rifampicin ...	172
Figure 5.19 The effect of rifampicin on PXR activity in HepaRG cells.....	172
Figure 5.21 Impact of Hypoxia upon gene and protein expression of PXR. ....	173
Figure 5.22 Impact of proinflammatory treatment upon PXR in HepaRG cells .....	174
Figure 5.23 Effect of hypoxia upon ERK1/2 protein expression in HepaRG cells .....	176
Figure 5.24 Effect of PD98059 on HepaRG cell viability .....	176
Figure 5.25 Effect of PD98059 treatment upon ERK1/2 in HepaRG cells.....	178
Figure 5.26 Effect of PD98059 treatment upon PXR in HepaRG cells.....	180
Figure 5.27 The effect of ERK1/2 inhibition by PD98059 upon CYP3A4 and CYP2C9 protein expression .....	184

## Chapter 6

Figure 6.1. The impact of hypoxia on CYP3A4 and CYP2C9 enzyme activity .....	206
Figure 6.2. Set 1 Scenario A simulation of population PK and PD profile of 100 mg single oral dose of sildenafil (n=1000) under normoxia (red) or hypoxia from time 0 (blue) .....	210
Figure 6.3. SE1 Scenariio B simulation of population PK and PD profile of 100 mg single oral dose of sildenafil (n=1000) under normoxia (red) or hypoxia lineary increases from time 0 to 4 h (blue).....	212
Figure 6.4. SET 1 Scenario C simulation of population PK and PD profile of 100 mg single oral dose of sildenafil (n=1000) under normoxia (red) or hypoxia increased in step function at 4 h (blue).....	213
Figure 6.5. Simulation of population PK of 100 mg single oral dose of sildenafil (n=1000) under normoxia or different SET 1 hypoxia scenarios .....	216
Figure 6.6. Simulation of population PK/PD profile of 100 mg single oral dose of sildenafil (n=1000) under normoxia or different SET 1 hypoxia scenarios .....	216
Figure 6.7. SET 2 Scenario A simulation of population PK and PD profile of 100 mg single oral dose of sildenafil (n=1000) under normoxia (red) or hypoxia (blue) from time 0 considering the change of $Cl_{int}$ and increase hepatic blood flow by 40% under hypoxia.....	218

Figure 6.8. Simulation of the effect of hepatic blood flow ( $Q_h$ ) alteration on predicted hepatic clearance ( $CL_{\text{hepatic}}$ ) of sildenafil where the hepatic intrinsic CL ( $CL_{\text{int}}$ ) is unchanged..... 222

## **Chapter 7**

Figure 7.1 Possible signaling pathways that downregulate CYP3A4 and CYP2C9 under hypoxia..... 239

# Index of Tables

## Chapter 1

Table 1.1 The changes of CYP450 isoforms expression under acute hypoxia (exposed to < 21% of O <sub>2</sub> for periods of < 1 week).....	19
---	----

## Chapter 2

Table 2.1 Primer used for the analysis of gene expression by RT-PCR.....	40
Table 2.2 TaqMan gene expression assay used.....	41
Table 2.3 Antibodies and their concentrations employed in Western blotting. ....	45

## Chapter 3

Table 3.1 General drug properties. ....	53
Table 3.2 Study characteristics. ....	56
Table 3.3 Changes in pharmacokinetics of different drugs under hypoxaemia. ....	61

## Chapter 4

Table 4.1 Comparative expression of CYP450 isoenzymes in primary human hepatocytes and hepatoma cell lines.....	91
---	----

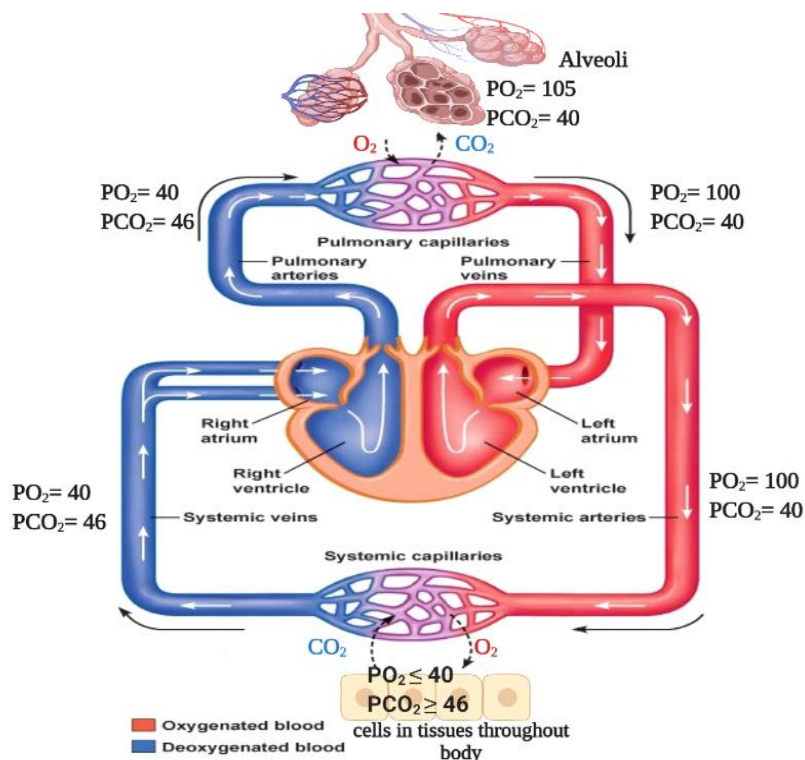
## Chapter 6

Table 6.1 PK Parameters used in Monte Carlo simulation. ....	200
Table 6.2 Key PK parameters used for Monte Carlo simulation summarised from Table 6.3 .....	207
Table 6.3 Summary of SET 1 simulation outcomes.....	214
Table 6.4 PK parameters used in Monte Carlo simulation SET 2.....	219
Table 6.5 Concentration-time outcomes, CL <sub>total</sub> , F <sub>total</sub> , E <sub>H</sub> comparing Scenarios A SET 1 versus SET2.....	219
Table 6.6 Excel-based ‘sensitivity analysis’ of the impact of changing Q <sub>h</sub> or CL <sub>int</sub> upon some key sildenafil PK parameters.....	223

## **Chapter 1: Introduction**

## 1.1 Arterial hypoxaemia

Arterial hypoxaemia is the state of low oxygen concentration in arterial blood. The oxygen level in the blood is proportional to the partial pressure of oxygen ( $PO_2$ ). Although the  $PO_2$  of arterial blood ( $PaO_2$ ) falls slowly with age, the lower limit of normal for an adult is usually accepted to be a  $PaO_2$  of 60 mmHg (8.0 kPa). Normal  $PaO_2$  in young, healthy people is about 95 mmHg; **Figure 1.1** shows the partial pressures of gases in the blood. Arterial hypoxaemia will lead to tissue hypoxia (otherwise known as anoxic hypoxia) due to insufficient oxygen delivery to body tissues (Collins and Shehabi, 2012). Tissues of the body depend on arterial oxygen for survival, growth, and function, with oxygen critical for oxidative phosphorylation which produces the fundamental energy substrate adenosine triphosphate (ATP) (Chance and Williams, 1956). There are two primary conditions of hypoxia associated with human exposure: **normobaric hypoxia** at normal barometric pressure equivalent to that at sea level – (sea level pressure 760 mmHg); **hypobaric hypoxia**, which is hypoxia occurring at low pressure- < 760 mmHg, such as at high altitude.



**Figure 1.1 Normal partial pressure of the gases in the blood.** Blood in the systemic veins, which is delivered to the lungs by pulmonary arteries, usually has a partial pressure of oxygen ( $PO_2$ ) of 40 mmHg and a partial pressure of carbon dioxide ( $PCO_2$ ) of 46 mmHg. After gas exchange in the alveoli of the lungs, blood in the pulmonary veins and systemic arteries has a  $PO_2$  of about 100 mmHg. Adapted from (Stanfield, 2017).



Hypobaric hypoxia is classified into acute hypoxia, chronic hypoxia, or chronic intermittent hypoxia (Richalet and Jimenez, 2015). In the context of high altitude, arterial hypoxaemia occurs in highlander populations that reside above 2,500 m and in lowlanders who migrate to high-altitude for occupational or recreational purposes (León-Velarde *et al.*, 2005). At sea level, arterial hypoxaemia occurs in patients suffering from pulmonary/cardiovascular medical conditions such as congestive heart failure and chronic obstructive pulmonary disease (Sarkar, Niranjana and Banyal, 2017). It is also actively elicited in the experimental setting in normobaric hypoxia low oxygen chambers (Fall *et al.*, 2018).

## 1.2 Pathophysiology of hypoxaemia

Excluding anaemias, there are several causes of hypoxaemia under normobaric conditions associated with cardiovascular and pulmonary systems. These include:

- **Ventilation /perfusion (V/Q) mismatch**
- **Right-to-left shunt**
- **Diffusion impairment**
- **Hypoventilation**

Additionally, hypoxaemia can occur under both normobaric and hypobaric conditions due to a **low fraction of inspired oxygen** ( $F_{iO_2}$ ).

### 1.2.1 Ventilation /perfusion (V/Q) mismatch

Ventilation /perfusion (V/Q) mismatch is the most commonly known cause of hypoxaemia which occurs when there is an imbalance between the amount of air reaching the alveoli (ventilation e.g., L/min) and the amount of blood reaching the alveoli (perfusion e.g., L/min) (Belda, Soro and Ferrando, 2013). This ratio of V/Q in a normal healthy human lung is ca. 0.8, i.e., a slightly lower ventilation flow compared to perfusion.

Asthma, COPD, bronchiectasis, cystic fibrosis, interstitial lung diseases, and pulmonary hypertension are common causes of hypoxaemia due to V/Q mismatch which can be associated with either pulmonary shunt mismatch or deadspace mismatch, or a combination of both, depending on the severity and specific pathophysiology of the condition (Sarkar, Niranjana and

Banyal, 2017). Other factors such as diffusion impairment, respiratory muscle fatigue, and right-to-left shunts can also contribute to hypoxaemia in these conditions.

There are two types of V/Q mismatch: **Pulmonary-shunt mismatch** and **Deadspace mismatch** (Figure 1.2).

**Pulmonary shunt mismatch** - A low V/Q ratio (e.g.,  $< 0.8$ ) develops when ventilation is diminished in proportion to perfusion. It causes hypoxaemia through reduced alveolar oxygen levels ( $PAO_2$ ) and subsequently leads to reduced arterial oxygen levels ( $PaO_2$ ). During chronic hypoxaemia, an important compensatory mechanism occurs to maintain the balance between ventilation and perfusion known as hypoxic pulmonary vasoconstriction (HPV). The human body will try to restrict perfusion in areas of the lungs with insufficient ventilation. Subsequently, the blood is diverted to the well-ventilated lung regions (West and Dollery, 1963; Orchard, De Leon and Sykes, 1983). However, chronic HPV causes vascular structural remodelling and subsequent development of sustained pulmonary hypertension (Leach and Treacher, 1995). The hypoxia mediates vasoconstriction by inhibiting the pulmonary artery voltage-gated  $K^+$  channels leading to intracellular  $K^+$  accumulation and cell depolarisation (Ward and Aaronson, 1999). This triggers the opening of the voltage-gated L-Type  $Ca^{2+}$  channels leading to  $Ca^{2+}$  influx and subsequently vasoconstriction (Ward and Aaronson, 1999; Aaronson *et al.*, 2006).

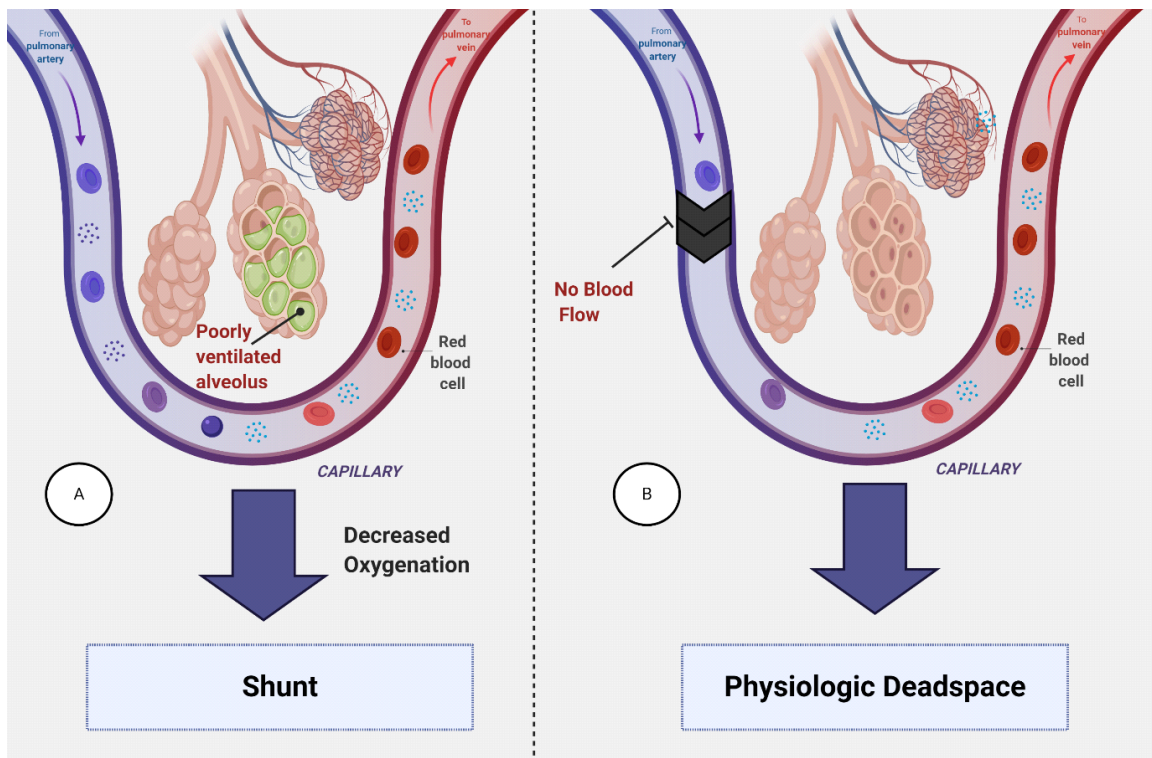


**Figure 1.2-Types of ventilation /perfusions (V/Q) mismatch. Fig 1.2A** In shunt, the alveoli are perfused but not ventilated while in physiologic dead space. **Fig 1.2B**, alveoli are ventilated but not perfused, which can be reversed as lung perfusion changes. Designed by D. Alablani – BioRender.

**Deadspace mismatch** - High V/Q ratio (e.g., > 0.8) develops when ventilation is in excess relative to perfusion, for example, in pulmonary embolism, which results in localised decreases in perfusion with the consequent rise in V/Q ratio. This is associated with dead space-like effects - the air in the affected area of the lung is not contributing to gas exchange and is essentially wasted - since the removal of CO<sub>2</sub> is reduced due to decreased perfusion (Pettersson and Glenn, 2014). Although the impact of a deadspace mismatch on blood oxygenation is minimal, it can cause hypoxaemia if the compensatory rise in total ventilation - which the amount of air that is inhaled and exhaled in the lung in a given amount of time to remove excess CO<sub>2</sub>- is absent. For example, in this deadspace effect, the blood is diverted from the low-perfusion areas of the lung, which can lead to the development of low V/Q in other regions of the lung. This will result in hypoxaemia unless a compensatory rise in total ventilation occurs (Sarkar, Niranjana and Banyal, 2017). The compensatory elevation of ventilation normalises the V/Q ratio for the low V/Q areas.

### 1.2.2 Right-to-left shunt

Right-to-left shunt is an extreme degree of V/Q mismatch where there is **no** ventilation (**V/Q ratio approaches 0**). A right-to-left shunt occurs as a result of various pulmonary diseases such as pneumonia, pulmonary oedema, acute respiratory distress syndrome, alveolar collapse, and pulmonary arteriovenous malformations (Sarkar, Niranjana and Banyal, 2017). The shunt passes the blood from the right to left side of the heart without undertaking productive gas exchange. In healthy individuals, a small effectively deoxygenated blood return to the left-side of the heart constitutively takes place (2–3% of cardiac output) through the bronchial veins draining into oxygenated pulmonary vein (**Figure 1. 3**).

### 1.2.3 Diffusion impairment

An impairment in the ability of the lung to transport oxygen into and out of the blood is a phenomenon at the alveolar-capillary membrane level. Two critical factors affect gas diffusion through this membrane. Specifically, the pressure gradient between the venous blood and alveolar gas and a thickening of the membrane. The thickening of the alveolocapillary membrane and diffusion impairment occurs with various pulmonary diseases such as pulmonary fibrosis, asbestosis, pneumoconiosis, diffuse lung lymph granulomatosis, and other conditions of the alveolar-capillary barrier. The degree of hypoxaemia in these disorders will be exacerbated by exercise (Belda, Soro and Ferrando, 2013) (**Figure 1. 3**).

### 1.2.4 Hypoventilation

Hypoventilation occurs due to dysfunction of the respiratory control at various levels such as the respiratory centre in the brainstem, in the spinal cord, in nerves supplying the respiratory muscles, at the neuromuscular junction and where respiratory muscles and the chest wall bellows are impacted. Hypoventilation does not produce significant hypoxaemia in the healthy lung, but in the presence of lung disease the resulting hypoxaemia can be severe (Sarkar, Niranjana and Banyal, 2017) (**Figure 1.3**).

### 1.2.5 Low Fraction of inspired oxygen ( $F_{iO_2}$ )

Low inspired oxygen levels in the surrounding environment may cause arterial hypoxaemia. A low fraction of inspired oxygen ( $F_{iO_2}$ ) is commonly observed in individuals ascending to high altitudes (above 2500 m), where the atmospheric oxygen levels are reduced. Additionally, situations such as smoke inhalation or being in proximity to fires, where combustion depletes the oxygen from the surrounding air, can also result in a decreased  $F_{iO_2}$  at sea level (Belda, Soro and Ferrando, 2013) (**Figure 1.3**).

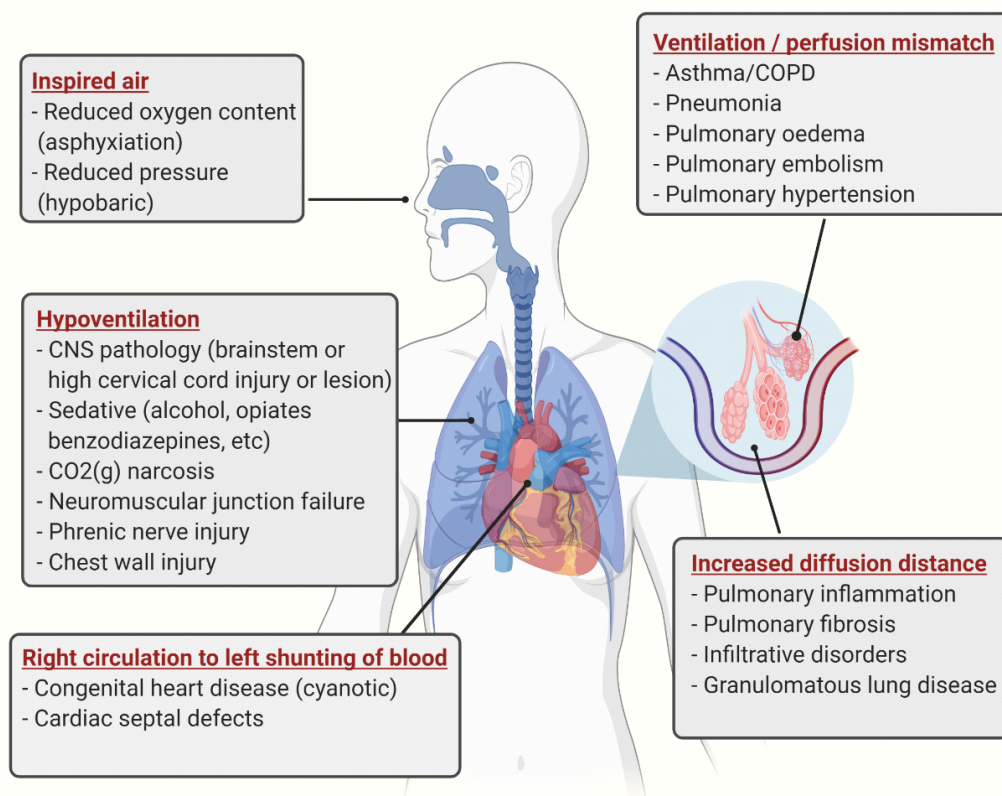


**Figure 1.3** Various mechanisms in hypoxaemia and associated medical conditions. Designed by D.Alablani - BioRender.

## 1.3 Measures of oxygenation

Within the field of physiology and clinical practice, a wide range of physiological and clinical measures have been established to evaluate tissue oxygen levels and determine whether they are potentially inadequate to meet the metabolic demands of the tissues. These measures serve as valuable indicators in assessing the sufficiency of oxygen supply for proper tissue function and homeostasis.

### 1.3.1 Arterial oxygen saturation ( $SpO_2$ and $SaO_2$ )

$SaO_2$  serves as a direct assessment of the proportion of oxygen-saturated haemoglobin (oxyhaemoglobin) in arterial blood, which can be determined through either an arterial blood gas test or pulse oximetry. On the other hand,  $SpO_2$  provides a non-invasive measurement of the percentage of oxyhaemoglobin in the capillary bed using co-oximetry with a pulse oximeter. A resting  $SaO_2$  level below or equal to 95%, or a desaturation of 5% or more during exercise, is regarded as indicative of an abnormal oxygen saturation (O'Driscoll *et al.*, 2017).

### 1.3.2 Arterial oxygen tension ( $PaO_2$ )

Oxygen undergoes diffusion from the alveolus into the pulmonary capillary and subsequently dissolves in the plasma. The amount of oxygen that dissolves into the plasma is determined by the arterial oxygen tension ( $PaO_2$ ).  $PaO_2$  is measured using an arterial blood gas test, and a value below 80 mmHg is regarded as abnormal (Theodore, 2020). This threshold assists in identifying deviations from the expected level of arterial oxygen tension and provides insights into an individual's respiratory function and gas exchange efficiency.

### 1.3.3 Alveolar to arterial (A-a) oxygen gradient

The **A-a oxygen gradient** represents the difference between the oxygen amount in the alveoli, known as the alveolar oxygen tension ( $PAO_2$ ), and the dissolved oxygen in the plasma. Its purpose is to aid in determining the underlying cause of hypoxemia. By measuring the A-a gradient, clinicians can narrow down whether the hypoxaemia is originating from extrapulmonary or intrapulmonary factors. An A-a gradient value exceeding 15 mmHg is considered abnormal. Elevated A-a gradient values typically indicate conditions such as ventilation-perfusion (V/Q) mismatch, right-to-left shunt, or impaired diffusion. Conversely, normal A-a gradient values falling within the range of 5 to 15 mmHg may suggest hypoventilation or low inspired oxygen as the primary contributors to the hypoxaemia (Theodore, 2020; Hantzidiamantis and Amaro, 2022).

### 1.3.4 $PaO_2/FiO_2$ ratio

The  **$PaO_2/FiO_2$  ratio** is a widely utilised measure of oxygenation, particularly in ventilated patients. It serves as a useful indicator of the severity of acute respiratory distress syndrome (ARDS). In normal circumstances, the  $PaO_2/FiO_2$  ratio ranges from 300 to 500 mmHg. However, values below 300 mmHg suggest impaired gas exchange, signifying abnormal

oxygenation. Furthermore, a  $\text{PaO}_2/\text{FiO}_2$  ratio below 200 mmHg indicates severe hypoxaemia, often observed in conditions such as severe pneumonia (Theodore, 2020).

### 1.3.5 Arterial to alveolar (a-A) oxygen ratio

The **a-A oxygen ratio**, calculated by dividing the  $\text{PaO}_2$  by the  $\text{PAO}_2$  ( $\text{PaO}_2/\text{PAO}_2$  ratio), serves as an important measure in assessing oxygenation status. The lower accepted limit of normal for this ratio ranges between 0.77 and 0.82 (Gilbert and Keighley, 1974).

### 1.3.6 Oxygenation index (OI)

The **oxygenation index (OI)** is a widely utilised parameter in neonates with persistent pulmonary hypertension of the newborn to assess the degree of hypoxaemia and guide treatment decisions. It plays a crucial role in determining the timing of interventions, such as the administration of inhaled nitric oxide, a vasodilator known for its ability to improve oxygenation. Effective management of hypoxaemia using inhaled nitric oxide has demonstrated positive outcomes, including reduced reliance on extracorporeal membrane oxygenation (ECMO) and a lower risk of chronic lung disease in newborns with persistent pulmonary hypertension (Trachsel *et al.*, 2005; Nelin and Potenziano, 2019). In healthy individuals, the normal OI value is typically less than 5. However, an OI value exceeding 25 indicates severe hypoxaemic respiratory failure (Theodore, 2020).

## 1.4 High altitude arterial hypoxaemia: complications and management

Arterial hypoxaemia occurring at high altitudes can lead to various medical illnesses. Acute mountain sickness (AMS) is a condition typically associated with acute exposure to altitude (defined as >2500 m) and is characterised by a range of non-specific symptoms (Brugniaux *et al.*, 2007). The **Lake Louise AMS** scoring system is used to diagnose and evaluate the severity of the symptoms associated with AMS. It comprises five indicators: headache, gastrointestinal upset, fatigue/weakness, dizziness/light-headedness and sleep disturbance. For each symptom, a score of 0 to 3 is assigned. In an individual acutely exposed to high altitude with a collective score on this system of  $\geq 3$ , (which must include the headache component) a diagnosis of AMS is made (Roach *et al.*, 2018). AMS resolves upon descent to sea level or with high altitude acclimatisation. However, AMS can progress to more severe conditions such as **high-altitude**

**pulmonary oedema (HAPE)** and **high-altitude cerebral oedema (HACE)**. HAPE is characterised by non-productive cough, dyspnoea and reduced exercise performance (Paralikar, 2012). HACE is marked by disturbances of consciousness that may develop into varying degrees of psychiatric change, confusion, ataxia of gait and ultimately to deep coma (Roach, Wagner and Hackett, 2016). A variety of drugs are used to manage AMS, such as acetazolamide, a carbonic anhydrase inhibitor considered the gold standard, and which is also used for prevention of HACE. Glucocorticoids such as dexamethasone are one of the first line treatments for HAPE and are used as an alternative to acetazolamide in AMS (Donegani *et al.*, 2016). Further, calcium-channel blockers like nifedipine and phosphodiesterase-5 (PDE-5) inhibitors such as sildenafil and tadalafil have been shown to decrease arterial hypoxaemia, pulmonary hypertension, the alveolar-arterial gradient and improve physical performance at high altitude (Bartsch *et al.*, 1991; Richalet *et al.*, 2005).

## **1.5 Hypoxia and physiological change that may be relevant to altered drug pharmacokinetics**

The primary goal of the current project was to explore drug pharmacokinetics (PK) under hypoxia. Pharmacokinetic processes can be defined as: **absorption** with relevant PK parameters being absorption half-life and first-order absorption rate constant:  $t_{1/2\text{ abs}}$ ,  $K_{\text{abs}}$ , respectively and the extent of bioavailability (F); **disposition**: which includes the distribution and elimination of a drug and with relevant parameters being  $V_d$  – volume of distribution,  $F_u$  – fraction unbound in plasma,  $F_{u_b}$  – fraction unbound in blood, CL – total body clearance,  $CL_u$  – total body clearance of unbound drug,  $CL_R$  – renal clearance, elimination half-life and first-order elimination rate constant  $t_{1/2}$ ,  $K$ , respectively. Parameters such as area under the curve plasma drug concentration-time profile (AUC), maximal or peak concentration ( $C_{\text{max}}$ ) and time to peak concentration ( $T_{\text{max}}$ ) and mean residence time of the drug (MRT) describe the exposure of the body to the administered drug reflect how much of the drug gains access to the systemic circulation ( $F \cdot \text{Dose}$ ), the drug's CL and the relative rate constants of absorption and elimination.

In Section 1.5.1 the effect of hypoxia on relevant organs/tissues is briefly reviewed and how the physiological changes under hypoxia impacted the PK and PD of drug. Section 1.5.2 review the effect of hypobaric hypoxaemia on the PK of several drugs in healthy humans.



## **1.5.1 Hypoxia and physiological systems**

### **1.5.1.1 Gastrointestinal system**

The impact of hypoxia upon gastrointestinal physiology relevant to drug pharmacokinetics remains unclear.

A study has investigated the effect of chronic hypobaric low oxygen levels (altitude of 5000 m) on food digestion and gastrointestinal absorption and was unable to establish any correlation between hypobaric hypoxia and malabsorption of carbohydrate, protein and fat (Kayser, 1992) ; similar results were seen for a study performed at lower altitude (3100 m to 4846 m; 11 days exposure) (Chesner, Small and Dykes, 1987). In contrast, Boyer and Blume report 48.5% decrease in fat absorption and 24.3% decrease in xylose secretion (used as a diagnostic agent to observe malabsorption) associated with severe hypoxaemia at higher elevation (6300 m) (Boyer and Blume, 1984).

Gastrointestinal complaints are frequently reported at high altitudes and have traditionally been attributed to delayed gastric emptying. Gastric mucosal blood flow measured by automated air gastric tonometry has been shown to decrease at high altitudes (Martin *et al.*, 2007), whereas, in contrast, studies using Doppler ultrasonography have reported increased mesenteric and hepatic venous blood flow subsequent to hypoxic vasodilatation (Kalson *et al.*, 2010). The subtle effects of a hypobaric hypoxic environment upon local capillary pressures and epithelial-luminal biochemistry including membrane carriers, metabolism and local intestinal secretions that influence pH remain unknown but could be highly relevant for oral drug absorption.

### **1.5.1.2 Respiratory and cardiovascular systems**

The pulmonary system is susceptible to acute and chronic changes in oxygen levels. The ventilation rate increases after acute exposure to hypoxia, while both ventilation rate and pulmonary volume - amount of air that can be held in the lungs at various stages of the breathing cycle are elevated following more chronic exposure to low oxygen levels (Monge and Leon-Velarde, 1991; Arancibia *et al.*, 2003). Increases in ventilation rate lead to a decrease of the partial pressure of carbon dioxide (PCO<sub>2</sub>) and a reduction of CO<sub>2</sub> in the circulation known as hypocapnia. The net result of hypocapnia is an elevation of blood pH, i.e., alkalosis. During the first few days of acute hypoxia exposure, bicarbonate levels in the blood decrease due to

increased excretion via the kidney to compensate for alkalosis. Associated with this is a reduction in plasma volume (detailed in section 1.5.1.4) (**Figure 1.4**).

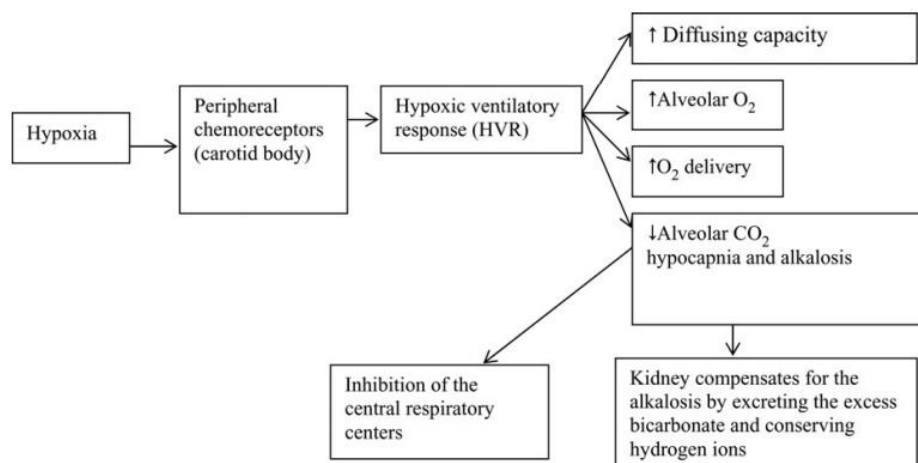


**Figure 1.4 Respiratory acclimatisation to hypoxia. Improved tissue oxygenation occurs through increased pulmonary ventilation and diffusion capacity.** Adapted from (Goldfarb-Rumyantzev and Alper, 2014).

However, the effect of these changes on drug pharmacokinetics is unknown and may depend on the specific drug characteristics, e.g., extent of the drug's volume of distribution ( $V_d$ ), how its ionic character is affected by pH changes, indeed how changed pH affects many aspects of the drug's plasma and/or tissue binding, its engagement with enzymes and carriers, and its passive permeation across membranes and barriers.

Exposure to acute hypobaric hypoxia in human volunteers is reported to increase cardiac output by approximately 22% and heart rate by 18% (Klausen, 1965; Naeije, 2010) (**Figure 1.5**). However, the response of the cardiovascular system to hypoxia is temporary, the cardiac output returning to baseline levels (ca. 4.7 L/min) after a few days of acclimatisation (Klausen, 1965; Vogel and Harris, 1967). Changes in cardiac output may affect drug absorption and disposition due to the alteration of organ perfusion (Hui *et al.*, 2016), particularly, this may occur for the elimination of high extraction ratio drugs.

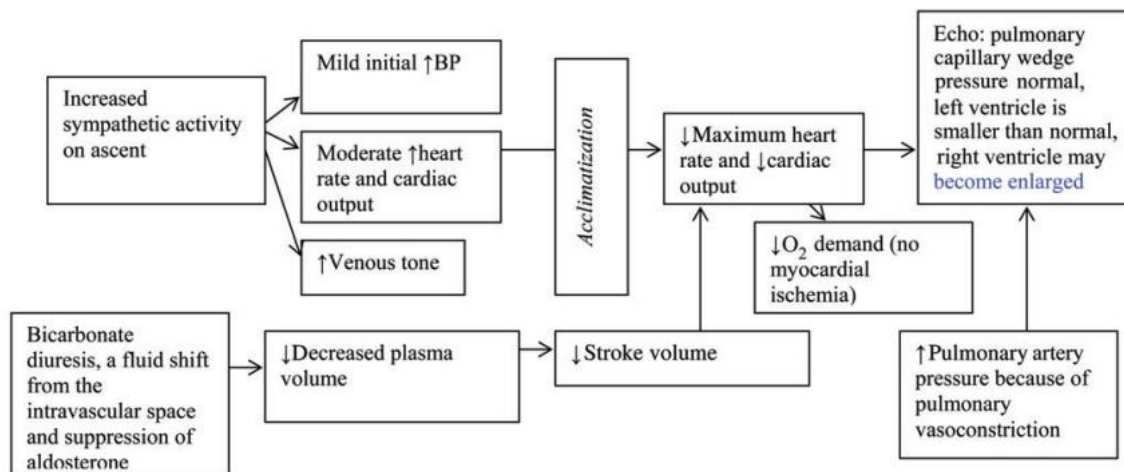


**Figure 1.5 Cardiovascular adaptation to hypoxia.** Adapted from (Goldfarb-Rumyantzev and Alper, 2014).

### 1.5.1.3 Haematological system

Hypoxia induces haematocrit (Hct) elevation through increased erythropoiesis and increased water loss from hyperventilation and the hypoxia-diuretic response (Mairbäurl, 1994; Jacobs *et al.*, 2012). Erythropoietin (EPT) released from the kidney as a response to the low oxygen level stimulates erythropoiesis (**Figure 1.6**). However, it takes about 2 to 3 days for new red blood cells to increase haematocrit. An increase in water vapour loss during hyperventilation may also result in a reduction of plasma water increasing Hct. The diuretic response can increase Hct within hours of hypoxia exposure (Hui *et al.*, 2016); a report found an increase of approximately 9% of Hct after acute exposure (16 h) to a high altitude of 3800 m (Li *et al.*, 2009). The increase of erythrocyte mass under hypoxia and altered plasma water volume could influence a drug's pharmacokinetic through erythrocyte/plasma water redistribution, altered plasma water/interstitial water volumes, changed glomerular filtration.

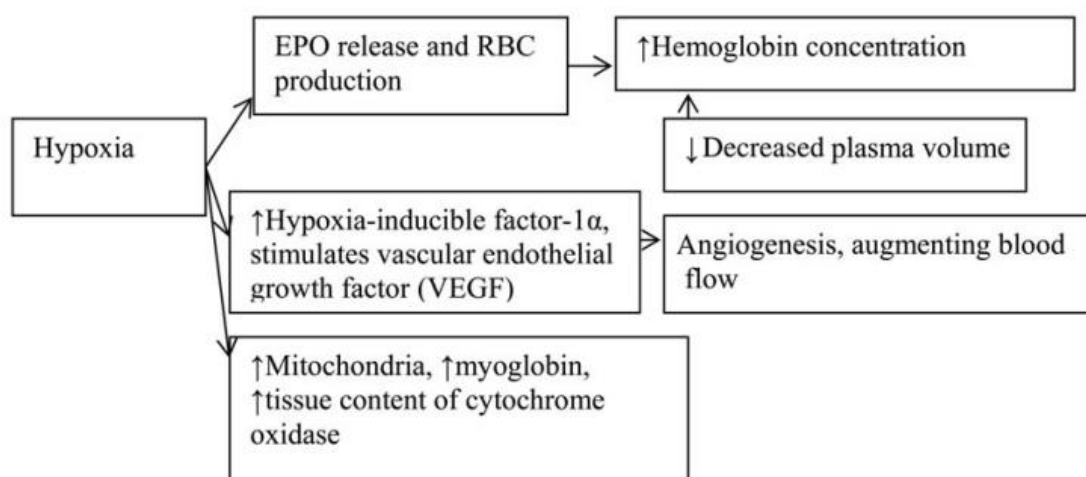


**Figure 1.6 Haematological response to hypoxia.** Adapted from (Goldfarb-Rumyantzev and Alper, 2014).

#### 1.5.1.4 Renal system

The effect of acute hypoxia on renal plasma flow, renal tubular secretion and reabsorption, glomerular filtration rate (GFR) and urine output still remains debatable and highly dependent on exposure time, as reported in a literature review of 2014 (Goldfarb-Rumyantzev and Alper, 2014). Some studies in humans suggest hypoxia (inhaled 10 -14% O<sub>2</sub>, 2 h exposure) produces only small non-significant changes in renal plasma flow and GFR (Berger *et al.*, 1949; Olsen *et al.*, 1992). In a longer hypoxia exposure time (4330 m, 24 h), a decrease by 17% in renal blood flow was reported (Steele *et al.*, 2020). In contrast, significant decreases in renal plasma flow and GFR have been demonstrated in chronic hypobaric hypoxia (Singh *et al.*, 2003; Pichler *et al.*, 2008). One of these studies reported a decrease in effective renal plasma flow of 38% upon chronic change from sea level to 5800 m, which had a causal association with increased Hct and blood viscosity (Singh *et al.*, 2003). Furthermore, hypoxia has been reported to act directly on the kidney, increasing local production of endothelin (Modesti *et al.*, 2006) and adrenomedullin (Haditsch *et al.*, 2007) which can suppress circulating antidiuretic hormone (ADH) and renin and aldosterone and potentially lead to a 1-3 L per day loss in body water (Jain *et al.*, 1980).

Respiratory alkalosis secondary to hypoxic tachypnoea promotes increased natriuresis, water diuresis, HCO<sub>3</sub><sup>-</sup> excretion and an overall fluid loss from the plasma water and hence plasma volume. This 'hypoxic diuretic response' is characterised by elevations in the renal excretion of sodium and water, in response to reduction in inspired oxygen (Jain *et al.*, 1980; Ge *et al.*,

2006) (**Figure 1.7**). Clearly changes in, for example, renal plasma flow, GFR and urinary pH can affect the renal clearance ( $CL_R$ ) of drugs and depending upon the importance of this route of elimination in a drug's overall clearance then this could affect substantially drug exposure levels.

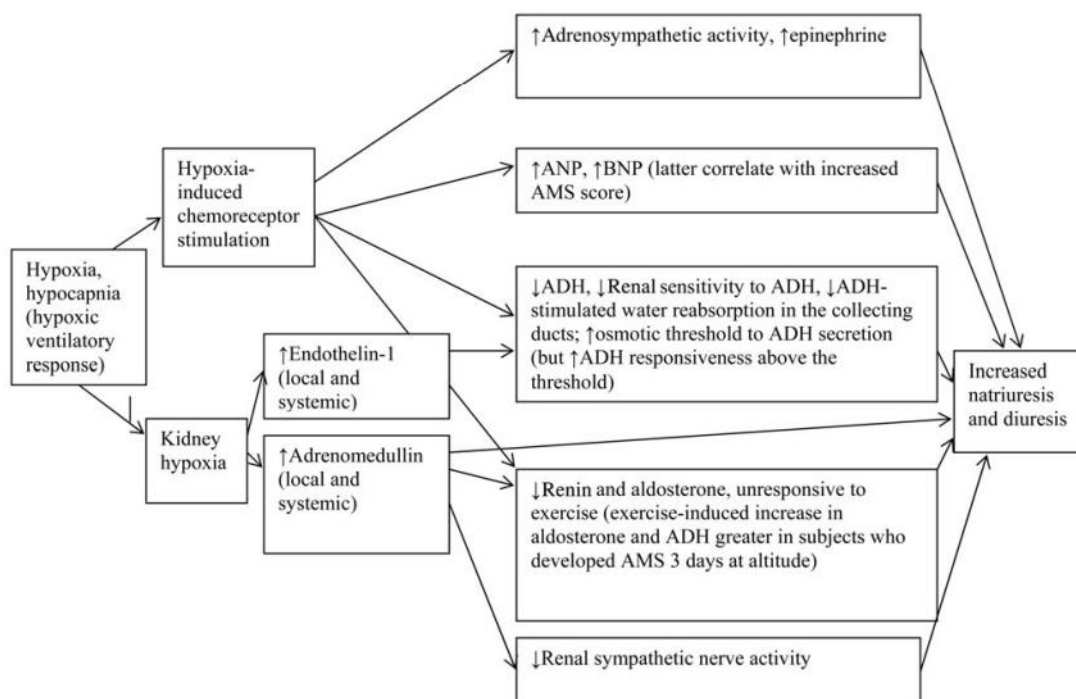


**Figure 1.7 Mechanism of hypoxic diuretic response leading to decreased plasma volume.** Adapted from (Goldfarb-Rumyantzev and Alper, 2014).

### 1.5.1.5 Cerebrovascular system

Exposure to hypoxia, be it normobaric or hypobaric in nature, causes an immediate rise in cerebrovascular blood flow (CVBF)- within the first 12 h of hypoxia- via cerebral vasodilation which normalises CVBF to pre-hypoxic values ca. 43 mL/100 g/min within three to five days of acclimatisation, even under continuous exposure to low levels of oxygen (Severinghaus *et al.*, 1966; Ainslie *et al.*, 2014).

For example, several studies have reported 40 to 70% increases in CVBF upon ascent to > 5000 m (Jensen *et al.*, 1990; Lucas *et al.*, 2011; Subudhi *et al.*, 2014; Willie *et al.*, 2014). Further, CVBF has been reported to increase by ca. 24% within the first 6-12 h (Severinghaus *et al.*, 1963), or 1 to 2 h (Jansen, Krins and Basnyat, 1999) of ascent from sea level to >3400 m. The onset of ventilatory acclimatisation coincides with the fall in CVBF, resulting in increases in

PaO<sub>2</sub> and reductions in PaCO<sub>2</sub> (Dempsey and Forster, 1982). Under higher, more normal, PaO<sub>2</sub> levels, vasodilation is attenuated, which reduces CVBF back toward normal. In addition to these factors, elevations in haematocrit over approximately two weeks act to decrease the initial rise in CVBF (Ainslie and Subudhi, 2014).

The magnitude of the change in CVBF resulting from hypoxia is dependent on four reflex mechanisms: i) hypoxic ventilatory response and hence the degree of respiratory alkalosis; ii) hypercapnic ventilatory response; iii) hypoxic cerebral vasodilatation, and iv) hypocapnic cerebral vasoconstriction (Severinghaus, 2001).

Alterations in drug distribution to the brain may occur as a consequence of changes in brain blood flow (Hui *et al.*, 2016). Furthermore, hypoxia-induced inflammatory reactions can increase the paracellular permeability and alter tight junction protein expression and/or localisation of tight junction of the blood-brain barrier (BBB) (Zhang *et al.*, 2000). A study conducted on rats exposed to acute hypoxia (6% O<sub>2</sub> for 30–60 min) showed an increase in vascular permeability of dextrans (4 and 10 kDa)—a tracer used to assess the BBB permeability and distribution - into the hippocampus and an enhancement in protein kinase C (PKC) activity (Willis, Meske and Davis, 2010). Therefore, hypoxia may enhance the distribution of low molecular central nervous system drugs to the brain.

### **1.5.1.6 Cytochrome P450**

Cytochrome P450 (CYP450) represents a superfamily of enzymes that consists of two main protein elements, a haem protein (CYP450) and flavoprotein (NADPH-CYP450) reductase containing both flavin mononucleotide (FMN) and flavin dinucleotide (FDN) (Dubey and Shaik, 2019). CYP450 enzymes are involved in what is known as phase I metabolism reactions, where functional group modifications are made to substrates to increase a substrate's polarity or access to phase II conjugation reactions; reactions which themselves add bulk and polarity to a molecule to further limit widespread tissue distribution and promote the efficiency of excretion.

CYP450 is located in many tissues throughout the body, however, it is in the liver where CYP450 enzymes are seen to display both the greatest diversity and in the highest concentrations. Within cells, CYP450 enzymes are located in the membranes of the endoplasmic reticulum (ER) and are involved in the metabolism of endogenous and exogenous molecules (Omura, 1999). The CYP1, CYP2, and CYP3 families account for 70% of the total hepatic P450 content and are responsible to a significant extent for the metabolism of

pharmaceutical actives (Weide and Steijns, 1999). The CYP3A4 member is the most abundant enzyme in the liver and is involved in the transformation of ca. 50% drugs that undergo metabolic conversion (Sevrioukova and Poulosa, 2013) (**Figure 1.8**). Extrahepatic CYP450 has been identified in a wide range of tissues, including the small intestine, pancreas, brain, lung, adrenal gland, kidney, bone marrow, mast cells, skin, ovary and testis (Krishna and Klotz, 1994; Chang and Kam, 1999). In the intestinal enterocyte for example CYP3A4 plays a role in reducing the extent of bioavailability of orally administered drugs.

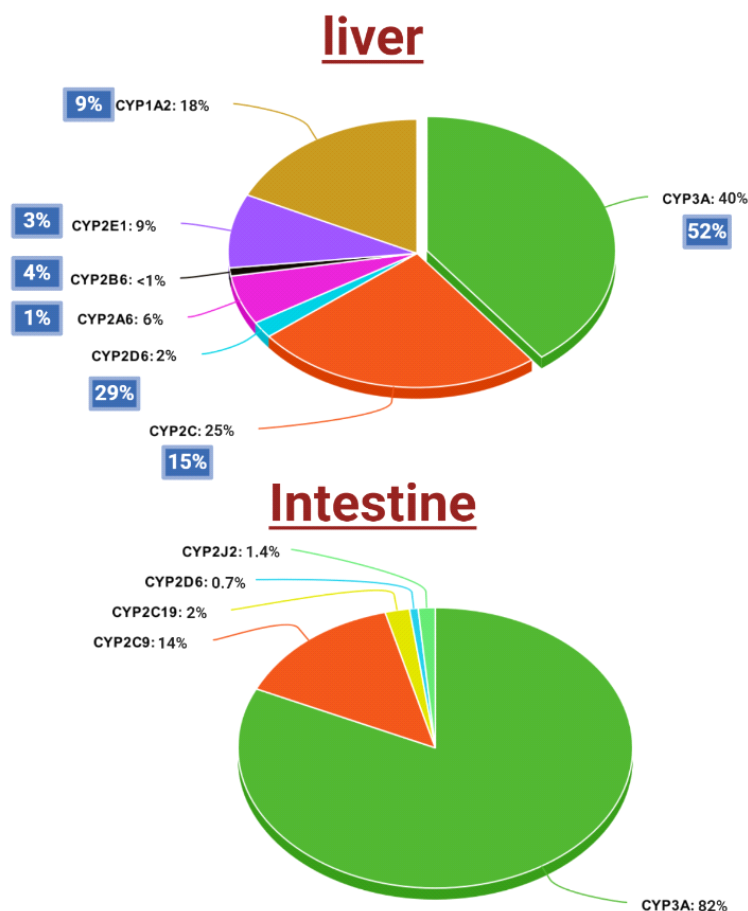


**Figure 1.8** Abundances of cytochrome P450 enzymes in the liver and small intestine. The pie charts indicate % hepatic and small intestine CYP isoform in human. The value in blue boxes corresponds to the % of clinically used drugs metabolised by each CYP. The data were adapted from (Yan and Caldwell, 2001; Donato and Castell, 2003; Paine *et al.*, 2006).

With parameters the organ clearance of drugs depends upon organ blood or plasma flow, the fraction of drug free in the blood or plasma and the intrinsic clearance of the drug associated with its ability for example to access across the cell membrane to the site of CYP450 enzymes in the endoplasmic reticulum and engage with the enzymes in reactions we commonly define by Michalis-Menten kinetics characterised  $V_{\max}/K_m$  constants and the context of the drug

concentrations at the enzyme site. Drugs can be categorised as high extraction ratio (ER) - $ER > 0.7$ -, low ER-  $ER < 0.3$ - or intermediate ER-  $ER 0.3$  to  $0.7$  - based on their pharmacokinetic properties, according to the Wilkinson and Shand model. High extraction ratio drugs, such as morphine, lidocaine and propranolol, are rapidly metabolised by the liver and have a low bioavailability. Low ER drugs, on the other hand, are metabolised more slowly by the liver and have a greater bioavailability. Warfarin, phenytoin and diazepam are some examples. The Wilkinson and Shand model also predict that the CL of high ER drugs is dependent on blood flow through the liver, whereas low ER drugs CL is dependent on enzyme activity (Wilkinson and Shand, 1975). Hypoxia may affect organ clearance at each of the above levels (Hui *et al.*, 2016).

In terms of CYP450 activities (**Table 1.1**), the effect of hypoxia on CYP450 is reported as time dependent (Proulx and Du Souich, 1995). These authors reporting in an animal study (rabbit) that exposure to low partial pressure of oxygen (12%) for 8 h decreased the concentration of CYP450, but only more prolonged exposures (up to 24 h of exposure) resulted in changes in functional substrate turnover. A number of animal studies have reported downregulation of CYP450 mRNA expression, enzyme activity and protein levels for a range of family members: CYP1A1 (Fradette *et al.*, 2002; Li, Wang, Li, Yuan, *et al.*, 2014; Wang *et al.*, 2017), CYP1A2 (Fradette *et al.*, 2002), CYP2B6 and CYP2C19 (Fradette and Souich, 2004), CYP2E1 (Li, Wang, Li, Zhu, *et al.*, 2014a) and CYP3A1 (Wang *et al.*, 2017). Other reports have shown that exposure to acute moderate hypoxia (exposure at 8 to 10% of O<sub>2</sub> for 24-48 h) upregulates the expression of CYP3A6 (Kurdi *et al.*, 1999; Fradette *et al.*, 2002, 2007a), CYP2D6 (Li, Wang, Li, Zhu, *et al.*, 2014a), CYP3A2 (Hori, Shimizu and Aiba, 2018) and CYP3A11 (Fradette *et al.*, 2007a). The expression of CYP2C9, when challenged by hypoxia, has been reported to be unchanged (Li, Wang, Li, Zhu, *et al.*, 2014a) or to decrease (Gola *et al.*, 2016) in rat, or to be upregulated in human endothelial cells (Michaelis *et al.*, 2005). Very pertinent to the current study is the downregulation of CYP3A4 expression reported in human liver cells in-vitro (HepaRG cells) (van Wenum *et al.*, 2018) and human fetal liver cells (Suzuki *et al.*, 2012) cultured under hypoxic conditions 3% O<sub>2</sub> (vs normoxia 21% O<sub>2</sub>) for 24-72 h.

Studies on human volunteers and patients are limited. Healthy humans living at sea level and subject to acute high-altitude exposure (4559 m) appear to experience only small decreases in CYP450 activity (i.e., as determined for substrates of CYP2D6, CYP3A4, CYP1A2 and CYP2C19) with little to no clinical significance (Jürgens *et al.*, 2002). Similarly, Streit *et al.* showed acute hypoxia at altitude (4500 m) does not impair the metabolism mediated by



## Chapter 1

CYP1A2 or CYP3A4 (Streit *et al.*, 2005) It is established, though, that hepatic blood flow significantly increases after exposure to hypoxia (Ramsøe *et al.*, 1970). This increase may compensate the reduction of CYP450 isoenzymes activity particularly if the drug has characteristics of a moderate to high hepatic extraction ratio drug.

Table 1.1 The changes of CYP450 isoforms expression under acute hypoxia (exposed to < 21% of O<sub>2</sub> for periods of < 1 week).

CYP450 isoforms												
Model	1A1	1A2	2B6	2C9	2C19	2D6	2E1	3A1	3A2	3A4	3A6	3A11
<b>Animal studies</b>	↓ (Fradette <i>et al.</i> , 2002; Li, Wang, Li, Yuan, <i>et al.</i> , 2014; Wang <i>et al.</i> , 2017)	↓ (Fradette <i>et al.</i> , 2002)	↓ (Fradette and Souich, 2004)	↓ (Gola <i>et al.</i> , 2016) ≈ (Li, Wang, Li, Yuan, <i>et al.</i> , 2014)	↓ (Fradette and Souich, 2004)	↑ (Li, Wang, Li, Yuan, <i>et al.</i> , 2014)	↓ (Li, Wang, Li, Zhu, <i>et al.</i> , 2014)	↓ (Wang <i>et al.</i> , 2017)	↑ (Hori, Shimizu and Aiba, 2018)		↑ (Kurdi <i>et al.</i> , 1999; Fradette <i>et al.</i> , 2002, 2007)	↑ (Fradette <i>et al.</i> , 2007)
<b>Human studies</b>		↑ (Jürgens <i>et al.</i> , 2002) ≈ (Streit <i>et al.</i> , 2005)			↑ (Jürgens <i>et al.</i> , 2002)	↓ (Jürgens <i>et al.</i> , 2002)				↓ (Jürgens <i>et al.</i> , 2002) ≈ (Streit <i>et al.</i> , 2005)		
<b>Model</b>	<b>1A1</b>	<b>1A2</b>	<b>2B6</b>	<b>2C9</b>	<b>2C19</b>	<b>2D6</b>	<b>2E1</b>	<b>3A1</b>	<b>3A2</b>	<b>3A4</b>	<b>3A6</b>	<b>3A11</b>
<b>In-vitro studies</b>				↑ (Michaelis <i>et al.</i> , 2005)						↓ (van Wenum <i>et al.</i> , 2018), (Suzuki <i>et al.</i> , 2012)		

↑ Upregulated; ↓ downregulated; ≈ unchanged.

### **1.5.2 Human studies exploring the impact of hypobaric hypoxia upon drug pharmacokinetics.**

The extent that drug pharmacokinetics and pharmacodynamics change at high altitude (>2500 m) remains unclear. It is complicated by a limited number of underpowered studies with participants exposed to different drugs, altitudes and exposure times. These studies have drawn different conclusions. There is a need for a series of well-controlled clinical research investigations.

In 2018, a Systematic Review and Meta-Analysis of the published literature on the impact of hypobaric hypoxia upon drug pharmacokinetics was published (Bailey, Stacey and Gumbleton, 2018). The analysis was restricted to human single-dose studies involving healthy males ( $21 \pm 3$  years; mean  $\pm$  S.D.) of Chilean or Chinese descent moving from low-altitude ( $\leq 600$  m) to terrestrial (not simulated) high-altitude ( $\geq 2,500$  m) in an acute manner ( $\leq 24$  h). Acute exposure avoided the complications of erythrocytosis that becomes evident during longer-term exposure at high-altitude. The analysis ultimately selected just six articles which met the inclusion criteria. However, reflective of the state of knowledge, the studies included were nevertheless generally underpowered and characterised by a high degree of intra-/inter-study variability. The limited selection of compounds exhibited diverse clearance pathways. The drugs involved in the analysis were: sulfamethoxazole (1200 mg PO,  $n = 20$ ) (Li *et al.*, 2009), acetazolamide (250 mg PO,  $n = 12$ ) (Ritschel *et al.*, 1998), lithium (300 mg PO,  $n = 7$ ) (Arancibia *et al.*, 2003), furosemide (40 mg PO,  $n = 12$ ) (Arancibia *et al.*, 2004), prednisolone (80 mg PO,  $n = 12$ ) (Arancibia *et al.*, 2005) and meperidine (0.75 mg/kg IM,  $n = 12$ ) (Ritschel *et al.*, 1996).

There was a consistent trend toward more prolonged oral absorption (i.e. longer absorption half-life) under acute high altitude exposure. Acute mountain sickness is often associated with gastrointestinal complaints, and there is some evidence that acute high-altitude exposure increases pre-prandial, with no effect on post-prandial, mesenteric and hepatic portal vein blood flows (Kalson *et al.*, 2010). Hypobaric-hypoxia may also impact upon gastric transit, local capillary pressures and epithelial-biochemistry, e.g., membrane carriers, metabolism, and local intestinal secretions, all of which could be highly relevant for the oral absorption of some drugs.

The meta-analysis reported a consistent trend for the ratio of the drug clearance/drug bioavailability (CL/F) parameter to be reduced under acute high-altitude conditions but for the

ratio of drug volume of distribution / drug bioavailability ( $V_d/F$ ) parameter to remain essentially unchanged. From this, the authors concluded that acute high-altitude was likely to have diminished CL, consistent with a trend for a longer elimination half-life ( $t_{1/2}$ ) under high-altitude conditions.

The six drugs in the analysis represented a diverse set of physicochemical and pharmacokinetic properties. The authors commented that a common mechanism underpinning high-altitude - induced changes in drug handling is not readily apparent. Decreases in drug CL through high-altitude exposure are often interpreted or assumed to involve diminished CYP450 activity.

While the drugs in the meta-analysis were predominantly highly protein-bound drugs, the impact of this upon pharmacokinetic parameters under challenge by hypoxia is a highly drug-individualised property. Changes in serum protein levels at high-altitude have been reported (Surks, 1966; Imoberdorf *et al.*, 2001; Li *et al.*, 2009), but the relevance in the acute setting is unclear. The plasma concentrations of total albumin and protein are reported to increase in people exposed to hypoxia, including that caused by high altitude, potentially leading to altered protein binding of the drug (Surks, 1966; Li *et al.*, 2009). Sulfamethoxazole is a drug highly bound to albumin (approximately  $F_u$  0.3). The protein binding of sulfamethoxazole is reported to be significantly higher in subjects exposed to acute ( $F_u$  0.2) high-altitude compared to that at sea-level ( $F_u$  0.34) (Li *et al.*, 2009). Similarly, a pharmacokinetic study of prednisolone suggested an increase of protein binding after acute hypoxia ( $F_u$  0.06) compared with under normal oxygen conditions at sea level ( $F_u$  0.43) (Arancibia *et al.*, 2005). Other studies have seen a decrease in the protein binding of meperidine and furosemide with increased  $F_u$  after acute exposure to hypoxia despite an increase of albumin levels (Ritschel *et al.*, 1996; Arancibia *et al.*, 2004). The furosemide study showed an increase of bilirubin concentration by 17.7% after acute exposure to hypoxia (Arancibia *et al.*, 2004). Bilirubin can compete with drug binding sites on albumin (Kazuo *et al.*, 1984; Hui *et al.*, 2016). Not unrelated, acute high-altitude exposure is associated with fluid extravasation, which may alter a drug's volume of distribution depending on if free drug concentrations or total drug concentrations are measured. However, a reduction in plasma volume under hypoxia exposure (acute exposure to a high altitude of 4360 m) has been reported to be associated with a small decrease in acetazolamide volume of distribution from a mean of 0.39 to 0.32 L·kg<sup>-1</sup>.

## Chapter 1

The drugs studied above, and indeed in other investigations, show a wide range of disposition characteristics, i.e. extensive vs limited metabolism, and with metabolism involving both CYP450 dependent and independent mechanisms, and where elimination depended upon a high or low extent of unchanged renal excretion. In terms of drug clearance (CL), the CL/F of lithium carbonate (Arancibia *et al.*, 2003) (no evidence of metabolism), lidocaine (Zhang *et al.*, 2016) (highly metabolised by CYP450) and prednisolone (Arancibia *et al.*, 2005) (metabolised and parent drug also renally excreted) have been shown to decline in subjects transiting to high altitude with acute reductions of inspired oxygen. Similarly, the CL/F of oral sulfamethoxazole (highly metabolised but not CYP450) was lower after exposure to 3800 m compared with subjects at an altitude of 400 m (Li *et al.*, 2009). Both increases in CL (acetazolamide - Ritschel *et al.*, 1998) and decreases in CL (meperidine - Ritschel *et al.*, 1996) have been reported as a consequence of acute high-altitude hypoxia (ca 4360 m). In the case of meperidine, at least part of the decrease in CL is attributed to reduced urinary pH occurring with an acute change from low to high altitude conditions and an associated reduced fraction of meperidine eliminated unchanged in the urine (Ritschel *et al.*, 1966; Gledhill, Beirne and Dempsey, 1975). Acetazolamide is a weak acid drug with a pKa of 7.2 excreted to a very large extent unchanged in the urine, with the expectation of a lower excretion associated with reduced urinary pH. Decreases in CL are not only observed in acute hypoxia, but also with chronic exposure to reduced oxygen. For example, 30-60% reductions of theophylline CL have been observed in patients suffering from chronic hypoxia-related diseases such as obstructive pulmonary disease, pulmonary oedema and pulmonary cardiopathy (Powell *et al.*, 1978).

Changes in drug pharmacokinetics arising from hypobaric hypoxia, and indeed normobaric hypoxia could predispose to incidental toxicity, especially for those drugs with a narrow therapeutic index. The clinical implications could be extensive, given prescribed prophylaxis against high-altitude illness as well as issues of ongoing chronic medication. Given that studies to date have been generally underpowered combined with small effect sizes characterised by a high degree of variability, a larger scale trial is needed to better define safer and more effective pharmacological effects under hypoxic conditions. Given the diverse nature of the drugs so far studied, a broader impact of the high-altitude environment upon the body's handling of pharmaceuticals is likely.

## 1.6 Hypoxia and inflammatory mediators

Hypoxia can elicit cellular and whole-body responses leading to changes in a wide variety of cytokines and other pro/anti-inflammatory mediators. However, the impact of such changes upon drug pharmacokinetics is not fully understood. Hypoxia is known to activate pro-and anti-inflammatory mediators. A study by Hartmann *et al.* showed in healthy volunteers who had climbed from low to high altitude (>3400 m) an increase in the serum levels of some of the cytokines associated with the acute phase response, i.e. interleukin-6 (IL-6), the soluble interleukin-6 receptor (sIL-6R) and C-reactive protein (Hartmann *et al.*, 2000). High-altitude cerebral oedema has been reported to be associated with increased blood-brain barrier (BBB) permeability due to hypoxia-stimulated release of inflammatory mediators (Zhou *et al.*, 2011). The authors reported an increase in serum TNF- $\alpha$  with exposure to hypoxia (5000 m) which triggered macrophage activation and a systemic inflammatory response, and activation of a cytokine cascade involving other secondary factors such as IL-1, IL-6 and IL-8. They concluded that TNF- $\alpha$  potentially alters the structure and function of the brain microvascular endothelial cells and causes dilatation of vascular smooth muscle leading to increased permeability of the BBB.

Hypoxia is recognised to modulate (both increase and decrease) the expression of several CYP450 isoforms (Du Souich and Fradette, 2011) via triggering the release of cytokines (IFN $\gamma$ , IL-1 $\beta$  and IL-2) responsible for the initiation of numerous signalling cascades, and production of reactive oxygen species (ROS) with downstream effects on activation of transcription factors including HIF-1, NF-kB, AP-1. In-vitro studies involving the incubation (24 h) of rabbit hepatocytes with serum subjected to hypoxaemia (PaO<sub>2</sub> 34 mmHg) resulted in decreases in CYP-1A1, -1A2, -2B4, -2C5 and -2C16 while increases were seen for CYP3A6 (Fradette *et al.*, 2007a).

## 1.7 Hypoxia and Reactive Oxygen Species (ROS)

Reactive oxygen species (ROS) represent a group of oxygen-derived species with one or more unpaired electrons in their outer orbital layer. ROS are formed in biological systems as by-products of the reduction of molecular oxygen. They are highly reactive and are able to bind to biological elements, including lipids, proteins and cell membranes, to bring about cell toxicity.

There are three broad classes of ROS: **hydroxyl radicals ( $\cdot\text{HO}$ )**, **superoxides ( $\text{O}\cdot^-$ )**, and **hydroperoxides ( $\text{ROOH}$ )**. ROS may also include several nitrogen-containing compounds or reactive nitrogen species (RNS), such as **nitric oxide ( $\text{NO}$ )**, **nitroxyl anion ( $\text{NO}^-$ )**, and **peroxynitrite ( $\text{ONOO}^-$ )** (Tafari *et al.*, 2016). ROS have a role in various cellular functions ranging from signal transduction pathways, defence against invading microorganisms and gene expression promoting cell growth or cell death (Lee, Giordano and Zhang, 2012). ROS are also recognised as secondary molecular messengers generated in response to growth factors, hormones, cytokines and extracellular ATP (Jefferson *et al.*, 2004).

ROS are produced by various enzyme systems. Two endogenous sources of ROS are the **CYP450 microsomal electron transport system** and the **mitochondrial electron transport chain**. Both use oxidases such as NADPH oxidase, and xanthine oxidase. In addition, ROS are produced by other mechanisms, including nitric oxide synthase and the lipoxygenase and cyclooxygenase systems (Cho, Seo and Kim, 2011; Hrycay and Bandiera, 2015). Given the high levels of CYP450 in the liver, it is clear this organ may be more exposed to higher levels of ROS. In normal cells, intracellular levels of ROS are maintained in-balance by antioxidants; oxidative stress occurs when this critical balance is disrupted. The endogenous antioxidant protective agents include several enzymes (*e.g.*, superoxide dismutase, catalase and glutathione peroxidase) (Cichoż-lach and Michalak, 2014) (**Figure 1.9**). Hypoxic conditions favour the increase of ROS and can impair the antioxidant mechanisms, *e.g.*, impairment of glutathione synthesis or superoxide dismutase, resulting in oxidative stress (Jefferson *et al.*, 2004; Tormos, Nebreda and Sastre, 2013; Cichoż-lach and Michalak, 2014). In cell signalling, ROS can act as a second messenger activating various signalling pathways such as protein kinase C (PKC), mitogen-activated protein kinase 1/2 (MEK1/2) and (ERK1/2) (Lee, Giordano and Zhang, 2012).

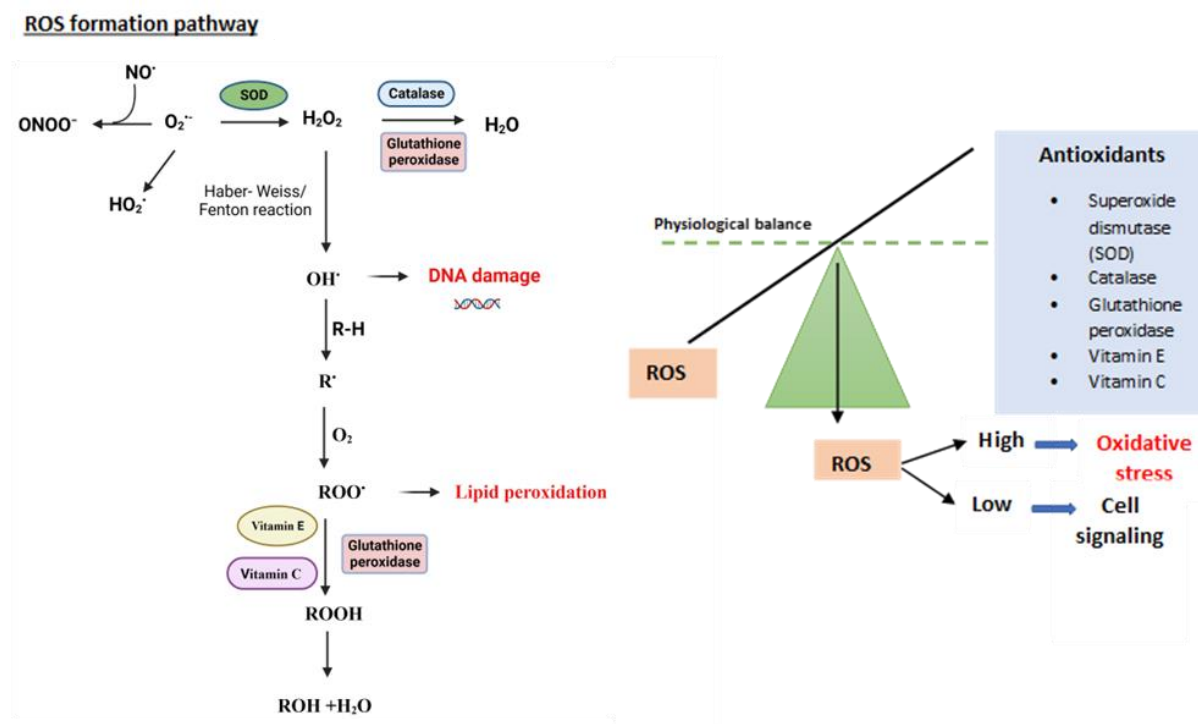


**Figure 1.9 ROS formation pathway and its physiological balance.** Peroxynitrite ( $ONOO^-$ ), nitric oxide ( $NO^\cdot$ ), superoxide dismutase (SOD), hydrogen peroxide ( $H_2O_2$ ), hydroxyl radical ( $OH^\cdot$ ), superoxide radical ( $O_2^{\cdot-}$ ), peroxy radicals ( $ROO^\cdot$ ). Designed by D.Alablani – BioRender

## 1.8 Hypoxia and Hypoxia-inducible factors (HIFs)

Hypoxia-inducible factors (HIFs) are oxygen-sensitive transcription factors that impact both oxygen delivery and the adaptation to oxygen deprivation. This is achieved by HIF regulating more than a hundred genes that are variously involved in a wide range of cellular functions, including, for example, the uptake and metabolism of glucose, angiogenesis, erythropoiesis, pH regulation and cell proliferation and apoptosis (Semenza, 2001; Rankin and Giaccia, 2008; Engelhardt, Patkar and Ogunshola, 2014).

HIF units are composed of **HIF-1 $\beta$** , also named as aryl-hydrocarbon receptor nuclear translocator (ARNT), that forms heterodimeric structures with one of three different oxygen-dependent inducible  $\alpha$ -subunits **HIF-1 $\alpha$** , **HIF-2 $\alpha$** , **HIF-3 $\alpha$** . The HIF-1 $\alpha$  is widely expressed in human tissues and subject to degradation under normoxia by the ubiquitin-proteasome pathway. HIF-2 $\alpha$  has a more restricted expression to specific tissues and cell types, including kidneys, small intestine, endothelium, lungs and heart (Gordan *et al.*, 2007; Engelhardt, Patkar and Ogunshola, 2014). The function of the HIF-3 $\alpha$  subunit in hypoxia regulation is not fully



understood, but its splice variant is known to inhibit the transcriptional activity of HIF-1 $\alpha$  (Ravenna, Salvatori and Russo, 2015).

Under normoxic conditions, oxygen regulates the HIF-1 $\alpha$  subunit by hydroxylation of the prolyl-hydroxylase enzyme domain (PHD2) in the HIF-1 $\alpha$  subunit. This hydroxylation then promotes the binding of the HIF-1 $\alpha$  subunit to Von Hippel-Lindau protein (VHL) which promotes the ubiquitination of the oxygen-dependent domain in HIF-1 $\alpha$ , which tags it for proteasomal degradation. However, under hypoxic conditions, the PHD2 enzyme domain is inhibited, preventing degradation and leading to stabilisation of the HIF-1 $\alpha$  subunit and the translocation of HIF-1 $\alpha$  from the cytoplasm into the nucleus. In the nucleus, the HIF-1 $\alpha$  subunit dimerises with HIF-1 $\beta$  subunit and co-activators such as p300/CBP, forming a functional HIF1 transcription factor. This HIF1 transcription factor binds to hypoxia-responsive elements (HREs) in promoter regions resulting in altered transcription, including, for example, the overproduction of factors involved in angiogenesis, erythropoiesis, proliferation and cellular metabolism aimed at reducing oxygen consumption and increasing oxygen delivery to tissues (Figure 1.10).

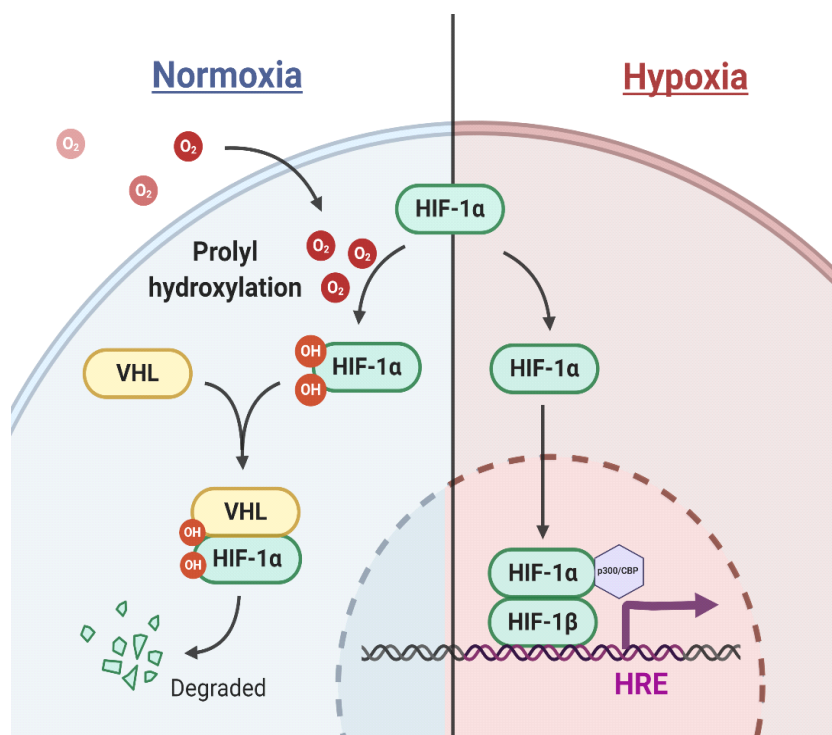


**Figure 1.10 The oxygen-dependent regulation of the transcription factor HIF-1 $\alpha$ .** Under normal oxygen level, HIF-1 $\alpha$  is hydroxylated by the PHD proteins in the presence of O<sub>2</sub>. VHL recognises and ubiquitinates the hydroxylated HIF-1 $\alpha$  and subsequent degradation by the proteasome. Under low levels of oxygen, PHD activity is inhibited, leading to stabilisation of HIF-1 $\alpha$ , translocation into the nucleus and dimerise with HIF-1 $\beta$ . This dimerised protein binds to the hypoxia response element (HRE) and activates its target genes. Designed by D. Ablani – BioRender.

In addition to hypoxia, several other factors may contribute to HIF-1 $\alpha$  stabilisation and nuclear translocation, including cytokine overproduction (IL-1 $\beta$ , TNF- $\alpha$ ), growth factors (EGF, TGF- $\alpha$ 1 and HGF) and ROS intermediates (Wenger, 2002). Furthermore, hypoxia increases the activity of serine-threonine kinases, for instance, the MAPK pathway (Seta and Millhorn, 2004) followed by nuclear translocation of NF- $\kappa$ B and binding to the proximal promoter of the HIF-1 $\alpha$  gene, triggering the transcriptional up-regulation of HIF-1 $\alpha$  (Gorlach and Bonello, 2008).

Of note, a quite complex relationship can exist between oxygen levels, HIF status and CYP450 regulation. For instance, hypoxia can downregulate CYP1A1/A2 by reducing the availability of aryl hydrocarbon receptors (Ahr). Hypoxia stabilises HIF-1 $\alpha$ , which is then dimerised with HIF-1 $\beta$  or Arnt. Since Arnt is also a heterodimerise partner of Ahr, the decrease of Arnt availability under hypoxia leads to a reduction of transactivation of CYP1A1/A2 (Chan *et al.*, 1999) (**Figure 1.11**).

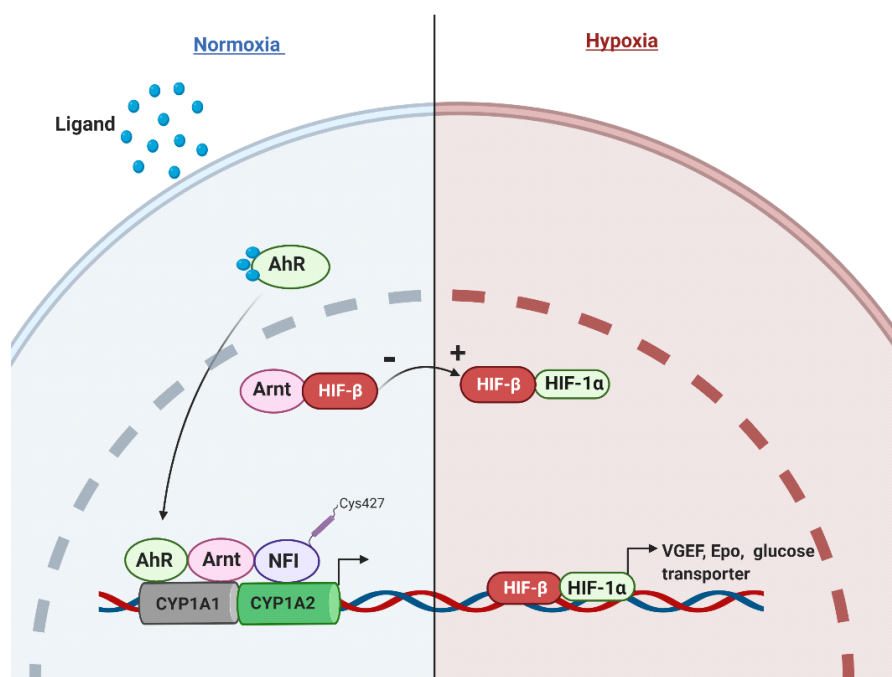


**Figure 1.11** signal transduction pathways activated by hypoxia result in upregulation of the genes responsible for cells survival and down-regulation of CYP1A1 /1A2 due to the reduction of aryl-hydrocarbon receptor nuclear translocator (ARNT) availability. AhR is the aryl hydrocarbon receptor, EPO is erythropoietin, HIF-1 $\beta$  is the hypoxia-inducible factor beta, HIF-1 $\alpha$  is the hypoxia-inducible factor-1 alpha, NFI is the nuclear factor 1, and VEGF is the vascular endothelial growth factor. Adapted from (Fradette and Souich, 2004) and by designed by D. Alablani – BioRender.

## 1.9 Sildenafil

Sildenafil, classified as a phosphodiesterase-5 (PDE-5) inhibitor, is a medication primarily prescribed for the treatment of erectile dysfunction and pulmonary arterial hypertension, as indicated by its approved uses. However, sildenafil has also been employed off-label for short-term treatment of conditions such as high-altitude pulmonary oedema and Raynaud phenomenon. Its off-label use has gained popularity among mountaineers, as sildenafil not only helps prevent high-altitude pulmonary oedema but also enhances exercise capacity and performance makes it an attractive option for athletes and individuals engaged in high-intensity activities (Ghofrani *et al.*, 2004).

In the planned MRHA-regulated clinical trial in volunteers developed to address under well controlled conditions the impact of hypoxia (experimentally - normobaric hypoxia) upon drug pharmacokinetics, sildenafil is the selected model agent.

### 1.9.1 Pharmacology of sildenafil

PDE5 is a cGMP-selective enzyme present in high concentrations in the lungs but also exists in other tissues. PDE5 degrades cyclic guanosine monophosphate (cGMP), which is a regulator of several cellular functions, the most relevant in this current work being vascular smooth muscle relaxation. Sildenafil, as an inhibitor of PDE5, therefore potentiates cGMP and hence potentiates vascular smooth muscle relaxation and vasodilation. In the lungs, dilatation of the blood vessels decreases pulmonary blood pressure and improves cardiac function (Ram *et al.*, 2018).

cGMP is produced from GTP by the action of the enzyme guanylate cyclase (GC). Both membrane-bound GC and soluble intracellular GC (sGC) exist, the latter typically activated by nitric oxide (NO).

### 1.9.2 Structure and physiochemical properties of sildenafil

The chemical name of sildenafil is (IUPAC name - 5-[2-ethoxy-5-(4-methylpiperazin-1-yl) sulfonylphenyl]-1-methyl-3-propyl-6H-pyrazolo[4,3-d] pyrimidin-7-one) and its empirical chemical formula is  $C_{22}H_{30}N_6O_4S$  (**Figure 1.12**). The molecular weight of sildenafil is 474.58 (g/mol) with melting point of 186 to 190°C. Its solubility is 3.5 to 4.5 mg/mL in water. Sildenafil citrate is twice as soluble in methanol than in water. Its solubility decreases with pH up to 9 when it starts to increase again.

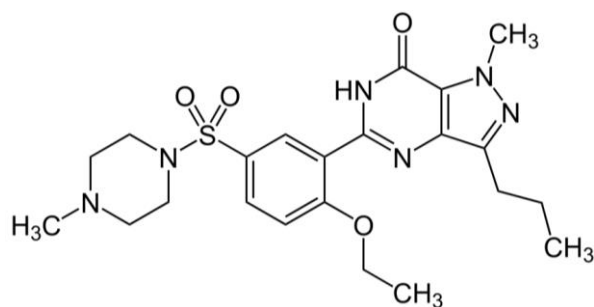


Figure 1.12 Chemical structure of Sildenafil.

Sildenafil has a basic functional group with a pKa 8.7 (NH-piperazine). A weak acidic moiety is, however, also present on the parent compound with pKa estimated 5.99 (HN-amide).

### 1.9.3 Metabolism of sildenafil

Sildenafil is eliminated predominantly by metabolism mediated by CYP450. The main enzymes responsible for metabolism are CYP3A4 (major route 79%) and CYP2C9 (minor route 20%). The major circulating metabolite is N-desmethyl sildenafil (UK-103,320), which has been shown to possess 50% of parent drug potency in the inhibition of PDE5, and is itself further metabolised (Goldenberg, 1998; Cheitlin *et al.*, 1999) (**Figure 1.13**). Plasma concentrations of N-desmethyl sildenafil are approximately 40% that of sildenafil, so the metabolite accounts for about 20% of the pharmacological effects of sildenafil (Cheitlin *et al.*, 1999). Three sildenafil metabolism pathways have been identified in man, which are piperazine N-demethylation, N,N<sup>2</sup>-deethylation and aliphatic hydroxylation. The piperazine N-desmethyl pathway gives rise to the major and active metabolite N-desmethyl sildenafil (Walker *et al.*, 1999).

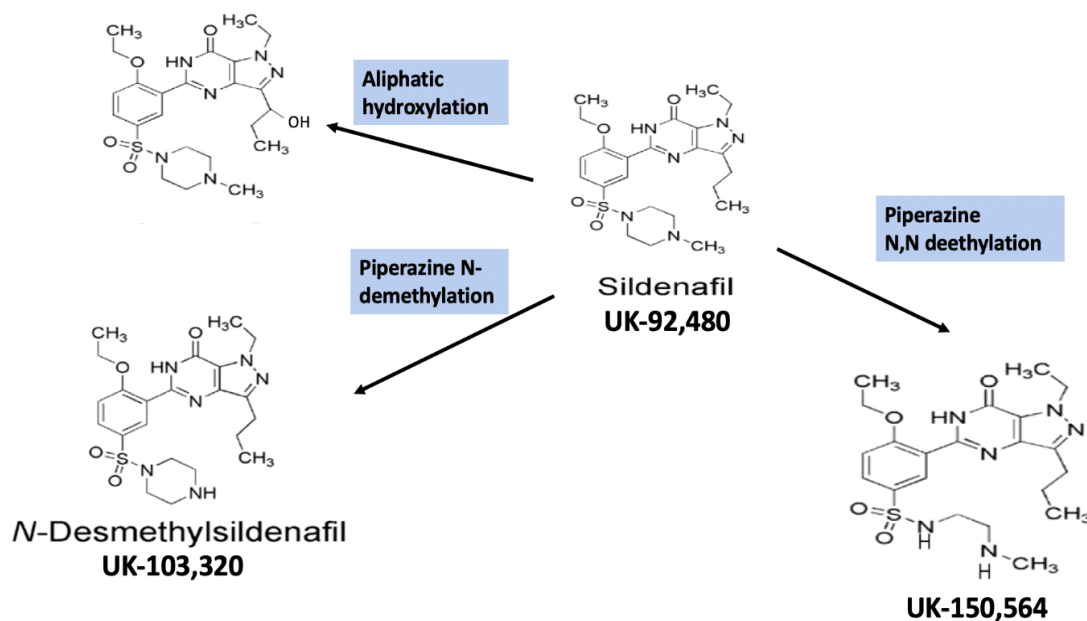


Figure 1.13 Metabolic pathways and metabolites of sildenafil.

### 1.9.4 Pharmacokinetics of sildenafil

Sildenafil pharmacokinetics are characterised by the following:

#### **Absorption:**

Peak concentrations of Sildenafil ( $C_{max}$ ) in healthy volunteers are reported to be 560 ng/mL with a single dose of 100 mg sildenafil oral capsule. Sildenafil is rapidly absorbed after oral administration reaching peak plasma concentrations within 1 h after dosing in the fasted state and with an oral bioavailability of 40%. Food has been shown to delay absorption, probably as a result of delayed gastric emptying, but with the extent of bioavailability not affected (Nichols, Muirhead and Harness, 2002). The 40% extent of oral bioavailability reflects both gut wall and hepatic first-pass metabolism. The first-order absorption rate constant was estimated as  $2.60 \text{ h}^{-1}$  (Milligan, Marshall and Karlsson, 2002). Sildenafil has been shown to display dose-proportional pharmacokinetics following oral administration (Boolell *et al.*, 1996; Muirhead *et al.*, 1996).

#### **Disposition:**

Sildenafil's estimated apparent volume of distribution after intravenous administration is 105 L. While ( $V_{ss}/F$ ) after oral administration is about 3.56 L/kg -310 L in an 87 kg person -

## Chapter 1

(Milligan, Marshall and Karlsson, 2002); taking these two independent measures would suggest a sildenafil  $F_{\text{oral}}$  in the (Milligan, Marshall and Karlsson, 2002) work of 34%.

The protein binding for sildenafil is 96%, i.e. a  $F_u$  of 0.04 (Nichols, Muirhead and Harness, 2002) and is independent of total drug concentrations.

The total body clearance (CL) for sildenafil is 41 L/h after intravenous administration in healthy subjects (Nichols, Muirhead and Harness, 2002). The population estimate for oral clearance (CL/F) in patients with erectile dysfunction was 58.5 L/h (Milligan, Marshall and Karlsson, 2002) with an elimination half-life ( $t_{1/2}$ ) reported to average 4 h (Nichols, Muirhead and Harness, 2002).

After either oral or intravenous administration, sildenafil is excreted as metabolites predominantly in the faeces (approximately 80% of the administered oral dose) and to a lesser extent in the urine (about 13% of the administered oral dose) (Muirhead *et al.*, 2002). According to an excretion study using [ $^{14}\text{C}$ ] labelled sildenafil in men following oral doses, it has been revealed that 79% of the radioactivity was excreted in the faeces while 12% was excreted in urine over 5 days (Walker *et al.*, 1999). This data was supported by another study conducted on post-mortem specimens; They found that the sildenafil and its metabolite concentrations were higher in bile than the kidney, liver, heart, and muscle specimens of two victims (Lewis, Johnson and Blank, 2000).

### **1.10 Project aim, hypothesis, and experimental objectives**

This thesis originally aimed to investigate the impact of acute hypoxaemia on drug pharmacokinetics through a well-controlled clinical trial involving healthy participants. The drug of interest for study was sildenafil. The primary hypothesis underlying the research was that acute arterial hypoxaemia could exert substantial effects on the pharmacokinetic profile of drugs.

The clinical trial was designed involving the pharmacokinetics (PK) and pharmacodynamics (PD) of a single oral dose of sildenafil in healthy participants under acute normobaric hypoxia conditions (12%  $\text{O}_2$ ). The necessary tasks to develop the trial were undertaken during the initial stages of this PhD (See Chapter 7 and Appendix 1).

## Chapter 1

As a result of COVID, the trial was suspended and the thesis thereafter had to take a change in direction, but one nevertheless retaining the focus on the original hypothesis but where more attention was given to underlying mechanisms through which hypoxia influences drug pharmacokinetics and simulated outcomes.

The understanding of how hypoxaemia affects drug pharmacokinetics and pharmacodynamics is currently limited to anecdotal human reports and non-clinical animal studies.

The **hypothesis** proposes that acute arterial hypoxaemia can lead to clinically significant changes in drug pharmacokinetics, affecting both oral absorption and drug disposition. These changes may necessitate dosage adjustments to maintain efficacy or prevent toxicity, particularly for drugs with a narrow therapeutic index. The clinical implications extend to individuals exposed to hypobaric hypoxaemia, such as lowlanders traveling to high-altitude regions for occupational, recreational, or religious purposes, as well as those experiencing normobaric hypoxaemia due to chronic pulmonary or cardiovascular diseases.

### **Modified Experimental Objectives:**

**Objective 1: Conduct a rapid systematic review and meta-analysis to investigate the effect of hypoxemia on drug pharmacokinetics in adults.**

**Chapter 3** applied strict inclusion criteria to ensure the inclusion of subjects diagnosed with hypoxaemia. A total of 10 studies were selected, comprising 6 studies conducted on patients with pulmonary diseases and four studies involving healthy individuals residing or ascending to high-altitude environments above 2500 m.

**Objective 2: Undertake mechanistic in-vitro studies to explore the effects of hypoxia on drug metabolism with in particular a focus on oxidative-nitrosative-inflammatory stress mediators.**

**Chapter 4** aims to characterise a hepatocyte model in order to study the impact of acute hypoxia on drug metabolism. The knowledge gained from this characterisation will be utilised in subsequent mechanistic studies and to inform the PK/PD Monte Carlo computational simulation. Different cell lines, such as HepG2 and HepaRG, along with various models including 2-dimensional and 3-dimensional models, were employed. Subsequently, the hepatocyte model was subjected to hypoxia, and the transcription, translation, and functional activity of CYP3A4 and CYP2C9 were examined. The

functional activity and transcription of ABC transporters under hypoxia were studied using Caco2 and HepG2 cell lines.

**Chapter 5** of this thesis aims to identify the mechanisms responsible for the downregulation of CYP3A4 and CYP2C9 under hypoxia, with a specific focus on pro-inflammatory cytokines and reactive oxygen species. The exposure of HepaRG cell lines to hypoxia facilitated the identification of inflammatory and pro-inflammatory mediators, as well as the generation of reactive oxygen species. The impact of these mediators on the transcription, translation, and functional activity of CYP3A4 and CYP2C9 was investigated. Furthermore, in this chapter, the MAPK/ERK signaling pathway and its downstream regulation of the nuclear receptor PXR were explored as potential mechanisms underlying the suppression of CYP3A4 and CYP2C9 under hypoxic condition.

**Objective 3: Simulate the PK/PD outcomes of sildenafil under acute hypoxia based on the existing literature and using in-vitro functional activity analysis of CYP3A4/2C9.**

**In Chapter 6**, the PK/PD profile of a 100 mg single oral dose of sildenafil was successfully simulated using PK parameters obtained from the literature. The effects of hypoxia on PK were modelled by incorporating in-vitro data on changes in hepatic cell metabolism/CL intrinsic involving CYP3A4 (responsible for 80% of sildenafil metabolism) and CYP2C9 (contributing to 20% of sildenafil metabolism), as well as changes in hepatic blood flows sourced from the literature.



## **Chapter 2: General Laboratory Material and Method for In-Vitro Work**

This chapter will look at the general material and methods used throughout the thesis. Later chapters will refer to these methods as appropriate. Specific materials and methods that are more specialised or limited to a single chapter will be described in detail in the respective chapter(s).

## **2.1 Cell culture**

### **2.1.1 HepG2 cells (Hepatocyte model)**

Human hepatocellular carcinoma cells (HepG2) were purchased from the European Collection of Authenticated Cell Cultures (ECACC 85011430). Cell lines were grown in Modified Eagle Medium (MEM) (Gibco; 11095080) supplemented with 10% fetal bovine serum (FBS) (Gibco; 10500064) and 1% penicillin-streptomycin (Gibco; 15140122) and were maintained in a humidified 37°C incubator with 5% CO<sub>2</sub>. Passage numbers between P5 to P8 were used in all experiments.

### **2.1.2 HepaRG cells (Hepatocyte model)**

Undifferentiated human bipotent progenitor cells (HepaRG) were purchased from Biopredic International (Rennes, France) and seeded in monolayer in 25 cm<sup>2</sup> flasks at a density of 0.02 x 10<sup>6</sup>/cm<sup>2</sup> to reach a confluency of 70-80% – this typically required 14 days of culture. The HepaRG cells were grown in a growth medium composed of: Williams' medium E (Gibco; A1217601) supplemented with GlutaMAX-I (Gibco; 35050038), 10% fetal bovine serum (Gibco 10500064), 1% (v/v) penicillin-streptomycin (Gibco; 15140122), 5 µg/mL insulin (Sigma-Aldrich; I0516) and 5 x 10<sup>-5</sup> M (i.e. 50 nM) hydrocortisone hemisuccinate (Sigma-Aldrich; H2270) and were incubated at 37°C in a humidified atmosphere of 5% CO<sub>2</sub>. After two weeks, the culture medium was altered with supplementation with 2% v/v DMSO (differentiation medium) (Sigma-Aldrich; D2650). The medium was renewed every 2 to 3 days. Passage numbers between P5 to P19 were used in all experiments.

### **2.1.3 Caco2 cells**

Human colonic carcinoma Caco2 epithelial cells were cultured in Dulbecco's modified Eagle's medium (DMEM) (Gibco 42430025) supplemented with 20% v/v fetal bovine serum (Gibco; 10500064), 1% (v/v) penicillin/streptomycin antibiotics (Gibco; 15140122) and 1% v/v MEM non-essential amino acids (Gibco; 1140035). Cells were incubated in a 37°C incubator with

5% CO<sub>2</sub> for 7–10 days until confluency. Passage numbers between P4 to P10 were used in all experiments.

### 2.1.4 3-Dimensional (3D) HepaRG cultures

After expansion and differentiation in 2D monolayers, HepaRG cells were detached using Accumax (Gibco 00466656), cells were counted and seeded at  $0.001 \times 10^6$  cells/cm<sup>2</sup> (96 well round bottom ultra-low attachment – ULA – plates; Costar; 7007). At day 31 (as shown in **Figure 2.1**) the differentiation media (Williams' medium E supplemented with GlutaMAX-I, 10% fetal bovine serum, 1% (v/v) penicillin-streptomycin, 5 µg/mL insulin,  $5 \times 10^{-5}$  M (i.e. 50 mM) hydrocortisone hemisuccinate and 2% DMSO) was switched to the same media but free from DMSO – named as growth media – and cells were allowed to grow as spherical cell aggregates for 10 days. On day 41 (**Figure 2.1**), the spheroids generated were treated for 72 h with a CYP3A4/2C9 enzyme inducer (25 µM rifampicin; Sigma Aldrich; R3501). On day 43, a competitive CYP3A4 enzyme inhibitor (1 µM ketoconazole; Sigma Aldrich PHR1385) was added to the appropriate treatment arms for 24 h before conducting the experiment on day 44 (**Figure 2.1**). These CYP450 modulating treatments- rifampicin and ketoconazole- were dissolved in DMSO to prepare a stock solution, and then the required treatment concentrations were prepared by diluting the stock solution into a growth media. The final concentration of DMSO added to the 3D culture media was 0.02%.

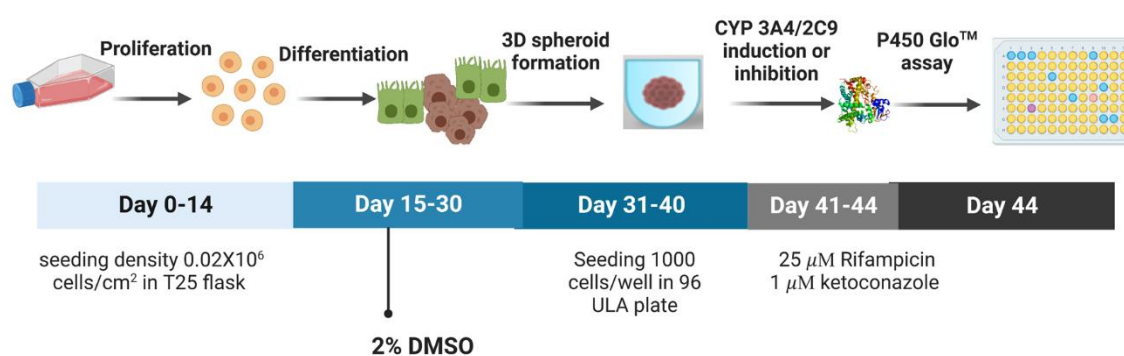


**Figure 2.1 Schematic protocol for HepaRG differentiation and spheroid formation.** HepaRG was seeded at a density of  $0.02 \times 10^6$  cells/cm<sup>2</sup> as a 2D monolayer and grown for two weeks. At day 15 the growth media was supplemented with 2% DMSO to differentiate the cells into hepatocyte and biliary cells. On day 31, the differentiated cells are detached and seeded at a density of 1000 cells/well in ultra-low attachment (ULA) plates to form spheroids. Following this on day 41 the spheroids were treated with rifampicin to induce the expression of CYP3A4 and CYP2C9 for three days. On day 43 ketoconazole was added to the respective treatment arms. The P450 GLO™ assay was conducted on day 44. The figure was created by D. Alablani -BioRender.

## 2.2 Cell staining and immunofluorescence

### 2.2.1 Live/ dead staining

After spheroids formation, (see **Figure 2.1**, day 38) spheroid were stained with a mixture of two dyes: 1 M calcein-AM (Invitrogen; C3099) and 1 mg/mL propidium iodide (PI) (Sigma Aldrich P4864). 2X concentration dye solutions were prepared in a culture medium immediately before use to working concentrations of 2  $\mu$ M calcein-AM and 8  $\mu$ g/mL PI. 40  $\mu$ l added directly to each well (each containing 1 spheroid) after aspirating 60  $\mu$ l of the media from a total of 100  $\mu$ l. Spheroids were incubated with dye for 1 h at 37 °C and 5% CO<sub>2</sub> before imaging using an EVOS™ M7000 microscope (ThermoFisher Scientific). The dye solution was not washed out, and care was taken during pipetting to avoid spheroid loss, disintegration, or displacement.

### 2.2.2 Immunofluorescent staining and microscopy

Cells were cultured at a density of 0.2 x10<sup>6</sup> cells/well on 35 mm glass bottom microwell dishes combined with coverslips (P35G-1.5-14-C, Mat Tek). The coverslips were coated with collagen to improve cell attachment. After cell differentiation, the media aspirated from the wells and the cells were gently washed with PBS (Gibco; 10010023) at room temperature. Afterwards, cells were fixed in 4% (w/v) paraformaldehyde in PBS for 10 min, washed in PBS for 2 min, permeabilised by 0.5% (v/v) Triton -100 in PBS (PBST) at room temperature for 5 min and blocked with 5% BSA in PBST. Subsequently, they were incubated overnight at 4°C with primary antibodies, washed out, and incubated for 1 h with secondary antibodies at room temperature. The cell nuclei were stained using Hoechst (1 $\mu$ g/mL) dye (Thermo Sci; 62249) and mounted in Antifade Mounting Medium (Vector ZB0420). The negative controls were incubated with secondary antibodies without the primary antibodies. Primary antibodies: rabbit anti-albumin (NBP1-32458, Novus biological), mouse anti-cytokeratin19 (Thermofisher; MA5-12613), rabbit anti-CYP2C9 (ab150364, Abcam), rabbit anti-CYP3A4 (Merck Life Science UK Limited; AB1254). Anti-mouse AlexaFluor 488 (Invitrogen; A-21200), anti-rabbit AlexaFluor 546 (Invitrogen; A11010), anti-rabbit AlexaFluor 488 (Invitrogen; A11034) were used as secondary antibodies. Cells were visualised by confocal microscopy using a Leica DMi8 inverted microscope equipped with: an HC PL APO lambda blue 63x1.40 oil-immersion objective – to visualise 2D monolayer; and with an HC PL APO CS 20x70 DRY UV objective

– to visualised 3D spheroids. The samples were illuminated with a 405 nm laser line for the excitation of the DAPI signal and with a white light laser tuned at 488 nm, and 543 nm for the excitation of AlexaFluor 488 and AlexaFluor 546, respectively. ImageJ was used to create the figures and analyse immunofluorescent intensity.

## 2.3 General assays

### 2.3.1 CYP450 enzymes activity measurement using P450-Glo™ assay

The CYP450 activity of the hepatocyte cell models was assessed using the P450-Glo™ assay (Promega, UK). Two luminogenic substrates were utilised: Luciferin-IPA (V9001; Promega) to quantify CYP3A4 enzyme activity, and Luciferin-H (V8791; Promega) to measure CYP2C9 enzyme activity. The non-lytic P450-Glo™ Assay was conducted following the manufacturer's protocol (Promega). HepaRG cells cultured in 2D monolayers were subjected to two rounds of washing with PBS, followed by incubation with 50 µl of cell culture medium containing either 3 µM Luciferin-IPA (for CYP3A4) or 100 µM Luciferin-H (for CYP2C9). Incubation was carried out at 37°C for 1 h or 4 h, respectively. Subsequently, 25 µL of the media supernatant was collected and transferred to opaque-white 96-well plates (Costar 3912). An additional 25 µL of the Luciferin detection reagent was added, and the samples were further incubated at room temperature for 20 min. Luminescence signals were then recorded using a plate reader (Infinite200 PRO; Tecan). To determine background luminescence, empty wells were prepared without cells, and Luciferin IPA or Luciferin H was incubated for 1 h or 4 h, respectively. Following this, 25 µL of the media was transferred to a white 96-well plate, and the Luciferin detection reagent was added. The background signal was subtracted from the sample measurements.

The number of viable cells remaining in the original 96-well plates was determined by the CellTiter-Glo luminescent cell viability assay (Promega G7570) – detailed in **section 2.3.2**. The luminescence measurements obtained using P450-Glo assays were normalised to the viable cell number to represent enzymatic activities.

For the assay conducted on 3D Spheroid HepaRG model, a modified protocol adapted from (Shin *et al.*, 2018) was applied. Spheroids were washed twice with phosphate-buffered saline (PBS) and incubated with 30 µL of cell culture medium containing the CYP3A4 or CYP2C9 substrate luciferin-IPA and Luciferin H, respectively. After a 1h incubation at 37°C, the

spheroids and its incubated substrate solution were transferred to a white opaque 96-well luminometer plate (Costar 3912), and 25  $\mu\text{L}$  of Luciferin detection reagent was added. The reaction mixture was triturated with a pipette to ensure cell lysis. After a 20 min incubation at room temperature, luminescence was measured using a plate reader (Infinite 200 PRO; Tecan).



**Figure 2.2** Chemical structures of substrate used in P450-Glo™ assay. Luciferin-IPA was used as substrate to measure CYP3A4 activity. Luciferin-H was used as substrate to measure CYP2C9 activity.

### 2.3.2 CellTiter-Glo luminescent cell viability assay

Cell viability of HepaRG was assessed by determining the adenosine triphosphate content of viable cells with the CellTiter-Glo Luminescent Cell Viability Assay (G7570, Promega, Southampton, UK). For the assay of 2D monolayer-cultured HepaRG, 100  $\mu\text{l}$  of CellTiter-Glo reagent was added to each well containing 100  $\mu\text{l}$  of cell culture medium. The contents were mixed for 2 min at room temperature on an orbital shaker to induce cell lysis and then incubated at room temperature for 10 min. Lysed solutions (100  $\mu\text{l}$ ) were transferred into clear 96-well plates. Luminescence was measured using a plate reader (Infinite 200 PRO; Tecan).

### 2.3.3 Rhodamine 6G and Hoechst 33342 accumulation assay in HEPG2 and Caco2 cells

Caco2 cells were seeded at a density of  $3 \times 10^4/\text{cm}^2$  in 12-well plates and grown for 21 days to achieve a differentiated state. HepG2 cells were seeded at a density of  $5 \times 10^5$  cells/mL. At the appropriate time, each well containing cells as above received either Rhodamine 6G (Sigma 252433) or Hoechst 33342 dyes at a final concentration of 5  $\mu\text{M}$  in DMEM media (free from phenol red and FBS). The plates were then incubated for another 60 min. After that, the uptake of dye was terminated by rinsing the plate three times with ice-cold PBS. In order to release the intracellular fluorescent Rhodamine 6G or Hoechst, cells were lysed with 20 mM Tris-HCL, pH 7.7, containing 0.2% sodium dodecyl sulphate (SDS). Cellular debris was removed

by centrifugation at high speed for 5 min. Aliquots (100 µl) of the supernatant were used for determining the cellular fluorescent intensity of Rhodamine 6G or Hoechst 33342 by a fluorescent plate reader (Infinite 200 PRO; Tecan).

The excitation/emission wavelength filter was 544/590 nm (for Rhodamine 6G) and 361/497 (for Hoechst 33342). The concentration of Rhodamine 6G or Hoechst 33342 in each sample was determined from the fluorescence measurements by the construction of a standard curve. The amount of Rhodamine 6G and Hoechst 33342 in the cell samples were normalised with the amount of protein in each sample (using 10 µl aliquots of the supernatant) as determined by the Pierce BCA method.

## **2.4 Molecular assessment for genes of interest**

### **2.4.1 RNA extraction**

RNeasy Mini kit (QIAGEN 74104 ) was used to isolate the total RNA from the HepaRG, HepG2 and Caco2 cells. Cells were detached from 25 cm<sup>2</sup> flasks after the confluency and differentiation, transferred into Eppendorf tubes, spun (5 min at 110 x g) into a pellet. The supernatant was removed, and cell pellets were then lysed in the Eppendorf tube with lysis solution (350 µl of RLT buffer). Then, 350 µl of 70% ethanol was added to the lysed cells and mixed well by pipet. The lysates were then transferred into collection tubes provided within the kit and which comprised silica filter cartridges. Lysates were centrifuged at 10000 x g for 15 sec. Wash solution 1 was added (700 µl of RW1 buffer - contain guanidine salt and ethanol), and collection tubes were again centrifuged at 10000 x g for 15 sec. A further two wash steps were undertaken using 500 µl of RPE buffer washes before eluting RNA. The elution step comprised the filter cartridge transfer into a new collection tube for the elution step. RNA-free water (30 µl) was added to each filter cartridge, and centerfuged at 10000 x g for 2 min. The extracted RNA were stored at -20°C until reverse transcription was performed. RNA quality was assessed using NanoDrop One Spectrophotometer (Thermo Scientific), which measures absorbance at 260 nm and 280 nm. A ratio of 2 is considered to be uncontaminated with genomic DNA and of good quality/purity. Total RNA samples showed high quality on Nanodrop technology with 260/280 ratios: 1.8-2.0.

### 2.4.2 Reverse transcription (cDNA synthesis)

Reverse transcription was carried out using a high-capacity cDNA reverse transcription kit (Applied Biosystems; 4368814). The following reagents were added to a 0.2 mL DNase and RNase free PCR tube; 1 µg total RNA, 10X RT buffer (2 µl), random hexamer primer (2 µl), dNTP mix (0.8 µl), reverse transcriptase (1 µl), RNase inhibitor (1 µl) and RNAase-free water (as needed to make a final volume of 20 µl). The following programme of the thermal cyclers (PTC-100 programmable thermal control, MJ research BioRad) was used; 25°C for 10 min, 37°C for 120 min, 85°C for 5 min, then cooled at 4°C for 10 min. Samples were stored at -20°C.

### 2.4.3 Primer design

Gene accession data for the mRNA of the desired genes were identified using nucleotide search function of National Centre for Biotechnology Information (NCBI). Primers for PCR were designed using BLAST and targeting across exon-exon boundaries. Melting temperatures ranged between 59 to 61°C, the GC content between 44-55% and the primer length between 18–24 bp with a product size of 100 to 200 bp. The primers were obtained from (Thermo Fisher Scientific). Hypoxanthine Phosphoribosyltransferase 1 (HPRT1) was used as an internal control. The primers used are listed in **Table 2.1**.

**Table 2.1** Primer used for the analysis of gene expression by RT-PCR

Gene	Forward	Reverse	Size (bp)
<b>Pro-inflammatory</b>			
<b>IL-6</b>	CTCAATATTAGAGTCTCAAC CCCCA	GAAGGCGCTTGTGGAGAAG G	146
<b>IL-1β</b>	CTCTTCGAGGCACAAGGCA CA	ATTTCACTGGCGAGCTCAGG T	112
<b>TNF- α</b>	CAGGTCCTCTTCAAGGGCC AA	GGGGCTCTTGATGGCAGAGA	120
<b>IL-12</b>	CAAGACCTCAGCCACGGTC A	GCACAGATGCCCATTCGCTC	101
<b>Nuclear receptor</b>			
<b>PXR</b>	GACATGTGAAGGATGCAAG G	CTCTCCAGGCACTTGCGCA	147
<b>Efflux transporters</b>			
<b>BCRP</b>	GACTTATGTTCCACGGGCCT	GGCTCTATGATCTCTGTGGC TTTA	175



<b>MRP2</b>	GGGATGAAAGGTCATCCTTT ACG	TCCAGGAATGAGGAATTCCA AAAAG	190
<b>MDR</b>	CAGATAAAAGAGAGGTGCA ACGG	CTGTGGCAAAGAGAGCGAAG	191
<b>Housekeeping gene (HKG)</b>			
<b>HPRT1</b>	AGCCCTGGCGTCGTGATTAG	TCGAGCAAGACGTTTCAGTCC T	141

#### 2.4.4 TaqMan gene expression assay

Doublex TaqMan gene expression assay was used to test the gene expression of CYP3A4 and CYP2C9. **Table 2.2** lists the three gene expression assay kits used, their product identifications, specific transcripts amplified and their specific dye.

**Table 2.2 TaqMan gene expression assay used**

Gene	Assay ID	Dye
<b>CYP3A4</b>	Hs00604506_m1	FAM-MGB
<b>CYP2C9</b>	Hs04260376_m1	VIC - MGB
<b>HPRT1</b>	Hs02800695_m1	VIC-MGB

Each kit contained gene-specific primers and fluorogenic probes that were pre-optimised by the manufacturer to yield  $100\% \pm 10\%$  amplification efficiency using human tissue RNA pools. The assay kits share the following general features: (a) forward and reverse primers are contained in different exons when multiple exons encode the transcript; (b) the reporter probe spans the exon-exon junction of the targeted transcript to prevent amplification of genomic DNA.

#### 2.4.5 Quantitative Polymerase Chain Reaction (qRT-PCR)

qRT-PCR was performed using a **PowerUp™ SYBR™ Green Master Mix** (Applied Biosystems; A25741). During PCR amplification, SYBR® Green employs a non-specific fluorescent dye that intercalates into double-stranded DNA. The amount of SYBR® Green bound to the DNA rises as the amount of amplified product increases, resulting in an increase

in fluorescence observed by qRT-PCR. The SYBR<sup>®</sup> Green approach is simple and inexpensive, but it may provide non-specific signals if other amplified products or impurities are present in the reaction. SYBR<sup>®</sup> Green's nonspecific binding makes them unsuitable for multiplex PCR. Each PCR tube contained 30 ng of cDNA, SYBR<sup>®</sup> Green Master mix (6 µl), forward and reverse primers (0.18 µl each) (**Table 2.1**) and RNA free water (as needed to make a final volume of 12 µl). The qRT-PCR conditions were as follows: denaturation at 95°C for 15 sec, annealing at 60°C for 15 sec, and extension at 72°C for 1 min for up to 40 cycles. The amplification was conducted using a QuantStudio<sup>™</sup> 5 Real-time PCR System (Applied Biosystems).

On the other hand, TaqMan is a unique approach that allows for multiplexing, which means that many target sequences may be identified in a single reaction. TaqMan employs a complementary fluorescence probe to the target sequence. A fluorescent dye is located at the 5' end of the probe, and a quencher is located at the 3' end. Taq polymerase cleaves the probe during PCR amplification, separating the dye from the quencher, resulting in a rise in fluorescence that may be measured in qRT-PCR. The **TaqMan gene expression assay** was performed using TaqMan Fast Advanced Master Mix (Applied Biosystems; 4444557) and 30 ng of cDNA. The manufacturer recommended amplification conditions were used: one cycle at 50°C for 2 min, then 95°C for 20 sec, followed by 40 cycles at 95°C for 3 sec and 60°C for 30 sec.

Assays using 'Singleplex' (single target amplified in each PCR reaction) and 'Duplex' (both CYP3A4 and CYP2C9 gene simplify simultaneously in a single PCR reaction) were validated by calculating amplification efficiency values for serial dilutions of cDNA in the PCR reactions. Furthermore, the expression of the target gene in Singleplex and Duplex PCR reactions in a serial dilution of cDNA was compared to confirm there are no differences in target gene expression between them.

For reliable normalisation of qRT-PCR experiments, one gene with steady expression in all used cell lines (HPRT1) was chosen as the housekeeping gene (HKG). For analysis, the  $\Delta\Delta C_t$  approach was utilised, which involves first calculating the  $\Delta C_t$  value by subtracting the cycle threshold ( $C_t$ ) values of the HKG gene from the  $C_t$  value of the target gene in each sample. Then, the  $\Delta\Delta C_t$  value is calculated by subtracting the  $\Delta C_t$  value of the control sample from the  $\Delta C_t$  value of the experimental sample.

## **2.5 Western blot**

### **2.5.1 Protein lysis and concentration determination**

Cells were detached and collected in a 15 mL centrifuge tube. The lysis buffer master mix was prepared by adding 10  $\mu$ l of EDTA and 10  $\mu$ l of Protease and Phosphatase Inhibitors (Thermo Fisher; 1861281/1861274) to 980  $\mu$ l of RIPA lysis buffer (Thermo Fisher; 89900). The cell lysate was prepared by adding 250  $\mu$ l of lysis buffer master mix to the cell pellet. The samples were kept on ice for 30 min, vortexed every 5 min and then centrifuged at 14000 x g for 15 min to pellet the cell debris. Afterwards, the supernatant was collected in a new microcentrifuge tube and stored at -20°C until required. The protein concentration of the lysate was determined with Pierce BCA protein assay kit (Thermo scientific; 23227) following the manufacturer's protocol. All samples were measured at 562 nm using an Infinite<sup>®</sup> 200 PRO Tecan plate reader. Protein concentrations were calculated using diluted albumin standards (Thermo scientific; 23209).

### **2.5.2 Sample preparation and gel electrophoresis**

The samples were prepared by adding the calculated amount of the 4X LDS sample buffer containing beta-mercaptoethanol as a reducing agent, water and 15 to 50  $\mu$ g of protein into microcentrifuge tubes. Samples were centrifuged at 110 xg for 10 sec, followed by heating at 95°C for 5 min. The Gel electrophoresis was performed with 12% Mini-PROTEAN<sup>®</sup> TGX<sup>™</sup> Precast Protein Gels (BIORAD; 4561045). The gel was placed in apparatus submerged in running buffer (0.25 mM Tris-HCL PH 8.3, 1.7 mM SDS and 96 mM glycine), and the samples were loaded in the gel well, as well as the marker. Electrophoresis was performed at 200 V for 40 min or until a good separation between bands was observed.

### **2.5.3 Transfer of protein from gel to membrane**

The semidry transfer method was carried out using Bio-Rad Trans-Blot Turbo Transfer System and Trans-Blot Turbo Transfer Pack Mini format 0.2  $\mu$ m Nitrocellulose (BIORAD; 1704158). The transfer was performed following the manufacturer's protocol. Briefly, the membrane and bottom stack were placed on the cassette base of Trans-Blot Turbo Transfer System, and the gel was placed on top of the membrane; then, the second wetted transfer stack was placed on top of the gel. The air bubbles were removed from the assembled sandwich with a blotting roller. The cassette lid was closed, then locked and inserted into Trans-Blot Turbo Transfer System. The system was programmed for transfer at 1.3 A constant, up to 25 V, for 7 min.

### **2.5.4 Immunodetection**

The membranes were blocked for non-specific interaction using 5 % milk diluted in washing buffer for 1 h at room temperature on a rocking platform. The membrane was then washed 3 times for 5 min in a washing buffer and incubated with primary antibody overnight at 4°C under a roller (**Table 2.3**). After that, the membranes were washed three times for 5 min each with washing buffer before incubation with the respective HRP-conjugated secondary antibodies for 60 min at room temperature (**Table 2.3**). The antibody-labelled proteins on the membrane were detected using Super Signal West Dura Extend Duration Substrate (Thermofisher; 34076). The membranes were scanned with ChemiDoc™ XRS+ System (Biorad). The optical density of the bands was calculated with ImageJ.

**Table 2.3 Antibodies and their concentrations employed in Western blotting.**

<b>Antigen</b>	<b>Conjugate</b>	<b>Predicted Mwt (kDa)</b>	<b>Dilution</b>	<b>Antibodies and Source</b>
<b>CYP 2C9</b>	-	55	1:1000	Rabbit polyclonal to CYP2C9 (abacam; ab4236)
<b>CYP 3A4</b>	-	50	1:1000	Rabbit monoclonal to CYP3A4 (Cell Signaling; D9U6N)
<b>PXR</b>	-	50	1:1000	Mouse polyclonal to PXR (abcam; ab118336)
<b>Phospho P44/42 MAPK (ERK1/2) (Thr202/Tyr204)</b>	-	42, 44	1:1000	Rabbit (Cell Signaling; 9101S)
<b>P44/42 MAPK (ERK1/2)</b>	-	42, 44	1:1000	Rabbit (Cell signaling; 9102S)
<b>GAPDH</b>	-	37	1:1000	GAPDH rabbit mAb detects endogenous levels of total GAPDH protein (Cell Signaling; 2118)
<b>β-Actin</b>	-	42	1:1000	Anti-β-actin antibody, mouse monoclonal (Sigma; A1978)
<b>Anti-rabbit IgG</b>	Horseradish peroxidase (HRP)	N/A*	1:10000	Anti-rabbit IgG, HRP-linked antibody (Cell Signaling; 7074)
<b>Anti-mouse IgG</b>	Horseradish peroxidase (HRP)	N/A	1:10000	Anti-mouse IgG, HRP-linked antibody (Cell Signaling; 7076S)

\*(N/A) Not available

**Chapter 3: The Impact of Hypoxaemia on Drug  
Pharmacokinetics in Adults: A Rapid Systematic  
Review and Meta-Analysis.**

### **3.1 Introduction**

Hypoxaemia is a state of decreased oxygen in arterial blood. This occurs in various acute and chronic respiratory and cardiovascular diseases and in high-altitude environments. At high altitudes, both atmospheric pressure and atmospheric partial pressure of oxygen are decreased, resulting in a reduced oxygen level dispersal into the blood, and a loss of arterial partial pressure and saturation of oxygen.

Altered drug disposition is well recognised in disease states affecting the organs we commonly think of as the major routes of elimination, the kidney or liver (Curry and Whelpton, 2010). However, little research has focused on the possible pharmacokinetic changes in humans that may accompany hypoxaemia despite the frequent occurrence of gas exchange abnormalities with chronic respiratory disease. Oxygen is essential for drug oxidation, for control of cellular redox state and for the synthesis of high-energy bonds used in phase2 conjugations, it is therefore not unreasonable to consider that clinically meaningful hypoxaemia may alter drug disposition in patients with chronic respiratory diseases (du Souich and Erill, 1978; Jones, 1981; Taburet, Tollier and Richard, 1990).

High altitudes can induce physiological changes and result in a hypobaric hypoxia response in several physiological systems, including the cardiovascular system, pulmonary system, gastrointestinal system, drug metabolism enzyme system, and renal excretory system (Brugniaux *et al.*, 2007; Goldfarb-Rumyantzev and Alper, 2014; Hui *et al.*, 2016). Physiological alterations induced by high-altitude stressors may affect the absorption, distribution, metabolism, and excretion (ADME) of drugs and alter drug pharmacokinetics to the extent that may require modifications of dosage regimens to ensure drug efficacy and safety.

#### **3.1.1 Aim and objectives**

This Chapter uses rapid systematic review methodology accompanied by a meta-analysis to evaluate the evidence for the effects of both normobaric hypoxaemia in respiratory disease and by using hypoxia chamber or hypobaric hypoxaemia at high altitude upon the pharmacokinetics (PK) of drugs in adults.

## 3.2 Methods

This review follows PRISMA reporting guidelines. The protocol was registered prospectively on the PROSPERO database (CRD42020215474) on 2<sup>nd</sup> November 2020.

### 3.2.1 Database and search strategy

A search of electronic databases was conducted from inception to 10 May 2023 by one reviewer (DJA). Four electronic databases were accessed: EMBASE (Ovid) (1947 to 2023 week 18), MEDLINE (Ovid) (1946 to 10 May 2023), SCOPUS (1963 to present) and Web of Science. The search strategy included the keywords and the subject heading for hypoxaemia, pharmacokinetics, respiratory diseases, high altitude. The search strategies and keywords for EMBASE, MEDLINE, Scopus and Web of Science are shown in **Appendix 4.1**. The search was restricted to English language and were re-run immediately before analysis. Initial search were conducted in Cochrane library to make sure there is no previous systematic review study has been published.

### 3.2.2 Selection and quality assessment

#### Review Inclusion Criteria

Studies were deemed eligible for meta-analysis based on the following criteria:

**(1) Study design:** RCT's and QUASI-experimental studies.

**(2) Participants:**

- Adults  $\geq 18$  years with hypoxaemia as defined as the partial pressure of arterial oxygen ( $\text{PaO}_2$ )  $< 80$  mmHg or a  $\text{PaO}_2/\text{FiO}_2$  ratio  $\leq 300$  mmHg or arterial oxygen saturation ( $\text{SaO}_2$ )  $\leq 95$  %.
- Hypoxaemia occurs in respiratory diseases such as (COPD, chronic or acute asthma, pneumonia, pulmonary oedema, pulmonary embolism, pulmonary hypertension, pulmonary fibrosis, granulomatous lung diseases) or as a result of ascending to high altitude or exposure to a low level of oxygen using hypoxia chamber.

**(3) Intervention:** any pharmacological treatment which has a therapeutic effect taken by oral, intramuscular or intravenous routes.



**(4) Comparator(s)/control:**

- Adult  $\geq 18$  years with pulmonary disease and controlled hypoxaemia ( $\text{PaO}_2$  is above 80 mmHg) due to oxygen therapy.
- Healthy volunteers who do not have pulmonary diseases and have normal  $\text{PaO}_2$  values (above 80 mmHg).
- Participants - healthy male or female lowlanders (living at sea-level).

**(5) Outcome measures:** Pharmacokinetic parameters including ( $F$ ,  $C_{\max}$ ,  $T_{\max}$ ,  $K_a$ ,  $t_{1/2a}$ ,  $K$ ,  $t_{1/2}$ ,  $CL$ ,  $V_d$ ,  $AUC_{0-t_{\text{last}}}$ ,  $AUC_{0-\infty}$ ), defined below in section 3.2.4.

**Review exclusion criteria:**

Studies were excluded that:

- Were performed on animals or in vitro.
- Were conducted on children (<18 years).
- Were on unrelated topics.
- Unpublished articles, dissertations, abstracts, and conference proceedings.
- Articles providing insufficient information relating to PK parameters.
- Studies that did not report the  $\text{PaO}_2$ ,  $\text{PaO}_2/\text{FiO}_2$ ,  $\text{SaO}_2$  levels, or did not mention the subjects are suffering from hypoxaemia.
- Studies published in languages other than English.

**Quality assessment**

The quality of each study eligible was evaluated by one examiner (DJA). Cardiff University's 'Specialist Unit for Review Evidence (SURE)' critical appraisal checklist were used to assess RCTs and quasi-experimental studies. The URL link to the checklist is: [SURE-CA-form-for-RCTs-and-other-experimental-studies\\_2018.pdf](#). This tool comprises 14 questions that address broad issues such as clearly defined research questions, methodology, and validity of results.

**3.2.3 Data management**

All the articles were imported into the Mendeley library. Duplicates were automatically screened and excluded. The articles were first screened by their titles and abstracts according to the eligibility criteria. The excluded studies were filed in a well-identified section – named as “exclusion 1”- of the Mendeley library. The full text of the remaining articles that met the

inclusion criteria, or presented a doubt in terms of eligibility, were uploaded and attached to the respective article citation in the Mendeley library. The full text papers were then read, and the ultimate decision on whether or not to include the studies in our rapid review was made. Excluded studies that did not meet our inclusion criteria are placed in a folder called "Exclusion 2" in Mendeley. The "Exclusion 2" folder was then subfolder into several files and titled according on the reason for the study's exclusion from our rapid review, such as conducted on children, PK outcomes are not reported, no normoxia control group etc. Using this approach, a single article can be classified into different files in case of multiple exclusion criteria.

### 3.2.4 Data extraction

The following information was extracted from selected studies by using structured data collection tables: author, publication year, experimental design, drug examined, dose, route of administration, sample size, age, body weight, underlying respiratory conditions, and PaO<sub>2</sub> level. Pharmacokinetic parameters including bioavailability (F), absorption rate constant ( $k_a$ ), volume of distribution ( $V_d$ ), absorption/elimination half-life ( $t_{1/2a}$  /  $t_{1/2}$ ), clearance (CL), elimination rate constant (K), time to peak plasma concentration ( $T_{max}$ ), area under the concentration-time curve (AUC)).

#### Definitions of PK Parameters

**K<sub>a</sub>**: rate of drug absorption from the site of administration into the systemic circulation

**t<sub>1/2a</sub>**: absorption half-life- the time it takes for half of the drug to be absorbed from the site of administration into the systemic circulation.

**F**: fraction of the administered dose which reaches the systemic circulation unchanged.

**C<sub>max</sub>**: maximum measured plasma concentration over the time span specified.

**T<sub>max</sub>**: time to the maximum measured plasma concentration.

**t<sub>1/2</sub>**: elimination half-life - the time it takes for the plasma concentration or the amount of drug in the body to be reduced by 50% .

**AUC<sub>0-t</sub>**: the area under the plasma concentration vs time curve, from time zero to "t".

**t<sub>last</sub>** – time corresponding to the last measured concentration C<sub>last</sub> .

## Chapter 3

**AUC<sub>0-∞</sub>**: the area under the plasma concentration vs time curve from time zero to infinity calculated as AUC<sub>0-t<sub>last</sub></sub> plus the extrapolated area from time t<sub>last</sub> to infinity calculated using C<sub>last</sub>/K .

**K**: the fraction of drug eliminated per unit time.

**CL**: volume of plasma from which a drug is completely cleared per unit time.

**V<sub>a</sub>**: also known as apparent volume of distribution- is the theoretical volume required to contain the total amount of an administered drug at the same concentration observed in blood plasma.

### 3.2.5 Statistical analysis

Statistical analyses were conducted using Review Manager (RevMan Version 5.3.5 for Windows, Cochrane Collaboration, Oxford, UK) to pool data for each of the PK parameters and associated variables. Continuous outcomes were presented as a standardised mean difference (SMD) and 95% confidence intervals (CI). Heterogeneity was evaluated using the chi-squared (Chi<sup>2</sup>), Higgins I<sup>2</sup> and Tau<sup>2</sup> statistics which assess the appropriateness of pooling individual study results. Random-effects models were applied if heterogeneity was evident (Chi<sup>2</sup> P < 0.10/ I<sup>2</sup> >50%); otherwise, fixed-effects models were used. Subgroup analyses were used when either statistical or clinical heterogeneity was evident. The Z test was used to test the statistic significant of overall effect size. Significance was established at P < 0.05, and data were presented as mean ± SD unless otherwise stated. Publication bias was assessed visually using a Funnel Plot.

## 3.3 Results

### 3.3.1 Study identification

Applying the search terms, a total of 1336 publications were retrieved through electronic database searches. After duplicates were removed and studies excluded by titles and abstracts, 42 articles were retrieved for detailed assessment. Of these, 32 articles were excluded (ten remained), because the studies were done on children, the primary outcomes (PK data) were not reported, because they did not report the laboratory measurement that indicates the patients under hypoxaemia such as PaO<sub>2</sub> or SaO<sub>2</sub> values or because there was no control group (**Figure 3.1**). A total of ten full-text articles were selected for meta-analysis (Cumming, 1976; Agnihotri *et al.*, 1978; Souich *et al.*, 1983; Cusack *et al.*, 1986; Du Souich *et al.*, 1989; Rowett *et al.*,

1996; Streit *et al.*, 2005; Li *et al.*, 2009; Zhang *et al.*, 2016; Thomas *et al.*, 2018), two were from Canada, two from the United States, one from the UK, one from Australia, one from Germany, two from China and one from India. The studies comprised of three cross-over RCTs, six non-RCTs, and one before and after study without control.

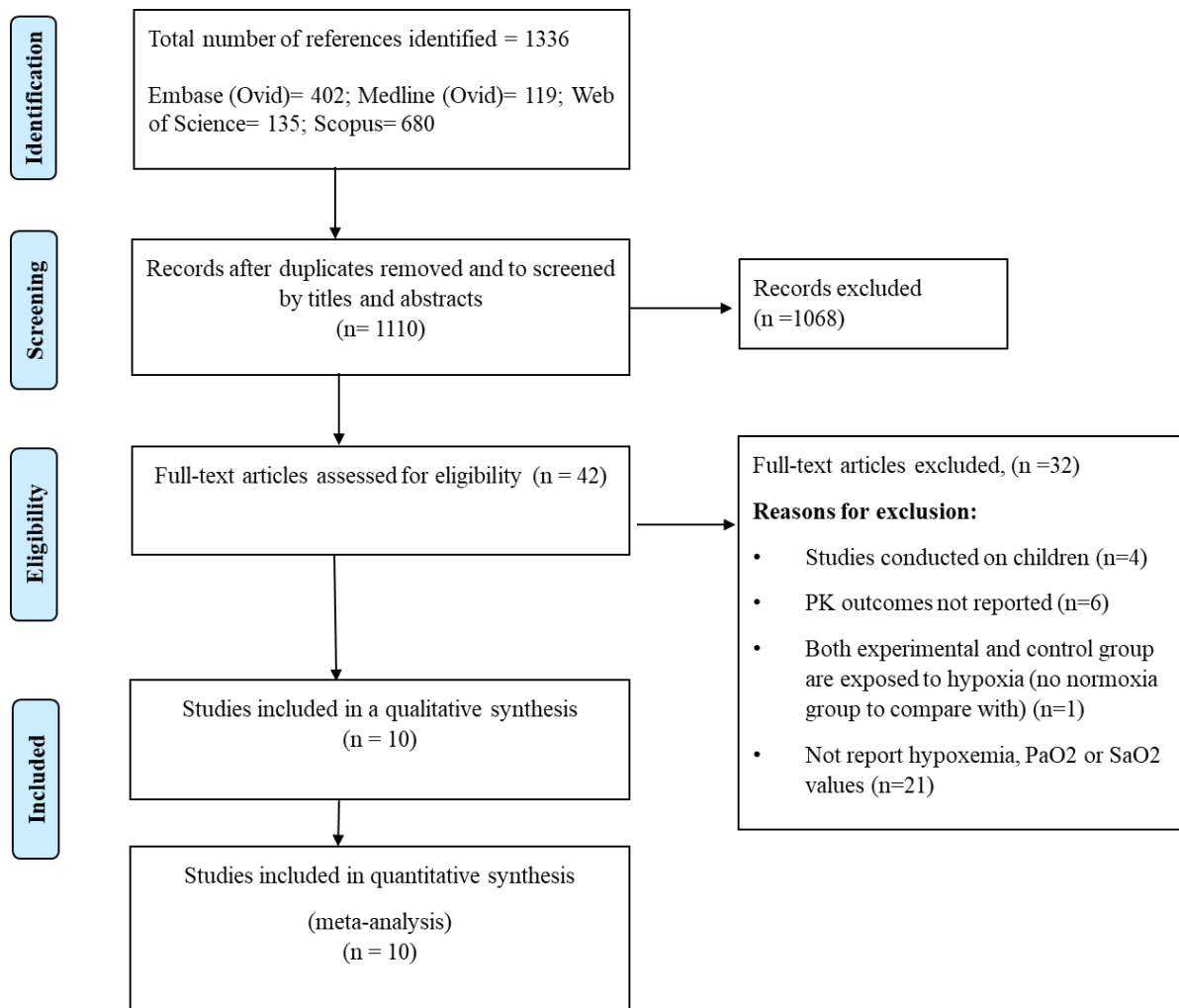


Figure 3.1 Flow chart of article searches and selection strategies.

### 3.3.2 Risk of bias

The SURE checklist was used because it offers an in-depth appraisal rather than relying on a summary score, which may not provide an adequate assessment of limitations specific to the individual study. All included studies were judged to be of moderate methodological quality (Appendix 4.3).

All studies were interpreted as having a clearly focused research question, an appropriate description of the interventions, a well-described method of data collection, outcome assessment and a consistent approach to reporting the conclusions (within the abstract and discussion).

For each criterion, most studies were interpreted as good quality, with the exception of research design (randomisation, intervention concealment and blinding). Most of the studies were reported as “NO” or “Unclear” (except for two studies Rowett *et al.*, 1996; Streit *et al.*, 2005) for the randomisation and the method of blinding being well described. This was expected as only three cross-over RCT studies were included in this review. The justification of sample size strategy were unclear in four of the studies (Cumming, 1976; Agnihotri *et al.*, 1978; Du Souich *et al.*, 1989; Rowett *et al.*, 1996). It was unclear if ethical approval was sought and received in four studies (Cumming, 1976; Agnihotri *et al.*, 1978; Souich *et al.*, 1983; Du Souich *et al.*, 1989). Conflicts of interest and sponsorships were reported in two studies (Souich *et al.*, 1983; Zhang *et al.*, 2016). In four studies, the authors did not identify any limitations (Cumming, 1976; Souich *et al.*, 1983; Cusack *et al.*, 1986; Du Souich *et al.*, 1989).

### 3.3.3 General characteristics of the included studies

This review includes ten studies published between 1976 and 2018 reporting PK data from participants with hypoxaemia evidenced by a reported low PaO<sub>2</sub> level (< 80 mmHg). However, the reasons for hypoxaemia varied. Six studies were related to patients with pulmonary disorders, which was the primary cause of hypoxaemia, while in four of the studies, hypoxaemia occurred due to ascending to high altitude areas. A total of 66 patients (58 males and eight females) were diagnosed with chronic respiratory disease and were receiving amongst the medications either antipyrine, sulfamethazine, theophylline or furosemide, which were administrated orally or intravenously. The PK of a single dose of verapamil, theophylline, sulfamethoxazole, lidocaine hydrochloride or alprazolam administrated either orally or intravenously (and in one study intramuscularly) were studied in 84 healthy male volunteers either living with (chronic) or acutely exposed ( $\leq 24$  h) to a high-altitude environment. The general properties of the drugs in these studies are shown in **Table 3.1**.

Table 3.1 General drug properties.

Drug	Antipyrine	Sulfamethazine	Theophylline	Furosemide	Verapamil	Sulfamethoxazole	Lidocaine hydrochloride	Alprazolam
<b>Action</b>	Analgesic and antipyretic	Anti-infective agent	phosphodiesterase inhibitor	Loop diuretic	Antiarrhythmic	Antibacterial agent	Analgesics and anaesthetics	Antianxiety agent
<b>Molecular mass</b>	188	278	180	330	455	253	234	309
<b>Protein binding (%)</b>	95-99	50-60	40, primarily to albumin	91-99, mainly to serum albumin	94	70	60-80	80
<b>Absorption (%)</b>	Rapidly absorbed	Rapidly absorbed	Rapidly absorbed	10 - 90	90	Rapidly absorbed	35	84-91
<b>Vd (L/kg)</b>	0.7	1.5-2	0.3 - 0.7	0.2	3.8	0.18	1.7	0.8-1.3
<b>t<sub>1/2</sub> (h)</b>	2-3	12-24	8	0.5-2	3-7	10	1.5-2	11.2
<b>Metabolism (%)</b>	90	Not available	90	10	80	80	90	90
<b>CL (L/h/kg)</b>	1.5	0.24-0.48	0.087	0.12	0.5-1	0.017	0.54	0.054
<b>Renal elimination (% unchanged)</b>	10	< 10	10-15	PO 50 IV 80	70	20	90	20
<b>CYP-450 substrate</b>	Substrate CYP3A4/1A2 /2C9/2E1	Non-substrate	Substrate CYP1A2/3A4	Non-substrate	Substrate CYP3A4/3A5/ 1A2/2C9/2C8	Minor pathway CYP2C9	Substrate CYP3A4 / 1A2/2B6/2C9/2D6	Substrate CYP3A4/3A5/3A7 /2C9

## Chapter 3

<b>P-glycoprotein substrate</b>	Non substrate	Non substrate	Non substrate	Non substrate	Substrate	Non substrate	Non substrate	Non-substrate
<b>cLogP</b>	1.18	0.43	-0.26	2.71	5.23	0.79	1.81	2.23
<b>PSA (Å<sup>2</sup>)</b>	29	97	69	122	63.95	98	32.34	43.07

Sources: The Drug Bank Database; Medscape.  $t_{1/2}$ , elimination half-life; cLogP (using ALOGPS), logarithm of compound's partition coefficient; PSA (using CHEMAXON), polars surface area; Å<sup>2</sup>, angstrom.

## Chapter 3

The pulmonary disease patients were  $63 \pm 3$  years old (mean  $\pm$  SD) and were compared with the same patients - each subject serves as their own control- after receiving oxygen therapy in a cross-over manner, with other patients with similar physical status but with normal PaO<sub>2</sub>, or with healthy participants. In high altitude studies, the participants were about 22 years old and healthy and were compared with healthy volunteers living at sea level altitude who has PaO<sub>2</sub> values. **Table 3.2** provides detailed information about the study characteristics.



Table 3.2 Study characteristics.

Studies	Drug	Dose/Administration	Sample (n) /sex	Age (years)	weight (kg)	Causes of hypoxaemia
(Cumming, 1976)	Antipyrine	600 or 1,200 mg/PO 1,000 mg/ IV	17 males	Adults, the exact age is not given	Not given	Pulmonary disorders
(Agnihotri <i>et al.</i> , 1978)		750 mg /PO	8 / seven males and one female	64 ± 7	60 ± 10	Obstructive airways disease and /or progressive massive fibrosis
(Souich <i>et al.</i> , 1983)	Sulfamethazine	10 mg/kg /PO	11 / eight males and three females	65.8 ±6.2	65 -82	Chronic obstructive lung diseases
(Cusack <i>et al.</i> , 1986)	Theophylline	Single dose isotope-enriched theophylline (10 mg, m/z 183) /IV + maintenance dose (m/z 180)/PO	10 males	64 ±2	63.3 ±3.3	Chronic obstructive pulmonary disease
(Du Souich <i>et al.</i> , 1989)		4 mg/kg /IV	10 /nine male and one female	58 ± 3	66.0 ± 3.2	Severe chronic obstructive lung disease
(Rowett <i>et al.</i> , 1996)	Furosemide	Day 2: 40 mg /PO +500 mg paracetamol Or Day 3: 20 mg/ IV + 500 mg paracetamol	10 / seven males and three females	64.6 ± 5.7	73.4 ± 14.6	Chronic respiratory failure
(Streit <i>et al.</i> , 2005)	Verapamil	5 mg / IV bolus over 10 min	10/ males	26 ± 4.	73.5 ± 8.7	Hypoxia chamber (12% oxygen). Equivalent to an altitude of 4500 m for 14 h.
	Theophylline	6 mg /kg / IV bolus over 20 min	10/ males			

Chapter 3

<b>(Li et al., 2009)</b>	Sulfamethoxazole	1500 mg/PO	20/ Han Chinese males (low altitude). 20/ Han Chinese males were living at high altitudes.	Low altitude group: 20.4 ± 1.1. High altitude group: 21.2 ± 1.3.	64.2 ± 5.9 (low altitude). 62.4 ± 8.2 (high altitude).	Ascending to an altitude of 3780 m for 16 h or more than 12 months.
<b>(Zhang et al., 2016)</b>	Lidocaine hydrochloride	10 mg / intramuscular	Low altitude group: 18/male. *Han high altitude group: 17/male. **Tibetan high-altitude group: 18/ male.	Low altitude group: 20.2 ± 0.94. Han high altitude group: 21.0 ± 0.97. Tibetan high-altitude group: 22.17 ± 0.96.	Low altitude group: 59.23 ± 4.46. Han high altitude group: 57.94 ± 5.54. Tibetan high-altitude group: 61.22 ± 4.53.	Resident at an altitude of 2,200–4,500 m.
<b>(Thomas et al., 2018)</b>	Alprazolam	1 mg /PO	Hypoxia group: 9/ male. Normoxia group: 15/ male.	20-60	Not given	Ascending to an altitude of 2500 m for 24 h.

Age expressed as mean ± SD or mean ±SE or as range, weight expressed as mean ± SD (or range); IV, intravenous; PO, oral route.

\*Han people are the largest ethnic group in China which are mostly live in Han region where the elevation ranging from sea level to about 2000 m above sea level.

\*\*Tibetan people are an ethnic group native to Tibet and surrounding areas, including parts of China, India, and Nepal are predominantly found in the Tibetan plateau, which is the highest plateau in the world, with an average altitude of over 4,000 meters above sea level

### 3.3.4 Systematic review

Ten studies were included in the Rapid Systematic Review. **Table 3.3** summarises the effect of hypoxaemia on pharmacokinetics.

#### 3.3.4.1 $C_{\max}$ , $T_{\max}$ , Area Under the Curve

The parameters  $C_{\max}$ ,  $T_{\max}$  and AUC were reported in nine studies. Of these only two studies found significant alteration of  $C_{\max}$  and/or AUC. Thomas *et al.* found a significant decrease of  $C_{\max}$  and AUC of oral alprazolam in a group of participants ascending to an altitude of 2500 m where hypoxaemia was compared with other groups ascending to the same altitude but who has a normal  $PaO_2$  values (non-hypoxic) (Thomas *et al.*, 2018). In contrast, the AUC of oral sulfamethoxazole were increased by 17.8% in healthy male subjects who had hypoxaemia after acute exposure to an altitude of 3,780 m, and when compared to those residing at an altitude of 400 m (Li *et al.*, 2009).

#### 3.3.4.2 Half-life ( $t_{1/2}$ ) and elimination rate constant (K)

In regard to the related elimination rate constant (K) (related to  $t_{1/2}$  by  $t_{1/2} = 0.693/K$ ) only two studies reported K under hypoxaemia and both of them were under high-altitude environments (Li *et al.*, 2009; Thomas *et al.*, 2018). The K of oral sulfamethoxazole was 11.8% and 17.1% lower (viz. prolonged  $t_{1/2}$ ) in the acute and chronic high altitude exposure groups (3780 m), compared with the low altitude group. In contrast, Thomas *et al.*, found an increase of K (viz. shorter  $t_{1/2}$ ) of oral alprazolam in groups of subjects with hypoxaemia ( $PaO_2$  mean  $\pm$  SD  $67.93 \pm 09.26$ ) at an altitude of 2500 m compared with other subjects at the same altitude but without hypoxaemia ( $PaO_2$   $87.57 \pm 2.10$ ) (Thomas *et al.*, 2018).

#### 3.3.4.3 Mean residence time (MRT)

The MRT was reported in three studies, all undertaken in high altitude environments (Li *et al.*, 2009; Zhang *et al.*, 2016; Thomas *et al.*, 2018). In healthy male subjects who presented hypoxaemia with exposure to high altitude of 3,780 m, the MRT of oral sulfamethoxazole was 9.0% higher after acute exposure and 7.8% higher after chronic exposure compared to those residing at an altitude of 400 m (Li *et al.*, 2009). Similarly, an increase in lidocaine hydrochloride MRT following intramuscular administration

has been observed in healthy native Han volunteers who lived at high altitudes (2,200–4,500 m) compared with Han volunteers at low altitudes (400 m) (Zhang *et al.*, 2016). In contrast, Thomas *et al.* observed a significant decrease of oral alprazolam MRT in a group of subjects with hypoxaemia (mean  $\pm$  SD 67.93  $\pm$  09.26) at an altitude of 2500 m compared with other subjects at the same altitude.

#### **3.3.4.4 Plasma Clearance (CL)**

The clearance of the drugs was reported in eight studies (Agnihotri *et al.*, 1978; Cusack *et al.*, 1986; Du Souich *et al.*, 1989; Rowett *et al.*, 1996; Streit *et al.*, 2005; Li *et al.*, 2009; Zhang *et al.*, 2016; Thomas *et al.*, 2018). Four of these studies (Agnihotri *et al.*, 1978; Cusack *et al.*, 1986; Du Souich *et al.*, 1989; Rowett *et al.*, 1996) involved patients with hypoxaemia and chronic pulmonary disease and found no significant alteration on the systemic clearance of antipyrine, theophylline and furosemide under hypoxaemia. Four studies (Streit *et al.*, 2005; Li *et al.*, 2009; Zhang *et al.*, 2016; Thomas *et al.*, 2018) involved healthy hypoxic subjects at high altitude environments or exposed to hypoxia using hypoxia chamber. Of these, only one study found a significant alteration of CL. The CL of oral sulfamethoxazole decreased by 17.8% in subjects acutely exposed to an altitude of 3780 m (for 16 h) compared to those in the baseline condition (at altitude of 400 m). However, the CL in subjects chronically exposed to high altitude (>1 year) were not altered (Li *et al.*, 2009).

#### **3.3.4.5 Volume of Distribution ( $V_d$ )**

The  $V_d$  under hypoxaemia was in nine studies (Agnihotri *et al.*, 1978; Souich *et al.*, 1983; Cusack *et al.*, 1986; Du Souich *et al.*, 1989; Rowett *et al.*, 1996; Streit *et al.*, 2005; Li *et al.*, 2009; Zhang *et al.*, 2016; Thomas *et al.*, 2018). Five of these studies (Agnihotri *et al.*, 1978; Souich *et al.*, 1983; Cusack *et al.*, 1986; Du Souich *et al.*, 1989; Rowett *et al.*, 1996) involved patients with hypoxaemic pulmonary disease. Of the nine only one study reveals an alteration of  $V_d$  under hypoxaemia. Souich and his colleagues found an increase in oral Sulfamethazine  $V_d$  by more than 50% in patients with hypoxaemia compared to healthy volunteers. The authors commented the increase of  $V_d$  occurs secondary to an increase in sulfamethazine unbound fraction (Souich *et al.*, 1983). In this study the oral bioavailability were estimated by measuring unchanged drug recovered from the urine by dividing the molar sum of sulfamethazine and its main

metabolite N-acetylsulfamethazine recovered in the urine by the molar dose of administered sulfamethazine then the  $V_d$  was estimated from  $V_d = F \cdot \text{dose} / \text{AUC} \cdot k$ .

#### **3.3.4.6 Bioavailability (F)**

Three studies reported the oral bioavailability in patients with chronic respiratory diseases and hypoxaemia (Souich *et al.*, 1983; Cusack *et al.*, 1986; Rowett *et al.*, 1996). Souich *et al* found a significant decrease of oral sulfamethazine bioavailability by 12% in patients with hypoxaemia compared with healthy control subjects. In this study the bioavailability was estimated by measuring unchanged drug recovered from the urine. Rowett *et al* reported non-significant 10 % decrease in furosemide oral bioavailability in chronic respiratory failure patient breathed room air compared with chronic respiratory failure patient received oxygen therapy. Nevertheless, Cusack *et al* found non-significant 7% increase in theophylline bioavailability in patients with chronic obstructive lung disease breathed room air compared with the same patients when switched to oxygen therapy.

**Table 3.3 Changes in pharmacokinetics of different drugs under hypoxaemia.**

Study	Drug	Experimental group	PaO <sub>2</sub> (mmHg)	Control group	PaO <sub>2</sub> (mmHg)	Effect of hypoxaemia on PK
(Cumming, 1976)	Antipyrine	Patients with pulmonary disorders	≤ 55	<ul style="list-style-type: none"> <li>Patients with a similar physical status of the experimental group but with normal PaO<sub>2</sub>.</li> <li>Healthy adults.</li> </ul>	>55	<ul style="list-style-type: none"> <li>Antipyrine t 1/2 increased by 120% in a group of patients predominantly with chronic hypoxaemia (PaO<sub>2</sub> of 55 mmHg and below) compared with other subjects without severe hypoxia (PaO<sub>2</sub> above 55 mmHg).</li> </ul>
(Agnihotri <i>et al.</i> , 1978)		Six patients with obstructive airways disease and two patients with progressive massive fibrosis	51 + 10	<ul style="list-style-type: none"> <li>The same patients in the experimental group received oxygen therapy.</li> </ul>	79 ± 17	<ul style="list-style-type: none"> <li>No evidence of impaired antipyrine metabolism in spite of hypoxia.</li> <li>Slight non-significant increase of CL in patients with hypoxaemia compared to control.</li> <li>30% decrease in apparent V<sub>d</sub>.</li> </ul>
(Souich <i>et al.</i> , 1983)	Sulfamethazine	Patient with Severe Chronic obstruction lung diseases	56 ± 3	<ul style="list-style-type: none"> <li>8 healthy male volunteers</li> </ul>	58 ± 7	<ul style="list-style-type: none"> <li>No differences were observed in the rate of sulfamethazine absorption.</li> </ul>

						<ul style="list-style-type: none"> <li>• Bioavailability was decreased.</li> <li>• <math>V_d</math> was more than 50% greater in the group of patients than in the control group secondary to an increase in sulfamethazine unbound fraction.</li> <li>• No differences were observed in sulfamethazine elimination.</li> </ul>
<b>(Cusack <i>et al.</i>, 1986)</b>	Theophylline	Patients with chronic obstructive lung disease on day 2 of room air breathing	$43 \pm 3$	<ul style="list-style-type: none"> <li>• Same patients on day 2 of supplemental oxygen 2 to 3 L /min</li> </ul>	$69 \pm 4$	<ul style="list-style-type: none"> <li>• Hypoxaemia do not alter theophylline clearance (<math>0.048 \pm 0.005</math> vs <math>0.050 \pm 0.004</math> L/h/kg).</li> <li>• Non-significant changed in bioavailability of theophylline (<math>0.81 \pm 0.04</math> vs <math>0.87 \pm 0.07</math>).</li> <li>• Unchanged in <math>V_d</math> at steady state (<math>0.450 \pm 0.021</math> vs <math>0.429 \pm 0.024</math> L/kg).</li> </ul>

						<ul style="list-style-type: none"> <li>• <math>V_d</math> inversely related to arterial pH during oxygen therapy (pH range, 7.32 to 7.44) and during room air breathing (pH range, 7.33 to 7.47).</li> </ul>
<b>(Du Souich <i>et al.</i>, 1989)</b>		Hypoxic patients with chronic obstructive lung disease	$54.9 \pm 1.3$	<ul style="list-style-type: none"> <li>• The same patients on experimental group on oxygen therapy</li> </ul>	$73.6 \pm 1.9$	<ul style="list-style-type: none"> <li>• Theophylline systemic clearance increased after oxygen therapy in only four of the ten patients which resulted in only a slight non-significant increase in the average value.</li> <li>• Theophylline <math>t_{1/2}</math> was not affected by oxygen therapy.</li> <li>• oxygen therapy did not affect the pattern of urinary excretion of theophylline or its metabolites (3-MX, 1,3-DMU and I-MU).</li> </ul>
<b>(Rowett <i>et al.</i>, 1996)</b>	Furosemide	Chronic respiratory failure patient breathed room air	$\leq 55$	<ul style="list-style-type: none"> <li>• Chronic respiratory failure patient received oxygen therapy</li> </ul>	$\geq 60$	<ul style="list-style-type: none"> <li>• No significant different of furosemide total plasma clearance during hypoxaemia 76.9 vs 62.4 mL · min.</li> </ul>



						<ul style="list-style-type: none"> <li>• Vd was not affected by hypoxaemia (121 mL · kg<sup>-1</sup> without and 109 mL · kg<sup>-1</sup> with oxygen; P &gt; 0.05).</li> <li>• Renal and non-renal CL were similar during hypoxaemia (31 and 38 mL · min<sup>-1</sup>, respectively) compared to respective values during supplemental oxygen delivery (29 and 32 mL · min<sup>-1</sup>).</li> <li>• The absolute bioavailability during hypoxaemia (0.62) was not different to that obtained during normoxia (0.56).</li> </ul>
<b>(Streit <i>et al.</i>, 2005)</b>	Verapamil	Healthy participants exposed to hypoxic chamber (breath 12% oxygen for 14 h).	41.2 ± 4.47	<ul style="list-style-type: none"> <li>• Healthy participants breathe a normal level of oxygen (21% O<sub>2</sub>).</li> </ul>	87.9 ± 6.61	<ul style="list-style-type: none"> <li>• Acute hypoxia did not alter the pharmacokinetics of verapamil.</li> </ul>
	Theophylline		43.2 ± 3.85		88.9 ± 5.32	<ul style="list-style-type: none"> <li>• Acute hypoxia did not alter the pharmacokinetics of theophylline.</li> </ul>
<b>(Li <i>et al.</i>, 2009)</b>	Sulfamethoxazole	Healthy Chinese male volunteers exposed to altitude of 3780 m either for 16 h (acute) or for	Acute exposure: 55.9 ± 5.11	<ul style="list-style-type: none"> <li>• Healthy Chinese male volunteers living at low altitude area (400 m).</li> </ul>	97.7 ± 5.77	<ul style="list-style-type: none"> <li>• The t<sub>1/2</sub> was 11.5% and 19.9% higher in the acute- and chronic-exposure groups,</li> </ul>

		more than 12 months (chronic).	Chronic exposure: $55.7 \pm 5.89$			<p>respectively, compared with the low-altitude group.</p> <ul style="list-style-type: none"> <li>MRT was 9.0% and 7.8% higher in the acute- (<math>P &lt; 0.05</math>) and chronic-exposure (<math>P &lt; 0.001</math>) groups, respectively, than in the low-altitude group.</li> <li>AUC was 17.8% higher and CL was 17.8% lower in the acute-exposure group compared with the low-altitude group (both, <math>P &lt; 0.05</math>)</li> <li>K were 11.8% and 17.1% lower in the acute- and chronic high altitude exposure groups versus low altitude groups.</li> </ul>
<b>(Zhang <i>et al.</i>, 2016)</b>	Lidocaine hydrochloride	<ul style="list-style-type: none"> <li>Healthy male native Han volunteers lived at high altitude (2,200–4,500 m).</li> <li>Healthy male native Tibetan volunteers lived</li> </ul>	<ul style="list-style-type: none"> <li>Han HA: <math>59.8 \pm 2.15</math></li> <li>Tibetan HA: <math>58.4 \pm 4.21</math></li> </ul>	<ul style="list-style-type: none"> <li>Healthy Han male volunteers living at low altitude (400 m).</li> </ul>	$97.4 \pm 1.32$	<ul style="list-style-type: none"> <li>In native Han group who live chronically in high altitude, the <math>t_{1/2}</math> was 29.8% higher, than in the low altitude group.</li> <li>Increase of MRT native Han group who live</li> </ul>

		at high altitude (2,200–4,500 m).				<p>chronically in high altitude.</p> <ul style="list-style-type: none"> <li>In native Tibetan group who live chronically in high altitude, the <math>t_{1/2}</math> was 29.8% higher than the low altitude group.</li> </ul>
<b>(Thomas <i>et al.</i>, 2018)</b>	Alprazolam	Healthy male volunteers ascending to altitude of 2500 m and have low PaO <sub>2</sub> value (hypoxia). Study duration: 24 h.	67.93± 09.26	<ul style="list-style-type: none"> <li>Healthy male volunteers ascending to altitude of 2500 m and have normal PaO<sub>2</sub> value (normoxia).</li> <li>Study duration: 24 h.</li> </ul>	87.57 ± 2.10	<ul style="list-style-type: none"> <li>The C<sub>max</sub> and AUC values were significantly reduced in hypoxia group than non-hypoxia group (21.26 ±1.40, p&lt;0.05).</li> <li>The elimination rate constant and clearance were significantly increased in hypoxia group (p&lt;0.05).</li> <li>The V<sub>d</sub> was not affected.</li> <li>MRT and t<sub>1/2</sub> was reduced in hypoxia group.</li> </ul>

PaO<sub>2</sub>; partial pressure of arterial oxygen which expressed as mean ± SD (or value); PK, pharmacokinetics; t<sub>1/2</sub>, elimination half-life; V<sub>d</sub>, volume of distribution; CL, clearance; (1,3-DMU)1,3-dimethyluric acid, (3-MX) 3-methylxantine; (I-MU), I-methyluric acid.

### 3.3.5 Meta-analysis

$\text{Chi}^2$  and Higgins  $I^2$  reveal significant heterogeneity ( $\text{Chi}^2 P < 0.10/ I^2 > 50\%$ ) in all of  $F$ ,  $\text{AUC}$ ,  $K$ ,  $t_{1/2}$ , and  $\text{MRT}$  as shown in forest blot (**Figure 3.4, 3.7, 3.8, 3.9 and 3.12**) respectively. The subgroup approach and random effect model were used to minimise heterogeneity between the studies included. Due to the clinical heterogeneity, e.g. characteristics of the study population between the studies, they were divided into two subgroups, the first group included studies done on patients with chronic respiratory diseases and the second subgroup included studies done on a healthy participant where hypoxaemia arose by exposure to either high altitude or via exposure to low oxygen in a hypoxia chamber which in contrast to high altitude is a normobaric hypoxia environment.

**Figure 3.2** presents a summary of the observed changes in each of the pharmacokinetic parameters occurring as a result of respiratory disease hypoxaemia. No statistical difference was observed in the pooled meta-analysis for  $V_d$ ,  $\text{CL}$ ,  $t_{1/2}$ ,  $F$ ,  $C_{\text{max}}$  and  $T_{\text{max}}$ .

Parameter	N/n	Total SMD	Total CI	P-value
V <sub>d</sub>	5/91	0.18	(-0.24, 0.60)	0.40
CL	4/76	0.10	(-0.35, 0.55)	0.67
t <sub>1/2</sub>	6/119	0.18	(-0.23, 0.59)	0.40
F	3/57	-0.58	(-1.56, 0.41)	0.25
C <sub>max</sub>	2/39	0.13	(-0.51, 0.77)	0.69
T <sub>max</sub>	2/39	-0.09	(-0.72, 0.54)	0.77

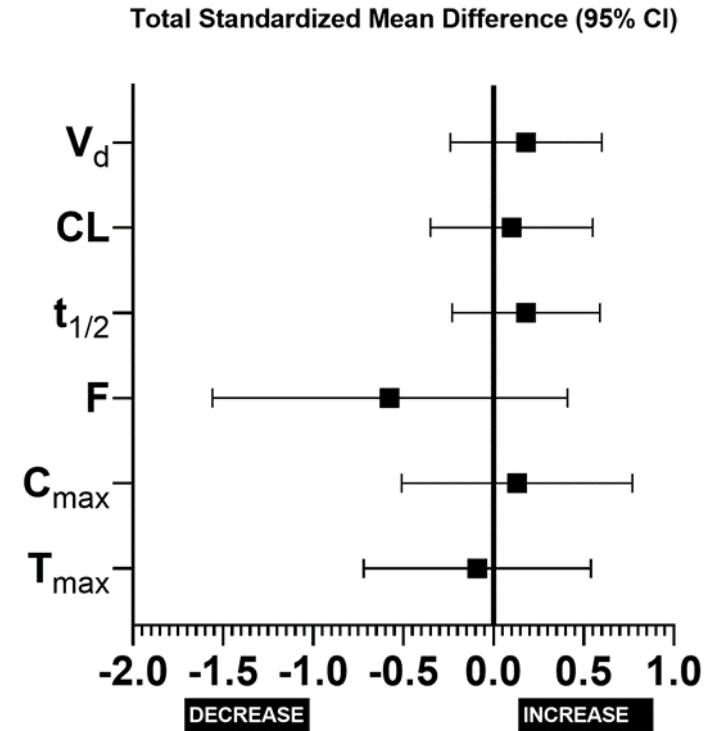


**Figure 3.2** A pooled meta-analysis of drug pharmacokinetics in patients with respiratory diseases and hypoxaemia. N/n, number of studies/participants; SMD, standardised mean difference; CL, confidence interval; V<sub>d</sub>, volume of distribution; CL, clearance; t<sub>1/2</sub>, elimination half-life; F, systemic bioavailability.

**Figure 3.3** shows the pooled forest plot of PK parameters for healthy volunteers' subgroup exposed to hypoxia by ascending to high-altitude or using hypoxia chamber at sea level. The CL showed statistical significance with a decrease in participants with hypoxaemia at high altitude areas (SMD: -0.37,  $P=0.05$ ). In contrast, no changes ( $P > 0.05$ ) were observed in the remaining parameters, notably  $C_{\max}$ ,  $T_{\max}$ , AUC, K,  $t_{1/2}$ ,  $V_d$ , and MRT. **Figure 3.5 to Figure 3.12** illustrate the forest plots for each of the pharmacokinetic parameters based on plasma analysis.

Parameter	N/n	Total SMD	Total CI	P-value
$C_{\max}$	4/119	-0.35	(-0.72, 0.02)	0.06
$T_{\max}$	4/119	0.06	(-0.31, 0.43)	0.75
$AUC_{0-t}$	4/139	-0.13	(-0.93, 0.68)	0.76
$V_d$	4/139	0.16	(-0.18, 0.50)	0.36
CL	4/119	-0.37	(-0.74, -0.00)	0.05
MRT	3/99	0.43	(-1.12, 1.99)	0.58
$t_{1/2}$	4/139	0.07	(-0.98, 1.12)	0.90
K	2/64	-0.15	(-2.00, 1.70)	0.88

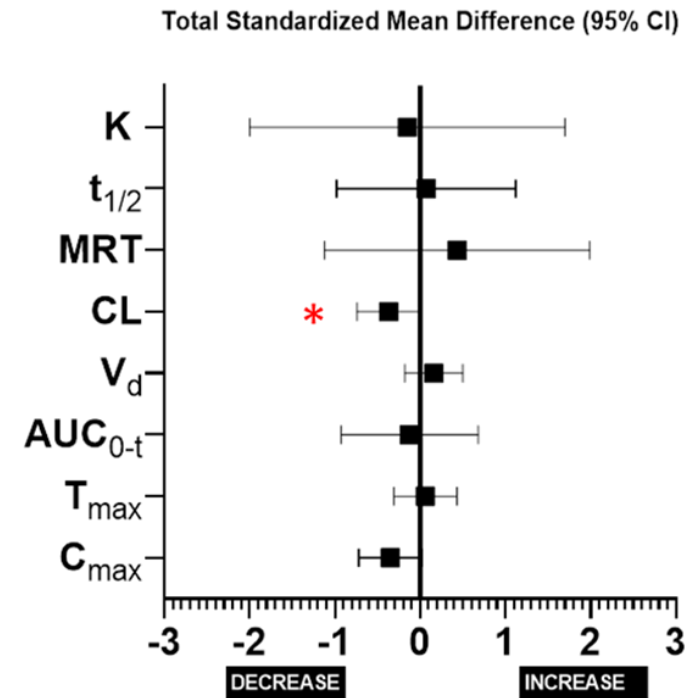


**Figure 3.3 Pooled meta-analysis of drug pharmacokinetics in healthy volunteers with hypoxaemia.** Values represented as sum or mean  $\pm$  SD; N/n, number of studies/participants; SMD, standardised mean difference; CI, confidence interval;  $C_{\max}$  maximum plasma drug concentration;  $T_{\max}$ , time to peak plasma concentration;  $AUC_{0-t}$ , area under the concentration-time curve;  $V_d$ , the volume of distribution; CL, clearance; MRT, mean residence time;  $t_{1/2}$ , elimination half-life; K, elimination rate constant.

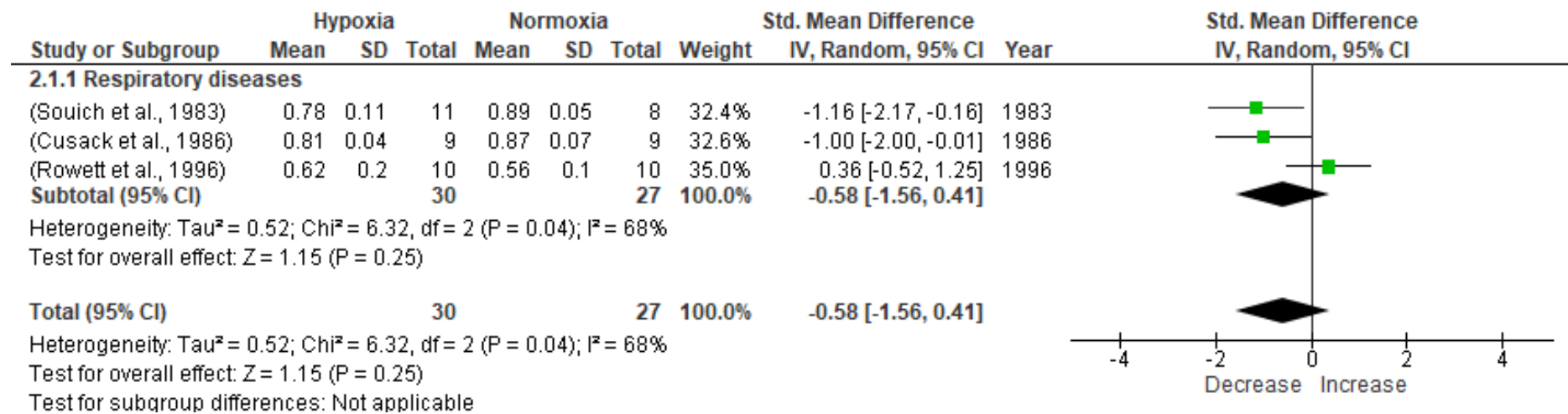


**Figure 3.4 Forest plot of bioavailability (F).** Green squares represent the standardised mean difference of each study, horizontal lines represent 95% confidence intervals (CI) and the black diamond represents the summary of standardised mean difference.



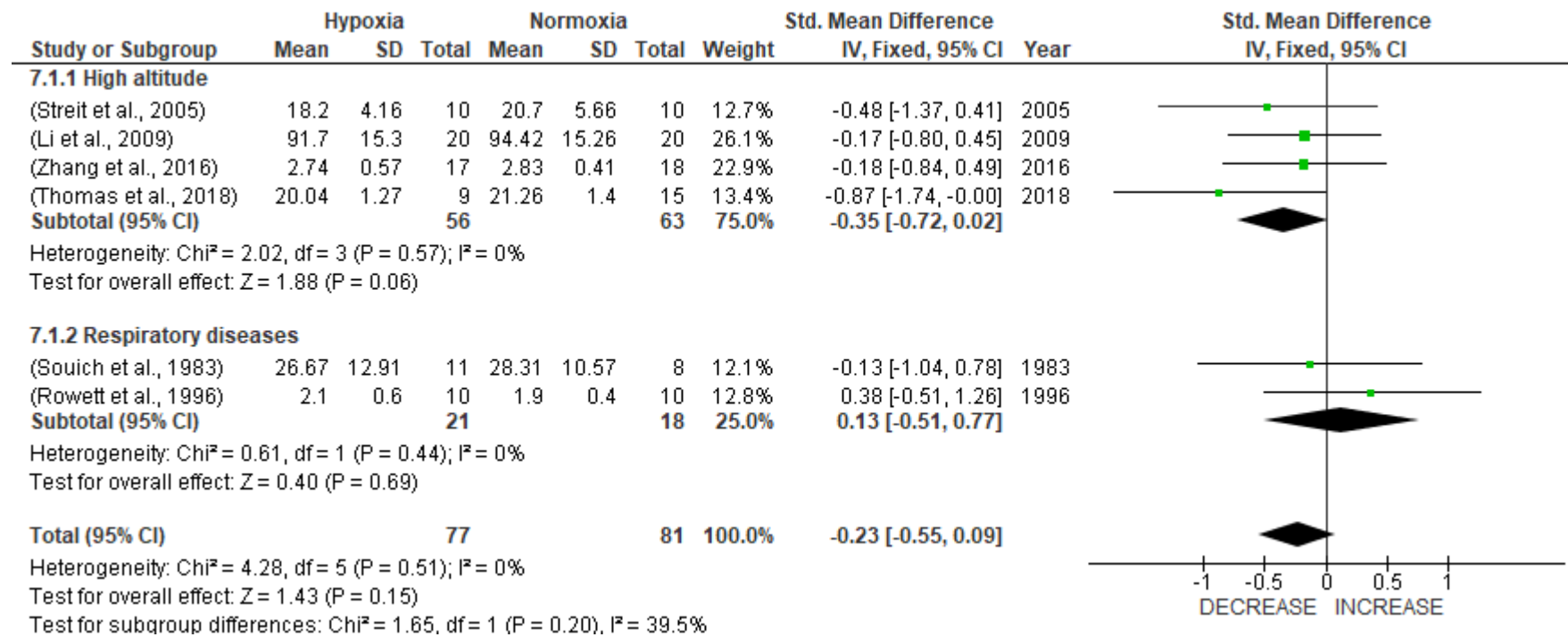


**Figure 3.5 Forest plot of maximum concentration (C<sub>max</sub>).** Green squares represent the standardised mean difference of each study, horizontal lines represent 95% confidence intervals (CI) and the black diamond represents the summary of standardised mean difference.

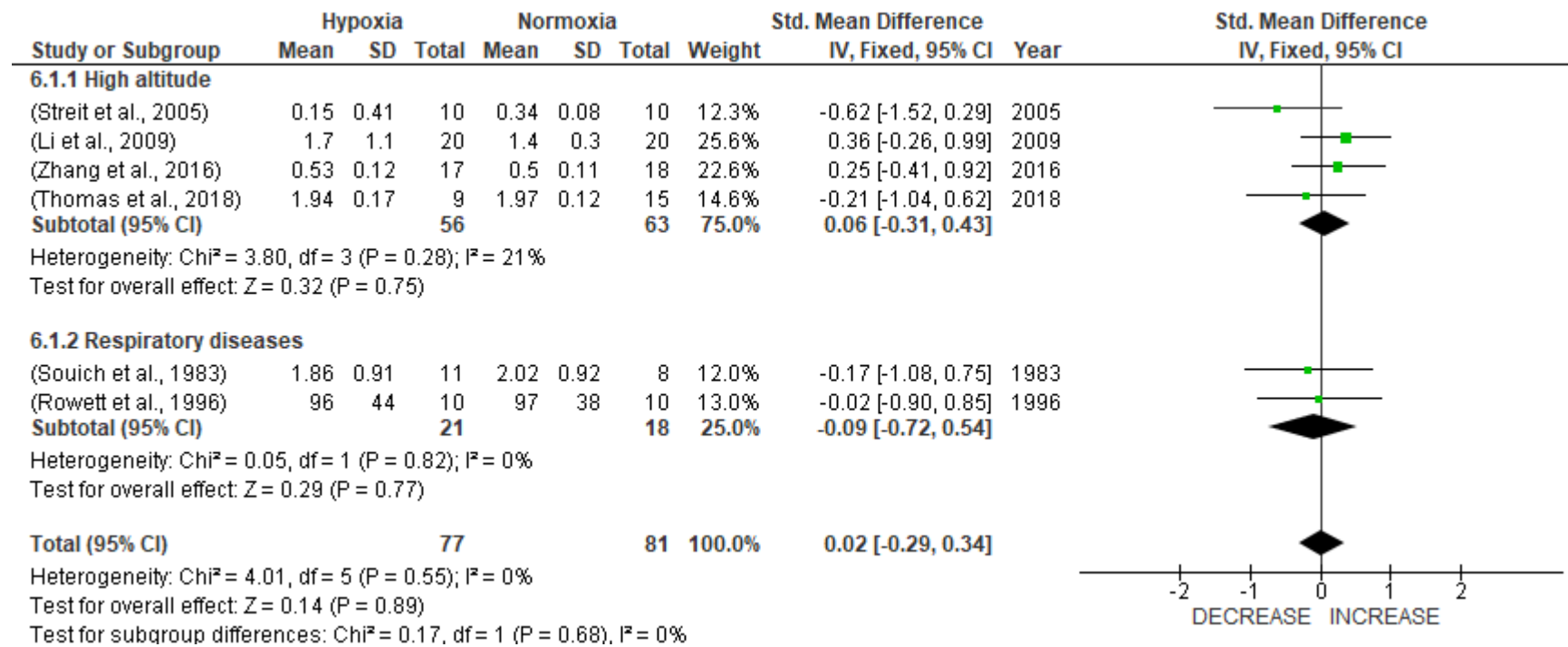


**Figure 3.6 Forest plot of time to maximum concentration (T<sub>max</sub>).** Green squares represent the standardised mean difference of each study, horizontal lines represent 95% confidence intervals (CI) and the black diamond represents the summary of standardised mean difference.

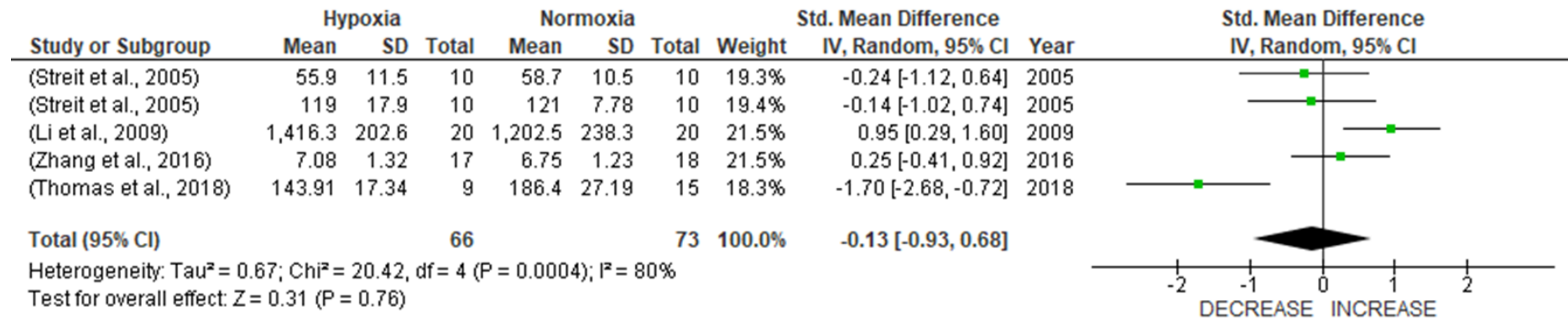


**Figure 3.7 Forest plot of area under the curve (AUC) at high-altitude.** Green squares represent the standardised mean difference of each study, horizontal lines represent 95% confidence intervals (CI) and the black diamond represents the summary of standardised mean difference. (Streit et al ,2005) study include two therapeutical interventions verapamil and theophylline.

Chapter 3

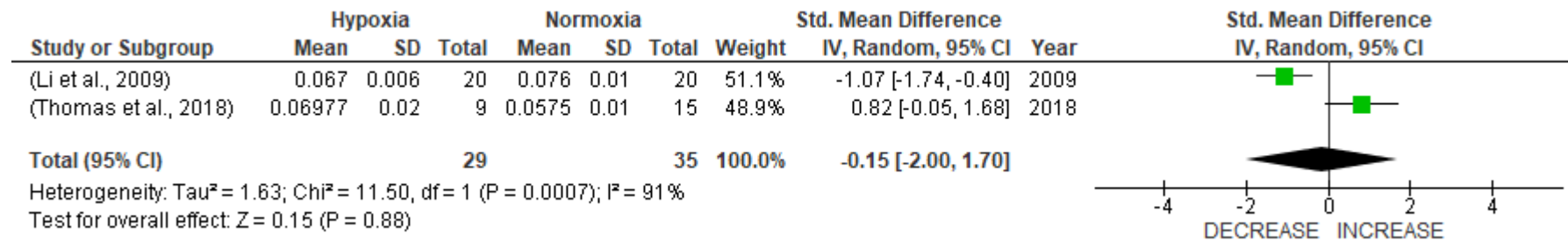


**Figure 3.8 Forest plot of elimination constant (K) at high-altitude.** Green squares represent the standardised mean difference of each study, horizontal lines represent 95% confidence intervals (CI) and the black diamond represents the summary of standardised mean difference.

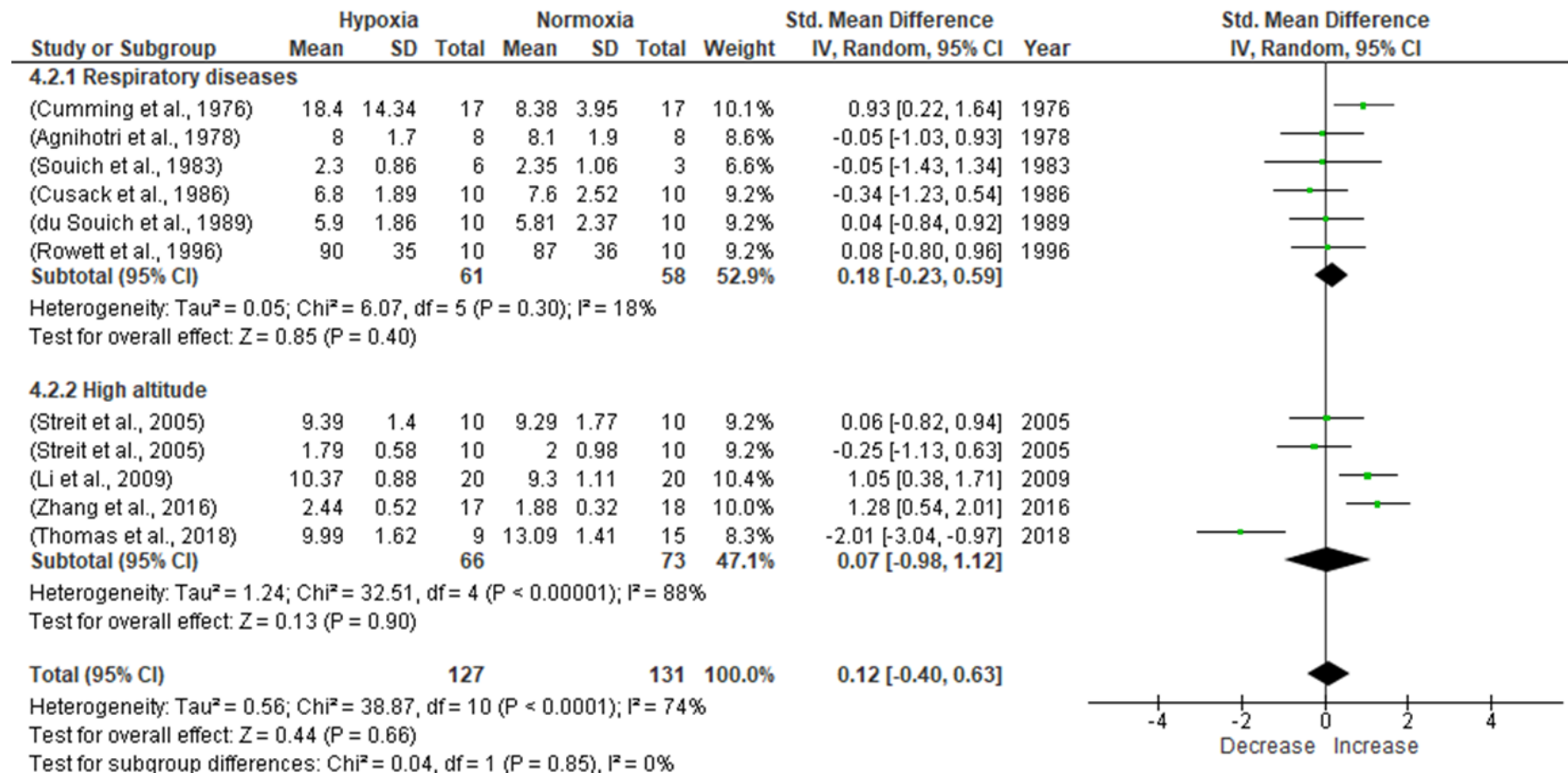


**Figure 3.9 Forest plot of elimination half-life (t 1/2).** Green squares represent the standardised mean difference of each study, horizontal lines represent 95% confidence intervals (CI) and the black diamond represents the summary of standardised mean difference. (Streit et al ,2005) study include two therapeutical interventions verapamil and theophylline.

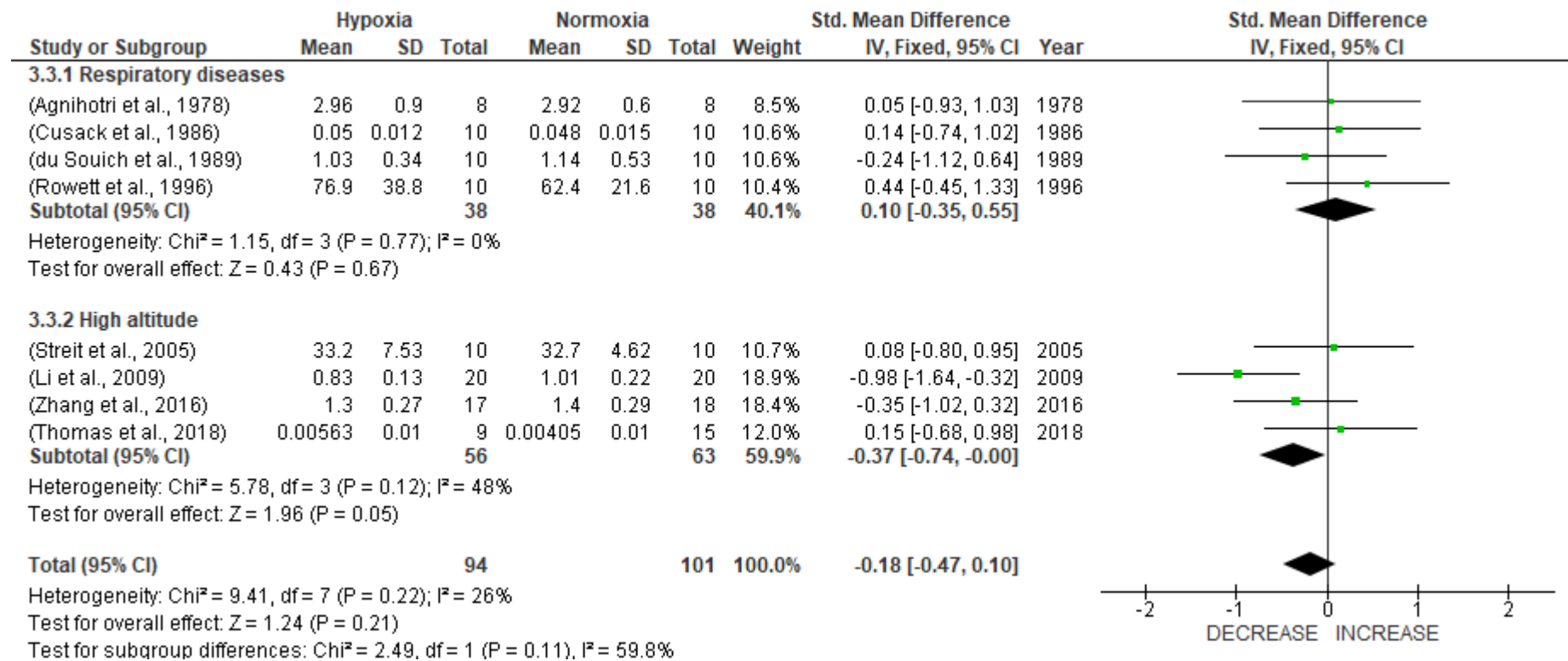


**Figure 3.10 Forest plot of clearance (CI).** Green squares represent the standardised mean difference of each study, horizontal lines represent 95% confidence intervals (CI) and the black diamond represents the summary of standardised mean difference.

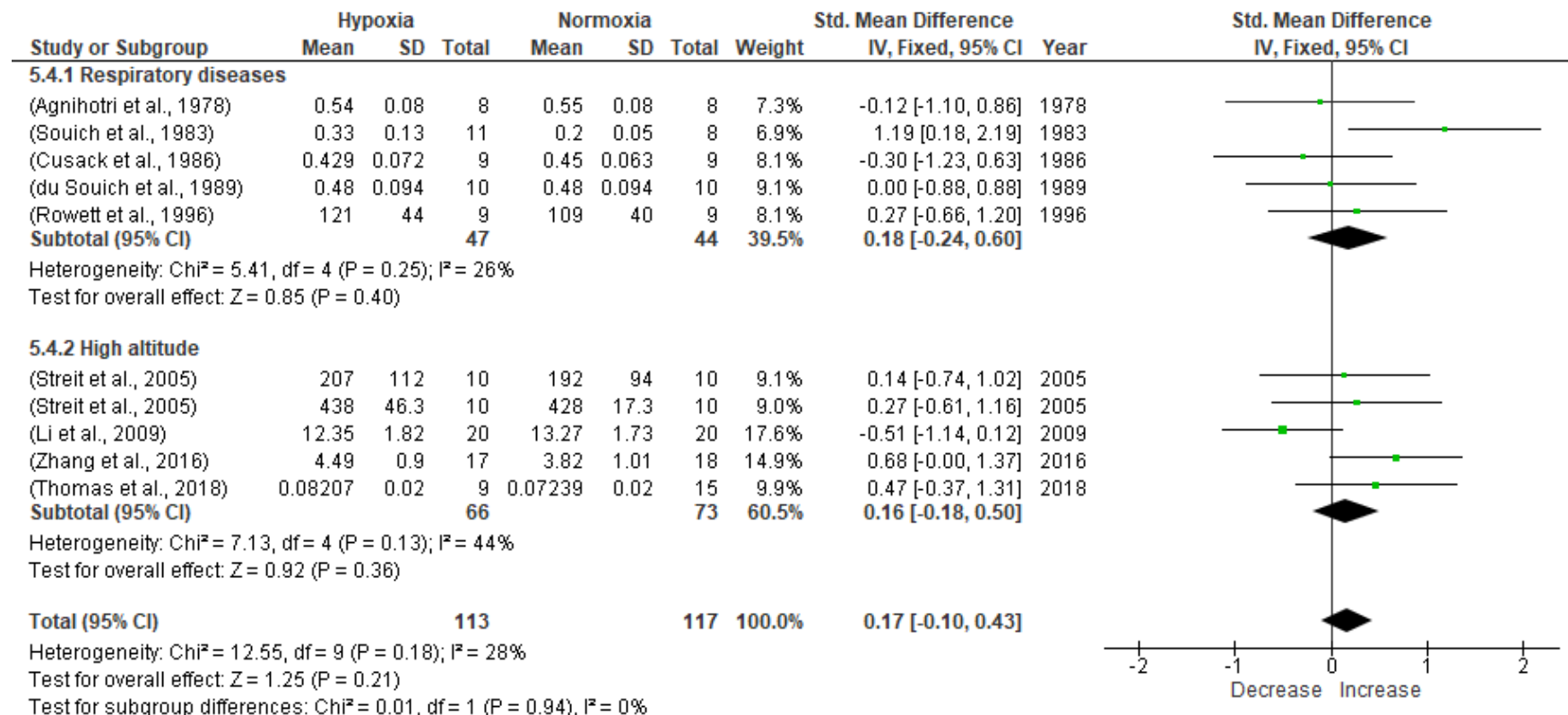


**Figure 3.11 Forest plot of volume of distribution ( $V_d$ ).** Green squares represent the standardised mean difference of each study, horizontal lines represent 95% confidence interval (CI) and the black diamond represents the summary of standardised mean difference. (Streit et al ,2005) study include two therapeutical interventions verapamil and theophylline.

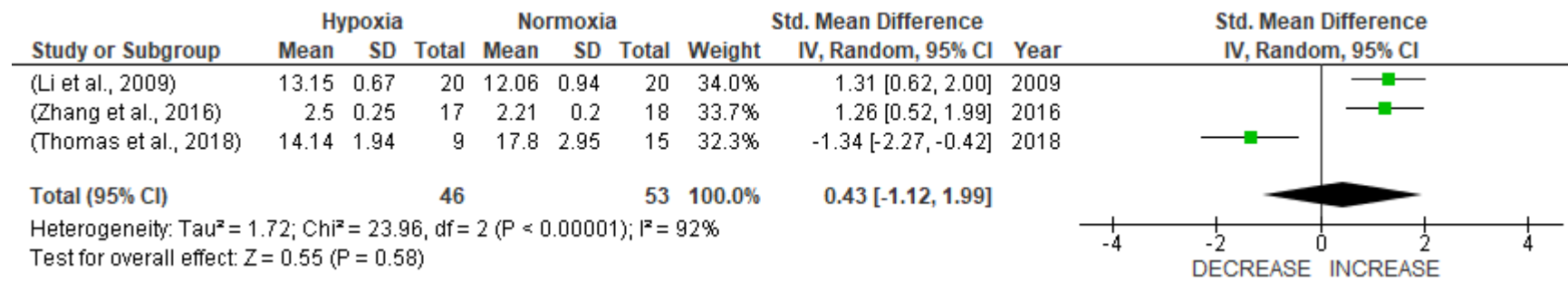


**Figure 3.12 Forest plot of mean residence time (MRT) at high-altitude.** Green squares represent the standardised mean difference of each study, horizontal lines represent 95% confidence intervals (CI) and the black diamond represents the summary of standardised mean difference.



### 3.3.6 Analysis of publication bias

**Figure 3.13** show the funnel plot for the assessment of publication bias. Publication bias was analysed for the meta-analysis of only for a single PK parameter, CL, as it was the parameter that included the highest number of studies  $n=8$ . No obvious publication bias was observed for the eight studies.

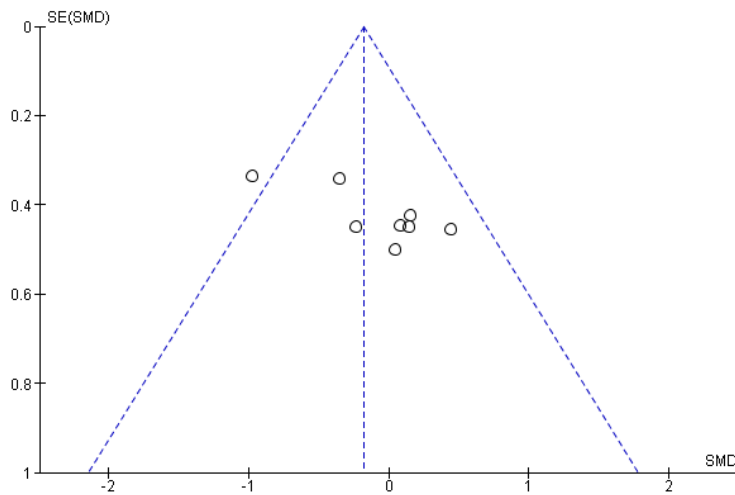


**Figure 3.13** Begg's funnel plot for the assessment of publication bias. SMD, standardised mean difference; SE, standard error.

### 3.4 Discussion and conclusions

In this chapter, a rapid systematic review and meta-analysis was conducted to answer the question of whether hypoxaemia has an impact on the PK of drugs in human adults, where hypoxaemia arises in patients with pulmonary disease or in healthy subjects with hypoxaemia conditions i.e., ascending to high altitude environments or in a very select manner in healthy volunteers experiencing a hypoxia chamber i.e., normobaric conditions.

This rapid systematic review and meta-analysis revealed some significant changes in PK parameters that define the absorption and disposition of the selection of medicinal drugs (which was limited) displaying diverse physicochemical and PK properties that may be indicative of a broader impact of the hypoxaemia upon the body's handling of pharmaceuticals. To the best of our knowledge, this is the first meta-analysis focusing on the effect of chronic hypoxaemia with respiratory disease on the PK of drugs. Importantly, the work's inclusion/exclusion criteria meant only those studies that evidenced hypoxaemia through the reporting of PaO<sub>2</sub> levels in the participants. This work differs in term of inclusion / exclusion criteria from the one other similar published meta-analysis (Bailey, Stacey and Gumbleton, 2018) which focused on subjects exposed to high-altitude hypoxaemia. Within this current work the analysis was also extended to include a subgroup of healthy participants who developed hypoxaemia after ascending to high altitude. Due to the high variability between the two sub-populations explored in this current work e.g., patients with pulmonary disease and healthy people at high altitude, these two subpopulations were not combined in our analysis, rather a meta-analysis was conducted for each group separately.

The analysis revealed a significant trend for the CL parameter to be reduced in healthy subjects with hypoxaemia due to ascending to high altitude or exposure to low level of oxygen by hypoxia chamber. This finding is supported by a recent systematic review and meta-analysis, which found a significant decrease in CL/F in healthy males exposed to low altitude followed by acute exposure to terrestrial high altitude (Bailey, Stacey and Gumbleton, 2018). Sulfamethoxazole CL data has a higher contribution to overall CL analyses. Sulfamethoxazole is well absorbed following oral administration, with peak plasma concentrations occurring within 1 to 4 h. It has a high protein-binding percentage (70-90%) and a considerable volume of distribution (about 13 L/kg).

## Chapter 3

Sulfamethoxazole is largely metabolised in the liver to its active form, N4-acetylsulfamethoxazole, via acetylation and glucuronidation pathways, with only a little fraction metabolised by the CYP450 system, notably CYP2C9 and CYP2C8. Sulfamethoxazole and its metabolites are mostly eliminated in the urine unaltered by glomerular filtration and tubular secretion. In healthy humans, the elimination half-life is around 9-11 h (Kaplan *et al.*, 1973).

At high altitudes, atmospheric pressure, and partial pressure of oxygen in the lung and arterial blood decrease, resulting in a fall in blood oxygen saturation. A physiological adaptation to compensate for the decrease in oxygen availability involves an increase in erythropoietin production, which can then increase haematocrit levels. Since sulfamethoxazole is predominantly eliminated by renal excretion, an increase in haematocrit might result in an increase in blood viscosity, which can reduce renal blood flow and the CL of sulfamethoxazole. This is because increased blood viscosity can obstruct blood flow through the glomerular capillaries, which are responsible for filtering medications from the blood into the urine. Research on healthy participants exposed to a high altitude of 4330 m for 24 h found a 17% decrease in renal blood flow, which was concurrent with an 11% decrease in renal oxygen delivery, an 11% decrease in GFR, and an increase in haematocrit levels (Steele *et al.*, 2020).

As reported in the sulfamethoxazole study, the increase in haematocrit during acute high altitude hypoxaemia resulted in a 20% rise in plasma protein content in acute high altitude vs, low altitude. Since the unbound drug is less accessible for renal excretion, the unbound fraction of the drug decreases and sulfamethoxazole clearance decreases. Increases in plasma total protein and albumin have also been observed in humans at high altitudes, resulting in higher drug protein binding (Surks, 1966; Li *et al.*, 2009).

Glucuronidase is a metabolic enzyme that is released by intestinal microflora as well as other organs such as the liver, kidney, and lung that catalyses the hydrolysis of glucuronic acid conjugates. Adak *et al* demonstrated that enzymes such as amylase, protease, alkaline phosphatase, and -glucuronidase are elevated which produced during microbial domestication at high altitudes, and that hypoxic environments at high altitudes may alter the composition and activity of intestinal microbiota, leading to gastrointestinal dysfunction (Adak *et al.*, 2013). Under acute high-altitude exposure, an increase in glucuronidase production from the intestinal microflora can result in

increased hydrolysis of the glucuronide conjugates, causing an increase in parent sulfamethoxazole to be released back into circulation a phenomenon known as enterohepatic recirculation. This may result in a decline in the CL of sulfamethoxazole.

The overall outcomes of our analysis in the chronic pulmonary disease subgroup show no significant change in any of the PK parameters included in the meta-analysis, which are bioavailability,  $C_{\max}$ ,  $T_{\max}$ ,  $V_d$ , CL and  $t_{1/2}$ . Chronic hypoxaemia patients may have compensatory mechanisms that aid to sustain organ function despite a reduction in oxygen supply. Chronic hypoxaemia, for example, can cause a rise in erythropoietin production and the formation of polycythaemia (defined by a haemoglobin of 17 g/dL in males and 15 g/dL in females), which can increase oxygen-carrying capacity and improve oxygenation (Zhang *et al.*, 2021). Chronic hypoxaemia has been linked to an increase in blood flow to many organs. In contrast to acute hypoxaemia, which reduces GFR and renal blood flow, the glomerular filtration rate appears to return to normal after chronic exposure to high altitude. In one study, the renal blood flow and filtration fraction were raised to maintain the glomerular filtration rate while renal plasma flow was decreased (Thron *et al.*, 1998). Acclimatization to chronic hypoxia may explain the unchanging PK of medication in our meta-analysis.

Some potential limitations that should be considered when interpreting the findings of this study are as follows: The majority of the participants in the Cumming, 1976; Agnihotri *et al.*, 1978 study were heavy smokers. Antipyrine is largely metabolised by the cytochrome P450 enzyme CYP2E1, although it is also processed by CYP1A2, CYP3A4, and other cytochrome P450 enzymes. Smoking may have an effect on the CYP enzymes, which are responsible for antipyrine metabolism, by increasing CYP activity and expression and shortening antipyrine  $t_{1/2}$ . A number of subjects in the (Cumming, 1976) study were using one or more of the following medications: aminophylline, diphenhydramine, diazepam, furosemide, allopurinol, acetaminophen, hydrochlorothiazide, and aminophylline. All of aminophylline, allopurinol, furosemide, and diazepam are CYP2E1 inhibitors and may inhibit antipyrine metabolism. Aminophylline may also induce CYP1A2 activity, whereas diazepam and furosemide induce CYP3A4 activity. Additionally, there may be a drug/drug interaction between these medications, for example. Diphenhydramine and furosemide may interact with diazepam and may enhance the sedative effect of diazepam. Furthermore, the number of subjects included was low and thus, our results might reflect small study effects. Two

## Chapter 3

studies (Li *et al.*, 2009; Zhang *et al.*, 2016) were carried out on Chinese male volunteers. It is unknown if the same findings would be seen in female or non-Chinese participants living at high elevations. Further clinical studies with larger sample sizes and different ethnicity are necessary to verify the conclusions of this study and provide more detailed recommendations.

Overall, under hypoxaemia, the analysis reveals impairment clearance within a limited sample of drugs that exhibit diverse ADME/PK characteristics. If these findings were to have more general applicability, then it could be envisaged that modifications in dosage regimens may be required guided by hypoxaemia status - this would be particularly true for drugs with a narrow therapeutic index.

**Chapter 4: Development of an in-vitro hepatocyte model to  
test the effect of hypoxia on CYP3A4 and CYP2C9**

## 4.1 Introduction

This chapter addresses the development of a hepatocyte model to be used in experiments exploring the impact of hypoxia on CYP450 levels and activity. The hepatocytes have relevance in terms of predicting intrinsic clearance ( $CL_{int}$ ) parameters for the pharmacokinetic simulation of total body clearance (CL) and first-pass metabolism (chapter 5) and for exploring mechanisms of hypoxia-induced changes in CYP450 levels and activity.

### 4.1.1 General overview of the liver

Two important blood vessels enter the liver, the hepatic portal vein and the hepatic artery. The hepatic portal vein carries nutrient rich blood from the small intestine while the hepatic artery carries oxygenated blood to the liver (**Figure 4.1 A**). Hepatocytes are the main parenchymal cells of the liver perfused with blood along the capillary spaces in the liver termed sinusoids. The large inter-cellular spaces between the sinusoidal (capillary) cells allow the hepatocytes to be in close contact with blood. The liver is organised into functional units called liver lobules which are separated by a sheet of connective tissue (Macswen *et al.*, 2002). The basal faces of adjoining hepatocytes possess inter-cellular junctional (tight junctional) complexes which surround channels termed canaliculi, which are the openings from the hepatocytes into the biliary system. Hepatocytes secrete metabolites, waste products, synthesised lipids and salts into the canaliculi which are either destined for excretion or utilisation in various biological processes. Bile is produced in the liver, secreted into the canaliculi for storage in the Gall bladder to then be later released into the intestine to aid digestion (**Figure 4.1 B**).

The liver is covered by a connective tissue capsule that acts as a support scaffold which branches and extends throughout the substance of the liver and covers the afferent blood vessels, lymphatic vessels and bile ducts that pass through the liver. The directional flow of mixed oxygenated and deoxygenated blood towards the central vein of the hepatic lobule creates a physiological oxygen gradient from the periportal to the perivenular areas of the parenchyma, with an oxygen pressure of 60-65 mmHg to 30-35 mmHg, respectively. Accordingly, the intracellular  $PO_2$  is about 15 mmHg lower, i.e. 45–50 mmHg in periportal cells and 15–20 mmHg in perivenous cells (Ungermann and Kietzmann, 2000). The periportal zone is less affected by small changes in oxygen levels during hypoxia since it has the maximum oxygen supply. In contrast the

perivenous zone receiving a more reduced level of oxygenated blood is more vulnerable to hypoxia-induced injury. This greater susceptibility in hypoxic conditions can impair the metabolic activity of the perivenous zone resulting in reduced protein synthesis, lipid metabolism, and bile production (Ungermann and Kietzmann, 2000; Cao *et al.*, 2014). Prolonged hypoxia in the perivenous or periportal zone can cause lipid peroxidation and cell death in severe cases (De Groot *et al.*, 1988; Anundi and De Groot, 1989).

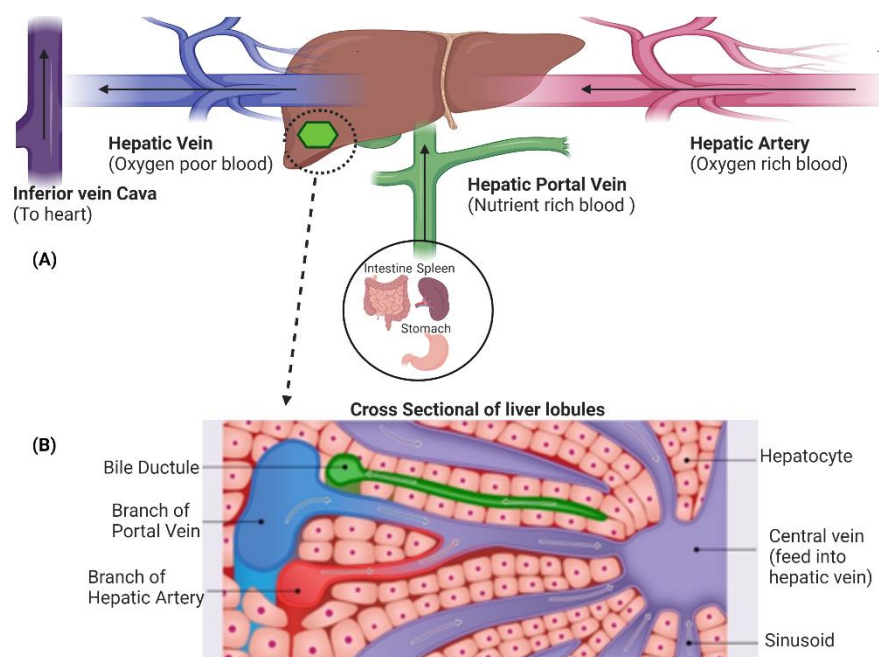


**Figure 4.1 Blood flow and structural organisation of the liver.** **Fig. 4.1A** the hepatic artery supplies the liver with about 25-30% of oxygenated blood while the hepatic vein transfers about 70-75% of blood with nutrients from the gastrointestinal system. After passing through the liver, the unoxygenated blood is conducted from the liver through the hepatic vein to the heart. **Fig. 4.1B** represents the structure of the functional unit of the liver, i.e. the hepatic lobules.

There are abundant studies that have used isolated hepatocytes and other cell types to study drug metabolism and CYP450 activity. This is reviewed in chapter 1 (section 1.5.1.6.). The evidence for how hypoxia impacts expression can sometimes be contradictory. As some further examples only offer such contradictory evidence: In an experiment involving the in-vitro incubation of hepatocytes from healthy rabbits exposed to the halogenated chemical phosgene ( $\text{COCl}_2$ ), which chemically mimics hypoxia, or when exposed in-vitro for 24 h to serum from rabbits experiencing hypoxemia ( $\text{PaO}_2$   $34 \pm 1$  mm Hg), increases in the expression of CYP3A6 and the



hypoxia marker HIF-1 $\alpha$  were observed (Fradette and Souich, 2004). In contrast, in highly differentiated human hepatoma HepaRG cells cultured for 24 h under severe hypoxic conditions (1% O<sub>2</sub>) the genes for CYP3A4, CYP1A2, CYP2E1 and CYP2C9, have been reported to be down-regulated (Shin *et al.*, 2018). It has been observed that in this hepatocyte cell line the activation of HIF-1 $\alpha$  occurs at oxygen concentrations between 0% and 1% (Doege *et al.*, 2005). Away from hepatocytes, in human endothelial and smooth muscle vascular cells, hypoxia (1% O<sub>2</sub> for 24 h) induced the up-regulation of CYP2C8 and CYP2C9 which in turn increased epoxyeicosatrienoic acid (EET) synthesis, eliciting vasodilation (Michaelis *et al.*, 2005). In bovine vascular endothelial cells (predominantly in the heart) hypoxia down-regulated CYP2J2, and decreased epoxidation of arachidonic acid to EET and as a consequence has a role in hypoxia increasing the risk of coronary events (Yang *et al.*, 2001).

#### 4.1.2 In-vitro metabolism models

In addition to whole animal experimentation, in-vitro models for ADME investigations are typically categorised into four main models: organ-/tissue-based; isolated cell-based (primary cultures, cell lines and iPSC); subcellular fractions-based (e.g., S9, cytosol and microsome); and isolated enzyme-based (purified and recombinant enzymes). **Figure 4.2** shows the balance of complexity, ease of application, ethical challenge, and the relative model comparability to the *in vivo* phenotypes (animals and human) for three of these commonly used model categories.

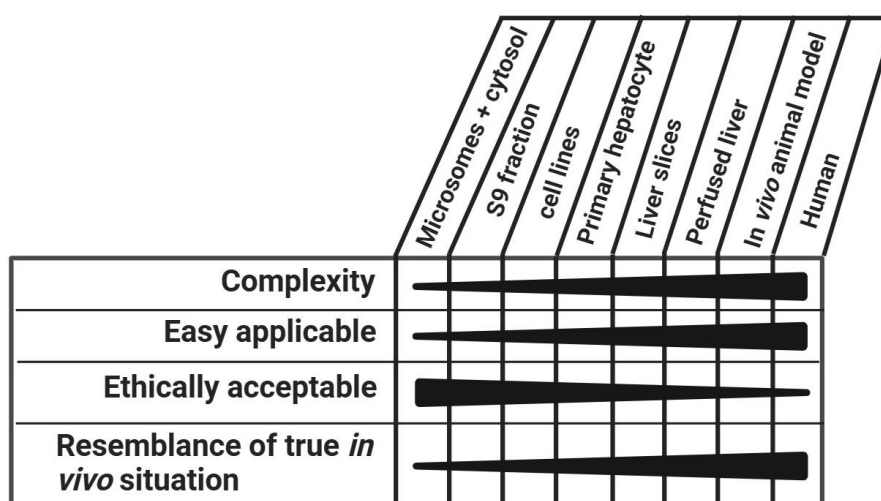


**Figure 4.2** Simple *in vitro* to more complex *in vivo* models to study drug metabolism. Adapted from (Brandon *et al.*, 2003).

#### **4.1.2.1 Organ-/tissue-level models**

The perfused organ can represent an in-vitro model close to the in vivo tissue. Within limits of tissue viability outside the intact organism, an isolated organ retains the complexity of tissue architecture although perfusion of the organ will inevitably be different in terms of the flow and pressure of the circulating media, as well as the autoregulation of vessel patency within the organ and the O<sub>2</sub> transfer capacity of the media used – noting some models have been perfused using whole blood. Organ models have greatest value outside the in-vivo situation when used for generating quantitative data on ADME. They can more directly relate to the in-vivo situation as well as offering some advantage for mechanistic studies. However, ethical issues appropriately relate to the use of animals as a source for organ/tissue models.

Tissue slices prepared from intact organs also retain much of the tissue architecture in so far as most of the cellular interactions within the tissue itself but lacking blood cell interactions. Perfusion is not present and the interstitial space will be compromised as a result. Oxygen and solute delivery to the cells within the tissue will in the tissue slice depend upon diffusional processes from the media into the tissue, parts of which will be deep-lying and where there will exist significant oxygen gradients from superficial to deeper parts of the section. Like the organ model, liver slices retain differentiated phenotype of hepatocytes and are utilised in metabolism and toxicological studies. The tissue slices retain both phase I and phase II enzymes and provide the potential for drugs to undergo a range of possible metabolic reactions.

Additional drawbacks of organ or tissue-slice based models include the labour-intensive nature of the preparation, a short viability period (for the organ – hours; for the slices - days), and for the slices in particular the damage to the cells on the outer edge of the slice is likely to result in inflammation and biotransformation impairment. The liver slice is infrequently used in drug metabolism studies (Brandon *et al.*, 2003; Parmentier *et al.*, 2007).

#### **4.1.2.2 Primary cell cultures, cell lines and iPSCs**

Primary cultured hepatocytes are a valuable model for xenobiotic metabolism studies and are competent in expressing both phase I and phase II metabolic enzymes. The model and metabolic profile enables drug metabolism investigations at quantitative and mechanistic levels that can be comparable to the in-vivo system (Ponsoda *et al.*, 2001).

However, the use of primary human cells in routine investigations is challenging due to the scarcity of human liver material, the high batch-to-batch functional variability, and potential phenotypic instability in-vitro even while it remains a primary culture (Brandon *et al.*, 2003).

An alternative cell-based model involves the use of hepatoma cell lines (derived from hepatocellular carcinomas) and recombinant immortalised hepatocyte cell lines. Both offer infinite cell replication with the possibility for phenotypic stability, although the immortalisation process itself can compromise a range of cellular functions. In both models, the interpretation of data is hindered by reduced (in some cases very minimal) expression of major CYP450 enzymes (Donato *et al.*, 2008).

**Table 4.1** presents the mRNA expression of various hepatoma cells compared to primary human hepatocytes. The cell lines in Table 4.1 were selected because they are the most often utilised cell types in metabolic studies with also data on mRNA expression in comparison to primary hepatocytes published. The data comes from a range of laboratories but with all investigations using the quantitative technique of SYBER green with qRT-PCR. For summarising data in Table 4.1 where multiple studies reported the expression of the same gene of interest, the average value of RNA expression was determined and shown; this is especially seen for the HepG2 cell line where more than a single reference was employed.

The **HepG2** cell line shows a lack of functional expression in almost all relevant CYP450 isoenzymes (Rodriguez-Antona *et al.*, 2002; Wilkening, Stahl and Bader, 2003). The authors reporting also the protein content and activity of most CYP450 isoenzymes were undetectable, and only very sensitive techniques such as qRT-PCR could detect and quantify the transcription levels of the respective genes (Rodriguez-Antona *et al.*, 2002). **BC2** is a human hepatocarcinoma-derived cell line. In a differentiated form, the cells express a number of relevant CYP450 isozymes at mRNA level (CYP1A2, 2A6, 2B6, 2C9, 2E1, and 3A4) (Donato *et al.*, 2008). **MZ-Hep1**, is a human hepatocellular carcinoma cell line, which like BC2 shows negligible levels of drug-metabolising enzymes and does not represent a viable alternative to primary hepatocytes (Rodriguez-Antona *et al.*, 2002). The hepatoma cell line, **HepaRG**, (Aninat *et al.*, 2006) has been shown to have a higher degree of similarity with primary hepatocytes in terms of morphology, genotypic profiles for metabolising enzymes

(phase I and II), and transporters, and also in nuclear receptors (AhR, PXR, CAR, PPAR- $\alpha$ ). HepaRG represents a reliable alternative to human hepatocytes for drug metabolism and toxicity studies.

**Table 4.1 Comparative expression of CYP450 isoenzymes in primary human hepatocytes and hepatoma cell lines.**

CYP450 enzymes	Hepatocyte models				
	Primary Hepatocyte	HepG2	MZ-Hep-1	BC2	HepaRG
<b>CYP1A1</b>	100	6.99	1.37	-	9.1
<b>CYP1A2</b>	100	0.03	0.03	0.01	-
<b>CYP2A6</b>	100	0.25	0.25	0.05	-
<b>CYP2B6</b>	100	0.50	0.09	0.16	34.6
<b>CYP2C9</b>	100	0.01	0.003	0.02	34.7
<b>CYP2C19</b>	100	0.05	0.05	0.07	-
<b>CYP2D6</b>	100	1.57	0.011	< 0.01	0.8
<b>CYP2E1</b>	100	0.04	0.006	0.07	3.5
<b>CYP3A4</b>	100	0.03	0.003	0.28	176
<b>CYP3A5</b>	100	1.16	0.03	2.49	-
<b>Key reference sources corresponding to cell model comparison</b>	-	(Rodriguez-Antona <i>et al.</i> , 2002; Wilkening, Stahl and Bader, 2003)	(Rodriguez-Antona <i>et al.</i> , 2002)	(Donato <i>et al.</i> , 2008)	(Aninat <i>et al.</i> , 2006)

\*Results are mean values of mRNA level expressed as a percentage (%) compared to primary hepatocytes.

Of note is advance in cell culture over recent decades with many more studies now using three-dimensional (3D) format. Much of the published information on the hepatocyte cell culture experiments have been undertaken in 2D-culture. While the 2D model provides some cell-cell contact it doesn't represent the extent of hepatocyte-hepatocyte cell-cell interactions seen in the intact tissue. The culture of hepatocytes in a 3D format may more closely resemble such interactions with likely impact upon gene expression (Berthiaume *et al.*, 1996). It is known that hepatocytes cultured in stirred bioreactors as 3D cultures produce tissue-like structures and maintain their liver-specific functions for a longer culture period and at a higher level than when cultured

in a 2D format (Leite *et al.*, 2011; Tostões *et al.*, 2012). The HepaRG cells as used in this Chapter were grown as 3D hepatocyte spheres.

Stem cells, specifically patient-derived pluripotent stem cells (iPSCs) obtained from various somatic cell types, have become a crucial resource for researchers exploring the regulatory mechanisms involved in hepatic development, the foundations of congenital diseases, and the intricacies of drug metabolism and toxicity. Hepatocytes derived from iPSCs offer a stable and easily accessible cell source, replacing the need for human primary hepatocytes or hepatoma cell lines in various applications. These applications include the investigation of issues related to lipid metabolism, protein accumulation, mitochondrial defects, and toxicity screening. It is important to note, however, that current differentiation protocols have not yet achieved hepatocytes that functionally match primary human liver cells, particularly concerning the expression of CYP450 enzymes crucial for drug metabolism. Nevertheless, newer differentiation methods, such as 3D co-culture of iPSC hepatocytes with cells from different lineages (e.g., hepatic endoderm and endothelial cells), show promise in improving hepatocyte metabolic function to more closely resemble the physiological characteristics of liver hepatocytes (Corbett & Duncan, 2019).

Variations in drug metabolism and transportation have been identified among different populations, indicating significant implications for inter-population differences in drug pharmacokinetics. These distinctions can be simulated in engineered cellular systems that incorporate cells derived from induced pluripotent stem cells (iPSCs), reflecting the genetic makeup of specific populations. Apart from facilitating population-specific investigations, iPSC hepatocytes can also manifest disease-causing mutations or conditions influencing hepatic drug clearance. Changes in metabolic induction may be linked to genetic factors, exemplified by instances such as rifampicin induction when P-glycoprotein is downregulated or CYP1A1 inducibility affected by mutations in the aromatic hydrocarbon receptor, a regulator of CYP enzymes alongside other transcription factors. However, the activity induction of enzymes like CYP3A4, CYP1A2, and CYP2C9 in iPSC hepatocytes is generally lower compared to primary hepatocytes (Dame & Ribeiro, 2021).

### 4.1.2.3 Subcellular fractions

Subcellular fractions are derived from centrifugation of tissue homogenates. Typically, centrifugation at ca. 9000 xg results in a liver S9 fraction (containing both microsomal and cytosolic fractions). The liver S9 fraction containing both microsomal and cytosolic fractions allows for availability of both phase I and phase II enzymes, including their cofactors. Clearly the cell structure and plasma membrane barrier and associated membrane transporters of the hepatocyte are lost. Ultracentrifugation at ca. 100,000 xg delivers a liver microsomal preparation representing isolated vesicles of hepatocyte endoplasmic reticulum (Parmentier *et al.*, 2007). Microsomes contain both phase I enzymes, such as CYP450s and certain phase II enzymes i.e., UGT responsible for glucuronidation which is also a microsomal located enzyme (**Figure 4.3**) (Brandon *et al.*, 2003).

Liver microsomes (membrane vesicles of the hepatocyte endoplasmic reticulum) contain membrane phase I enzymes, namely CYP450s, flavine-containing monooxygenases (FMO), esterases, amidases, and epoxide hydrolases, and phase II enzymes such as UGTs (**Figure 4.3**) (Parmentier *et al.*, 2007). The S9 fraction has lower enzyme activities compared to microsomes (Brandon *et al.*, 2003) but nevertheless, both the liver S9 and microsome fractions have been heavily exploited in drug metabolism and drug-drug interaction studies.

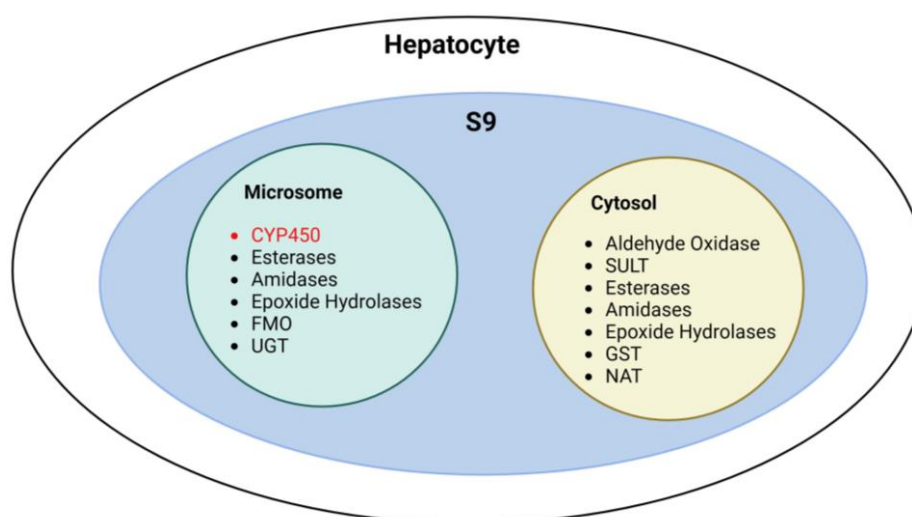


**Figure 4.3 Metabolic enzymes in subcellular S9 fraction.** (FMO); Flavin Monooxygenases, (UGT); Uridine Glucuronide Transferase, (SULT); Sulfotransferase, (GST); glutathione S-Transferases, (NAT); N-Acetyltransferases.

#### 4.1.2.4 Isolated Enzymes

Microsomes containing specific individual human CYP450s and UGTs have long been extremely important methodological options for in-vitro drug biotransformation studies (Brandon *et al.*, 2003; Venkatakrishnan *et al.*, 2005; Knoche *et al.*, 2022). With recombinant DNA technology a variety of recombinant expression systems have been developed, including insect, bacterial, yeast, and mammalian models, which have allowed for both transient and stable expression of isolated and catalytically active CYP450s (Friedberg *et al.*, 1999; Hiratsuka, 2012; Shang *et al.*, 2023). This provided investigators with the ability to study a single specific human CYP450 or UGT isoenzyme. While this presented a significant advantage in some aspects, particularly qualitatively, e.g. identifying if a single enzyme has capacity to metabolise a given molecule and in developing structure-activity relationships (SAR), an obvious drawback is the single enzyme model's functional predictability to the intact cell, let alone organ-level model. For example, any quantitative measures derived from a single enzyme will lack the context of how a drug would be handled faced with multiple simultaneous metabolic pathways. There clearly is the potential for over- or even under-estimation of the metabolic biotransformation (Brandon *et al.*, 2003). An approach where individual human CYP450s are reconstituted into a phenotypic 'cocktail' of enzymes, even with transporters, e.g., P-gp, has developed over the last 10-20 years (Darnaud *et al.*, 2023).

### 4.1.3 Aim and Objectives

#### Aim:

This chapter aims to characterise a hepatocyte cell model to study the effect of acute hypoxia on drug metabolism with the information gained to be later utilised in further mechanistic and quantitative studies in this thesis.

The work is focused on CYP3A4 and CYP2C9 isoforms as they are responsible for the metabolism of sildenafil which is the model drug approved for this PhD's work in the original clinical trial planned and prepared for pre-COVID and which has subsequently transformed here into work involving computational PK-PD simulations (Chapter 5). The clinical trial, while not, a part of this substantive component of this thesis, is nevertheless still to be undertaken, with the thesis work informing the design.

**Objectives:**

- 1. Characterise an in-vitro human hepatocyte model that expresses functional levels of CYP3A4 and CYP2C9 allowing for mechanistic investigations and also for data generation for pharmacokinetic predictive simulations.**

The cell model work to involve:

- Two-dimensional (2D) cell culture of HepG2 and HepaRG cells under normoxic conditions (21% O<sub>2</sub>)
- Three-dimensional (3D) cell culture of HepaRG under normoxic conditions (21% O<sub>2</sub>) and confirmation of the differentiation of the HepaRG cells and their structural arrangement in 3D culture as well as the resulting live-/dead-cell ratio (reflecting a potential ‘necrotic core’).

- 2. Investigate the effect of hypoxia on the functional expression of CYP3A4 and CYP2C9.**

The cell model work to involve:

- 2D and 3D cell culture HepaRG under normoxic vs hypoxic conditions (1% O<sub>2</sub>).
- Quantification of CYP3A4/CYP2C9 expression (mRNA, protein) and functional enzyme activity (substrate turnover).

In addition, as part of early studies not explicitly involving CYP450, the work explored the impact of hypoxia on ABC efflux transporters. Here both HepG2 and Caco2 cells were cultured in 2D under normoxic (21% O<sub>2</sub>) or hypoxic (1% O<sub>2</sub>) conditions. The functional expression of ABC transporters (P-glycoprotein, BCRP and MDR-1) under the above conditions were explored.

## **4.2 Material and Methods**

### **4.2.1 Cell culture**

#### **4.2.1.1 Two-dimensional (2D) monolayer**

Human hepatocellular carcinoma cells (HepG2) and undifferentiated HepaRG cells and Caco2 cells were grown as described in **Chapter 2, sections 2.1.1, 2.1.2 and 2.1.3**, respectively. Hypoxic conditions were achieved by incubating cells in a hypoxia



chamber (Baker Ruskinn PhO2x box) with 5% CO<sub>2</sub> and 1% O<sub>2</sub> balanced with N<sub>2</sub> at 37°C.

#### 4.2.1.2 Three-dimensional (3D) cultures and cell treatments

After expansion and full differentiation in 2D monolayers, HepaRG cells were trypsinised, counted, and seeded at 1000 cells per well onto 96-well round bottom ultra-low attachment (ULA) plates (Corning) (**Figure 4.4**). Growth media (free from DMSO) was then used, and the cells were allowed to aggregate and form a sphere for ten days. On day ten (Day 40 in Figure 4.4) spheroids were treated for 72 h with either CYP3A4/2C9 enzyme inducer 25 µM rifampicin or CYP3A4 enzyme inhibitor 1 µM ketoconazole (all from Sigma Aldrich) (**Figure 4.4**). All treatments were dissolved in DMSO to prepare a stock solution, and then the required treatment concentrations were prepared by diluting the stock solution into a growth media.

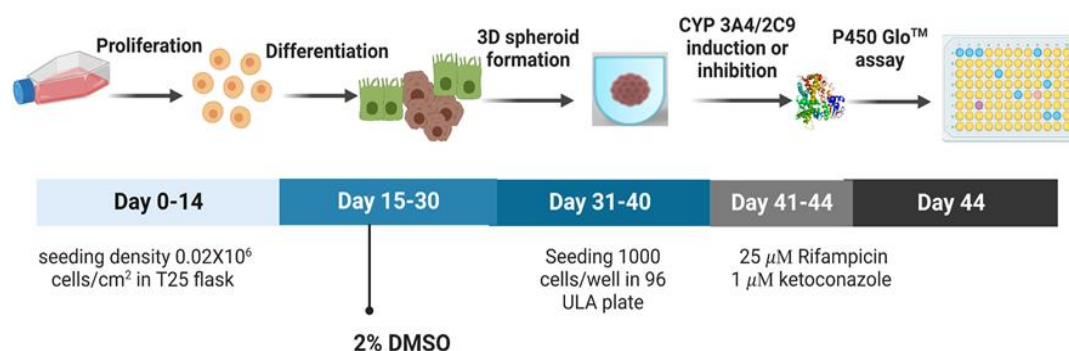


**Figure 4.4 Schematic protocol for HepaRG differentiation and spheroid formation.** HepaRG cells were seeded at a density of  $0.02 \times 10^6$  cells/cm<sup>2</sup> as a 2D monolayer and grown for two weeks. The growth media was then supplemented with 2% DMSO for 15 days to differentiate the cells into hepatocyte and biliary cells. On day 31, the differentiated cells were trypsinized and seeded at a density of 1000 cells/well in ultra-low attachment (ULA) plates to form spheroids. Subsequently, the spheroids were treated with rifampicin to induce the expression of CYP3A4 and CYP2C9, or with ketoconazole as a competitive inhibitor of CYP3A4. The cell spheroids were subjected to the P450 GLO™ assay for measuring functional CYP450 activity.

#### 4.2.2 Live/dead staining and viability assay

After spheroid formation (see **Figure 4.4**, day 40), the spheroids were stained with a mixture of two dyes: 1M calcein-AM (from InVitrogen) and 1 mg/mL propidium iodide (PI) (from Sigma Aldrich) as per the protocol described in **Chapter 2 section 2.2.1**.

For differentiated HepaRG cells grown in 2D monolayer format, the effect of hypoxia, rifampicin and ketoconazole treatment on cell viability were tested using CellTiter Glo assay as per the protocol described in **Chapter 2 section 2.3.2**.

### **4.2.3 CYP3A4 and CYP2C9 expression**

For the functional expression of CYP450s a bioluminescent assay was undertaken. This involved the seeding of a 2D monolayer of undifferentiated HepaRG cells in white-walled collagen-coated culture plates with clear bottoms (BioCoat® 96-well plates, Corning) at a density of 9000 cells/well. After two weeks the media was changed to differentiation media and kept in the culture for another two weeks. In order to induce the expression of CYP3A4 and CYP2C9 enzymes, the cells were treated with either 25 µM rifampicin for 72 h or just the vehicle (0.02% DMSO). In 3D model, HepaRG spheroids was cultured and treated as stated in section 4.2.1.2. The CYP activity were measured in HepaRG cultured in 2D monolayer or in 3D format using P450-Glo™ assays (Promega, UK). Two luminogenic substrates were used, Luciferin-IPA and Luciferin-H to measure the CYP3A4 and CYP2C9 enzymes activity, respectively. The detailed protocol was described in **Chapter 2 section 2.3.1**.

Expression levels as judged by immunofluorescence microscopy were undertaken in the HepaRG cells cultured at a density of  $0.2 \times 10^6$  cells/well on 35 mm glass bottom microwell dishes combined with coverslips (P35G-1.5-14-C, Mat Tek). The immunofluorescent microscopy was performed as described in **Chapter 2, section 2.2.2**. The coverslips were coated with collagen to improve cell attachment. After cells differentiation, the media was aspirated from the wells and the cells were gently washed with PBS at room temperature.

### **4.2.4 Isolation of RNA and quantitative real-time reverse transcription PCR (qRT-PCR)**

Total RNA from Caco2, HepG2 and HepaRG (either cultured as 2D monolayer or 3D spheroid) was isolated using a RNeasy system (QIAGEN) and was determined by measuring the absorbance of the RNA at 260 nm. All RNA samples had A260/A280 ratios higher than 1.8, indicating purity. The RNA was then reverse transcribed into cDNA, as described in **Chapter 2, section 2.4.2**.

Doublex TaqMan gene expression assay was used for HepaRG 3-D spheroids due to the limited number of spheroids and extracted RNA. The gene expression assay kits used, and qRT-PCR methodology are described in detail in **Chapter 2, section 2.4.4 and section 2.4.5**.

### **4.2.5 Protein extraction and Western blot**

The HepG2 and HepaRG cells cultured as 2D monolayer were trypsinised and collected in a 15 mL centrifuge tube. The lysis buffer master mix was prepared by added 10 µl of EDTA and 10 µl of Protease and Phosphatase Inhibitors to 980 µl of lysis buffer (RIPA, Thermo Fisher). Protein extraction, western blot, and related antibodies were illustrated in **Chapter 2 sections 2.5**.

### **4.2.6 Rhodamine 6G and Hoechst 33342 accumulation assay**

Two fluorescent dyes were used to evaluate the activity of the efflux transporters P-gp and BCRP under hypoxia: Rhodamine 6G, a substrate for P-gp, and Hoechst, a substrate for BCRP. Caco2 cells were seeded at a density of  $3 \times 10^4/\text{cm}^2$  in 12-well plates and grown for 21 days to achieve differentiation. HepG2 cells were seeded at a density of  $5 \times 10^5$  cells/mL and grown for seven days. Cells were then incubated in a hypoxia chamber (Baker Ruskinn PhO2x box) with 5% CO<sub>2</sub> and 1% O<sub>2</sub> balanced with N<sub>2</sub> at 37°C or kept in normoxia (21% O<sub>2</sub>, 5 % CO<sub>2</sub> at 37 °C). The accumulation assay is described in detail in **Chapter 2, section 2.3.3**.

### **4.2.7 Statistics**

All data analyses were carried out using GraphPad Prism 5 (GraphPad Software, San Diego, CA). All experiments were performed with three to 12 technical replicates from a minimum of three independent biological experiments. Results were expressed as mean  $\pm$  SEM. Comparisons between multiple groups were performed with one-way ANOVA followed by a post hoc test. If the data were not normally distributed, Kruskal-Wallis Test (nonparametric ANOVA) followed by Dunn's Multiple Comparisons Test was used. Samples with two groups only were compared using unpaired t-test. If the data were not normally distributed, Mann-Whitney U-test was used. P <0.05 was considered significant.

## 4.3 Results and Discussion

### 4.3.1 HepG2 cells as an in-vitro hepatocyte model: Studies under normoxia

The aim of this work was to characterise in the Cardiff laboratory a human in-vitro model to explore the effects of hypoxia on xenobiotic metabolism via CYP3A4 and CYP2C9 isoenzymes; which respectively account for 30% and 13% of hepatic metabolism of clinically used drugs (Zanger and Schwab, 2013). The characterised model to be later used in PK-PD simulations (Chapter 5) and mechanistic studies on the effects of hypoxia (Chapter 6). These particular CYP450 enzymes also metabolise sildenafil (a drug the PhD programme prior to Covid had identified to include in a clinical trial of the effects of hypoxia on PK-PD) converting it into the active metabolite N-desmethyl sildenafil.

HepG2 was the initial cell model explored. HepG2 is a human hepatoma cell line that has been commonly used as an in-vitro model to study drug metabolism (Cui *et al.*, 2016). Although HepG2 cells have relatively low basal CYP450 expression levels, they do appear to provide good inter-experimental consistency and avoid the disadvantages of primary human hepatocytes, which show high inter-individual donor variation and a rapid decline of metabolic enzyme expression with time in culture (Yokoyama *et al.*, 2018). Using standard light microscopy, the morphology of HepG2 cells illustrated in **Figure 4.5**.

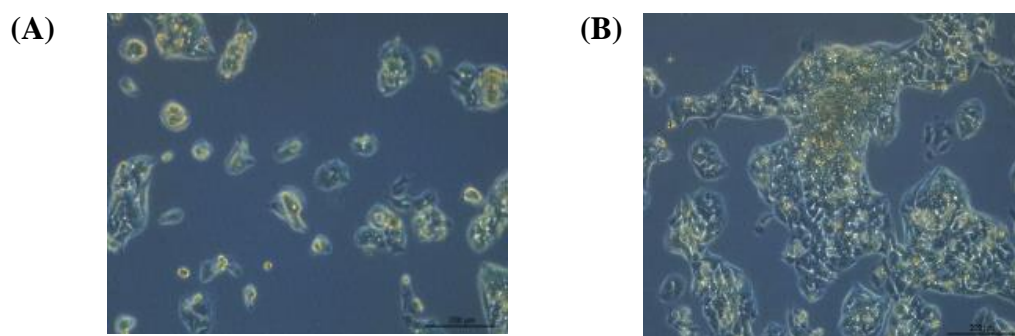


**Figure 4.5 HepG2 cell morphology.** The cells seeded at a density of  $5 \times 10^4$  cells/cm<sup>2</sup>. HepG2 grow as adherent, epithelial-like cell monolayers in small aggregates. **Fig. 4.5A** day 2 of culture cells initially attach in patches or small aggregates. **Fig. 4.5B** by day 5 of culture growth is extended across the attachment area with occasionally the cells forming multiple-layered aggregates. Images by phase contrast microscopy (x10 magnification). Scale bar 200  $\mu$ m.

The low CYP450s in HepG2 cells appears to be due to changes in transcriptional regulation, potentially reversible by co-transfection of hepatic transcription factors or pre-treatment with

chemical inducers (Rodriguez-Antona *et al.*, 2002). It is recognised that CYP450 enzymes can be induced in the HepG2 model by several drugs, for example, rifampicin (Maglich *et al.*, 2003; Chen *et al.*, 2004). Rifampicin is an agent used in mycobacterial and gram+ve infections, and which acts as an antibacterial via inhibition of DNA-dependent RNA polymerase. Its actions as an inducer are via its activation of the Pregnane X receptor (PXR), a member of the orphan nuclear receptor, which in turn mediates the induction of CYP3A4 and CYP2C9 (Maglich *et al.*, 2003; Chen *et al.*, 2004), as well as glucuronosyltransferases and p-glycoprotein activities. Confirming the effects of rifampicin in the HepG2 model ahead of further potential experimentation with this cell line, we found the HepG2 cells to express CYP3A4 and CYP2C9 transcripts under basal conditions (**Figure 4.6 C**) and when the cells were exposed to increased concentrations of rifampicin the expression of the CYP450 transcripts increases, with rifampicin pre-treatment inducing the expression of CYP3A4 mRNA by up to 3.7-fold, and CYP2C9 increased by up to 4.8-fold, when treated with 100  $\mu$ M rifampicin.

Cell lysates from HepG2 cells were also prepared for Western blot analyses. Under basal expression conditions, HepG2 cells failed to display a signal for CYP3A4 (**Figure 4.6 A**) and CYP2C9 (**Figure 4.6 B**). Even at the highest level of rifampicin pre-treatment (100  $\mu$ M), only a very faint signal was observed for CYP3A4 protein and an inconclusive signal for CYP2C9. This lack of protein expressions compared to the findings with the transcripts could arise due to post-transcriptional regulation, such as RNA splicing, RNA stability or transport, and translation efficiencies directly from what are likely low transcript levels. As for the lack of an obvious induction effect upon the CYP450 protein, this could be due to the time point at which the protein expression was studied was not sufficient to detect the increase in protein levels, for example CYP3A4 protein  $t_{1/2}$  is ca. three days on average. Here, at two days following rifampicin exposure the inductive impact of rifampicin would still be less than 50% of the ultimate increase if the sampling times were extended for 4-5 x  $t_{1/2}$ . Protein synthesis and degradation rates are dynamic processes, and it is possible that an increase in mRNA expression is followed by a delay in protein synthesis. The same Western blot conditions used here were also adopted for the HepaRG cell line where good signals were observed using similar protein loading.

While the 'low' CYP450 expression may be viewed as predictable from literature (see **Table 4.1**), exploring the use of this cell line was appropriate simply because of the potential ease of use it provides and the substantial literature available for comparison. However, even with

rifampicin treatments the lack of any meaningful impact on protein expression (and hence functional activity) limited the utility of HepG2 for future functional investigations.

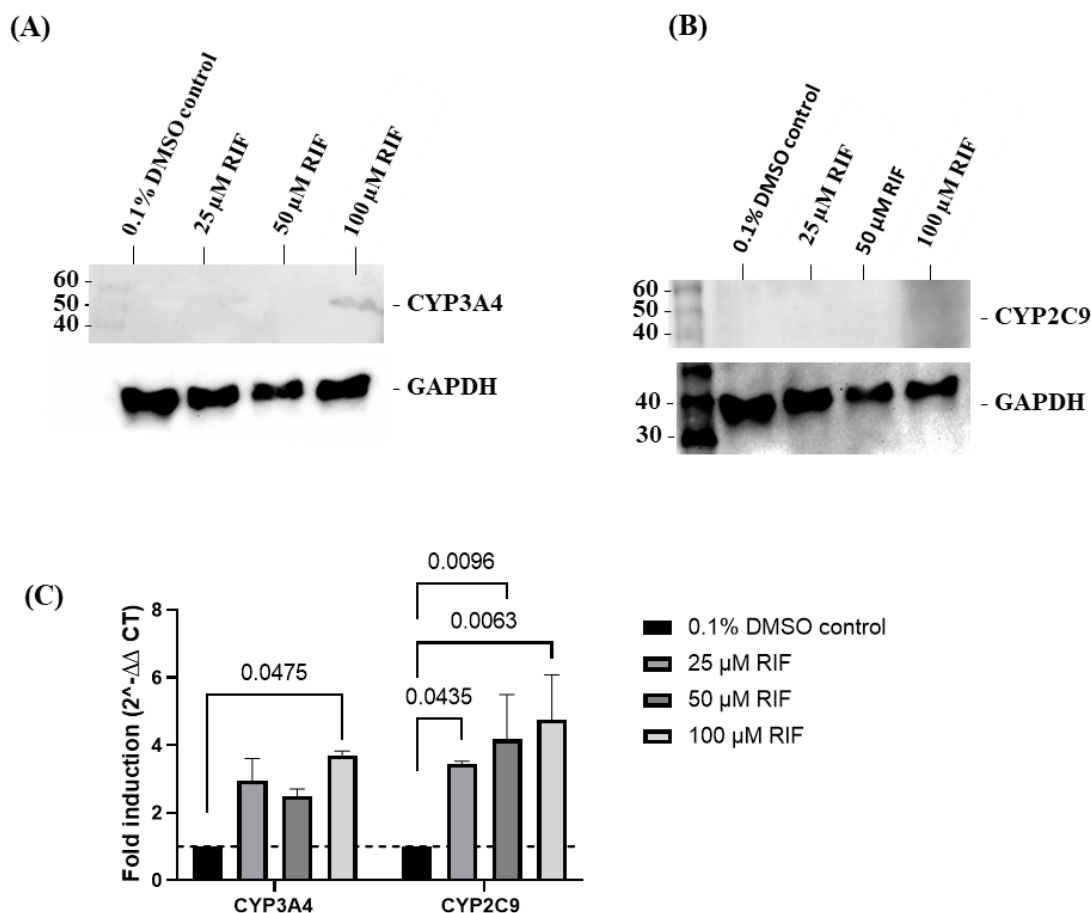


**Figure 4.6 Induction of CYP3A4 and CYP2C9 in HepG2 cells after 48 h.treatment with CYP450 inducer rifampicin (RIF) at 0 to 100 μM concentrations.** **Fig. 4.6A** and **Fig. 4.6B** show Western blots for CYP3A4 and CYP2C9, respectively with loading of 50 μg of extracted cell lysate protein separation by SDS-PAGE, electrotransfer to nitrocellulose membrane, and immunoblot with anti-CYP3A4 (50 kDa) and anti-CYP2C9 (55 kDa) antibodies. GAPDH (37 kDa) was used as an internal control for protein loading. **Fig. 4.6C** shows mRNA expression for CYP3A4 and CYP2C9 following RNA extraction, reverse transcription and 30ng loading of cDNA for qPCR analysis. Gene expression was normalised to the house-keeper gene (HPRT1) and then to the control (0.1 % DMSO)-treated cells. Bars represent mean ± SEM. N=3 independent experiments. One-way ANOVA with Bonferroni test.

### 4.3.2 HepaRG cells as an in-vitro hepatocyte model: Studies under normoxia

#### 4.3.2.1 HepaRG cells cultured in 2D monolayer format

HepaRG cells are being increasingly adopted as an alternative to HepG2 cells and primary human hepatocytes for preclinical hepatotoxicity and metabolic studies (Legendre *et al.*, 2009;

Andersson, 2017). The HepaRG human cell line was established from a tumour of a female patient with hepatocarcinoma. The HepaRG cell model provides a more consistent gene expression and to date is reported as phenotypically stable; it overcomes the donor variability seen with the use of primary human hepatocytes. When passaged at low density, the cells are reported to differentiate into both hepatocytes and biliary epithelial cells and are thus considered to have a progenitor or mixed progenitor phenotype(s) (Gripon *et al.*, 2002).

To show the differentiation of HepaRG cells into the two populations of hepatocyte cells and cholangiocyte cells, this work followed the literature and used two markers, albumin and cytokeratin 19 (CK19) for the respective cell types. These markers were selected as they have been initially reported as specific markers for hepatocytes and biliary cells (Marion, Hantz and Durantel, 2010; Gunness *et al.*, 2013; Higuchi *et al.*, 2016).

After four days of monolayer culture, HepaRG cells exhibited an epithelial morphology (**Figure 4.7 A**). In this culture format the cells were in the proliferative phase for approximately seven days after plating, reaching confluency by day 14 (**Figure 4.7 B**). At day 14, two morphologically distinct cell populations emerged: cholangiocyte-like cells - large and flat cells with a clear cytosol, a regular polygonal shape; and hepatocyte-like cells - smaller with a granular and dark cytosol, prominent nuclei and visible nucleoli. From day 14 the cultures were continued with media supplemented with 2% DMSO for a further two weeks – this supplementation triggering further differentiation. The mechanism by which DMSO induces the differentiation of tumour cells is poorly understood. DMSO stimulates albumin and  $\alpha$  - fetoprotein production in transformed hepatocytes and hepatocarcinoma cells (Higgins and Borenfreund, 1980; Su and Waxman, 2004) and aids in the maintenance of differentiated adult rat hepatocytes, as evidenced by the production of liver-specific plasma proteins, including consistent production and secretion of albumin at high levels (Su and Waxman, 2004). Clusters of hepatocyte-like cells appeared with the trend to organise into trabeculae-like (plate-like) hepatocellular structures which also displayed regions of bile canaliculi-like structures surrounded by some biliary-like cells (**Figure 4.7 C and D**). The presence of two morphologically distinct populations at the end of the differentiation period supporting evidence of the bidirectional differentiation process.

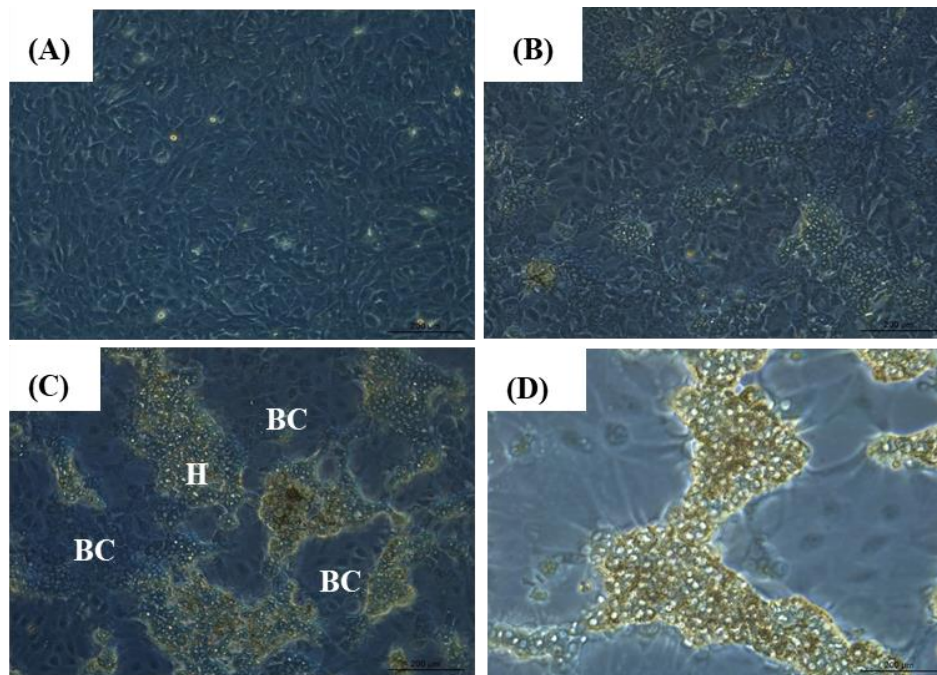


**Figure 4.7 Morphology of HepaRG cells.** Cells were imaged by phase-contrast microscopy (x10 magnification) at different stages of the culture: **Fig. 4.7A** proliferation phase (day 4); **Fig. 4.7B** confluence (day 14); and **Fig. 4.7C** and **Fig. 4.7D** differentiated phase day 30. showing HepaRG cells differentiated to either hepatocyte like cells (H) or biliary like cells (BC). Media was supplemented from day 15 with 2% DMSO to differentiate the cells. Scale bar 200  $\mu$ m.

The profile of a hepatocyte marker, albumin, and biliary cell marker, CK19, was assessed by immunofluorescent microscopy (**Figure 4.8.**). Cell-associated albumin was detected in all phases of the culture, (Days 4 -30, from the early proliferative phase through to the full differentiated stage) but the signal became stronger as the cells reached confluency on Day 14 (**Figure 4.8C**). By day 30 the clustering of hepatocyte-like cells was more evident and the presence of albumin was highly restricted to the hepatocyte clusters and was only faintly detected in biliary-like cells. It should be noted the albumin source in the media was bovine and not a source cross-reacting with the anti-albumin antibody.

The marker CK19 was again detected in all phases of culture. On days 4 and 14 of culture CK19 were detected (**Figure 4.8 B**; **Figure 4.8 C**) but by day 30 the CK19 expression was more intense and became concentrated in a specific area, surrounding the hepatocyte colonies (**Figure 4.8 D**) – this spatial separation is best seen with the merged images. This pattern is consistent with the HepaRG differentiating into two distinct cell populations - hepatocytes and biliary cells.



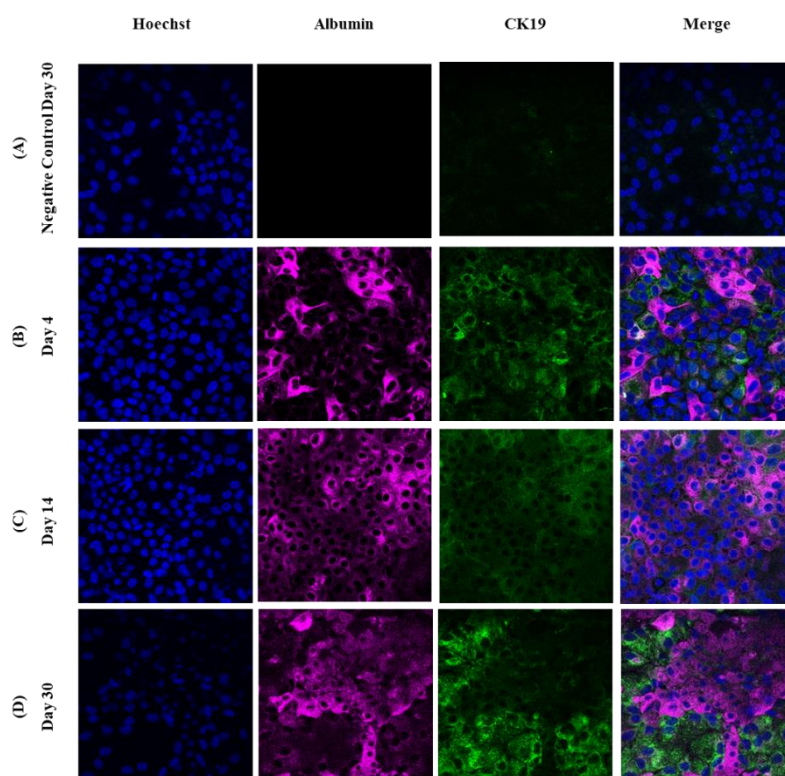


**Figure 4.8 Expression of hepatocyte and biliary cells specific marker on HepaRG cells.** The detection of hepatocyte (albumin +ve) and biliary cells (CK19 +ve) performed using immunofluorescent microscopy. Albumin and CK19 were detected in all phases of culture. Nuclei stained with Hoechst. **Fig. 4.8A** Negative control sample stained with only secondary antibodies. **Fig. 4.8B** Day 4 proliferation phase of culture. Albumin signal is already strong **Fig. 4.8C** Day 14 - cells approaching stationary phase of culture. **Fig. 4.8D** Day 30 the full differentiation state after cells cultured in a growth media supplemented with 2% DMSO. Cell rearrangement is evident occurs with signals for albumin and CK19 restricted in specific areas.

To assess the CYP450 expression status of the 3A4 and 2C9 isoforms - important for this current work - the RNA from HepaRG cultured cells in 2D monolayer (and for comparison from the HepG2) cells was extracted, and 30 ng of cDNA used for qPCR.

**Figures 4.9A and 4.9B** show, respectively, that CYP3A4 and CYP2C9 mRNA expression were considerably greater in HepaRG cells at basal conditions than in HepG2 cells. When HepaRG cells were treated with 25  $\mu$ M rifampicin, the expression of CYP3A4 and CYP2C9 increased ten-fold and five-fold, respectively, which contrasts with the lower responsiveness of the HepG2 to the inducer. The greater degree of differentiation in the HepaRG cells explain the higher (compared to HepG2) CYP450 expression levels.

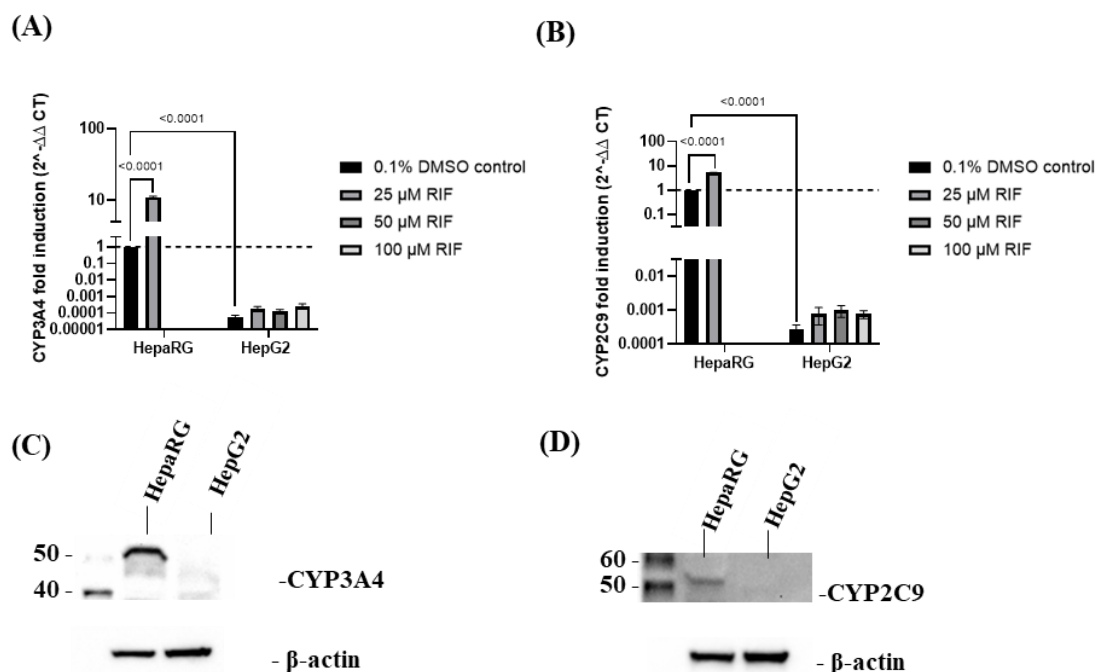


**Figure 4.9 Comparison between HepG2 and HepaRG CYP3A4 and CYP2C9 mRNA and protein expression.** RNA was extracted from four experimental groups of HepG2 cells: 0.1% DMSO vehicle control 25, 50, and 100 μM rifampicin (RIF) treatment for 48 h. RNA was extracted from two experimental groups of HepaRG cells: 0.1% DMSO vehicle control and 25 μM rifampicin treatment for 48 h. 30 ng of cDNA was used in qPCR experimentation **Fig. 4.9A** shows the expression of CYP3A4 mRNA in 0.1% DMSO vehicle control and rifampicin treated groups. **Fig. 4.9B** shows the expression of CYP2C9 mRNA in 0.1% DMSO vehicle control and rifampicin treated groups. The gene expression was normalised to the housekeeping gene (HPRT1) and then to the respective controls. Bars represent mean ± SEM. N=3 independent experiments. Statistics undertaken by One-way ANOVA followed by post-hoc Dunnett test. **Fig. 4.9C** and **Fig. 4.9D** represent Western blot analysis for CYP3A4 (50 kDa) and CYP2C9 (55 kDa). β-actin (42 kDa) as internal control for protein loading. Western blot images represent one of the three independent experiments with similar results.

Following HepaRG and HepG2 cell lysate preparation and loading of 50 μg total protein for Western blot analyses (**Figures 4.9C** and **Figure 4.9D**). The HepaRG cells displayed relative strong and consistent signals for the expression of both CYP3A4 and CYP2C9 seen as distinct bands corresponding to their designated molecular weights, 50 kDa and 55 kDa, respectively. In contrast, no visible band(s) was observed in the HepG2 cell line for either CYP3A4 or CYP2C9; although a much weaker band at 40 and 45 kDa was seen for CYP3A4. On the basis of CYP450 mRNA and protein expression data and responsiveness to rifampicin, the HepaRG cell line appeared to represent a more appropriate model to employ for this project's future investigations. The current findings appear to be consistent with previous research, which found that differentiated HepaRG cells express various cytochrome P450 enzymes (CYP450s) (e.g., CYP1A2, CYP2B6, CYP2C9, CYP2E1, and CYP3A4) at a higher level and exhibit other

metabolic functions (e.g. phase II enzymes and membrane transporters) normally found in the liver, all of which have supported HepaRG cells as a relevant model for primary human hepatocytes (Guillouzo *et al.*, 2007; Kanebratt and Andersson, 2008; Turpeinen *et al.*, 2009).

#### 4.3.2.2 HepaRG cells cultured in 3D format as spheroids.

HepaRG cells can grow to and survive as spheroids in culture. This has been described using various methods including hanging drops (Drewitz *et al.*, 2011), bioreactors (Leite *et al.*, 2012), functional polymers (Higuchi *et al.*, 2016) and ULA plates. In this current work the ULA plate method was chosen on the basis of ease and reproducibility of results (Gunness *et al.*, 2013). **Figure 4.10A** shows a scheme for HepaRG cell growth and differentiation to form a spheroid. Cells are initially grown as monolayers (with 2% DMSO differentiation between Day 15-30). On day 30 of culture, the differentiated HepaRG cells are then seeded at 1000 cells/ well into ULA plates with the progressive formation of a spheroid. **Figure 4.10B** shows images of spheroid formation monitored over 10 days (days 31-40). From day 33 to 35 onward individual cells appeared to aggregate into a compact spheroid structure which is very clearly formed by day 40 in culture.

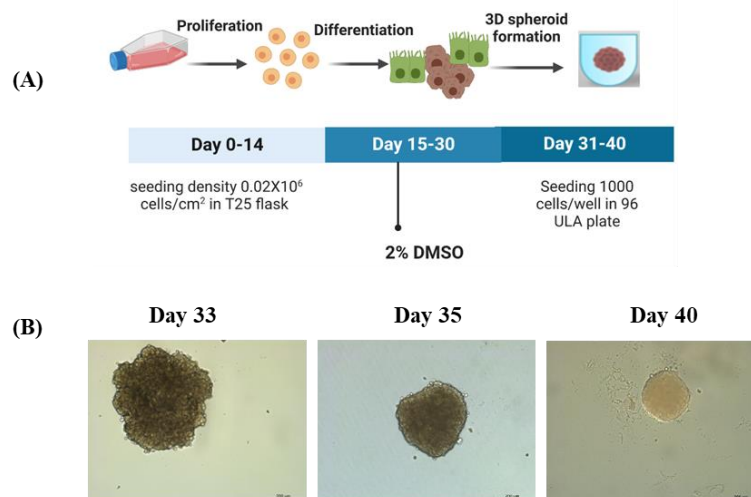


**Figure 4.10 Formation of 3D HepaRG spheroid.** **Fig. 4.10A** scheme of HepaRG cell growth. After cell differentiation at day 30 of culture the cells were trypsinised and seeded into ultra-low attachment (ULA) plates at density of 1000 cells/well. **Fig. 4.10B** spheroid formation was monitored over 10 days after seeding by light microscopy. By day 40 of ULA culture, a compact and spheroidal cell mass was observed. Scale bars represent 200 μm.

## Chapter 4

In spheroid culture, after prior differentiation in the monolayer format, the HepaRG cells do not proliferate and spheroid size is solely dependent upon the seeding density in the ULA plate and the forces that serve to cause cell aggregation. To explore different ULA plate seeding densities, HepaRG cells were plated at 1,000 to 50,000 cells / ULA well and allowed to aggregate for 10 days. The objective was to identify an optimal cell density that maximises cell number in a spheroid (e.g., for functional studies) without the spheroid displaying areas of necrosis from poor oxygen diffusion, particularly to the inner core of the spheroid.

Calcein-AM is a cell-permeable dye that is converted to fluorescent (green) calcein by intracellular esterase present within viable cells. PI is a cell non-permeable dye that stains DNA and which only enters cells when cell membrane integrity is disrupted, as in 'dead' cells. The live/dead analysis of the HepaRG spheroids is represented in **Fig. 4.11** and shows as cell seeding density increases and the spheroids become larger and there is an increase in the number of dead cells (red). This is seen most profoundly in the 50,000 cells seeding. Even at a density of 4,000 cell/well a necrotic core becomes evident. Most of the cells remain viable (green) in spheroids seeded at 1,000 and 2,000 cells/well.

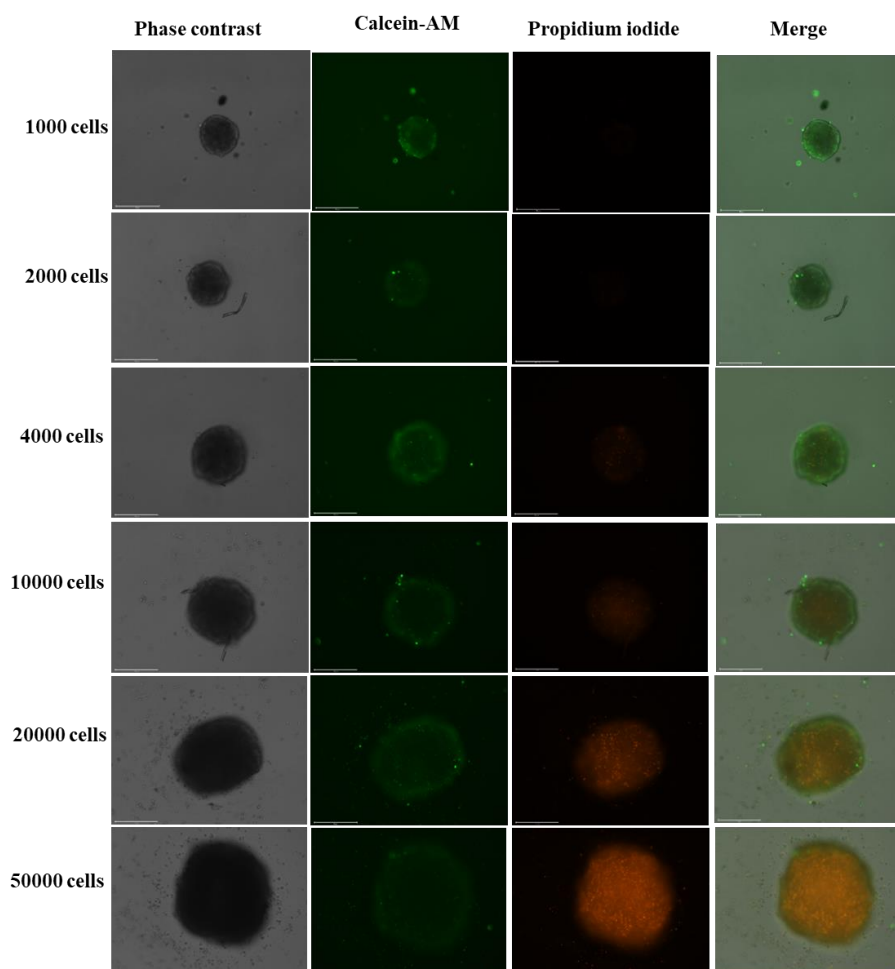


**Figure 4.11** Representative images of a developing ‘necrotic core’ in HepaRG cells with increases in ULA plate cell seeding densities. HepaRG cells were differentiated following the standard protocol. After cell differentiation at day 30 of culture, the cells were trypsinised and seeded into ultra-low attachment (ULA) plates to form spheroid at densities of 1000, 2000, 4000, 10000, 20000 and 50000 cells/ ULA well and kept to form spheroids for 10 days. On day 11 spheroids were incubated with a mixture of Calcein-AM to measure the live cells (green) and propidium iodide to measure dead cells and the generation of a necrotic core (red). Scale bar 275  $\mu\text{m}$ .

HepaRG spheroids grown to a diameter  $> 250 \mu\text{m}$  have been reported to display an hypoxic core (Ramaiahgari *et al.*, 2017). As the necrotic core of the HepaRG spheroids started to appear at a seeding density 4,000 cells/well, the focus was on the lower seeding densities and the size of spheroids when seeding at 1000 and 2000 cells/ ULA well; Here the spheroid size was measured at day 10 in ULA plates using ImageJ software. The mean diameter  $\pm$  SD of spheroid when seeding was at 1000 cells/well was  $237 \mu\text{m} \pm 22$ , while the mean diameter  $\pm$  SD of spheroid seeding at 2000 cells/well was  $309 \mu\text{m} \pm 34.7$  (**Figure 4.12**).

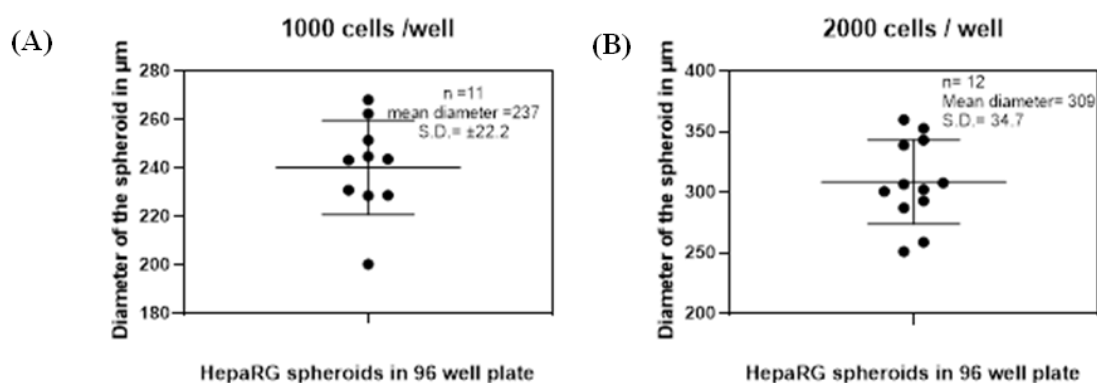


**Figure 4.12 Measurement of HepaRG 3D spheroid diameter after 10 days in ULA plate culture.** HepaRG cells were differentiated following the standard protocol. After cell differentiation at day 30 of culture, the cells were trypsinised and seeded into ultra-low attachment (ULA) plates to form spheroid at densities of 1000, 2000 cells/ ULA well and kept to form spheroids for 10 days. At day 11 spheroids diameters were measured by image j. **Fig. 4.12A** 1000 cells/well led to an average size of a spheroid of 237 μm. **Fig. 4.12B** 2000 cells/well led to average size of a spheroid of 309 μm.

The current work supports HepaRG cells cultured at 1000 cells/ ULA to form an organised reproducible spherical structure presenting minimal risk for compromising xenobiotic metabolism studies.

To determine the arrangement of the two cellular populations – hepatocyte and biliary cells - within the 3D spheroid model, HepaRG spheroids were fixed with 4% paraformaldehyde and stained with rabbit anti-albumin antibody and mouse anti-CK19 antibody. Confocal microscopy of the spheroids was performed using an inverted Leica TSC SP5 microscope equipped with x20 and x70 objective lens (reaching a maximum depth of ca. 36μm into the spheroid ‘tissue’); confocal analysis was undertaken across 23 Z-stacks with a Z-step size of 1.98 μm. **Figure 4.13** shows the signal for the biliary cell marker, CK19, increasing in intensity when moving through the depth of the spheroid (from 9.9 to 27.7 μm in depth) closer toward the spheroid interior, although this would still represent a comparative peripheral depth of field compared to the full diameter of the spheroid (ca 300 μm); the albumin signal remained of similar intensity across the Z-stack. Again, what is apparent is the distinct distribution of cell types within a given Z-stack (see merged channel), a feature retained in the 3D model as it was in the 2D model. This finding is agrees with Leite et al, who showed a similar pattern of hepatic and biliary cell arrangement in HepaRG spheroid model cultured using a spinner (Leite *et al.*, 2012).

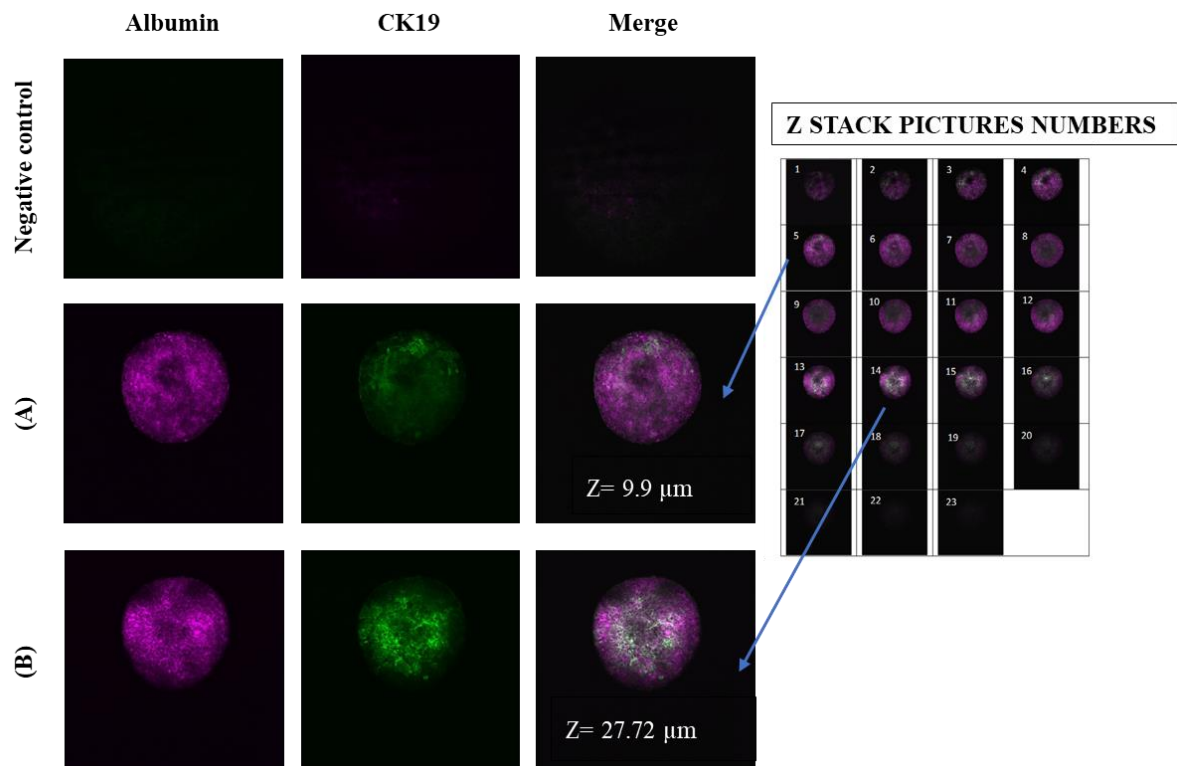


**Figure 4.13 Cell arrangement within HepaRG 3D culture. 23 Z-stack images taken (step size  $1.98 \mu\text{m}$ ) Immunofluorescence signals show two types of cell patterns.** HepaRG cells were differentiated following the standard protocol. After cell differentiation at day 30 of culture, the cells were trypsinised and seeded into ultra-low attachment (ULA) plates to form spheroid at densities of 2000 cells/ ULA well and kept to form spheroids for 10 days. On day 11 spheroids were fixed with 4% paraformaldehyde and stained with hepatocyte marker albumin (magenta) and with biliary cells marker CK 19 (green) antibodies. **Fig. 4.11A** images at a depth of  $9.9 \mu\text{m}$  into spheroid showing strong albumin signal. **Fig.4.11B** images taken at a of  $27.7 \mu\text{m}$  depth and showing increased CK19 signal. Albumin signal appearing to retain strength of signal as the imaging moved toward the interior of spheroid. The negative control sample was stained with only secondary antibodies anti-mouse AlexaFluor 488 and anti-rabbit AlexaFluor 546. The Insert show the precise Z-step used in the main Figure.

### 4.3.2.3 HepaRG cells: CYP3A4 and CYP2C9 functional expression in 2D monolayer vs 3D spheroid model

Still under normoxia conditions, a direct comparison of CYP450 functional expression was undertaken comparing the 2D monolayer format of differentiated HepaRG cells and the 3D spheroid model of differentiated HepaRG cells. In these experiments rifampicin (25  $\mu$ M for 72 h) was used as an enzyme inducer for both CYP3A4 and CYP2C9, and ketoconazole (1  $\mu$ M for 72 h) as a competitive inhibitor for CYP3A4 in particular. The viability of the HepaRG cells (at least in 2D format) was not altered by exposure to these interventions (**Figure 4.14**).

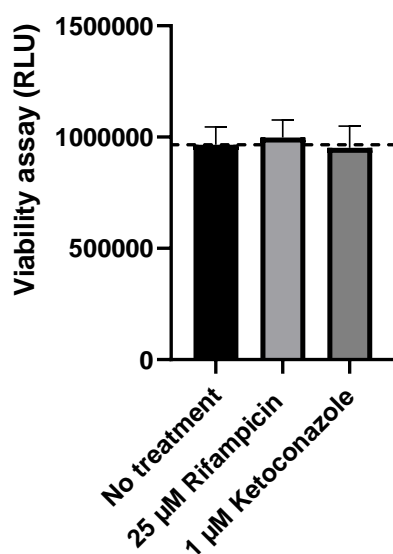


**Figure 4.14 Viability assay of rifampicin and ketoconazole treatment in HepaRG monolayer.** HepaRG cells were differentiated following the standard protocol. After differentiation cells were treated with 25  $\mu$ M of rifampicin or 1  $\mu$ M ketoconazole for 72 h and viability was determined by CellTiter Glo assay. Untreated cells were used as control. Statistics by one way ANOVA.

RNA was isolated from HepaRG cells grown either as 2D monolayers or 3D spheroids, with 30 ng of cDNA (qPCR) used to evaluate CYP3A4 and CYP2C9 gene transcript expression. **Figure 4.15** shows the expression of CYP3A4 and CYP2C9 transcripts to be significantly lower in the 3D spheroid model than in the 2D monolayer model. This dose reflects absolute lower level recorded in the 3D spheroid format as the data is referenced (internally controlled for) in both models against the house-keeping gene HPRT1. Therefore, explanations varying extraction efficiencies between the models are unlikely to be the explanation. One possibility is the absence of DMSO in the spheroid model at day 30 to 40. The DMSO if present during this time has detrimental impact upon cell viability (Appendix 3.1, Supplementary figure 3.1.1) and hence its absence from the protocols. However, it is also recognised to promote basal expression of CYP450 as reported by the Kanebratt and Andersson study where the expression



of several CYP450 enzymes including CYP3A4 considerably decreased within the first day after removal of DMSO from the culture medium, although thereafter levels were stable but remained low. reported for e.g., CYP1A, CYP2C, CYP2E1, and CYP3A4 (Kanebratt and Andersson, 2008).

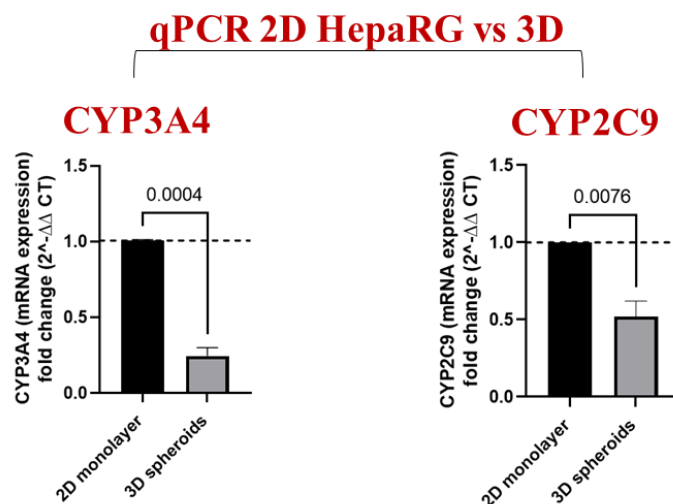


**Figure 4.15 CYP3A4 and CYP2C9 mRNA transcript gene expression in HepaRG cultured in 2D monolayer and 3D spheroid formats.** The gene expression was normalised to the house keeping gene (HPRT1) and then to the cells cultured in a 2D monolayer model. Bars represent mean  $\pm$  SEM. N=3 independent experiments. T-test was used for statistical analysis.

The P450-Glo<sup>TM</sup> substrate assay allows evaluation of the functional activities of CYP3A4 and CYP2C9. The assay uses luminescence generated from CYP450 isoenzyme-specific Luciferin derivatives as the luminogenic probes. **Figure 4.16** shows data for this functional assay for HepaRG cells when comparing the 2D and 3D format, and between the CYP3A4 and CYP2C9 isoforms.

In the HepaRG cells in 2D, as expected rifampicin significantly enhanced CYP3A4 functional activity and ketoconazole significantly decreased CYP3A4 -mediated turnover of the substrate (**Figure 4.16A**). The inductive effects of rifampicin on CYP2C9 were less clear, not achieving statistical difference compared to control. Similarly, ketoconazole had no significant effect on CYP2C9 in the 2D model, although a trend was present (**Figure 4.16B**). The above observations for the impact of competition with ketoconazole is consistent with the wider understanding with ketoconazole a well recognised competitive inhibitor for CYP3A4 which is the enzyme responsible for the production of the major ketoconazole metabolite. There is no

reported involvement of CYP2C9 in ketoconazole metabolism; this absence of an effect on CYP2C9 providing some further confirmation of the specificity of the luminogenic probes.

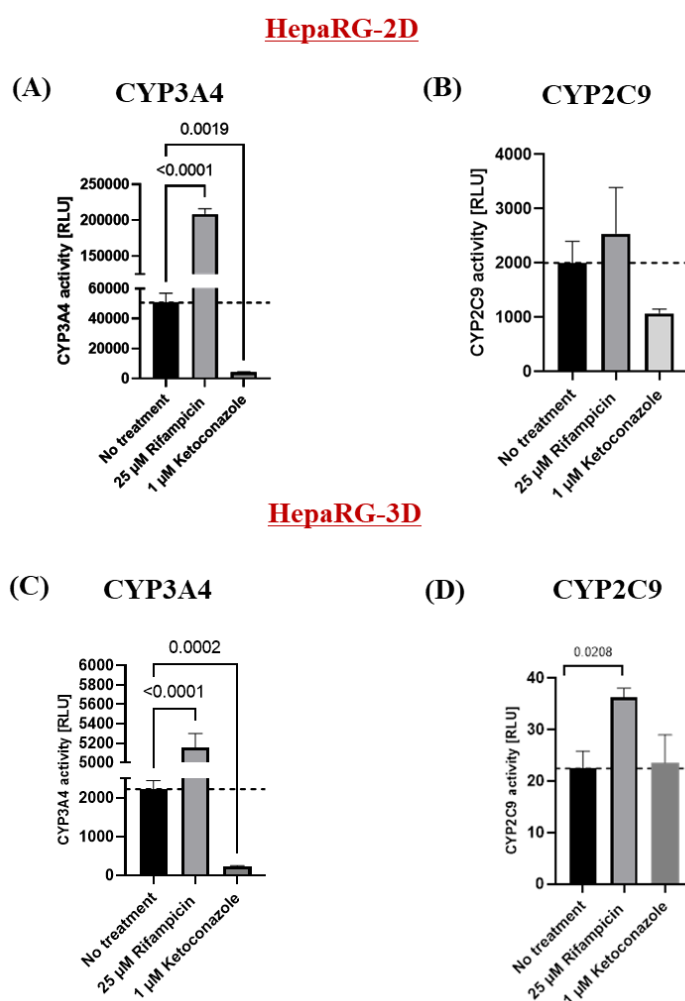


**Figure 4.16** CYP3A4 and CYP2C9 activity in HepaRG cultured as monolayer (2D) and in spheroid formats (3D). Data presented as relative luminescent unit (RLU). Activities measured using P450-Glo™ (Promega). Cells treated with enzyme inducer rifampicin or enzyme inhibitor ketoconazole and compared to no-treatment control. **Fig. 4.16A** and **Fig. 4.16B** shows CYP3A4 and CYP2C9 functional activity, respectively, in 2D monolayer HepaRG model. **Fig. 4.16C** and **Fig. 4.16D** show CYP3A4 and CYP2C9 activity, respectively, in 3D spheroid HepaRG model. All experiments were performed with three to ten technical replicates from three independent experiments. Bars represent mean  $\pm$  SEM. One way ANOVA and post-hoc Dunnett test used for statistical analysis.

Similarly, in the 3D spheroid model, ketoconazole had no effect upon CYP2C9 functional activity but significantly reduced the turnover of the CYP3A4 substrate. Rifampicin pre-treatment here significantly increased both CYP3A4 and CYP2C9 functional activity by approximately x2-fold, which for CYP3A4 is less than that seen for the 2D-model which saw increases of approximately x4-fold (**Figure 4.16C**, **Figure 4.16D**). This data shows the

applicability of the P450-Glo™ test and the appropriateness if necessary of 2D monolayer model at least in terms of CYP450 function and modulation.

### 4.3.3 HepaRG cells as an in-vitro hepatocyte model: Studies under hypoxia

#### 4.3.3.1 HepaRG cells: Effect of hypoxia (1 % O<sub>2</sub>) on CYP3A4 and CYP2C9 in 2D cell monolayer format

One of the objectives of this thesis (Chapter 6) was to investigate the mechanisms through which hypoxia alters CYP450 expression. Here, this section of work further supports the evidence for the use of the HepaRG cell model in this later context. Specifically, in this section the use of the HepaRG 2D monolayer format to study the effects of hypoxia (1% O<sub>2</sub>) on CYP3A4 and CYP2C9 activity.

HepaRG Cells in 2D monolayer format were subjected to hypoxia (1% O<sub>2</sub>) for 4, 6, and 24 h, and cell viability assessed using a CellTiter-Glo luminescent assay. The viability of the HepaRG cells (at least in 2D format) was not altered by exposure to hypoxia (**Figure 4.17**).

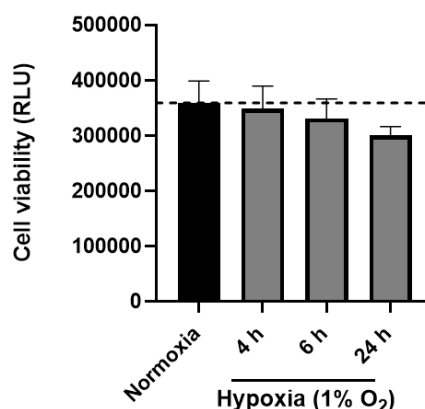


**Figure 4.17 Effect of hypoxia (1% O<sub>2</sub>) on HepaRG cell viability in 2D cell format.** HepaRG cultured as 2D monolayer. After differentiation on day 30 of culture cells exposed to hypoxia (1% O<sub>2</sub>) for 4, 6 and 24 h. Viability was determined by CellTiter Glo assay. HepaRG cells cultured under normoxia were used as control. Statistics by one way ANOVA.

**Figure 4.18** shows both protein (Western blot) and mRNA transcript levels (TaqMan qRT-PCR) for CYP3A4 and CYP2C9 in HepaRG monolayers exposed to 1% O<sub>2</sub> for up to 24 h. By 24 h of hypoxia exposure significant decreases in both CYP3A4 and CYP2C9 transcript levels were seen (**Fig. 4.18C and 4.18D**) approximately 70-80% and 60-70% decreases, respectively compared to corresponding controls. The impact of hypoxia upon transcript levels was not significantly evident with the shorter hypoxia exposure times. The reduced transcript levels by 24 h were also reflected in protein expression by Western blot (**Fig. 4.18A and 4.18B**) and by immunofluorescence staining (**Fig.4.19 and 4.20**).

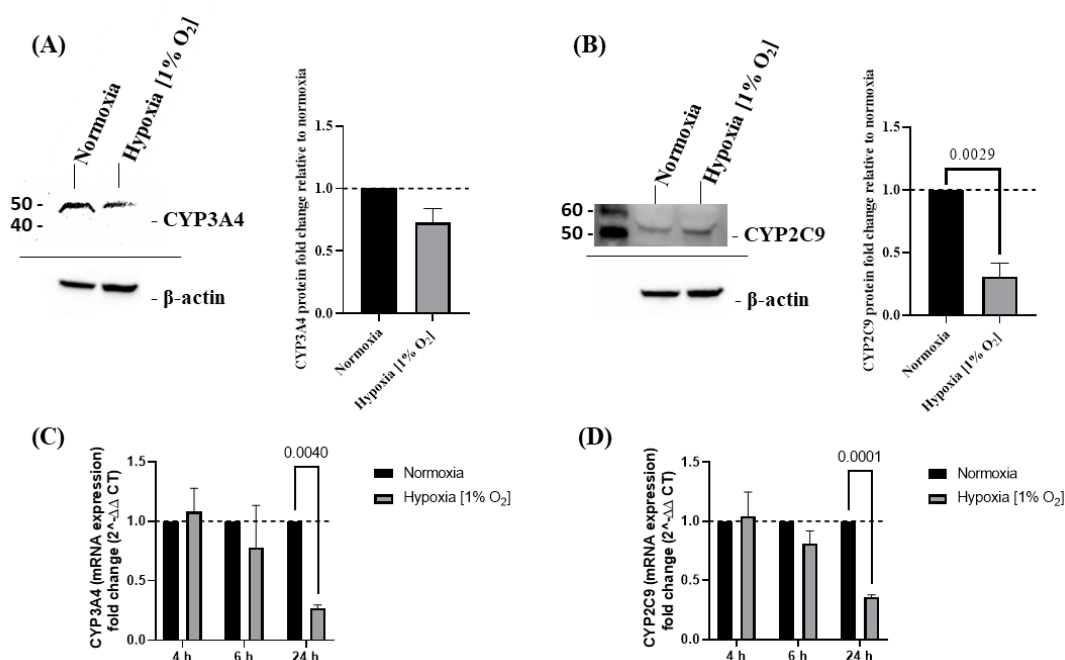


**Figure 4.18** Effect of hypoxia (1% O<sub>2</sub>) on CYP3A4 and CYP2C9 expression in HepaRG cells grown in 2D monolayer format. **Fig. 4.18A** and **Fig. 4.18B** respectively represent the Western blot analysis of CYP3A4 (50 kDa) and CYP2C9 (55 kDa) after exposure of cells to 1% O<sub>2</sub> for 24 h and the corresponding densitometry normalised to β-actin (42 kDa). Western blot bars represent one of the three independent experiments with similar results. **Fig. 4.18C** and **Fig. 4.18D** represent the qRT-PCR analysis of CYP3A4 and CYP2C9, respectively. Gene expression normalised to housekeeping gene (HPRT1) and then to cells culture under normoxia (black bar). Bars represent mean ± SEM. N=3 independent experiments. One-way ANOVA and post-hoc Bonferroni test was used for statistical analysis.

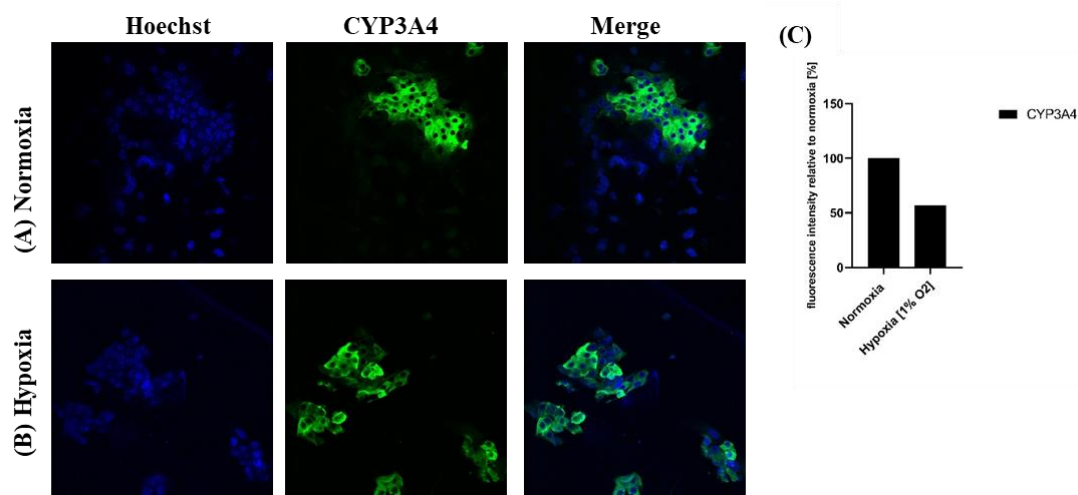


**Figure 4.19 Immunofluorescent microscopy of 2D monolayer HepaRG cells and the effect of hypoxia on CYP3A4.** HepaRG monolayer were differentiated following the standard protocol. After differentiation (day 30 of culture) cells were exposed to 1% O<sub>2</sub> for 24 h or kept in normoxia (21% O<sub>2</sub>). The cells were fixed with 4% paraformaldehyde and stained with anti- CYP3A4 antibody followed by AlexaFluor 488 secondary antibody. Nuclei stained with Hoechst. **Fig. 4.19A** immunofluorescent microscopy images for CYP3A4 in HepaRG cells under normoxia. **Fig. 4.19B** immunofluorescent microscopy images for CYP3A4 in HepaRG cells cultured under hypoxia. **Fig. 4.19C** Fluorescence densitometry for CYP3A4 quantified by ImageJ. N=1.

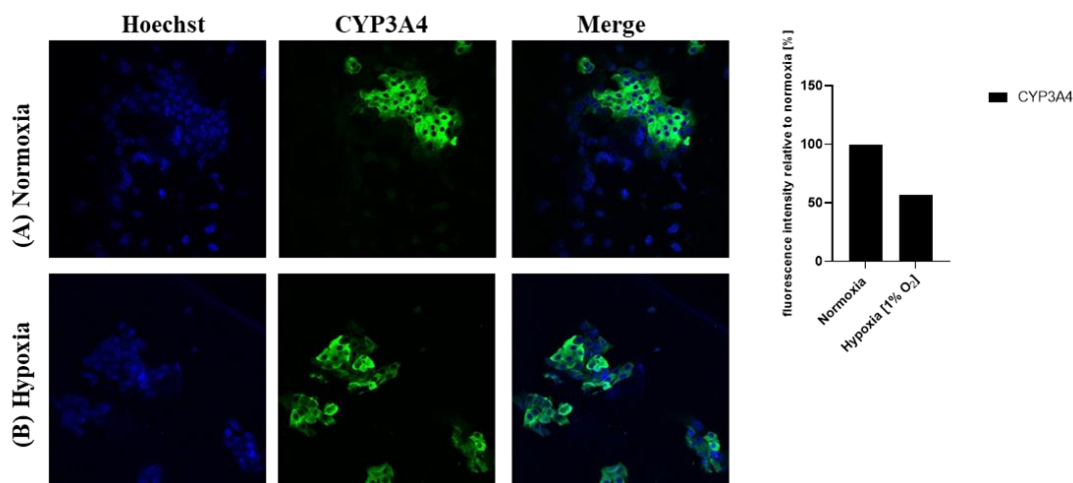


**Figure 4.20 Immunofluorescent microscopy of 2D monolayer HepaRG cells and the effect of hypoxia on CYP2C9.** HepaRG monolayer were differentiated following the standard protocol. After differentiation (day 30 of culture) cells were exposed to 1% O<sub>2</sub> for 24 h or kept in normoxia (21% O<sub>2</sub>). The cells were fixed with 4% paraformaldehyde and stained with anti- CYP2C9 antibody followed by AlexaFluor 488 secondary antibody. Nuclei stained with Hoechst. **Fig. 4.20A** immunofluorescent microscopy images for HepaRG cells under normoxia stained with only secondary antibody AlexaFluor 488 as a negative control. **4.20B** immunofluorescent microscopy images for CYP2C9 in HepaRG cells cultured under normoxia. **Fig. 4.20C** immunofluorescent microscopy images for CYP2C9 in HepaRG cells cultured under hypoxia. **Fig. 4.20D** Fluorescence densitometry for CYP2C9 quantified by ImageJ. N=1.

**Figure 4.19** shows the fluorescence intensity images (immunofluorescence staining) for CYP3A4 in HepaRG cells under normoxia and also after 24 h of hypoxia. While not as quantitative as the qRT-PCR data, or perhaps the Western blot, the immunofluorescence staining is consistent in showing a reduced intensity with hypoxia. **Figure 4.20** shows the

corresponding fluorescence intensity images for CYP2C9 in HepaRG cells and similarly showing a loss of immunofluorescence staining with hypoxia. Together these further show hypoxia to impact the ultimate translation of the CYP450 enzymes. This is consistent with Legendre *et al.*, reporting hypoxia-induced (1% O<sub>2</sub> for 24 h) suppression (at protein and mRNA level) of numerous phase I metabolic enzymes in HepaRG monolayer culture (Legendre *et al.*, 2009).

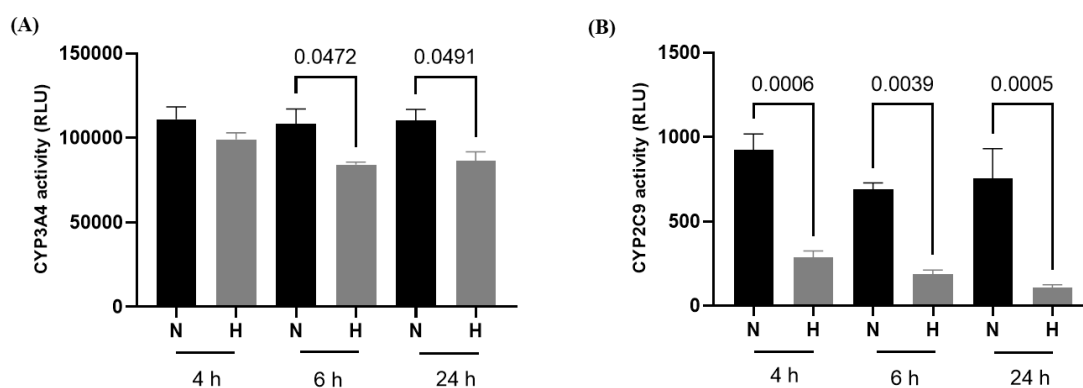


**Figure 4.21 Effect of hypoxia (1% O<sub>2</sub> for 4, 6 or 24 h) on CYP3A4 and CYP2C9 activity in HepaRG 2D monolayer** HepaRG cells were differentiated following the standard protocol. After differentiation cells were exposed to hypoxia (H; grey bars) for 4, 6 or 24 h. HepaRG cultured under normoxia (N; black bar) were used as a control. **Fig. 4.20A** and **Fig. 4.20B** functional activity of CYP3A4 and CYP2C9, respectively, as assessed by the P450-Glo™ assay. CYP activity is shown as a relative luminescent unit (RLU). Bars represent the mean ± SEM of three independent experiments each with at least six replicates. One-way ANOVA test and post-hoc Bonferroni was used for analysis.

Importantly, Figure 4.21 A and Figure 4.21 B show, respectively, functional data for substrate turnover (P450-Glo™ substrate assay) by CYP3A4 and CYP2C9 and the impact of hypoxia. The P450-Glo™ substrates use in the assay are isoenzyme-specific/-selective derivatives of d-Luciferin which are converted by the respective CYP isoenzyme(s) into d-Luciferin for the luminescent readout. Not all the derivatives of the d-Luciferin derivatives show isoenzyme specificity. However, for CYP3A4 the d-Luciferin substrate is Luc-IPA which shows a high degree of selectivity with only a minimal reactivity with CYP3A5 and 3A7. For CYP2C9 the d-Luciferin substrate is Luc-H which is specific and reacting only with CYP2C9 (Westerink and Schoonen, 2007). Comparing in Figure 4.21 the CYP3A4 and CYP2C9 RLU shows the latter to produce approximately x100-fold less luminescence (e.g., normoxia bars - CYP3A4 100,000 RLU vs CYP2C9 1,00 RFU). This should not be interpreted in an absolute sense as the substrates will have different kinetics for catalysis ( $K_m$ ,  $V_{max}$ ) and the RLU are not calibrated

and reported in respect to absolute enzyme levels. A further context may be from the raw data corresponding qRT-PCR data (e.g. **Fig. 4.18C** and **D** - 24 h normoxia):- while not quantitative in the absolute sense, the raw 'cycle threshold' (CT) values normalised the house keeping gene (HPRT1, which can be expected to remain constant) show a  $\Delta$ CT for CYP3A4 that is only ca 80% greater than the  $\Delta$ CT for CYP2C9. Practically the P450-Glo™ substrate assay allows for treatment comparisons (e.g., with or without inhibitor etc.) within a given isoenzyme and not absolute comparisons across isoenzymes.

While the earlier qRT-PCR data (**Fig 4.18C** and **Fig. 4.18D**) showed a trend (not statistically significant) for decreased transcript for both genes as early as 6 h into hypoxia exposure, **Figure 4.21** shows statistically significant functional decreases in substrate turnover earlier than the 24 h hypoxia timepoint, i.e. ca. 30% fall as early as 6 h for CYP3A4 and ca. 70% fall at 6 h for CYP2C9. Such functional decreases in catalysis under hypoxia at earlier times will more likely reflect changes in the availability of oxygen and other co-factors in the catalysis reaction. At earlier periods of hypoxia exposure the availability of reactants within the catalytic path that will likely have more of an impact upon catalysis activity than transcriptional change in CYP450 enzyme(s). For CYP450, the catalysis of substrate essentially involves a stoichiometric reaction with an electron donor, typically using NADPH, other co-factors and O<sub>2</sub> itself. With longer periods of hypoxia the transcriptional and translational impacts upon CYP450-mediated catalysis may become more evident. The reduction of functional activity with hypoxia even by 6 h was greater for CYP2C9 compared with CYP3A4. This may be due to the fact that CYP3A4 can utilise redox partners such as cytochrome b5 or cytochrome P450 reductase to support its activity (Voice et al., 1999; Yamazaki et al., 1997). These redox partners can transfer electrons to or from the enzyme, helping to drive the catalytic cycle even in the absence of oxygen (Guengerich, 2018).

Collectively, the above data shows that CYP3A4 and CYP2C9 functional gene expression was significantly decreased by hypoxia (1% O<sub>2</sub>) and the appropriateness if necessary of 2D monolayer model at least in terms of CYP450 function and modulation.

### **4.3.3.2 HepaRG cells: Effect of hypoxia (1% O<sub>2</sub>) on CYP3A4 and CYP2C9 in 3D cell spheroid format**

Here HepaRG 3D spheroids were used to confirm the effect of hypoxia (1% O<sub>2</sub>) on CYP3A4 and CYP2C9 activity ahead of the potential use of this format model in later experiments.

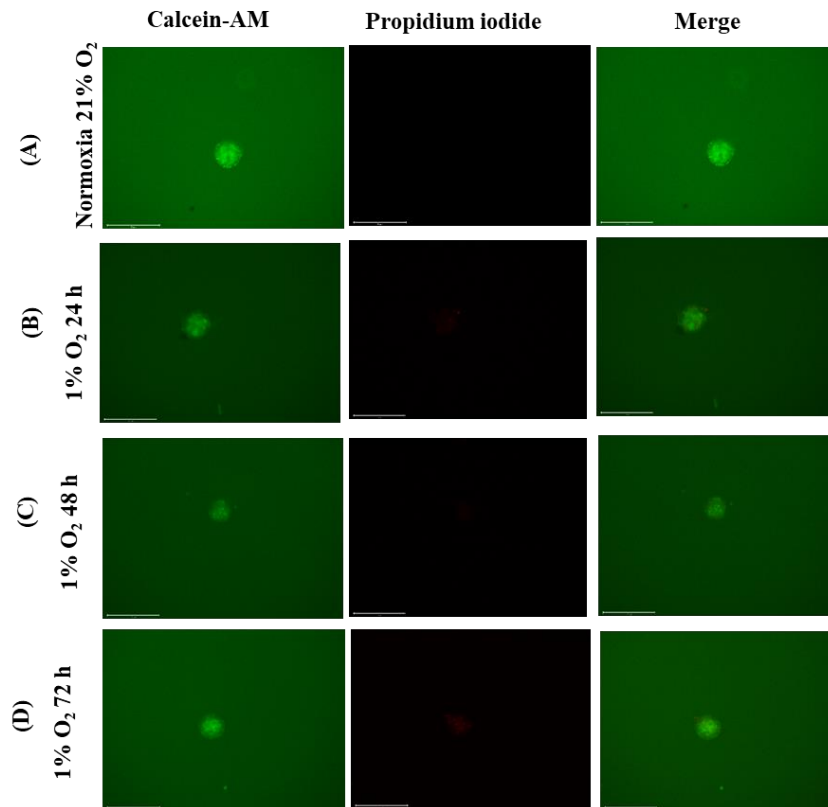


**Figure 4.22 Representative images of HepaRG 3D spheroid viability at 1% O<sub>2</sub> over a 72 h exposure period.** HepaRG spheroids were cultured under: **Fig. 4.21A** normoxia (21% O<sub>2</sub>) serving as the control; **Fig. 4.21B** 24 h of hypoxia (1% of O<sub>2</sub>); **Fig. 4.21C** 48 h of hypoxia (1% of O<sub>2</sub>); **Fig. 4.21 D** 72 h of hypoxia (1% of O<sub>2</sub>). At the end of the exposure periods spheroids were incubated with a mixture of calcein-AM to measure the live cells (green) and propidium iodide (red) to measure the dead cells. Scale bar 275  $\mu$ m.



HepaRG spheroids (1000 cells/well) were subjected for 24, 48, and 72 h exposure to (1% O<sub>2</sub>). The spheroids were incubated with a combination of calcein-AM (green) to measure living cells and propidium iodide (red) to detect dead cells and the development of cell necrosis was monitored. **Figure 4.22** shows the vast majority of the cells to remain viable across the full hypoxia exposure period. At 72 h some evidence of weak PI staining was apparent particularly in the spheroid core (**Figure 4.22D** – bottom row).

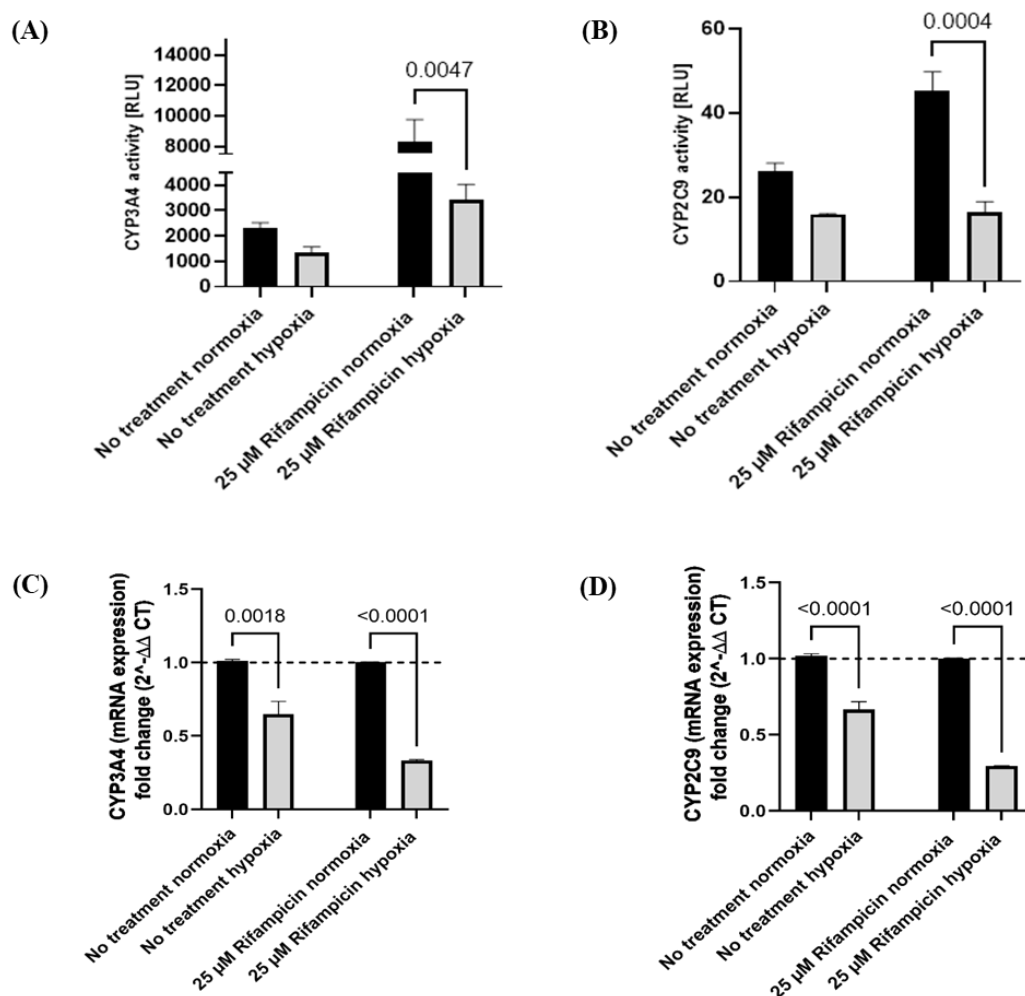


**Figure 4.23 Effect of hypoxia (1% O<sub>2</sub> for 24 h) on CYP3A4 and CYP2C9 activity and transcript expression in HepaRG 3D spheroids.** HepaRG spheroids were treated for 48 h with the enzyme inducer rifampicin after which the spheroids were subjected to a further 24 h of rifampicin treatment either under normoxia or hypoxia. Spheroids cultured under normoxia were used as a control. **Fig. 4.23A** and **Fig. 4.23B** functional activity of CYP3A4 and CYP2C9, respectively, as assessed by the P450-Glo™ assay. CYP activity is shown as a relative luminescent unit (RLU). **Fig. 4.23C** and **Fig. 4.23D** qRT-PCR for CYP3A4 and CYP2C9, respectively. Gene expression was normalised to house-keeping gene (HPTR1) and then to normoxia control. Bars represent the mean ± SEM of three independent experiments. One way ANOVA test was used for analysis.

The effect of 1% O<sub>2</sub> hypoxia on CYP3A4 and CYP2C9 functional activity and gene expression was then studied. Although longer hypoxia exposure times, notably 48 h, showed the HepaRG spheroids to retain viability, the current analysis was undertaken with hypoxia (1% O<sub>2</sub>)

exposure for 24 h only. This reflecting the purpose of the work to explore the effects of acute hypoxia exposure (at or less than 24 h).

In **Figure 4.23** the study groups included rifampicin treatment involving pre-incubation with rifampicin (48 h + 24 h) for an initial 48 hours under normoxia, followed by another 24 h incubation under normoxia or hypoxia – this latter 24 h representing the additional hypoxia vs normoxia comparisons. **Figures 4.23C** and **4.23D** show the effects of hypoxia for 24 h upon mRNA transcript levels (qRT-PCR) for CYP3A4 and CYP2C9, respectively. In both the absence and presence of rifampicin hypoxia significantly reduced the respective transcript levels compared to the corresponding normoxia (21% O<sub>2</sub>) control; the statistical significance shown above the corresponding comparisons. For CYP3A4 and CYP2C9 the results were similar: in the absence of rifampicin the hypoxia exposure for 24 h reduced the transcript levels by ca. 35%, while following rifampicin pre-treatment, hypoxia exposure reduced transcript level by ca 70%. Functional assessment is shown in **Figures 4.23A** and **4.23B** and demonstrates rifampicin under normoxia to enhance both CYP3A4 (ca. 400%) and CYP2C9 (ca. 40%) functional activity. The relatively low impact of rifampicin to induce CYP2C9 was also seen in the HepaRG 2D format and reflecting the lower responsiveness of this gene to rifampicin as well as the longer t<sub>1/2</sub> reported at ca 100 h (Yang *et al.*, 2008). Unlike studies with HepaRG cells in the 2D format, the impact of hypoxia on function in the 3D format was only evident (with statistical significance) following rifampicin pre-treatment. This likely due hypoxia-mediate reductions more noticeable in cells where CYP3A4 and CYP2C9 activity is initially higher. Here hypoxia (1% O<sub>2</sub> for 24 h) reduced function by ca. 60% for both CYP3A4 and CYP2C9.

Collectively the current work with HepaRG cells supports hypoxia decreasing the CYP3A4 and CYP2C9 transcriptional and translational expression while also decreasing functional activity. Further that the HepaRG cells may serve as a model for future PK-PD simulation and mechanistic studies in this thesis. In particular the 2D format while allowing greater ease of culture may also allow studies to be conducted without the need for enzyme induction using rifampicin. The observations made in this chapter are supported by several in-vitro and in-vivo animal studies. For example, an in-vitro study with HepaRG cells hypoxia resulted in decreases in the mRNA expression of CYP1A2, CYP2C9, CYP3A4, and CYP2E1 (Legendre *et al.*, 2009). In HepG2 cells exposed to acute hypoxia the expression of CYP1A2, CYP2C9, CYP2E1, CYP3A4 were decreased via PXR and CAR regulatory pathways (Duan *et al.*, 2020). Gola et al showed that after 7 and 14 days of exposure of rats to a simulation altitude of 7,620

m (hypoxia), CYP2C9 protein expression downregulated with reductions in ibuprofen metabolism. These authors also observed increases in pro-inflammatory cytokines IL-1 $\beta$ , IL-2, IFN- $\gamma$ , TNF- $\alpha$  associated with the reduced CYP2C9 expression (Gola *et al.*, 2016). An animal study at 4,300 m altitude found that acute hypoxia (24 h) decreased CYP3A4 protein expression by 1.6-fold in rats. This decrease in CYP3A4 enzyme was associated with alterations in sildenafil pharmacokinetics, including a decrease in CL by 69%,  $V_d$  by 46%, and an increase in  $t_{1/2}$  by 44%,  $C_{max}$  by 133%, and AUC by 213%. The reduction in CYP3A4 protein, according to the author, is the main cause of sildenafil PK change under acute hypoxia (Zhang and Wang, 2022). The mechanism of reduction CYP3A4 and CYP2C9 under acute hypoxia will be studied in Chapter 6.

#### **4.3.4 Effect of acute hypoxia on ABC transporters**

Initial, early pilot investigations for the study of hypoxia on drug absorption and disposition (not explicitly involving CYP450) the work here explored the impact of hypoxia on ABC efflux transporters involving P-glycoprotein (P-gp or MDR-1), multidrug-resistance-associated protein2 (MRP2), and breast cancer resistance protein (BCRP). These ATP-binding cassette (ABC) transporters, amongst other transporters, have a role in drug absorption and disposition and may be subject to hypoxia-induced changes. For example, the co-ordinated regulation and function of CYP3A4 and P-gp, and their related functional substrate overlap (Wacher, Wu and Benet, 1995). The ABC transporters are located in key absorption-disposition barriers, for example: on the apical surface of epithelial cells of the large and small intestine; apical hepatocyte membrane facing the biliary canaliculi which eventually merge to form bile ductiles; luminal membrane of renal proximal tubules; luminal capillary surface of brain microvascular cells, as well as in other barriers such as in the lung (Chan, Lowes and Hirst, 2004; Gameiro *et al.*, 2017; Li *et al.*, 2019).

Here both HepG2 and Caco2 (a human colon cancer line) were used in pilot experiments where they were cultured in 2D format under normoxic (21% O<sub>2</sub>) or hypoxic (1% O<sub>2</sub>) conditions, and with the functional expression of ABC transporters (P-glycoprotein, BCRP and MDR-1) explored; these cells have been used previously to study ABC drug transporters (Gutmann *et al.*, 1999; Rigalli *et al.*, 2012). **Figure 4.24** shows the impact of hypoxia (1% for 24 h) upon transcript expression (qRT-PCR) and function (dye cellular uptake and efflux) for the ABC transporters in the Caco2 and HepG2 cells.

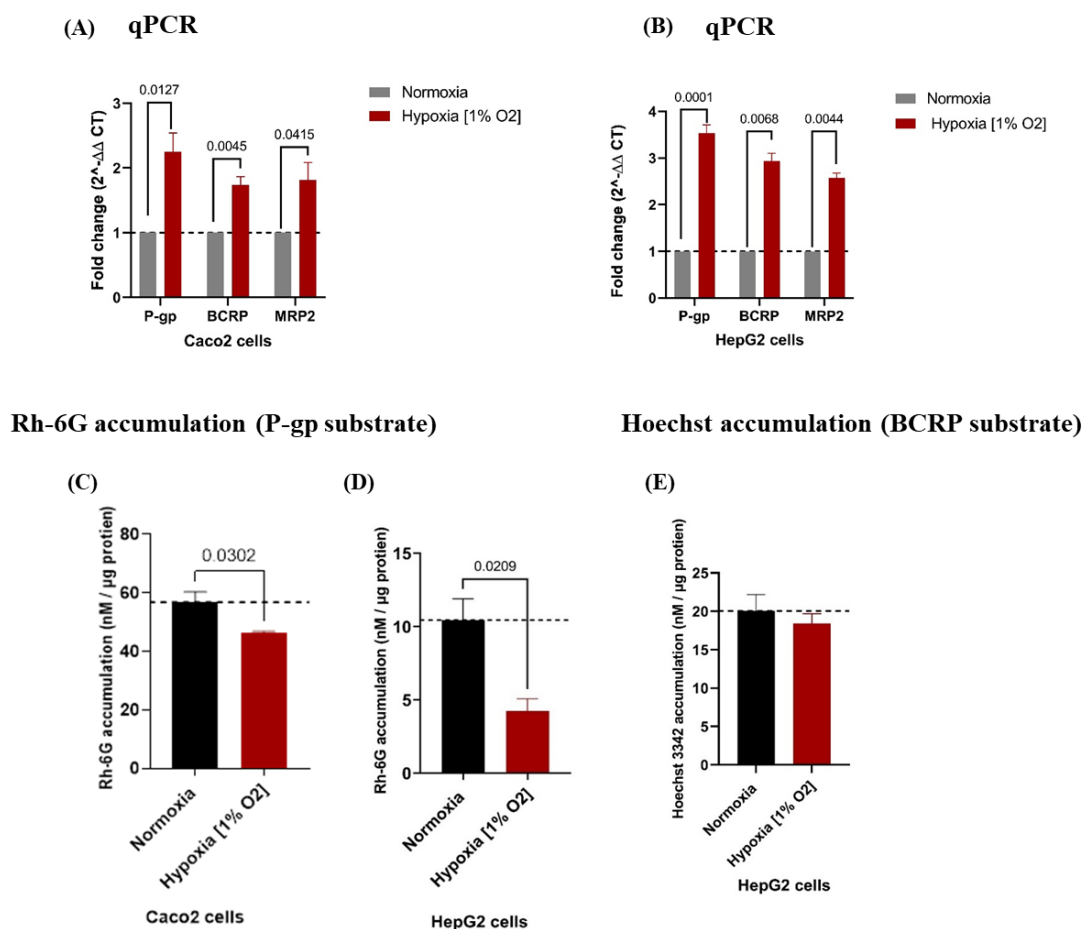


**Figure 4.24 Effect of hypoxia on ABC transporter expression and functional activity.** Caco2 cells were differentiated for 21 days and HepG2 were grown for 7 days and then were exposed to either normoxia (21% O<sub>2</sub>) or hypoxia (1% O<sub>2</sub>) for 24 h. **Fig. 4.24A** qRT-PCR for P-gp, BCRP and MRP-2 in Caco2 cells; **Fig. 4.24B** qRT-PCR for P-gp, BCRP and MRP-2 in HepG2 cells N=3 experiment each with three replicates. One way ANOVA used for analysis. **Fig. 4.24C** accumulation of the dye and P-gp substrate Rhodamine-6G (R-6G) in Caco2 cells and **Fig. 4.24D** in HepG2 cells; **Fig. 4.24E** accumulation of the dye and BCRP substrate Hoechst 33342 in HepG2 cells. Histogram bars represent the mean ± SEM of three independent experiments. T-test were used for analysis.

Caco2 cells were cultured for 21 days to differentiate them into columnar polarized epithelial cells similar to enterocytes of the small intestine. In all cases 24 h of hypoxia significantly increased the gene expression of ABC transporters in the Caco2 cells (**Figure 4.24A**) of: P-gp by ca. 2-fold; BCRP by 1.7-fold; MRP-2 by 1.8-fold. Similarly, in HepG2 cells hypoxia

significantly increased the gene expression (**Figure 4.24B**) of: P-gp by 3.5-fold; BCRP by 2.9-fold; MRP2 by 2.5-fold.

Increased ABC transporter transcript levels arising from hypoxia have been reported previously. For example, BCRP mRNA expression was upregulated by either hypoxia or the iron-chelator deferoxamine (Krishnamurthy *et al.*, 2004). The deferoxamine stabilizes HIF1- $\alpha$  by inhibiting a prolyl-hydroxylase involved in tagging HIF1- $\alpha$  for proteasomal degradation. Both the protein and mRNA expression of P-gp and MRP1 were significantly increased in the intestine, liver, and kidneys of rats after exposure to simulated high-altitude environment of 5000 m for 24 h (Luo *et al.*, 2016). Furthermore, several studies have reported upregulation of P-gp under hypoxia in different cell lines, including human lung adenocarcinoma A549 cell line (Xia *et al.*, 2004) and in HepG2 human hepatocellular carcinoma cell line (Zhu *et al.*, 2005). Several pathways have been discussed in the literature regarding P-gp upregulation under hypoxia: under normoxia, NF- $\kappa$ B dimers form a complex with inhibitory factor (IkB $\alpha$ ) maintaining the former in an inactive state. Under hypoxia, IkB kinases (IKK) activated during oxidative stress led to degradation of IkB $\alpha$ , activation of NF- $\kappa$ B, and their transfer into the nucleus allowing transcriptional induction of ABC transporters, for example, MDR1 (Deng *et al.*, 2001; Bentires-Alj *et al.*, 2003; Li *et al.*, 2015). Other research has shown ROS activation under hypoxia-induced phosphorylation of JNK tyrosine and threonine residues leads to increased transcription activity of c-Jun and its interaction with nuclear HIF-1. Binding of HIF-1 to HIF-Responsive Elements (HREs) on the MDR1 promoter results in increased MDR-1 expression (Comerford, Cummins and Taylor, 2004; Liu *et al.*, 2007).

The hypoxia-induced increase in P-gp transcripts in this current work was associated with hypoxia-associated increases in P-gp transporter function (**Figures 4.24**). Here the fluorescent dyes Rhodamine 6G (Rh-6G) and Hoechst 33342 were used as substrates for P-gp and BCRP, respectively (Gameiro *et al.*, 2017). Rh-6G having a higher affinity to P-gp than Rhodamine-123 (Eytan *et al.*, 1997) which is also a commonly used P-gp substrate. As shown in **Figures 4.24C** and **4.24D**, in both Caco2 and HepG2 cells, respectively, exposure to hypoxia 1% O<sub>2</sub> for 24 h resulted in the cells having significantly less accumulation of the P-gp substrate Rh-6G, indicative of increased P-gp efflux function. In contrast in the HepG2 cells the transport of the BCRP substrate, Hoechst 33342, showed no statistically significant functional difference between normoxia and hypoxia conditions (**Fig. 4.24E**), despite the BCRP RNA transcript shown to be increased with hypoxia.

One possible reason for this difference between transcript and function for BCRP could be its relative low expression in HepG2 (Brandon *et al.*, 2006), that would allow detection of change using a highly sensitive technique like qPCR but not when function is tested using a dye-based assay. Further, the lack of correlation between BCRP mRNA expression and function has been reported previously in an acute myeloid leukaemia cell line – this was postulated to be associated with post-transcriptional ABCG2 gene regulation including mRNA destabilisation (Suvannasankha *et al.*, 2004).

While hypoxia-induced reductions appear to decrease the chemical oxidation potential of cells by reducing CYP450 activity, the acute exposure of hypoxia induces increases in the for example P-gp expression and function. This may serve the cell as hypoxia can cause toxic metabolites and reactive oxygen species (ROS) to accumulate intracellularly causing cell damage and impairing cellular function (Hernansanz-Agustín and Enríquez, 2021). At least with acute hypoxia, ABC transporters may be initially upregulated to counter this accumulation and increase the efflux of toxic metabolites and ROS and hence protect cells from oxidative stress and damage. Expression of P-glycoprotein is regulated in a redox-sensitive manner with expression promoted by hypoxia-inducible factor-1 $\alpha$  (HIF-1 $\alpha$ ) and inhibited by intracellular reactive oxygen species (ROS) (Wartenberg *et al.*, 2005). BCRB transporters were found to be induced in pluripotent stem cells under hypoxia by HIF-1 pathway enhancing cell survival by reducing the accumulation of protoporphyrin a toxic haem metabolite in the cells (Krishnamurthy *et al.*, 2004).

## 4.4 Conclusions

This chapter has successfully characterised a hepatocyte cell model for studying the effects of acute hypoxia on drug metabolism. The findings have provided valuable insights that will be utilised in further mechanistic and quantitative studies conducted in this thesis.

- The HepG2 cell line was found to be unsuitable due to low mRNA expression of CYP2C9/CYP3A4 and undetectable protein levels, even with pre-treatment of the enzyme inducer rifampicin. On the other hand, the HepaRG cell line demonstrated high and stable levels of CYP3A4 and CYP2C9, making it a viable model for subsequent experiments.

## Chapter 4

- Optimisation of the 3D format revealed that a seeding density of 1000 cells per well was optimal, while the 2D monolayer format of HepaRG cells provided greater ease of use, higher expression levels of CYP3A4/CYP2C9, and facilitated the extraction of RNA and protein for consistent functional studies.
- It was determined that hypoxia at 1% O<sub>2</sub> did not negatively impact the viability of HepaRG cells, confirming its suitability for hypoxia experimental studies. The investigation revealed that hypoxia (1% O<sub>2</sub>, 24 h) led to reduced functional activity, transcription, and translation of CYP3A4 and CYP2C9 in the HepaRG cell line.
- Hypoxia increased the gene expression of P-gp, BCRP, and MRP2, as well as enhanced the functional activity of P-gp in the HepG2 and Caco2 cell lines.

Based on these findings, the HepaRG cell line in the 2D format will be utilised as the model of choice for investigating the mechanisms underlying the suppression of CYP3A4 and CYP2C9 activity under acute hypoxia (Chapter 6). Furthermore, the changes in CYP450 activity under acute hypoxia will inform the PK-PD simulations for sildenafil (Chapter 5).

Overall, this chapter has laid the foundation for further investigations into the impact of acute hypoxia on drug metabolism and will contribute to a better understanding of the mechanisms underlying PK/PD alterations in hypoxic conditions.

**Chapter 5: Mechanism of REDOX regulation and  
CYP450 alteration under hypoxia**



## 5.1 Introduction

### 5.1.1 Reactive Oxygen Species (ROS)

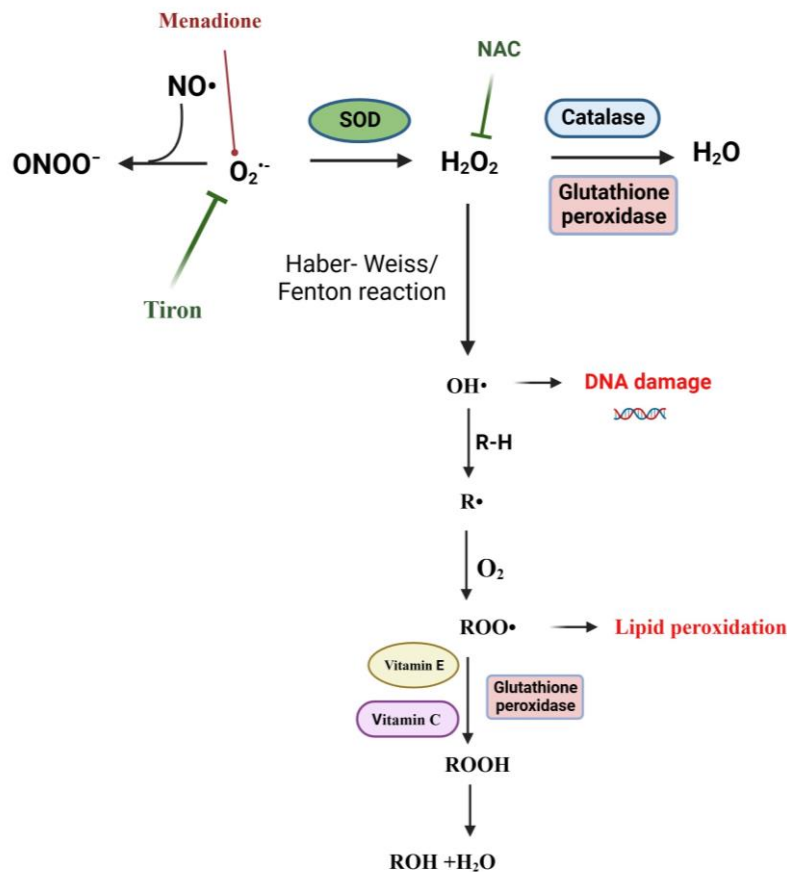


**Figure 5.1 ROS formation pathway.** including peroxynitrite ( $ONOO^-$ ), nitric oxide ( $\cdot NO$ ), hydrogen peroxide ( $H_2O_2$ ), hydroxyl radical ( $OH\cdot$ ), superoxide radical ( $O_2^{\cdot-}$ ), peroxy radicals ( $ROO\cdot$ ).

Figure 5.1 shows the key ROS molecules mentioned in this work, their synthesis and decomposition routes. ROS are produced in various cellular compartments, including the cytoplasm, cell membrane, endoplasmic reticulum, mitochondria, and peroxisome (Forrester *et al.*, 2018). Among these compartments, mitochondria play a prominent role in generating approximately 90% of ROS within cells (Tirichen *et al.*, 2021). Mitochondria in particular have a prominent role in producing superoxide anions, which represent the most abundant type of ROS (Zorov, Juhaszova and Sollott, 2014). Although the superoxide anion itself does not exhibit significant reactivity in biological systems, it can cause damage to haem moieties or enzymes containing iron-sulphur centres, such as aconitase, in the citric acid cycle. This damage results in the release of ferrous ions ( $Fe^{+2}$ ) which subsequently can react with hydrogen

peroxide ( $\text{H}_2\text{O}_2$ ), leading to the generation of hydroxyl radicals through a process known as the Fenton process (Guo and Che, 2012). The diffusion of hydroxyl radicals from the mitochondrial matrix to the intermembrane space is restricted due to their extremely high reactivity and consequently short lifespan. Moreover, the superoxide radical anions can interact with nitric oxide (NO) produced within the mitochondria and hence gives rise to the formation of the harmful oxidant ONOO<sup>-</sup>. Notably, ONOO<sup>-</sup> exhibits higher reactivity compared to its precursor molecules (Alvarez *et al.*, 2003; Guo and Che, 2012; Möller *et al.*, 2019).

The primary site of ROS generation within mitochondria is the electron transport chain (ETC) during the process of oxidative phosphorylation, where molecular oxygen ( $\text{O}_2$ ) undergoes reduction to water ( $\text{H}_2\text{O}$ ). The ETC is situated in the inner membrane of mitochondria, in close proximity to the mitochondrial matrix, and consists of five major protein complexes known as complexes I, II, III, IV, and V. Leakage of electrons during their transport within the ETC occurs at specific sites, namely the flavin mononucleotide (FMN) site of complex I and the Q cycle of complex III, resulting in the production of superoxide ( $\text{O}_2^{\cdot-}$ ) as the primary ROS species within mitochondria (Li *et al.*, 2013; Chenna *et al.*, 2022). Research suggests that approximately 0.2% to 2.0% of the consumed  $\text{O}_2$  by mitochondria generates  $\text{O}_2^{\cdot-}$  (Li *et al.*, 2013). Complex I predominantly produces  $\text{O}_2^{\cdot-}$  on the matrix side of the inner membrane, while complex III-derived  $\text{O}_2^{\cdot-}$  is produced both towards the inner-membrane space and the matrix (Muller, Liu and Van Remmen, 2004; Guo and Che, 2012). Subsequently,  $\text{O}_2^{\cdot-}$  can move from the intermembrane space to the cytoplasmic surface of the outer membrane of mitochondria through a specific voltage-dependent anion channel (VDAC) (Han *et al.*, 2003); due to its short half-life and charged nature, the diffusion of  $\text{O}_2^{\cdot-}$  through the lipid portion of mitochondrial membranes is highly unfavorable.

There are inconsistencies in published studies regarding the nature of ROS generation under hypoxia, this is possibly due to variances in the cellular and subcellular models used for study, as well as the inability of the available technology to reliably assess ROS levels.

Endothelial cell plasma membranes have been reported to produce less  $\text{H}_2\text{O}_2$  in hypoxia than in normoxia (Zulueta *et al.*, 1995; López-Barneo, Pardal and Ortega-Sáenz, 2001). Similarly, the generation of the OH<sup>•</sup> in the perinuclear endoplasmic reticulum (via the Fenton reaction of  $\text{H}_2\text{O}_2$  with iron  $\text{Fe}^{2+}$ ) is shown to be reduced in HepG2 cells under hypoxia (8%  $\text{O}_2$ , 24 h) compared to normoxia (Liu *et al.*, 2004).

Alternatively, several groups have observed an increase of total intracellular ROS levels under hypoxia in several different cell models and using different technologies (Chandel *et al.*, 1998; Guzy *et al.*, 2005; Mansfield *et al.*, 2005). For example, the exposure of pulmonary artery smooth muscle cells to hypoxia significantly increased indicator of intracellular ROS by fivefold compared to normoxic cells (Killilea *et al.*, 2000). Hypoxic embryonic ventricular myocytes increased intracellular ROS by threefold over that of normoxic cells (Yao *et al.*, 1999). Similar results were seen in hypoxic human lung epithelial cells (1% O<sub>2</sub>, 24 h), where a significant increase of ROS production in hypoxia has been reported (Li, Wright and Jackson, 2002).

### 5.1.2 Regulation of CYP450 by ROS

The effect of ROS on CYP450 is not extensively studied in the literature, but reports exist that relate to CYP1A1, CYP3A4 and CYP2E1 isoforms. Most of the published studies agree that ROS negatively regulates the expression CYP450 isoforms. For example, in the HepG2 cell line the expression of CYP1A1 and CYP2E1 is downregulated by exogenous H<sub>2</sub>O<sub>2</sub> treatment and glutathione depletion. This downregulation of CYP1A1 and CYP2E1 was suppressed by applying catalase, an anti-oxidant enzyme catalysing the decomposing of H<sub>2</sub>O<sub>2</sub> to water and oxygen (Morel and Barouki, 1998; Morel, Mermod and Barouki, 1999; Morel, De Waziers and Barouki, 2000). In contrast, Nagai and collaborators reported an increase in the mRNA and protein levels of CYP3A4 induced by H<sub>2</sub>O<sub>2</sub> treatment in human K562 erythroleukemic cells (Nagai, Kato and Tamura, 2004).

While the ROS mechanism(s) regulating CYP450 under hypoxia remain to be fully elucidated, **Figure 5.2** illustrates the possible pathways involved in this regulation of CYP450s upon ROS production under hypoxia. Specifically:

- A)** Hypoxia causes increased ROS leading to oxidative stress which activates HIF-1 $\alpha$  by inactivating its inhibitor, HIF prolyl hydroxylase. HIF-1 $\alpha$  heterodimerises with HIF-1 $\beta$  and binds to the promoter of target genes leading to a decrease in the expression of transcription factors (CAR and PXR) that would normally promote the expression of the CYP3A4 and CYP2C9.
- B)** ROS activates protein kinase C (PKC) that phosphorylates mitogen-activated protein kinase, kinase1/2 (MEK1/2), followed by activation of extracellular signal-regulated

kinase1/2 (ERK1/2) which then promotes the nuclear translocation of the transcription nuclear factor-kB (NF-kB). After binding to main target genes, NF-kB triggers the inflammatory cascade and downregulates CYP450 isoforms.

- C) ROS acts directly on CYP450 isoforms, reducing enzyme activity. Hypoxia induces a decrease in glutathione and other cellular antioxidants and an increase in lipid peroxidation end-products in the liver as a result of the formation of reactive oxygen intermediates (ROI), such as superoxide anion and H<sub>2</sub>O<sub>2</sub>. ROI may bind to CYP450 associate Fe<sup>2+</sup>, leading to the destruction of the haem group, which is essential for the catalytic activity of CYP450, and hence CYP450 inactivation.

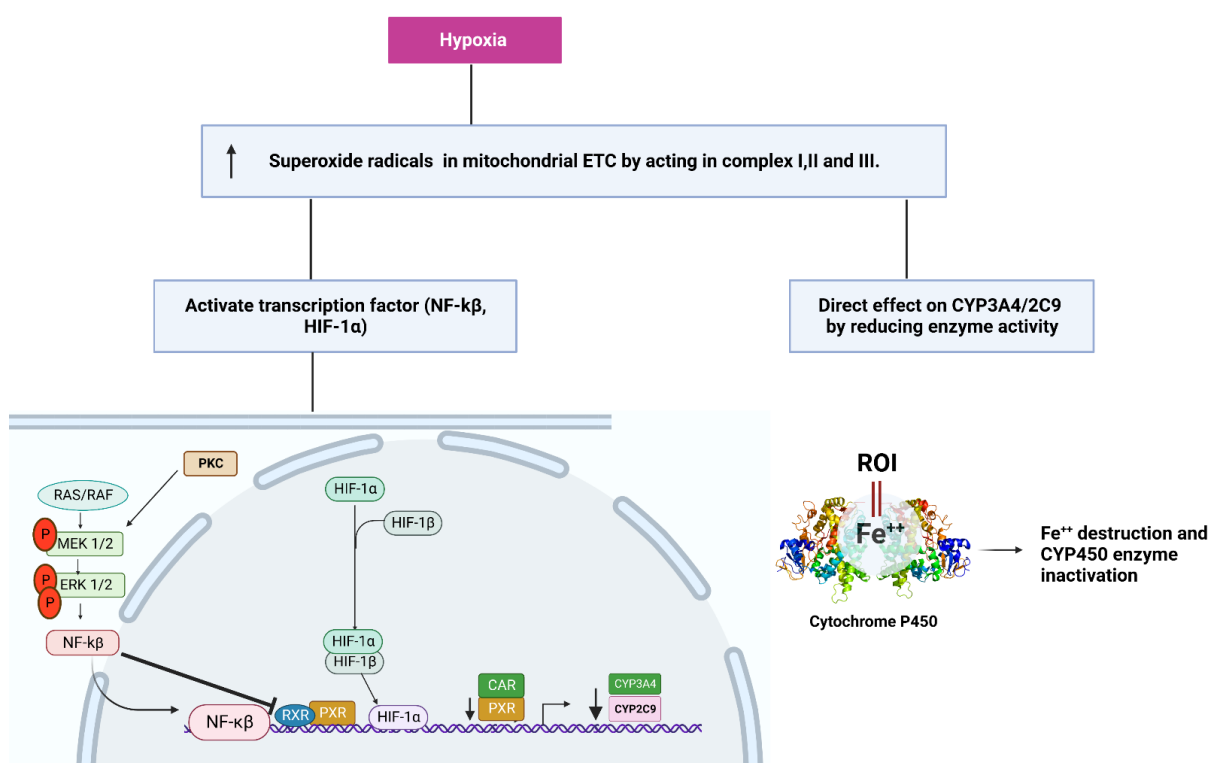


**Figure 5.2 Possible signal transduction pathways mediated by ROS that regulate CYP450 isoforms under hypoxia.** ETC: electron transport chain; NF-kB: Nuclear factor kappa-light-chain-enhancer of activated B cells; HIF-1α: Hypoxia-inducible factor 1-alpha; HIF-1β: Hypoxia-inducible factor 1-beta; PKC: protein kinases C ; MEK: Mitogen-Activated protein Kinase; ERK: Extracellular signal Regulated Kinase; RXR: Retinoid X Receptor; PXR: Pregnane X Receptors; CAR: Constitutive Androstane Receptor; ROI: reactive oxygen intermediate; Fe<sup>2+</sup>: iron or haem. Designed by D.Alablani- BioRender.

### 5.1.3 Hypoxia, inflammation, nuclear receptors and CYP450s

The hypothesis of hypoxia-induced inflammation has gained widespread acceptance in the hypoxia signalling field. Individuals exposed to hypoxia are more likely to experience inflammation, whether they have pulmonary-cardiovascular conditions or are healthy

individuals exposed to hypoxic conditions such as in acute mountain sickness. The inflammatory response markers interleukin-6 (IL-6), IL-6 receptors, and C-reactive protein (CRP) are all found to increase in the blood of healthy subjects who have spent three days at an altitude of more than 3400 m (Hartmann *et al.*, 2000). Numerous studies in rodents and humans have shown that induced-hypoxia is associated with inflammation characterised by an increase in oxidative stress, increased pulmonary NF- $\kappa$ B expression and in circulating pro-inflammatory cytokines IL-1, IL-6, and TNF- $\alpha$  (Mazzeo, 2005; de Gonzalo-Calvo *et al.*, 2010; Sarada *et al.*, 2012). Hypoxia has been repeatedly shown to promote the production of cytokines such as IL-1 $\beta$ , TNF- $\alpha$ , and interferon-gamma (IFN- $\gamma$ ), as well as hypoxia-induced factor 1 (HIF-1 $\alpha$ ) (Wenger, 2002; Cokic *et al.*, 2014; Merry *et al.*, 2015). Endothelial cells exposed to hypoxic conditions (PO<sub>2</sub> ~12–14 mmHg) display increased transcriptional and translational levels of IL-1 and IL-8 (Karakurum *et al.*, 1994).

Overwhelmingly, the evidence points to hypoxia leading to a reduced CYP450 functional expression involving an inflammatory element. The pro-inflammatory cytokine IL-6 is strongly linked to causing a reduced CYP450 enzyme activity under hypoxia, while IL-1, TNF- $\alpha$ , and IFN- $\gamma$  may have a less inhibitory effect (Morgan, 2001, 2009). However, the effects on individual isoenzymes can be divergent, and in particular in reports for CYP3A6 (Fradette *et al.*, 2002). When hepatocytes were incubated with serum from rabbits exposed to acute hypoxia (8% O<sub>2</sub> for 24 h, PaO<sub>2</sub> 34mm Hg), CYP1A1 and CYP1A2 gene expression and protein activity decreased; a decrease attenuated by co-exposure with IFN- $\gamma$  and IL-1 antibodies (Fradette *et al.*, 2007a). In contrast, this study demonstrated an increase in CYP3A6 gene expression and protein activity with hypoxia, potentially due to the influence of erythropoietin (Fradette *et al.*, 2007a). Kurdi *et al.*, using animal models, reported a reduction in theophylline metabolic clearance by 15% to 28%, caused by either hypoxia or inflammatory stimuli. This reduction involved the suppression of CYP1A1/1A2, while observing an upregulation of CYP3A6 (Kurdi *et al.*, 1999).

The nuclear receptor superfamily codes for transcription factors that convert extracellular and intracellular signals into cellular responses via the respective transcription factor binding to (via cognate DNA-binding domain), and functionally activating/suppressing the transcription of target genes. The family includes steroids and non-steroid receptors. The superfamily includes amongst many others the Pregnane X Receptor (PXR) and the Constitutive Androstane Receptor (CAR). Both CAR and PXR function as sensors for toxic by-products of endogenous molecules and of exogenous xenobiotics. Their activation as transcription factors

is aimed at enhancing the removal of potentially toxic molecules. Both PXR and CAR are recognised as playing a key role in regulating CYP450 in the liver. For example, PXR is reported as the primary inducer of CYP3A expression, whereas CAR influences the transcription of CYP2B, CYP1A, and CYP3A (Handschin and Meyer, 2003; Tien and Neglishi, 2006). Both have been shown to regulate CYP2C9, CYP2C19, and CYP2C18, in a series of gene knockdown studies (Chen *et al.*, 2004; Hu, Bi and Huang, 2011). As CYP450s are target genes for PXR and CAR, how hypoxia affects these receptors with then downstream impacts on CYP450 activity, is an important consideration. However, the mechanism(s) by which hypoxia regulates CYP450 via PXR and CAR are not fully known.

In HepaRG cells acute hypoxia (1% O<sub>2</sub>, 24 h) has been shown to reduce the mRNA expression of CYP1A2, CYP2C9, CYP3A4, CYP2E1 with concurrent reductions in PXR, and CAR (Legendre *et al.*, 2009). Yu and colleges using a rat model for intermittent hypoxia with emphysema reported inflammatory cytokines activated NF- $\kappa$ B in the liver, reducing the transcription of PXR and CAR and reducing their translocation into the nucleus with the consequence of suppressed CYP3A transcription (Yu *et al.*, 2017). PHD (Prolyl hydroxylases) are enzymes whose activity is modulated by substrates such as oxygen and a number of co-factors. In normoxia, hypoxia-inducible factor (HIF1)- $\alpha$  is rapidly degraded via the ubiquitin-proteasome pathway and which involves the action of PHDs to label (hydroxylate) the HIF1- $\alpha$  for this degradation. PHD inhibitors stabilise HIF-1 $\alpha$  even in normoxia (i.e., mimic the effect of hypoxia) and hence promote HIF-1 $\alpha$  translocation to the nucleus and it action to affect the transcription of target genes. Takano *et al.* studied the impact of PHD inhibitors in normoxic human hepatocytes, and found the inhibitor suppressed gene expression of CYP3A4, CYP2B6 which was correlated with the suppression of both PXR, CAR, and the suppression of the nuclear family member retinoid X receptor (RXR); retinoids are recognised to induce certain CYP450s via transactivation of RXR. The authors linked the decrease in CYP450 through HIF-1 $\alpha$  stabilisation to the decreases in CAR, PXR, and RXR (Takano *et al.*, 2021).

In addition to PXR and CAR, several other nuclear receptors have been implicated in the regulation of CYP3A4 under hypoxic conditions. Hepatocyte nuclear factor 4 alpha (HNF4 $\alpha$ ), peroxisome proliferator-activated receptor alpha (PPAR $\alpha$ ), and vitamin D receptor (VDR) are among the nuclear receptors that have demonstrated involvement in the regulation of CYP3A4 expression.

HNF4 $\alpha$  has been found to be closely associated with the expression of the CYP3A4 gene in the adult liver, suggesting its prominent role in regulating the basal expression of CYP3A4 (He *et al.*, 2016). Interestingly, studies have observed a reduction in HNF4 $\alpha$  gene expression in HepG2 cells subjected to severe hypoxia. This decrease in HNF4 $\alpha$  gene expression coincides with a significant decline in HNF4 $\alpha$  protein levels, resulting in weakened DNA-binding activity within the HepG2 cells. The precise mechanism underlying the inhibition of the HNF4 $\alpha$  gene by hypoxia remains unclear. While potential binding sites for HIF-1 (hypoxia-inducible factor 1) have not been identified in the promoter region of the HNF4 $\alpha$  gene, studies have detected three potential HIF-1 binding sites in the 3' untranslated region (UTR) and a putative hypoxia response element (HRE) in various introns (Mazure, Trong and Danan, 2001). Further investigations are necessary to unravel the intricate molecular pathways involved in the hypoxia-induced suppression of the HNF4 $\alpha$  gene and its consequent impact on CYP3A4 expression.

PPAR $\alpha$ , also known as NR1C1, is predominantly expressed in the liver and plays a crucial role as a primary sensor in regulating various biological processes such as lipid homeostasis, energy metabolism, immune modulation, and inflammatory responses (Wahli and Michalik, 2012; Yuan *et al.*, 2020). By forming a heterodimer with RXR $\alpha$ , PPAR $\alpha$  binds to specific DNA regions called PPAR $\alpha$  response elements.

A research study focused on the human hepatic CYP3A4 gene identified three functional PPAR $\alpha$ -binding regions (PBR-I, -II, and -III) located within a 12 kb region upstream of the gene (Thomas *et al.*, 2013). This discovery established a direct association between PPAR $\alpha$  and the transcriptional regulation of CYP3A4 in hepatocytes. Furthermore, evidence supports the notion that PPAR $\alpha$  serves as a novel genetic determinant for the CYP3A4 gene. The significance of this relationship was reinforced by shRNA-mediated knockdown experiments targeting the PPAR $\alpha$  gene in primary human hepatocytes, which resulted in a substantial reduction of over 50% in CYP3A4 expression levels (Klein *et al.*, 2012).

In conditions characterised by hypoxia, such as low oxygen levels, the expression of PPAR $\alpha$  in the liver is known to be down-regulated through mechanisms involving hypoxia-inducible factors (HIFs) (Li *et al.*, 2017). Similarly, during severe hypoxia in rat ventricular cardiac myocytes incubated in an environment containing 95% nitrogen and 5% carbon dioxide, the binding activity of peroxisome proliferator-activating receptor alpha (PPAR $\alpha$ ) with RXR $\alpha$  is diminished due to a reduction in RXR $\alpha$  expression (Huss, Levy and Kelly, 2001).

The vitamin D receptor (VDR) is primarily located within the cytosol of cells that exhibit sensitivity to vitamin D<sub>3</sub>. Upon binding of 1,25-D<sub>3</sub> to VDR, a complex is formed, which subsequently forms a heterodimer with RXR. This complex translocates to the cell nucleus, where it binds to specific DNA sequences known as vitamin D responsive elements (VDREs). Consequently, the transcriptional activity of relevant genes is either activated or repressed (Qin and Wang, 2019). Notably, the CYP3A4 gene can be induced by 1,25-(OH)<sub>2</sub>D<sub>3</sub> through the activation of VDR, as observed in both HepG2 cells and normal differentiated primary human hepatocytes (Drocourt *et al.*, 2002; Elizondo and Medina-Díaz, 2003).

An important observation is the shared presence of similar responsive elements, namely ER6, DR3 (dNR1), and DR4 (eNR3A4), within the promoter region of the CYP3A4 gene for both VDR and PXR (Pavek *et al.*, 2010; Qin and Wang, 2019). This finding suggests a potential functional connection between these transcription factors. It has been demonstrated that the expression of VDR is down-regulated in human endothelial cells exposed to a hypoxic mimicking environment through CoCl<sub>2</sub> treatment (Zhong *et al.*, 2014). This down-regulation aligns with the similar decrease observed in placental trophoblasts (Ma *et al.*, 2012).

Furthermore, it is worth noting that the formation of a heterodimer between VDR and RXR is required for their activation, a requirement that is also shared by PXR and CAR and PPAR $\alpha$ . This highlights the possibility of interplay and potential interference among these four transcriptional factors under hypoxic condition.

#### **5.1.4 MAPK/ ERK and the regulation of PXR nuclear receptor and CYP450**

The extracellular signal-regulated kinase 1/2 (ERK) belongs to the mitogen-activated protein kinase (MAPK) family, which plays a central role in transducing extracellular signals to intracellular targets. The MAPK cascades, of which ERK is a crucial member, are pivotal signaling elements that regulate fundamental cellular processes, including cell proliferation, differentiation, and stress responses (Roskoski, 2012; Guo *et al.*, 2020). Various stimuli, such as cytokines, viruses, ligands of G-protein-coupled receptors, mitochondrial reactive oxygen species (ROS), and, in some reports, hypoxia, exert regulatory control by activating the ERK/MAPK signaling pathway (Minet *et al.*, 2000a; Jones and Bergeron, 2004; Osorio-Fuentealba *et al.*, 2009; Bhagatte, Lodwick and Storey, 2012; Schroyer *et al.*, 2018; Guo *et al.*,



2020). These stimuli modulate the activation of ERK/MAPK, thereby influencing downstream signaling events and cellular responses. The activation of the ERK/MAPK pathway can be achieved through distinct mechanisms including  $\text{Ca}^{2+}$  activation, receptor tyrosine kinases, notably Ras, provide another mode of activation. Ras activation initiates a cascade of signaling events, culminating in ERK activation. Protein kinase C (PKC)-mediated activation represents an additional mechanism by which the ERK/MAPK pathway can be stimulated. Lastly, G protein-coupled receptors, a diverse class of cell surface receptors, can activate the pathway and initiate ERK signaling (Guo *et al.*, 2020).

The activation of ERK can have direct phosphorylation effects on various nuclear receptors, typically occurring at serine and threonine residues surrounded by proline. This post-translational modification plays a significant role in regulating transcriptional processes, resulting in either positive or negative regulation of gene expression (Zassadowski *et al.*, 2012). In the case of human PXR, Lichti-Kaiser *et al.* (2009) conducted an in-silico study and identified serine 350 as a potential site for direct phosphorylation by a MAPK. However, it has been reported that the direct phosphorylation of PXR can exert negative effects on its transcriptional activity. This negative impact can manifest in multiple ways. Firstly, the phosphorylation event can induce alterations in the subcellular localisation pattern of PXR. This change in localisation can disrupt the appropriate interaction of PXR with corepressors or coactivators, which are crucial for modulating its transcriptional activity (Wang *et al.*, 2012). Additionally, direct phosphorylation of PXR can impair its ability to form heterodimers with retinoid X receptor  $\alpha$  (RXR $\alpha$ ), thereby interfering with the functional regulation of target genes (Wang *et al.*, 2012).

As mentioned earlier, the PXR pathway plays a pivotal role in governing drug-metabolising enzymes, such as CYP3A4 and CYP2C9. Notably, stimuli such as hypoxia, ROS, and cytokines have been identified as activators of the MAPK/ERK signaling pathway, which has been associated with detrimental effects on the transcriptional activity of PXR. Therefore, it is important to explore the potential connection between PXR and the downregulation of CYP450 enzymes in hypoxic conditions, particularly with regards to the involvement of the ERK signaling pathway. However, it is important to acknowledge the scarcity of studies that have specifically investigated this association under hypoxic conditions. Although a limited number of reports conducted under normoxic conditions have suggested a potential positive influence of inhibiting the ERK pathway on the regulation of CYP450 enzymes. Smutny and colleagues treated HepG2 cell and primary human hepatocytes with U0126, MEK1/2 inhibitor which is

upstream kinases of ERK1/2 and found an induction in CYP3A4, CYP3A5 and CYP3A7 mRNA expression (>100-fold) in HepG2 cells and CYP3A4 mRNA expression in primary human hepatocytes. The induction of CYP genes by U0126 was specific to certain genes and sensitive to a transcriptional inhibitor. Gene reporter assays revealed that U0126 activates a CYP3A4 promoter construct containing PXR response elements (PXREs), and this induction is dependent on intact PXREs. U0126 was identified as an atypical ligand for the nuclear receptor PXR and was found to up-regulate the expression of several nuclear receptors includes HNF4 $\alpha$ , CAR, VDR and PXR while down-regulating the expression of the corepressor small heterodimer partner (SHP). The study highlights the potential of U0126 as a selective inducer of CYP3A genes in HepG2 cells through direct activation of PXR and indirect down-regulation of SHP (Smutny *et al.*, 2014).

### 5.1.5 Aim and Objectives

The primary aim of this chapter is to further investigate the mechanisms underlying the decrease in CYP3A4 and CYP2C9 activity caused by hypoxia, expanding upon the findings from Chapter 4 and 5. Specifically, this exploration will focus on examining the role of oxidative stress, inflammatory mediators, and the nuclear transcription factor PXR. Moreover, a novel aspect of this study is the investigation of the potential involvement of the MAPK/ERK pathway as a signaling pathway responsible for the downregulation of PXR, CYP3A4, and CYP2C9 under hypoxic conditions. This research aims to shed light on these mechanisms and their interplay, providing valuable insights into the impact of hypoxia on drug metabolism.

#### **Objectives:**

**1. Investigate the nature and magnitude of reactive oxygen species generated as a result of hypoxia and explore how modulation of ROS influences CYP3A4/CYP2C9 expression.**

This objective performed in HepaRG cells under normoxia and hypoxia measured ROS levels, modulation of ROS by specific interventions e.g. anti-oxidants and quantified the impacts on CYP3A4/CYP2C9 mRNA expression (qRT-PCR), protein level (Western blot) and functional activity (P450-Glo™ assay).

**2. Investigate the nature and magnitude of inflammatory mediators generated as a result of hypoxia (1% O<sub>2</sub>), as well as the influence of such mediators directly applied to the cell model upon CYP3A4/CYP2C9.**

This objective performed in HepaRG cells under normoxia and hypoxia evaluated the mRNA expression of pro-inflammatory cytokines (qRT-PCR) and the cellular response to the application of exogenously applied cytokines (TNF- $\alpha$  and IL-6) with quantification of the impacts on CYP3A4/CYP2C9 mRNA expression (qRT-PCR), protein level (Western blot).

### **3. Investigate the involvement of the MAPK/ERK signaling pathway in the hypoxia-induced downregulation of CYP3A4 and CYP2C9 via the nuclear receptor PXR.**

This objective performed in HepaRG cells under normoxia and hypoxia quantified the expression of ERK1/2 and nuclear receptors PXR (Western blot), and the impact of modulating the MEK/ERK pathway and assessing the expression of PXR, CYP3A4 and CYP2C9 (Western blot).

## **5.2 Methods**

### **5.2.1 Cell culture and treatments**

HepaRG cells were differentiated following the standard protocol (detailed in **chapter 2, section 2.1.2**) and treated with 10 ng/mL IL-6 for 72 h or 10 ng/mL TNF- $\alpha$  for 24 h (all from Peprotech; 20006 / 30001A) under normoxia (21 % O<sub>2</sub>, 5% CO<sub>2</sub> and 37°C). Menadione (Sigma Aldrich; M5750) was employed as a ROS inducer in the ROS assays, while N-acetylcysteine (NAC) (Sigma Aldrich; A7250) and Tiron (1,2-dihydroxybenzene-3,5-disulfonate) (Abcam; ab146234) were utilised as ROS scavengers. The MEK1/2 inhibitor PD98059 (Cell Signaling; 9900) was used for MEK/ERK pathway studies with working concentrations ranged from 5 to 50  $\mu$ M. Hypoxic conditions were achieved by incubating cells in a hypoxia chamber (Baker Ruskinn PhO2x box) with 5% CO<sub>2</sub> and 1% O<sub>2</sub> balanced with N<sub>2</sub> at 37°C.

### **5.2.2 Primer design and Quantitative Real-Time Reverse Transcription PCR (qRT-PCR)**

The primer design and the qRT-PCR are detailed in **sections 2.4 of Chapter 2**.

### 5.2.3 Western blot

Protein lysis and quantification, Western blot, and associated antibodies were described in **sections 2.5 of Chapter 2.**

### 5.2.4 Cell viability

The cell viability was accessed by CellTiter-Glo<sup>®</sup> Luminescent assay- detailed in **Chapter 2 section 2.3.2**- or Presto Blue<sup>™</sup> assay. HepaRG cells were seeded at a density of 9000 cells/well in 96-well black side/clean bottom plates (Greiner; 655087) and allowed to grow and differentiate for one month, following the standard protocol. Cells were treated with different concentrations of menadione or TNF- $\alpha$  for 24 h, IL-6 for 72 h, NAC or Tiron for 48 h, or PD98059 for 25 h. Control cells were cultured in standard media without treatment. Media without cells was used as a blank. After treatment, cell viability was accessed.

The PrestoBlue assay has gained widespread recognition within the academic and research communities owing to its utilisation of resazurin-based solutions that are permeable to cellular membranes. This popularity is primarily attributed to its exceptional sensitivity, safety, simplicity, and flexibility concerning measurement techniques. Moreover, a notable advantage of this assay is its broad applicability, extending to the examination of various cell types, including mammalian, bacterial, plant, and fish cells. These assays are designed to assess the enzymatic and irreversible reduction of resazurin to resorufin by metabolically-active cells. The quantity of resorufin produced as a result of cell incubation with resazurin is directly correlated to the number of viable cells and can be quantified either through colometric or fluorometric methods. However, among these options, fluorescence detection is considered the method of choice, as it provides the necessary level of sensitivity required for accurate and precise measurements of cell viability (Luzak, Siarkiewicz and Boncler, 2022).

The Presto Blue cell assay (Invitrogen; A13261) was performed according to the manufacturer's guidelines. In summary, 10  $\mu$ l of 10x Presto Blue reagent was diluted with 90  $\mu$ l of standard culture media and added directly to each well containing the cells. The cells were then incubated for 1 h under standard culture conditions at 37°C, while being protected from light. Subsequently, the fluorescence intensity was measured using a microplate reader (Infinite 200 PRO; Tecan) equipped with standard fluorescence filter sets (excitation=560 nm, emission=590 nm).

### **5.2.5 H<sub>2</sub>O<sub>2</sub> measurement assay (ROS-Glo H<sub>2</sub>O<sub>2</sub> assay)**

HepaRG cells were seeded at a cell density of 9000 cells/well in 96-well white side/clean bottom plates (Nunc™; 10158721) and allowed to grow and differentiate for one month, following the standard protocol. ROS-Glo H<sub>2</sub>O<sub>2</sub> assay (Promega; G8820) was used to measure ROS by monitoring the production of hydrogen peroxide (H<sub>2</sub>O<sub>2</sub>) as various ROS converting into H<sub>2</sub>O<sub>2</sub> inside the cells as end product. The cells were exposed to either 21% O<sub>2</sub> or 1% O<sub>2</sub> (5 % CO<sub>2</sub>, 37°C) for 24 h, then incubated with H<sub>2</sub>O<sub>2</sub> substrate solution for 6 h (20 µl H<sub>2</sub>O<sub>2</sub> substrate solution and 80 µl of media in each well). After that, 100 µl of ROS-Glo detection solution was added to each well and incubated for 20 min at room temperature. This detection solution also is lytic such that all H<sub>2</sub>O<sub>2</sub> is released into the media. Upon the introduction of ROS-Glo™ Detection Reagent comprising Ultra-Glo™ Recombinant Luciferase and d-cysteine, the precursor undergoes a transformative process facilitated by d-cysteine, resulting in the conversion of the precursor into luciferin. Subsequently, the produced Luciferin engages in a chemiluminescent reaction with Ultra-Glo™ Recombinant Luciferase, yielding a luminescent signal that corresponds to the concentration of H<sub>2</sub>O<sub>2</sub>; the luminescence recorded using a microplate reader (Infinite® 200 PRO; Tecan).

### **5.2.6 Total ROS detection (Total ROS detection Kit)**

Total oxidative stress derived from HepaRG cells cultured under hypoxia were measured by total ROS Detection Kit (Enzo Life Science, 51010). This kit enables the detection of peroxynitrite (ONOO<sup>-</sup>), hydroxyl radical (·OH), nitric oxide (·NO), and peroxy radicals (ROO<sup>·</sup>) using a DCF-DA probe that interacts with a wide spectrum of ROS/RNS to produce a green fluorescent product. Briefly, HepaRG cells were seeded at a density of 9000 cells/well in 96-well black side/clean bottom plates (Greiner, 655087) and allowed to grow and differentiate for one month following the standard protocol. The Oxidative Stress Detection reagent (green) was used to measure ROS. This reagent is cell permeable and crosses the outer mitochondrial membrane. It becomes fluorescent upon reaction with the above listed ROS molecules. The ROS detection mix was prepared by adding 4 µl of the oxidative stress detection reagent in 10 mL of culture medium (w/o serum). A 100 µl aliquote of the ROS detection mix was then added to each well and the cells were cultured under either hypoxia (1% O<sub>2</sub>, 5% CO<sub>2</sub>, at 37 °C) or normoxia (21% O<sub>2</sub>, 5% CO<sub>2</sub>, at 37°C) for 24 h. Plates were read (bottom reading) after 24 h

incubation without removing the detection mix, using a microplate reader (Infinite® 200 PRO; Tecan). Standard fluorescein (excitation=490 nm, emission=528 nm) filter sets were used.

### **5.2.7 Mitochondrial superoxide measurement (MitoSOX assay).**

MitoSOX was created by combining the triphenylphosphonium ion (TPP<sup>+</sup>), a lipophilic cation known for its ability to accumulate different cargo molecules into the negatively-charged mitochondrial matrix, with dihydroethidium. Dihydroethidium is an existing probe utilised for detecting superoxide within cells. Upon oxidation by superoxide, dihydroethidium undergoes a transformation into the specific oxidation product known as 2-hydroxyethidium (Roelofs *et al.*, 2015). HepaRG cells were seeded in 24-well plates at a density of 5500 cells /well and cultured for a total of four weeks, involving two weeks of growth followed by an additional two weeks of differentiation, adhering to the established protocol. Subsequently, differentiated cells were subjected to a hypoxic environment (1% O<sub>2</sub>, 5% CO<sub>2</sub>, 37°C) for a duration of 24 h. To assess mitochondrial superoxide levels, MitoSOX Red (M36008, Invitrogen) dye was employed as the indicator.

A stock solution of the MitoSOX reagent was prepared by dissolving 50 µg of MitoSOX in 13 µl of dimethylsulfoxide (DMSO) to create a 5 mM MitoSOX reagent stock. From this stock, a 5 µM MitoSOX reagent working solution was prepared in HepaRG media without phenol red and fetal bovine serum (FBS). Subsequently, the cells were exposed to the 5 µM MitoSOX reagent working solution for 30 min, under two distinct conditions: normoxia (21% O<sub>2</sub>) and hypoxia (1% O<sub>2</sub> for 24 h). Following the incubation period, MitoSOX was removed, and the cells were washed thrice with warm HepaRG media, free from FBS and phenol red. The fluorescent images were acquired using Confocal microscopy (Leica TCS SP5), and ImageJ software was employed for subsequent analysis.

In addition, an alternative assessment method using a plate reader was employed to quantify the fluorescent signal indicative of superoxide production. HepaRG cells were seeded in black transparent-bottom 96-well plates at a density of 9000 cells /well and cultured for a total of four weeks, including two weeks of growth followed by two weeks of differentiation. Subsequently, the cells were incubated with the 5 µM MitoSOX reagent working solution for 30 min, and after two washes with media devoid of phenol red or FBS, the fluorescent signal

was measured using bottom reading in an Infinite 200 PRO Tecan microplate reader. Standard fluorescein filter sets (excitation=510 nm, emission=580 nm) were employed for this purpose. The MitoSOX fluorescent signal was normalised to the protein content in each well, determined through the Pierce BCA method.

**Figure 5.3** shows a summary of the three assays used to measure the different ROS species.

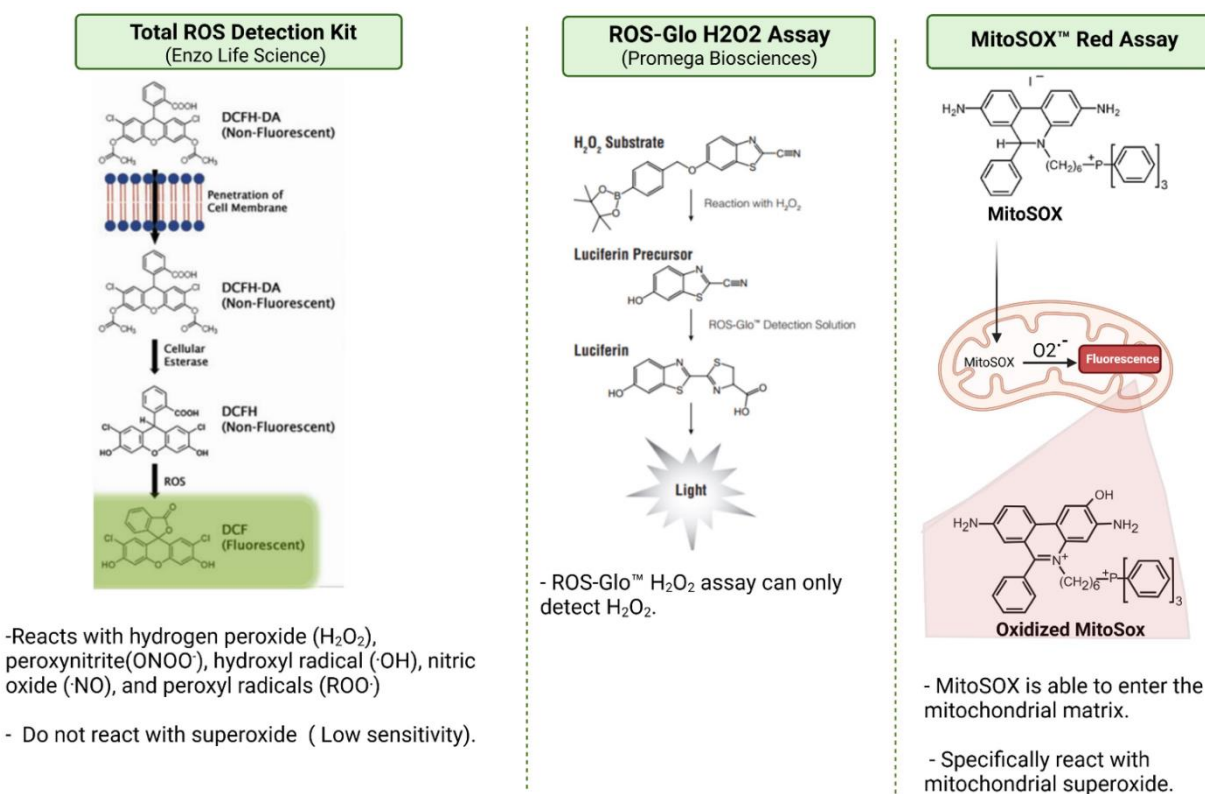


**Figure 5.3** Summary of different assays used to measure ROS.

## 5.2.8 Statistics

All data analyses were carried out using GraphPad Prism 5 (GraphPad Software, San Diego, CA). All experiments were performed with three to twelve technical replicates from a minimum of three independent biological experiments. Results were expressed as mean  $\pm$  SEM. The normality of the data was tested using Shapiro-Wilk test. If the data pass the normality test ( $P$  value  $> 0.05$ ), One-way ANOVA were performed. If the data did not pass the normality test, Kruskal-Wallis followed by Dunn's test were used. Samples with two groups only were compared using unpaired t-test if its normally distributed or with Mann-Whitney U-

test if not pass the normality test. In all cases, data was considered significant when P-value < 0.05.

## 5.3 Results and Discussion

In **Chapter 4**, we demonstrated that acute hypoxia decreased CYP3A4 and CYP2C9 expression in our hepatocyte model HepaRG. Here the mechanism(s) by which CYP3A4 and CYP2C9 regulation may be altered under hypoxia are explored. The mechanisms to be explored involved activation of ROS and RNS (reactive nitrogen species) and inflammatory mediators, as well as examining the MAPK/ERK signalling pathway, a putative mechanism responsible for hypoxia-induced dysregulation of CYP450.

### 5.3.1 Effect of acute hypoxia on REDOX generation

The impact of hypoxia upon ROS production was investigated using three different assays.

- **ROS-Glo H<sub>2</sub>O<sub>2</sub>** a luminescence-based assay specifically detecting hydrogen peroxide (H<sub>2</sub>O<sub>2</sub>).
- **Total ROS detection kit** a fluorescence molecular probe assay for the detection a wide range of ROS/RNS including peroxynitrite (ONOO<sup>-</sup>), hydroxyl radical (<sup>•</sup>OH), nitric oxide (<sup>•</sup>NO), H<sub>2</sub>O<sub>2</sub> and peroxy radicals (ROO<sup>•</sup>).
- **MitoSox assay** a fluorescence-based assay specifically detecting mitochondrial superoxide radical (O<sub>2</sub><sup>•-</sup>).

**Figure 5.4** shows H<sub>2</sub>O<sub>2</sub> production (ROS-Glo H<sub>2</sub>O<sub>2</sub> assay) in HepaRG cells exposed to hypoxia (1% O<sub>2</sub>) for 4, 6, and 24 h. Within the HepaRG cells hypoxia induced significant decreases (>75% decreases) in H<sub>2</sub>O<sub>2</sub> levels at all the studied time points compared of cells maintained under normoxia. The assay used in Figure 6.4 is lytic in nature and therefore detects H<sub>2</sub>O<sub>2</sub> levels from intracellular as well as extracellular sources. H<sub>2</sub>O<sub>2</sub> is the most stable of the ROS species.

Changes in H<sub>2</sub>O<sub>2</sub> levels may be viewed as indicative of general alterations in the ROS levels within the cellular environment. For example, H<sub>2</sub>O<sub>2</sub> can rapidly diffuse across cellular membranes including plasma membranes and subcellular organelles (Winterbourn, 2013). The permeability of H<sub>2</sub>O<sub>2</sub> across membranes is influenced by the composition of the membrane such as lipid rafts, by mechanical changes in the membrane such as those resulting from



osmotic stretching of lipid bilayers and via membrane proteins that facilitate  $\text{H}_2\text{O}_2$  diffusion, including aquaporins (Bienert, Schjoerring and Jahn, 2006; Lennicke *et al.*, 2015); it has been demonstrated that human aquaporin 8 (AQP8) enables the passage of  $\text{H}_2\text{O}_2$  through membranes (Marchissio *et al.*, 2012).

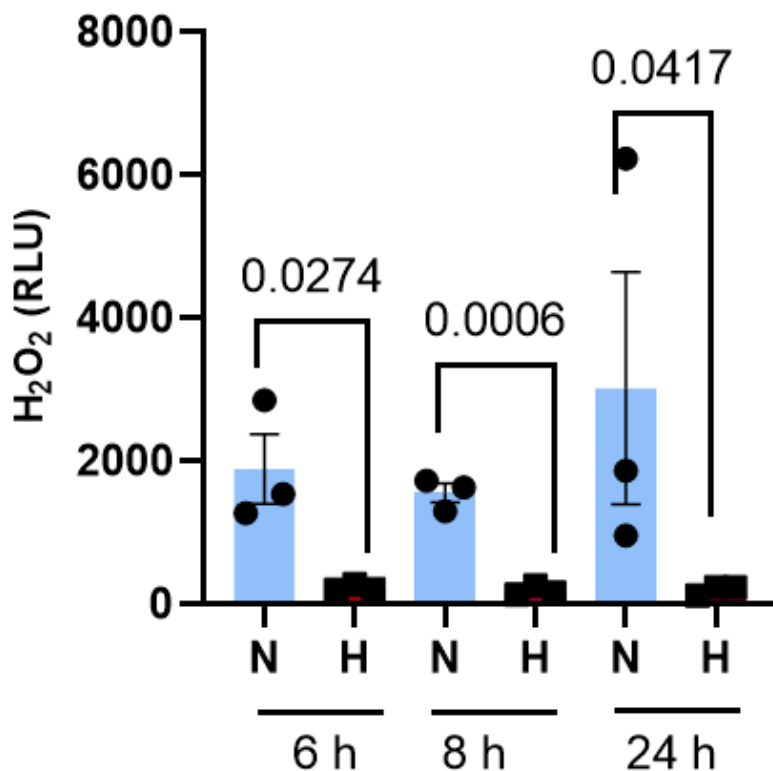


**Figure 5.4 Impact of hypoxia upon  $\text{H}_2\text{O}_2$  generation.** HepaRG cells were differentiated following the standard protocol. After differentiation cells were exposed to hypoxic conditions (1%  $\text{O}_2$ ; H - black bars) for 6, 8 or 24 h and the  $\text{H}_2\text{O}_2$  level were measured by ROS-Glo  $\text{H}_2\text{O}_2$  assay. Cells cultured under normoxia (21%  $\text{O}_2$ ; N - blue bars) were used as a control. This assay is lytic and hence measures total  $\text{H}_2\text{O}_2$  intracellular and extracellular. Bars represent mean  $\pm$  SEM. N=3 independent experiments with at least six replicates each experiment. Statistics by One-way ANOVA test.

Moreover, the phosphorylation and glycosylation states of membrane proteins also impact the membrane permeability of  $\text{H}_2\text{O}_2$  (Lennicke *et al.*, 2015).  $\text{H}_2\text{O}_2$  serves as a common transformation product for a range of ROS molecules. For instance, superoxide dismutase (SOD) enzymatically converts superoxide into  $\text{O}_2$  and  $\text{H}_2\text{O}_2$  (Andrés *et al.*, 2022) (Figure 6.1).

**Figure 5.5** shows the results using the Total ROS detection assay, which measures  $\text{H}_2\text{O}_2$  and other radicals including peroxynitrite, hydroxyl radical, nitric oxide and peroxy radicals. Again, this data shows a significant reduction in ROS levels after 24 h of hypoxia conditions with the decreases in ROS paralleling the decreases in oxygen levels. When compared to cells

cultured in normoxia (21% O<sub>2</sub> = 1452 ±107 RFU) the hypoxia challenge (1% O<sub>2</sub> = 949 ±24.6 RFU) reduced ROS levels by 35%.

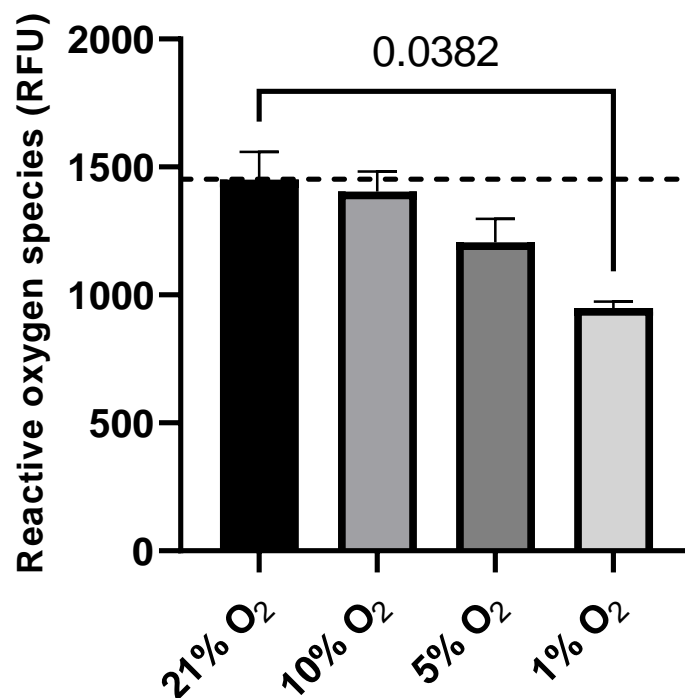


**Figure 5.5 Impact of hypoxia upon ROS production in HepaRG cells.** HepaRG cells were differentiated following the standard protocol. After differentiation cells were subjected to different levels of hypoxia (10%, 5% or 1% O<sub>2</sub>; grey bars) for 24 h and ROS measured using total ROS detection Kit. HepaRG Cells culture under normoxia (21% O<sub>2</sub>; black bar) were used as a control. Bars represent mean ± SEM. N=3 independent experiments with at least six replicates each experiment. Statistics by Kruskal Wallis and post hoc Dunn's test.

Both the **Figures 5.4** and **5.5** show a decrease in cellular ROS levels under hypoxia. Fandrey and colleagues had earlier reported the endogenous production of H<sub>2</sub>O<sub>2</sub> in HepG2 cells to be decreased in cells under hypoxia (Fandrey, Frede and Jelkmann, 1994). Extracellular H<sub>2</sub>O<sub>2</sub> levels in bovine pulmonary artery endothelial cells subjected to hypoxia (3% O<sub>2</sub> for 2 h) have also been shown to be 30% lower than in normoxia (20 % O<sub>2</sub>) (Zulueta *et al.*, 1995). Hypoxia exposure (1% O<sub>2</sub>) of an acute short term nature (20 min) through to a more prolonged (72 h) duration leads to significant reductions in intracellular ROS levels in skin fibroblasts by up to 75% (Sgarbi *et al.*, 2017). Similarly, brief exposure of fibroblasts or 143B osteosarcoma cells to low oxygen levels, as low as 0.5% for 20 min, results in reductions in ROS levels which progressively declined as the hypoxia was extended over 24 h (Sgarbi *et al.*, 2018). Many other researchers have reported in various cell types similar reductions in ROS production under hypoxia, primarily originating from the mitochondrial electron transport chain. For example,

in vascular smooth muscle cells (Waypa *et al.*, 2010), in human fibrosarcoma and human lung cells (Tuttle *et al.*, 2007).

There are, however, contrasting findings which show an increase in ROS levels upon exposure to acute hypoxia. Chandel *et al.* explored how hypoxia may activate the transcription of erythropoietin, glycolytic enzymes, and vascular endothelial growth factor. They reported hypoxia (1.5% O<sub>2</sub>) in Hep3B hepatoma cells leads to transcriptional activation via a mitochondria-dependent signalling process involving increased ROS. Fundamentally, the depletion of mitochondrial DNA in these cells led to an inability to generate ROS following hypoxia exposure, thereby implicating the indispensability of intact mitochondria in the induction of hypoxia-stimulated ROS production (Chandel *et al.*, 1998). These authors also observed a diminished expression of genes targeted by hypoxia-inducible factor 1 (HIF-1) in mitochondria-depleted cells under hypoxic conditions, highlighting the involvement of ROS in HIF-1 $\alpha$  stabilisation. Similarly, hypoxia is reported to increase H<sub>2</sub>O<sub>2</sub> generation in rat aortic smooth muscle cells and relevant to the work Chandel *et al.*, inhibition of mitochondrial respiration with rotenone treatment resulted in reduced ROS levels (Sato *et al.*, 2005). Lluís *et al.* reported a rise in ROS levels in HepG2 cell and cultured rat hepatocytes exposed to 5% oxygen. The rise in ROS levels attenuated when mitochondrial complexes I and II were disrupted. These authors also demonstrated that targeted inhibition of mitochondrial glutathione (GSH), a peptide serving a protective function against oxidant-induced cell death, resulted in reduced cellular survival subsequent to hypoxia-induced ROS generation (Lluís *et al.*, 2005). In MCF7 breast cancer cells cultured in 3D spheroid configuration within a microfluidic device exposure to various low levels of O<sub>2</sub> (1% to 5%) for 3 h resulted in increases in intracellular production of ROS compared to cells maintained under normoxic conditions (20% O<sub>2</sub>) (Berger Fridman *et al.*, 2021).

Possible reasons for the discrepancy in the impact of acute hypoxia upon ROS levels may relate to the kinetics of response relative to sampling time, e.g. superoxide production is much greater in the initial minutes of hypoxia (Hernansanz-Agustín *et al.*, 2014, 2017), and there is some evidence that discrepancy in ROS measurements can be attributed to variations in the timing of the measurements taken (Hernansanz-Agustín and Enríquez, 2021). Variations in ROS measurements/responsiveness can also arise from the use of different experimental models, of diverse cell lines and different animal models, or different types of biological samples (tissues, blood, etc.). Models may also exhibit variations in cellular antioxidant capacity, metabolic adaptations, and cellular redox state, which all may influence ROS production. Furthermore,

the choice of measurement method can be critical. Different techniques like fluorescence-based probes, electron paramagnetic resonance (EPR) spectroscopy, and biochemical assays possess unique advantages, limitations, sensitivities/specificities.

**Figure 5.6.** shows the results of hypoxia in the HepaRG cells using the MitoSox assay which detects mostly mitochondrial superoxide radicals (Mukhopadhyay *et al.*, 2007). The results show an increase in fluorescent signal (an increase in superoxide radical) in the HepaRG cells subjected to hypoxia (1% O<sub>2</sub> for 24 h) (**Figure 5.6**). A previous study in myoblast cells exposed to 1% O<sub>2</sub> showed a similar increase in mitochondrial superoxide generation utilising this MitoSox assay (Zhou *et al.*, 2019).

The mechanism of hypoxia-induced mitochondrial superoxide production has recently been reviewed (Hernansanz-Agustín and Enríquez, 2021): Within the electron transport chain, specifically in complex I and complex III, superoxide is generated within the mitochondrial matrix. During the initial minutes of hypoxia, complex I undergoes an activation to deactivation transition, involving a conformational change in some of its component subunits. The transition characterises a dormant state of complex I, where it is unable to carry out its enzymatic activity and, therefore, cannot pump H<sup>+</sup> ions into the mitochondrial intermembrane space. As complex I becomes inactive during acute hypoxia, the mitochondrial matrix becomes more acidic due to an increase in H<sup>+</sup> ion levels. This acidity leads to the partial dissolution of calcium phosphate precipitates within the matrix. The H<sup>+</sup> ions react with phosphate ions (PO<sub>4</sub><sup>3-</sup>) in the calcium phosphate precipitates, forming more soluble compounds such as hydrogen phosphate (HPO<sub>4</sub><sup>2-</sup>) or dihydrogen phosphate (H<sub>2</sub>PO<sub>4</sub><sup>-</sup>) and releasing free Ca<sup>+2</sup> ions. The elevation in matrix Ca<sup>+2</sup> levels activates the mitochondrial Ca<sup>+2</sup>/Na<sup>+</sup> antiporter located in the inner mitochondrial membrane, facilitating the entry of Na<sup>+</sup> ions into the mitochondrial matrix. The accumulation of Na<sup>+</sup> in the matrix interacts with phospholipids of the inner leaflet of the mitochondrial intermembrane space. This interaction promotes the formation of phospholipid aggregates, reducing the fluidity of the mitochondrial intramembrane space. Consequently, the decrease in fluidity impairs the transfer of ubiquinol between complex II and complex III, leading to an uncoupling of the free Coenzyme (CoQ) cycle with the result that superoxide generation at complex III is promoted.

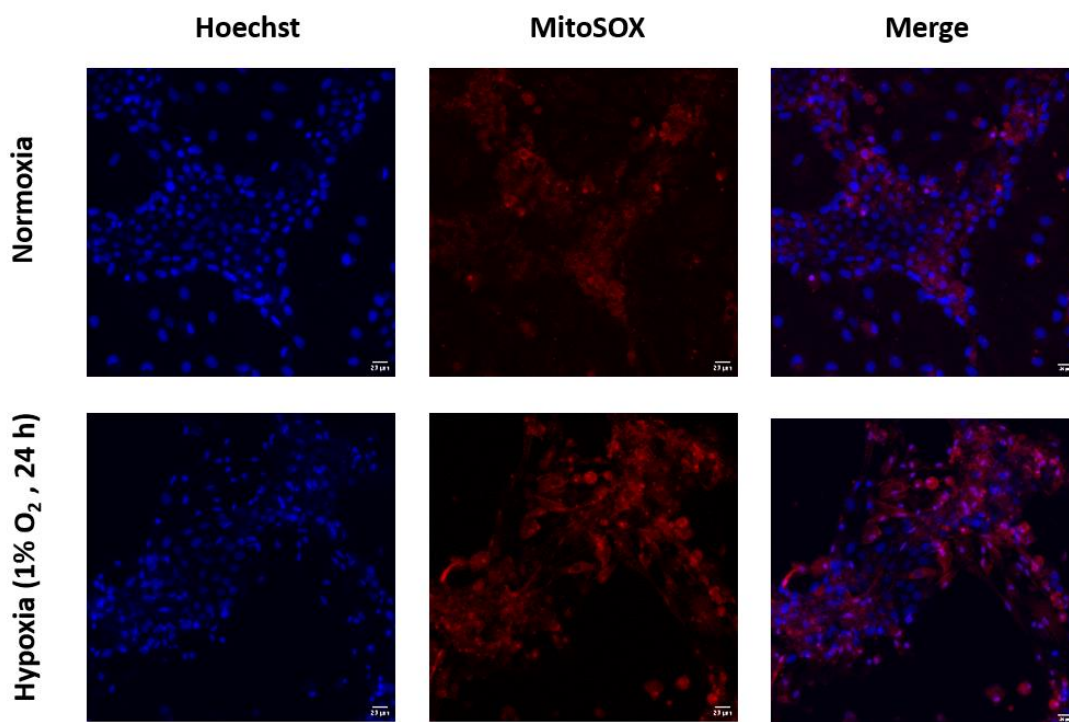


**Figure 5.6 Impact of hypoxia on mitochondrial superoxide radical generation in HepaRG cells.** HepaRG cells were differentiated following the standard protocol. Differentiated cells were exposed to 1% O<sub>2</sub> for 24 h. Cells cultured in standard conditions (21% O<sub>2</sub>) were used as a control. By Mitosox Red assay the superoxide radical generation in the mitochondria was measured and live cell imaging carried out using 40X magnification lens. Scale bar: 20 μm.

In these investigations the responsiveness of reactive oxygen species (ROS) to hypoxia did vary in direction, i.e. in Figures 5.4., 5.5. hypoxia reduced ROS, while in Figure 5.6. hypoxia increased ROS. Several potential explanations may be considered. The assays employed target distinct subcellular compartments, e.g. MitoSOX specifically quantifies superoxide radicals within the mitochondrial matrix, while the Total ROS and ROS-Glo assays measure ROS levels in various cellular compartments, encompassing the cytoplasm and other organelles. Variations in the localisation of ROS production and the sites of detection may contribute to the observed inconsistencies. It is important to acknowledge that the concentration of superoxide radicals in the mitochondrial matrix is estimated to be 5 to 10 times higher compared to the cytosol (Cadenas and Davies, 2000). Furthermore, certain assays may be susceptible to interference from other cellular components. For instance, sodium pyruvate, a salt derived from the conjugate anion form of pyruvic acid, is commonly included in commercially available cell culture media to enhance the cells' ability to metabolise glucose and generate energy. Studies have demonstrated that media containing pyruvate tend to exhibit reduced production of

hydrogen peroxide ( $H_2O_2$ ), likely due to the scavenging capacity of pyruvate towards  $H_2O_2$  (Long and Halliwell, 2009). Considering that pyruvate is a constituent of the William E medium employed for culturing our hepatocyte model (HepaRG cells), its potential scavenging effects could influence the measured levels of  $H_2O_2$ .

Hepatocytes can display distinct differences in ROS levels upon exposure to hypoxia; hepatocytes are classified into peri-portal (PP) and peri-venous (PV) subpopulations. In a study by Bhogal *et al.*, isolated human PV hepatocytes exhibited a notable increase in intracellular ROS accumulation during hypoxia (0.1%  $O_2$  for 24 h), as measured using the fluorescent probe 2',7'-dichlorofluorescein-diacetate. Conversely, isolated human PP hepatocytes did not exhibit an increase in intracellular ROS accumulation under the same hypoxic conditions. Numerous studies have identified the mitochondria as the main source of ROS during hypoxia. These authors inhibited mitochondrial complex I using rotenone, an inhibitor of this complex. They observed a significant reduction in ROS accumulation in PV hepatocytes exposed to hypoxia when mitochondrial complex I was inhibited by rotenone (Bhogal *et al.*, 2011). This discrepancy in ROS generation between PP and PV hepatocytes even in in-vitro likely attributed to variances in the concentration of the antioxidant glutathione between hepatocyte subpopulations. The PV hepatocytes possessing lower levels of intracellular glutathione compared to PP hepatocytes (Kera *et al.*, 1988). In the in-vivo context, it has also been shown that Kupffer cells located in the PV liver region are more prominently activated during ischemia, releasing ROS and causing hepatocyte damage. These collective findings suggest that the PV region of the liver serves as the primary site for hepatic inflammation and ROS generation during hypoxic liver injury (Taniai *et al.*, 2004).

Based on the aforementioned discussion, it is anticipated that superoxide, hydroxyl radicals, hydrogen peroxide, and peroxynitrite (formed from the reaction between superoxide and nitric oxide) will be present in all compartments of mitochondria, including the mitochondrial matrix, intermembrane space, and cytosol. The concentration of  $O_2^-$  in the mitochondrial matrix is estimated to be 5 to 10 times higher than in the cytosol (Cadenas and Davies, 2000). In experiments conducted with intact skeletal muscle mitochondria, it was observed that Complex III exhibited a direct release of  $O_2^-$  outside of the mitochondria matrix. However, measurements of hydrogen peroxide production indicated that this extramitochondrial release would only explain 50% of the total electron leak, even in mitochondria lacking the enzyme Superoxide dismutase-1 (SOD1), and enzyme that catalyses the dismutation of superoxide radicals to oxygen and hydrogen peroxide. The authors propose that the remaining 50% of the

electron leak is likely attributed to the release of O<sub>2</sub><sup>-</sup> into the mitochondrial matrix (Muller, Liu and Van Remmen, 2004).

In human studies the general consensus is that high-altitude hypoxia leads to a reduction in antioxidant activity, an increase in ROS production, and the subsequent induction of oxidative damage. A study utilising Electron Paramagnetic Resonance (EPR) showed acute (up to 72 h) and sub-acute (over 72 h) hypoxemia led to a significant 38% increase in ROS production in blood and urine from lowlander human subjects exposed to high altitude (3269 m) (Mrakic-Sposta *et al.*, 2021). Moreover, there was a 17% decrease in antioxidant capacity and oxidative damage to proteins, lipids, and DNA. Additionally, inflammatory markers, including IL-6 and neopterin concentration (an indicator of renal function), were found to be elevated (Mrakic-Sposta *et al.*, 2021).

The same laboratory reported a study in lowlander human subjects who had ascended to high altitude (5140 m). The subjects displayed a disturbance in redox status with increases in plasma/urine ROS levels (by 19%) and NO metabolites (by 28%). Indicators of oxidative damage, such as 15-F<sub>2</sub>t-IsoP, were elevated, as were markers of cellular immune system activation, e.g. urinary neopterin, pro-inflammatory prostanoid levels (including TXB<sub>2</sub>, PGE<sub>2</sub>, and 15-deoxy-delta<sup>12,14</sup>-PGJ<sub>2</sub>). Conversely, there was a downregulation of omega-3 polyunsaturated fatty acids (PUFAs) and anti-inflammatory CYP450 EPA-derived mediators, such as DiHETEs. The downregulation indicating a suppression of anti-inflammatory mechanisms at high altitudes (Mrakic-Sposta *et al.*, 2022).

### **5.3.2 Impact of menadione, NAC and Tiron on ROS generation in HepaRG Cells**

One objective of this chapter was to investigate the influence of ROS on CYP3A4 and CYP2C9. To assess this, ROS levels were manipulated using an inducer such as menadione or an antioxidant such as N-acetyl cysteine or Tiron.

Menadione (2-methyl-1,4-naphthoquinone) also known as vitamin K<sub>3</sub>, is a toxic quinone used experimentally for investigating mechanisms involved oxidative damage. It generates a large amount of intracellular superoxide anion by redox cycling. The process of redox cycling involves the one-electron reduction of oxidants, leading to the generation of ROS. Menadione metabolism induces the generation of ROS while concurrently depleting NAD(P)H levels

(Criddle *et al.*, 2006). Various reductive enzymes, such as microsomal NADPH-cytochrome P450 reductase and mitochondrial NADH-ubiquinone oxidoreductase (complex I), have the ability to metabolise quinones (inc. menadione) through one-electron reduction reactions. This process leads to the formation of unstable semiquinones, which can readily engage in redox cycling when molecular oxygen is present. Consequently, the quinones are regenerated, accompanied by the production of ROS. Menadione reduction at Complex I of the mitochondrial respiratory chain contributes to approximately 50% to menadione metabolism. This metabolism converts menadione to its reduced form, menadiol. This reduced form is typically conjugated with glutathione to produce inert metabolite that can be eliminated from the body. However, menadiol is not stable under oxidative conditions and quickly undergoes autoxidation at normal pH levels. This autoxidation process initially results in the formation of a semiquinone form ( $\text{MNSQ}^{\cdot-}$ ) through a one-electron oxidation reaction, which then reacts with oxygen to generate superoxide ( $\text{O}_2^{\cdot-}$ ) and hydrogen peroxide ( $\text{H}_2\text{O}_2$ ) (Baran *et al.*, 2010; Xing *et al.*, 2018).

N-acetyl cysteine (NAC) functions as a glutathione precursor; it penetrates cells, interacts, and detoxifies free radicals non-enzymatically. It is deacetylated to form cysteine, which promotes the synthesis of glutathione, one of the most important intracellular antioxidants, improving the activity of superoxide dismutase (SOD) (Cotgreave, 1996).

Tiron (1,2-dihydroxybenzene-3,5-disulfonate) is a vitamin E derivative that functions as a metal chelator as well as a direct hydroxyl radical ( $\cdot\text{HO}$ ) and superoxide ( $\text{O}_2^{\cdot-}$ ) scavenger (Krishna *et al.*, 1992).

**Figure 5.7.** shows initial experiments to determine the optimum and non-toxic concentration of menadione in HepaRG cells ahead of menadione use to induce ROS as part of a series of experiments examining possible mechanisms underpinning ROS impact on CYP450 expression. HepaRG cells were treated with menadione at 2.5  $\mu\text{M}$  to 2000  $\mu\text{M}$  concentrations for 24 h. Menadione concentrations up to 50  $\mu\text{M}$  did not affect the viability of HepaRG cells as judged by the Presto Blue assay which relies on the reductive metabolism of the cell to reduce resazurin to resorufin (see section 6.2.4). Concentrations at 100  $\mu\text{M}$  or more showed a loss of cell viability. This preliminary work identified concentration of 25  $\mu\text{M}$  or 50  $\mu\text{M}$  menadione for use to induce the ROS in the HepaRG cells.



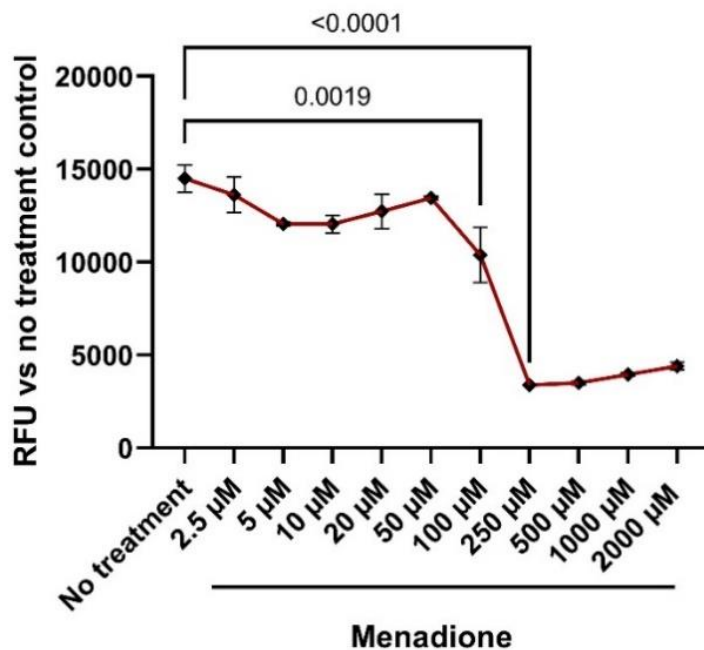


**Figure 5.7 Effect of menadione treatment on HepaRG viability.** HepaRG cells were differentiated following the standard protocol. After differentiation cells were treated with different concentration of menadione for 24 h at standard culture condition. Untreated cells were used as a control. By PrestoBlue assay the cell viability was determined. Black diamond represent mean  $\pm$  SEM. N=3 independent experiments with at least six replicates each experiment. Statistics by Kruskal-Wallis and post hoc Dunn's test.

Menadione treatment (50  $\mu$ M) was used to induce ROS in the HepaRG cells, confirmed by using the ROS-Glo  $H_2O_2$  and the MitoSox assays. **Figure 5.8A**, shows under normoxic conditions the menadione treatment considerably increases  $H_2O_2$  production (ROS-Glo  $H_2O_2$  assay) as early as 8 h after exposure and by up to 8-fold, with increases in ROS evident across the 24 h experiment; the ROS-Glo  $H_2O_2$  assay to assess the impact of menadione on ROS production was not applied under hypoxic conditions. Mostly due to the very significant decrease in the luminescent signal (ROS-Glo  $H_2O_2$  assay) observed in these cells during hypoxia (**Figure 5.4**.) The concern being the loss of sensitivity of the assay to accurately detect changes in ROS production ROS-Glo  $H_2O_2$  assay upon menadione exposure under low-oxygen conditions. Using the MitoSox assay under normoxia a clear increase in menadione-induced increase in superoxide was evident. With hypoxia and 'No Treatment' the most obvious outcome was that hypoxia appears to induce some superoxide compared to normoxia 'No Treatment'. The impact under hypoxia of menadione on superoxide generation is less clear (**Figure 5.8B**.), although there is a suggestion of a small increase from the qualitative assessment of the images.

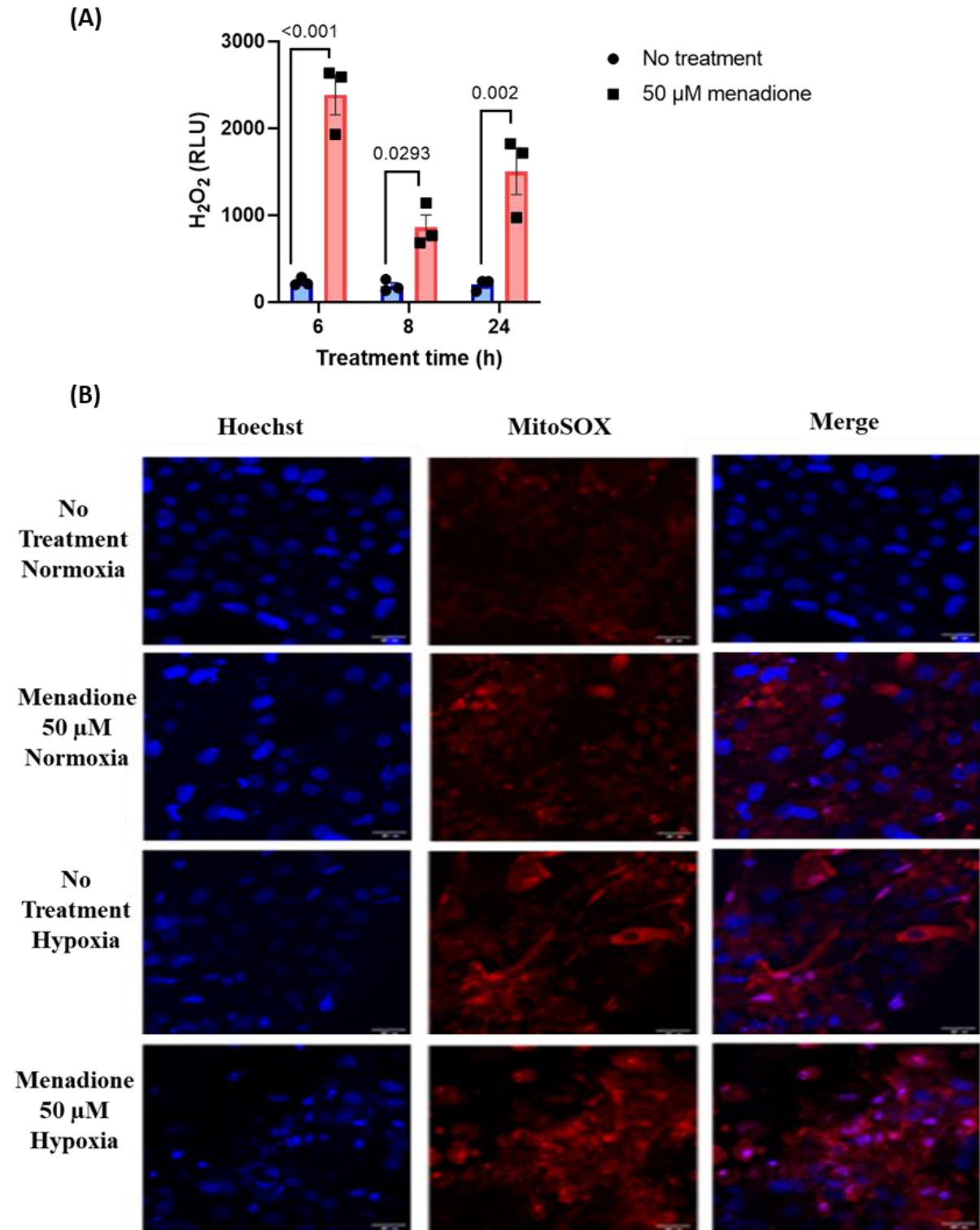


**Figure 5.8 Effect of menadione on  $H_2O_2$  and superoxide radical generation.** HepaRG cells were differentiated following the standard protocol. After differentiation cells were treated with 50  $\mu$ M menadione for 6, 8 or 24 h under normoxia (21%  $O_2$ ). By ROS-Glo  $H_2O_2$  assay  $H_2O_2$  generation was studied **Fig.5.8A**. Untreated cells were used as a respective control. Bars represent mean  $\pm$  SEM. N=3 independent experiments with at least six replicates each experiment. Statistics by One-way ANOVA and Bonferroni test. Differentiated cells were exposed to 1%  $O_2$  for 24 h or cultured in standard conditions (21%  $O_2$ ) and treated with 50  $\mu$ M menadione for 24 h. Untreated cells were used as a control. By Mitosox Red assay **Fig.5.8B** the superoxide radical generation in the mitochondria was measured and live cell imaging carried out using 40X magnification lens. Scale bar: 20  $\mu$ m.

Similar experiments ahead of examining possible mechanisms underpinning ROS impact on CYP450 expression were undertaken with the ROS scavengers, NAC and Tiron. First the cell viability was tested using the CellTiter Glo assay, an assay which uses ATP to estimate the number of viable cells. **Figure 5.9A** and **Figure 5.9B** show that NAC (10 mM) or Tiron (10 and 20 mM) treatment for 48 h under normoxic and hypoxic conditions (1% O<sub>2</sub>, 24 h), respectively, has no significant impact on HepaRG cell viability.

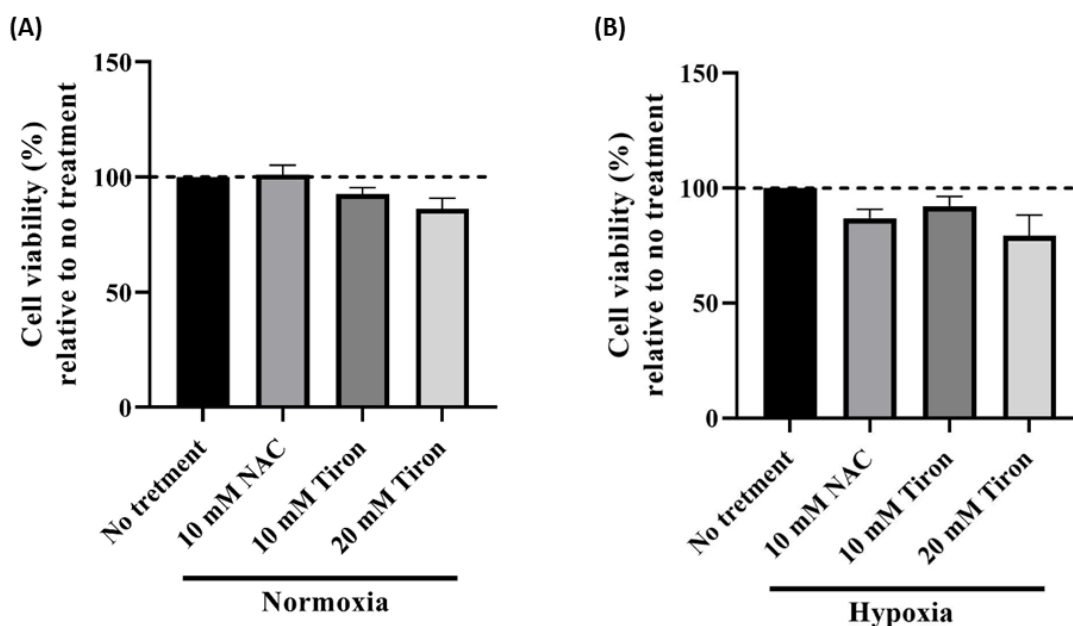


**Figure 5.9 Effects of NAC and Tiron treatment on HepaRG cell viability.** HepaRG cells were differentiated following the standard protocol. After differentiation cells were treated with 10 mM of NAC or 10 mM and 20 mM of Tiron, for 48 h at normoxic or hypoxic (1% O<sub>2</sub>, 24 h) conditions. Untreated cells were used as a control. By CellTiter Glo assay the cell viability was determined. Data presented as % relative to no treatment group. Bars represent mean  $\pm$  SEM. N=3 independent experiments with at least six replicates each experiment. Statistics by one way ANOVA and Bonferroni's post hoc test.

The efficacy of NAC as a ROS scavenger in HepaRG cells was investigated using the total ROS detection Kit. NAC treatment even at a concentration of 5 mM effectively reduces ROS levels in normoxic HepaRG cells (**Figure 5.10A**). Similarly, with lower oxygen levels, 10%, 5%, or 1% O<sub>2</sub>, NAC successfully scavenged ROS, to varying extents as shown in **Figure 5.10B**; but where the efficiency to scavenge ROS diminishes with reduced O<sub>2</sub> levels, reflecting an increasingly higher ROS burden in the cell under hypoxia.

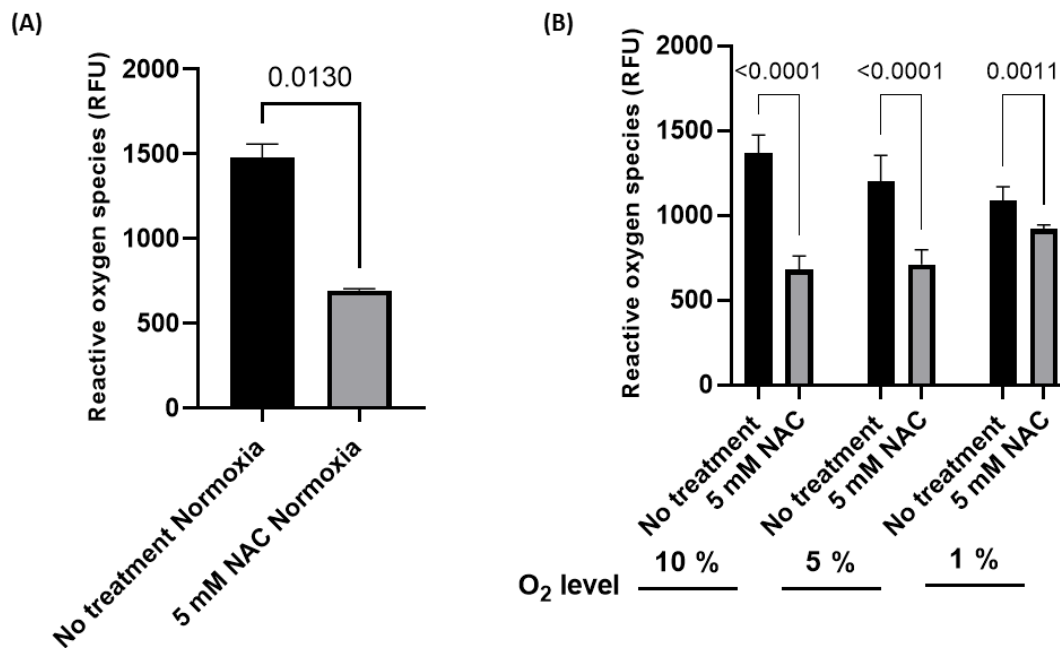


**Figure 5.10** Effect of NAC on ROS scavenger under normoxia and hypoxia. HepaRG cells were differentiated following the standard protocol. After differentiation cells were treated with 5 mM NAC for 24 h and ROS generation assessed by ROS detection Kit under normoxia **Fig.5.10A** or under exposure to various levels of hypoxia (10%, 5% or 1% O<sub>2</sub>) **Fig.5.10B**. Untreated cells culture with the respective O<sub>2</sub> concentration were used as a control. Bars represent mean  $\pm$  SEM. N=3 independent experiments with at least six replicates each experiment. Statistics by T-test **Fig.5.10A**, or one-way ANOVA and Bonferroni test **Fig.5.10B**.

The ability of Tiron to scavenge superoxide radicals in HepaRG cells was assessed using the MitoSox assay. Cells were treated with Tiron at concentrations of 10 mM and 20 mM for 48 h, under normoxia and hypoxia (1% O<sub>2</sub>, for 24 h). Two approaches were used: a quantitative measurement using a plate reader and a visualization of the fluorescent signal through confocal microscopy. **Figure 5.11A** and **5.11B** shows that Tiron treatment at a concentration of 20 mM significantly reduced (20-25%) the levels of superoxide radicals under both normoxic and hypoxic conditions compared to respective untreated control groups. However, the use of a lower Tiron concentration of 10 mM appeared not exhibit scavenger activity in either normoxic and hypoxic conditions, as observed through confocal microscopy (**Figure 5.11C**). However, the confocal images lacks the quantitative rigour of the cytometric plate-reader approach.

Tiron is recognised as an antioxidant that localises and accumulates within the mitochondria. Here, Tiron effectively scavenges ROS at source (Abdel-Magied *et al.*, 2019). Tiron's mode of action involves direct oxidation with superoxide, leading to the generation of a semiquinone radical independent of oxygen concentration (Taiwo, 2008). Additionally, Tiron demonstrates metal chelation capabilities, particularly in interactions with iron, which have been linked to

its potential to confer protection against cytotoxicity (Taiwo, 2008; Abdel-Magied *et al.*, 2019). There is no substantiating evidence to support that Tiron inhibits cytochrome P450.

Tiron is a hydrophilic molecule where part of the process at least in membrane permeation could be mediated by a specific transporter(s) (Vorobjeva and Pinegin, 2016). Paky *et al.* explored the impact of Tiron upon superoxide production in an isolated perfused rabbit lung under normoxic conditions. They found Tiron treatment induced a dose-dependent decline in superoxide levels, reaching maximal inhibition at 20 mM. Higher concentrations of Tiron (20 to 80 mM) failed to lead to any greater scavenging (Paky *et al.*, 1993) with the authors speculating this reflecting a saturation of the membrane transporter and/or superoxide generation taking place in a cellular compartment that remains inaccessible to Tiron.

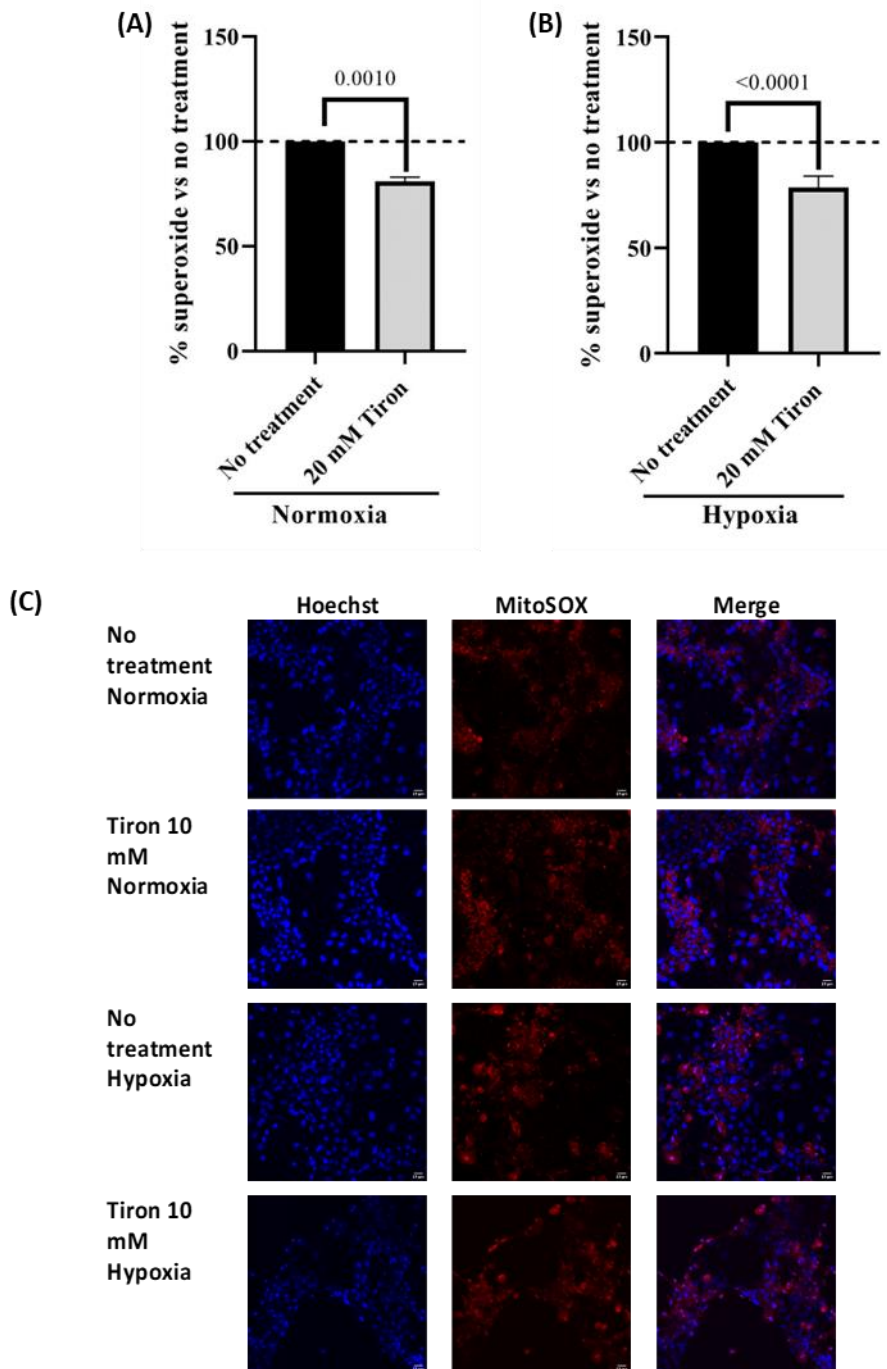


**Figure 5.11 Effect of Tiron on ROS scavenger under normoxia and hypoxia using MitoSox assay.** HepaRG cells were differentiated following the standard protocol. After differentiation, cells were treated with 10 mM or 20 mM Tiron for 48 h, and ROS generation was assessed using the MitoSox assay. Two methodological approaches were used: First, cells exposed to normoxia (**Fig.5.11A**) or hypoxia (1% O<sub>2</sub>, 24 h) (**Fig.5.11B**) and treated with 20 mM Tiron were compared to the no-treatment control. The MitoSox fluorescent signal was obtained using a plate reader with excitation at 510 nm and emission at 580 nm. Data are presented as percentages, and the bars represent the mean  $\pm$  SEM. N=3 independent experiments were conducted, each with three to eight replicates. Statistical analysis was performed using the T-test. The second methodological approach involved visualizing the fluorescent signal from superoxide radical generation after incubation with the MitoSox assay using confocal microscopy. **Fig.5.11C** presents the results after treatment with 10 mM Tiron under both normoxia and hypoxia conditions. Untreated cells were used as a control. Live cell imaging was carried out using a 40X magnification lens. The scale bar represents 20  $\mu$ m.

### 5.3.3 Impact of ROS on CYP3A4 and CYP2C9 expression in HepaRG Cells

Here the impact of ROS manipulation on CYP3A4 and CYP2C9 was examined. HepaRG cells were cultured under hypoxia (1% O<sub>2</sub>) and treated with either the ROS inducer menadione or the antioxidants N-acetyl cysteine (NAC), a global ROS scavenger, or Tiron which specifically scavenges superoxide and hydroxyl radicals.

As shown in **Figure 5.12A**, differentiated HepaRG under hypoxia show a reduction in the level of CYP3A4 mRNA transcript compared to normoxia conditions. Menadione treatment at concentration of 50 µM for 24 h further reduced CYP3A4 mRNA expression by 13%, compared with hypoxia alone. Under hypoxia-driven decreases in CYP3A4 mRNA, treatment with NAC (10 mM) and with Tiron (10 and 20 mM) saw CYP3A4 levels restored to some extent to greater than that in the hypoxia alone control although still less than the levels under normoxia. With NAC (10 mM) the mRNA expression of CYP3A4 increased by 8%, compared hypoxia control. With Tiron, 10 and 20 mM concentrations the CYP3A4 mRNA levels increased by 7% and 13%, respectively.

**Figure 5.12B** is Western blot data representative from one of three independent experiments. Under hypoxia CYP3A4 protein level was reduced, compared to normoxia. Maintaining the HepaRG cells under hypoxia, menadione treatment further suppressed the protein levels of CYP3A4. Consistent with the qRT-PCR data, Tiron (10 and 20 mM) treatments restored the CYP3A4 levels to at least greater than the hypoxia control. The highest concentration of Tiron (20 mM) was able to recover CYP3A4 to similar levels observed in cells cultured under normoxia. Notably, a statistically significant distinction was evident between the normoxia group and all other hypoxia treatment groups, with only the 20 mM Tiron concentration being highlighted in Figure 5.12A to maintain the emphasis on the primary focus, which is the hypoxia condition.

The corresponding functional activity of CYP3A4 in the HepaRG cells is shown in **Figure 5.12C**. Here the data is shown as CYP450 activity (RLU) normalised to cell viability (RLU). Hypoxia caused a significant decrease (ca more than 50% decline) in functional activity which was further decreased by 25 µM menadione. In functional activity experiments, a low concentration of menadione (25 µM) was employed, as this level was deemed adequate to induce an effect. This efficacy could arise from the drug's direct engagement with the enzyme's active or allosteric sites, causing a swift alteration in enzymatic activity. In contrast, the intricate nature of mRNA expression and protein levels involves multifaceted cellular

processes, impacted by factors like transcription, RNA stability, mRNA quantities, translation efficiency, protein stability, and degradation. Consequently, achieving changes in gene expression and protein levels might necessitate higher drug concentrations or extended exposure durations to effectively influence these processes.

The decrease caused by hypoxia alone was partially restored by treatment with NAC 10 mM and Tiron (10 and 20 mM). For example, Tiron (20 mM) increasing activity to within 25% of the normoxia level. Shown in the insert to Figure 5.12C is the viability data which did not show any statistically significant differences with the treatments, although a trend for NAC and 20 mM Tiron in particular to be lower than normoxia and hypoxia controls.

The investigation encompassed the assessment of mRNA expression and functional activity of CYP3A4 under normoxic conditions following treatment with menadione, NAC, and TIRON. The mRNA data, outlined in **Appendix 3.2 and Supplementary Figure 3.2.1A**, displayed a notable outcome. Specifically, a 24-h exposure to 50  $\mu$ M menadione substantially decreased CYP3A4 expression by 40% compared to the untreated control. However, in contrast to hypoxic results, NAC treatment exhibited no significant alteration in CYP3A4 expression. Conversely, Tiron treatment revealed a dose-dependent reduction in CYP3A4 expression, with the 10 mM Tiron-treated group showing a 24% reduction and the 20 mM Tiron-treated group showing a 43% reduction compared to the untreated control.

Furthermore, the functional activity of CYP3A4 under normoxic conditions was depicted in **Appendix 3.2 Supplementary Figure 3.2.1B**. A 24-h treatment with 25  $\mu$ M menadione led to a significant 24% decrease in CYP3A4 activity. This reduction aligned with the mRNA expression data under normoxia. Similarly, a 48-h exposure to 10 mM NAC had no significant impact on CYP3A4 activity. In contrast, Tiron treatment for 48 h demonstrated a substantial concentration-dependent decline in CYP3A4 activity. Specifically, the 10 mM Tiron-treated group displayed a 20% reduction, while the 20 mM Tiron-treated group exhibited a 30% reduction in CYP3A4 activity compared to the untreated control. Tiron treatment could potentially disrupt the balance of ROS, impacting the signaling pathways that regulate CYP3A4 expression. It's possible that excessive antioxidant activity from Tiron might interfere with ROS-mediated signaling pathways responsible for maintaining CYP3A4 levels. These observations emphasize that maintaining proper levels of reactive oxygen species (ROS) is crucial for effective cell signaling and the regulation of CYP expression. Disturbances in ROS balance, whether caused by hypoxia-induced oxidative stress or reductive stress (resulting in a



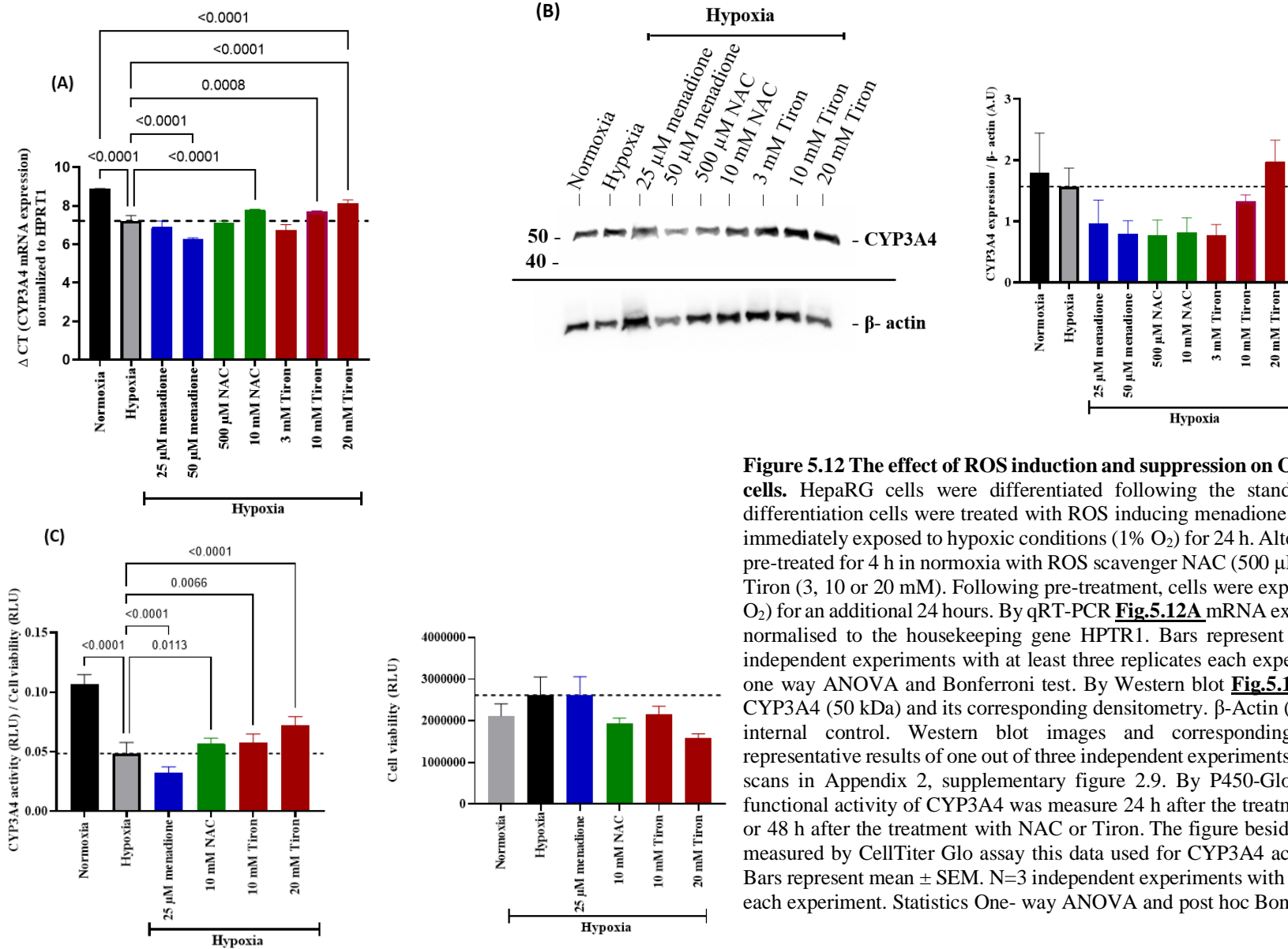


**Figure 5.12** The effect of ROS induction and suppression on CYP3A4 in HepaRG cells. HepaRG cells were differentiated following the standard protocol. After differentiation cells were treated with ROS inducing menadione (25 and 50 μM) and immediately exposed to hypoxic conditions (1% O<sub>2</sub>) for 24 h. Alternatively, cells were pre-treated for 4 h in normoxia with ROS scavenger NAC (500 μM or 10 mM) or with Tiron (3, 10 or 20 mM). Following pre-treatment, cells were exposed to hypoxia (1% O<sub>2</sub>) for an additional 24 hours. By qRT-PCR **Fig.5.12A** mRNA expression of CYP3A4 normalised to the housekeeping gene HPTR1. Bars represent mean ± SEM. N=3 independent experiments with at least three replicates each experiment. Statistics by one way ANOVA and Bonferroni test. By Western blot **Fig.5.12B** protein levels of CYP3A4 (50 kDa) and its corresponding densitometry. β-Actin (42 kDa) was used as internal control. Western blot images and corresponding densitometry are representative results of one out of three independent experiments. Original membrane scans in Appendix 2, supplementary figure 2.9. By P450-Glo™ assay **Fig.5.12C** functional activity of CYP3A4 was measure 24 h after the treatment with menadione or 48 h after the treatment with NAC or Tiron. The figure beside is the cell viability measured by CellTiter Glo assay this data used for CYP3A4 activity normalization. Bars represent mean ± SEM. N=3 independent experiments with at least six replicates each experiment. Statistics One- way ANOVA and post hoc Bonferroni test.

decrease below the normal level), can have a negative impact on the activity and expression of CYP450 enzymes. Preserving the delicate ROS equilibrium is essential for upholding the functional integrity of these crucial drug-metabolising enzymes.

As depicted in **Figure 5.13A**, differentiated HepaRG cells subjected to hypoxia demonstrated a decrease in CYP2C9 mRNA transcript levels compared to normoxia conditions. Upon treatment with menadione at concentrations of 25  $\mu$ M and 50  $\mu$ M for 24 h, there was a further reduction in CYP2C9 mRNA expression by 8% and 14%, respectively, compared to hypoxia alone.

In response to hypoxia-induced reductions in CYP2C9 mRNA, treatment with the global ROS scavenger NAC (10 mM) for 28 h, and with Tiron (10 and 20 mM), which specifically scavenges superoxide and hydroxyl radicals, led to a partial restoration of CYP2C9 levels. However, the levels remained lower than those observed under normoxia conditions. NAC (10 mM) increased the mRNA expression of CYP2C9 by 12% compared to the hypoxia control. Treatment with Tiron at 10 mM and 20 mM concentrations resulted in a 6% and 33% increase in CYP3A4 mRNA levels, respectively. The comparison between the normoxia group and all the other alternative hypoxia treatment groups revealed a significant statistical differentiation. However, Figure 5.13A displays only the statistics pertaining to the 20 mM Tiron concentration, thereby ensuring the preservation of the primary focus on the hypoxic state.

**Figure 5.13B** presents Western blot data from one of three independent experiments. Under hypoxia, the protein level of CYP2C9 was reduced compared to normoxia. Menadione treatment during hypoxia further suppressed the protein levels of CYP2C9. NAC at low concentration (500  $\mu$ M) was able to recover CYP2C9 to similar levels observed in cells cultured under normoxia. Interestingly, neither NAC at high dose (10 mM) nor Tiron (20 mM) treatments were able to fully restore CYP2C9 levels to those observed in the hypoxia control.

In **Figure 5.13C**, the corresponding functional activity of CYP2C9 (RLU) normalised to cell viability (RLU) in the HepaRG cells is shown. Hypoxia caused a significant decrease (over 80% decline) in functional activity, which was further decreased by 25  $\mu$ M menadione. Treatment with Tiron (10 and 20 mM) partially restored the decrease caused by hypoxia, with Tiron (20 mM) increasing the activity to within 34% of the normoxia level. Illustrated in the inset of Figure 5.13C are the viability results, which did not display any statistically notable distinctions among the treatments. Nevertheless, there is a tendency, especially for NAC and

20 mM Tiron, to demonstrate slightly diminished values when contrasted with the normoxia and hypoxia control sets.

In **Appendix 3.2, Supplementary Figure 3.2.2A**, the data regarding CYP2C9 mRNA expression under normoxia is presented. A substantial reduction of 68% was observed in response to 50  $\mu$ M menadione treatment for 24 h, as compared to the untreated control. Under normoxic conditions, CYP2C9 mRNA levels in HepaRG cells remained relatively unchanged upon treatment with either 500  $\mu$ M or 10 mM NAC for 28 h. Conversely, treatment with Tiron (3, 10, or 20 mM) for 28 h displayed a dose-dependent reduction in CYP2C9 expression. Specifically, CYP2C9 expression was downregulated by 45% in the 10 mM Tiron-treated group and by 70% in the 20 mM Tiron-treated group, relative to the untreated control. Moving on to **Appendix 3.2, Supplementary Figure 3.2.2B**, the functional activity of CYP2C9 under normoxia is illustrated. Exposure to 25  $\mu$ M menadione for 24 h resulted in a marginal decline in CYP2C9 activity, approximately 20% lower than the untreated control; however, this change did not achieve statistical significance. In contrast to the mRNA expression data observed under normoxia, Tiron treatment led to an increase in CYP2C9 activity in a concentration-dependent manner. Specifically, CYP2C9 activity saw a rise of 40% in the 10 mM Tiron-treated group and a 60% increase in the 20 mM Tiron-treated group, as compared to the untreated control. Notably, treatment with 10 mM NAC did not demonstrate any discernible positive impact on CYP2C9 activity.

Taken together, the data for CYP3A4 and CYP2C9 shows that under hypoxia, ROS may at least partially regulate CYP450 expression and that antioxidant interventions can restore/preserve some of the hypoxia-induced diminished CYP450 activity. Other research has observed contrasting outcomes of ROS exposure. For example, H<sub>2</sub>O<sub>2</sub> treatment under normoxia increased CYP3A4 mRNA and protein levels in human K562 erythroleukemic cells (Nagai, Kato and Tamura, 2004). In contrast, research conducted in HepG2 cells under normoxia revealed that exogenous H<sub>2</sub>O<sub>2</sub> treatment, leading to mitochondrial oxidative stress, adversely affects the mRNA expression of CYP1A1 and CYP2E1. This effect is mitigated by the antioxidant catalase (Morel and Barouki, 1998; Morel, Mermoud and Barouki, 1999; Morel, De Waziers and Barouki, 2000). Induction of oxidative stress by H<sub>2</sub>O<sub>2</sub> can downregulate CYP450 gene expression through haem degradation (Guengerich, 1978) or by oxidising the haem thiolate cysteine ligand to a sulphenic acid. In the active site of CYP450 enzymes, a crucial haem thiolate cysteine ligand is present. This haem group, containing iron, establishes a coordinated thiolate linkage (Fe-S-C) with a cysteine residue within the protein, playing a

fundamental role in facilitating the enzymatic activity of cytochrome P450 enzymes. Notably, direct oxidation of the haem-thiolate center has been observed in human recombinant P450s 1A2, 2C8, 2D6, and 3A4 when subjected to H<sub>2</sub>O<sub>2</sub> treatment, leading to an adverse impact on their functional activity. The oxidation process involves the formation of a disulphide bond (sulphenylation) with the thiolate part of the haem-thiolate cysteine ligand, causing reversible enzyme inactivation. Sulphenic acid production occurs through redox relays utilising peroxiredoxins or at specific sites with elevated oxidant production (e.g., NADPH oxidase, mitochondria), facilitating direct diffusion across plasma membranes (Albertolle *et al.*, 2018).

In the context of normoxic conditions characterised by well-maintained levels of ROS for cell signaling, the utilisation of vitamin E analogs such as Tiron and glutathione precursors like NAC has the potential to disrupt the delicate equilibrium between oxidants and antioxidants within cellular environments. This disruption manifests as an excessive abundance of reducing agents, including GSH and NAD(P)H, coupled with diminished concentrations of pivotal oxidants like O<sub>2</sub><sup>•-</sup> and H<sub>2</sub>O<sub>2</sub>, giving rise to a state known as reductive stress (Mladenov *et al.*, 2023). This reductive stress, in turn, results in attenuated cellular metabolism, compromised mitochondrial functionality, impaired cellular proliferation, and compromised protein disulphide bond formation in the endoplasmic reticulum (Zhang and Tew, 2021). While there is no direct evidence concerning reductive stress's immediate influence on CYP450, it is conceivable that reductive stress can impact proper protein folding, possibly yielding misfolded or non-functional CYP450 enzymes. Additionally, reductive stress may induce epigenetic modifications, like DNA methylation or histone modifications (Pérez-Torres *et al.*, 2020), potentially influencing gene expression related to CYP450. In a study involving primary human cardiac stem cells cultivated under physiological oxygen levels (5% O<sub>2</sub>) and treated with a high-dose antioxidant cocktail comprising ascorbate, L-glutathione, and  $\alpha$ -tocopherol acetate, the addition of these antioxidants significantly decreased ROS levels, exacerbating DNA damage quantified by  $\gamma$ -H2AX formation, a microscopic structure indicative of DNA damage, and concurrently diminishing DNA repair enzymes (Li and Marbán, 2010). This underscores the essential requirement for maintaining physiologically balanced intracellular ROS levels to activate DNA repair pathways and uphold genomic stability in stem cells.

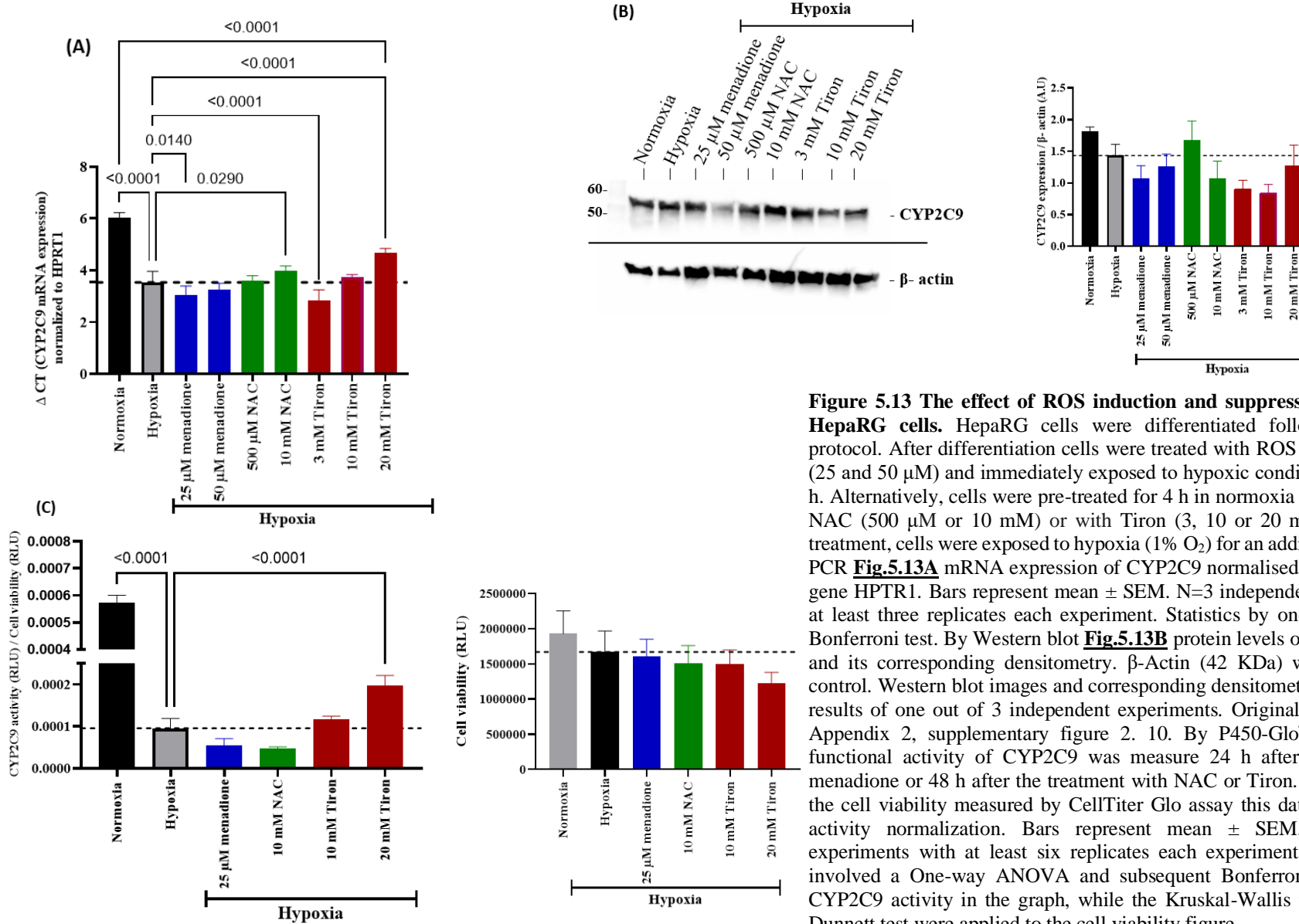


**Figure 5.13** The effect of ROS induction and suppression on CYP2C9 in HepaRG cells. HepaRG cells were differentiated following the standard protocol. After differentiation cells were treated with ROS inducing menadione (25 and 50  $\mu$ M) and immediately exposed to hypoxic conditions (1% O<sub>2</sub>) for 24 h. Alternatively, cells were pre-treated for 4 h in normoxia with ROS scavenger NAC (500  $\mu$ M or 10 mM) or with Tiron (3, 10 or 20 mM). Following pre-treatment, cells were exposed to hypoxia (1% O<sub>2</sub>) for an additional 24 h. By qRT-PCR **Fig.5.13A** mRNA expression of CYP2C9 normalised to the housekeeping gene HPTR1. Bars represent mean  $\pm$  SEM. N=3 independent experiments with at least three replicates each experiment. Statistics by one way ANOVA and Bonferroni test. By Western blot **Fig.5.13B** protein levels of CYP2C9 (55 KDa) and its corresponding densitometry.  $\beta$ -Actin (42 KDa) was used as internal control. Western blot images and corresponding densitometry are representative results of one out of 3 independent experiments. Original membrane scans in Appendix 2, supplementary figure 2. 10. By P450-Glo™ assay **Fig.5.13C** functional activity of CYP2C9 was measure 24 h after the treatment with menadione or 48 h after the treatment with NAC or Tiron. The figure beside is the cell viability measured by CellTiter Glo assay this data used for CYP2C9 activity normalization. Bars represent mean  $\pm$  SEM. N=3 independent experiments with at least six replicates each experiment. Statistical analysis involved a One-way ANOVA and subsequent Bonferroni test for assessing CYP2C9 activity in the graph, while the Kruskal-Wallis test followed by the Dunnett test were applied to the cell viability figure.

### 5.3.4 Hypoxia induces transcription of proinflammatory-related cytokines by HepaRG cells

It is relatively well-established that there is intercommunication between hypoxia and the generation of ROS, which in turn affects the activation and regulation of cytokines involved in inflammatory reactions (Ranneh *et al.*, 2017; Chelombitko, 2018). For instance, under hypoxic conditions, the stabilisation of HIF-1 $\alpha$  leads to increased ROS production from the mitochondrial electron transport chain (Wang and Semenza, 1993; Chandel *et al.*, 2000). Subsequently, ROS can directly induce the production of cytokines or activate the NF- $\kappa$ B pathway, which then triggers cytokine production (Kim, Seo and Kim, 2000). Moreover, HIF-1 $\alpha$  plays a role in regulating cytokine production either directly or indirectly through NF- $\kappa$ B pathway activation (Jeong *et al.*, 2003; Walmsley *et al.*, 2005). Tumour Necrosis Factor Receptor-Associated Periodic Syndrome (TRAPS) is characterised as an autoinflammatory disorder resulting from missense mutations occurring in the type 1 TNF receptor (TNFR1). These mutations lead to a failure in interacting with TNF and consequently, its accumulation within the endoplasmic reticulum. Notably, an escalation in mitochondrial ROS levels has been observed in human peripheral blood mononuclear cells carrying TNFR1 mutations associated with TRAPS, as opposed to cells derived from healthy donors. ROS mediate increased mitogen-activated protein kinases (MAPK) and the subsequent production of inflammatory cytokines. Of significance, the inhibition of ROS has been demonstrated to effectively suppress MAPK activity, subsequently leading to a reduction in the production of key inflammatory cytokines such as IL-6 and TNF (Bulua *et al.*, 2011). A related study demonstrated that ROS inhibitors also rendered MAPK ineffective (Kamata *et al.*, 2005). These studies collectively highlight a substantial interplay between ROS and pro-inflammatory mediators, primarily involving the NF- $\kappa$ B, HIF1- $\alpha$ , and MAPK cascades.

Here is the investigation of pro-inflammatory cytokines expression under acute hypoxia in our hepatocyte model HepaRG, ahead of study on the regulation of CYP450 by cytokines. A panel of proinflammatory-related cytokines (IL-12, IL-6, IL-1 $\beta$ , and TNF- $\alpha$ ) was evaluated by qRT-PCR in HepaRG cells exposed to 1% O<sub>2</sub> for 6, 24 and 72 h. These particular pro-inflammatory cytokines were selected because they are known as biomarkers for the acute inflammatory response seen under acute high altitude hypoxia (Hartmann *et al.*, 2000; Heinrich *et al.*, 2018; Lundeberg *et al.*, 2018). **Figure 5.14** shows the HepaRG cells under prolonged hypoxic conditions (72 h) displayed significant increase in mRNA levels for all of the studied cytokines,

IL-12 (3-fold increase), IL-1 $\beta$  (1.6-fold increase), IL-6 (15-fold increase) and TNF- $\alpha$  (3-fold increase) when compared to normoxia (21% O<sub>2</sub>) conditions. In addition: an increase in TNF- $\alpha$  gene expression (2-fold) was seen also at 24 h under 1% O<sub>2</sub>; a downregulation of IL-1 $\beta$  (2-fold) was observed at 6 h.

Similar findings have been reported in various studies. For example, endothelial cells exposed to acute hypoxia showed elevated IL-6 transcription (Yan *et al.*, 1995). Hypoxaemia (5% O<sub>2</sub>, 60 min) in mice stimulated the production of IL-1 $\beta$ , IL-6, and TNF- $\alpha$  in plasma (Ertel *et al.*, 1995), and a similar panel of cytokines was elevated in rat cardiac myocytes exposed to PO<sub>2</sub> of 30 to 40 mmHg for 4 h (Yamauchi-Takihara *et al.*, 1995). In a study examining the consequences of acute hypoxia in humans, Klausen *et al.* found that blood IL-6 levels significantly increased, while other pro-inflammatory cytokines remained unaffected (Klausen *et al.*, 1997). Additionally, purified stromovascular cells (SVFs) derived from obese human subjects were cultured for 24 h under normoxic or hypoxic conditions (1% O<sub>2</sub>). The supernatant fractions were then analysed using ELISA. The results indicated that TNF- $\alpha$  secretion increased by 1-fold in response to hypoxia, whereas IL-10 and chemokine (C-C motif) ligand 2 (CCL2) secretion decreased by approximately 0.67-fold. However, IL-6 secretion remained unchanged. A similar pattern of cytokine production was observed at shorter culture times of 6 and 12 h, but the overall production levels were lower, likely due to the progressive accumulation of cytokines in the culture supernatant over the culture period (O'Rourke *et al.*, 2011). In fibroblast-like synoviocytes (FLSs) isolated from rheumatoid arthritis patients and exposed to hypoxia (1% O<sub>2</sub> for 6, 12 or 24 h), there was a notable increase in the mRNA expression of IL-6 and IL-8 by approximately 2 to 2.5 fold at 12 h and 24 h of hypoxia exposure. Moreover, the promoter activity in cells exposed to hypoxia for 12 h demonstrated a significant upregulation of IL-6 and IL-8 by about 3-fold. However, despite these changes at the mRNA and promoter levels, using ELISA to detect the protein expression in the cell culture supernatant did not reveal any significant alterations compared to the normoxia control (Wang *et al.*, 2023). A study investigated the mRNA expression of IL-6 and TNF- $\alpha$  in normal peritoneum and adhesion fibroblasts under both normal and hypoxic conditions (2% O<sub>2</sub>, 24 h), using samples obtained from the same patients. In response to hypoxia, IL-6 mRNA levels were found to be upregulated in both normal peritoneal and adhesion fibroblasts, showing a 1.4-fold and 1-fold increase, respectively, compared to normoxia. Similarly, TNF- $\alpha$  mRNA exhibited upregulation under hypoxia, with a 1.5-fold increase in normal peritoneal fibroblasts

and a 1.2-fold increase in adhesion fibroblasts when compared to normoxia (Ambler *et al.*, 2012).

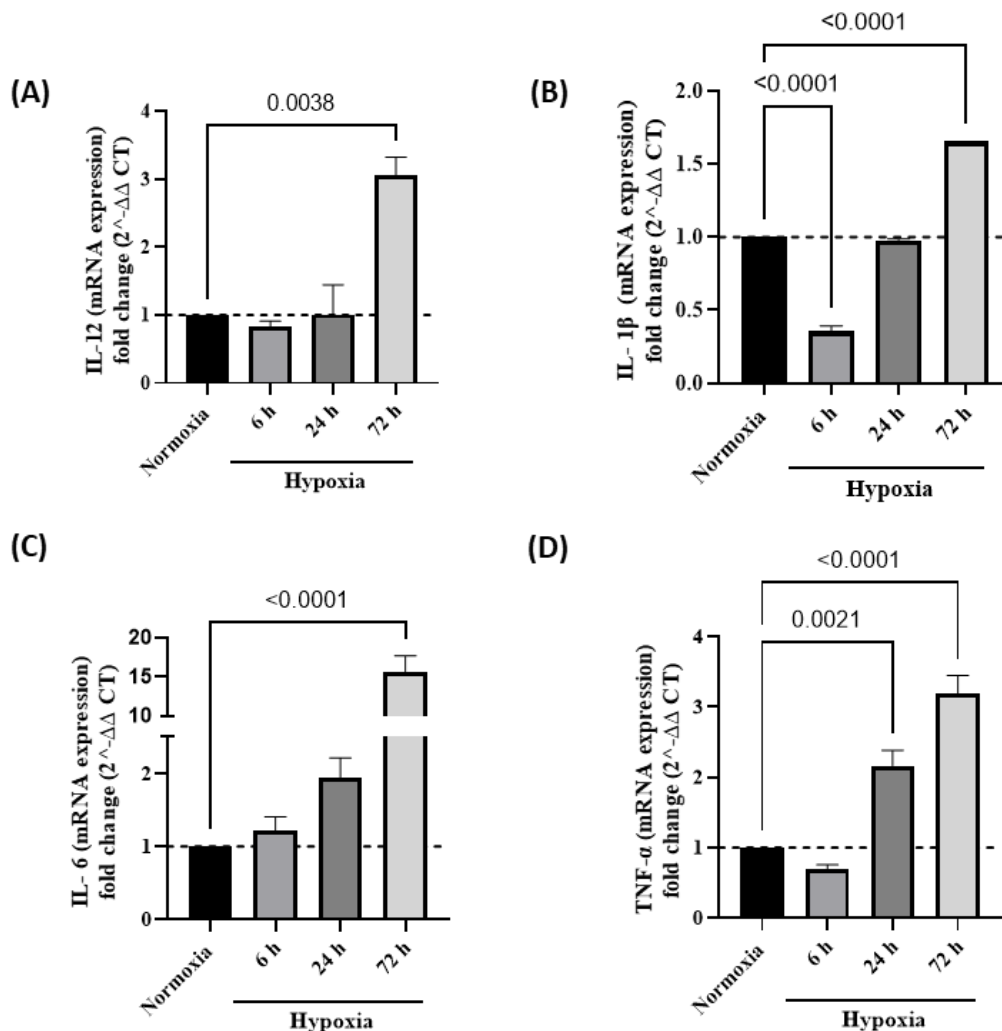


**Figure 5.14** Gene expression of proinflammatory-related mediators in HepaRG cultured at normoxic (21% O<sub>2</sub>) or hypoxic (1% O<sub>2</sub> for 6, 24 or 72 h) conditions. HepaRG cells were differentiated following the standard protocol. After differentiation cells were exposed to hypoxia (grey bars) for 6, 24 or 72 h. HepaRG cultured under normoxia were used as a control. By qRT-PCR **Fig. 5.14A** mRNA expression of IL-12. **Fig. 5.14B** mRNA expression of IL-1β. **Fig. 5.14C** mRNA expression of IL-6. **Fig. 5.14D** mRNA expression of TNF-α. The gene expression was normalised to the housekeeping gene (HPRT1) and cells that were culture under normoxia. Bars represent mean ± SEM. N=3 independent experiments. Statistics by One-way ANOVA and post hoc Dunnett test.

### 5.3.5 Impact of pro-inflammatory cytokines on CYP3A4 and CYP2C9 expression in HepaRG cells under normoxia conditions

Here the aim was to study the effect of exposure to inflammatory cytokines upon HepaRG cells expression of CYP450 under normoxia conditions. The cytokines IL-6 and TNF-α were



selected based on earlier qRT-PCR data (**Figure 5.14**) which showed these cytokines to have the more profound and/or quicker response to hypoxia challenge.

HepaRG cells were differentiated and treated with 10 ng/mL IL-6 for 72 h. Thereafter CYP3A4 and CYP2C9 gene and protein expression were evaluated using qRT-PCR and Western blot, respectively. A concentration of 10 ng/mL was used based on previous studies on hepatocytes which found this concentration is sufficient to induce maximum effects on CYP450 gene expression (Aitken and Morgan, 2008; Klein *et al.*, 2015).

The viability of HepaRG exposed to IL-6 (10 ng/mL) for 72 h remained unaffected as shown in **Figure 5.15**.

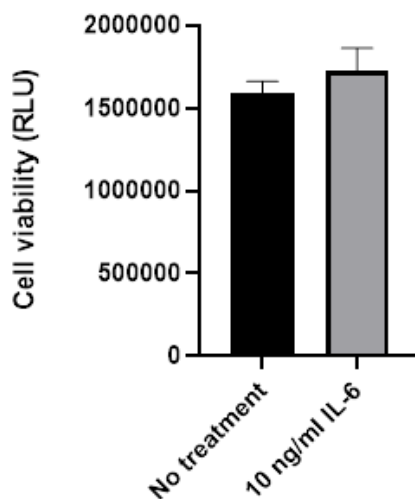


**Figure 5.15 Cell viability of HepaRG cells upon IL-6 treatment.** HepaRG cells were differentiated following the standard protocol. After differentiation cells were treated with 10 ng/mL of IL-6 for 72 h in standard culture conditions (21% O<sub>2</sub>, 5% CO<sub>2</sub>, 37°C). Untreated cells were used as a control. By CellTiter Glo assay, the cell viability was determined. Bars represent mean ± SEM. N=3 independent experiments with at least six replicates each experiment. Statistics by unpaired T-test.

The treatment of HepaRG cells with the pro-inflammatory cytokine IL-6 led to the suppression of mRNA expression of CYP3A4 (2.5-fold) and CYP2C9 (5-fold), compared with untreated cells (**Figures 5.16A** and **5.16B**, respectively). Similar effects were observed for CYP3A4 and CYP2C9 protein expression following exposure to IL-6, where CYP3A4 protein expression was decreased by ca. 5-fold, and the signal for CYP2C9 was imperceptible (with experiments repeated) (**Figures 5.16C** and **5.16D**, respectively).

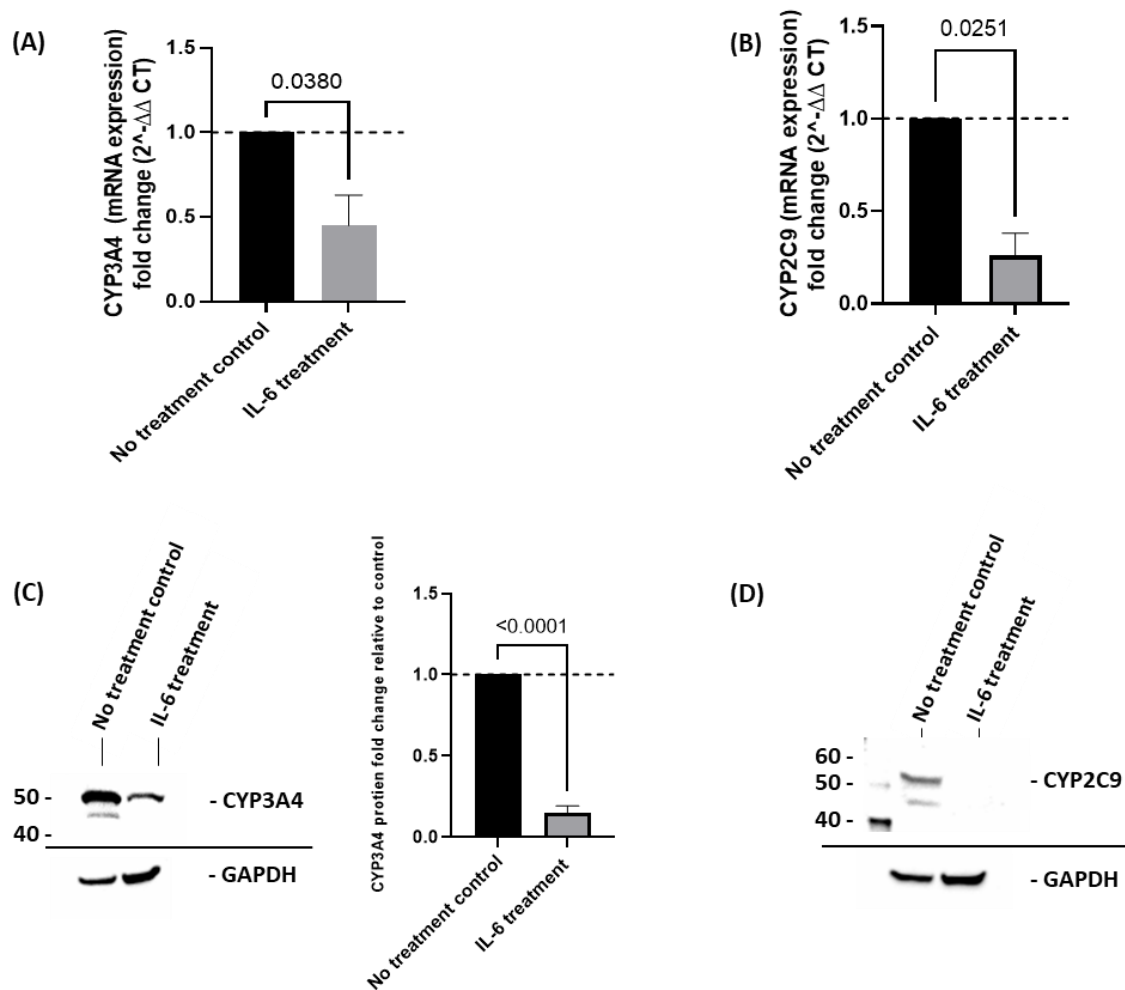


**Figure 5.16** The effect of IL-6 treatment on CYP3A4 and CYP2C9 mRNA and protein expression in HepaRG cells. HepaRG cells were differentiated following the standard protocol. After differentiation cells were treated with 10 ng/mL of IL-6 for 72 h under standard condition (21% O<sub>2</sub>). Untreated cells were used as a control. By qRT-PCR **Fig.5.16A** mRNA expression of CYP3A4. **Fig.5.16B** mRNA expression of CYP2C9. Bars represent mean  $\pm$  SEM. N=3 independent experiments with at least three replicates each experiment. By Western blot **Fig.5.16C** protein levels of CYP3A4 (50 kDa) and **Fig.5.16D** CYP2C9 (55 kDa). GAPDH (37 kDa) was used as internal control. Western blot images representative results of one out of three independent experiments. Original membrane scans in Appendix 2, supplementary figure 2.5 and 2.6. Statistics by unpaired T-test.

A similar set of experiments for TNF $\alpha$  is shown in **Figures 5.17 and 5.18**. After 24 h of treatment with 10 ng/mL TNF $\alpha$ , the gene and protein expression of CYP3A4 and CYP2C9 under normoxia were evaluated by qRT-PCR and Western blot, respectively. Prior hepatocyte studies determined this concentration to be adequate to generate maximal effects on CYP450

gene expression and a concentration of 10 ng/mL was chosen (Aitken and Morgan, 2008; Klein *et al.*, 2015). Furthermore, this concentration had no effect on HepaRG viability (**Figure 5.17**).

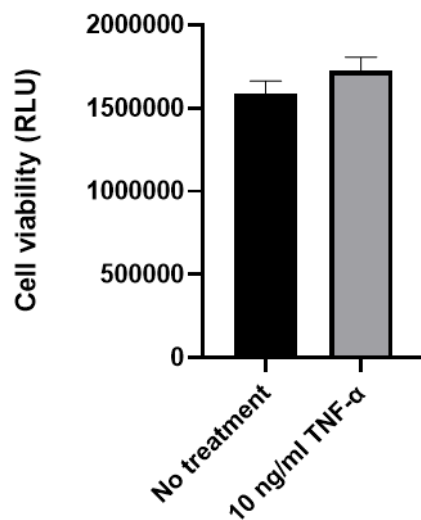


**Figure 5.17 Cell viability of HepaRG cells upon TNF- $\alpha$  treatment.** HepaRG cells were differentiated following the standard protocol. After differentiation cells were treated with 10 ng/mL of TNF- $\alpha$  for 24 h in standard culture conditions (21% O<sub>2</sub>, 5% CO<sub>2</sub>, 37 C°). Untreated cells were used as a control. By CellTiter Glo assay, the cell viability was determined. Bars represent mean  $\pm$  SEM. N=3 independent experiments with at least six replicates each experiment. Statistics by unpaired T-test.

The effect of the treatment with TNF- $\alpha$  upon CYP3A4 and CYP2C9 gene and protein expression is shown in Figure 5.18. TNF $\alpha$  exposure led to a marked suppression in the mRNA levels of CYP3A4 (by 25-fold) and CYP2C9 (by 11-fold), as shown in **Figures 5.18A** and **5.18B**, respectively. Similar effects were observed at protein level, where TNF- $\alpha$  decreased the levels of CYP3A4 and CYP2C9, by ca 50% and 30% (**Figures 5.18C** and **5.18D**, respectively).

In hepatocytes and hepatomas, Jover and colleagues investigated the mechanisms by which IL-6 inhibits the expression of CYP3A4 observing that IL-6 caused a moderate increase in the transcription factor C/EBP $\beta$  (CCAAT- enhancer binding protein  $\beta$ ), as well as a significant increase in the translation of C/EBP $\beta$ -LIP, a 20-kDa C/EBP $\beta$  isoform lacking a transactivation domain. The LIP isoform suppresses the expression of human CYP3A4 by competing with other constitutive C/EBP-activating factors, particularly C/EBP $\alpha$  (Jover *et al.*, 2002). Chondrocyte 1 (DEC1) is a transcription factor that has a vital role in cell development including cellular differentiation, lineage commitment, and sex determination (Massari and Murre, 2000). Mao *et al.* found increased DEC1 expression in human hepatocytes treated with IL-6, accompanied by a continual decrease in CYP3A4 expression. The authors suggest that

DEC1 binds to the CCCTGC sequence in the CYP3A4 promoter to form the CCCTGC-DEC1 complex, suppressing CYP3A4 expression and activity (Mao *et al.*, 2012). It is of note that DEC1 expression significantly rises in response to environmental stimuli such as hypoxia (Miyazaki *et al.*, 2002).

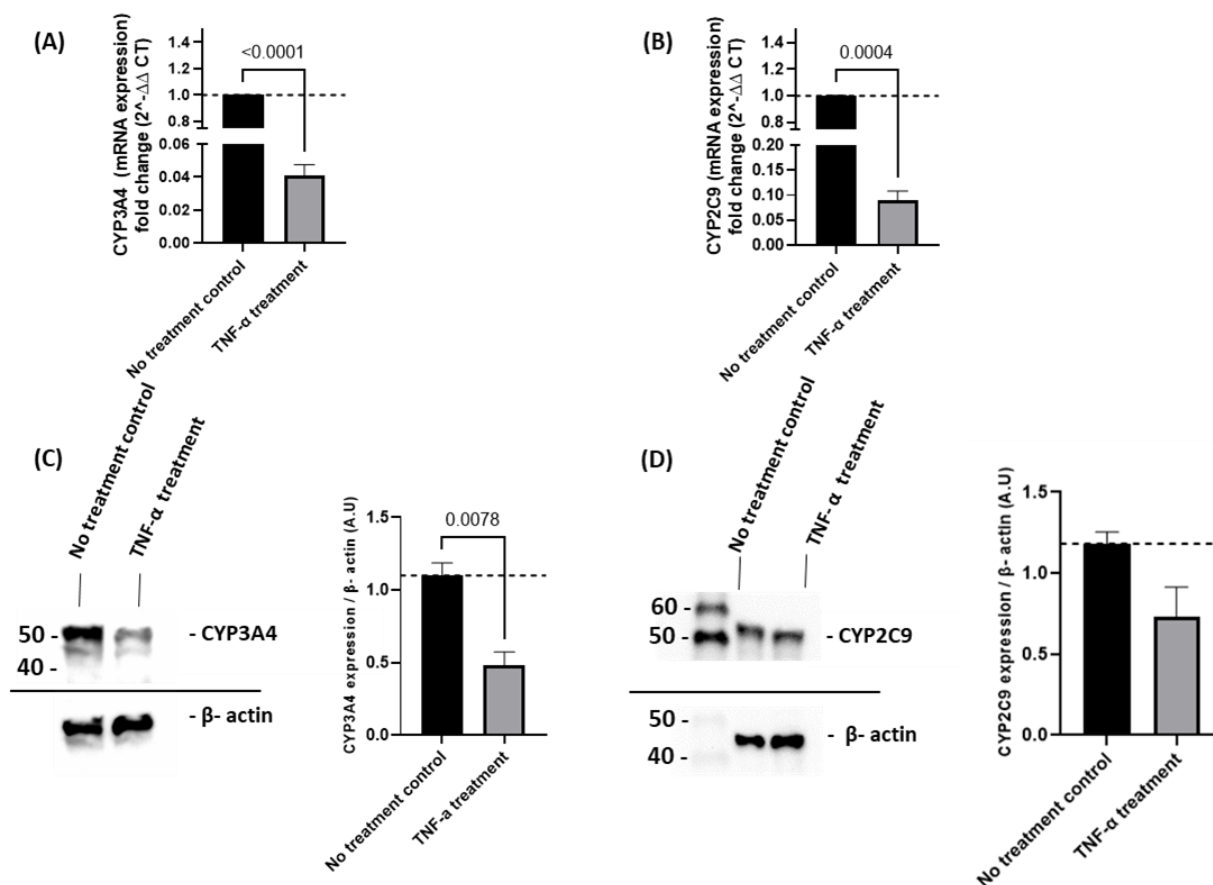


**Figure 5.18** The effect of TNF- $\alpha$  on CYP3A4 and CYP2C9 mRNA expression and protein level in HepaRG cells. HepaRG cells were differentiated following the standard protocol. After differentiation cells were treated with 10 ng/mL of TNF- $\alpha$  for 24 h under normoxia. Untreated cells were used a control. By qRT-PCR **Fig.5.18A** mRNA expression of CYP3A4. **Fig.5.18B** mRNA expression of CYP2C9. Bars represent mean  $\pm$  SEM. N=3 independent experiments with at least three replicates each experiment. By Western blot **Fig.5.18C** protein levels of CYP3A4 (50 kDa) and **Fig.5.18D** CYP2C9 (55 kDa).  $\beta$ -Actin (42 kDa) was used as internal control. Western blot images representative results of one out of three independent experiments. Original membrane scans in Appendix 2, supplementary figure 2.7 and 2.8. Statistics by unpaired T-test.

Regarding TNF- $\alpha$  regulation of CYP3A4, one study found that LPS and pro-inflammatory cytokines (TNF $\alpha$ ) enhanced the expression of NF- $\kappa$ B, which forms heterodimers with the retinoid X receptor- $\alpha$  (RXR- $\alpha$ ). The formation of an NF- $\kappa$ B-RXR- $\alpha$  heterodimer consumes RXR- $\alpha$ , disrupting the interaction of PXR and RXR- $\alpha$  and so repressing CYP3A4 transcription (Gu *et al.*, 2006). The PXR and RXR- $\alpha$  are essential regulators of CYP3A4 transcription. They form a heterodimeric complex that binds to specific response elements in the promoter

region of the CYP3A4 gene. This binding event activates the transcription of CYP3A4, leading to increased production of the CYP3A4 enzyme.

Other CYP isoforms, such as CYP1A1, have been the focus of studies demonstrating that NF- $\kappa$ B activation is a crucial event leading to the inhibition of CYP1A1 gene expression in TNF $\alpha$  treated hepatocytes (Ke *et al.*, 2001). Although the NF- $\kappa$ B pathway was not a primary focus of this thesis, it holds potential significance in the context of cytokine release under hypoxic conditions and the subsequent downregulation of CYP450 in our HepaRG cell model. Both hypoxia and the observed overproduction of mitochondrial ROS could potentially act as stimuli for the NF- $\kappa$ B pathway (Morgan and Liu, 2010; D'ignazio and Rocha, 2016). Upon activation, NF- $\kappa$ B acts as a master regulator of inflammatory signalling, inducing the release of cytokines (Oliver, Taylor and Cummins, 2009). As described in a recent systematic review study, this cytokine release can subsequently lead to the downregulation of CYP3A4 and CYP2C9 (Gatti and Pea, 2022). This downregulation primarily occurs through the negative regulation of transcription factors PXR and CAR (de Jong *et al.*, 2020).

### **5.3.6 PXR regulates CYP3A4 and CYP2C9 and is downregulated by hypoxia and pro-inflammatory cytokines treatment**

To explore further the mechanism by which hypoxia and stressors generated under hypoxia, such as pro-inflammatory cytokines, suppress CYP3A4 and CYP2C9, we hypothesised that hypoxia and cytokines inhibit CYP3A4 and CYP2C9 via the nuclear receptor PXR.

To first demonstrate that PXR regulates CYP3A4 and CYP2C9, we treated our hepatocyte model, HepaRG cells, with the PXR inducer rifampicin (25  $\mu$ M, for 48 h). This concentration has no effect on HepaRG viability, as demonstrated in our prior work (Chapter 4 **Figure 4.14**). Rifampicin binds to PXR and triggers conformational changes that cause co-repressors to dissociate and co-activators, such steroid receptor coactivator 1 (SRC-1) and SRC-3, to be recruited, resulting in chromatin remodelling and subsequent transcriptional activation (Pondugula, Dong and Chen, 2009). **Figure 5.19** shows rifampicin treatment increased PXR protein levels in the HepaRG cells. In a sequential study, differentiated HepaRG cells were then treated with 25  $\mu$ M rifampicin for 48 h which significantly increased the expression of CYP3A4 (11-fold) and CYP2C9 (5-fold) compared with no treatment HepaRG cells. Showing at least indirectly that PXR induction in the HepaRG cells correlates with increased CYP3A4

and CYP2C9 mRNA expression (**Figures 5.20A** and **5.20B**) in agreement with CYP3A4 and CYP2C9 regulation through PXR.

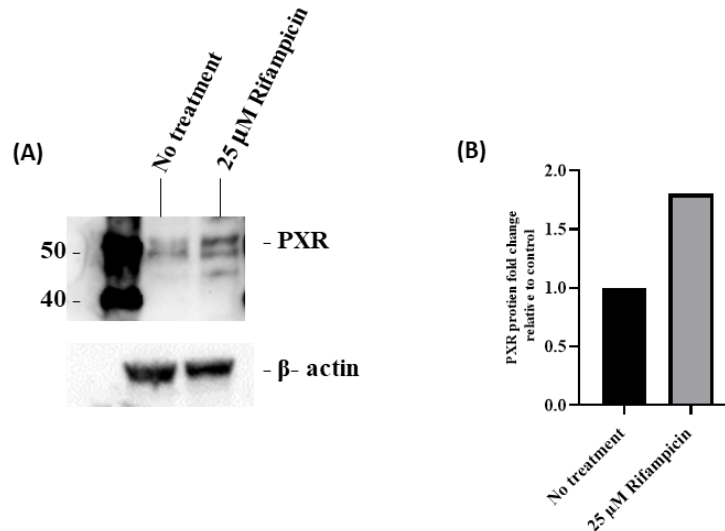


**Figure 5.20 The effect of rifampicin on PXR activity in HepaRG cells.** HepaRG cells were differentiated following the standard protocol. After differentiation cells were treated with 25 μM of rifampicin for 48 h. Untreated cells were used as control. By Western blot **Fig.5.19A** protein levels of PXR (50 kDa) and its corresponding densitometry **Fig.5.19B**. β-Actin (42 kDa) was used as internal control. N=1.

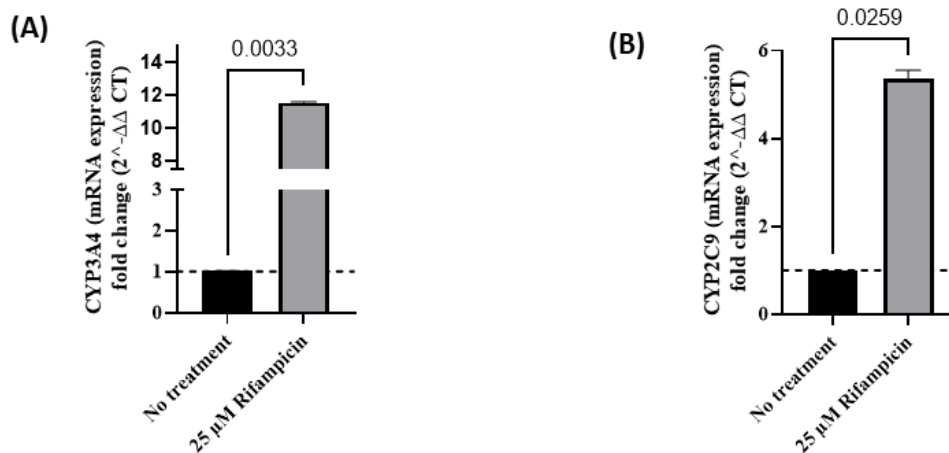


**Figure 5.19 Regulation of CYP3A4 and CYP2C9 expression by PXR ligand rifampicin.** HepaRG cells were differentiated following the standard protocol. After differentiation cells were treated with 25 μM of rifampicin for 48 h under normoxia. Untreated cells were used as a control. By qRT-PCR **Fig.5.20A** mRNA expression of CYP3A4 normalised to the housekeeping gene HPTR1. **Fig.5.20B** mRNA expression of CYP2C9 normalised to the housekeeping gene HPTR1. Bars represent mean ± SEM. N=3 independent experiments with at least three replicates each experiment. Statistics by unpaired T-test.

To further the study of the impact of hypoxia and pro-inflammatory cytokines, IL-6 and TNF- $\alpha$ , to suppress CYP3A4 and CYP2C9 via PXR, HepaRG cells were differentiated and (i) exposed to 1% O<sub>2</sub> for 24 hrs with PXR mRNA and protein expression examined; (ii) treated with 10 ng/mL IL-6 for 72 hrs or with 10 ng/mL TNF- $\alpha$  for 24 hrs under normoxia and again the mRNA and protein expression assessed .

As shown in **Figure 5.21A** the hypoxic environment (1% O<sub>2</sub>) decreased the PXR gene (mRNA) expression in HepaRG cells by 6-fold compared with cells cultured under normoxia. Along with suppression of the mRNA transcripts, hypoxia also significantly downregulated PXR protein levels (**Figure 5.21B** and **C**). This is in agreement with Legendre *et al.* who showed suppression in PXR mRNA expression in HepaRG cells exposed to 24 hr at 1% O<sub>2</sub> (Legendre *et al.*, 2009).

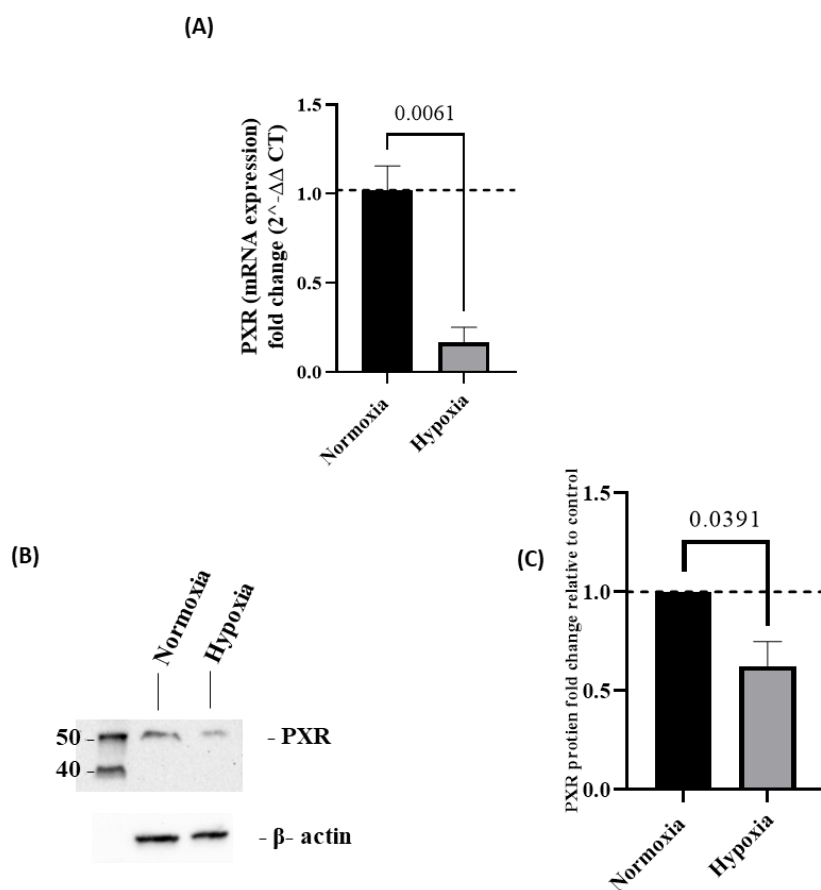


**Figure 5.21 Impact of Hypoxia upon gene and protein expression of PXR.** HepaRG cells were differentiated following the standard protocol. After differentiation cells were exposed to hypoxia (1% O<sub>2</sub>) for 24 h. Cells cultured under standard conditions (21% O<sub>2</sub>) were used as a control. By qRT-PCR **Fig.5.21A** mRNA expression of PXR normalised to the housekeeping gene HPTR1 then to normoxia control. Bars represent mean  $\pm$  SEM. N=3 independent experiments with at least three replicates each experiment. By Western blot **Fig.5.21B** protein levels of PXR (50 kDa).  $\beta$ -Actin (42 kDa) was used as internal control. **Fig.5.21C** densitometry for western blot images. Western blot images representative results of one out of three independent experiments. Original membrane scans in Appendix 2, supplementary figure 2.12. Statistics by unpaired T-test.

The impact of pro-inflammatory environment created by IL-6 or TNF- $\alpha$  treatment under normoxia upon mRNA expression of PXR in HepaRG is shown in **Figure 5.22A** and **B**. Exposure of HepaRG cells to TNF- $\alpha$  and IL-6 treatments significantly suppressed the gene expression of PXR by 5.6-fold and 1.8-fold, respectively. Overall, the findings support a view that hypoxia and pro-inflammatory cytokines downregulate CYP3A4 and CYP2C9 via PXR downregulation.

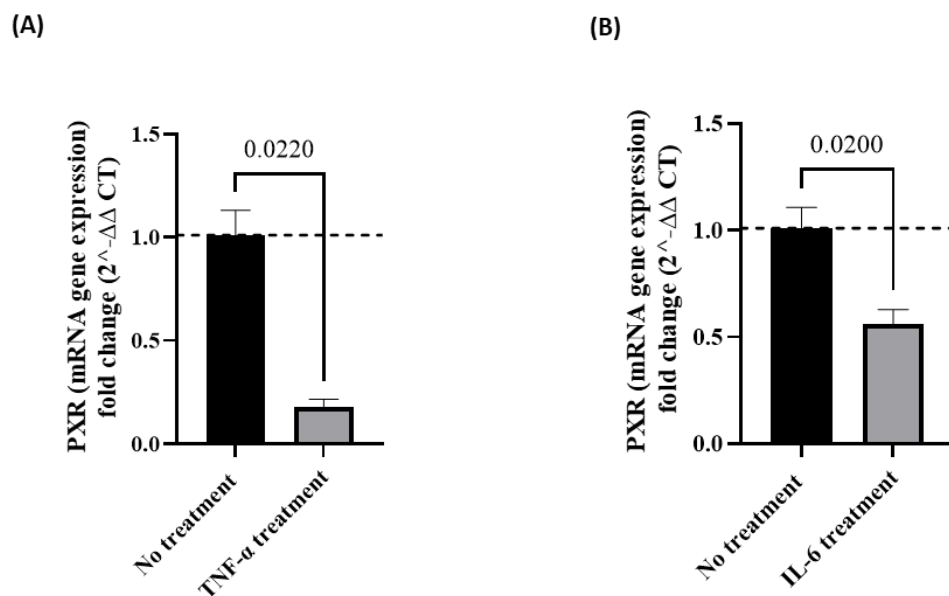


**Figure 5.22 Impact of proinflammatory treatment upon PXR in HepaRG cells.** HepaRG cells were differentiated following the standard protocol. After differentiation cells were treated with 10 ng/mL TNF- $\alpha$  **Fig.5.22A** for 24 hrs or with 10 ng/mL IL-6 **Fig.5.22B** for 72 hrs under normoxia. Untreated cells were used as a control. By qRT-PCR **Fig.5.22A** and **Fig.5.22B** are mRNA expression of PXR normalised to the housekeeping gene HPTR1 and then to untreated control. Bars represent mean  $\pm$  SEM. N=3 independent experiments with at least three replicates each experiment. Statistics by unpaired T-test.

### 5.3.7 MAPK/ERK, PXR and hypoxia

Mitogen-activated protein kinases (MAPKs) are serine/threonine kinases that play an important role in transducing extracellular signals, beginning with activation of cell surface receptors and to regulation of transcriptional factors and downstream kinases (Min, He and Hui, 2011). The extracellular signal-regulated kinase (ERK) is a subfamily member of MAPKs, activated directly by the upstream kinase, MAPK/ERK kinase (MEK) which catalyses the phosphorylation of human ERK at Tyr204/187 and then Thr202/185 (Roskoski, 2012). ERK1/2 signaling pathway can be activated in response to a diverse range of stimuli, including growth factors, cytokines (Lewis, Shapiro and Ahn, 1998; Roux and Blenis, 2004),



mitochondrial ROS (Bhagatte, Lodwick and Storey, 2012; Schroyer *et al.*, 2018) and in some studies under hypoxia (Minet *et al.*, 2000b; Jones and Bergeron, 2004; Osorio-Fuentealba *et al.*, 2009).

In our earlier work in this chapter, we found an increase in pro-inflammatory cytokines and in superoxide production under hypoxia, which are recognised as stimuli for ERK1/2. At the same time, we observed a decrease in PXR expression under hypoxia and with cytokine exposure. The hypothesis here is that hypoxia may activate MAPK/ERK signaling pathway, which ultimately downregulates CYP3A4 and CYP2C9 via negative regulation of the nuclear receptor PXR. We first examined the ERK1/2 phosphorylation under hypoxia to confirm the activation of this pathway. The MEK/ERK pathway was then inhibited by PD98059, a highly selective non-competitive reversible allosteric binding site inhibitor of MEK and hence the downstream MAP kinase cascade. This inhibition of MEK was followed by analysis of PXR, CYP3A4 and CYP2C9 protein expression in HepaRG cells subjected to hypoxia.

#### **5.3.7.1 ERK 1/2 phosphorylation under hypoxia**

HepaRG cells were exposed to either normoxia (21 % O<sub>2</sub>) or hypoxia (1% O<sub>2</sub> for 24 hrs) after which cells were lysed for total protein extraction, and 45 µg total protein loaded for SDS-PAGE Western blot. The activation of ERK pathway was assessed by using anti-phospho antibodies to detect the ERK phosphorylation at Thr 202 and Tyr 204 residues. **Figure 5.23A** shows the Western blot membrane of phosphorylated and total ERK1/2 and the loading control β-actin. A small (ca 20%) increase in ERK1/2 phosphorylation was observed under hypoxia compared to normoxia control (**Figure 5.23B**). This is in agreement with Minet *et al.* reporting an increase in ERK1/2 phosphorylation under hypoxia (1% O<sub>2</sub> for 2 h) in human microvascular endothelial cells and suggests ERK1 activation involvement in hypoxia-induced HIF-1 transactivation (Minet *et al.*, 2000b).

#### **5.3.7.2 PD98059 inhibits ERK 1/2 activation in HepaRG cells**

PD98059 is a selective noncompetitive cell-permeable inhibitor of the MEK/ERK pathway that acts by inhibiting MEK1/2 activation by upstream kinases, the PD98059 acting as a negative allosteric modulator. Using CellTiter Glo assay, the viability of HepaRG cells treated with PD98059 at concentrations ranging from 5 to 50 µM for 25 hrs was confirmed under normoxia ; **Figure 5.24**, shows viability of HepaRG cells was not affected with PD98059 treatments up to 50 µM.

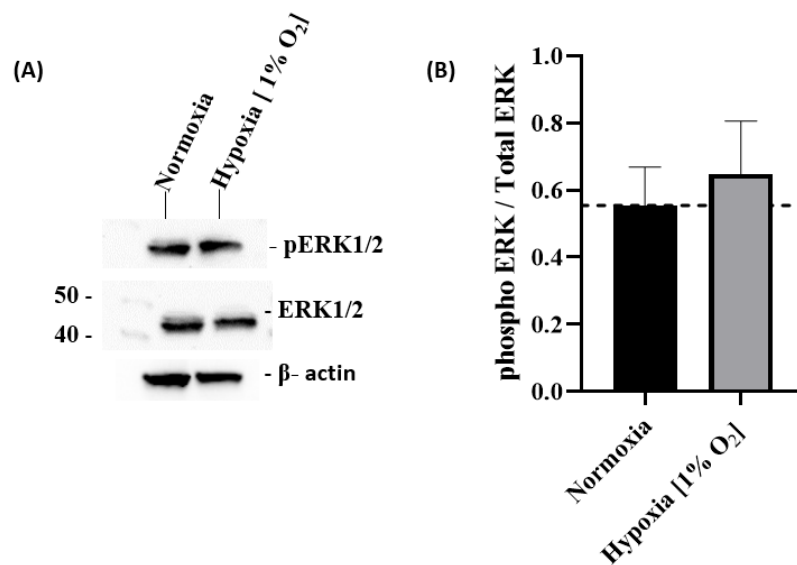


**Figure 5.23 Effect of hypoxia upon ERK1/2 protein expression in HepaRG cells.** HepaRG cells were differentiated following the standard protocol. After differentiation cells were exposed to hypoxia (1% O<sub>2</sub>) for 24 h. Cell cultured under normoxia were used as a control. By Western blot **Fig.5.23A** protein levels pERK1/2 (42/44 kDa), total ERK1/2 (42/44 kDa), and internal control β-actin (42 kDa). **Fig.5.23B** pERK1/2 densitometry quantification Western blot images representative one out of four independent experiments. Original membrane scans in Appendix 2, supplementary figure 2.18. Statistics by unpaired T-test.

**Figure 5.23** showed hypoxia led to higher levels of activated ERK1/2. The efficacy of PD98059 to inhibit ERK1/2 activation in HepaRG cells is shown in **Figure 5.25**. Here the cells were treated with PD98059 at concentrations of 5, 10, 25 and 50 μM for 1 h in normoxia conditions followed by an additional 24 h of co-incubation either under normoxia (**Figures 5.25A,B**) or hypoxia (1% O<sub>2</sub>) (**Figures 5.25C,D**). PD98059 treatment inhibited ERK1/2

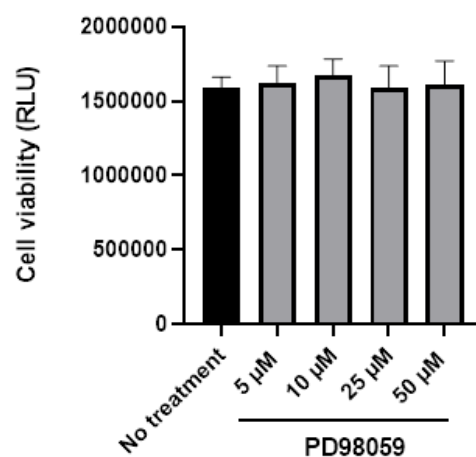


**Figure 5.24 Effect of PD98059 on HepaRG cell viability.** HepaRG cells were differentiated following the standard protocol. After differentiation cells were treated with increasing concentration of PD98059 for 25 h at normoxia. Untreated cells were used as a control. By CellTiter Glo assay the cell viability was determined. Bars represent mean ± SEM. N=3 independent experiments with at least six replicates each experiment. Statistics by one way ANOVA and post hoc Bonferroni test.

phosphorylation in a dose-dependent manner in both normoxia and hypoxia conditions. Under normoxic conditions, a significant reduction (50% decrease) was observed at a concentration of 5  $\mu\text{M}$ , whereas under hypoxic conditions, a higher concentration of 10  $\mu\text{M}$  is required to achieve an equivalent level of inhibition (50%). The data in Figure 5.23 suggests an increased activation of ERK 1/2 under hypoxia, contributing to its enhanced resistance to inhibition. Consequently, a greater dose of PD98059 may be needed to effectively suppress ERK 1/2 activity in the presence of hypoxia. It is less plausible that the diminished intracellular metabolism of PD98059 is due to hypoxia-induced CYP450 inhibition since no studies have demonstrated the involvement of CYP450 in the metabolism of PD98059. Overall, our results confirmed the efficacy of PD98059 to inhibit MEK and subsequently ERK1/2 phosphorylation in our hepatocyte model HepaRG.

### **5.3.7.3 PD98059 enhances PXR expression**

This chapter has so far show hypoxia to increase ERK activation and decrease PXR expression. Inhibition of ERK activation by use PD98059 was demonstrated under both hypoxia and normoxia. Next was the demonstration of the effects of PD98059 upon PXR expression.

PXR is a nuclear receptor that has a vital role in CYP3A4 and CYP2C9 transcriptional activation. PXR is predominantly located in the cytoplasm; however, upon activation, it translocate into the nucleus, forms a heterodimer with retinoid X receptor  $\alpha$  (RXR), and binds to several specific response elements in the 5' upstream region of CYP3A4 gene (Kawana *et al.*, 2003; Pondugula, Dong and Chen, 2009). The purpose here was to examine the involvement in ERK activation under hypoxia as a possible mechanism for the downregulation of PXR, and then the downregulation of CYP3A4 and CYP2C9. The hypothesis being hypoxia-induced ERK pathway activation will phosphorylate PXR, preventing PXR translocation into the nucleus and thereby suppressing CYP3A4/CYP2C9 transcription activation. Note: measurement of phospho-PXR levels was not possible (see below) and total PXR levels was the surrogate.

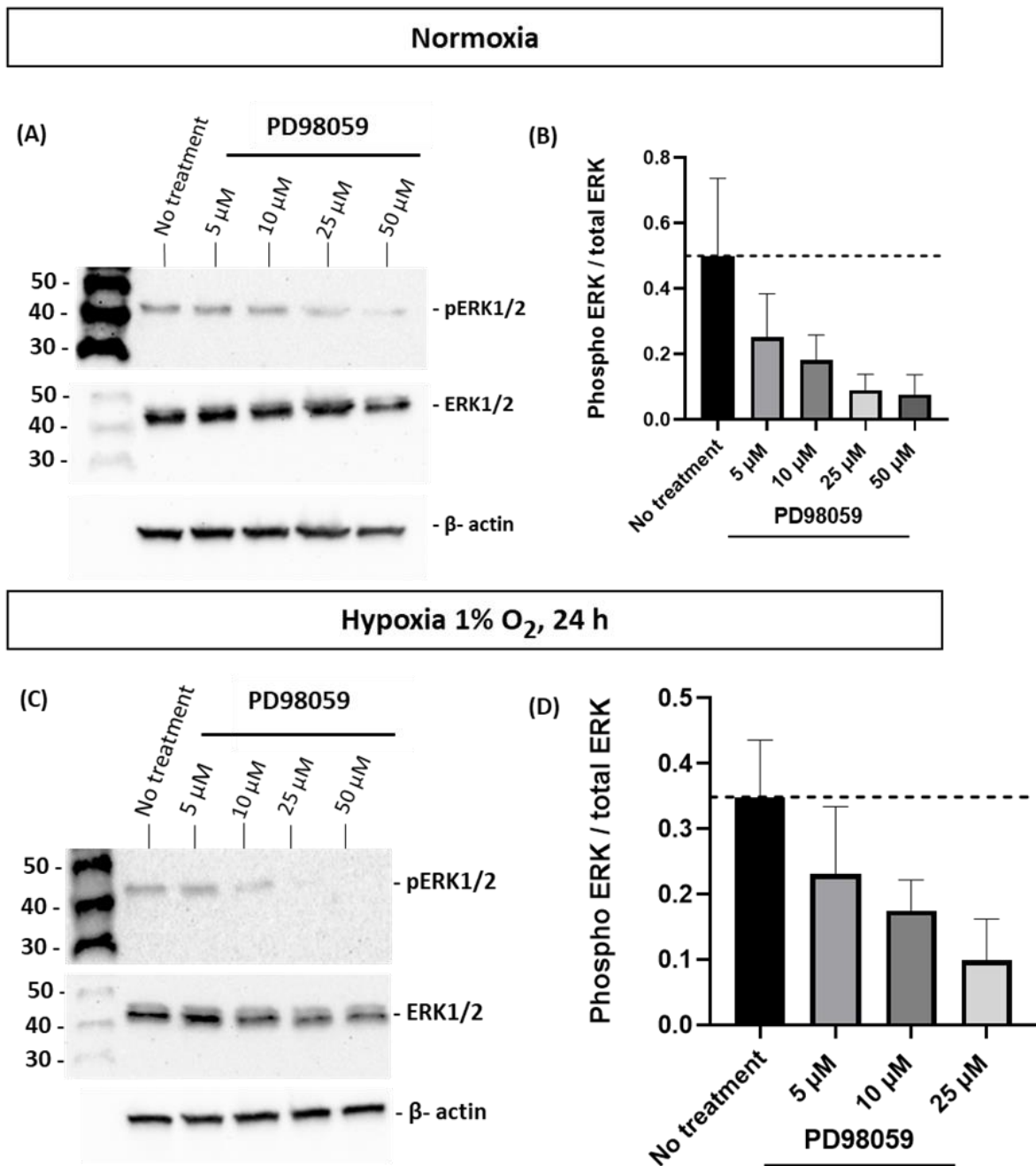


**Figure 5.25 Effect of PD98059 treatment upon ERK1/2 in HepaRG cells.** HepaRG cells were differentiated following the standard protocol. After differentiation cells were pre-exposed to 5, 10, 25, or 50  $\mu$ M of PD98059 under normoxia for one hour. After the initial incubation, cells were kept in normoxia (21% O<sub>2</sub>) or transferred to the hypoxia chamber (1% O<sub>2</sub>) for additional 24 h. By Western blot protein levels pERK1/2 (42/44 kDa), total ERK1/2 (42/44 kDa), and internal control  $\beta$ -actin (42 kDa) of cells cultured under normoxia **Fig.5.25A** or under hypoxia **Fig.5.25C**, pERK1/2 densitometry quantification when cells were cultured under normoxia **Fig.5.25B** or under hypoxia **Fig.5.25D**. Western blot images representative results of one out of three independent experiments. Original membrane scans in Appendix 2, supplementary figure 2.13 and 2.14. Statistics by one way ANOVA and post hoc Bonferroni test.

HepaRG cells were treated for 1 h under normoxia with various concentrations of PD98059 (5  $\mu$ M to 50  $\mu$ M) followed by an additional 24 h treatment co-incubation under either normoxia or hypoxia (1% O<sub>2</sub>). **Figure 5.26** shows the effects of PD98059 to upon the protein expression of total PXR (i.e. using an antibody that detects the total form of PXR); even though testing the phosphorylation of PXR is important to support our hypothesis, it was limited by the lack of commercially available of a phospho-PXR antibody in the market. Nevertheless, an increase in total PXR protein expression with PD98059 treatment was observed in both normoxia (**Figure 5.26A,B**) and hypoxia (**Figure 5.26C,D**), with 25-50  $\mu$ M PD98059 concentrations leading to an increase of up to 53% (normoxia) and up to 166% (hypoxia).

The activation of ERK may directly phosphorylate an array of nuclear receptors, which generally occurs at serine and threonine amino acid residues surrounded by proline, and leading to negative or positive transcriptional regulation (Zassadowski *et al.*, 2012). Lichti-Kaiser *et al.* identified human PXR to be a target for direct phosphorylation by a MAPK at serine350 (Lichti-Kaiser *et al.*, 2009) with negative effects on PXR transcriptional activity and by altering its pattern of subcellular localisation, affecting its interaction with co-repressors or co-activators or decrease the ability of PXR to form heterodimers with retinoid X receptor  $\alpha$  (Wang *et al.*, 2012). Based on total protein in whole cell lysates Figure 5.26 reflects direct transcriptional/translational impacts.

#### **5.3.7.4 PD98059 enhances CYP450 expression**

This chapter has so far show hypoxia to decrease CYP450 expression, to increase ERK activation and decrease PXR expression. Inhibition of ERK activation by PD98059 was demonstrated under both hypoxia and normoxia. Further, PD98059 increased the expression of PXR. Having also demonstrated that rifampicin induced increases in PXR were associated with increased CYP450 expression we explored here how PD98059 (as an inhibitor of ERK activation) affects the expression of CYP3A4 and CYP2C9.

Similar to earlier studies, HepaRG cells were treated for 1 h under normoxia with PD98059 (5  $\mu$ M to 50  $\mu$ M) followed by an additional 24 h co-incubation under normoxia or hypoxia (1% O<sub>2</sub>), and the cell lysates were subjected to Western blot.

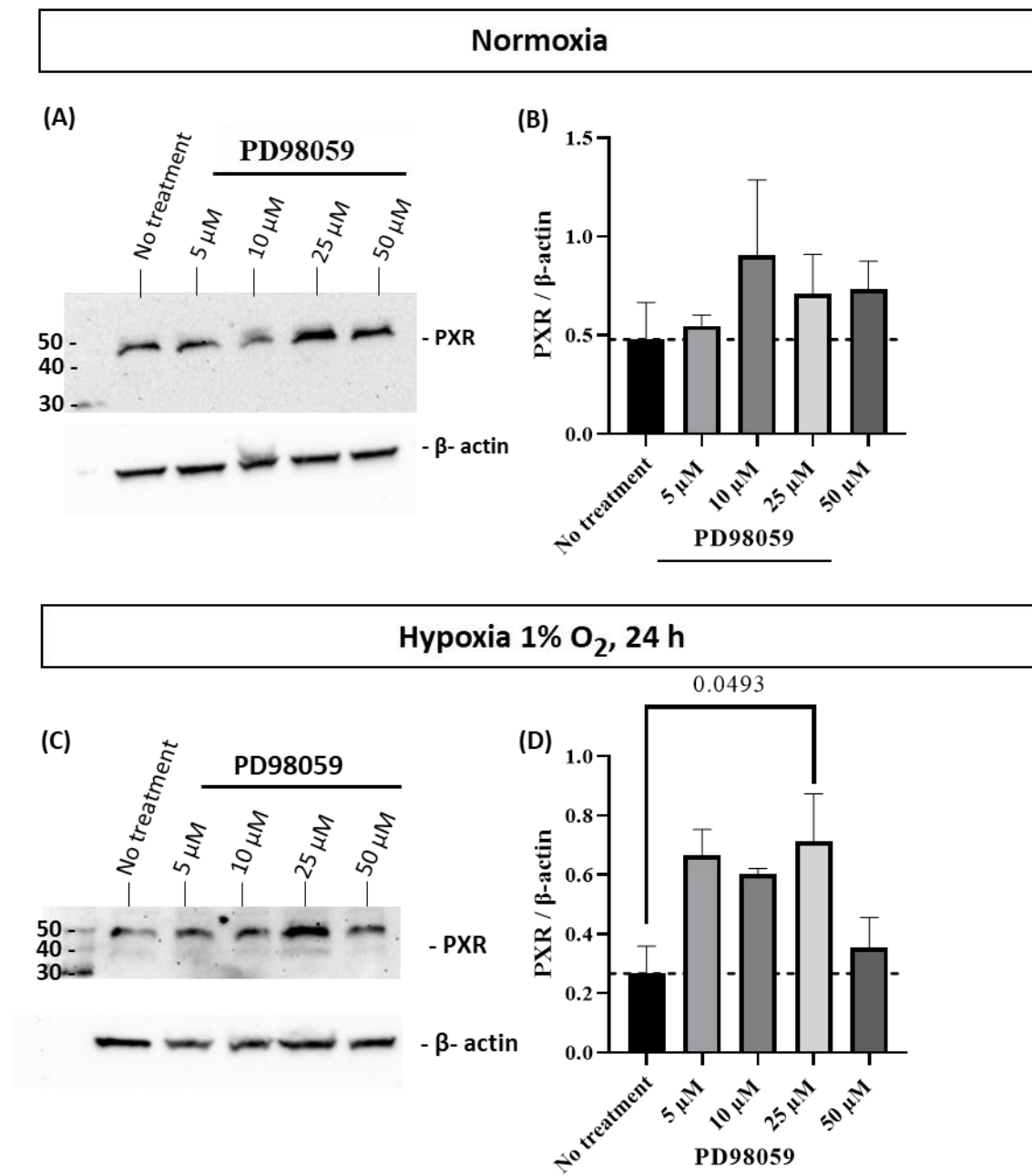


**Figure 5.26 Effect of PD98059 treatment upon PXR in HepaRG cells.** HepaRG cells were differentiated following the standard protocol. After differentiation cells were pre-exposed to 5, 10, 25, or 50  $\mu$ M of PD98059 under normoxia for one hour. After the initial incubation, cells were kept in normoxia (21% O<sub>2</sub>) or transferred to the hypoxia chamber (1% O<sub>2</sub>) for additional 24 h. By Western blot protein levels PXR (50 kDa) and internal control  $\beta$ -actin (42 kDa) of cells cultured under normoxia **Fig.5.26A** or under hypoxia. **Fig.5.26C**. PXR densitometry quantification when cells were cultured under normoxia **Fig.5.26B** or under hypoxia **Fig.5.26D**. Western blot images representative results of one out of three independent experiments. Original membrane scans in Appendix 2, supplementary figure 2.15 and 2.16. Statistics by one way ANOVA and post hoc Bonferroni test.

**Figure 5.27A** shows under normoxia, the treatment with PD98059 resulted in elevated CYP3A4 expression at all concentrations employed, with the exception of the 50  $\mu\text{M}$  concentration. Likewise, under normoxic conditions, PD98059 induced upregulation in CYP2C9 expression at all concentrations tested, except for the 50  $\mu\text{M}$  concentration. **Figure 5.27B** shows that in hypoxia the CYP2C9 expression level was increased above control at all concentrations of PD98059 applied. The impact of PD98059 treatment in hypoxia upon CYP3A4 was less clear; increases were seen at 5-10  $\mu\text{M}$  but decreases relative to control were evident at 25-50  $\mu\text{M}$  PD98059. This pattern was not seen for the impact of PD98059 upon PXR expression in hypoxia (Figure 5.26C,D) which used PD98059 concentrations up to 50  $\mu\text{M}$ , although greater inhibition was evident at 50  $\mu\text{M}$  here also. It is unlikely to be a toxicity issue *per se* in hypoxia as the responses to PD98059 at 50  $\mu\text{M}$  in hypoxia (Figure 5.27B) showed a significant restoration in CYP2C9 expression compared to control. While the link to the present data, specifically why CYP3A4 levels declined in hypoxia with higher PD98059 concentrations, was not explored in this current work, early studies with PD98059 (Alessi *et al.*, 1995) showed it to display differential inhibition in the phosphorylation of MEK1 and MEK2. Specifically, in a range of cell types (mouse Swiss 3T3 fibroblasts, human KB fibroblasts, and PC12 cells) PD98059 inhibition in the activation of MEK2 was weaker than MEK1, i.e. PD98059 is a more potent inhibitor of MEK1 activation with effects on MEK1 seen at lower concentrations of PD98059 ( $\text{IC}_{50} = 2\text{-}7 \mu\text{M}$ ), whereas MEK2 activation requires higher concentrations of PD98059 ( $\text{IC}_{50} = 50 \mu\text{M}$ ). It could be that inhibition of MEK1 (at lower concentrations has the more protective role for CYP3A4 under hypoxia. Indeed, a similar profile whereby lower concentrations of PD98059 were more effective for restoring CYP3A4 was also seen in normoxia (Figure 5.27A). For this to be relevant there would need to be distinct signalling emerging from activation of MEK1 and MEK2 that ultimately impact CYP3A4 expression in opposing directions, i.e. activation of MEK1 repressing CYP3A4 while activation of MEK2 can play a part in maintaining CYP3A4 expression.

The MAPK pathway features a wide diversity of activators, substrates and functions. Its regulation is complex and downstream signal specificity arises from a combination of pathways (Braicu *et al.*, 2019). Isoforms of the same enzyme can display not fully overlapping signalling and functional outcomes. This is true for MEK1 and MEK2 which display divergent homologies in some of their regulatory regions that impacts function. For example, MEK1 supports phosphorylation by the serine/threonine protein kinase PAK1 which is associated with enhanced signalling through Raf-MEK-ERK (Coles and Shaw, 2002). Some examples of

divergent roles so far identified include: Unique activation patterns of MEK1 and MEK2 in hepatocytes occurring in response to the addition of EGF to culture media during cell plating, with MEK1 activated immediately whereas MEK2 is activated only after 24 h in culture (Rescan *et al.*, 2001). MEK1 activation preferentially driving proliferation, whereas in the same cell type MEK2 activation induces growth arrest (Ussar and Voss, 2004). This may be related to the independent finding that MEK1 and MEK2 regulate distinct sorting of ERK2 to different intracellular compartments, with MEK1-activated ERK2 accumulating in the nucleus and induces proliferation whereas MEK2-activated ERK2 retained in the cytoplasm (Skarpen *et al.*, 2008). In pancreatic cancer cells inhibition of MEK1 limits cell proliferation, while MEK2 inhibition alters cell morphology and invasive ability (Zhou *et al.*, 2010).

Noting the results described above, if we consider the lower concentration of PD98059, i.e. 5 and 10  $\mu\text{M}$ , the data clearly shows an increase in CYP3A4 and CYP2C9 protein expression above control in both normoxia and hypoxia conditions, which supports at least the partial involvement of the MEK/ERK pathway in hypoxia-induced downregulation of CYP450. To our knowledge, this study is the first that explores the regulation of PXR and CYP3A4/2C9 by ERK pathway in HepaRG cells under hypoxia using PD98059 as an inhibitor. A study under normoxia using U0126, a prototypical MEK1/2 inhibitor (working via activation of PXR), has been shown to upregulate CYP3A4 mRNA expression in HepG2 cells. An outcome reported to occur via dual mechanisms: direct binding of U0126 to the PXR ligand binding domain, which results in steroid receptor coactivator-1 recruitment and the binding of PXR to nuclear receptor response elements within the CYP3A4 promoter. A second indirect mechanism restores CYP3A4 expression by downregulating small heterodimer partner (SHP) corepressor expression (Smutny *et al.*, 2014). A recent investigation has revealed that within 3D spheroid cultures of primary human hepatocytes under normoxia, the application of AZD1208 – a compound that hinders the phosphorylation of ERK1/2 at Tyr204, thus inhibiting the MAPK/ERK signaling cascade – leads to a substantial 3.5-fold increase in the mRNA expression of CYP3A4 and CYP2B6, along with a 2-fold increase in CYP2C9 mRNA when compared to untreated controls. Furthermore, the protein expression and functional activity of CYP3A4 exhibited significant augmentation following AZD1208 treatment. Concurrently, by employing small interfering RNA (siRNA)-mediated knockdown of PXR, the researchers additionally demonstrated the involvement of PXR in the induction of CYP3A4 and CYP2B6. As a result, they proposed the idea of inhibiting PXR through modulation of the MAPK/ERK pathway (Hendriks *et al.*, 2020). Research centered on the MAPK/ERK signaling pathway and



the subsequent regulation of PXR and CYP450 in the context of hypoxia is currently limited. In a laboratory-based study, rabbit hepatocytes were exposed to serum obtained from rabbits experiencing hypoxemia or chemically induced hypoxia using CoCl<sub>2</sub>. This exposure led to the activation of protein expression in CYP3A6, HIF1- $\alpha$ , and c-jun. Inhibition of MEK1/2 phosphorylation, indicating the deactivation of ERK1/2 through PD98059, impedes the up-regulation of CYP3A6 and inhibits the increase of c-jun. However, it does not hinder the increase in HIF-1 $\alpha$  levels or its binding to the CYP3A6 oligonucleotide probe. The increase in CYP3A6 induced by serum from rabbits experiencing hypoxia appears to occur independently of CAR and PXR (Fradette and Du Souich, 2003).

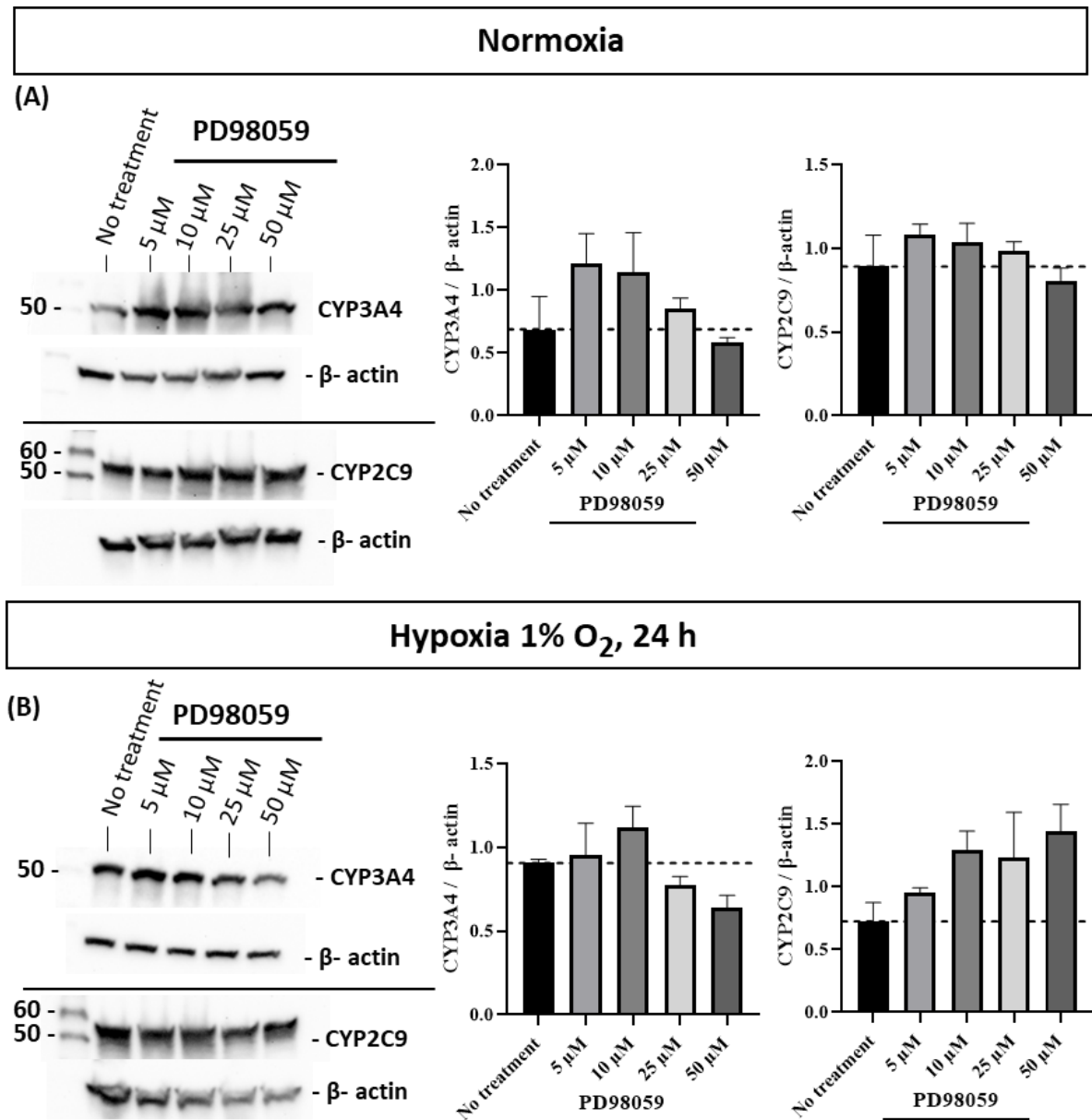


**Figure 5.27 The effect of ERK1/2 inhibition by PD98059 upon CYP3A4 and CYP2C9 protein expression.** HepaRG cells were differentiated following the standard protocol. After differentiation cells were pre-exposed to 5, 10, 25, or 50  $\mu$ M of PD98059 under normoxia for one hour. After the initial incubation, cells were kept in normoxia (21% O<sub>2</sub>) or transferred to the hypoxia chamber (1% O<sub>2</sub>) for additional 24 h. By Western blot protein levels of CYP3A4 (50 kDa) and CYP2C9 (55 kDa) under normoxia [Fig.5.27A](#) or hypoxia [Fig.5.27B](#).  $\beta$ -actin (42 kDa) was used as internal control. Bars represents densitometry quantification of CYP3A4 and CYP2C9. Western blot images representative results of one out of three independent experiments. Original membrane scans in Appendix 2, supplementary figure 2.17. Statistics by one way ANOVA and post hoc Bonferroni test.

## 5.4 Conclusions

This chapter explores the mechanism by which hypoxia downregulates CYP450, focusing on stressors, i.e. inflammatory mediators and ROS, and studying the PXR and ERK pathways. The work in this chapter has resulted in the following findings:

- Different assays show different direction of ROS production under hypoxia in HepaRG cells. Hypoxia had the capacity to increase the production of mitochondrial superoxide as measured by Mitosox assay. While using fluorogenic probe and luminescence-based detection assays shows a decrease in the production of peroxynitrite, hydroxyl radical, nitric oxide, hydrogen peroxide and peroxy radicals.
- Hypoxia has the capacity to upregulate the transcription levels of pro-inflammatory cytokines IL-12, IL-6, IL-1 $\beta$ , and TNF- $\alpha$  in HepaRG cells.
- IL-6 and TNF- $\alpha$  negatively regulate CYP3A4 and CYP2C9 transcription and translation.
- ROS modulation using the inducer menadione deteriorates CYP3A4 and CYP2C9 levels, while the antioxidants NAC or Tiron protect CYP3A4 and CYP2C9 mRNA, protein expression and functional activity under hypoxia.
- Hypoxia and pro-inflammatory cytokines IL-6 and TNF- $\alpha$  negatively regulate PXR mRNA and protein levels.
- ERK1/2 pathway seems to be activated under hypoxia in HepaRG cells.
- Using PD98059 as an inhibitor of ERK1/2, we have shown an enhancement in PXR protein expression under hypoxia, suggesting that ERK 1/2 activation under hypoxia may negatively regulate PXR.
- By employing PD98059 as an inhibitor of the ERK1/2 pathway, we have observed a certain degree of upregulation in CYP3A4 and CYP2C9 at low treatment doses under hypoxic conditions. This observation suggests that the MEK/ERK pathway could potentially serve as a mechanism for the downregulation of CYP450 in hypoxia through the regulation of PXR.

**Chapter 6: Acute arterial hypoxaemia and its impact  
on drug pharmacokinetics in humans; a  
pharmacokinetic-pharmacodynamic Monte Carlo  
simulation study**

## 6.1 Introduction

Acute exposure to hypoxia has the capacity to alter the pharmacokinetics (PK) of drugs; the PK providing quantitative parameters that define a drug's absorption and disposition. As stated in Chapter 3, very limited well-controlled evidence exists that helps define the probable impacts of acute hypoxia upon drug PK, a need which led to our clinical trial preparations involving sildenafil. That work was aimed on acute hypoxia experienced by millions of lowlanders who travel to terrestrial high altitudes and that risk acute mountain sickness. This is a condition that can be managed by sildenafil, a selective inhibitor of cGMP-specific phosphodiesterase type 5. However, the impact upon clinical arterial hypoxaemia upon a drug's PK in respiratory and cardiovascular patients also remains a hugely under-examined area, again lacking a strong evidence base.

In the context of clinical arterial hypoxaemia, however, Rowett *et al* (1996) reported a quite unique study involving ten patients with controlled *cor pulmonale* and compensated respiratory failure, each requiring continuous 24 h supplemental oxygen to correct the hypoxaemia. In this cross-over design the patients experienced controlled periods where supplemental oxygen was withheld (inducing 'clinical hypoxaemia', PaO<sub>2</sub> 50 mmHg) or administered oxygen to maintain normoxaemia (PaO<sub>2</sub> 60 mmHg). With each patient receiving oral and IV furosemide, the authors found the acute hypoxaemia periods not to change furosemide pharmacokinetics in respect to unchanged total clearance (bound or free), renal clearance (amount excreted unchanged), volume of distribution or the absolute extent of oral bioavailability (Rowett *et al.*, 1996). In this context, furosemide elimination pharmacokinetics is extensively dependent upon the kidneys (approximately 85% elimination by the kidneys following an IV dose), both in terms of renal metabolism (ca. 40% of total elimination) and renal excretion of unchanged drug (ca. 45% of total elimination). As highlighted in Chapter 3, however, there still remains the need to explore how hypoxia/hypoxaemia impacts upon drug PK both acutely and chronically and particularly so for drugs eliminated extensively by metabolism. Sildenafil was chosen for our clinical trial work not only for its use by mountaineers to manage acute mountain sickness but also, in contrast to furosemide, because its clearance depends extensively upon metabolism in the liver and involves CYP3A4, an isoenzyme involved in the elimination of a large number of approved and clinical experimental drugs.

In the absence of being able to conduct the sildenafil clinical trial and based upon both literature PK data for sildenafil and this thesis' experimental data of how hypoxia affects CYP450

function, a PK simulation was undertaken to allow some possible scenarios to be explored. Further, the probability outcome for these scenarios would be invaluable for improved trial design (e.g. dosing, PK and PD sample timings) ahead of the restart in the near future of the sildenafil hypoxia PK-PD clinical trial.

This chapter utilises the approach of Monte Carlo simulation to model the probability of different PK outcomes. Monte Carlo simulation is a widely used approach in PK-PD (Goutelle *et al.*, 2009; Bradley *et al.*, 2010; Trang, Dudley and Bhavnani, 2017; Girdwood *et al.*, 2022). It is a form of probability analysis, where a model (in this case PK and PD) is constructed that integrates different variables, e.g. drug clearance (CL), extent of bioavailability (F) etc., each with their own probability distribution. These variables are entered into the respective PK and/or PD model and upon each re-run of the model (typically 1000s of times) different values are assigned to the variable in question. The averaged outcome (the estimate), which in this work is represented by estimated sildenafil plasma concentration vs. time profiles, and the variance around this estimate(s) allows consideration of the range of possibilities and the probability of their occurrence.

### 6.1.1 Aim and Objectives

The aim of this chapter is to estimate, by Monte Carlo simulation, the pharmacokinetics and pharmacodynamics of a 100 mg single oral dose of sildenafil in adults exposed to hypoxaemia in a range of scenarios including acute exposure.

#### Objectives

1. Undertake literature survey: for sildenafil PK parameters and the variability of these PK parameters. Similarly, the PD parameters e.g.,  $IC_{50}$  for sildenafil in its action to inhibit the enzyme phosphodiesterase 5 (PDE5), the predominant PDE target for sildenafil and whose inhibition in vascular smooth muscle leads to relaxation; for the effect of acute hypoxia on hepatic and renal blood flows, data which may be incorporated into the simulations.
2. Explore and quantify the alteration of CYP3A4 and CYP2C9 functional activity under hypoxia conditions using an in-vitro hepatocyte model. Make use of this in-vitro data to in the simulation of sildenafil hepatic intrinsic clearance ( $Cl_{int}$ ) under exposure to acute hypoxia.
3. Simulate different sets/scenarios of PK/PD outcomes for a 100 mg single oral dose of sildenafil in 'healthy adults' exposed to hypoxia.

- **SET 1:** simulate the PK/PD profile of sildenafil over a 24 h period where the hypoxia intervention causes a reduction in sildenafil hepatic intrinsic clearance ( $CL_{int}$ ) (estimated from experimental in-vitro data in this thesis). This Set includes three scenarios:
  - **Scenario A:** Normoxia vs, hypoxia where the effects of hypoxia to reduce hepatic metabolism are already maximal before the 24 h PK-PD simulation begins, i.e., before the single oral dose administration of sildenafil. This scenario may depict mountaineers taking sildenafil only after they have already ascended to 2,500 metres and they are already experiencing hypoxaemia. This would also be a relevant simulation where drugs are newly prescribed to patients experiencing hypoxaemia. Further, it would be a scenario of a laboratory clinical research study, where a volunteer enters a normobaric experimental hypoxia chamber, experience the full effects of hypoxaemia and then be administered sildenafil.
  - **Scenario B:** Normoxia vs, hypoxia where the effects of hypoxia upon hepatic metabolism gradually arise from time 0 of the simulation (i.e. the point at which the single oral dose administration of sildenafil occurs) through to 4 h into the simulation, at which time the effects of hypoxia to reduce sildenafil  $CL_{int}$  are at a maximum level. This progressive four-hrs increase in the effects of hypoxia upon  $CL_{int}$  follow a simple linear relationship with time. This scenario may depict mountaineers taking sildenafil at the start of the ascent and then experiencing progressive reductions in oxygen levels over the following 4 h as they ascend in altitude.
  - **Scenario C:** Normoxia vs, hypoxia where the effects of hypoxia upon hepatic metabolism occur in an immediate in a ‘step-function’ and maximal manner at 4 h into the simulation (i.e., 4 h after the single oral dose administration of sildenafil). This scenario may depict a laboratory clinical research study where a volunteer enters a normobaric experimental hypoxia chamber at 4 h after the administration of oral sildenafil (i.e. instantly switched from normoxia to hypoxia) and at this point experience the full/maximal effects of hypoxaemia.

- **SET 2:** This set of simulation investigate the PK-PD profile of sildenafil under hypoxic conditions, considering the simultaneous decrease in hepatic clearance ( $CL_{int}$ ) and the alteration of hepatic blood flow. In this scenario, the maximal physiological effects are already established prior to the start of the 24-h PK-PD simulation.
  - **Scenario A:** Normoxia vs, hypoxia - In this scenario, apart from the maximal decrease in  $CL_{int}$ , there is an additional 40% increase in hepatic blood flow.

## 6.2 Method

### 6.2.1 Literature search

#### 6.2.1.1 Pharmacokinetic parameters for sildenafil

Here the aim was to identify from the published literature a consensus for sildenafil PK parameters following IV and oral administration, parameters that would underpin the simulation studies. The following key terms were used to search the PubMed database: “Sildenafil” OR “PDE5 inhibitors” AND “pharmacokinetics”. Studies included were those involving healthy adult human volunteers given single oral and/or IV dosages of sildenafil. The search yielded 794 publications, and after screening the title and abstract, ten related papers were chosen. Five of these studies met the inclusion criteria and which were then used to define the PK parameters of sildenafil. These studies were (Walker *et al.*, 1999; Milligan, Marshall and Karlsson, 2002; Muirhead *et al.*, 2002; Nichols, Muirhead and Harness, 2002; Vachier *et al.*, 2011). Four of the five studies reported sildenafil PK after IV administration (Walker *et al.*, 1999; Muirhead *et al.*, 2002; Nichols, Muirhead and Harness, 2002; Vachier *et al.*, 2011), while all four of the five studies reported sildenafil PK in oral tablet dosage form (**Table 6.1**).



Table 6.1 Pharmacokinetics parameters of sildenafil following a single oral or IV dose.

Parameters	Walker <i>et al.</i> , 1999		Muirhead <i>et al.</i> , 2002		Nichols, Muirhead, and Harness <i>et al.</i> 2002		Vachieri <i>et al.</i> , 2011	Milligan, Marshall and Karlsson, 2002
	Oral tablet (n=3)	IV bolus (n=3)	Oral tablet (n=3)	IV bolus (n=3)	Oral tablet (n=12)	IV bolus (n=12)	IV bolus (n=10)	Oral tablet (n=450)
Dosage form/sample size	Oral tablet (n=3)	IV bolus (n=3)	Oral tablet (n=3)	IV bolus (n=3)	Oral tablet (n=12)	IV bolus (n=12)	IV bolus (n=10)	Oral tablet (n=450)
Dose (mg)	50	25	50	25	50	50	10	50
C <sub>max</sub> (ng/mL)	212	-	207	-	159	-	-	157
T <sub>max</sub> (h)	1.2	-	1.14	-	1.46	-	-	1.03
K <sub>a</sub> (h <sup>-1</sup> )	-	-	-	-	-	-	-	2.60
t <sub>1/2</sub> elimination (h)	3.7	2.4	3.19	2.18	4.07	3.92	3.2	3.67
CL (L/h)	-	*25.2	-	**26	-	40.8	32.2	***57.4
K (h <sup>-1</sup> )	0.04	-	-	-	0.17	0.18	-	-
fu (fraction unbound)	0.04	-	-	-	-	-	-	-
F (oral bioavailability %)	38	-	-	-	41	-	-	41
V <sub>c</sub> (L)	-	*84	-	-	-	234	137.3	***297
AUC (ng /mL.h)	-	-	729	971	530	1291	329.7	950
Urinary excretion (%) (Parent and metabolites)	12	13	12.28	13.05	-	-	-	-
Variability in CL/F between subjects (%)	-	-	-	-	-	-	-	29
Variability in V/F between subjects (%)	-	-	-	-	-	-	-	20
Variability in F between subjects (%)	-	-	-	-	****3.5	-	-	-

\*Value reported in the study as mL/min /kg for CL and L/kg for V<sub>c</sub>. The units were converted to L/h for CL and L for V<sub>c</sub>

\*\* Value was calculated using CL=Dose/AUC<sub>0-∞</sub>

\*\*\* Value presented as CL/F and V/F

\*\*\*\*The variability in F is calculated from the 90% confidence interval (CI) provided in Nichols *et al.* 2002 using: F variability = (upper CI - lower CI )/3.29 ; where upper CI = 47.3% and lower CI = 35.6%. The value 3.29 is the factor used to calculate the variability corresponding to a 90% confidence interval.

### 6.2.1.2 IC<sub>50</sub> of sildenafil

Here, the aim was to identify from the published literature a consensus for sildenafil PD. Five studies were identified that reported the IC<sub>50</sub> of sildenafil in its inhibition of PDE5: (Boolell *et al.*, 1996; Saenz De Tejada *et al.*, 2001; Corbin, Francis and Webb, 2002; Bischoff, 2004; Wang *et al.*, 2013) **Table 6.2** summarises the IC<sub>50</sub> of sildenafil PD values. The average IC<sub>50</sub> of 5.22 nM (= 2.48 ng/mL) was used in the simulation and taken to correspond to free (unbound) drug concentrations and not total concentrations.

**Table 6.2 IC<sub>50</sub> of Sildenafil**

Model	IC <sub>50</sub> for PDE5 (nm)	Study
PDE5 isozymes extracted from human corpus cavernosum	3.5	(Corbin, Francis and Webb, 2002)
PDE5 isozymes extracted from human corpus cavernosum	3.9	(Boolell <i>et al.</i> , 1996)
Recombinant human PDE5 enzyme	5.2	(Wang <i>et al.</i> , 2013)
PDE5 isozymes extracted and purified from human platelets	6.6	(Saenz De Tejada <i>et al.</i> , 2001)
Recombinant human PDE5 enzyme	8.5	(Bischoff, 2004)

### 6.2.1.3 Renal blood flow changes under acute hypoxia

The need to model the effect of acute hypoxia upon renal blood flow was less clear than that for changes in hepatic flow. Two studies have measured renal blood flow after short exposure to hypoxia (10 to 14% O<sub>2</sub> for 2 h). These studies found an increase in renal blood flow but critically no change in GFR (Berger *et al.*, 1949; Olsen *et al.*, 1993). Another study was conducted over a longer duration of hypoxia, 24 h in healthy subjects ascending to an altitude of 4330 m. Here a decrease in renal blood flow by 17% was observed. This reduction was considered by the author to arise from an increase in vasoconstriction, renal vascular resistance, and a decrease in renal oxygen supply (Steele *et al.*, 2020). As renal clearance, at least under normoxia, contributes little (ca, 13%) to overall sildenafil total clearance, and the impact upon GFR of any such changes in blood flow were not evidenced, the effects of hypoxia upon renal blood and sildenafil were not simulated in this current work.

### 6.2.1.4 Hepatic blood flow changes under hypoxia

Here the aim was to identify from the published literature a consensus for the effects of acute hypoxia upon hepatic blood flow. One study examined the impact of hypoxia on hepatic portal vein (HPV) blood flow in humans. A 40% increase in HPV blood flow and a 97% rise in pre-prandial superior mesenteric artery blood flow was seen in 12 healthy subjects ascending to an altitude of 4392 m for 24 h. These changes arising from increased vessel diameter, flow velocity and heart rate (Nicholas S Kalson *et al.*, 2010) .

### 6.2.2 In-vitro CYP3A4 and CYP2C9 functional activity assay

Using the 2D model, HepaRG cells were cultured for a period of two weeks, followed by an additional two weeks of differentiation, achieved by supplementing the medium with 2% DMSO (as outlined in **Chapter 2, Section 2.1.2**). The HepaRG cells were subjected to the following conditions: a) normoxia, representing normal oxygen levels (21%), serving as the control for each time point in the experiment; b) hypoxia (1% O<sub>2</sub> for 4 h); c) hypoxia (1% O<sub>2</sub> for 6 h); and d) hypoxia (1% O<sub>2</sub> for 24 h). To assess CYP functional activity, the P450-Glo™ assays (Promega, UK) were employed, following the procedures outlined in **Chapter 2, Section 2.3.1**.

### 6.2.3 Determination of CL-based parameters for simulation

With all of the following PK parameters obtained from the literature as a mix or calculated as below on the basis either an absolute value, e.g. L/h, or provided per kg body, e.g. mL/min/kg then conversion between the two used for an average body weight 70 kg.

#### NORMOXIA

**Total body Clearance (CL)** From the literature 40.8 L/h (= 9.71 mL/min/kg) (Nichols, Muirhead and Harness, 2002).

**Renal CL (CL<sub>renal</sub>)** at 13% of total body CL (Nichols, Muirhead and Harness, 2002).

$$CL_{\text{renal}} = CL \cdot 0.13 \quad \dots \text{Eq. 6.1}$$

Hence from Eq 6.1 CL<sub>renal</sub> is 5.3 L/h (= 1.26 mL/min/kg)

**Hepatic CL (CL<sub>hepatic</sub>)** at 87% of total body CL.

$$CL_{\text{hepatic}} = CL \cdot 0.87 \quad \dots \text{Eq. 6.2}$$

## Chapter 6

Hence from Eq 6.2  $CL_{\text{hepatic}}$  is 35.5 L/h (= 8.45 mL/min/kg)

**Hepatic intrinsic CL ( $CL_{\text{int}}$ )** The hepatic intrinsic CL ( $CL_{\text{int}}$ ) was calculated from:

Initially realising that organ Clearance can be first defined as a function of blood flow (Q) and Extraction ratio (E) as below:

$$CL_{\text{hepatic}} = Q_h \cdot E_h$$

From this:

$$CL_{\text{hepatic}} = \frac{Q_h \cdot f_u \cdot CL_{\text{int}}}{Q_h + (f_u \cdot CL_{\text{int}})} \dots \text{Eq. 6.3}$$

Where  $E_H = \frac{f_u \cdot CL_{\text{int}}}{Q_h + (f_u \cdot CL_{\text{int}})}$  and  $CL_{\text{int}}$  is from rearranging Eq. 6.3 to obtain Eq. 6.4:

$$CL_{\text{int}} = \frac{-CL_{\text{hepatic}} \cdot Q_h}{((CL_{\text{hepatic}} \cdot f_u) - (Q_h \cdot f_u))} \dots \text{Eq. 6.4}$$

$$CL_{\text{int}} = 356.96 \text{ mL/min/kg} = \text{ca. } 1499 \text{ L/h}$$

Where:

$Q_h$  = total hepatic blood flow = 20.7 mL/min/kg (= 86.94 L/h for a 70 kg individual (Davies and Morris, 1993; Naritomi *et al.*, 2001).

$f_u$  = fraction unbound = 0.04 (Walker *et al.*, 1999).

$CL_{\text{hepatic}}$  = Hepatic Clearance = 8.45 mL/min/kg

## **HYPOXIA**

### **Hepatic intrinsic Clearance under hypoxia ( $CL_{\text{int} \parallel}$ )**

Using in-vitro CYP3A4 and CYP2C9 functional activity measurements data, there was 18% decrease of activity in CYP3A4 and a 75% decrease of activity in CYP2C9 (see **Section 6.3.1, Figure 6.1**) The approach to modelling the effect on hypoxia upon hepatic intrinsic clearance to obtain  $CL_{\text{int} \parallel}$  and hence hepatic clearance under hypoxia ( $CL_{\text{hepatic} \parallel}$ ) and total body clearance under hypoxia ( $CL_{\parallel}$ ) made use of a residual factor for hypoxia  $RF_{\text{hypoxia}}$ ; where

$$RF_{\text{hypoxia}} = \text{Adjustment for CYP3A4} + \text{Adjustment for CYP2C9}$$

Where 'Adjustment for CYP3A4' = Fraction sildenafil metabolism via CYP3A4 reported under normoxia \* [1 – mean hypoxia-induced fractional reduction in in-vitro metabolism via CYP3A4]

$$= 0.8 * (1 - 0.18) = 0.656$$

## Chapter 6

Where 'Adjustment for CYP2CP' = Fraction sildenafil metabolism via CYP2C9 reported under normoxia \* [1 – mean hypoxia-induced fractional reduction in in-vitro metabolism via CYP2C9]

$$= 0.2 * (1 - 0.75) = 0.050$$

Hence  $RF_{\text{hypoxia}} = 0.706$  or 0.71

Therefore:

$$CL_{\text{int} \parallel} = CL_{\text{int}} \cdot RF_{\text{hypoxia}} \dots \text{Eq. 6.5}$$

Hence  $CL_{\text{int} \parallel} = 253.44 \text{ mL/min/kg} = 1064 \text{ L/h}$  Representing a 29% reduction with hypoxia

### Hepatic CL under hypoxia ( $CL_{\text{hepatic} \parallel}$ )

Assuming no change in hepatic blood flows with hypoxia then

$$CL_{\text{hepatic} \parallel} = \frac{Q_h \cdot f_u \cdot CL_{\text{int} \parallel}}{Q_h + (f_u \cdot CL_{\text{int} \parallel})} \dots \text{Eq. 6.6}$$

Hence  $CL_{\text{hepatic} \parallel} = 28.57 \text{ L/h}$  (= 6.80 mL/min/kg), a 19.5% decrease compared to normoxia.

Where:

$Q_h$  = total hepatic blood flow = 20.7 mL/min/kg (= 86.94 L/h for a 70 kg individual)

$f_u = 0.04$

$CL_{\text{int} \parallel} = 253.44 \text{ mL/min/kg}$  which equates to 1064 L/h for 70 kg individual

### Total body Clearance (CL) under hypoxia ( $CL_{\parallel}$ )

Under the condition that hypoxia does not change  $CL_{\text{renal}}$  then total body Clearance (CL) under hypoxia ( $CL_{\parallel}$ ) is:

$$CL_{\parallel} = CL_{\text{hepatic} \parallel} + CL_{\text{renal}} \dots \text{Eq. 6.7}$$

Therefore  $CL_{\parallel} = 33.87 \text{ L/h}$ , i.e., a 16.98 % reduction compared to normoxia

Where:

$CL_{\text{renal}} = 5.3 \text{ L/h}$  (= 1.26 mL/min/kg), i.e., unchanged from normoxia

$CL_{\text{hepatic} \parallel} = 28.57 \text{ L/h}$  (= 6.80 mL/min/kg)

### **Hepatic CL under hypoxia where hepatic blood flow is also altered**

In another scenario the total hepatic blood flow was considered to change under hypoxia. With consequence for  $CL_{\text{hepatic } \parallel}$  and  $CL_{\parallel}$ . Here a relevant study was that of (Nicholas S. Kalson *et al.*, 2010) observing a pre-prandial increased in Hepatic Portal Vein (HPV) blood flow by 40% in 12 healthy subjects after 24 h at 4392 m. In this simulation we initially a 40% increase applied it to total hepatic blood flow ( $Q_h$ ) to simulate the effects of hypoxia.

Hence, we determined a revised total hepatic blood flow taking into account hypoxia -induced changes. This revised total hepatic blood flow denoted as:  $Q_h$  (adjustment factor) and parameterised by multiplying  $Q_h$  by the relevant adjustment factor. For example, for a 40% increase in  $Q_h$  the adjustment factor is 1.4. Hence,  $Q_{h\ 1.4} = Q_h \times 1.4$ .

The revised hepatic clearance under hypoxia where total hepatic blood flow is increased by 40% in addition to the previous changes in intrinsic clearance is therefore:

$$CL_{\text{hepatic } \parallel 1.4} = \frac{Q_{h\ 1.4} \cdot f_u \cdot CL_{\text{int } \parallel}}{Q_{h\ 1.4} + (f_u \cdot CL_{\text{int } \parallel})} \dots \text{Eq. 6.8}$$

Where:

$Q_{h\ 1.4}$  = total hepatic blood flow adjusted for a 40% increase = 28.98 mL/min/kg which equates to 121.7 L/h for 70 kg individual

$f_u = 0.04$

$CL_{\text{int } \parallel} = 253.44$  mL/min/kg which equates to 1064 L/h for 70 kg individual

Hence, hypoxia which reduces intrinsic hepatic clearance (as determined previously) and increases hepatic blood flow by 40% results in a revised hepatic clearance of:

$CL_{\text{hepatic } \parallel 1.4} = 31.53$  L/h (=7.50 mL/min/kg), i.e., an overall 11% decrease compared to the respective normoxia value for  $CL_{\text{hepatic}}$  of 35.5 L/h (or 8.45 mL/min/kg).

### **Total CL under hypoxia where hepatic blood flow is also altered**

Here the total clearance now also accounts for altered hepatic blood flow as well as changes to hepatic intrinsic clearance. For example, the revised total clearance under hypoxia where total hepatic blood flow is increased by 40% in addition to the previous changes in intrinsic clearance is therefore:

$$CL_{\parallel 1.4} = CL_{\text{hepatic } \parallel 1.4} + CL_{\text{renal}} \dots \text{Eq. 6.9}$$

$CL_{||1.4} = 36.83 \text{ L/h}$  (= 8.77 mL/min/kg), i.e., an overall 10% decrease compared to the respective normoxia value of  $CL$  of 40.8 L/h (= 9.71 mL/min/kg)

Where:

$CL_{\text{hepatic } ||1.4} = 31.53 \text{ L/h}$  (=7.50 mL/min/kg)

$CL_{\text{renal}} = 5.3 \text{ L/h}$  (= 1.26 mL/min/kg), i.e., unchanged from normoxia

## 6.2.4 Determination of extent of oral bioavailability parameters for simulation

### NORMOXIA

#### Extent of oral bioavailability ( $F_{\text{total}}$ )

From the literature  $F_{\text{total}} = 0.41$  (Milligan, Marshall and Karlsson, 2002; Nichols, Muirhead and Harness, 2002).

To isolate the loss of drug due to 1<sup>st</sup> pass metabolism in the liver *versus* loss of drug due to permeation/stability factors in the lumen of the gastro-intestinal tract we used:

$$F_{\text{total}} = F_{\text{lumen}} \cdot F_{\text{hepatic}} \dots \text{Eq. 6. 10}$$

Here to determine  $F_{\text{hepatic}}$  we first calculated a hepatic extraction ratio  $E_H$  for sildenafil as determined from:

$$E_H = \frac{CL_{\text{hepatic}}}{Q_h} \dots \text{Eq. 6. 11}$$

$$= \frac{35.5 \text{ L/h}}{86.94 \text{ L/h}} = 0.408 = \text{ca. } 0.41$$

From this:

$F_{\text{hepatic}} = 1 - E_H = 1 - 0.41 = 0.59$  which means 59% of sildenafil presented to the liver on 1<sup>st</sup>-pass avoids 1<sup>st</sup>-pass metabolism and reaches the general circulation.

Hence:

$$F_{\text{lumen}} = \frac{F_{\text{total}}}{F_{\text{hepatic}}} \dots \text{Eq. 6. 12}$$

$$= \frac{0.41}{0.59} = 0.69$$

The above means 69% of the oral dose of sildenafil escapes loss in the lumen of the gastro-intestinal tract and accesses the Hepatic Portal Vein (HPV). Of this, 59% of whatever reaches the liver via the HPV then avoids 1<sup>st</sup>-pass hepatic metabolism and reaches the general circulation. Overall, this provides for a 41% extent of oral bioavailability i.e.,  $F_{\text{total}} = F_{\text{lumen}} \times F_{\text{hepatic}}$  and in fractional terms  $0.41 = 0.69 \times 0.59$

## **HYPOXIA**

### **Extent of oral bioavailability ( $F_{\text{total,||}}$ ) under hypoxia but where there is no hypoxia-induced change in hepatic blood flow**

First, we calculate sildenafil hepatic extraction ratio under hypoxia ( $E_{H||}$ )

$$E_{H||} = \frac{CL_{\text{hepatic||}}}{Q_h} \dots \text{Eq. 6.13}$$

$$= \frac{28.57 \text{ L/h}}{86.94 \text{ L/h}} = 0.328 = \text{ca. } 0.33$$

Hence by using:

$$F_{\text{hepatic||}} = 1 - E_{H||} \dots \text{Eq. 6.14}$$

$$F_{\text{hepatic||}} = 1 - 0.33 = 0.67$$

That is 67% of whatever reaches the liver via the HPV avoids 1<sup>st</sup>-pass hepatic metabolism. If we assume that hypoxia has had no effect upon the loss of drug from the gastro-intestinal lumen then  $F_{\text{lumen}}$  remains unchanged from the normoxia parameterisation i.e.  $F_{\text{lumen}} = 0.69$

Hence from:

$$F_{\text{total||}} = F_{\text{lumen}} \cdot F_{\text{hepatic||}} \dots \text{Eq. 6.15}$$

$$F_{\text{total||}} = 0.69 \cdot 0.67 = 0.46$$

The means 69% of the oral dose of sildenafil escapes loss in the lumen of the gastro-intestinal tract and accesses the Hepatic Portal Vein (HPV). Of this, 67% of whatever reaches the liver via the HPV then avoids 1<sup>st</sup>-pass hepatic metabolism and reaches the general circulation (i.e., reduced 1<sup>st</sup> pass metabolism in hypoxia). Overall, this provides for a 46% extent of oral bioavailability i.e.,  $F_{\text{total}} = F_{\text{lumen}} \times F_{\text{hepatic}}$  and in fractional terms  $0.46 = 0.69 \times 0.67$ . Because of a reduced 1<sup>st</sup> pass metabolism in the liver due to hypoxia the total extent of oral bioavailability increases from 41% in normoxia to 46% in hypoxia.



**Extent of oral bioavailability ( $F_{\text{total} \parallel 1.4}$ ) under hypoxia and where alterations in hepatic blood flow also arise (e.g., increased flow by 40% - hence a  $Q_h$  (adjustment factor) of 1.4)**

Here the total extent of oral bioavailability now also accounts for altered hepatic blood flow as well as changes to hepatic intrinsic clearance, i.e., 1<sup>st</sup>-pass extraction. For example, Eq. 6.8 which defines the impact of such changes through hypoxia upon hepatic clearance, where specifically hepatic blood flow increases by 40%.

In this section by  $F_{\text{total} \parallel 1.4}$  defines the total extent of bioavailability under hypoxia where total hepatic blood flow is increased by 40% in addition to previous changes in hepatic clearance.

In the case of a 40% increase in hepatic blood flow, **Eq. 6.8** provided a  $CL_{\text{hepatic} \parallel 1.4}$  of 31.53 L/h (=7.50 mL/min/kg),

Where:

$Q_{h1.4}$  = total hepatic blood flow adjusted for a 40% increase = 28.98 mL/min/kg which equates to 121.7 L/h for 70 kg individual.

Therefore, a hepatic extraction ratio under hypoxia where both intrinsic clearance is decreased, and hepatic blood flow increased by 40% can determined from:

$$E_{H \parallel 1.4} = \frac{CL_{\text{hepatic} \parallel 1.4}}{Q_{h1.4}} \dots \text{Eq. 6. 16}$$

$$= \frac{31.53 \text{ L/h}}{121.7 \text{ L/h}} = 0.259 = \text{ca. } 0.26$$

Hence by using:

$$F_{\text{hepatic} \parallel 1.4} = 1 - E_{H \parallel 1.4} \dots \text{Eq. 6. 17}$$

$$F_{\text{hepatic} \parallel 1.4} = 1 - 0.26 = 0.74$$

That is 74% of whatever reaches the liver via the HPV avoids 1<sup>st</sup>-pass hepatic metabolism. If we assume again that hypoxia has had no effect upon the loss of drug from the gastro-intestinal lumen then  $F_{\text{lumen}}$  remains unchanged from the normoxia parameterisation i.e.,  $F_{\text{lumen}} = 0.69$

Hence from:

$$F_{\text{total} \parallel 1.4} = F_{\text{lumen}} \cdot F_{\text{hepatic} \parallel 1.4} \dots \text{Eq. 6. 18}$$

$$F_{\text{total} \parallel 1.4} = 0.69 * 0.74 = 0.51$$

The means 69% of the oral dose of sildenafil escapes loss in the lumen of the gastro-intestinal tract and accesses the Hepatic Portal Vein (HPV). Of this, 74% of whatever reaches the liver via the HPV then avoids 1<sup>st</sup>-pass hepatic metabolism and reaches the general circulation (i.e. reduced 1<sup>st</sup> pass metabolism in hypoxia arising from both reduced intrinsic hepatic clearance and increased hepatic blood flow). Overall, this provides for a 51% extent of oral bioavailability i.e.  $F_{\text{total}} = F_{\text{lumen}} \times F_{\text{hepatic}}$  and in fractional terms  $0.51 = 0.69 \times 0.74$ . Because of the additional impact of hypoxia to increase hepatic blood (40%) the total extent of oral bioavailability is now 51% *versus* 46% when hypoxia was affecting hepatic intrinsic clearance alone *versus* 41% under normoxia.

### 6.2.5 Monte Carlo simulation

As stated earlier, a Monte Carlo simulation approach depends upon a model into which different variables/parameters are introduced to provide an integrated estimate of the model outcome. The model and variables are seen in Eq. 6.19 to 6.24 and Table 6.3. Each variable/parameter has its own probability distribution with the Monte Carlo simulation repeatedly re-run drawing each time on a different random set of values (inputs) associated with the probability distributions. The result is a set of possible outcomes (estimates). The model and all simulations were created using R software (version 4.1.2) and RStudio.

The area under the curve of simulated data (AUC<sub>0-∞</sub>; synonymous as AUC) were calculated. All the simulation plots were performed using ‘ggplot2’ package in R software and presented as median with 5<sup>th</sup> - 95<sup>th</sup> percentile confidence interval.

**Table 6.1 PK Parameters used in Monte Carlo simulation.**

Parameter	Normoxia	Hypoxia	Hypoxia + Q <sub>h</sub> change (increase by 40 %)	Description
$K_a$ [h <sup>-1</sup> ]	2.60	2.60	2.60	Oral absorption rate
$V_c$ [L]	234	234	234	Apparent Volume of Distribution (central)
CL [L/h]	40.8	-	-	Total Clearance
CL <sub>  </sub> [L/h]	-	33.9	-	
CL <sub>  1.4</sub> [L/h]	-	-	36.8	
CL <sub>int</sub> [L/h]	1499	-	-	Hepatic intrinsic CL

$CL_{int \parallel}$ [L/h]	-	1064	-	
$CL_{int \parallel 1.4}$ [L/h]	-	-	1064	
$CL_{hepatic}$ [L/h]	35.5	-	-	Hepatic clearance
$CL_{hepatic \parallel}$ [L/h]	-	28.6	-	
$CL_{hepatic \parallel 1.4}$ [L/h]	-	-	31.5	
$CL_{renal}$ [L/h]	5.3	5.3	5.3	Renal clearance
$Q_h$ [L/h]	86.9	-	-	Total hepatic blood flow
$Q_{h \parallel}$ [L/h]	-	86.9	-	
$Q_{h \parallel 1.40}$ [L/h]	-	-	121.7	
$E_H$	0.41	-	-	Hepatic extraction ratio
$E_{H \parallel}$	-	0.33	-	
$E_{H \parallel 1.4}$	-	-	0.26	
$F_{total}$	0.41	-	-	Total fraction of oral dose absorbed to the systemic circulation
$F_{total \parallel}$	-	0.46	-	
$F_{total \parallel 1.4}$	-	-	0.51	
$F_{lumen}$	0.69	0.69	0.69	Fraction of drug bioavailable to the Liver from the GI lumen
$F_{hepatic}$	0.59	-	-	Fraction of drug presented to the Liver from the GI lumen which is then bioavailable to the systemic circulation.
$F_{hepatic \parallel}$	-	0.67	-	
$F_{hepatic \parallel 1.4}$	-	-	0.74	
				Note $F_{total} = F_{lumen} + F_{hepatic}$

Where:  $\parallel$  indicates parameter value under hypoxia;  $\parallel 1.4$  indicates parameter value increased  $Q_h$  by 40% (i.e. 1.4) by hypoxia.

### **PK-PD Model**

A one-compartment linear elimination and a first-order absorption were used. The differential equations for the model are displayed below:

$$\frac{d}{dt}(\text{gut}) = -K_a * \text{gut} \dots \text{Eq. 6.19}$$

$$\frac{d}{dt}(\text{plasma}) = K_a * \text{gut} * F_{total} - \left( \frac{CL_{total}}{V_c} \right) * \text{plasma} \dots \text{Eq. 6.20}$$

Where “gut” is the amount of the drug in the GI lumen, “plasma” is the amount of drug in systemic circulation, “ $K_a$ ” is the fractional rate constant describing the loss of the drug from the GI lumen (**Eq. 6.19**) which together with  $F_{total}$  (**Eq. 6.20**) helps define the fractional rate constant for absorption.  $F_{total}$  represents the total fraction of the dose of drug, i.e., amount of the drug in the GI lumen that ultimately is bioavailable to the systemic circulation.  $CL_{total}/V_c$  defines the fractional rate constant for elimination, i.e., irreversible loss from the systematic circulation where  $V_c$  is the apparent volume of distribution; it is defined as central for the purposes of the simulation model which assumes only a single disposition compartment.

Monte Carlo simulations were performed to predict the time-course of unbound sildenafil concentrations in the plasma what can be viewed healthy volunteers exposed to hypoxia – “*virtual subjects*”; 1000 virtual subjects were administrated a 100 mg single oral dose tablet of sildenafil.

#### To simulate sildenafil PK under normoxia

From **Eq. 6.19**

$$\frac{d}{dt}(\text{gut}) = -K_a * \text{gut} \dots \text{Eq. 6.21}$$

From **Eq. 6.20**

$$\frac{d}{dt}(\text{plasma}) =$$

$$K_a * \text{gut} * F_{total} - \left( \frac{\left[ \frac{Q_h * f_u * CL_{int}}{Q_h + (f_u * CL_{int})} \right] + CL_{renal}}{V_c} \right) * \text{plasma} \dots \text{Eq. 6.22}$$

**To simulate sildenafil PK under hypoxia** where hypoxia affected only  $CL_{int}$  (i.e. without effects upon  $Q_h$ )

**Eq. 6.21** remains the same.

From **Eq. 6.20** however:

$$\frac{d}{dt}(\text{plasma}) =$$

$$K_a * \text{gut} * F_{\text{total}||} - \left( \frac{[\frac{Q_{h||} * f_u * CL_{\text{int}||}}{Q_{h||} + (f_u * CL_{\text{int}||})}] + CL_{\text{renal}}}{V_c} \right) * \text{plasma} \dots \text{Eq. 6.23}$$

The  $CL_{\text{int}}$  was corrected using the residual factor ( $RF_{\text{hypoxia}}$ ) as described in **Eq. 6.5**. Hence  $CL_{\text{int}||}$  (i.e.  $CL_{\text{int}}$  under hypoxia) is derived from  $CL_{\text{int}} * RF_{\text{hypoxia}}$ .  $Q_h$  is assumed unchanged in this scenario although is denoted by the hypoxia subscript  $||$ . See Table 6.3 for parameter values.

While from **Eq. 6.13**, **Eq. 6.14**, **Eq. 6.15** and **Eq. 6.6**

$$F_{\text{total}||} = \left( 1 - \frac{[\frac{Q_{h||} * f_u * CL_{\text{int}||}}{Q_{h||} + (f_u * CL_{\text{int}||})}]}{Q_{h||}} \right) * F_{\text{lumen}} \dots \text{Eq. 6.24}$$

Where the term in large round brackets is the hepatic extraction ratio under hypoxia, i.e.  $E_{H||}$ . The  $F_{\text{lumen}}$  is the Fraction of drug bioavailable to the Liver from the GI lumen,  $Q_{h||}$  is the total blood flow to the liver under hypoxia but here is considered to remain unchanged from the normoxia parameter (see Table 6.3).

Where simulations also included the impact of hypoxia upon hepatic blood flow (**SET 2** simulations) the respective parameters substituted into **Eq. 6.23** and **Eq. 6.24** representing a 40% increase in  $Q_h$  under hypoxia (**SET 2 Scenario A**) were:  $Q_{h||1.4}$ ,  $CL_{\text{int}||1.4}$  and  $F_{\text{total}||1.4}$  (See **Table 6.3**).

As stated in **Section 6.1.1**. in detail, two sets of simulations for the dosing of a single 100 mg sildenafil table dose.

**SET 1** comprised three scenarios involving normoxia and hypoxia comparisons, where: **Scenario A** - the maximal effects of hypoxia on hepatic metabolism were already present before the start of the 24-h PK-PD simulation; **Scenario B** - the effects of hypoxia on hepatic metabolism gradually developed from the beginning of the simulation reaching maximum impact at the 4 h; **Scenario C** - where the effects of hypoxia on hepatic metabolism occurred abruptly in a ‘step-function’ and on maximum intensity at 4 h into the simulation.

**SET 2** comprised a single scenario **Scenario A** involving normoxia and hypoxia comparisons, where both a simultaneous decrease in hepatic  $CL_{\text{int}}$  and an alteration in total hepatic blood flow were simulated with the maximal physiological effects established prior to the 24-h PK-

PD simulation. Specifically, hypoxia induced the maximal decrease in  $CL_{int}$  as in SET 1 but with a concurrent 40% increase in total hepatic blood flow.

**The PD model** consisted of a basic Emax model to relate the concentration of drug a  $C_{(t)}$  to the observed response expressed as a percentage change in response to inhibition PDE5. In this model, Emax is the maximum change in response the drug can produce (100%),  $EC_{50}$  is the value of  $C_{(t)}$  producing 50% of the Emax value:

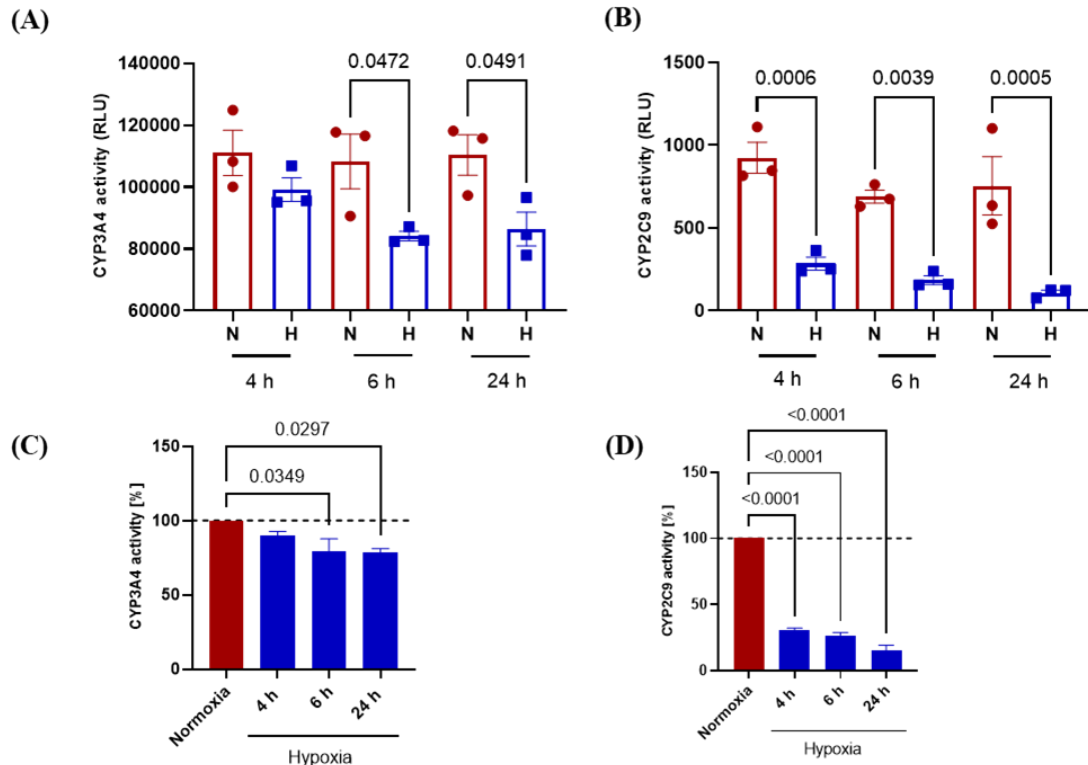
$$E_{(t)} = \frac{E_{max} * C_{(t)}}{EC_{50} + C_{(t)}} \dots \text{Eq. 6. 25}$$

$EC_{50}$  was taken as the  $IC_{50}$  of sildenafil obtained from an average PDE5  $IC_{50}$  from various published studies (Saenz De Tejada et al., 2001; Corbin, Francis and Webb, 2002; Gupta, Kovar and Meibohm, 2005; Mehrotra et al., 2007; Wang et al., 2013). The average  $IC_{50}$  of 5.22 nM (= 2.48 ng/mL) was used and taken to represent the  $IC_{50}$  of the free (unbound) drug concentration not total (free + bound) concentration.

## 6.3 Results and Discussion

### 6.3.1 In-vitro CYP3A4 CYP2C9 functional activity measurements toward setting intrinsic Clearance parameters for simulation

The functional turnover activity of CYP3A4 and CYP2C9 in human hepatocyte HepaRG was examined using P450-Glo™ assays to determine the fraction of alteration in hepatic  $Cl_{int}$  under hypoxia. This assay employs specific substrates, Luciferin IPA for CYP3A4 and Luciferin H for CYP2C9. These substrates are converted by P450s to Luciferin, which then reacts with luciferase to produce light that is directly proportional to the activity of the P450. To produce hypoxia HepaRG cells were exposed to 1%  $O_2$  for time intervals (4, 6 and 24 h) with the P450 activity under hypoxia then compared to normoxia controls (21%  $O_2$ ). **Figure 6.1A** shows the absolute changes in CYP3A4-induced luminescence, with **Figure 6.1C** showing the corresponding relative % change. At 6 and 24 h of hypoxia CYP3A4 activity was significantly reduced by 21% and 22%, respectively, compared to the relative normoxia control. **Figures 6.1B and 6.1D** show the comparable data for CYP2C9 where hypoxia respectively reduces activity by 69%, 73%, and 84% at 4, 6 and 24 h compared to normoxia control. The average reduction across all time points for CYP3A4 was 18%, while for CYP2C9 it was 75%. The figure also shows how the Residual Factor<sub>hypoxia</sub> (RF) (see **Eq. 6.5.**) was determined and which reflected the different contributions of CYP3A4 (0.8, 80%) and CYP2C9 (0.2, 20%) to hepatic metabolism of sildenafil. Specifically, based on the averaged decreases in P450s from the in-vitro experiments the hepatic intrinsic clearance under hypoxia ( $Cl_{int||}$ ) was reduced by 29% to a value that was 71% (0.71) of the normoxia control (detailed in **section 6.2.3**).



Duration of hypoxia (1% O <sub>2</sub> )	4 h	6 h	24 h	Average
CYP3A4 % reduction vs normoxia	-10	-21	-22	-18
CYP2C9 % reduction vs normoxia	-69	-73	-84	-75

$$RF_{\text{hypoxia}} = \underbrace{\{[0.8 \cdot (1 - 0.18)] + [0.2 \cdot (1 - 0.75)]\}}_{71\%}$$

$Cl_{\text{int} \parallel}$  is 71 % of  $Cl_{\text{int}}$  or **hypoxia** resulted in 29% reduction in  $Cl_{\text{int} \parallel}$  vs  $Cl_{\text{int}}$

**Figure 6.1. The impact of hypoxia on CYP3A4 and CYP2C9 enzyme activity.** HepaRG cells were differentiated following the standard protocol. After differentiation, cells were exposed to hypoxia (1% O<sub>2</sub>) for 4, 6 and 24 h. Cells cultured under normoxia (21% O<sub>2</sub>) were used as a control. P450 Glo™ assay was used to assess CYP450 activity. **Fig.6.1A** - CYP3A4 activity presented as relative luminescent unit (RLU). **Fig. 6.1 B** CYP2C9 activity presented as relative luminescent unit (RLU). **Fig. 6.1C** and **Fig.6.1D** – respectively, CYP3A4 and CYP2C9 activity presented as % of normoxia. . Bars represents mean ± SEM. N=3 independent experiments with at least six replicates each experiment. One-way ANOVA with Bonferroni test was used for analysis. Hepatic intrinsic clearance under hypoxia ( $Cl_{\text{int} \parallel}$ ) was determined using a residual factor for hypoxia ( $RF_{\text{hypoxia}}$ ).  $RF_{\text{hypoxia}}$  was calculated by considering the contributions of CYP3A4 (0.8) and CYP2C9 (0.75) in sildenafil metabolism, along with the average decrease in the activity of CYP3A4 and CYP2C9 across all time periods. ( $Cl_{\text{int}}$ ) is hepatic intrinsic clearance under normoxia.



### 6.3.2 Monte Carlo simulation SET 1:

Here the PK/PD simulations are set to run over a 24 h period where the hypoxia intervention causes a reduction in sildenafil hepatic intrinsic clearance ( $CL_{int}$ ) (estimated from experimental in-vitro data). There are three different scenarios within SET 1. The PK parameters utilised in this SET 1 are shown in **Table 6.4**.

**Table 6.2 Key PK parameters used for Monte Carlo simulation summarised from Table 6.3**

Parameter	Normoxia	Hypoxia	Description
$K_a$ [ $h^{-1}$ ]	2.60	2.60	Oral absorption rate
$V_c$ [L]	234	234	Apparent volume of distribution (central)
$CL$ [L/h]	40.8	-	Total clearance under normoxia and hypoxia (  )
$CL_{  }$ [L/h]	-	33.9	
$F_{total}$	0.41	-	Extent of oral bioavailability or total fraction of oral dose absorbed to the systemic circulation under normoxia and hypoxia (  )
$F_{total  }$	-	0.46	

#### **6.3.2.1 SET 1 Scenario A - the maximal effect of hypoxia on hepatic metabolism is already present before the start of the 24-h PK-PD simulation**

The PK/PD profile of a single oral 100 mg sildenafil tablet in 1000 subjects was simulated under normoxia and cellular hypoxia, where the effects of hypoxia upon hepatic cell metabolism to bring about a hypoxia-induced reduction in intrinsic hepatic clearance ( $CL_{int||}$ ) were informed by the in-vitro experiments as described above. The in-vitro data predicted a decrease in intrinsic hepatic clearance under hypoxia by 29% compared to normoxia control. This decrease in intrinsic hepatic clearance would be predicted to lead to a reduction in total clearance (hepatic+ renal) of sildenafil under hypoxia by 17% and an increase in sildenafil extent of oral bioavailability by 12% (**Eq. 6.6** and **6.7**).

In this ‘SET 1 Scenario A’ simulation comparison between normoxia and hypoxia assumed the maximal effects of hypoxia on hepatic metabolism were already established prior to the start of the 24-h PK-PD simulation. This scenario would be relevant to a mountaineer taking sildenafil only after ascending to 2,500 m and experiencing hypoxaemia. It is also applicable

under normobaric conditions when, for example a newly prescribed medication is taken by a patient with a clinical condition(s) leading to hypoxaemia. It may also be relevant to a laboratory clinical research study where a volunteer enters a normobaric experimental hypoxia chamber, experiences the full effects of hypoxaemia, and subsequently is administered sildenafil.

The PK-PD vs time simulation profiles for SET 1 Scenario A are shown in **Figure 6.2**. The simulated concentration-time profiles for unbound concentrations of sildenafil following a 100 mg single oral dose are shown in **Figure 6.2A** under normoxia and hypoxia; the dotted horizontal line shows the unbound concentration of sildenafil equivalent to the  $IC_{50}$  (in-vitro literature data of 2.48 ng/mL) for sildenafil inhibition of PDE5. The adjacent table in the Figure shows some relevant outcome parameters. In all simulations the absorption rate constant ( $K_a$ ) and volume of distribution were assumed to remain unchanged (**Table 6.3**). Of note is that sildenafil absorption from an immediate release (IR) tablet is known to be rapid (Table 6.1) with the  $K_a$  set in this work at  $2.60\text{ h}^{-1}$  (i.e.,  $t_{1/2}$  absorption of ca. 0.266 h or ca. 16 min). This means that the absorption process would have been 73% complete at 0.5 h into the simulation, 93% complete at 1 h and > 99% at 2 h into the simulation.

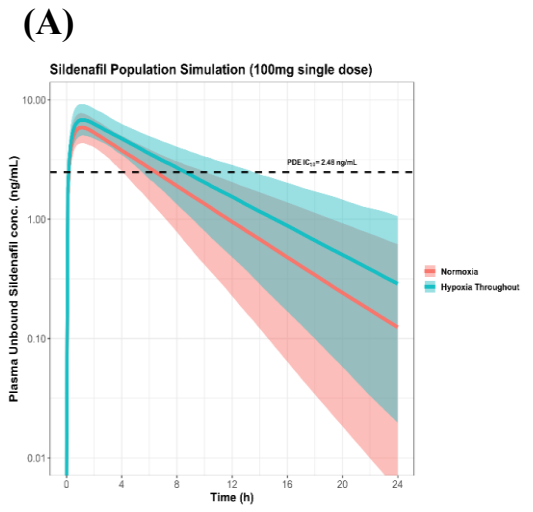
As expected from the hypoxia-induced decrease in clearance ( $CL\ 40.8\text{ L/h}$  vs  $CL_{\parallel}\ 33.9\text{ L/h}$ ; **Tables 5.3 and 5.4**), the hypoxia profile in **Figure 6.2A** displayed a more prolonged terminal slope. Based on respective clearance and volume parameters (**Table 6.3**), the  $t_{1/2}$  for elimination under normoxia would be 3.99 h while in hypoxia the  $t_{1/2}$  would be 4.82 h. As this scenario simulates the maximum hypoxia present from the point at which sildenafil was administered the effect of hypoxia upon oral first-pass (i.e. to increase  $F_{total}$ ) would be maximal and hence and the increased extent of bioavailability ( $F_{total}\ 0.41$  vs,  $F_{total\parallel}\ 0.46$ ; **Tables 5.3 and 5.4**). The combined effects of hypoxia, increasing  $F_{total}$ , and the decreased  $CL$ , therefore, resulting in a higher exposure to sildenafil seen by a greater  $AUC_{0-\infty}$  (40.5 vs 53.6, a 32% increase) and higher  $C_{max}$  (5.88 vs 6.80, a 16% increase). A reduced elimination rate constant ( $K$ ) (prolonged  $t_{1/2}$ ) has the potential to prolong  $T_{max}$ , although such a change in  $T_{max}$  tends to be greater for drugs showing slower absorption processes (smaller  $K_a$ ); here only a slight change in  $T_{max}$  was seen with the prolonged  $t_{1/2}$ .

The implications of hypoxia on the concentration vs, time profiles in respect to the pharmacodynamic  $IC_{50}$  (2.48 ng/mL) can also be seen in table with a 58% and a 34% increase

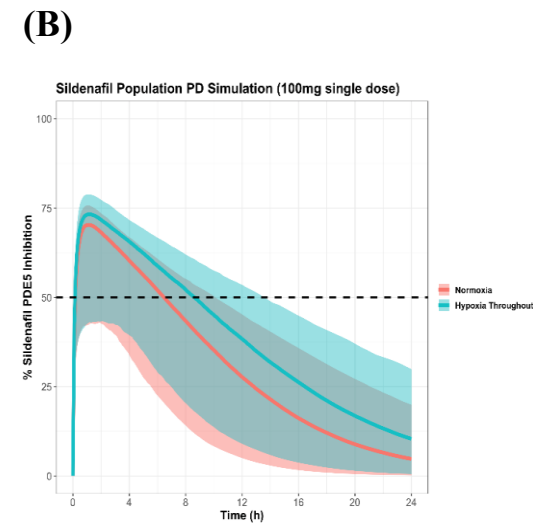
respectively, in the exposure ( $AUC_{(\text{concentration vs time})}$ ) and the time of sildenafil concentrations above the  $IC_{50}$  (**Figure 6.2A**).

The corresponding simulated effect-time profiles are shown in **Figure 6.2B** based on the  $E_{max}$  model earlier described (**Eq. 6.24**). Here we see the consequence of the hypoxia-induced change in PK with a 24% increase in the  $AUC_{(\text{effect vs time})}$  profile, a 51% increase in the  $AUC_{(\text{effect vs time})}$  above the  $EC_{50}$  and a 34% increase in time above the  $EC_{50}$ . The  $EC_{50}$  is directly related to the  $IC_{50}$  parameter in that: - the PD model (basic  $E_{max}$ ) used considers the  $EC_{50}$  to represent the effect at 50% of the maximal effect, and for this to be achieved when 50% of the total pharmacodynamic receptors are occupied. The concentration at which  $EC_{50}$  is achieved would be equivalent in the current PK-PD simulations to the  $IC_{50}$ , which represents the concentration delivering 50% of the maximal inhibition and hence in receptor theory the point at which 50% of the total available receptors are occupied.

In the current PD simulations, the  $EC_{50}$  and  $E_{max}$  parameters were assumed not to change as a result of hypoxia. Existing research on the effect of hypoxia on PDE5 is limited and primarily relates to gene expression data, with little to no information available on the functional activity of PDE5 under hypoxic conditions. The study of Vignozzi *et al.* conducted using human penile smooth muscle cells exposed to 1.5%  $O_2$  for 24 h or 48 h reported a significant decrease in PDE5 mRNA expression by approximately 40% and 50%, respectively (Vignozzi *et al.*, 2006). The work of Lin *et al.* used rat cavernous smooth muscle cells exposed to cobalt chloride ( $CoCl_2$ ), a substance inducing chemical hypoxia through stabilisation of HIF-1/-2. They reported cells exposed to 300  $\mu M$   $CoCl_2$  for 24 h and 48 h downregulated PDE5 mRNA expression (Lin *et al.*, 2003). These reports provide some evidence that hypoxia may affect the level of PDE5 gene expression and potentially in the cellular levels of the enzyme. Based on receptor theory this may reduce the  $IC_{50}$  while also reducing the maximal possible effect that the PDE5 enzyme can display in its degradation of cyclic GMP in the smooth muscle cells that line blood vessels. The consequence therefore may be to enhance the impact of hypoxia-induced PK changes upon sildenafil's pharmacodynamics or diminish the impact. It would depend on the dose administered, the extent to which sildenafil's PK is altered and how the altered concentrations relate to the hypoxic  $IC_{50}$  ( $EC_{50}$ ) and  $E_{max}$ . In the current SET 1 Scenario A simulation (where the  $IC_{50}$  ( $EC_{50}$ ) and  $E_{max}$  remain unaffected by hypoxia) under normoxia only 9.6% of the total  $AUC_{(\text{effect vs time})}$  profile was above the  $EC_{50}$  which is increased to only 11.7% in the hypoxia arm. This implies that under



PK parameters	Normoxia	Hypoxia SET 1 Scenario A 'Hypoxia from time zero'	% differences to normoxia
	Median (Q5, Q95)	Median (Q5, Q95)	
Time above IC50 (h)	6.50 (4.10, 10.2)	8.70 (5.50, 13.6)	34 % increase
AUC above IC50 (ng/mL . h)	10.8 (4.40, 22.1)	17.1 (7.58, 34.8)	58 % increase
AUC (0-∞) (ng/mL . h)	40.5 (24.0, 65.0)	53.6 (31.2, 85.6)	32 % increase
C <sub>max</sub> (ng/ml)	5.88 (4.34, 7.91)	6.80 (4.94, 9.22)	16 % increase
T <sub>max</sub> (h)	1.10 (1.10, 1.20)	1.20 (1.10, 1.30)	9 % increase



PD parameters	Normoxia	Hypoxia SET 1 Scenario A 'Hypoxia from time zero'	% differences to normoxia
	Median (Q5, Q95)	Median (Q5, Q95)	
Time above EC50 (h)	6.50 (4.10, 10.2)	8.70 (5.50, 13.6)	34 % increase
AUC above EC50 (% . h)	74.0 (0.00, 133)	112 (0.00, 199)	51 % increase
AUC (0-∞) (% . h)	769 (301, 1106)	955 (375, 1288)	24 % increase

**Figure 6.2. Set 1 Scenario A simulation of population PK and PD profile of 100 mg single oral dose of sildenafil (n=1000) under normoxia (red) or hypoxia from time 0 (blue).** Fig 6.2A displays a simulation of an unbound concentration of 100 mg single oral dose of sildenafil over time and the adjacent table present the PK parameters of sildenafil in both normoxia and hypoxia groups and the % of median differences relative to normoxia. Fig 6.2B displays a simulation of % of sildenafil to inhibit PDE5 over 24 h in both normoxia and hypoxia groups. The adjacent table presents the PD parameters of sildenafil in both groups and the % of median relative to normoxia. The red in the figures is a simulation of 100 mg of sildenafil under normoxia while the blue is a simulation of 100 mg of sildenafil, incorporating revised predicted 'hypoxia' parameters for CL<sub>||</sub> and F<sub>total ||</sub>. The thick line is the median and the ribbon is 5<sup>th</sup> to 95<sup>th</sup> percentile.

the simulated PK conditions used in this particular scenario the effect of hypoxia on PDE could

enhance the impact of the PK changes.

### **6.3.2.2 SET 1 Scenario B - the maximal effect of hypoxia on hepatic metabolism is developed in a progressive linear manner between time 0 h and 4 h of the PK-PD simulation**

This simulation involved normoxia vs hypoxia groups administered a single oral 100 mg dose of sildenafil, where the effects of hypoxia upon hepatic metabolism gradually increase from time 0 of the simulation (i.e. normoxia and the timepoint of administration of the single oral dose of 100 mg sildenafil) through to 4 h into the simulation; at 4 h the effects of hypoxia to reduce sildenafil intrinsic hepatic clearance are at a maximum, i.e. a 29% reduction under hypoxia vs, normoxia (**Tables 5.3 and 5.4**). This progressive four-hour decrease in intrinsic hepatic clearance followed a simple linear profile with time 0 through to 4 h. This scenario may depict mountaineers taking sildenafil at the start of the ascent and then experiencing progressive reductions in oxygen levels over the following hours as they ascend in altitude.

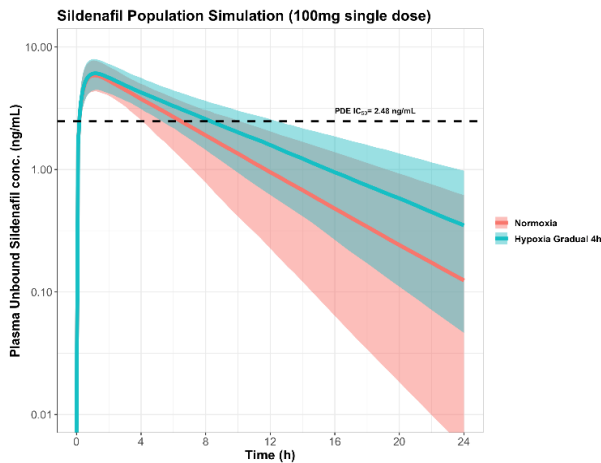
The PK-PD simulations for SET 1 Scenario B are shown in **Figure 6.3**. The simulated concentration-time profiles are shown in **Figure 6.3A** under normoxia and hypoxia. As may be expected, the gradual onset of hypoxia now results in a lesser impact on all outcome parameters (adjacent table in Figure 6.3) compared to the SET 1 Scenario A. Compared to normoxia the increases in  $AUC_{0-\infty}$  and  $C_{max}$  were not as great, 26% and 3%, respectively. With absorption that is 93% complete at 1 h and > 99% at 2 h into the simulation, the impact of hypoxia upon the extent of bioavailability will in this second scenario be particularly diminished. The implications of hypoxia on the concentration vs time profiles in respect to the  $IC_{50}$  (2.48 ng/mL) can also be seen in the Table with 28% increases in the exposure ( $AUC_{(concentration\ vs\ time)}$ ) and the time of sildenafil concentrations above the  $IC_{50}$  (**Figure 6.3A**).

The corresponding simulated effect-time profiles are shown in **Figure 6.3B**. Here we see the hypoxia-induced changes in PK resulted in a 25% increase in the  $AUC_{(effect\ vs\ time)}$  profile, and 28% increases in the  $AUC_{(effect\ vs\ time)}$  above the  $EC_{50}$  and in the time above the  $EC_{50}$ .

### **6.3.2.3 SET 1 Scenario C - the maximal effects of hypoxia on hepatic metabolism occur abruptly in a ‘step-function’ at 4 h into the PK-PD simulation.**

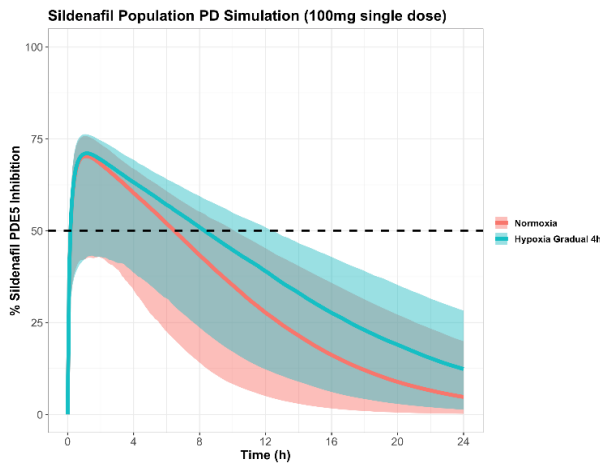
Here the effects of hypoxia upon hepatic metabolism occur in an immediate and maximal manner at 4 h into the simulation (i.e. 4 h after the single oral dose administration of 100 mg sildenafil). This scenario can be seen as a representation of a laboratory clinical research study,

(A)



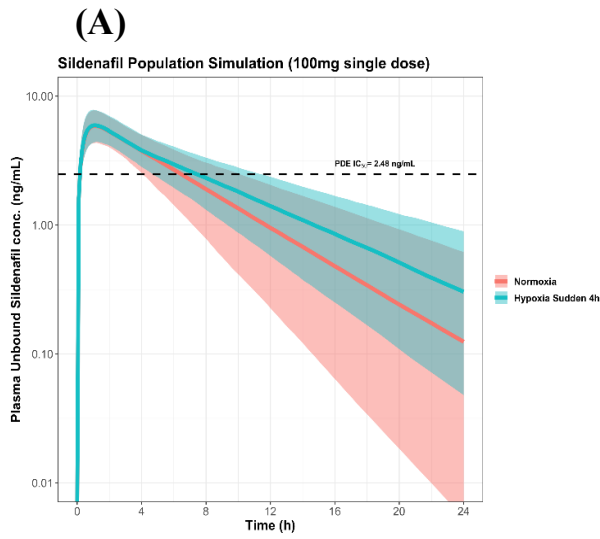
PK parameters	Normoxia	Hypoxia SET 1 Scenario B 'Hypoxia increases from time zero to 4 h'	% differences to normoxia
	Median (Q5, Q95)	Median (Q5, Q95)	
Time above IC50 (h)	6.5 (4.10, 10.2)	8.30 (5.30, 12.4)	28 % increase
AUC above IC50 (ng/mL . h)	10.8 (4.40, 22.1)	13.8 (5.96, 27.1)	28 % increase
AUC (0-∞) (ng/mL . h)	40.5 (24.0, 65.0)	50.9 (31.1, 75.9)	26 % increase
C <sub>max</sub> (ng/ml)	5.88 (4.34, 7.91)	6.08 (4.48, 8.12)	3 % increase
T <sub>max</sub> (h)	1.10 (1.10, 1.20)	1.10 (1.10, 1.20)	0 %

(B)

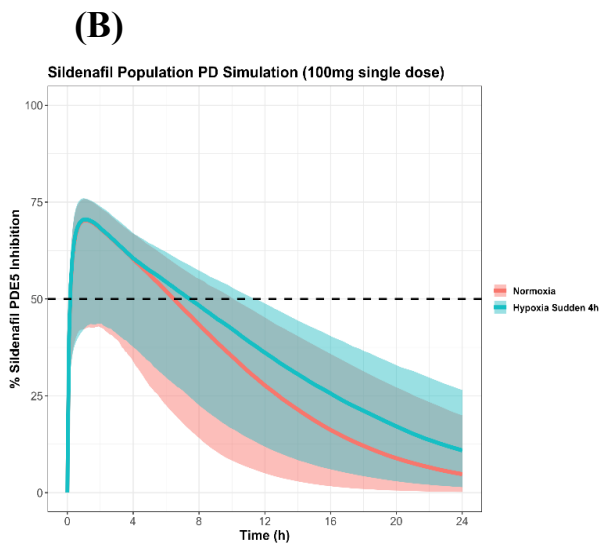


PD parameters	Normoxia	Hypoxia SET 1 Scenario B 'Hypoxia increases from time zero to 4 h'	% differences to normoxia
	Median (Q5, Q95)	Median (Q5, Q95)	
Time above EC50 (h)	6.50 (4.10, 10.2)	8.30 (5.30, 12.4)	28 % increase
AUC above EC50 (% . h)	74.0 (0.00, 133)	95.0 (0.00, 165)	28 % increase
AUC (0-∞) (% . h)	769 (301, 1106)	958 (417, 1232)	25 % increase

**Figure 6.3. SE1 Sceniaro B simulation of population PK and PD profile of 100 mg single oral dose of sildenafil (n=1000) under normoxia (red) or hypoxia lineary increases from time 0 to 4 h (blue). Fig. 6.3A displays a simulation of an unbound concentration of 100 mg single oral dose of sildenafil over time. The adjacent table presents the PK parameters of sildenafil in both normoxia and hypoxia groups and the % of median differences between them. Fig. 6.3B displays a simulation of % of sildenafil to inhibit PDE5 over 24 h in both normoxia and hypoxia groups. The adjacent table presents the PD parameters of sildenafil in both groups and the % of median differences relative to normoxia. The red represents a simulation of 100 mg of sildenafil under normoxia, while the blue is a simulation of 100 mg of sildenafil administrated under normoxia and then lineary transition to full hypoxia (incorporating revised hypoxia parameters, i.e., CL<sub>||</sub> and F<sub>total||</sub>) over 4 h. The thick line is the median, and the ribbon is the 5<sup>th</sup> to 95<sup>th</sup> percentile.**



PK Parameters	Normoxia Median (Q5, Q95)	Hypoxia SET 1 Scenario C 'Hypoxia increases in step function' at 4 h' Median (Q5, Q95)	% differences to normoxia
Time above IC50 (h)	6.50 (4.10, 10.2)	7.50 (4.80, 11.5)	15 % increase
AUC above IC50 (ng/mL . h)	10.8 (4.40, 22.1)	10.9 (4.61, 22.9)	0.9 % increase
AUC (0-∞) (ng/mL . h)	40.5 (24.0, 65.0)	45.8 (26.6, 69.6)	13 % increase
C <sub>max</sub> (ng/ml)	5.88 (4.34, 7.91)	5.81 (4.45, 7.85)	1.2 % decrease
T <sub>max</sub> (h)	1.10 (1.10, 1.20)	1.10 (1.00, 1.10)	0 %



PD Parameters	Normoxia Median (Q5, Q95)	Hypoxia SET 1 Scenario C 'Hypoxia increases in step function' at 4 h' Median (Q5, Q95)	% differences to normoxia
Time above EC50 (h)	6.50 (4.10, 10.2)	7.50 (4.80, 11.5)	15 % increase
AUC above EC50 (% . h)	74.0 (0.00,133)	80.0 (0.00,146)	8 % increase
AUC (0-∞) (% . h)	769 (301,1106)	907 (408, 1186)	18 % increase

**Figure 6.4. SET 1 Scenario C simulation of population PK and PD profile of 100 mg single oral dose of sildenafil (n=1000) under normoxia (red) or hypoxia increased in step function at 4 h (blue).** Fig.6.4A displays a simulation of an unbound concentration of 100 mg single oral dose of sildenafil over time. The adjacent table presents the PK parameters of sildenafil in both normoxia and hypoxia groups and the % of median differences relative to normoxia. Fig.6.4B displays a simulation of % of sildenafil to inhibit PDE5 over 24 h in both normoxia and sudden hypoxia groups. The adjacent table presents the PD parameters of sildenafil in both groups and the % of median differences relative to normoxia. The red represents a simulation of 100 mg of sildenafil under normoxia, while the blue is a simulation of 100 mg of sildenafil administered under normoxia and then transition to full hypoxia (incorporate revised hypoxia parameter, i.e., CL<sub>||</sub> and F<sub>total ||</sub>) occurs immediately in step function at 4 h. The thick line is the median, and the ribbon is the 5<sup>th</sup> to 95<sup>th</sup> percentile.

where a volunteer enters a normobaric experimental hypoxia chamber four h after taking oral sildenafil. At which point, there is an instant transition from normoxia to hypoxia, resulting in a rapid reduction of clearance and potentially increase in the extent of bioavailability.

The PK-PD simulations for SET 1 Scenario C are shown in **Figure 6.4**. The simulated concentration-time profiles are shown in **Figure 6.4A** under normoxia and hypoxia. Here with the lag time of 4 h prior to the introduction of hypoxia, the impact upon  $AUC_{0-\infty}$  and  $C_{max}$  was even less evident. With absorption even at 2 h into the simulation > 99% complete the only hypoxia-induced PK change influencing the respected concentration-time profile is the changes to clearance from 4 h to 24 h into the simulation. The implications of hypoxia on the concentration vs time profiles in respect to the  $IC_{50}$  (2.48 ng/mL) can also be seen in the adjacent Table which reflects essentially no impact upon both the exposure ( $AUC_{(concentration\ vs\ time)}$ ) and the time of sildenafil concentrations above the  $IC_{50}$  (**Figure 6.4A**). The corresponding simulated effect-time profiles are shown in **Figure 6.4B**. Here we see the hypoxia-induced changes in PK resulted in slightly more obvious differences in the effect-time profile (than that seen in the concentration-time profile) reflecting the changing concentrations against a non-linear PD model; the differences to normoxia are however not meaningful.

**Table 6.5** summarises the concentration-time and effect-time outcomes from the SET 1 simulations. **Figures 6.5** and **6.6** summarise, respectively, the combined concentration - time and the combined effect - time profiles arising from the simulations of the SET1 scenarios. The profiles reflect the simulated unbound concentrations of sildenafil, the concentrations that by convention relate to concentrations free at the receptor site and it will be the free concentrations which will have most relevance to the in-vitro experimental conditions used to derive any in-vitro  $IC_{50}$  parameters. Fraction unbound ( $F_u$ ) for sildenafil is 0.04, i.e., 96% is bound to plasma protein. In most situations with changes in drug dose and concentration the  $F_u$  of a drug is assumed to remain constant, and hence total drug concentration is effectively a biomarker for the free drug concentration. However, interventions can alter  $F_u$  and change the relationship between measured total drug concentration and the concentration of free drug. Such interventions would include for example protein binding drug-drug interactions or disease changes affecting for example the synthesis or excretion of plasma proteins involved in drug binding. The simulation scenarios undertake in this work assumed  $F_u$  to remain constant (i.e., 0.04) unaffected by hypoxia. This assumption is discussed further in a later part of this chapter.

**Table 6.3 Summary of SET 1 simulation outcomes**



<b>SET 1 simulation outcomes</b>	<b>Normoxia</b>	<b>Hypoxia SET 1 Scenario A</b>  'Hypoxia from time zero'	<b>Hypoxia SET 1 Scenario B</b>  'Hypoxia increases from time zero to 4 h'	<b>Hypoxia SET 1 Scenario C</b>  'Hypoxia increases in 'step function' at 4 h'
	Median (Q5, Q95)	Median (Q5, Q95)  % difference to normoxia	Median (Q5, Q95)  % difference to normoxia	Median (Q5, Q95)  % difference to normoxia
<b>AUC</b> <sub>0-∞</sub> (ng . mL <sup>-1</sup> . h) concentration-time profile	40.5 (24.0, 65.0)	53.6 (31.2, 85.6)  32 % increase	50.9 (31.1, 75.9)  26 % increase	45.8 (26.6, 69.6)  13 % increase
<b>C</b> <sub>max</sub> (ng . mL <sup>-1</sup> )	5.88 (4.34, 7.91)	6.80 (4.94, 9.22)  16 % increase	6.08 (4.48, 8.12)  3 % increase	5.81 (4.45, 7.84)  1.2 % decrease
<b>T</b> <sub>max</sub> (h)	1.10 (1.00, 1.20)	1.20 (1.10, 1.30)  9 % increase	1.10 (1.10, 1.20)  0 %	1.10 (1.00, 1.10)  0 %
<b>AUC</b> <sub>above IC50</sub> (ng . mL <sup>-1</sup> . h)	10.8 (4.40, 22.1)	17.1 (7.58, 34.8)  58 % increase	13.8 (5.96, 27.1)  28 % increase	10.9 (4.61, 22.9)  0.9 % increase
<b>Time</b> <sub>above IC50</sub> (h)	6.50 (4.10, 10.2)	8.70 (5.50, 13.6)  34 % increase	8.30 (5.30, 12.4)  28 % increase	7.50 (4.80, 11.5)  15 % increase
<b>AUC</b> <sub>0-∞</sub> (% . h) effect-time profile	769 (301, 1106)	955 (375, 1288)  24 % increase	958 (417,1232)  25 % increase	907 (804, 1186)  18 % increase
<b>AUC</b> <sub>above EC50</sub> (% . h)	74 (0.00, 133)	112 (0.00, 199)  51 % increase	95 (0.00, 165)  28 % increase	80 (0.00, 146)  8 % increase
<b>Time</b> <sub>above EC50</sub> (h)	6.50 (4.10, 10.2)	8.70 (5.50, 13.6)  34 % increase	8.30 (5.30, 12.4)  28 % increase	7.50 (4.80, 11.5)  15 % increase

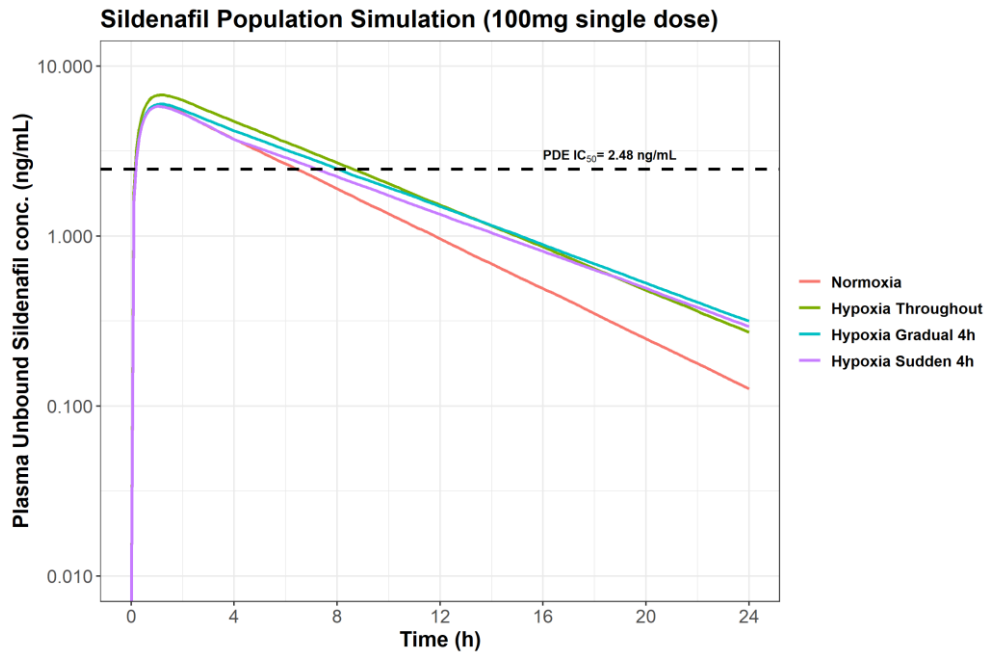


**Figure 6.5. Simulation of population PK of 100 mg single oral dose of sildenafil (n=1000) under normoxia or different SET 1 hypoxia scenarios.** The figure displays the unbound concentration - time profile of 100 mg single oral dose of sildenafil collectively for: normoxia; SET 1 A (hypoxia throughout); SET 1 B (gradual hypoxia over 4 h); or SET 1 C (sudden 'step-change' hypoxia at 4 h). The dotted line shows the  $IC_{50}$  for PDE inhibition from the literature of 2.48 ng/mL.

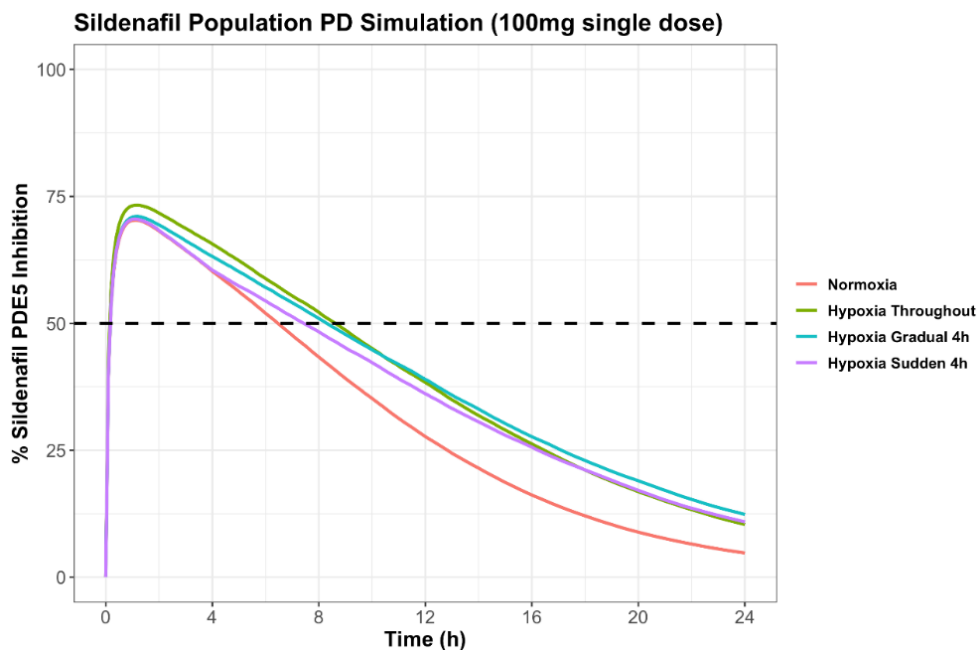


**Figure 6.6. Simulation of population PK/PD profile of 100 mg single oral dose of sildenafil (n=1000) under normoxia or different SET 1 hypoxia scenarios.** The figure displays the effect - time profile of 100 mg single oral dose of sildenafil collectively for: normoxia; SET 1 A (hypoxia throughout); SET 1 B (gradual hypoxia over 4 h); or SET 1 C (sudden 'step-change' hypoxia at 4 h). The dotted line shows the  $EC_{50}$  for PDE inhibition set at 50% of the  $E_{max}$ .

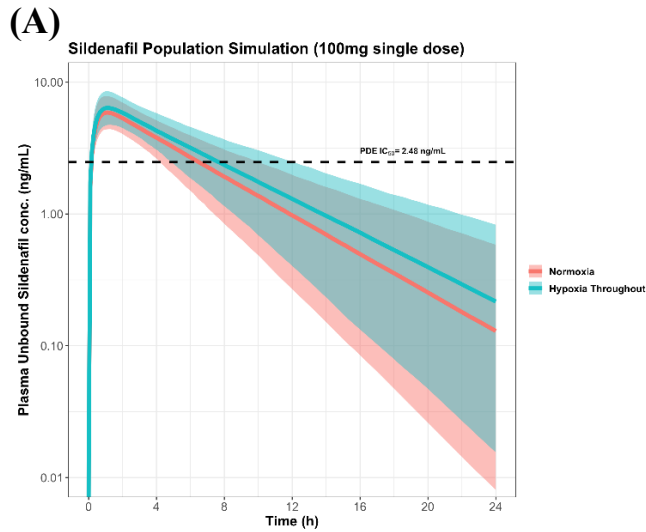
### 6.3.3 Monte Carlo simulation SET 2:

Here the PK/PD simulations ran over a 24 h period where, as in the SET 1 simulations hypoxia intervention causes a reduction in sildenafil hepatic intrinsic clearance ( $CL_{int}$ ) (estimated from experimental in-vitro data), but in addition for the SET 2 simulations the impact of hypoxia to alter total hepatic blood flow ( $Q_h$ ). The relevant equations relating to hypoxia-induced changes in total hepatic blood flow and how they then drive the simulated data is shown in **Eqs. 6.8, 6.9, 6.16, 6.23, 6.24**.

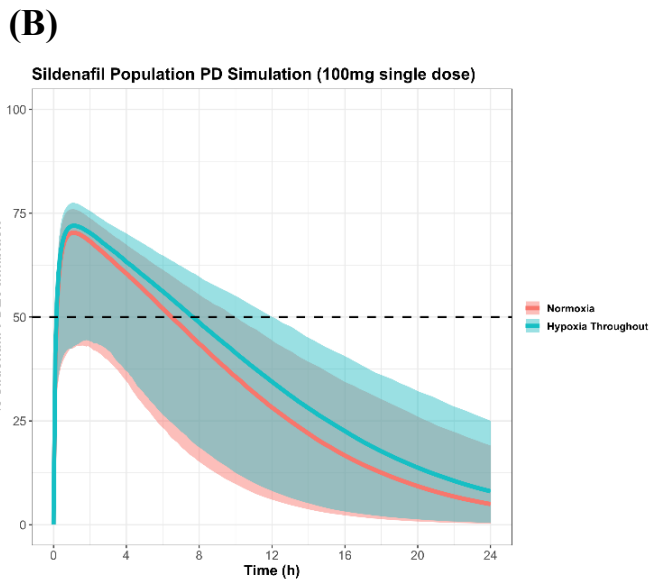
**6.3.3.1 SET 2 Scenario A - the maximal effect of hypoxia is established prior to the 24-h PK-PD simulation with, in addition to the hypoxia-induced a maximal decrease in hepatic intrinsic clearance (as in SET 1 Scenario A), there is now also a hypoxia-induced increase in  $Q_h$  by 40%**

The PK parameters utilised in the SET 2 Scenario A are shown in **Table 6.6**. The PD parameters for SET 2 remain the same as in SET 1 (**Eq. 6.25**).

The PK-PD simulations for SET 2 Scenario A are shown in **Figure 6.7**. The simulated concentration-time profiles are shown in **Figure 6.7A** under normoxia and hypoxia. The adjacent table in the Figure shows increases (except for  $T_{max}$ ) in all the relevant concentration – time outcome parameters arising from hypoxia, although some of these increases are very minor. The increases reflect here the combined impact of reducing hepatic intrinsic clearance and increasing total hepatic blood flow. A comparison of the concentration-time outcomes can be usefully made to the SET 1 Scenario A simulation which was the same except it lacked the hypoxia-induced 40% increase in total hepatic blood flow; **Table 6.7** makes this comparison.



PK parameters	Normoxia	Hypoxia SET 2 Scenario A 'Hypoxia from time zero'	% differences to normoxia
	Median (Q5, Q95)	Median (Q5, Q95)	
Time above IC50 (h)	6.50 (4.30, 10.1)	7.70 (4.90, 12.1)	18 % increase
AUC above IC50 (ng/mL . h)	10.8 (4.51, 22.2)	14.2 (6.25, 28.9)	31 % increase
AUC (0-∞) (ng/mL . h)	40.6 (23.3, 64.9)	48.2 (27.8, 76.3)	19 % increase
C <sub>max</sub> (ng/ml)	5.88 (4.41, 7.85)	6.38 (4.75, 8.56)	9 % increase
T <sub>max</sub> (h)	1.10 (1.10, 1.30)	1.10 (1.10, 1.30)	0 %



PD parameters	Normoxia	Hypoxia SET 2 Scenario A Hypoxia from time zero'	% differences to normoxia
	Median (Q5, Q95)	Median (Q5, Q95)	
Time above EC50 (h)	6.50 (4.30, 10.1)	7.70 (4.90, 12.1)	18 % increase
AUC above EC50 (% . h)	75.0 (0.00, 136)	94.0 (0.00, 171)	25 % increase
AUC (0-∞) (% . h)	776 (315, 1095)	883 (355, 1209)	14 % increase

**Figure 6.7. SET 2 Scenario A simulation of population PK and PD profile of 100 mg single oral dose of sildenafil (n=1000) under normoxia (red) or hypoxia (blue) from time 0 considering the change of  $Cl_{int}$  and increase hepatic blood flow by 40% under hypoxia. Fig. 6.7A displays a simulation of an unbound concentration of 100 mg single oral dose of sildenafil over time, and the table presents the PK parameters of sildenafil in both normoxia and hypoxia groups and the % of median differences between them. Fig. 6.7B displays a simulation of % of sildenafil to inhibit PDE5 over 24 h in both normoxia and hypoxia groups. The table presents the PD parameters of sildenafil in both groups and the % of median differences between them. The red represents a simulation of 100 mg of sildenafil under normoxia while the blue is a simulation of 100 mg of sildenafil, Incorporating revised predicted 'hypoxia' parameters for hepatic CL and oral bioavailability and an increase in  $Q_h$  blood flow by 40%. The thick line is the median, and the ribbon is the 5<sup>th</sup> to 95<sup>th</sup> percentile.**

Table 6.4 PK parameters used in Monte Carlo simulation SET 2

PK Parameter	Normoxia	Hypoxia	Description
$K_a$ [ $h^{-1}$ ]	2.60	2.60	Oral absorption rate
$V_c$ [L]	234	234	Apparent volume of distribution (central)
$CL$ [L/h]	40.8	-	Total clearance under normoxia and hypoxia with 40 % increase in hepatic blood flow ( $\parallel_{1.4}$ )
$CL_{\parallel_{1.4}}$ [L/h]	-	36.8	
$F_{total}$ [fraction]	0.41	-	Extent of oral bioavailability or total fraction of oral dose absorbed to the systemic circulation under normoxia and hypoxia with 40 % increase in hepatic blood flow ( $\parallel_{1.4}$ )
$F_{total \parallel_{1.4}}$ [fraction]	-	0.51	

Table 6.5 Concentration-time outcomes,  $CL_{total}$ ,  $F_{total}$ ,  $E_H$  comparing Scenarios A SET 1 versus SET2.

	Normoxia SET 1 Scenario A = SET 2 Scenario A	Hypoxia SET 1 Scenario A	Hypoxia SET 2 Scenario A
$AUC_{0-\infty}$ (ng. $mL^{-1} \cdot h$ ) concentration-time profile	40.5	53.6	48.2
$C_{max}$ (ng . $mL^{-1}$ )	5.88	6.80	6.38
$T_{max}$ (h)	1.10	1.20	1.10
$AUC_{above IC50}$ (ng. $mL^{-1} \cdot h$ )	10.8	17.1	14.2
$Time_{above IC50}$ (h)	6.50	8.70	7.70
$CL_{total}$ (L/h)	40.8	33.9	36.8
$F_{total}$	0.41	0.46	0.51
$E_H$	0.41	0.33	0.26

**Table 6.7** shows a further increase in  $F_{\text{total}}$  (the  $F_{\text{total}}$  shifting from 0.46 to 0.51) as hypoxia in SET 2 now also affects total hepatic blood flow; a 40% increase in  $Q_h$ . In our simulations we assumed that hypoxia did not alter the extent of bioavailability from the lumen ( $F_{\text{lumen}}$  of 0.69; see **Eqs. 6.10 - 6.12**). Rather it is the impact of hypoxia on hepatic extraction ratio ( $E_H$ ) and hence hepatic first-pass bioavailability ( $F_{\text{hepatic}}$ ) that led to the overall increase in  $F_{\text{total}}$ . Changes in hepatic blood flow ( $Q_h$ ) independent of  $F_u$  and  $CL_{\text{int}}$  may affect the hepatic extraction ratio  $E_H$  (see **Eqs. 6.3 and 6.4**). Hypoxia-induced decreases in the intrinsic hepatic clearance ( $CL_{\text{int}}$ ) alone, without changes in  $Q_h$ , reduced the  $E_H$  (SET 1 Scenario A i.e.  $E_H$  decreased from 0.41 in normoxia to 0.33 in hypoxia; see **Eqs. 6.10 - 6.15**). With the additional impact of the 40% increase in hepatic blood flow (SET 2 Scenario A) the  $E_H$  was further reduced ( $= 0.26$ ; see **Eqs. 6.16 - 6.18**). The relatively smaller impact upon  $E_H$  of a 40% increase in  $Q_h$  (i.e. 21% decrease with  $E_H$  0.33 to  $E_H$  0.26) reflects the magnitude of the  $CL_{\text{int}}$  parameter, (253 mL/min/kg in hypoxia) versus that of  $Q_h$  (29.0 mL/min/kg). Nevertheless, on hepatic first-pass the hypoxia-induced increases in  $Q_h$  will increase the transit of drug molecules through liver sinusoids, reducing residence time in the liver and leading to a slightly less efficient hepatic extraction ( $E_H$ ) and greater  $F_{\text{hepatic}}$  with a corresponding effect upon  $F_{\text{total}}$  (i.e.  $F_{\text{total}} = F_{\text{lumen}} + F_{\text{hepatic}}$  where  $F_{\text{hepatic}} = 1 - E_H$ ). In addition to the impact of changes in  $Q_h$  upon  $E_H$ ,  $Q_h$  is a variable in an organ's clearance more directly, i.e.  $CL_{\text{hepatic}} = Q_h \times E_H$  (Wilkinson and Shand, 1975). Here the  $CL_{\text{hepatic}}$  for drugs displaying a high extraction ratio (ca.  $E_H > 0.7$ ) being more influenced by changes in  $Q_h$  than if the drug displayed a low (ca.  $E_H < 0.3$ ) or intermediate extraction ratio.

The liver receives its blood supply from two primary sources: 70%-80% of the blood entering the liver is partially deoxygenated venous blood supplied by the hepatic portal vein (HPV) and which drains blood to the liver from the gastrointestinal tract (apart from the lower section of rectum), spleen, pancreas, and gallbladder. The portal vein receives tributaries from the superior and inferior mesenteric veins, splenic vein, gastric vein, and cystic vein. Parts of the diaphragm also drain into the portal vein via the Sappey veins. The hepatic artery accounts for the remaining 20-30% of the liver blood flow providing oxygenated blood (Greenway and Stark, 1917; Schenk *et al.*, 1962; Granger and Kviety, 2004; Vollmar and Menger, 2009).

There is limited research on the effects of acute hypoxia upon hepatic blood flow, with only one study (Nicholas S. Kalson *et al.*, 2010) investigating HPV blood flow in this context. Their study involved 12 healthy volunteers who ascended to an altitude of 4392 m for 24 h. They observed pre-prandial HPV blood flow to increase by 40%, along with a 97% increase in

superior mesenteric artery blood flow compared to sea-level measurements. The authors attributed these changes to an increase in vessel diameter, flow velocity, and heart rate under hypoxia. Contrasting findings were reported in another study involving nine adults exposed to a shorter duration of hypoxia (2 h) (equivalent to 4300 m) within a hypobaric chamber. This study revealed a decrease of 15% in superior mesenteric artery blood flow compared to normoxic conditions (Loshbaugh, Loeppky and Greene, 2006).

It is the work of Kalson et al., reporting a 40% increase in HPV that formed the basis for the simulations in SET 2 Scenario A. Clearly there is a need for further research to fully understand the effects of hypoxia on hepatic blood flow and its implications for drug metabolism and response. To explore a little more the potential impacts for sildenafil, a simulation was undertaken restricted solely to changes in  $Q_h$  (i.e. simulations did not include changes to intrinsic clearance ( $CL_{int}$ ) or  $F_u$ ), and how these  $Q_h$  changes would affect the hepatic clearance of sildenafil. The sildenafil hepatic  $CL_{int}$  was held constant at 357 mL/min/kg (= normoxic value) and the  $F_u$  held constant at 0.04. The  $Q_h$  was varied around the initial value of 20.7 mL/min/kg. These initial parameters resulted in a sildenafil hepatic clearance ( $CL_{hepatic}$ ) of 8.45 mL/min/kg (Eq. 6.4).

**Figure 6.8** shows the outcome of the simulations where the y-axis is sildenafil  $CL_{hepatic}$  and the x-axis ( $\text{Log}_{10}$  scale) is  $Q_h$ . The initial  $Q_h$  value (i.e., corresponding to Factor change = 1) is shown by the vertical black dashed line.  $Q_h$  changes simulated around the initial value ranged from a reduction in  $Q_h$  to 10% of initial (Factor change = 0.1) to a 300% increase over initial (Factor change = 3). The vertical green dashed line in **Figure 6.8** shows the Factor change = 1.4 representing a 40% increase in  $Q_h$ .

**Figure 6.8** shows the predicted impact of varying  $Q_h$  alone upon sildenafil  $CL_{hepatic}$ . Noting the  $\text{Log}_{10}$  scale for the x-axis, the Figure shows that changes in  $Q_h$  do not result in proportional changes in sildenafil  $CL_{hepatic}$ . e.g. increasing  $Q_h$  alone by 40% (Factor Change = 1.4) results in respective ca.12% increase in  $CL_{hepatic}$  to 9.49 mL/min/kg. Sildenafil, with a hepatic first-pass extraction ratio of 0.41 falls into the category of drugs with intermediate hepatic extraction. Therefore, changes in hepatic blood flow have a more limited impact on sildenafil's hepatic clearance. However, small changes in hepatic blood flow can have a notable effect on the clearance of medications with high extraction ratios ( $E_H > 0.7$ ), such as rifampicin and phenobarbital.

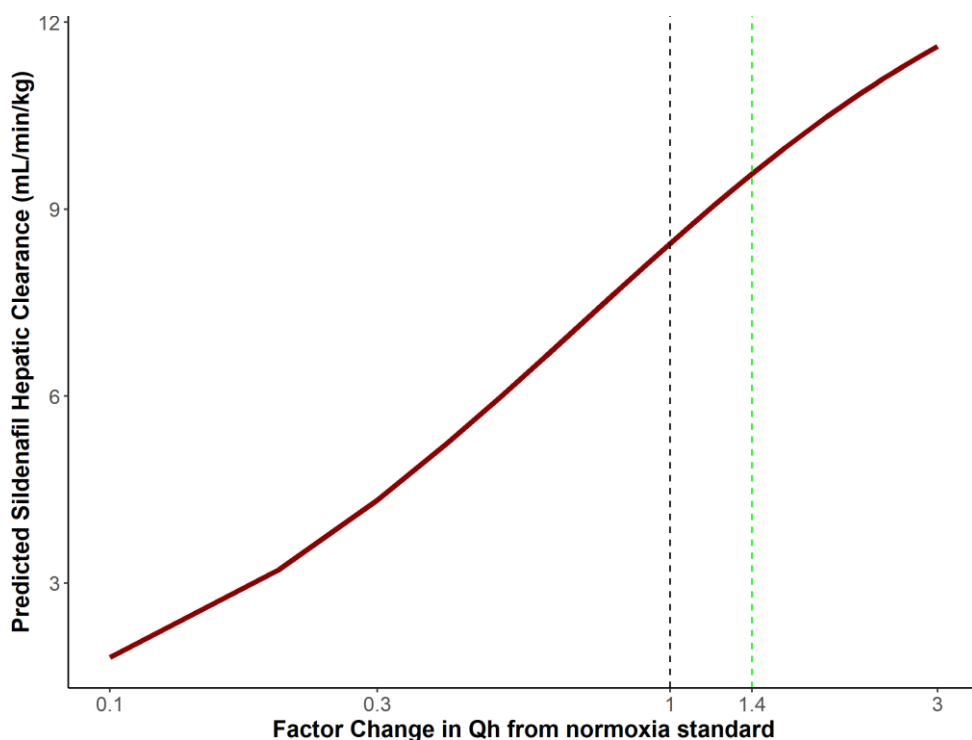


**Figure 6.8. Simulation of the effect of hepatic blood flow ( $Q_h$ ) alteration on predicted hepatic clearance ( $CL_{hepatic}$ ) of sildenafil where the hepatic intrinsic CL ( $CL_{int}$ ) is unchanged.** The change in  $Q_h$  (Log10 scale) represented as a factor, where 1 corresponds to the normal  $Q_h$  of 20.7 mL/min/kg. In the Figure, the vertical black dashed line represents this normal  $Q_h$  (Factor change = 1), while the vertical dashed green line represents an increase in  $Q_h$  by 40% (Factor change = 1.4).

The above simulations were performed using R and RStudio, a programming language/platform for statistical computing and graphical presentation of the outcomes (Gandrud, 2013). R software is widely used in pharmacokinetics and health decision sciences due to its flexibility and extensive collection of packages and functions for data analysis, modelling, and visualisation (Jaki and Wolfsegger, 2011; Jalal *et al.*, 2017). R is also used for population pharmacokinetic modelling using nonlinear mixed-effects models and in the evaluation of different dosing regimens using packages such as ‘mrgsolve’, as well as visualisation packages such as ‘ggplot2’ and ‘ggpubr’.

To further exemplify how sildenafil clearance and extent of oral bioavailability are influenced by changes in  $Q_h$  or  $CL_{int}$ , an Excel-based ‘sensitivity analysis’ was undertaken (**Table 6.8**).



**Table 6.6** Excel-based ‘sensitivity analysis’ of the impact of changing  $Q_h$  or  $CL_{int}$  upon some key sildenafil PK parameters

$Q_h$ mL/min/kg (% decrease from initial)	$CL_{int}$ mL/min/kg (remains unchanged)	$E_H$ (%) difference	$CL_{hepatic}$ mL/min (%) difference	$F_{hepatic}$ (%) difference	$F_{total}$ (%) difference	$AUC_{0-\infty}$ ng/mL . h (%) difference
20.7	357	0.41	592	0.59	0.41	40.0
18.6 (-10%)	357	0.43 (6.29)	566 (-4.34)	0.57 (-4.34)	0.39 (-4.34)	39.8 (-0.59)
16.6 (-20%)	357	0.46 (13.4)	537 (-9.26)	0.54 (-9.26)	0.37 (-9.26)	39.5 (-1.31)
14.5 (-30%)	357	0.50 (21.6)	503 (-14.9)	0.50 (-14.9)	0.35 (-14.9)	39.2 (-2.22)
12.4 (-40%)	357	0.53 (31.0)	465 (-21.4)	0.47 (-21.4)	0.32 (-21.4)	38.7 (-3.41)
10.4 (-50%)	357	0.58 (42.0)	420 (-29.0)	0.42 (-29.0)	0.29 (-29.0)	38.0 (-5.03)
$Q_h$ mL/min/kg (remains unchanged)	$CL_{int}$ mL/min/kg (% decrease from initial)	$E_H$ (%) difference	$CL_{hepatic}$ mL/min (%) difference	$F_{hepatic}$ (%) difference	$F_{total}$ (%) difference	$AUC_{0-\infty}$ ng/mL . h (%) difference
20.7	357	0.41	592	0.59	0.41	40.0
20.7	321 (-10%)	0.38 (-6.17)	555 (-6.17)	0.62 (4.26)	0.43 (4.26)	44.1 (10.2)
20.7	286 (-20%)	0.36 (-12.9)	515 (-12.9)	0.64 (8.89)	0.44 (8.89)	49.1 (22.6)
20.7	250 (-30%)	0.33 (-20.2)	472 (-20.2)	0.67 (14.0)	0.47 (14.0)	55.4 (38.3)
20.7	214 (-40%)	0.29 (-28.3)	424 (-28.3)	0.71 (19.5)	0.49 (19.5)	63.5 (58.6)
20.7	179 (-50%)	0.26 (-37.2)	372 (-37.2)	0.74 (25.6)	0.51 (25.6)	74.4 (85.7)

The first two columns in **Table 6.8** represent the ‘inputs’  $Q_h$  and  $CL_{int}$  into the ‘sensitivity analysis’ and the columns to the left represent the the outcomes of  $E_H$ ,  $CL_{hepatic}$  and  $F_{hepatic}$ ,  $F_{total}$  and  $AUC_{0-\infty}$ . In the top-half of table the  $CL_{int}$  remains unchanged (357 mL/min/kg, equivalent to the normoxia  $CL_{int}$  as used for SET A) but with decreases in  $Q_h$  from 20.7 to 10.4 mL/min/kg, i.e. a 50% decrease; in the bottom-half of table the  $Q_h$  remains unchanged (20.7 mL/min/kg,

$Q_h$  value used for SET A simulations) but there are decreases in  $CL_{int}$  from 357 to 179 mL/min/kg, i.e. a 50% decrease.

The  $E_H$  outcome (column 3) shows when  $Q_h$  alone is decreased ( $CL_{int}$  held constant) then the  $E_H$  increases as predicted from **Eq 6.3**, and which may be viewed as arising from the longer residence time of drug passing through the liver sinusoids. When  $Q_h$  is held constant and  $CL_{int}$  is decreased then  $E_H$  decreases because of the dominant impact here of  $CL_{int}$ . The consequence for the extent of bioavailability across the liver is a corresponding decrease and increase in  $F_{hepatic}$  i.e. ( $F_{hepatic} = 1 - E_H$ ). The intermediate nature of sildenafil with a hepatic extraction ratio of 0.41 is reflected in both the cases of reduced  $Q_h$  or reduced  $CL_{int}$  by reductions in  $CL_{hepatic}$ , but where decreases in  $CL_{int}$  (through  $E_H$ , i.e.  $CL_{hepatic} = Q_h * E_H$ ) drive a slightly greater reduction in  $CL_{hepatic}$  than those arising from the decreases in  $Q_h$  alone. Overall, the impact of changes in  $Q_h$  and  $CL_{int}$  upon exposure to sildenafil, reflected in the  $AUC_{0-\infty}$  can be seen the final column. Here very significant impacts are seen in  $AUC_{0-\infty}$  when  $CL_{int}$  is reduced i.e., increases in  $AUC_{0-\infty}$  by 75% compared to initial. Here reductions in  $CL_{int}$  both increase the  $F_{total}$  and reduce the  $CL_{total}$ , with the impact to increase  $AUC_{0-\infty}$  predicted by **Eq. 6.26**.; the reverse would be true for increases in  $CL_{int}$  which would both decrease the  $F_{total}$  and increase the  $CL_{total}$ .

$$AUC_{0-\infty} = \frac{Dose \cdot F_{total}}{CL_{total}} \dots \text{Eq. 6. 26}$$

In this current work renal blood flow was assumed to remain constant with hypoxia. Although this may not be the case, the renal route plays only a minor role in sildenafil elimination with approximately 13% of the parent drug excreted in urine (Walker *et al.*, 1999; Muirhead *et al.*, 2002). One study reported a 24 h exposure to high altitude (4,330 m) led to a 17% reduction in renal blood flow (Steele *et al.*, 2020). Based on 13% of the drug eliminated by the renal route we may estimate a renal clearance of sildenafil of ca 5.3 L/h, which if subject to a 17% would result in a renal CL of 4.39 L/h, i.e., a 0.9-1.0 L/h change which in the context of the total CL (ca 40 L/h) is negligible. Further, some other studies report an increase in renal blood flow with hypoxia which may not impact excretion. For example, two studies observed a 10% to 14% increase in renal blood flow during a 2 h hypoxic exposure although glomerular filtration rate was maintained (Berger *et al.*, 1949; Olsen *et al.*, 1992).

This current Excel-based ‘sensitivity analysis’ and the R-based PK/PD simulations may indirectly help shape the possibilities of how hypoxia can affect the PK/PD of sildenafil, a drug

in widespread use amongst mountaineers. Currently, no human clinical research studies on sildenafil PK/PD under hypoxia have been published; an original aim of this thesis was to conduct such a study.

The only direct evidence is an animal study (Zhang and Wang, 2022) on the PK of sildenafil in rats (dose by oral solution gavage of 4.8 mg/kg) and involving three groups: a low-altitude group (50 m) and two hypoxia high-altitude groups, one at 2300 m for 24 h ‘Acute exposure’ (H1) and the other at 4300 m for 24 h ‘Acute exposure’ (H2). In both hypoxia high-altitude groups, a significant downregulation (30-40%) of protein expression for CYP3A4 was reported in the rat liver. The  $AUC_{0-24h}$  for sildenafil in the H2 in particular was significantly increased (313%) and both the CL and volume of distribution were significantly decreased compared to the low-altitude group by 70% and 47%, respectively; these primary disposition parameters will actually represent CL/F and V/F as no IV dosing arm was provided. As in our simulation, the increase in AUC is likely to be the result of both a decreased CL and increased  $F_{total}$ .

The decreased volume of distribution seen in the above animal study contrasted to this chapter’s simulation work where the volume of distribution was set to remain constant under hypoxia. Alterations in drug plasma protein binding ( $F_u$ ) can influence not only a drug’s clearance but also its volume of distribution. In the animal study above the H2 group displayed moderately but statistically significant raised plasma albumin levels compared to animals at low altitude (Zhang and Wang, 2022). An increase in albumin levels has also been observed in humans exposed to high altitude environments and been implicated in the increased protein binding of drugs (Surks, 1966; Li *et al.*, 2009). Sulfamethoxazole, a drug with moderately high plasma protein binding (ca, 70%), showed significantly increased protein binding in subjects acutely exposed to high altitude (mean  $\pm$  SD: 80.43  $\pm$  4.03%) compared to baseline conditions (mean  $\pm$  SD: 65.74  $\pm$  2.88%) at low altitude (Li *et al.*, 2009). Similarly, acute high altitude exposure was found to affect protein binding of prednisolone with an increase in protein binding observed after exposure to high altitude (mean  $\pm$  SD: 75  $\pm$  6.9%) compared to sea level conditions (mean  $\pm$  SD: 57  $\pm$  1.8%) (Arancibia *et al.*, 2005).

Hypoxia has also been shown to stimulate erythropoiesis through the release of erythropoietin from the kidneys and increased water vapour loss due to hyperventilation. These physiological responses result in an elevation in haematocrit and an increase in red blood cell production, as well as a reduction in plasma volume observed in individuals exposed to high altitudes (Mairbäurl, 1994; Jacobs *et al.*, 2012; Hui *et al.*, 2016). These changes, along with alterations

in capillary hydrostatic and interstitial osmotic pressures, which contribute to fluid transfer from the intravascular to the extravascular compartment, can potentially enhance drug-protein binding while reducing a drug's volume of distribution.

The impact of acute hypoxia on acid-base balance is also a consideration. Hypobaric hypoxaemia (as in a high altitude setting) can lead to respiratory alkalosis, characterised by hyperventilation and subsequent hypocapnia. To counterbalance this effect, the kidneys decrease bicarbonate levels through excretion, thereby mitigating the increase in body pH (Hui *et al.*, 2016). The influence of increased blood pH on pharmacokinetics is uncertain and may vary depending on the specific characteristics of the drug. Additionally, a systematic review and meta-analysis study highlighted that certain factors like hypobaric hypoxaemia, exercise, and cold exposure can lower the pH in the gut (Bailey, Stacey and Gumbleton, 2018). This decrease in gut pH can have implications for weak basic drugs such as sildenafil, which has a pKa value of 7.61. In an acidic environment, weak basic drugs are more prone to ionisation, resulting in a greater proportion of cationic drug molecules. The cationic form of the drug exhibits reduced solubility and diminished ability to traverse cell membranes compared to the non-ionised form. Consequently, the absorption of weak basic drugs may be impaired when the gut environment is acidic.

## 6.4 Conclusions

The findings of this study provide important insights into the PK/PD profile of sildenafil under hypoxic conditions. Based on the simulations conducted, the following conclusions can be drawn:

- Acute hypoxia has the potential to alter the PK/PD profile of sildenafil and may have relevance in clinical scenarios and for other drugs, including alterations in PK/PD during normobaric hypoxaemia.
- Altered hepatic blood flow under hypoxia was found to have a minimal effect on the overall PK/PD changes observed, while a decrease in hepatic clearance ( $CL_{int}$ ) had a significant impact. This suggests that the modulation of  $CL_{int}$  plays a major role in the observed changes in sildenafil PK/PD under hypoxic conditions.

PK/PD simulations offer a valuable framework for exploring and understanding the potential physiological variables that can influence drug outcomes and quantifying the extent of such outcomes. Furthermore, these simulations can guide the design of clinical trials, determine optimal dosage administration timing, and aid in dose adjustments for patients with normobaric hypoxaemia or individuals experiencing hypobaric hypoxaemia.

Based on the PK/PD simulations conducted on sildenafil, the following recommendations can be made:

- In populations exposed to hypoxia, such as climbers, to avoid pharmacological side effects or toxicity, it is advisable to administer medications metabolised by CYP3A4 and CYP2C9, including sildenafil, as a prophylaxis at sea level prior to ascending to high altitudes, rather than taking the drug after exposure to hypoxia.
- In individuals at high altitudes or patients with acute hypoxaemia who require drug administration at a specific time, dosage modifications should be considered, especially for drugs with a narrow therapeutic index.

These recommendations aim to ensure the safe and effective use of sildenafil and other medications in populations exposed to hypoxia. However, further research and clinical trials are warranted to validate these recommendations and explore the applicability of PK/PD simulations in optimising drug therapy under hypoxic conditions.

## **Chapter 7: Summary Discussion and Future Work**

## Chapter 7

Arterial hypoxaemia, characterised by low partial pressure of oxygen (PaO<sub>2</sub>) levels below 80 mmHg, is commonly observed in individuals with pulmonary disorders as well as in populations residing at high altitudes for various purposes, such as mountaineering or occupational activities (Monge and Leon-Velarde, 1991; Sarkar, Niranjana and Banyal, 2017). It has been reported that 25-85% of individuals travelling to high altitudes experience hypoxaemia-related symptoms, ranging from mild acute mountain sickness to severe complications like high-altitude cerebral oedema and high-altitude pulmonary oedema, which often require medical intervention (Fiore, Hall and Shoja, 2010). The onset of hypoxaemia triggers a series of physiological responses aimed at maintaining oxygen delivery to vital organ systems. However, these responses can also lead to the generation of free radicals and activation of oxidative-inflammatory stress pathways both systemically and locally (Ertel *et al.*, 1995; Klausen *et al.*, 1997; Lemos *et al.*, 2013; Bailey *et al.*, 2019; Gaur *et al.*, 2021).

The presence of arterial hypoxaemia and the associated physiological adjustments, including redox and haemodynamic changes, have the potential to influence the pharmacokinetics (PK) and pharmacodynamics (PD) of medications administered acutely or chronically in these individuals (Hui *et al.*, 2016). Nevertheless, the precise impact of hypoxaemia on drug PK and PD remains uncertain due to limited and underpowered studies that have investigated different drugs, altitudes, and exposure durations, yielding inconsistent findings. Therefore, there is a crucial need for well-controlled clinical research investigations to comprehensively explore the effects of hypoxaemia on drug response. Understanding how hypoxaemia influences drug PK and PD is of utmost importance for optimizing therapeutic interventions in individuals exposed to hypoxic conditions. Such knowledge can aid in the development of appropriate dosage adjustments and treatment strategies to ensure drug efficacy and minimise the risk of adverse effects. Moreover, the findings from these investigations may have broader implications for individuals with pulmonary disorders or those residing in high-altitude regions, as well as for patients undergoing therapeutic interventions in hypoxic environments.

This thesis **originally** aimed to investigate the impact of acute hypoxaemia on drug pharmacokinetics through a well-controlled clinical trial involving healthy participants. The drug of interest for study was sildenafil, chosen as a representative model drug. Sildenafil, a pharmaceutical agent primarily acting as a phosphodiesterase-5 inhibitor, is clinically used for the management of pulmonary hypertension. Furthermore, it has demonstrated efficacy in preventing or attenuating altitude-induced pulmonary vasoconstriction, a critical factor contributing to the development of high-altitude pulmonary oedema (HAPE) (Zhao *et al.*,

## Chapter 7

2001). The primary hypothesis underlying the research was that acute arterial hypoxaemia, a common consequence of high-altitude environments and certain pulmonary disorders, could exert substantial effects on the pharmacokinetic profile of drugs. Consequently, it was anticipated that dosage modifications may be warranted to optimize drug therapy in the context of hypoxic conditions. By investigating the specific case of sildenafil, the thesis aimed to shed light on the broader implications of hypoxaemia on drug pharmacokinetics and, consequently, on patient care in hypoxic settings.

The clinical trial was designed with sufficient statistical power to investigate the pharmacokinetics (PK) and pharmacodynamics (PD) of a single oral dose of sildenafil in healthy participants under acute normobaric hypoxia conditions (12% O<sub>2</sub>). The necessary tasks to develop the trial were undertaken during the initial stages of this PhD and involved my work on obtaining ethical approval, developing a protocol that adheres to the requirements of the Medicines and Healthcare products Regulatory Agency (MHRA), completing good clinical practice (GCP) training, working with GLP laboratory on the bioanalysis of sildenafil were all successfully accomplished (see **Appendix 1**). Further, as part of the background to the protocol design a Rapid systematic Review and Meta analysis on hypoxaemia and altered drug PK was undertaken and reported in **Chapter 3**.

As a result of COVID the trial was suspended and the thesis thereafter had to take a change in direction, but one nevertheless retaining the focus on the original hypothesis but where more attention was given to underlying mechanisms through which hypoxia influences drug pharmacokinetics and simulated outcomes (**Chapters 4, 5 and 6**).

To comprehensively assess the impact of both acute and chronic hypoxaemia on drug pharmacokinetics, a rapid systematic review and meta-analysis were conducted, as described in **Chapter 3**. A total of ten studies were included in the analysis, comprising six studies conducted in patients with pulmonary diseases and four studies involving healthy individuals exposed to hypoxaemia either through simulated hypoxia chambers or by ascending to high-altitude environments exceeding 2500 m. The meta-analysis findings revealed no significant changes in pharmacokinetic (PK) parameters, including volume of distribution (V<sub>d</sub>), elimination half-life (t<sub>1/2</sub>), clearance (CL), and bioavailability, in patients with respiratory diseases and chronic hypoxaemia. This meta-analysis represents the first study of its kind investigating the effect of chronic hypoxaemia in patients with respiratory diseases on drug pharmacokinetics. In contrast, a significant decrease in CL was observed in healthy individuals



## Chapter 7

experiencing acute hypoxaemia. The observed decrease in CL among healthy individuals with acute hypoxaemia is consistent with the findings of a previous systematic review and meta-analysis published by Bailey, Stacey, and Gumbleton in 2018. Bailey *et al.*'s study focused specifically on the impact of hypobaric hypoxia on drug pharmacokinetics and was limited to human single-dose studies involving healthy males of Chilean or Chinese descent who transitioned from low-altitude ( $\leq 600$  m) to terrestrial high-altitude environments ( $\geq 2500$  m) in an acute manner within a 24-h timeframe. The analysis included six articles meeting the inclusion criteria and concluded that acute high-altitude exposure was likely to result in decreased clearance and a trend towards a longer elimination half-life ( $t_{1/2}$ ) under high-altitude conditions. In contrast to Bailey *et al.*'s study, our meta-analysis employed more stringent inclusion criteria by specifically selecting studies that reported participants' arterial partial pressure of oxygen ( $\text{PaO}_2$ ) levels to confirm the presence of hypoxaemia, defined as a  $\text{PaO}_2 < 80$  mmHg. Additionally, our rapid review encompassed studies involving various routes of drug administration, including oral, intramuscular, and intravenous routes, while Bailey *et al.*'s study was restricted to the oral route alone.

A reduction in blood oxygen levels has been shown to influence drug clearance (CL) by modulating the expression of various phase I metabolising enzymes. The specific impact on each enzyme varies, subsequently influencing the response of individual drugs. Several animal studies have reported that acute hypoxia leads to downregulation of CYP450 mRNA expression, enzyme activity, and protein levels for a wide range of CYP450 isoforms, including CYP1A1, CYP1A2, CYP2B6, CYP2C19, CYP2E1, and CYP3A1 (Fradette *et al.*, 2002; Fradette and Souich, 2004; Li, Wang, Li, Zhu, *et al.*, 2014b; Shi *et al.*, 2017). Conversely, acute hypoxia has been found to upregulate the expression of CYP3A6, CYP2D6, CYP3A2, and CYP3A11 (Kurdi *et al.*, 1999; Fradette *et al.*, 2002, 2007b; Fradette and Souich, 2004; Li, Wang, Li, Zhu, *et al.*, 2014b; Hori, Shimizu and Aiba, 2018).

Furthermore, hypoxaemia can affect drug disposition by influencing hepatic blood flow, which in turn impacts the rate at which drugs are delivered to the liver for metabolism. This effect is particularly relevant for drugs with a high hepatic extraction ratio, such as lidocaine, propranolol, and isoproterenol. Acute hypoxaemia-induced vasoconstriction, mediated by sympathetic nerve system activation, increased renal vascular resistance, and decreased renal oxygen delivery, leads to a reduction in renal blood flow (Olsen *et al.*, 1993; Steele *et al.*, 2020). Consequently, drugs primarily excreted through the renal route may be affected. For

## Chapter 7

instance, sulfamethoxazole, a drug primarily excreted in the urine, exhibited a significant 18% decrease in clearance in participants exposed to an altitude of 3780 m for 16 h (Li *et al.*, 2009).

Moreover, high-altitude exposure has been associated with an increase in plasma total protein and albumin levels in humans, resulting in enhanced drug-protein binding (Surks, 1966; Li *et al.*, 2009). This elevation in plasma proteins under hypoxic conditions can impact the clearance of drugs with high plasma protein binding, as there will be less unbound free drug available for hepatic metabolism and renal excretion.

**Chapter 4** employed quantitative reverse transcription-polymerase chain reaction (qRT-PCR) and Western blot experiments (**Figure 4.7**) to assess the expression levels of critical genes, including CYP3A4 and CYP2C9, in HepG2 cells. Despite treatment with the enzyme inducer rifampicin at high concentrations, the expression of these genes remained low or nearly undetectable in HepG2 cells. This finding suggests that HepG2 cells have limited potential as functional liver cells. Consequently, the HepaRG cell line was selected as the in-vitro model for investigating the effects of hypoxia on CYP450 enzymes and subsequent mechanistic studies. The utilisation of the HepaRG cell line aligns with the observations of Yokoyama *et al.*, who reported significantly higher phase I metabolising enzyme activity in HepaRG cells compared to HepG2 cells, equivalent to that observed in primary human hepatocytes (Yokoyama *et al.*, 2018). Furthermore, HepaRG cells exhibit more hepatocyte-like characteristics, including higher expression levels of CYP450 enzymes, bile canaliculi structures, and bile acid transporters, when compared to HepG2 cells (Le Vee *et al.*, 2006; Guillouzo *et al.*, 2007). These attributes support the suitability of HepaRG cells for investigating the effect of hypoxia on CYP450 enzymes and associated CL alterations.

Subsequently, the spheroid 96-well ultra-low attachment (ULA) plate culture technique was employed, offering advantages such as reduced cell requirement and increased throughput. The gene expression of CYP3A4 and CYP2C9 was assessed in both 3D spheroids and 2D monolayer models. Surprisingly, the mRNA levels of CYP3A4 and CYP2C9 were found to be more significant in the 2D monolayer model, as depicted in **Chapter 4, Figure 4.16**. However, these findings contradict those reported by Takahashi *et al.*, who observed considerably higher mRNA levels of CYP1A2, CYP2B6, and CYP3A4 in 3D spheroids of HepaRG cells generated using the hanging drop technique, compared to the 2D monolayer HepaRG cells (Takahashi *et al.*, 2015). An explanation for this discrepancy may lie in the methodology employed for spheroid formation. In our study, differentiated cells were used to seed the spheroids, with the

## Chapter 7

withdrawal of dimethyl sulfoxide (DMSO) supplement from the culture media to facilitate 3D spheroid formation. Optimisation experiments conducted previously revealed that DMSO supplementation at 2% induced cell death and debris, as observed through microscopic examination (see **Appendix 3, Supplementary Figure 3.1.1**). According to the study by Kanebratt and Andersson, the expression of various CYP450 enzymes, including CYP3A4 and CYP2C9, in HepaRG cells significantly decreased on the first day following the removal of DMSO from the culture media, and although levels stabilised afterward, they remained low (Kanebratt and Andersson, 2008). Considering the greater ease of use, higher expression levels of CYP3A4 and CYP2C9, improved extraction of RNA and protein, and consistent conduct of functional studies, the 2D monolayer format appears to be more suitable. The utilisation of a complex model such as 3D spheroids seems unnecessary at present. However, if the 3D spheroid model is to be employed in future studies, further optimisation research will be required to address the observed discrepancies and enhance its applicability.

The impact of hypoxia on the CYP3A4 and CYP2C9 isoenzymes was further investigated in this thesis. In **Chapter 4**, utilising the HepaRG 2D monolayer as the experimental model, we demonstrated that acute hypoxia exposure (1% O<sub>2</sub> for 24 h) led to a repression of both gene and protein expressions, as well as functional activity, of CYP3A4 and CYP2C9. Remarkably, this repression in functional activity and gene expression was evident as early as 4 h following the onset of hypoxia exposure. These findings align with the observations made by Legendre *et al.*, who reported a suppression of several phase I metabolic enzymes, including CYP3A4 and CYP2C9, at the mRNA and protein levels in HepaRG monolayer cultures exposed to 1% O<sub>2</sub> for 24 h (Legendre *et al.*, 2009).

While the clinical trial could not proceed a Monte Carlo PK-PD simulation was employed (**Chapter 5**) to model the probability of various outcomes based on available literature data on the PK properties of sildenafil and experimental data regarding the potential effects of hypoxia on the function of CYP3A4 and CYP2C9 enzymes. By integrating this information into the simulation model, it was possible to explore potential scenarios and estimate the likelihood of different outcomes under hypoxic conditions. The utilisation of PK simulation provides valuable insights into the expected outcomes under different circumstances. These insights, combined with the probability outcomes generated through the Monte Carlo simulation approach, will contribute to the refinement of the trial design for the future resumption of the sildenafil PK-PD clinical trial. This adaptive approach allows for the optimisation of trial

## Chapter 7

parameters and decision-making in light of the observed effects of hypoxia on drug metabolism, despite the absence of direct clinical data obtained from the planned trial.

To feed into the simulation (i.e. hepatic  $CL_{int}$ ) the impact of effects of acute hypoxia (1%  $O_2$  for 24 h) on the functional activity of CYP3A4 and CYP2C9 enzymes was evaluated using our in-vitro hepatocyte model, HepaRG cells. The results revealed a significant reduction of 18% and 75% in the functional activity of CYP3A4 and CYP2C9, respectively, under hypoxic conditions. This finding indicates that acute hypoxia has a suppressive effect on the metabolic activity of these important drug-metabolising enzymes. Moreover, we aimed to assess the impact of hypoxia on the pharmacokinetics (PK) of sildenafil, a model drug used in this study. Through careful estimation, we observed that acute hypoxia resulted in notable changes in the PK parameters of sildenafil. The total clearance (CL) and hepatic intrinsic clearance ( $CL_{int}$ ) of sildenafil were decreased by 17% and 29%, respectively, under hypoxic conditions. Additionally, the total bioavailability of the drug was found to increase by 12% during acute hypoxia.

The Monte Carlo simulations involved 1,000 'subjects'. Notably, our findings revealed that acute hypoxia had a significant impact on the PK of sildenafil. Compared to the normoxia control simulations, the hypoxia simulations exhibited increased values for key PK parameters, including area under the concentration-time curve (AUC) above the half-maximal inhibitory concentration ( $IC_{50}$ ), maximum concentration ( $C_{max}$ ), and half-life ( $t_{1/2}$ ). These changes in PK parameters were also reflected alterations in the simulated pharmacological effects of sildenafil, as indicated by the increased area under the effect-time curve AUC above the half-maximal effective concentration ( $EC_{50}$ ). The decreased hepatic clearance ( $CL_{int}$ ) under hypoxic conditions was identified as a crucial factor influencing the PK/pharmacodynamic (PD) relationship of sildenafil.

In an alternative simulation scenarios, the combined effects were investigated of reduced hepatic clearance ( $CL_{int}$ ) and changes in hepatic portal vein blood flow under hypoxic conditions. The results demonstrated that changes in blood flow had minimal impact on the overall pharmacokinetics of sildenafil. However, the simulations revealed that hypoxia primarily affected the PK parameters of sildenafil through the reduction of hepatic  $CL_{int}$ , resulting in decreased total clearance (CL) and increased drug bioavailability. Based on these simulation findings, it can be inferred that dosage adjustments may be necessary for adults with hypoxaemia, particularly when administering medications with a narrow therapeutic window.

## Chapter 7

These adjustments would ensure the maintenance of therapeutic efficacy while minimising the potential risks of drug toxicity. Additionally, our study provides valuable insights for future clinical trials involving sildenafil under hypoxic conditions, which can aid in the design of optimized protocols to account for the influence of hypoxia on drug pharmacokinetics and pharmacodynamics.

It is important to note that there is currently no research available on the effects of hypoxia specifically on the PK of sildenafil in human subjects. However, a recent animal study conducted on rats exposed to an altitude of 4300 m for 24 h demonstrated significant changes in the PK profile of sildenafil. The study reported a 213% increase in the area under the concentration-time curve ( $AUC_{0-24}$ ), a 44.27% increase in half-life ( $t_{1/2}$ ), and a 133.67% increase in maximum concentration ( $C_{max}$ ). Additionally, the clearance (CL) and apparent volume of distribution ( $V_d$ ) decreased by 69.13% and 46.75%, respectively (Zhang and Wang, 2022). The authors of this study attributed the observed changes in sildenafil PK to a decrease in the levels of CYP3A4 protein. While the animal study provides valuable insights into the potential impact of hypoxia on sildenafil PK, further research is required to validate these findings in humans. Conducting controlled studies involving human subjects exposed to hypoxic conditions would provide more accurate and clinically relevant information regarding the PK alterations of sildenafil.

In **Chapter 6**, we investigated the mechanisms that may underpin the hypoxia-induced downregulation of CYP3A4 and CYP2C9 isoenzymes. Various mechanism pathways were studied focusing on ROS, cytokines and nuclear receptors PXR. We showed that hypoxia exposure (1%  $O_2$  for 24 h or 48 h) upregulated cytokine gene expression (IL-6 and TNF- $\alpha$ ) to higher extent in HepaRG cells. Treating the cells with these cytokines resulted in repression in CYP3A4 and CYP2C9 gene and protein expression, indicating a potential regulatory role of IL-6 and TNF- $\alpha$  in modulating CYP450 enzymes under hypoxic conditions. These findings align with previous in vitro studies that demonstrated a similar effect on gene expression and enzyme activities in HepaRG cells exposed to IL-6 or TNF- $\alpha$  (Klein *et al.*, 2015; Febvre-James *et al.*, 2018).

Moreover, the assessment of reactive oxygen species (ROS) revealed disparate outcomes. Specifically, our results demonstrated an elevation in mitochondrial superoxide generation, primarily derived from the electron transport chain reaction, under hypoxic conditions. Conversely, reactive oxygen radicals (other than superoxide) originating from various

## Chapter 7

molecular sources such as NADPH oxidase in the plasma membrane, endoplasmic reticulum, and peroxisomes, exhibited a reduction in ROS generation during hypoxia. These findings are consistent with the research conducted by Zhou *et al.*, who observed an increase in mitochondrial superoxide generation in myoblast cells exposed to 1% O<sub>2</sub>, as detected by the MitoSOX red assay (Zhou *et al.*, 2019). Additionally, studies have demonstrated that endothelial cell plasma membranes produce less extracellular H<sub>2</sub>O<sub>2</sub> under hypoxic conditions compared to normoxic conditions (Zulueta *et al.*, 1995; López-Barneo, Pardal and Ortega-Sáenz, 2001).

We demonstrated that ROS may play a role in the regulation of CYP3A4 and CYP2C9 under hypoxia. With the induction of superoxide through menadione treatment the functional activity, gene expression, and protein expression of CYP3A4 and CYP2C9 were suppressed. Conversely, the utilisation of Tiron, a known superoxide scavenger, exerts a protective effect on these isoenzymes. Specifically, under hypoxic conditions, treatment with Tiron leads to a dose-dependent upregulation of the functional activity, gene expression, and protein expression of CYP3A4 and CYP2C9. However, under normoxic conditions, we observed a downregulation of CYP3A4 and CYP2C9 mRNA expression, as well as a decrease in the functional activity of CYP3A4 following Tiron treatment. These observations highlight the importance of maintaining ROS levels within a normal range for proper cell signaling and regulation of CYP expression. Any disruption in ROS homeostasis, whether it be an increase during hypoxia-induced oxidative stress or a decrease below the normal level resulting in reductive stress, may have deleterious effects on the activity and expression of CYP3A4 and CYP2C9 isoenzymes. Thus, maintaining the delicate balance of ROS is crucial for preserving the functional integrity of these important drug-metabolising enzymes.

In light of the observed decrease in functional activity of CYP3A4 and CYP2C9 under hypoxic conditions, an important question arises regarding the potential signaling pathway through which hypoxia negatively regulates these enzymes. We propose a hypothesis that hypoxia, along with the release of cytokines and reactive oxygen species (ROS), activates the MEK/ERK pathway, leading to the phosphorylation of nuclear receptors known as pregnane X receptors (PXR). Phosphorylation of PXR inhibits its translocation into the nucleus and binding to DNA response elements, resulting in downregulation of CYP3A4 and CYP2C9 expression.

## Chapter 7

We investigated the mRNA and protein expression of PXR under hypoxic conditions, as well as with the treatment of IL-6 or TNF- $\alpha$ , two pro-inflammatory cytokines commonly released under hypoxic conditions. Our findings revealed a decrease in the expression of PXR at both the mRNA and protein levels in response to hypoxia and cytokine treatment. The downregulation of PXR expression is a significant finding considering that CYP3A4 and CYP2C9 are target genes of PXR, as evidenced by the enhancement of their mRNA levels and functional activity following treatment with the PXR inducer rifampicin. These observations strongly suggest a potential connection between hypoxia, nuclear receptors (such as PXR), and the regulation of CYP450 enzymes.

Previous research by Lichti-Kaiser *et al.* conducted an in-silico study of consensus phosphorylation sites for common protein kinases and identified human PXR as a target for direct phosphorylation by a MAPK (Lichti-Kaiser *et al.*, 2009). However, direct phosphorylation of PXR has been reported to negatively affect its transcriptional activity by altering its subcellular localisation or disrupting its interaction with corepressors or coactivators (Wang *et al.*, 2012). Building upon this knowledge, we hypothesise that the MAPK/ERK signaling pathway may play a role in the downregulation of PXR under hypoxic conditions, subsequently leading to the suppression of CYP3A4 and CYP2C9. To test this hypothesis, we initially examined the expression of ERK1/2 proteins under acute hypoxia and observed a slight increase in their expression. Subsequently, we treated HepaRG cells, our hepatocyte model, with MAPK/ERK inhibitors PD98059 and observed an upregulation of PXR protein. Furthermore, treating HepaRG cells with PD98059 under hypoxic conditions resulted in an increase in CYP3A4 and CYP2C9 protein expression, suggesting that the ERK pathway may play a role in CYP450 regulation via PXR. These results provide support for our hypothesis and indicate the existence of a connection between hypoxia, the MEK/ERK pathway, PXR, and the downregulation of CYP3A4 and CYP2C9.

**In summary**, our findings have several important implications:

- Acute hypoxaemia can potentially impair the clearance (CL) of drugs metabolised by CYP3A4 and CYP2C9. Therefore, drugs used in patients with hypoxaemia to treat high-altitude illness or manage cardiopulmonary diseases may require closer monitoring or dose adjustment to maintain therapeutic efficacy and prevent potential toxicity.

## Chapter 7

- The HepaRG cell line serves as a promising in-vitro model for studying drug metabolism, and our study highlights the negative regulation of CYP3A4 and CYP2C9 under acute hypoxia conditions. This model can be useful in elucidating the underlying mechanisms of drug metabolism modulation in hypoxic conditions.
- Hypoxia promotes the release of inflammatory mediators such as TNF- $\alpha$  and IL-6, as well as reactive oxygen species (ROS), which may play a negative role in the regulation of CYP3A4 and CYP2C9 under hypoxic conditions. These factors could potentially contribute to the observed downregulation of these enzymes.
- Antioxidants such as N-acetylcysteine (NAC) and Tiron may have a protective effect on CYP3A4 and CYP2C9 enzymes under hypoxia. Therefore, the supplementation of antioxidants in hypoxaemic conditions may help mitigate the decrease in intrinsic clearance observed under hypoxia.
- Our research suggests a potential involvement of the MAPK/ERK signaling pathway in the downregulation of CYP3A4 and CYP2C9 under hypoxia. This pathway, along with the phosphorylation of nuclear receptor PXR, appears to be linked to the regulation of these enzymes. Further investigation of this signaling pathway may provide valuable insights into the mechanisms underlying the hypoxia-mediated modulation of drug metabolism.

### **Future work:**

While the simulation work presented in this thesis has provided valuable insights into the effect of hypoxia on the pharmacokinetics of sildenafil, further research is needed to validate these findings in clinical practice. Conducting a large-scale randomized controlled trial in humans is crucial to assess the real-world implications of our simulation results. Sildenafil can serve as an excellent model drug for investigation in this clinical trial. Additionally, it is important to extend the pharmacokinetic research to other commonly used drugs for treating or preventing high-altitude illness, including calcium channel blockers (such as nifedipine and flunarizine), steroids (such as budesonide and dexamethasone), and medications commonly prescribed for pre-existing cardiovascular and pulmonary diseases, such as antiplatelets, statins, and beta-blockers.

In the clinical trial, it is essential to measure the fractional unbound levels of drugs under hypoxaemia, especially for drugs that exhibit high plasma protein binding. This is particularly relevant considering the observed increase in plasma protein levels under hypobaric



## Chapter 7

hypoxaemia. Methods such as equilibrium dialysis, ultrafiltration, or ultracentrifugation can be employed for plasma fractionation. Furthermore, assessing the generation of cytokines (using ELISA tests), reactive oxygen species (ROS) (using electron paramagnetic resonance), and nitric oxide (using ozone-based chemiluminescence) in the blood of participants exposed to hypoxia will provide insights into the stressors altered by hypoxia and their potential impact on the pharmacokinetics and pharmacodynamics of drugs.

To fully comprehend the mechanism underlying the downregulation of CYP3A4 and CYP2C9 under hypoxia, additional studies are warranted. While the role of PXR in the regulation of these enzymes under hypoxia has been highlighted in **Chapter 6**, further investigation is required to explore other potential signaling pathways, such as the HIF-1 $\alpha$  pathway and the NF-kB pathway (as depicted in **Figure 7.1**). Moreover, it is important to evaluate the effects of the downregulation of nuclear receptors on drug transporters or phase 2 drug-metabolising enzymes to gain a comprehensive understanding of how hypoxia impacts drug clearance. These additional studies will provide valuable insights into the intricate mechanisms through which hypoxia influences drug metabolism and clearance.

By undertaking these future research endeavors, we can further enhance our understanding of the impact of hypoxia on drug pharmacokinetics and develop more precise guidelines for drug dosing and management in hypoxaemic patients. Ultimately, this knowledge will contribute to the advancement of personalized medicine and optimize therapeutic outcomes for individuals facing hypoxaemia-related conditions.

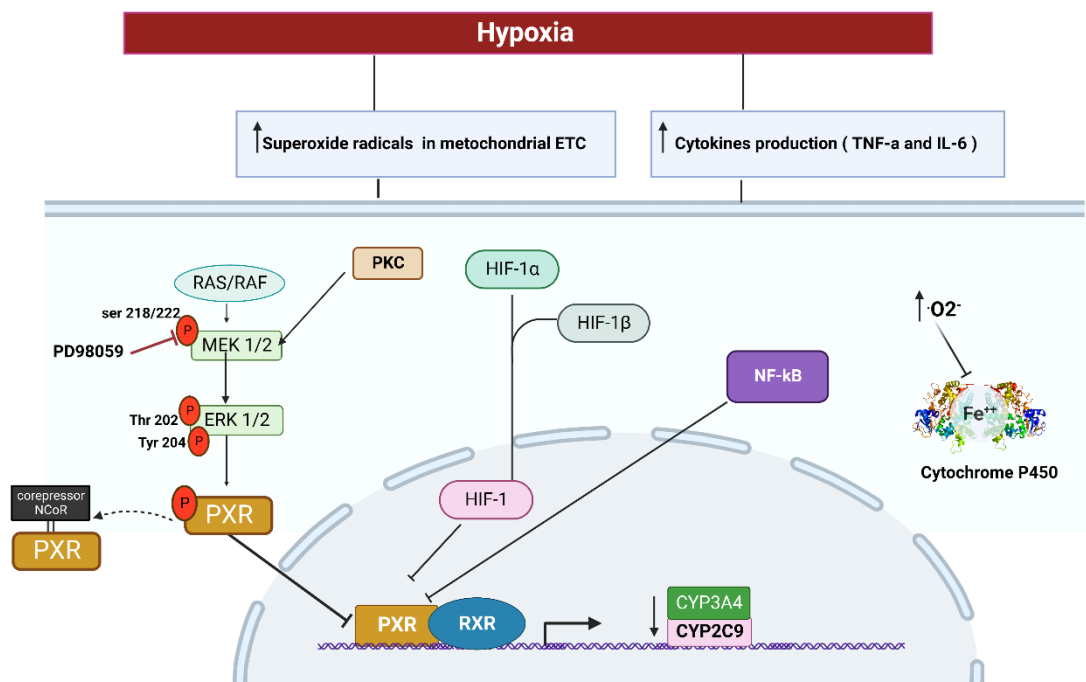


**Figure 7.1 Possible signaling pathways that downregulate CYP3A4 and CYP2C9 under hypoxia.** Hypoxia triggers the generation of stressors, including superoxide radicals from the mitochondrial electron transport chain, as well as the production of cytokines such as TNF- $\alpha$  and IL-6. Low oxygen levels and increased redox production contribute to the stabilisation and activation of nuclear transcription factors, such as HIF-1 $\alpha$ . HIF-1 $\alpha$  forms a heterodimer with HIF-1 $\beta$  and translocate into the nucleus, leading to the downregulation of PXR and subsequently CYP3A4 and CYP2C9. Another potential mechanism involves the activation of nuclear receptors NF- $\kappa$ B, which promotes cytokine production and modulates PXR nuclear receptors by interfering with PXR-RXR interaction. Additionally, increased production of superoxide radicals under hypoxia can directly affect CYP450 isoforms, impairing enzyme function and causing RNA and protein damage. Hypoxia-induced reduction in cellular antioxidants, such as glutathione, along with elevated lipid peroxidation end-products, can result from the formation of reactive oxygen intermediates (ROI) like superoxide anion and H<sub>2</sub>O<sub>2</sub> in the liver. ROI may bind to the iron (Fe<sup>2+</sup>) associated with CYP enzymes, leading to haem destruction and inactivation of CYP enzymes. Furthermore, hypoxia and ROS can activate PKC, which subsequently phosphorylates the MAPK pathway and nuclear receptors PXR. This phosphorylation promotes the binding of PXR to corepressors, limiting its translocation into the nucleus.

## References:

- Aaronson, P.I. *et al.* (2006) 'Hypoxic pulmonary vasoconstriction: mechanisms and controversies', *J Physiol*, 570(1), pp. 53–58.
- Abdel-Magied, N. *et al.* (2019) 'Modulating effect of tiron on the capability of mitochondrial oxidative phosphorylation in the brain of rats exposed to radiation or manganese toxicity', *Environmental Science and Pollution Research*, 26, pp. 12550–12562.
- Adak, A. *et al.* (2013) 'Dynamics of predominant microbiota in the human gastrointestinal tract and change in luminal enzymes and immunoglobulin profile during high-altitude adaptation', *Folia Microbiologica*, 58(6), pp. 523–528.
- Agnihotri, S.N. *et al.* (1978) 'Chronic pulmonary disease and antipyrine disposition', *British journal of clinical pharmacology*, 5(3), pp. 275–277.
- Ainslie *et al.* (2014) 'Cerebral Blood Flow at High Altitude', *High altitude medicine & biology*, 15(2), pp. 133–140.
- Ainslie, P.N. and Subudhi, A.W. (2014) 'Cerebral blood flow at high altitude', *High Altitude Medicine & Biology*, 15(2), pp. 133–140.
- Aitken, A.E. and Morgan, E.T. (2008) 'Gene-Specific Effects of Inflammatory Cytokines on Cytochrome P450C, 2B6 and 3A4 mRNA Levels in Human Hepatocytes', *Drug Metab Dispos*, 35(9), pp. 1687–1693.
- Albertolle, M.E. *et al.* (2018) 'Sulfenylation of human liver and kidney microsomal cytochromes P450 and other drug-metabolizing enzymes as a response to redox alteration', *Molecular and Cellular Proteomics*, 17(5), pp. 889–900.
- Alessi, D.R. *et al.* (1995) 'PD 098059 is a specific inhibitor of the activation of mitogen-activated protein kinase kinase in vitro and in vivo', *Journal of Biological Chemistry*, 270(46), pp. 27489–27494.
- Alvarez, S. *et al.* (2003) 'Oxygen dependence of mitochondrial nitric oxide synthase activity', *Biochemical and Biophysical Research Communications*, 305(3), pp. 771–775.
- Ambler, D.R. *et al.* (2012) 'Effects of hypoxia on the expression of inflammatory markers IL-6 and TNF- $\alpha$  in human normal peritoneal and adhesion fibroblasts', *Systems Biology in Reproductive Medicine*, 58(6), pp. 324–329.

- Andersson, T.B. (2017) ‘Evolution of novel 3D culture systems for studies of human liver function and assessments of the hepatotoxicity of drugs and drug candidates’, *Basic and Clinical Pharmacology and Toxicology*, 121(4), pp. 234–238.
- Andrés, C.M.C. *et al.* (2022) ‘Chemistry of Hydrogen Peroxide Formation and Elimination in Mammalian Cells, and Its Role in Various Pathologies’, *Stresses*, 2(3), pp. 256–274.
- Aninat, C. *et al.* (2006) ‘Expression of cytochromes P450, conjugating enzymes and nuclear receptors in human hepatoma HepaRG cells’, *Drug Metabolism and Disposition*, 34(1), pp. 75–83.
- Anundi, I. and De Groot, H. (1989) ‘Hypoxic liver cell death: Critical PO<sub>2</sub> and dependence of viability on glycolysis’, *American Journal of Physiology - Gastrointestinal and Liver Physiology*, 257(1), pp. G59-64.
- Arancibia, A. *et al.* (2003) ‘Pharmacokinetics of lithium in healthy volunteers after exposure to high altitude.’, *International Journal of Clinical Pharmacology and Therapeutics*, 41(5), pp. 200–206
- Arancibia, A. *et al.* (2004) ‘Effects of high altitude exposure on the pharmacokinetics of furosemide in healthy volunteers .’, 42(6), pp. 1–2.
- Arancibia, A. *et al.* (2005) ‘Pharmacokinetics of prednisolone in man during acute and chronic exposure to high altitude .’, *Int J Clin Pharmacol Ther*, 43(2), pp. 1–2.
- Bailey, D.M. *et al.* (2019) ‘Exaggerated systemic oxidative-inflammatory-nitrosative stress in chronic mountain sickness is associated with cognitive decline and depression’, *Journal of Physiology*, 597(2), pp. 611–629.
- Bailey, D.M., Stacey, B.S. and Gumbleton, M. (2018) ‘A Systematic Review and Meta-Analysis Reveals Altered Drug Pharmacokinetics in Humans During Acute Exposure to Terrestrial High Altitude—Clinical Justification for Dose Adjustment?’, *High Altitude Medicine & Biology*, 19(2), pp. 141–148.
- Baran, I. *et al.* (2010) ‘Effects of Menadione, Hydrogen Peroxide, and Quercetin on Apoptosis and Delayed Luminescence of Human Leukemia Jurkat T-Cells’, *Cell Biochemistry and Biophysics*, 58(3), pp. 169–179.
- Bartsch, P. *et al.* (1991) ‘Prevention of high-altitude pulmonary edema by nifedipine’, *N Engl J Med*, 325(18), pp. 1284–1289.

- Belda, F.J., Soro, M. and Ferrando, C. (2013) 'Trends in Anaesthesia and Critical Care Pathophysiology of respiratory failure', *Trends in Anaesthesia and Critical Care*, 3(5), pp. 265–269.
- Bentires-Alj, M. *et al.* (2003) 'NF- $\kappa$ B transcription factor induces drug resistance through MDR1 expression in cancer cells', *Oncogene*, 22(1), pp. 90–97.
- Berger, E.Y. *et al.* (1949) 'The effect of anoxic anoxia on the human kidney.', *The Journal of clinical investigation*, 28(4), pp. 648–652.
- Berger Fridman, I. *et al.* (2021) 'High throughput microfluidic system with multiple oxygen levels for the study of hypoxia in tumor spheroids', *Biofabrication*, 13(3), pp. 3–17.
- Berthiaume, F. *et al.* (1996) 'Effect of extracellular matrix topology on cell structure, function, and physiological responsiveness: Hepatocytes cultured in a sandwich configuration', *FASEB Journal*, 10(13), pp. 1471–1484.
- Bhagatte, Y., Lodwick, D. and Storey, N. (2012) 'Mitochondrial ROS production and subsequent ERK phosphorylation are necessary for temperature preconditioning of isolated ventricular myocytes', *Cell Death and Disease*, 3(7), pp. 1–11.
- Bhogal, R.H. *et al.* (2011) 'Variable responses of small and large human hepatocytes to hypoxia and hypoxia/reoxygenation (H-R)', *FEBS Letters*, 585(6), pp. 935–941.
- Bienert, G.P., Schjoerring, J.K. and Jahn, T.P. (2006) 'Membrane transport of hydrogen peroxide', *Biochimica et Biophysica Acta*, 1758(8), pp. 994–1003.
- Bischoff, E. (2004) 'Potency, selectivity, and consequences of nonselectivity of PDE inhibition', *International Journal of Impotence Research*, 16(1), pp. S11–S14.
- Boolell, M. *et al.* (1996) 'Sildenafil: an orally active type 5 cyclic GMP-specific phosphodiesterase inhibitor for the treatment of penile erectile dysfunction', *Int J Impot Res*, (2), pp. 47–52.
- Boyer, S.J. and Blume, F.D. (1984) 'Weight loss and changes in body composition at high altitude', *J Appl Physiol Respir Environ Exerc Physiol*, 57:(5), pp. 1580–1585.
- Bradley, J.S. *et al.* (2010) 'Pharmacokinetics, pharmacodynamics, and Monte Carlo simulation: Selecting the best antimicrobial dose to treat an infection', *Pediatric Infectious Disease Journal*, 29(11), pp. 1043–1046.

- Braicu, C. *et al.* (2019) 'A comprehensive review on MAPK: A promising therapeutic target in cancer', *Cancers*, 11(10), pp. 1–25.
- Brandon, E.F.A. *et al.* (2003) 'An update on in vitro test methods in human hepatic drug biotransformation research: Pros and cons', *Toxicology and Applied Pharmacology*, 189(3), pp. 233–246.
- Brandon, E.F.A. *et al.* (2006) 'Validation of in vitro cell models used in drug metabolism and transport studies; Genotyping of cytochrome P450, phase II enzymes and drug transporter polymorphisms in the human hepatoma (HepG2), ovarian carcinoma (IGROV-1) and colon carcinoma (CaCo-2, LS)', *Toxicology and Applied Pharmacology*, 211(1), pp. 1–10.
- Brugniaux, J.V. *et al.* (2007) 'Cerebrovascular responses to altitude', *respiratory physiology & neurobiology*, 158(2–3), pp. 212–223.
- Bulua, A.C. *et al.* (2011) 'Mitochondrial reactive oxygen species promote production of proinflammatory cytokines and are elevated in TNFR1-associated periodic syndrome (TRAPS)', *Journal of Experimental Medicine*, 208(3), pp. 519–533.
- Cadenas, E. and Davies, K.J.A. (2000) 'Mitochondrial free radical generation, oxidative stress, and aging', *Free radical biology and medicine*, 29(3–4), pp. 222–230.
- Cao, R. *et al.* (2014) 'Hypoxia induces dysregulation of lipid metabolism in HepG2 cells via activation of HIF-2 $\alpha$ ', *Cellular Physiology and Biochemistry*, 34(5), pp. 1427–1441.
- Chan, L.M.S., Lowes, S. and Hirst, B.H. (2004) 'The ABCs of drug transport in intestine and liver: Efflux proteins limiting drug absorption and bioavailability', *European Journal of Pharmaceutical Sciences*, 21(1), pp. 25–51.
- Chan, W.K. *et al.* (1999) 'Cross-talk between the Aryl Hydrocarbon Receptor and Hypoxia Inducible Factor Signaling Pathways', *THE JOURNAL OF BIOLOGICAL CHEMISTRY*, 274(17), pp. 12115–12123.
- Chance, B. and Williams, G.R. (1956) 'The respiratory chain and oxidative phosphorylation', *Advances in Enzymology and Related Areas of Molecular Biology*, 17, pp. 65–134.
- Chandel, N. *et al.* (1998) 'Mitochondrial reactive oxygen species trigger hypoxia-induced transcription', *Proceedings of the National Academy of Sciences of the United States of America*, 95, pp. 11715–11720.

- Chandel, N.S. *et al.* (2000) 'Reactive oxygen species generated at mitochondrial Complex III stabilize hypoxia-inducible factor-1 $\alpha$  during hypoxia: A mechanism of O<sub>2</sub> sensing', *Journal of Biological Chemistry*, 275(33), pp. 25130–25138.
- Chang, G.W.M. and Kam, P.C.A. (1999) 'The physiological and pharmacological roles of cytochrome P450 isoenzymes', *Anaesthesia*, 54(1), pp. 42–50.
- Cheitlin, M.D. *et al.* (1999) 'ACC / AHA expert consensus document use of sildenafil (viagra) in patients with cardiovascular disease writing group members', *J Am Coll Cardiol*, 33, pp. 273–282.
- Chelombitko, M.A. (2018) 'Role of Reactive Oxygen Species in Inflammation: A Minireview', *Moscow University Biological Sciences Bulletin*. Pleiades Publishing, pp. 199–202.
- Chen, Y. *et al.* (2004) 'Induction of human CYP2C9 by rifampicin, hyperforin, and phenobarbital is mediated by the pregnane x receptor', *Journal of Pharmacology and Experimental Therapeutics*, 308(2), pp. 495–501.
- Chenna, S. *et al.* (2022) 'Mechanisms and mathematical modeling of ROS production by the mitochondrial electron transport chain', *American Journal of Physiology - Cell Physiology*, 323(1), pp. C69–C83.
- Chesner, I.M., Small, N.A. and Dykes, P.W. (1987) 'Intestinal absorption at high altitude', *Postgraduate Medical Journal*, 63, pp. 173–175.
- Cho, K., Seo, J. and Kim, J. (2011) 'Bioactive Lipxygenase Metabolites Stimulation of NADPH Oxidases and Reactive Oxygen Species', *Molecules and Cells*, 32(1), pp. 1–5.
- Cichoż-lach, H. and Michalak, A. (2014) 'Oxidative stress as a crucial factor in liver diseases', *World J Gastroenterol*, 20(25), pp. 8082–8091.
- Cokic, B.B.B. *et al.* (2014) 'Nitric oxide and hypoxia stimulate erythropoietin receptor via MAPK kinase in endothelial cells', *Microvascular Research*, 92, pp. 34–40.
- Coles, L.C. and Shaw, P.E. (2002) 'PAK1 primes MEK1 for phosphorylation by Raf-1 kinase during cross-cascade activation of the ERK pathway', *Oncogene*, 21, pp. 2236–2244.
- Collins, D.W. and Shehabi, Y. (2012) 'Arterial hypoxemia', in J.-L. Vincent and J.B. Hall (eds) *Encyclopedia of Intensive Care Medicine*. Berlin, Heidelberg: Springer Berlin Heidelberg, pp. 257–266.

- Comerford, K.M., Cummins, E.P. and Taylor, C.T. (2004) 'c-Jun NH<sub>2</sub>-terminal kinase activation contributes to hypoxia-inducible factor 1 $\alpha$ -dependent P-glycoprotein expression in hypoxia', *Cancer Research*, 64(24), pp. 9057–9061.
- Corbin, J.D., Francis, S.H. and Webb, D.J. (2002) 'Phosphodiesterase type 5 as a pharmacologic target in erectile dysfunction', *Urology*, 60(02), pp. 4–11.
- Corbett, J. L., and Duncan, S. A. (2019) 'iPSC-Derived Hepatocytes as a Platform for Disease Modeling and Drug Discovery' *Frontiers in Medicine*, 6(265), pp.1–12.
- Cotgreave, I.A. (1996) 'N-acetylcysteine: pharmacological considerations and experimental and clinical applications.', *Advances in pharmacology*, 38, pp. 205–227.
- Criddle, D.N. *et al.* (2006) 'Menadione-induced reactive oxygen species generation via redox cycling promotes apoptosis of murine pancreatic acinar cells', *Journal of Biological Chemistry*, 281(52), pp. 40485–40492.
- Cui, H. *et al.* (2016) 'In Vivo And In Vitro Study On Drug-drug Interaction Of Lovastatin And Berberine From Pharmacokinetic And Hepg2 Cell Metabolism Studies', *Molecules*, 21(4), pp. 1–12.
- Cumming, J.F. (1976) 'The effect of arterial oxygen tension on antipyrine half-time in plasma', *Clinical Pharmacology & Therapeutics*, 19(4), pp. 468–471.
- Curry, S.H. and Whelpton, R. (2010) *Drug Disposition and Pharmacokinetics: From Principles to Applications*, John Wiley & Sons, Ltd.
- Cusack, B.J. *et al.* (1986) 'Theophylline clearance in patients with severe chronic obstructive pulmonary disease receiving supplemental oxygen and the effect of acute hypoxemia', *American Review of Respiratory Disease*, 133(6), pp. 1110–1114.
- Dame, K., and Ribeiro, A. J. S. (2021) 'Microengineered systems with iPSC-derived cardiac and hepatic cells to evaluate drug adverse effects', *Experimental Biology and Medicine*, 246(3), pp. 317–331.
- Darnaud, L. *et al.* (2023) 'Phenotyping Indices of CYP450 and P-Glycoprotein in Human Volunteers and in Patients Treated with Painkillers or Psychotropic Drugs', *Pharmaceutics*, 15(3), pp. 1–25.



- Davies, B. and Morris, T. (1993) 'Physiological parameters in laboratory animals and humans', *Pharmaceutical Research*, pp. 1093–1095.
- Dempsey, J.A. and Forster, H.V. (1982) 'Mediation of ventilatory adaptations', *Physiological Reviews*, 62(1), pp. 262–346.
- Deng, L. *et al.* (2001) '2-acetylaminofluorene up-regulates rat mdr1b expression through generating reactive oxygen species that activate NF- $\kappa$ B pathway', *Journal of Biological Chemistry*, 276(1), pp. 413–420.
- D'ignazio, L. and Rocha, S. (2016) 'Hypoxia induced NF- $\kappa$ B', *Cells*, 5(1), pp. 2–8.
- Doerge, K. *et al.* (2005) 'Inhibition of mitochondrial respiration elevates oxygen concentration but leaves regulation of hypoxia-inducible factor (HIF) intact', *Blood*, 106(7), pp. 2311–2317.
- Donato, M.T. *et al.* (2008) 'Cell lines: a tool for in vitro drug metabolism studies.', *Current drug metabolism*, 9(1), pp. 1–11.
- Donato, M.T. and Castell, J. V (2003) 'Strategies and Molecular Probes to Investigate the Role of Cytochrome P450 in Drug Metabolism Focus On In Vitro Studies', *Clinical Pharmacokinetics*, 42(2), pp. 153–178.
- Donegani, E. *et al.* (2016) 'Drug use and misuse in the mountains: A UIAA MedCom consensus guide for medical professionals', *High Altitude Medicine & Biology*, 17(3), pp. 157–184.
- Drewitz, M. *et al.* (2011) 'Towards automated production and drug sensitivity testing using scaffold-free spherical tumor microtissues', *Biotechnology Journal*, 6(12), pp. 1488–1496.
- Drocourt, L. *et al.* (2002) 'Expression of CYP3A4, CYP2B6, and CYP2C9 is regulated by the vitamin D receptor pathway in primary human hepatocytes', *Journal of Biological Chemistry*, 277(28), pp. 25125–25132.
- Duan, Y. Bin *et al.* (2020) 'Regulation of High-Altitude Hypoxia on the Transcription of CYP450 and UGT1A1 Mediated by PXR and CAR', *Frontiers in Pharmacology*, 11(September), pp. 1–16.
- Dubey, K.D. and Shaik, S. (2019) 'Cytochrome P450 the wonderful nanomachine revealed through dynamic simulations of the catalytic cycle', *Accounts of Chemical Research Sason*, 52(2), pp. 389–399.

- Elizondo, G. and Medina-Díaz, I.M. (2003) 'Induction of CYP3A4 by 1 $\alpha$ ,25-dihydroxyvitamin D3 in HepG2 cells', *Life Sciences*, 73(2), pp. 141–149.
- Engelhardt, S., Patkar, S. and Ogunshola, O.O. (2014) 'Cell-specific blood-brain barrier regulation in health and disease: A focus on hypoxia', *British Journal of Pharmacology*, 171(5), pp. 1210–1230.
- Ertel, W. *et al.* (1995) 'Hypoxemia in the absence of blood loss or significant hypotension causes inflammatory cytokine release', *American Journal of Physiology - Regulatory Integrative and Comparative Physiology*, 269(1), pp. R160–R166.
- Eytan, G.D. *et al.* (1997) 'Efficiency of P-glycoprotein-mediated exclusion of rhodamine dyes from multidrug-resistant cells is determined by their passive transmembrane movement rate', *European Journal of Biochemistry*, 248(1), pp. 104–112.
- Fall, L. *et al.* (2018) 'Redox-regulation of haemostasis in hypoxic exercising humans: a randomised double-blind placebo-controlled antioxidant study', *Journal of Physiology*, 596(20), pp. 4879–4891.
- Fandrey, J., Frede, S. and Jelkmann, W. (1994) 'Role of hydrogen peroxide in hypoxia-induced erythropoietin production', *Biochemical Journal*, 303(2), pp. 507–510.
- Febvre-James, M. *et al.* (2018) 'The jak1/2 inhibitor ruxolitinib reverses interleukin-6-mediated suppression of drug-detoxifying proteins in cultured human hepatocytes', *Drug Metabolism and Disposition*, 46(2), pp. 131–140.
- Fiore, D.C., Hall, S. and Shoja, P. (2010) 'Altitude Illness: Risk Factors, Prevention, Presentation, and Treatment', *American family physician*, 82(9), pp. 1103–1110.
- Forrester, S.J., K.D.S. *et al.* (2018) 'Reactive Oxygen Species in Metabolic and Inflammatory Signaling', *Circulation research*, 122(6), pp. 877–902.
- Fradette, C. *et al.* (2002) 'Hypoxia-induced down-regulation of CYP1A1/1A2 and up-regulation of CYP3A6 involves serum mediators', *British Journal of Pharmacology*, 137(6), pp. 881–891.
- Fradette, C. *et al.* (2007a) 'Animal models of acute moderate hypoxia are associated with a down-regulation of CYP1A1, 1A2, 2B4, 2C5, and 2C16 and up-regulation of CYP3A6 and P-glycoprotein in liver', *Drug Metabolism and Disposition*, 35(5), pp. 765–771.

- Fradette, C. *et al.* (2007b) ‘Animal models of acute moderate hypoxia are associated with a down-regulation of CYP1A1, 1A2, 2B4, 2C5, and 2C16 and up-regulation of CYP3A6 and P-glycoprotein in liver’, *Drug Metabolism and Disposition*, 35(5), pp. 765–771.
- Fradette, C. and Souich, P. (2004) ‘Effect of Hypoxia on Cytochrome P450 Activity and Expression’, *Current Drug Metabolism*, 5(3), pp. 257–271.
- Fradette, C. and Du Souich, P. (2003) ‘Hypoxia-inducible factor-1 and activator protein-1 modulate the upregulation of CYP3A6 induced by hypoxia’, *British Journal of Pharmacology*, 140(6), pp. 1146–1154.
- Friedberg, T. *et al.* (1999) ‘Merits and limitations of recombinant models for the study of human P450-mediated drug metabolism and toxicity: An intralaboratory comparison’, *Drug Metabolism Reviews*, 31(2), pp. 523–544.
- Gameiro, M. *et al.* (2017) ‘Cellular models and in vitro assays for the screening of modulators of P-gp, MRP1 and BCRP’, *Molecules*, 22(4), pp. 4–6.
- Gandrud, C. (2013) *Reproducible research with R and R studio*, CRC Press.
- Gatti, M. and Pea, F. (2022) ‘The Cytokine Release Syndrome and/or the Proinflammatory Cytokines as Underlying Mechanisms of Downregulation of Drug Metabolism and Drug Transport: A Systematic Review of the Clinical Pharmacokinetics of Victim Drugs of this Drug–Disease Interaction Under Different Clinical Conditions’, *Clinical Pharmacokinetics*. Adis, pp. 1519–1544.
- Gaur, P. *et al.* (2021) ‘High-altitude hypoxia induced reactive oxygen species generation, signaling, and mitigation approaches’, *International Journal of Biometeorology*, 65(4), pp. 601–615.
- Ge, R. *et al.* (2006) ‘Urine acid-base compensation at simulated moderate altitude’, *High Alt Med Biol*, 7(1), pp. 64–71.
- Ghofrani, H.A. *et al.* (2004) ‘Sildenafil Increased Exercise Capacity during Hypoxia at Low Altitudes and at Mount Everest Base Camp’, *Annals of Internal Medicine*, 141(3), pp. 169–177.
- Gilbert, R. and Keighley, J. (1974) ‘The arterial-alveolar oxygen tension ratio. An index of gas exchange applicable to varying inspired oxygen concentrations.’, *American Review of Respiratory Disease*, 109(1), pp. 142–145.

- Girdwood, S.T. *et al.* (2022) ‘Population Pharmacokinetic Modeling of Total and Free Ceftriaxone in Critically Ill Children and Young Adults and Monte Carlo Simulations Support Twice Daily Dosing for Target Attainment’, *Antimicrobial Agents and Chemotherapy*, 66(1), pp. 1–17.
- Gledhill, N., Beirne, G.J. and Dempsey, J.A. (1975) ‘Renal response to short-term hypocapnia in man’, *Kidney International*, 8(6), pp. 376–384.
- Gola, S. *et al.* (2016) ‘Evaluation of hepatic metabolism and pharmacokinetics of ibuprofen in rats under chronic hypobaric hypoxia for targeted therapy at high altitude’, *Journal of Pharmaceutical and Biomedical Analysis*, 121, pp. 114–122.
- Goldenberg, M.M. (1998) ‘Safety and efficacy of sildenafil citrate in the treatment of male erectile dysfunction’, *Clinical therapeutics*, 20(6), pp. 1033–1048.
- Goldfarb-Rumyantzev, A.S. and Alper, S.L. (2014) ‘Short-term responses of the kidney to high altitude in mountain climbers’, *Nephrology Dialysis Transplantation*, 29(3), pp. 497–506.
- de Gonzalo-Calvo, D. *et al.* (2010) ‘Differential inflammatory responses in aging and disease: TNF- $\alpha$  and IL-6 as possible biomarkers’, *Free Radical Biology and Medicine*, 49(5), pp. 733–737.
- Gordan, J.D. *et al.* (2007) ‘HIF-2  $\alpha$  Promotes Hypoxic Cell Proliferation by Enhancing c-Myc Transcriptional Activity’, *Cancer Cell*, 11, pp. 335–347.
- Gorlach, A. and Bonello, S. (2008) ‘The cross-talk between NF- $\kappa$ B and HIF-1: further evidence for a significant’, *Biochem. J*, 412(3), pp. 17–19.
- Goutelle, S. *et al.* (2009) ‘Population modeling and Monte Carlo simulation study of the pharmacokinetics and antituberculosis pharmacodynamics of rifampin in lungs’, *Antimicrobial Agents and Chemotherapy*, 53(7), pp. 2974–2981.
- Granger, D.N. and Kvietys, P.R. (2004) ‘Circulation, Overview’, in *Encyclopedia of Gastroenterology*, pp. 351–355.
- Greenway, C. V and Stark, R.D. (1917) ‘Hepatic Vascular Bed’, *Physiological reviews*, 51(1), pp. 23–65.
- Gripon, P. *et al.* (2002) ‘Infection of a human hepatoma cell line by hepatitis B virus’, *Proceedings of the National Academy of Sciences*, 99(24), pp. 15655–15660.

- De Groot, H. *et al.* (1988) 'Lipid peroxidation and cell viability in isolated hepatocytes in a redesigned oxystat system: Evaluation of the hypothesis that lipid peroxidation, preferentially induced at low oxygen partial pressures, is decisive for CCl<sub>4</sub> liver cell injury', *Archives of Biochemistry and Biophysics*, 264(2), pp. 591–599.
- Gu, X. *et al.* (2006) 'Role of NF- $\kappa$ B in regulation of PXR-mediated gene expression: A mechanism for the suppression of cytochrome P-450 3A4 by proinflammatory agents', *Journal of Biological Chemistry*, 281(26), pp. 17882–17889.
- Guengerich, F.P. (1978) 'Destruction of Heme and Hemoproteins Mediated by Liver Microsomal Reduced Nicotinamide Adenine Dinucleotide Phosphate-Cytochrome P-450 Reductase', *Biochemistry*, 17(17), pp. 3633–3639.
- Guengerich, F.P. (2018) 'Mechanisms of Cytochrome P450-Catalyzed Oxidations', *ACS Catalysis*, 8(12), pp. 10964–10976.
- Guillouzo, A. *et al.* (2007) 'The human hepatoma HepaRG cells : A highly differentiated model for studies of liver metabolism and toxicity of xenobiotics', *Chemico-Biological Interactions*, 168, pp. 66–73.
- Gunness, P. *et al.* (2013) '3D organotypic cultures of human heparg cells: A tool for in vitro toxicity studies', *Toxicological Sciences*, 133(1), pp. 67–78.
- Guo, C.-H. and Che, P.-C. (2012) 'Mitochondrial Free Radicals, Antioxidants, Nutrient Substances, and Chronic Hepatitis C', in *Antioxidant Enzyme*. InTech, pp. 237–264.
- Guo, Y. *et al.* (2020) 'ERK/MAPK signalling pathway and tumorigenesis (Review)', *Experimental and Therapeutic Medicine*, 19(3), pp. 1997–2007.
- Gupta, M., Kovar, A. and Meibohm, B. (2005) 'The clinical pharmacokinetics of phosphodiesterase-5 inhibitors for erectile dysfunction', *Journal of Clinical Pharmacology*, 45(9), pp. 987–1003.
- Gutmann, H. *et al.* (1999) 'Evidence for Different ABC-Transporters in Caco-2 Cells Modulating Drug Uptake', *Pharmaceutical Research*, 103(3), pp. 239–248.
- Guzy, R.D. *et al.* (2005) 'Mitochondrial complex III is required for hypoxia-induced ROS production and cellular oxygen sensing', *Cell Metabolism*, 1(6), pp. 401–408.

- Haditsch, B. *et al.* (2007) 'Renal Adrenomedullin and High Altitude Diuresis', *Physiol. Res.*, 56, pp. 779–787.
- Han, D. *et al.* (2003) 'Voltage-dependent anion channels control the release of the superoxide anion from mitochondria to cytosol', *Journal of Biological Chemistry*, 278(8), pp. 5557–5563.
- Handschin, C. and Meyer, U.R.S.A. (2003) 'Induction of Drug Metabolism: The Role of Nuclear Receptors', *Pharmacological reviews*, 55(4), pp. 649–673.
- Hantzidiamantis, P. and Amaro, E. (2022) *Physiology, Alveolar to Arterial Oxygen Gradient, StatPearls*.
- Hartmann, G. *et al.* (2000) 'High altitude increases circulating interleukin-6, interleukin-1 receptor antagonist and c-reactive protein', *CYTOKINE*, 12(3), pp. 246–252.
- He, H. *et al.* (2016) 'Developmental regulation of CYP3A4 and CYP3A7 in Chinese Han population', *Drug Metabolism and Pharmacokinetics*, 31(6), pp. 433–444.
- Heinrich, E.C. *et al.* (2018) 'Increased Levels of Interleukin-6 (IL-6) in Andean Males with Chronic Mountain Sickness and Sea-Level Participants After One Day at High Altitude May Reflect Differences in IL-6 Regulation', *The FASEB Journal*, 32, pp. lb479–lb479.
- Hendriks, D.F.G. *et al.* (2020) 'Clinically Relevant Cytochrome P450 3A4 Induction Mechanisms and Drug Screening in Three-Dimensional Spheroid Cultures of Primary Human Hepatocytes', *Clinical Pharmacology and Therapeutics*, 108(4), pp. 844–855.
- Hernansanz-Agustín, P. *et al.* (2014) 'Acute hypoxia produces a superoxide burst in cells', *Free Radical Biology and Medicine*, 71, pp. 146–156.
- Hernansanz-Agustín, P. *et al.* (2017) 'Mitochondrial complex I deactivation is related to superoxide production in acute hypoxia', *Redox Biology*, 12, pp. 1040–1051.
- Hernansanz-Agustín, P. and Enríquez, J.A. (2021) 'Generation of reactive oxygen species by mitochondria', *Antioxidants*, 10(3), pp. 1–18.
- Higgins, P.J. and Borenfreund, E. (1980) 'Enhanced albumin production by malignantly transformed hepatocytes during in vitro exposure to dimethylsulfoxide', *Biochimica et Biophysica Acta (BBA)-Nucleic Acids and Protein Synthesis*, 610(1), pp. 174–180.

- Higuchi, Y. *et al.* (2016) 'Functional polymer-dependent 3D culture accelerates the differentiation of HepaRG cells into mature hepatocytes', *Hepatology Research*, 46(10), pp. 1045–1057.
- Hiratsuka, M. (2012) 'In vitro assessment of the allelic variants of cytochrome P450', *Drug Metabolism and Pharmacokinetics*, 27(1), pp. 68–84.
- Hori, Y., Shimizu, Y. and Aiba, T. (2018) 'Altered hepatic drug-metabolizing activity in rats suffering from hypoxemia with experimentally induced acute lung impairment', *Xenobiotica*, 48(6), pp. 576–583.
- Hrycay, E.G. and Bandiera, S.M. (2015) 'Involvement of Cytochrome P450 in Reactive Oxygen Species Formation and Cancer', *In Advances in Pharmacology*, 74, pp. 35–84.
- Hu, B.F., Bi, H.C. and Huang, M. (2011) 'Advances in the research of pregnane X receptor and constitutive androstane receptor', *Yao xue xue bao = Acta pharmaceutica Sinica*, 46(10), pp. 1173–1177.
- Hui, L. *et al.* (2016) 'Effects of high altitude exposure on physiology and pharmacokinetics.', *Current drug metabolism*, 17(6), pp. 559–65.
- Huss, J.M., Levy, F.H. and Kelly, D.P. (2001) 'Hypoxia inhibits the peroxisome proliferator-activated receptor  $\alpha$ /retinoid X receptor gene regulatory pathway in cardiac myocytes: A mechanism for O<sub>2</sub>-dependent modulation of mitochondrial fatty acid oxidation', *Journal of Biological Chemistry*, 276(29), pp. 27605–27612.
- Imoberdorf, R. *et al.* (2001) 'Enhanced synthesis of albumin and fibrinogen at high altitude', *Journal of Applied Physiology*, 90(2), pp. 528–537.
- Jacobs, R.A. *et al.* (2012) 'Red blood cell volume and the capacity for exercise at moderate to high altitude', *Sports Med*, 42(8), pp. 643–663.
- Jain, S. *et al.* (1980) 'Body fluid compartments in humans during acute high-altitude exposure', *Aviation, space, and environmental medicine*, 51(3), pp. 234–236.
- Jaki, T. and Wolfsegger, M.J. (2011) 'Estimation of pharmacokinetic parameters with the R package PK', *Pharmaceutical Statistics*, 10(3), pp. 284–288.
- Jalal, H. *et al.* (2017) 'An Overview of R in Health Decision Sciences', *Medical Decision Making*, 37(7), pp. 735–746.

- Jansen, G.F., Krins, A. and Basnyat, B. (1999) 'Cerebral vasomotor reactivity at high altitude in humans', *Journal of Applied Physiology*, 86(2), pp. 681–686.
- Jefferson, J.A. *et al.* (2004) 'Increased Oxidative Stress Following Acute and Chronic High Altitude Exposure', *High altitude medicine & biology*, 5(1), pp. 61–69.
- Jensen, J.B. *et al.* (1990) 'Cerebral blood flow in acute mountain sickness', *Journal of Applied Physiology*, 69(2), pp. 430–433.
- Jeong, H.J. *et al.* (2003) 'Expression of proinflammatory cytokines via HIF-1 $\alpha$  and NF- $\kappa$ B activation on desferrioxamine-stimulated HMC-1 cells', *Biochemical and Biophysical Research Communications*, 306(4), pp. 805–811.
- Jones, D.P. (1981) 'Hypoxia and drug metabolism', *Biochemical Pharmacology*, 30(10), pp. 1019–1023.
- Jones, N.M. and Bergeron, M. (2004) 'Hypoxia-induced ischemic tolerance in neonatal rat brain involves enhanced ERK1/2 signaling', *Journal of Neurochemistry*, 89(1), pp. 157–167.
- de Jong, L.M. *et al.* (2020) 'Distinct effects of inflammation on cytochrome P450 regulation and drug metabolism: Lessons from experimental models and a potential role for pharmacogenetics', *Genes*, 11(12), pp. 1–24.
- Jover, R. *et al.* (2002) 'Down-regulation of human CYP3A4 by the inflammatory signal interleukin-6: molecular mechanism and transcription factors involved.', *The FASEB journal : official publication of the Federation of American Societies for Experimental Biology*, 16(13), pp. 1799–1801.
- Jürgens, G. *et al.* (2002) 'Acute hypoxia and cytochrome P450-mediated hepatic drug metabolism in humans', *Clinical Pharmacology and Therapeutics*, 71(4), pp. 214–220.
- Kalson, Nicholas S *et al.* (2010) 'Do changes in gastro-intestinal blood flow explain high-altitude anorexia?', *Birmingham Medical Research Expeditionary S*, 40(8), pp. 735–741.
- Kalson, Nicholas S. *et al.* (2010) 'Do changes in gastro-intestinal blood flow explain high-altitude anorexia?', *European Journal of Clinical Investigation*, 40(8), pp. 735–741.
- Kamata, H. *et al.* (2005) 'Reactive oxygen species promote TNF $\alpha$ -induced death and sustained JNK activation by inhibiting MAP kinase phosphatases', *Cell*, 120(5), pp. 649–661.



- Kanebratt, K.P. and Andersson, T.B. (2008) 'Evaluation of HepaRG cells as an in vitro model for human drug metabolism studies', *Drug Metabolism and Disposition*, 36(7), pp. 1444–1452.
- Kaplan, S.A. *et al.* (1973) 'Pharmacokinetic profile of trimethoprim-sulfamethoxazole in man', *Journal of Infectious Diseases*, 128(3), pp. S547–S555.
- Karakurum, M. *et al.* (1994) 'Hypoxic induction of interleukin-8 gene expression in human endothelial cells', *Journal of Clinical Investigation*, 93(4), pp. 1564–1570.
- Kawana, K. *et al.* (2003) 'Molecular mechanism of nuclear translocation of an orphan nuclear receptor, SXR', *Molecular Pharmacology*, 63(3), pp. 524–531.
- Kayser, B. (1992) 'Nutrition and high altitude exposure', *International journal of sports medicine*, 13, pp. S129–S129.
- Kazuo, M. *et al.* (1984) 'Classification of drugs on the basis of bilirubin-displacing effect on human serum albumin', *Chemical and pharmaceutical bulletin*, 32(6), pp. 2414–2420.
- Ke, S. *et al.* (2001) 'Mechanism of Suppression of Cytochrome P-450 1A1 Expression by Tumor Necrosis Factor- $\alpha$  and Lipopolysaccharide', *Journal of Biological Chemistry*, 276(43), pp. 39638–39644.
- Kera, Yoshio *et al.* (1988) 'Glutathione replenishment capacity is lower in isolated perivenous than in periportal hepatocytes', *Biochem. J*, 254(2), pp. 411–417.
- Killilea, D.W. *et al.* (2000) 'Free radical production in hypoxic pulmonary artery smooth muscle cells', *American Journal of Physiology-Lung Cellular and Molecular Physiology*, 279(2), pp. 408–412.
- Kim, H., Seo, J.Y. and Kim, K.H. (2000) 'NF- $\kappa$ B and cytokines in pancreatic acinar cells.', *Journal of Korean medical science*, 15, pp. S53–S54.
- Klausen, K. (1965) 'Cardiac output in man in rest and work during and after acclimatization to 3 , 800 rd', *Journal of applied physiology*, 21(2), pp. 609–616.
- Klausen, T. *et al.* (1997) 'Hypoxemia increases serum interleukin-6 in humans', *European Journal of Applied Physiology and Occupational Physiology*, 76(5), pp. 480–482.
- Klein, K. *et al.* (2012) 'PPARA: A novel genetic determinant of CYP3A4 in vitro and in vivo', *Clinical Pharmacology and Therapeutics*, 91(6), pp. 1044–1052.

- Klein, M. *et al.* (2015) 'A systematic comparison of the impact of inflammatory signaling on absorption, distribution, metabolism, and excretion gene expression and activity in primary human hepatocytes and HepaRG Cells', *Drug Metabolism and Disposition*, 43(2), pp. 273–283.
- Knoche, L. *et al.* (2022) 'LC-HRMS-Based Identification of Transformation Products of the Drug Salinomycin Generated by Electrochemistry and Liver Microsome', *Antibiotics*, 11(2), pp. 1–12.
- Krishna, C.M. *et al.* (1992) 'The catecholic metal sequestering agent 1,2-dihydroxybenzene-3,5-disulfonate confers protection against oxidative cell damage', *Archives of Biochemistry and Biophysics*, 294(1), pp. 98–106.
- Krishna, D.R. and Klotz, U. (1994) 'Extrahepatic metabolism of drugs in humans', *Clinical pharmacokinetics*, 26(2), pp. 144–160.
- Krishnamurthy, P. *et al.* (2004) 'The stem cell marker Bcrp/ABCG2 enhances hypoxic cell survival through interactions with heme', *Journal of Biological Chemistry*, 279(23), pp. 24218–24225.
- Kurdi, J. *et al.* (1999) 'Effect of hypoxia alone or combined with inflammation and 3-methylcholanthrene on hepatic cytochrome P450 in conscious rabbits', *British Journal of Pharmacology*, 128(2), pp. 365–373.
- Leach, R.M. and Treacher, D.F. (1995) 'Clinical aspects of hypoxic pulmonary vasoconstriction', *Experimental Physiology*, 80(5), pp. 865–875.
- Lee, J., Giordano, S. and Zhang, J. (2012) 'Autophagy, mitochondria and oxidative stress: cross-talk and redox signalling', *Biochem. J.*, 441, pp. 523–540.
- Legendre, C. *et al.* (2009) *Drug-metabolising enzymes are down-regulated by hypoxia in differentiated human hepatoma HepaRG cells: HIF-1 $\alpha$  involvement in CYP3A4 repression*, *European Journal of Cancer*. Elsevier Ltd.
- Leite, S.B. *et al.* (2011) 'Merging bioreactor technology with 3D hepatocyte-fibroblast culturing approaches: Improved in vitro models for toxicological applications', *Toxicology in Vitro*, 25(4), pp. 825–832.
- Leite, S.B. *et al.* (2012) 'Three-Dimensional HepaRG Model As An Attractive Tool for Toxicity Testing', 130(1), pp. 106–116.

- Lemos, V.D.A. *et al.* (2013) 'Can High Altitude Influence Cytokines and Sleep?', *Mediators of inflammation*, pp. 1–8.
- Lennicke, C. *et al.* (2015) 'Hydrogen peroxide - Production, fate and role in redox signaling of tumor cells', *Cell Communication and Signaling*, 13(1), pp. 1–19.
- León-Velarde, F. *et al.* (2005) 'Consensus statement on chronic and subacute high altitude diseases', *HIGH ALTITUDE MEDICINE & BIOLOGY*, 6(2), pp. 147–156.
- Lewis, R.J., Johnson, R.D. and Blank, C.L. (2000) 'A novel method for the determination of sildenafil (viagra®) and its metabolite (UK-103, 320) in postmortem specimens using LC / MS / MS and LC / MS / MS / MS', *Office of Aviation Medicine*, pp. 1–12.
- Lewis, T.S., Shapiro, P.S. and Ahn, N.G. (1998) 'Signal transduction through MAP kinase cascades', *Advances in Cancer Research*, 74, pp. 137–139.
- Li, C., Wright, M.M. and Jackson, R.M. (2002) 'Reactive species mediated injury of human lung epithelial cells after hypoxia-reoxygenation', *Experimental Lung Research*, 28(5), pp. 373–389.
- Li, C.Y. *et al.* (2019) 'Major glucuronide metabolites of testosterone are primarily transported by MRP2 and MRP3 in human liver, intestine and kidney', *Journal of Steroid Biochemistry and Molecular Biology*, 191(April), p. 105350.
- Li, D. *et al.* (2017) 'Hepatic hypoxia-inducible factors inhibit PPAR $\alpha$  expression to exacerbate acetaminophen induced oxidative stress and hepatotoxicity', *Free Radical Biology and Medicine*, 110, pp. 102–116.
- Li, T.S. and Marbán, E. (2010) 'Physiological levels of reactive oxygen species are required to maintain genomic stability in stem cells', *Stem Cells*, 28(7), pp. 1178–1185.
- Li, W. *et al.* (2015) 'MDR1 will play a key role in pharmacokinetic changes under hypoxia at high altitude and its potential regulatory networks', *Drug Metabolism Reviews*, 47(2), pp. 191–198.
- Li, X. *et al.* (2013) 'Targeting mitochondrial reactive oxygen species as novel therapy for inflammatory diseases and cancers', *Journal of Hematology and Oncology*. BioMed Central Ltd.

- Li, X., Wang, X., Li, Y., Yuan, M., *et al.* (2014) 'Effect of exposure to acute and chronic high-altitude hypoxia on the activity and expression of CYP1A2, CYP2D6, CYP2C9, CYP2C19 and NAT2 in rats', *Pharmacology*, 93(1–2), pp. 76–83.
- Li, X., Wang, X., Li, Y., Zhu, J., *et al.* (2014a) 'The Activity, Protein, and mRNA Expression of CYP2E1 and CYP3A1 in Rats after Exposure to Acute and Chronic High Altitude Hypoxia', *High Altitude Medicine & Biology* [Preprint].
- Li, X., Wang, X., Li, Y., Zhu, J., *et al.* (2014b) 'The Activity, Protein, and mRNA Expression of CYP2E1 and CYP3A1 in Rats after Exposure to Acute and Chronic High Altitude Hypoxia', *High Altitude Medicine & Biology*, 15(4), pp. 491–496.
- Li, X.Y. *et al.* (2009) 'Comparison of the pharmacokinetics of sulfamethoxazole in male chinese volunteers at low altitude and acute exposure to high altitude versus subjects living chronically at high altitude: An open-label, controlled, prospective study', *Clinical Therapeutics*, 31(11), pp. 2744–2754.
- Lichti-Kaiser, K. *et al.* (2009) 'A systematic analysis of predicted phosphorylation sites within the human pregnane X receptor protein', *Journal of Pharmacology and Experimental Therapeutics*, 331(1), pp. 65–76.
- Lin, G. *et al.* (2003) 'Up and down-regulation of phosphodiesterase-5 as related to tachyphylaxis and priapism', *Journal of Urology*, 170(2 II), pp. 15–19.
- Liu, M. *et al.* (2007) 'PO<sub>2</sub>-dependent differential regulation of multidrug resistance 1 gene expression by the c-Jun NH<sub>2</sub>-terminal kinase pathway', *Journal of Biological Chemistry*, 282(24), pp. 17581–17586.
- Liu, Q. *et al.* (2004) 'A Fenton reaction at the endoplasmic reticulum is involved in the redox control of hypoxia-inducible gene expression', *Proceedings of the National Academy of Sciences of the United States of America*, 101(12), pp. 4302–4307.
- Lluis, J.M. *et al.* (2005) 'Critical role of mitochondrial glutathione in the survival of hepatocytes during hypoxia', *Journal of Biological Chemistry*, 280(5), pp. 3224–3232.
- Long, L.H. and Halliwell, B. (2009) 'Artefacts in cell culture: Pyruvate as a scavenger of hydrogen peroxide generated by ascorbate or epigallocatechin gallate in cell culture media', *Biochemical and Biophysical Research Communications*, 388(4), pp. 700–704.

- López-Barneo, J., Pardal, R. and Ortega-Sáenz, P. (2001) 'Cellular mechanism of oxygen sensing', *Annual review of physiology*, 63(1), pp. 259–287.
- Loshbaugh, J., Loeppky, J. and Greene, E. (2006) 'Effects of acute hypobaric hypoxia on resting and postprandial superior mesenteric artery blood flow', *High Alt Med Biol*, 7(1), pp. 47–53.
- Lucas, S.J.E. *et al.* (2011) 'Alterations in cerebral blood flow and cerebrovascular reactivity during 14 days at 5050 m', *J Physiol*, 589(3), pp. 741–753.
- Lundeberg, J. *et al.* (2018) 'Increased Cytokines at High Altitude: Lack of Effect of Ibuprofen on Acute Mountain Sickness, Physiological Variables, or Cytokine Levels', *High Altitude Medicine and Biology*, 19(3), pp. 249–258.
- Luo, B.F. *et al.* (2016) 'Effect of hypoxia on expressions of MDR1 and MRP2 in rats', *Journal of Southern Medical University*, 36(9), pp. 1169–1172.
- Luzak, B., Siarkiewicz, P. and Boncler, M. (2022) 'An evaluation of a new high-sensitivity PrestoBlue assay for measuring cell viability and drug cytotoxicity using EA.hy926 endothelial cells', *Toxicology in Vitro*, 83, pp. 1–9.
- Ma, R. *et al.* (2012) 'Expressions of vitamin D metabolic components VDBP, CYP2R1, CYP27B1, CYP24A1, and VDR in placentas from normal and preeclamptic pregnancies', *American Journal of Physiology - Endocrinology and Metabolism*, 303(7).
- Macsween, R.M.N. *et al.* (2002) *Pathology of the Liver*. Fourth ed. Harcourt.
- Maglich, J.M. *et al.* (2003) 'Identification of a novel human constitutive androstane receptor (CAR) agonist and its use in the identification of CAR target genes', *The American Society for Biochemistry and Molecular Biology*, 278(19), pp. 17277–17283.
- Mairböurl, H. (1994) 'Red blood cell function in hypoxia at altitude and exercise', *Int J Sports Med*, 15(2), pp. 51–63.
- Mansfield, K.D. *et al.* (2005) 'Mitochondrial dysfunction resulting from loss of cytochrome c impairs cellular oxygen sensing and hypoxic HIF- $\alpha$  activation', *Cell Metabolism*, 1(6), pp. 393–399.

- Mao, Z. *et al.* (2012) 'DEC1 binding to the proximal promoter of CYP3A4 ascribes to the downregulation of CYP3A4 expression by IL-6 in primary human hepatocytes', *Biochemical Pharmacology*, 84(5), pp. 701–711.
- Marchissio, M.J. *et al.* (2012) 'Mitochondrial aquaporin-8 knockdown in human hepatoma HepG2 cells causes ROS-induced mitochondrial depolarization and loss of viability', *Toxicology and Applied Pharmacology*, 264(2), pp. 246–254.
- Marion, M.-J., Hantz, O. and Durantel, D. (2010) 'The HepaRG cell line: biological properties and relevance as a tool for cell biology, drug metabolism, and virology studies', *Methods in Molecular Biology*, 640(1), pp. 72–261.
- Martin, D. *et al.* (2007) 'Increased Gastric–End Tidal PCO<sub>2</sub> Gap during Exercise at High Altitude Measured by Gastric Tonometry', *High altitude medicine & biology*, 8(1), pp. 550–55.
- Massari, M.E. and Murre, C. (2000) 'Helix-Loop-Helix Proteins: Regulators of Transcription in Eucaryotic Organisms', *Molecular and Cellular Biology*, 20(2), pp. 429–440.
- Mazure, N.M., Trong, L.N. and Danan, J.L. (2001) 'Severe Hypoxia Specifically Downregulates Hepatocyte Nuclear Factor-4 Gene Expression in HepG2 Human Hepatoma Cells', *Tumor biology*, 22(5), pp. 310–317.
- Mazzeo, R.S. (2005) 'Altitude, exercise and immune function', *Exercise Immunology Review*, 11(303), pp. 6–16.
- Mehrotra, N. *et al.* (2007) 'The role of pharmacokinetics and pharmacodynamics in phosphodiesterase-5 inhibitor therapy', *International Journal of Impotence Research*, 19(3), pp. 253–264.
- Merry, H.E. *et al.* (2015) 'Functional roles of tumor necrosis factor-alpha and interleukin 1-beta in hypoxia and reoxygenation', *Annals of Thoracic Surgery*, 99(4), pp. 1200–1205.
- Michaelis, U.R. *et al.* (2005) 'Cytochrome P450 epoxygenases 2C8 and 2C9 are implicated in hypoxia-induced endothelial cell migration and angiogenesis', *Journal of Cell Science*, 118, pp. 5489–5498.
- Milligan, P. a, Marshall, S.F. and Karlsson, M.O. (2002) 'A population pharmacokinetic analysis of sildenafil citrate in patients with erectile dysfunction.', *British journal of clinical pharmacology*, 53(1), pp. 45S-52S.

- Min, L., He, B. and Hui, L. (2011) 'Mitogen-activated protein kinases in hepatocellular carcinoma development', *Seminars in Cancer Biology*, 21(1), pp. 10–20.
- Minet, E. *et al.* (2000a) 'ERK activation upon hypoxia: Involvement in HIF-1 activation', *FEBS Letters*, 468(1), pp. 53–58.
- Minet, E. *et al.* (2000b) 'ERK activation upon hypoxia: Involvement in HIF-1 activation', *FEBS Letters*, 468(1), pp. 53–58.
- Miyazaki, K. *et al.* (2002) 'Identification of functional hypoxia response elements in the promoter region of the DEC1 and DEC2 genes', *Journal of Biological Chemistry*, 277(49), pp. 47014–47021.
- Mladenov, M. *et al.* (2023) 'Oxidative Stress, Reductive Stress and Antioxidants in Vascular Pathogenesis and Aging', *Antioxidants*, 12(5), pp. 2–29.
- Modesti, P.A. *et al.* (2006) 'Role of endothelin-1 in exposure to high altitude acute mountain sickness and endothelin-1 ( ACME-1 ) study', *American Heart Association*, 114, pp. 1410–1416.
- Möller, M.N. *et al.* (2019) 'Diffusion and transport of reactive species across cell membranes', *Advances in Experimental Medicine and Biology*, 1127, pp. 3–19.
- Monge, C. and Leon-Velarde, F. (1991) 'Physiological adaptation to high altitude : oxygen transport in mammals and birds', *PHYSIOLOGICAL REVIEWS*, 71(4), pp. 1135–1172.
- Morel, Y. and Barouki, R. (1998) 'Down-regulation of cytochrome P450 1A1 gene promoter by oxidative stress: Critical contribution of nuclear factor 1', *Journal of Biological Chemistry*, 273(41), pp. 26969–26976.
- Morel, Y., Mermoud, N. and Barouki, R. (1999) 'An Autoregulatory Loop Controlling CYP1A1 Gene Expression: Role of H<sub>2</sub>O<sub>2</sub> and NFI', *Molecular and Cellular Biology*, 19(10), pp. 6825–6832.
- Morel, Y., De Waziers, I. and Barouki, R. (2000) 'A repressive cross-regulation between catalytic and promoter activities of the CYP1A1 and CYP2E1 genes: Role of H<sub>2</sub>O<sub>2</sub>', *Molecular Pharmacology*, 57(6), pp. 1158–1164.
- Morgan, E.T. (2001) 'Regulation of cytochrome P450 by inflammatory mediators: Why and how?', *Drug Metabolism and Disposition*, 29(3), pp. 207–212.

- Morgan, E.T. (2009) 'Impact of infectious and inflammatory disease on cytochrome P450-mediated drug metabolism and pharmacokinetics', *Clin. Pharmacol Ther*, 85(4), pp. 434–438.
- Morgan, M.J. and Liu, Z. (2010) 'Crosstalk of reactive oxygen species and NF- $\kappa$ B signaling', *Nature Publishing Group*, 21(1), pp. 103–115.
- Mrakic-Sposta, S. *et al.* (2021) 'Effects of acute and sub-acute hypobaric hypoxia on oxidative stress: a field study in the Alps', *European Journal of Applied Physiology*, 121(1), pp. 297–306.
- Mrakic-Sposta, S. *et al.* (2022) 'OxInflammation at High Altitudes: A Proof of Concept from the Himalayas', *Antioxidants*, 11(368), pp. 1–11.
- Muirhead, G.J. *et al.* (1996) 'Pharmacokinetics of sildenafil (Viagra), a selective cGMP PDE5 inhibitor, after single oral doses in fasted and fed healthy volunteers', *Br J Clin Pharmacol*, 42(2), p. 268P.
- Muirhead, G.J. *et al.* (2002) 'Comparative human pharmacokinetics and metabolism of single-dose oral and intravenous sildenafil', *BrJ Clin Pharmacol*, 53, pp. 13S-20S.
- Mukhopadhyay, P. *et al.* (2007) 'Simultaneous detection of apoptosis and mitochondrial superoxide production in live cells by flow cytometry and confocal microscopy', *Nature protocols*, 2(9), pp. 2295–2301.
- Muller, F.L., Liu, Y. and Van Remmen, H. (2004) 'Complex III releases superoxide to both sides of the inner mitochondrial membrane', *Journal of Biological Chemistry*, 279(47), pp. 49064–49073.
- Naeije, R. (2010) 'Physiological Adaptation of the Cardiovascular System to High Altitude', *Progress in Cardiovascular Diseases*, 52(6), pp. 456–466.
- Nagai, F., Kato, E. and Tamura, H.O. (2004) 'Oxidative stress induces GSTP1 and CYP3A4 expression in the human erythroleukemia cell line, K562', *Biological and Pharmaceutical Bulletin*, 27(4), pp. 492–495.
- Naritomi, Y. *et al.* (2001) 'Prediction of human hepatic clearance from in vivo animal experiments and in vitro metabolic studies with liver microsomes from animals and humans', *Drug Metabolism and Disposition*, 29(10), pp. 1316–1324.



- Nelin, L.D. and Potenziano, J.L. (2019) 'Inhaled nitric oxide for neonates with persistent pulmonary hypertension of the newborn in the CINRGI study: time to treatment response', *BMC Pediatrics*, 19(1), pp. 1–7.
- Nichols, D.J., Muirhead, G.J. and Harness, J.A. (2002) 'Pharmacokinetics of sildenafil after single oral doses in healthy male subjects: absolute bioavailability; food effects and dose proportionality', *British journal of clinical pharmacology*, 53, pp. 5S-12S.
- O'Driscoll, B.R. *et al.* (2017) 'BTS guideline for oxygen use in adults in healthcare and emergency settings', *Thorax*, 72(6), pp. i1-90.
- Oliver, K.M., Taylor, C.T. and Cummins, E.P. (2009) 'Hypoxia. Regulation of NFκB signalling during inflammation: The role of hydroxylases', *Arthritis Research and Therapy*, 11(1), pp. 1–8.
- Olsen, N. *et al.* (1992) 'Effects of acute hypoxia on renal and endocrine function at rest and during graded exercise in hydrated subjects', *J Appl Physiol*, 37(5), pp. 2036–2043.
- Olsen, N. V. *et al.* (1993) 'Renal hemodynamics, tubular function, and response to low-dose dopamine during acute hypoxia in humans', *Journal of Applied Physiology*, 74(5), pp. 2166–2173.
- Omura, T. (1999) 'Forty years of cytochrome P450', *Biochemical and Biophysical Research Communications*, 266(3), pp. 690–698.
- Orchard, C.H., De Leon, R.S. and Sykes, M.K. (1983) 'The relationship between hypoxic pulmonary vasoconstriction and arterial oxygen tension in the intact dog', *J. Physiol*, 338(1), pp. 61–74.
- O'Rourke, R.W. *et al.* (2011) 'Hypoxia-induced inflammatory cytokine secretion in human adipose tissue stromovascular cells', *Diabetologia*, 54(6), pp. 1480–1490.
- Osorio-Fuentealba, C. *et al.* (2009) 'Hypoxia stimulates via separate pathways ERK phosphorylation and NF-κB activation in skeletal muscle cells in primary culture', *Journal of Applied Physiology*, 106(4), pp. 1301–1310.
- Paine, M.F. *et al.* (2006) 'The human intestinal cytochrome P450 "PIE"', *DRUG METABOLISM AND DISPOSITION*, 34(5), pp. 880–886.

- Paky, A. *et al.* (1993) 'Endogenous production of superoxide by rabbit lungs: effects of hypoxia or metabolic inhibitors', *Journal of applied physiology*, 74(6), 74(6), pp. 2868–2874.
- Paralikar, S. (2012) 'High altitude pulmonary edema - clinical features , pathophysiology , prevention and treatment', *Indian journal of occupational and environmental medicine*, 16(2), pp. 59–62.
- Parmentier, Y. *et al.* (2007) 'In vitro studies of drug metabolism', in, pp. 231–257.
- Pavek, P. *et al.* (2010) 'Intestinal cell-specific vitamin D receptor (VDR)-mediated transcriptional regulation of CYP3A4 gene', *Biochemical Pharmacology*, 79(2), pp. 277–287.
- Pérez-Torres, I. *et al.* (2020) 'Oxidative, reductive, and nitrosative stress effects on epigenetics and on posttranslational modification of enzymes in cardiometabolic diseases', *Oxidative Medicine and Cellular Longevity*, 2020, pp. 2–18.
- Petersson, J. and Glenny, R.W. (2014) 'Gas exchange and ventilation – perfusion relationships in the lung', *European Respiratory Journal*, 44(4), pp. 1023–41.
- Pichler, J. *et al.* (2008) 'Glomerular filtration rate estimates decrease during high altitude expedition but increase with Lake Louise acute mountain sickness scores', *Acta Physiol*, 192(1), pp. 443–450.
- Pondugula, S.R., Dong, H. and Chen, T. (2009) 'Phosphorylation and Protein-protein Interactions in PXR- mediated CYP3A Repression', *Expert Opin Drug Metab Toxicol*, 5(8), pp. 861–873.
- Ponsoda, X. *et al.* (2001) 'Drug biotransformation by human hepatocytes. In vitro/in vivo metabolism by cells from the same donor', *Journal of Hepatology*, 34(1), pp. 19–25.
- Powell, J. *et al.* (1978) 'Theophylline disposition in acutely hospitalized patients the effect of smoking, heart failure, severe airway obstruction, and pneumonia', *Am Rev Respir Dis*, 118(2), pp. 229–38.
- Proulx, M. and Du Souich, P. (1995) 'Acute Moderate Hypoxia in Conscious Rabbits: Effect on Hepatic Cytochrome P450 and on Reactive Oxygen Species', *Journal of Pharmacy and Pharmacology*, 47(5), pp. 392–397.
- Qin, X. and Wang, X. (2019) 'Role of vitamin D receptor in the regulation of CYP3A gene expression', *Acta Pharmaceutica Sinica B*, 9(6), pp. 1087–1098.

- Ram, E. *et al.* (2018) 'Sildenafil for pulmonary hypertension in the early postoperative period after mitral valve surgery', *Journal of Cardiothoracic and Vascular Anesthesia*, 33(6), pp. 1648–1656.
- Ramaiahgari, S.C. *et al.* (2017) 'Three-dimensional (3D) HepaRG spheroid model with physiologically relevant xenobiotic metabolism competence and hepatocyte functionality for liver toxicity screening', *Toxicological Sciences*, 159(1), pp. 124–136.
- Ramsøe, K. *et al.* (1970) 'Liver function and blood flow at high altitude', *Journal of Applied Physiology*, 28(6), pp. 725–727.
- Rankin, E. and Giaccia, A. (2008) 'The role of hypoxia-inducible factors in tumorigenesis', *Cell Death Differ*, 15(4), pp. 678–685.
- Ranneh, Y. *et al.* (2017) 'Crosstalk between reactive oxygen species and pro-inflammatory markers in developing various chronic diseases: a review', *Applied Biological Chemistry*. Springer Netherlands, pp. 327–338.
- Ravenna, L., Salvatori, L. and Russo, M.A. (2015) 'HIF3  $\alpha$ : the little we know', *FEBS Journal*, 283(6), pp. 993–1003.
- Rescan, C. *et al.* (2001) 'Mechanism in the Sequential Control of Cell Morphology and S Phase Entry by Epidermal Growth Factor Involves Distinct MEK/ERK Activations', *Molecular Biology of the Cell*, 12, pp. 725–738.
- Richalet, J. and Jimenez, D. (2015) 'Chilean miners commuting from sea level to 4500 m: a prospective study', *HIGH ALTITUDE MEDICINE & BIOLOGY*, 3(2), pp. 195–166.
- Richalet, J.P. *et al.* (2005) 'Sildenafil inhibits altitude-induced hypoxemia and pulmonary hypertension', *American Journal of Respiratory and Critical Care Medicine*, 171(3), pp. 275–281.
- Rigalli, J.P. *et al.* (2012) 'Regulation of Biotransformation Systems and ABC Transporters by Benznidazole in HepG2 Cells: Involvement of Pregnane X-Receptor', *PLoS Neglected Tropical Diseases*, 6(12), pp. 1–10.
- Ritschel, W. *et al.* (1966) 'Urinary excretion of meperidine and normeperidine in man upon acute and chronic exposure to high altitude', *Methods Find Exp Clin Pharmacol*, 18(1), pp. 49–53.

- Ritschel, W.A. *et al.* (1996) 'Pharmacokinetics of meperidine in healthy volunteers after short and long-term exposure to high altitude', *The Journal of Clinical Pharmacology*, 36(7), pp. 610–616.
- Ritschel, W.A. *et al.* (1998) 'Pharmacokinetics of acetazolamide in healthy volunteers after short- and long-term exposure to high altitude.', *Journal of clinical pharmacology*, 38(6), pp. 533–539.
- Roach, R.C. *et al.* (2018) 'The 2018 lake louise acute mountain sickness score', *HIGH ALTITUDE MEDICINE & BIOLOGY*, 19(1), pp. 4–6.
- Roach, R.C., Wagner, P.D. and Hackett, P.H. (2016) *Hypoxia, Advances in Experimental Medicine and Biology*.
- Rodriguez-Antona, C. *et al.* (2002) 'Cytochrome P450 expression in human hepatocytes and hepatoma cell lines: molecular mechanisms that lower expression in cultured cells', *Xenobiotica*, 32(6), pp. 505–520.
- Roelofs, B.A. *et al.* (2015) 'Low micromolar concentrations of the superoxide probe MitoSOX uncouple neural mitochondria and inhibit complex IV', *Free Radical Biology and Medicine*, 86, pp. 250–258.
- Roskoski, R. (2012) 'ERK1/2 MAP kinases: Structure, function, and regulation', *Pharmacological Research*, 66(2), pp. 105–143.
- Roux, P.P. and Blenis, J. (2004) 'ERK and p38 MAPK-Activated Protein Kinases: a Family of Protein Kinases with Diverse Biological Functions', *Microbiology and Molecular Biology Reviews*, 68(2), pp. 320–344.
- Rowett, D. *et al.* (1996) 'The effect of hypoxaemia on drug disposition in chronic respiratory failure', *European Journal of Clinical Pharmacology*, 50(1–2), pp. 77–82.
- Saenz De Tejada, I. *et al.* (2001) 'The phosphodiesterase inhibitory selectivity and the in vitro and in vivo potency of the new PDE5 inhibitor vardenafil', *International Journal of Impotence Research*, 13(5), pp. 282–290.
- Sarada, S.K.S. *et al.* (2012) 'Nifedipine inhibits hypoxia induced transvascular leakage through down regulation of NFkB', *Respiratory Physiology and Neurobiology*, 183(1), pp. 26–34.

- Sarkar, M., Niranjana, N. and Banyal, P. (2017) 'Mechanisms of hypoxemia', *Lung India*, 34(1), p. 47.
- Sato, H. *et al.* (2005) 'Mitochondrial reactive oxygen species and c-Src play a critical role in hypoxic response in vascular smooth muscle cells', *Cardiovascular Research*, 67(4), pp. 714–722.
- Schenk, W.G. *et al.* (1962) 'Direct Measurement of Hepatic Blood Flow in Surgical Patients', *Annals of Surgery*, 156(3), pp. 463–471.
- Schroyer, A.L. *et al.* (2018) 'MLK3 phosphorylation by ERK1/2 is required for oxidative stress-induced invasion of colorectal cancer cells', *Oncogene*, 37(8), pp. 1031–1040.
- Semenza, G.L. (2001) 'HIF-1 and mechanisms of hypoxia sensing', *Curr Opin Cell Biol*, 13(2), pp. 167–171.
- Seta, K.A. and Millhorn, D.E. (2004) 'Oxygen Sensing in Health and Disease Functional genomics approach to hypoxia signaling', *J Appl Physiol*, 96(2), pp. 765–773.
- Severinghaus, J. (2001) *High altitude, an exploration of human adaptation*. Edited by E. Hornbein TF, Schoene RB. New York, Basel: Marcel Dekker: CRC Press.
- Severinghaus, J.W. *et al.* (1963) 'Respiratory suggesting control at high altitude active transport regulation of CSF pH ', *Journal of applied physiology*, 18(6), pp. 1155–1166.
- Severinghaus, J.W. *et al.* (1966) 'Cerebral Blood Flow In Man at High Altitude', *Circulation Research*, 19(2), pp. 274–282.
- Sevrioukova, I.F. and Poulos, T.L. (2013) 'Understanding the mechanism of cytochrome P450 3A4: recent advances and remaining problems', *Dalton Trans*, 42(9), pp. 3116–3126.
- Sgarbi, G. *et al.* (2017) 'Hypoxia decreases ROS level in human fibroblasts', *International Journal of Biochemistry and Cell Biology*, 88(March), pp. 133–144.
- Sgarbi, G. *et al.* (2018) 'Hypoxia and IF1 expression promote ROS decrease in cancer cells', *Cells*, 7(7), pp. 1–12.
- Shang, T. *et al.* (2023) 'Heterologous Expression of Recombinant Human Cytochrome P450 (CYP) in Escherichia coli: N-Terminal Modification, Expression, Isolation, Purification, and Reconstitution', *BioTech*, 12(1), p. 17.

- Shi, L.X. *et al.* (2017) ‘Hepatic Cyp1a2 expression reduction during inflammation elicited in a rat model of intermittent hypoxia’, *Chinese Medical Journal*, 130(21), pp. 2585–2590.
- Shin, D.S. *et al.* (2018) ‘Quantitative evaluation of cytochrome P450 3A4 inhibition and hepatotoxicity in HepaRG 3-D spheroids’, *International Journal of Toxicology*, 37(5), pp. 393–403.
- Singh, M. *et al.* (2003) ‘Blood gases, hematology, and renal blood flow during prolonged mountain sojourns at 3500 and 5800 m.’, *Aviat Space Environ Med.*, 74(5), pp. 533–6.
- Skarpen, E. *et al.* (2008) ‘MEK1 and MEK2 regulate distinct functions by sorting ERK2 to different intracellular compartments’, *The FASEB Journal*, 22(2), pp. 466–476.
- Smutny, T. *et al.* (2014) ‘U0126, a mitogen-activated protein kinase kinase 1 and 2 (MEK1 and 2) inhibitor, selectively up-regulates main isoforms of CYP3A subfamily via a pregnane X receptor (PXR) in HepG2 cells’, *Archives of Toxicology*, 88(12), pp. 2243–2259.
- Souich, P. *et al.* (1983) ‘Influence of Chronic Obstructive Lung Disease on the Disposition of an Acidic Drug (Sulfamethazine)’, *Archives of Internal Medicine*, 143(2), pp. 233–236.
- Du Souich, P. *et al.* (1989) ‘Theophylline disposition in patients with GOLD with and without hypoxemia’, *Chest*, 95(5), pp. 1028–1032.
- du Souich, P. and Erill, S. (1978) ‘Metabolism of procainamide in patients with chronic heart failure, chronic respiratory failure and chronic renal failure’, *European Journal of Clinical Pharmacology*, 14(1), pp. 21–27.
- Du Souich, P. and Fradette, C. (2011) ‘The effect and clinical consequences of hypoxia on cytochrome P450, membrane carrier proteins activity and expression’, *Expert Opinion on Drug Metabolism & Toxicology*, 7(9), pp. 1083–1100.
- Stanfield, C.L. (2017) ‘Principles of Human Physiology, Sixth Edition’, in *Pearson Education*.
- Steele, A.R. *et al.* (2020) ‘Global REACH 2018: Renal oxygen delivery is maintained during early acclimatization to 4,330 m’, *American Journal of Physiology - Renal Physiology*, 319(6), pp. F1081–F1089.
- Streit, M. *et al.* (2005) ‘Cytochrome P 450 enzyme-mediated drug metabolism at exposure to acute hypoxia ( corresponding to an altitude of 4 , 500 m )’, *Eur J Clin Pharmacol*, pp. 39–46.

- Su, T. and Waxman, D.J. (2004) 'Impact of dimethyl sulfoxide on expression of nuclear receptors and drug-inducible cytochromes P450 in primary rat hepatocytes', *Archives of Biochemistry and Biophysics*, 424(2), pp. 226–234.
- Subudhi, A.W. *et al.* (2014) 'AltitudeOmics : effect of ascent and acclimatization to 5260 m on regional cerebral oxygen delivery', *Exp Physiol*, 99(5), pp. 772–781.
- Surks, M.I. (1966) 'Metabolism of human serum albumin in man during acute exposure to high altitude ( 14 , 100 Feet )', *Journal of Clinical Investigation*, 45(9), pp. 1442–1451.
- Suvannasankha, A. *et al.* (2004) 'Breast cancer resistance protein (BCRP/MXR/ABCG2) in acute myeloid leukemia: Discordance between expression and function', *Leukemia*, 18(7), pp. 1252–1257.
- Suzuki, E. *et al.* (2012) 'Effects of Hypoxia-inducible Factor-1 $\alpha$  Chemical Stabilizer, CoCl<sub>2</sub> and Hypoxia on Gene Expression of CYP3As in Human Fetal Liver Cells', *Drug Metabolism and Pharmacokinetics*, 27(4), pp. 398–404.
- Taburet, A.M., Tollier, C. and Richard, C. (1990) 'The Effect of Respiratory Disorders on Clinical Pharmacokinetic Variables', *Clinical Pharmacokinetics*, 19(6), pp. 462–490.
- Tafari, M. *et al.* (2016) 'The Interplay of Reactive Oxygen Species, Hypoxia, Inflammation, and Sirtuins in Cancer Initiation and Progression', *Oxidative Medicine and Cellular Longevity*, 2016.
- Taiwo, F.A. (2008) 'Mechanism of tiron as scavenger of superoxide ions and free electrons', *Spectroscopy*, 22(6), pp. 491–498.
- Takahashi, Y. *et al.* (2015) '3D spheroid cultures improve the metabolic gene expression profiles of HepaRG cells', *Bioscience Reports*, 35(3), pp. 1–7.
- Takano, H. *et al.* (2021) 'Downregulation of CYP1A2, CYP2B6, and CYP3A4 in human hepatocytes by prolyl hydroxylase domain 2 inhibitors via hypoxia-inducible factor- $\alpha$  stabilization', *Drug Metabolism and Disposition*, 49(1), pp. 20–30.
- Taniai, H. *et al.* (2004) 'Susceptibility of murine periportal hepatocytes to hypoxia-reoxygenation: Role for NO and Kupffer cell-derived oxidants', *Hepatology*, 39(6), pp. 1544–1552.
- Theodore, A.C. (2020) *Measures of oxygenation and mechanisms of hypoxemia -*, *UpToDate*.

- Thomas, A. *et al.* (2018) 'The Hypoxic Ventilatory Response And Hepatic CYP3A4 Upregulation In Human At High Altitude', *International Journal of Pharmaceutical Sciences and Research*, 9(2), pp. 687–692.
- Thomas, M. *et al.* (2013) 'Direct Transcriptional Regulation of Human Hepatic Cytochrome P450 3A4 (CYP3A4) by Peroxisome Proliferator–Activated Receptor Alpha (PPAR  $\alpha$ )', *Molecular Pharmacology*, 83(3), pp. 709–718.
- Thron, C.D. *et al.* (1998) 'Renovascular adaptive changes in chronic hypoxic polycythemia', *Kidney International*, 54(6), pp. 2014–2020.
- Tien, E. s. and Neglishi, M. (2006) 'Nuclear receptors CAR and PXR in the regulation of hepatic metabolism', *Xenobiotica*, 36(10–11), pp. 1152–1163.
- Tirichen, H. *et al.* (2021) 'Mitochondrial Reactive Oxygen Species and Their Contribution in Chronic Kidney Disease Progression Through Oxidative Stress', *Frontiers in Physiology*. Frontiers Media S.A., pp. 1–12.
- Tormos, A.M., Nebreda, A.R. and Sastre, J. (2013) 'p38 MAPK : A dual role in hepatocyte proliferation through reactive oxygen species', *Free radical research*, 47(11), pp. 905–916.
- Tostões, R.M. *et al.* (2012) 'Human liver cell spheroids in extended perfusion bioreactor culture for repeated-dose drug testing', *Hepatology*, 55(4), pp. 1227–1236.
- Trachsel, D. *et al.* (2005) 'Oxygenation index predicts outcome in children with acute hypoxemic respiratory failure', *American Journal of Respiratory and Critical Care Medicine*, 172(2), pp. 206–211.
- Trang, M., Dudley, M.N. and Bhavnani, S.M. (2017) 'Use of Monte Carlo simulation and considerations for PK-PD targets to support antibacterial dose selection', *Current Opinion in Pharmacology*, 36, pp. 107–113.
- Turpeinen, M. *et al.* (2009) 'Functional expression, inhibition and induction of CYP enzymes in HepaRG cells', *Toxicology in Vitro*, 23(4), pp. 748–753.
- Tuttle, S.W. *et al.* (2007) 'Detection of reactive oxygen species via endogenous oxidative pentose phosphate cycle activity in response to oxygen concentration: Implications for the mechanism of HIF-1 $\alpha$  stabilization under moderate hypoxia', *Journal of Biological Chemistry*, 282(51), pp. 36790–36796.



- Ungermann, K. and Kietzmann, T. (2000) 'Oxygen : Modulator of Metabolic Zonation and Disease of the Liver', *Hepatology*, 31(2), pp. 255–260.
- Ussar, S. and Voss, T. (2004) 'MEK1 and MEK2, different regulators of the G1/S transition', *Journal of Biological Chemistry*, 279(42), pp. 43861–43869.
- Vachieri, J.L. *et al.* (2011) 'Safety, tolerability and pharmacokinetics of an intravenous bolus of sildenafil in patients with pulmonary arterial hypertension', *British Journal of Clinical Pharmacology*, 71(2), pp. 289–292.
- Le Vee, M. *et al.* (2006) 'Functional expression of sinusoidal and canalicular hepatic drug transporters in the differentiated human hepatoma HepaRG cell line', *European Journal of Pharmaceutical Sciences*, 28(1–2), pp. 109–117.
- Venkatakrishnan, K. *et al.* (2005) 'Drug Metabolism and Drug Interactions: Application and Clinical Value of In Vitro Models', *Current Drug Metabolism*, 4(5), pp. 423–459.
- Vignozzi, L. *et al.* (2006) 'Effect of chronic tadalafil administration on penile hypoxia induced by cavernous neurotomy in the rat', *Journal of Sexual Medicine*, 3(3), pp. 419–431.
- Vogel, J.A. and Harris, C.W. (1967) 'Cardiopulmonary responses of resting during early exposure to high altitude', *Journal of Applied Physiology*, 22(6), pp. 1124–1128.
- Vollmar, B. and Menger, M.D. (2009) 'The hepatic microcirculation: Mechanistic contributions and therapeutic targets in liver injury and repair', *Physiological Reviews*, 89(4), pp. 1269–1339.
- Vorobjeva, N. V. and Pinegin, B. V. (2016) 'Effects of the antioxidants Trolox, Tiron and Tempol on neutrophil extracellular trap formation', *Immunobiology*, 221(2), pp. 208–219.
- Wacher, V.J., Wu, C.Y. and Benet, L.Z. (1995) 'Overlapping substrate specificities and tissue distribution of cytochrome P450 3A and P-glycoprotein: implications for drug delivery and activity in cancer chemotherapy', *Molecular carcinogenesis*, 13(3), pp. 129–134.
- Wahli, W. and Michalik, L. (2012) 'PPARs at the crossroads of lipid signaling and inflammation', *Trends in Endocrinology and Metabolism*, 23(7), pp. 351–363.
- Walker, D.K. *et al.* (1999) 'Pharmacokinetics and metabolism of sildenafil in mouse, rat, rabbit, dog and man', *Xenobiotica*, 29(3), pp. 297–310.

- Walmsley, S.R. *et al.* (2005) 'Hypoxia-induced neutrophil survival is mediated by HIF-1 $\alpha$ -dependent NF- $\kappa$ B activity', *Journal of Experimental Medicine*, 201(1), pp. 105–115.
- Wang, G. *et al.* (2023) 'Hypoxia and TNF- $\alpha$  Synergistically Induce Expression of IL-6 and IL-8 in Human Fibroblast-like Synoviocytes via Enhancing TAK1/NF- $\kappa$ B/HIF-1 $\alpha$  Signaling', *Inflammation*, 46(3), pp. 912–924.
- Wang, G.L. and Semenza, G.L. (1993) 'Characterization of hypoxia-inducible factor 1 and regulation of DNA binding activity by hypoxia', *Journal of Biological Chemistry*, 268(29), pp. 21513–21518.
- Wang, R. *et al.* (2017) 'The effects of metronidazole on Cytochrome P450 Activity and Expression in rats after acute exposure to high altitude of 4300 m', *Biomedicine and Pharmacotherapy*, 85, pp. 296–302.
- Wang, Y.M. *et al.* (2012) 'Role of CAR and PXR in xenobiotic sensing and metabolism', *Expert Opinion on Drug Metabolism and Toxicology*, 8(7), pp. 803–817.
- Wang, Z. *et al.* (2013) 'The selectivity and potency of the new PDE5 inhibitor TPN729MA', *Journal of Sexual Medicine*, 10(11), pp. 2790–2797.
- Ward, J.P. and Aaronson, P.I. (1999) 'Mechanisms of hypoxic pulmonary vasoconstriction: can anyone be right?', *Respiration physiology*, 115(3), pp. 261–271.
- Wartenberg, M. *et al.* (2005) 'Reactive oxygen species-linked regulation of the multidrug resistance transporter P-glycoprotein in Nox-1 overexpressing prostate tumor spheroids', *FEBS Letters*, 579(20), pp. 4541–4549.
- Waypa, G.B. *et al.* (2010) 'Hypoxia triggers subcellular compartmental redox signaling in vascular smooth muscle cells', *Circulation Research*, 106(3), pp. 526–535.
- Weide, J. Van Der and Steijns, L.S.W. (1999) 'Cytochrome P450 enzyme system: genetic polymorphisms and impact on clinical pharmacology', *Ann Clin Biochem*, 36(6), pp. 722–729.
- Wenger, R.H. (2002) 'Cellular adaptation to hypoxia : O<sub>2</sub> -sensing protein hydroxylases , hypoxia-inducible transcription factors , and O<sub>2</sub> -regulated gene expression', *The FASEB Journal*, 16, pp. 1151–1162.
- van Wenum, M. *et al.* (2018) 'Oxygen drives hepatocyte differentiation and phenotype stability in liver cell lines', *Journal of Cell Communication and Signaling*, 12(3), pp. 575–588.

- Voice, M. W., Zhang, Y., Wolf, C. R., Burchell, B., & Friedberg, T. (1999). Effects of Human Cytochrome b 5 on CYP3A4 Activity and Stability in Vivo. *Archives of Biochemistry and Biophysics*, 366(1), 116–124.
- West, J.B. and Dollery, C.T. (1963) ‘Distribution of blood flow in isolated lung ; relation to vascular and alveolar pressures’, *Journal of Applied Physiology*, 19(4), pp. 713–724.
- Westerink, W.M.A. and Schoonen, W.G.E.J. (2007) ‘Cytochrome P450 enzyme levels in HepG2 cells and cryopreserved primary human hepatocytes and their induction in HepG2 cells’, *Toxicology in Vitro*, 21(8), pp. 1581–1591.
- Wilkening, S., Stahl, F. and Bader, A. (2003) ‘COMPARISON OF PRIMARY HUMAN HEPATOCYTES AND HEPATOMA CELL LINE HEPG2 WITH REGARD TO THEIR BIOTRANSFORMATION PROPERTIES’, *Drug Metabolism and Disposition*, 31(8), pp. 1035–1042.
- Wilkinson, G. and Shand, DG. (1975) ‘Commentary: a physiological approach to hepatic drug clearance’, *Clin Pharmacol Ther*, 18(4), pp. 377–390.
- Willie, C.K. *et al.* (2014) ‘Regional cerebral blood flow in humans at high altitude : gradual ascent and 2 wk at 5 , 050 m’, *J Appl Physiol* 116.:, 116(7), pp. 905–910.
- Willis, C.L., Meske, D.S. and Davis, T.P. (2010) ‘Protein kinase C activation modulates reversible increase in cortical blood-brain barrier permeability and tight junction protein expression during hypoxia and posthypoxic reoxygenation’, *Journal of Cerebral Blood Flow and Metabolism*, 30(11), pp. 1847–1859.
- Winterbourn, C.C. (2013) ‘The biological chemistry of hydrogen peroxide’, in *Methods in Enzymology*. Academic Press Inc., pp. 3–25.
- Xia, S. *et al.* (2004) ‘Effects of hypoxia on expression of P-glycoprotein and multidrug resistance protein in human lung adenocarcinoma A549 cell line.’, *Zhonghua yi xue za zhi*, 84(8), pp. 663–666.
- Xing, G. *et al.* (2018) ‘Oxidant Generation Resulting from the Interaction of Copper with Menadione (Vitamin K3)—a Model for Metal-mediated Oxidant Generation in Living Systems’, *Journal of Inorganic Biochemistry*, 188, pp. 38–49.
- Yamauchi-Takahara, K. *et al.* (1995) ‘Hypoxic stress induces cardiac myocyte-derived interleukin-6’, *Circulation*, 91(5), pp. 1520–1524.

- Yamazaki, H., Gillam, E. M. J., Dong, M.-S., Johnson, W. W., Guengerich, F. P., & Shimada, T. (1997). Reconstitution of Recombinant Cytochrome P450 2C10(2C9) and Comparison with Cytochrome P450 3A4 and Other Forms: Effects of Cytochrome P450-P450 and Cytochrome P450-b 5 Interactions 1 Multiple forms of cytochrome P450 (P450 or CYP) 4. *ARCHIVES OF BIOCHEMISTRY AND BIOPHYSICS*, 342(2), 329–337.
- Yan, S.. F. *et al.* (1995) ‘Induction of interleukin 6 (IL-6) by hypoxia in vascular cells. Central role of the binding site for nuclear factor-IL-6’, *Journal of Biological Chemistry*, 270(19), pp. 11463–11471.
- Yan, Z. and Caldwell, G.W. (2001) ‘Metabolism Profiling , and Cytochrome P450 Inhibition & Induction in Drug Discovery’, *Current Topics in Medicinal Chemistry*, 1(5), pp. 403–425.
- Yang, B. *et al.* (2001) ‘Overexpression of cytochrome P450 CYP2J2 protects against hypoxia-reoxygenation injury in cultured bovine aortic endothelial cells’, *Molecular Pharmacology*, 60(2), pp. 310–320.
- Yang, J. *et al.* (2008) ‘Cytochrome P450 Turnover: Regulation of Synthesis and Degradation, Methods for Determining Rates, and Implications for the Prediction of Drug Interactions’, *Current Drug Metabolism*, 9(5), pp. 384–393.
- Yao, Z. *et al.* (1999) ‘Role of reactive oxygen species in acetylcholine-induced preconditioning in cardiomyocytes’, *American Journal of Physiology - Heart and Circulatory Physiology*, 277(6), pp. H2504–H2509.
- Yokoyama, Y. *et al.* (2018) ‘Comparison of drug metabolism and its related hepatotoxic effects in HepaRG, cryopreserved human hepatocytes, and HepG2 cell cultures’, *Biological and Pharmaceutical Bulletin*, 41(5), pp. 722–732.
- Yu, H. *et al.* (2017) ‘Altered gene expression of hepatic cytochrome P450 in a rat model of intermittent hypoxia with emphysema’, *Molecular Medicine Reports*, 16(1), pp. 881–886.
- Yuan, X. *et al.* (2020) ‘Transcriptional regulation of CYP3A4 by nuclear receptors in human hepatocytes under hypoxia’, *Drug Metabolism Reviews*, 52(2), pp. 225–234.
- Zanger, U.M. and Schwab, M. (2013) ‘Pharmacology & Therapeutics Cytochrome P450 enzymes in drug metabolism : Regulation of gene expression , enzyme activities , and impact of genetic variation’, *Pharmacology and Therapeutics*, 138(1), pp. 103–141.

- Zassadowski, F. *et al.* (2012) 'Regulation of the transcriptional activity of nuclear receptors by the MEK/ERK1/2 pathway', *Cellular Signalling*, 24(12), pp. 2369–2377.
- Zhang, J. *et al.* (2016) 'Pharmacokinetics of lidocaine hydrochloride metabolized by CYP3A4 in chinese han volunteers living at low altitude and in native han and tibetan chinese volunteers living at high altitude', *Pharmacology*, 97(3–4), pp. 107–113.
- Zhang, J. *et al.* (2021) 'Secondary polycythemia in chronic obstructive pulmonary disease: prevalence and risk factors', *BMC Pulmonary Medicine*, 21(1), pp. 1–12.
- Zhang, J. and Wang, R. (2022) 'Changes in CYP3A4 Enzyme Expression and Biochemical Markers Under Acute Hypoxia Affect the Pharmacokinetics of Sildenafil', *Front. Physio*, 13, pp. 1–9.
- Zhang, L. and Tew, K.D. (2021) 'Reductive stress in cancer', in *Advances in Cancer Research*. Academic Press Inc., pp. 383–413.
- Zhang, W. *et al.* (2000) 'Inflammatory activation of human brain endothelial cells by hypoxic astrocytes in vitro is mediated by IL-1 $\beta$ ', *Journal of Cerebral Blood Flow and Metabolism*, 20(6), pp. 967–978.
- Zhao, L. *et al.* (2001) 'Sildenafil Inhibits Hypoxia-Induced Pulmonary Hypertension', *Circulation*, 104(4), pp. 424–428.
- Zhong, W. *et al.* (2014) 'Activation of vitamin D receptor promotes VEGF and CuZn-SOD expression in endothelial cells', *Journal of Steroid Biochemistry and Molecular Biology*, 140, pp. 56–62.
- Zhou, L. *et al.* (2010) 'MEK1 and MEK2 isoforms regulate distinct functions in pancreatic cancer cells', *Oncology Reports*, 24(1), pp. 251–255.
- Zhou, Q. *et al.* (2011) 'Increased permeability of blood-brain barrier caused by inflammatory mediators is involved in high altitude cerebral edema', *Scientific Research and Essays*, 6(3), pp. 607–615.
- Zhou, X.L. *et al.* (2019) 'Interactions between cytosolic phospholipase A2 activation and mitochondrial reactive oxygen species production in the development of ventilator-induced diaphragm dysfunction', *Oxidative Medicine and Cellular Longevity*, 2019, pp. 1–11.

Zhu, H. *et al.* (2005) 'Involvement of hypoxia-inducible factor-1-alpha in multidrug resistance induced by hypoxia in HepG2 cells', *Journal of experimental & clinical cancer research: CR*, 24(4), pp. 565–574.

Zorov, D.B., Juhaszova, M. and Sollott, S.J. (2014) 'Mitochondrial Reactive Oxygen Species (ROS) and ROS-Induced ROS Release', *Physiol Rev*, 94(3), pp. 909–950.

Zulueta, J.J. *et al.* (1995) 'Release of hydrogen peroxide in response to hypoxia-reoxygenation: role of an NAD(P)H oxidase-like enzyme in endothelial cell plasma membrane', *American journal of respiratory cell and molecular biology*, 12(1), pp. 41–49.

## **Appendices**

**Appendix 1- clinical trial protocol and all required documents for MHRA approval.**



**NEUROVASCULAR RESEARCH  
LABORATORY UNIVERSITY OF SOUTH  
WALES**

**CLINICAL TRIAL PROTOCOL**

**Arterial hypoxaemia and its impact on the pharmacokinetics-  
pharmacodynamics of sildenafil; a randomised, double-blind, placebo-  
controlled trial.**

**Document type:** Clinical Trial Protocol **EudraCT**  
**number:** to complete once registered **Clinical**  
**trial phase:** I

**Release date:** to complete once registered.

**Funding:** University of South Wales/ Prince Sattam bin Abdulaziz University /Cardiff University



# Appendix 1

## Table of Contents

<b>1. Introduction</b>	
1.1. Background.....	10
1.2. Purpose and hypothesis of the research study .....	10
<b>2. Study objective and endpoints</b>	
<b>3. Investigational plan</b>	
3.1. Study design .....	11
3.2. Study setting.....	12
3.3. Risks and benefits.....	12
<b>4. Population</b>	
4.1 Inclusion criteria .....	14
4.2 Exclusion criteria .....	15
<b>5. Treatment</b>	
5.1 Investigational and control drugs .....	16
5.2 Randomization .....	17
5.3 Blinding.....	17
5.4 Treating the subjects.....	17
5.4.1 Subjects numbering.....	17
5.4.2 Dispensing the investigation drug .....	17
5.4.3 Handling of study treatment .....	18
5.4.4 Instruction for prescribing and taking study medication .....	18
5.4.5 Concomitant medication.....	18
5.4.6 Prohibited medication and lifestyle .....	18
5.5 Study completion and discontinuation.....	18
5.5.1 Study completion and post -study follow up .....	18
5.5.2 Discontinuation of the study .....	19
5.5.3 Withdrawal of informed consent.....	19
5.5.4 Loss of follow- up.....	19

## Appendix 1

### 6. Visit schedule and assessment

6.1 Subjects demographics/ other baseline characteristics.....	23
6.2 Physical examination.....	23
6.3 Cardiovascular Screening Assessment .....	23
6.4 Stature and Mass .....	23
6.5 Haemodynamic and Respiratory Assessments.....	23
6.6 Haematology.....	24
6.7 Assessment of acute mountain sickness (AMS).....	24
6.8 Other assessments .....	24
6.8.1 Pharmacokinetics .....	24
6.8.2 Other biomarkers.....	25

### 7. Safety monitoring

7.1 Adverse event .....	25
7.2 Serious adverse events (SAE).....	25
7.2.1 Definition of SAE .....	25
7.2.2 SAE reporting.....	26
7.2.3 Reporting of study treatment errors including misuse /abuse .....	26

### 8. Data review and database management

8.2Site monitoring.....	26
8.2Data collection .....	27
8.2Data management.....	27

### 9. Data analysis

9.1 Subject demographics and baseline characteristics .....	28
9.2 Hypothesis .....	28
9.3 Pharmacokinetics.....	28
9.4 Sample size calculation .....	28

### 10. Ethical considerations

10.1 Regulatory and ethical compliance .....	29
10.2 Informed consent .....	29
10.3 Protocol amendments.....	29

## **Appendix 1**

10.4 Confidentiality .....	29
10.5 Declaration of interests.....	29
10.6 Dissemination policy.....	29

## **References**

## Appendix 1

### List of Tables

Table 1: Assessment Schedule.....	17
Table 2: Other assessments.....	19
Table 3: Guidance for capturing the study treatment errors including misuse/abuse.....	26

### List of Figures

Figure 1: Schematic of experimental design and testing protocol.....	11
--	----

### List of abbreviations

AFR	Ascorbate free radical
AEs	Adverse Events
AMS	Acute mountain sickness
AUC	Area under the curve
C <sub>max</sub>	Peak concentration
CRFs	Case report /Record Forms
CL/F	Oral clearance
ESQ-C	Environmental Symptoms Questionnaire - Cerebral Symptoms Questionnaire
EMA	European Medicines Agency
EPR	Electron paramagnetic resonance
Fu	Fraction unbound in plasma
gfap	Glial fibrillary acidic protein
HAH	High altitude headache
hsELISA	High sensitivity enzyme linked immunosorbent
HPLC	High-performance liquid chromatography
Hb	Haemoglobin
Hct	Haematocrit
K <sub>a</sub>	Absorption rate constant
K	Elimination rate constant
LLS	Lake Louise Score
LOOH	Lipid hydroperoxides
LCMS	Liquid chromatography mass spectrometry
NSE	Neuron-specific enolase

## Appendix 1

NFL	Neurofibrillary filament light chain
NO	Nitric oxide
O&NS	Oxidative and nitrosative stress
OBC	Ozone-based chemiluminescence
PK	Pharmacokinetic measurements
RBC	Red blood cell
SpO <sub>2</sub>	Peripheral arterial oxygen saturation
T <sub>max</sub>	Time to peak concentration
t <sub>1/2a</sub>	Absorption half-life
t <sub>1/2</sub>	Elimination half life
Uhcl-1	Ubiquitin C-terminal hydrolase L1
UV spec	Ultraviolet spectroscopy
V/F	Oral volume of distribution

## Appendix 1

### Glossary of terms

$AUC_{0-t_{last}}$	The area under the concentration time-curve from time zero to the last measurable time point.
$AUC_{0-\infty}$	Area under the concentration time-curves from time zero to infinity
$C_{max}$	The highest concentration of the drug observed after dose of drug.
Enrolment	Time of participant entry into the study after the informed consent obtained.
Investigational drug	The drug whose PK/PD proprieties are subject to investigation into the study.
$K_a$	Fractional rate of drug absorption from the site of administration into the systemic circulation
$K$	The rate at which an investigational drug is removed from the body
Subject ID	A unique number given to the participant once they signed the informed consent
$T_{max}$	The time when $C_{max}$ observed.
$t_{1/2}$	Apparent terminal half-life

**Protocol summary**

<b>Full title</b>	Arterial hypoxaemia and its impact on the pharmacokinetics-pharmacodynamics of sildenafil; a randomised, double-blind, placebo-controlled trial.
<b>Brief title</b>	A study to investigate the effect of low oxygen levels on the uptake of Sildenafil.
<b>Sponsor and clinical phase</b>	University of South Wales/ Phase I
<b>Investigation type</b>	Drug
<b>Study type</b>	Pharmacokinetic
<b>Purpose and rational</b>	To determine the effect of acute hypoxia (low oxygen levels) on the pharmacokinetics (PK) and pharmacodynamics (PD) of Sildenafil in healthy male volunteers. This is clinically relevant given that millions of lowlanders who sojourn to terrestrial high-altitude are prescribed medication to prevent illness notwithstanding patients with diseases of the circulation characterised by arterial hypoxaemia. However, to what extent acute hypoxia impacts drug PK-PD remains unclear.
<b>Primary Objective(s)</b>	To determine if acute hypoxia alters the PK of a single dose of Sildenafil (100 mg) in healthy volunteers.
<b>Secondary Objective(s)</b>	To determine potential mechanisms that may explain any changes in Sildenafil PK. These include the analysis of regional blood flow (cerebral, pulmonary, hepatic and renal), minute ventilation, partial pressures of end-tidal oxygen and carbon dioxide, heart rate, blood pressure, plasma volume shifts, blood brain barrier integrity and oxidative-nitrosative stress.
<b>Study design</b>	The project will be a randomised, double-blind, placebo-controlled study to investigate the influence of acute hypoxia on the PK-PD of orally administered Sildenafil (100 mg). All visits will take place at the Neurovascular Research Laboratory, University of South Wales. An initial pre-screening visit (Visit 1) will involve a medical health screening to determine participant eligibility. Participants will

## Appendix 1

	<p>be randomly assigned to either Group 1 (Sildenafil Group) or Group 2 (Placebo Group) and will be required to attend two more visits (Visit 2 and 3) which will last approximately. ~10 hours each (separated by at least one week). One of these visits will be under conditions of low oxygen levels (hypoxia: 12% O<sub>2</sub>) achieved using a normobaric environmental chamber, whilst the other visit will be under normal conditions (normoxia: 21% O<sub>2</sub>). Following 60 minutes of rest, participants will receive a drug (Group 1: 100 mg of Sildenafil; Group 2: Placebo). Repeated blood sampling and measurements of cerebral, pulmonary, hepatic and renal blood flow and cardiorespiratory parameters will be conducted at various time points (<b>Figure 1</b>).</p>
<p><b>Population</b></p>	<p>Group 1 - 15 healthy male volunteers aged 18 – 35 years. Group 2 - 15 healthy male volunteers aged 18 – 35 years.</p>
<p><b>Inclusion criteria</b></p>	<ul style="list-style-type: none"> <li>- Male</li> <li>- Older than 17 years of age or younger than 36 years of age.</li> <li>- No underlying medical condition</li> <li>- No history of elevated blood pressure (&gt;140 mmHg systolic or &gt;90 mmHg diastolic) or low blood pressure (&lt;90 mmHg systolic or &lt;50 mmHg diastolic)</li> <li>- No personal or direct familial history of cardiovascular disease</li> <li>- No liver problems or hepatic impairment -</li> <li>- No bleeding disorders.</li> <li>- No severe cardiovascular disorders such as unstable angina or severe cardiac failure).</li> <li>- No History of stroke or myocardial infarction.</li> <li>- No known history of inherited eye disease or loss of vision due to non-arteritic anterior ischaemic optic neuropathy (NAION)</li> <li>- No known history of hereditary degenerative retinal disorders such as retinitis pigmentosa.</li> <li>- No physical deformity of the penis</li> <li>- Have not consumed medication in last 4 weeks, excluding paracetamol/non-steroidal anti-inflammatory medication.</li> <li>- Not a regular recreational drug user within the previous 10 years</li> <li>- Non-smoker (past or present)</li> <li>- Willing to consent to disclose information regarding their general health.</li> </ul>



## Appendix 1

	<ul style="list-style-type: none"> <li>- No history of acute mountain/altitude sickness</li> <li>- Haven't donated blood in the past 3 months</li> <li>- No history of anaemic and/or iron insufficiency and/or sickle cell anaemia</li> <li>- No known allergic reaction to Sildenafil, tradename VIAGRA®, REVATIO®</li> <li>- Lactose tolerant (due to the sildenafil supplement and placebo listing lactose as an active ingredient)</li> <li>- Assessed to be fit to participate following clinical review by the medical supervisor.</li> <li>- Prior to attending the laboratory for Visit 2 and 3, completed a 12-hour overnight fast and having followed a low nitrite-nitrate diet, avoided vigorous exercise, alcohol, and caffeine 24-hours prior to arrival.</li> <li>- Engages in moderate aerobic exercise (e.g. running, cycling) for more than 150 minutes, three times per week.</li> </ul>
<p><b>Exclusion criteria</b></p>	<ul style="list-style-type: none"> <li>- Female</li> <li>- Younger than 18 years of age or older than 35 years of age.</li> <li>- known underlying medical condition</li> <li>- Brachial blood pressure (&gt;140 mmHg systolic or &gt;90 mmHg diastolic) or low blood pressure (&lt;90 mmHg systolic or &lt;50 mmHg diastolic)</li> <li>- Personal or direct familial history of cardiovascular disease</li> <li>- Liver problems or hepatic impairment</li> <li>- Bleeding disorders</li> <li>- severe cardiovascular disorders such as unstable angina or severe cardiac failure.</li> <li>- History of stroke or myocardial infarction.</li> <li>- Inherited eye disease or loss of vision due to non-arteritis anterior ischaemic optic neuropathy (NAION)</li> <li>- known history of hereditary degenerative retinal disorders such as retinitis pigmentosa.</li> <li>- Physical deformity of the penis</li> <li>- Consumed medication in the last 4 weeks, excluding paracetamol/non-steroidal anti-inflammatory medication</li> <li>- Regular recreational drug use within the previous 10 years</li> <li>- Smoker (past or present)</li> <li>- Choose not to disclose information regarding their general health</li> <li>- Previously experienced acute mountain/altitude sickness</li> <li>- Donated blood in the past 3 months</li> <li>- Known to be anaemic and/or have an iron insufficiency and/or have sickle cell anaemia</li> <li>- Known allergic reaction to Sildenafil, tradename VIAGRA®, REVATIO®</li> </ul>

## Appendix 1

	<ul style="list-style-type: none"> <li>- Lactose intolerant due to the sildenafil supplement and placebo listing lactose as an active ingredient.</li> <li>- Does not engage in moderate aerobic exercise (e.g. running, cycling) for more than 150 minutes, three times per week.</li> <li>- Assessed to be unfit to participate following clinical review by the medical supervisor.</li> </ul> <p>Once enrolled into the study, the following exclusion criteria will apply:</p> <ul style="list-style-type: none"> <li>- Clinical AMS (combined total LL score (self assessment + clinical scores) of <math>\geq 5</math> points and ESQ-C score <math>\geq 0.7</math> points)</li> <li>- Headache score (<math>&gt;70</math>)</li> <li>- Blood pressure (<math>&gt;180</math> mmHg or <math>&lt;90</math> mmHg systolic blood pressure and/or <math>&gt;120</math> mmHg diastolic blood pressure)</li> <li>- Heart Rate (<math>&gt;</math> predicted maximum heart rate [<math>220 - \text{age in years}</math>])</li> <li>- Oxygen Saturation (<math>&lt;70\%</math>)</li> <li>- If researchers are unable to find a suitable vein or failing to cannulate the participant on two consecutive occasions</li> <li>- If participants feel they are unable to continue the study as a result of an unrelated injury or change in personal circumstances</li> <li>- Participant chooses to voluntarily withdraw from the study</li> </ul>
<b>Study treatment</b>	<p>Group 1 - Single oral dose of 100 mg Sildenafil on two occasions (Visit 2 and 3)</p> <p>Group 2 - Single oral dose of Placebo on two occasions (Visit 2 and 3)</p>
<b>Key assessment</b>	<p>Venous blood samples to derive PK parameters for Sildenafil and its major metabolite N-desmethylsildenafil.</p> <p>PK parameters include <math>C_{\max}</math>, <math>T_{\max}</math>, <math>K_a</math>, <math>t_{1/2a}</math>, <math>K</math>, <math>t_{1/2}</math>, <math>CL/F</math>, <math>V/F</math>, <math>AUC_{0-t_{\text{last}}}</math> and <math>AUC_{0-\infty}</math>.</p>
<b>Other assessment</b>	<p>Cerebral blood flow will be measured in the internal carotid and vertebral artery using Duplex ultrasound. Duplex ultrasound will also be used to measure pulmonary, hepatic and renal blood flow. Cardiorespiratory measurements will include minute ventilation, partial pressures of end-tidal oxygen and carbon dioxide (capnography), heart rate (3 lead echocardiogram) and blood pressure (finger photoplethysmography). Blood samples will facilitate the assessments of plasma volume shifts (haemoglobin, haematocrit), blood-brain-barrier integrity</p>

	(S100 $\beta$ , neuron- specific enolase, neurofibrillary filament light chain, tau protein, glial fibrillary acidic protein, ubiquitin C-terminal hydrolase L 1), and oxidative-nitrosative stress (DNA oxidation, lipid hydroperoxides, ascorbate free radical, nitric oxide bioavailability).
--	--

## 1. Introduction

### 1.1. Background

Acute exposure to hypoxia (low oxygen levels) is associated with altering drugs' pharmacokinetics (PK) properties that define the absorption and disposition of medicinal drugs subsequent to free radical-mediated alterations in cytochrome P (CYP)-450 activity, pH, protein binding, distribution volume and perfusion. This is clinically relevant given that millions of lowlanders who sojourn to terrestrial high- altitude are prescribed medication to prevent illness notwithstanding patients with diseases of the circulation characterised by arterial hypoxaemia. However, to what extent acute hypoxia impacts drug PK remains unclear and there are no published studies to date describing changes in the PK of Sildenafil, a widely prescribed selective inhibitor of cGMP-specific phosphodiesterase type 5 (D. M. Bailey, Stacey, & Gumbleton, 2018). Closer patient monitoring and dose adjustments to maintain therapeutic efficacy and avoid incidental toxicity may be required if arterial hypoxaemia can alter Sildenafil PK properties.

### 1.2. Purpose and hypothesis of the research study

The purpose of this study is to determine the effect of acute hypoxia on the PK parameters of Sildenafil/ N-desmethylsildenafil in healthy volunteers. We hypothesise that acute hypoxia will alter the mean of PK parameters of Sildenafil and/or N- desmethylsildenafil, when compared to the normoxia condition. Secondly, the study aims to determine any potential mechanisms that may explain any changes in Sildenafil/ N-desmethylsildenafil PK during hypoxia exposure. We hypothesise that acute hypoxia will alter regional blood flow (cerebral, pulmonary, hepatic and renal), minute ventilation, partial pressures of end-tidal oxygen and carbon dioxide, heart rate, blood pressure, plasma volume shifts, blood brain barrier integrity and oxidative- nitrosative stress in both the Sildenafil and Placebo group (the placebo group highlighting the influence of acute hypoxia independently of the effects of Sildenafil).

## 2. Study objective and endpoints

**Primary Objective:** To determine if acute hypoxia alters the PK of a single dose of Sildenafil (100 mg) in healthy volunteers.

**Primary End Point:** Venous blood samples will be obtained to derive PK parameters for Sildenafil and its major metabolite N-desmethylsildenafil. PK parameters include:  $C_{max}$ ;  $T_{max}$ ;  $K_a$ ;  $t_{1/2a}$ ;  $K$ ;  $t_{1/2}$ ;  $CL/F$ ;  $V/F$ ;  $AUC_{0-t_{last}}$ ; and  $AUC_{0-\infty}$ .

**Secondary Objective:** To determine potential mechanisms that may explain any changes in Sildenafil/ N-desmethylsildenafil PK. These include the analysis of regional blood flow

## Appendix 1

(cerebral, pulmonary, hepatic and renal), minute ventilation, partial pressures of end-tidal oxygen and carbon dioxide, heart rate, blood pressure, plasma volume shifts, blood brain barrier integrity and oxidative-nitrosative stress.

**Secondary End Point:** Cerebral blood flow will be measured in the internal carotid and vertebral artery using Duplex ultrasound. Duplex ultrasound will also be used to measure pulmonary, hepatic and renal blood flow. Cardiorespiratory measurements will include minute ventilation, partial pressures of end-tidal oxygen and carbon dioxide (capnography), heart rate (3 lead echocardiogram) and blood pressure (blood pressure sphygmomanometer). Venous blood sampling will also facilitate the assessment of plasma volume shifts (haemoglobin, haematocrit), blood-brain-barrier integrity (S100 $\beta$ , neuron-specific enolase, neurofibrillary filament light chain, tau protein, glial fibrillary acidic protein, and ubiquitin C-terminal hydrolase L1) and oxidative-nitrosative stress (DNA oxidation, lipid hydroperoxides, ascorbate free radical and nitric oxide bioavailability).

### 3. Investigational plan

#### 3.1. Study design

The study will be a randomised, double-blind, placebo-controlled design to investigate the influence of acute hypoxia on the PK-PD parameters of orally administered Sildenafil (100 mg) and is outlined in **Figure 1**. All visits will take place at the Neurovascular Research Laboratory, University of South Wales. An initial pre- screening visit will involve written informed consent (Appendix 3) being obtained from the participant, followed by a medical health screening to determine participant eligibility. All potential participants will be assigned a Subject ID and entered into the recruitment and screening log (Appendix 8). A letter will be sent to the participant's general practitioner (Appendix 5) informing them of the study along with a copy of the participant information sheet. Contact details and details of the participant's general practitioner will be recorded in the personal details form (Appendix 9). The general practitioner will inform Dr Coulson of any reasons the participant cannot partake in the study. Participants will be randomly assigned to either Group 1 or Group 2 and will be required to attend two more visits (Visit 2 and 3) which will last approximately 10 hours each (separated by at least one week). One of these visits will be under conditions of low oxygen levels (hypoxia: 12% O<sub>2</sub>) achieved using a normobaric environmental chamber, whilst the other visit will be under normal conditions (normoxia: 21% O<sub>2</sub>). Following 60 minutes of rest, participants will receive a drug administration (Group 1: 100 mg of Sildenafil [Sildenafil Teva]; Group 2: Placebo [placebo-world: lactose tablet]) whilst blindfolded to maintain blinding. Repeated blood sampling and measurements of cerebral, pulmonary, hepatic and renal blood flow and cardiorespiratory parameters will be conducted at various time points (**Figure 1**). This experimental design will allow for a maximum of two participants to be examined simultaneously.

## Appendix 1

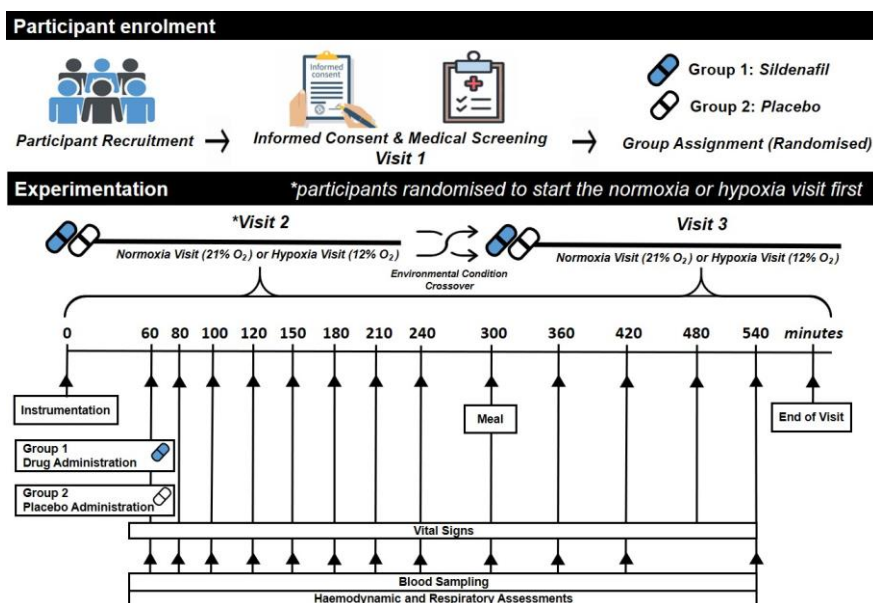


**Figure 1. Schematic of experimental design and testing protocol.**

### 3.2. Study setting

The study will take place at the Neurovascular Research Laboratory, University of South Wales, Faculty of Life Science and Education, Glyntaff Campus, CF37 4AT.

### 3.3. Risks and benefits

All participants will receive a medical screening including an assessment of cerebral, pulmonary, renal and hepatic blood flow. Participants will also benefit from experiencing simulated high-altitude in an environmental chamber. The risk to the participant will be minimised by adhering to a strict eligibility and exclusion criteria, a medical screening and continual clinical monitoring. The main risks associated with the proposed project is the hypoxic environment and Sildenafil administration (outlined in detail below). Lower risks were identified as incidental findings associated with the haemodynamic and cardiorespiratory assessments, venous blood sampling. Both low and high risks expected in this study have been detailed below:

**Hypoxic environment:** There is a risk of experiencing acute mountain sickness (AMS) in the proposed study as symptoms typically present within 6 hours of exposure to 12 % O<sub>2</sub> (equivalent to 4,500 m terrestrial altitude) (D. M. Bailey et al., 2009). Symptoms will be assessed using a combination of HAH Visual Analogue Score (HAH), Lake Louise Score (LLS) and the ESQ-Cerebral Symptoms Questionnaire (ESQ) (Appendix 13) every 60 minutes during visits 2 and 3 and recorded in the participant's Case Report Form (Appendix 6). Clinical AMS will be defined if a participant presents with a combined total LL score (self-assessment + clinical scores) of  $\geq 5$  points and ESQ-C score  $\geq 0.7$  points (D.M. Bailey et al., 2006). Additionally, heart rate, oxygen saturation, and blood pressure will also be monitored every 60 minutes throughout each visit.

Thresholds for termination of testing are as follows:

- Clinical AMS (combined total LL score (self-assessment + clinical scores) of  $\geq 5$  points and ESQ-C score  $\geq 0.7$  points)
- Headache score ( $>70$ )
- Heart Rate ( $>$  predicted maximum heart rate  $[220 - \text{age}]$ )

## Appendix 1

- Oxygen Saturation (<70%)
- Blood pressure (>180 mmHg or <90 mmHg systolic blood pressure and/or >120 mmHg diastolic blood pressure)

In the event any of these thresholds are exceeded, testing will be immediately terminated and the participant removed to the normoxic control environment for recovery, as recommended (West, 2007). AMS scores, headache scores, heart rate, oxygen saturation and blood pressure will be monitored every 5 minutes for the following 30 minutes or until normal. Additionally, at both 2 and 48 hours after leaving the laboratory, participants will receive a follow-up phone call from the medical supervisor to assess their health status. Should symptoms persist, the participant will be recommended to visit their general practitioner. However, given the capability to rapidly remove participants from the hypoxic environment (i.e. normobaric hypoxia in a laboratory rather than hypobaric hypoxia associated with terrestrial high-altitude), the risks of any lasting symptoms are very unlikely.

***Sildenafil administration:*** Sildenafil has been used without serious incident previously in studies involving hypoxia and exercise (Appendix 12; Ghofrani et al., 2004; Hsu et al., 2006; Kjaergaard et al., 2007; Ricart et al., 2005), including a previous study conducted at the University of South Wales (#7070LSE). The low risk of an adverse effect is reduced further due to the participants selected being young and healthy and the exclusion of other concurrent medication. In the unlikely event of an allergic reaction (incidence not known), a medical supervisor will be in attendance with a resuscitation kit. If the medical supervisor deems it necessary, the participant will be transported immediately to the nearest accident and emergency department (Royal Glamorgan Hospital, Ynys Maerdy, Llantrisant). Participants will be instructed to not eat any grapefruit products and organic nitrates while taking sildenafil, to avoid any impact on PK parameters (Jetter et al., 2002) such as hypotension, which was reported as a clinically significant symptom when combined with Sildenafil (Webb, Freestone, Allen, & Muirhead, 1999). Participants will be directed to read the Sildenafil leaflet (Summary of Product Characteristics, Appendix 11) alongside the participant information sheet (Appendix 2) which contains these risks, prior to consent. A medical supervisor will be in attendance throughout each experimental visit to monitor the participant's health during hypoxia exposure and Sildenafil administration.

***Duplex ultrasound assessments:*** Participants will be required to wear a hospital gown to maintain personal dignity whilst performing the pulmonary, hepatic and renal ultrasound assessments (access is required to the chest and stomach area).

***Venous blood sampling:*** There will be transient discomfort from needle insertion for the cannula. This is unavoidable but can be mediated to an extent by the cannula only being inserted by a suitably qualified medical supervisor.

***Incidental findings:*** In the unlikely event of discovering a clinically significant abnormality during either visit, if urgent attention is required, participant will be referred to the accident and emergency (A and E) department at the Royal Glamorgan Hospital and will be treated as a medical emergency. If any non-life-threatening abnormalities are detected, the individual will be referred by the medical supervisor for an outpatient echocardiogram and 12 lead ECG for review in Dr Coulson's Clinic at the University Hospital, Llandough, of which standard healthcare practice includes care of the individuals' health and wellbeing. Additionally, the participant will be excluded from the study and advised to visit their general practitioner for further consultation.

***Time commitment:*** The pre-screening visit will last approximately ½ hour and Visit 2 and 3 will each last ~10 hours each, yielding a cumulative time commitment of ~ 20 ½ hours of total time commitment. This is outlined in the participant information sheet (Appendix 2)

## Appendix 1

and participants will be reminded again on the day of each visit, the duration of time they will be required for that day.

**General environmental risks:** There are also several minor risks associated with this project with regards to general laboratory equipment and procedures, which have also been identified and assessed (please see Appendix 10).

### 4. Population

The study population will consist of young healthy male volunteers aged 18 – 35 years old.

#### 4.1. Inclusion criteria

To be eligible for inclusion into the study, all participants population must adhere to the following criteria:

- Male
- Older than 17 years of age or younger than 36 years of age.
- No underlying medical condition
- No history of elevated blood pressure (>140 mmHg systolic or >90 mmHg diastolic) or low blood pressure (<90 mmHg systolic or <50 mmHg diastolic)
- No personal or direct familial history of cardiovascular disease
- No liver problem or hepatic impairment
- No bleeding disorders
- No severe cardiovascular disorders such as unstable angina or severe cardiac failure).
- No History of stroke or myocardial infarction
- No known history of inherited eye disease or loss of vision due to non-arteritic anterior ischaemic optic neuropathy (NAION)
- No known history of hereditary degenerative retinal disorders such as retinitis pigmentosa
- No physical deformity of the penis
- Have not consumed medication in last 4 weeks, excluding paracetamol/non-steroidal anti-inflammatory medication
- Not a regular recreational drug user within the previous 10 years
- Non-smoker (past or present)
- Willing to consent to disclose information regarding their general health
- No history of acute mountain/altitude sickness
- Haven't donated blood in the past 3 months
- No history of anaemic and/or iron insufficiency and/or sickle cell anaemia
- No known allergic reaction to Sildenafil, tradename VIAGRA®, REVATIO®
- Lactose tolerant (due to the sildenafil supplement and placebo listing lactose as an active ingredient)
- Assessed to be fit to participate following clinical review by a medical supervisor.
- Prior to attending the laboratory for Visit 2 and 3, completed a 12-hour overnight fast and having followed a low nitrite-nitrate diet, avoided vigorous exercise, alcohol and caffeine 24-hours prior to arrival.
- Provide written informed consent

#### 4.2. Exclusion criteria

A participant with the following criteria will be excluded from the study:

## Appendix 1

- Female
- Younger than 18 years of age or older than 35 years of age.
- Has a known underlying medical condition
- Elevated blood pressure (> 150 mmHg systolic or > 90 mmHg diastolic) or low blood pressure (< 90 mmHg systolic or < 50 mmHg diastolic)
- Personal or direct familial history of cardiovascular disease
- A liver problem or hepatic impairment
- A bleeding disorders
- Severe cardiovascular disorders such as unstable angina or severe cardiac failure.
- Known history of stroke or myocardial infarction
- Inherited eye disease or loss of vision due to non-arteritic anterior ischaemic optic neuropathy (NAION)
- Known history of hereditary degenerative retinal disorders such as retinitis pigmentosa
- A physical deformity of the penis
- Consumed medication in last 4 weeks, excluding paracetamol/non-steroidal anti-inflammatory medication
- Regular recreational drug use within the previous 10 years
- Smoker (past or present)
- Choose not to disclose information regarding their general health
- Previously experienced acute mountain/altitude sickness
- Donated blood in the past 3 months
- Known to be anaemic and/or have an iron insufficiency and/or sickle cell anaemia
- Known allergic reaction to Sildenafil, tradename VIAGRA®, REVATIO®
- Lactose intolerant due to the sildenafil supplement and placebo listing lactose as an active ingredient.
- Assessed to be unfit to participate following clinical review by a medical supervisor.
- Prior to attending the laboratory for Visit 2 and 3, the participant has not completed a 12-hour overnight fast and having followed a low nitrite-nitrate diet, avoided vigorous exercise, alcohol and caffeine 24-hours prior to arrival.
- Not willing to provide written informed consent

Once recruited into the study, the following exclusion criteria will apply:

- Clinical AMS (combined total LL score (self assessment + clinical scores) of  $\geq 5$  points and ESQ-C score  $\geq 0.7$  points)
- Headache score (>70)
- Blood pressure (>180 mmHg or <90 mmHg systolic blood pressure and/or >120 mmHg diastolic blood pressure)
- Heart Rate (> predicted maximum heart rate [220 – age in years])
- Oxygen Saturation (<70%)
- If researchers are unable to find a suitable vein or failing to cannulate the participant on two consecutive occasions
- If participants feel they are unable to continue the study as a result of an unrelated injury or change in personal circumstances
- Participant chooses to voluntarily withdraw from the study

## 5. Treatment

### 5.1. Investigational and control drugs



## Appendix 1

Group 1 will receive one oral dose of 100 mg Sildenafil on two occasions (Visit 2 and 3).

Group 2 will receive one oral dose of Placebo (lactose) on two occasions (Visit 2 and 3).

### 5.2. Randomisation

Following the pre-screening visit (Visit 1) eligible participants will be randomised into Group 1 or Group 2. Participants will then be randomised to complete the normoxia or hypoxia condition first for Visit 2 (e.g. normoxia visit). Visit 3 will consist of the other condition (e.g. hypoxia visit). Randomisation will be achieved via a fair coin toss (heads = Group 1, tails = Group 2; then, heads = normoxia visit first, tails = hypoxia visit first).

### 5.3. Blinding

The participants and the investigators analysing the data will remain blind to treatment groups (Group 1/ Group 2) from the time of randomisation until the data has been analysed.

To ensure successful blinding, the following methods will be used:

- The randomisation data (stored in the randomisation log – Appendix 22) will be strictly confidential and only accessible by the Chief Investigator (Dr Coulson) and Medical Supervisor until the un-blinding time.
- The randomisation codes associated with the participant treatment groups will only be disclosed following data analysis, in the case of participant emergencies or at the conclusion stage of the study.
- Participants will be blindfolded during placebo/sildenafil administration to avoid any issues associated with differences in markings, colour or shape of the tablets.

### 5.4. Treating the subjects

#### 5.4.1. Subjects numbering

Prior to any medical screening (Visit 1) participants will be given a unique subject ID. All subject ID's will start with "SIL" and will be followed by a three-digit number between **001** and **100**. The first participant recruited into the study will be **SIL001**. Once a number has been assigned for a participant, it will not be used again.

#### 5.4.2. Dispensing the investigation drug

Sildenafil Teva (100 mg) will be obtained by generic prescription. Administration of Sildenafil will be conducted by the Medical Supervisor, who will be present throughout the study.

#### 5.4.3. Handling of study treatment

Both Sildenafil and the Placebo tablets will be received by Dr Coulson at Neurovascular Research Laboratory at the University of South Wales. All tablets will be kept in a secure location (University of South Wales, GK002) only accessible by the research team. A substance storage and withdrawal log (Appendix 15) will be updated throughout the study duration.

#### 5.4.4. Instruction for prescribing and taking study medication

The University Hospital of Wales will supply the investigators with Sildenafil based on Dr Coulson's prescription. The participants will be provided with medication packs containing either one tablet of Sildenafil (100 mg) or one tablet of Placebo in Visit 2 and 3. Following

## Appendix 1

a 12 hour overnight fast, participants will consume an oral dose of Sildenafil or Placebo with 200 mL of water after 60 minutes of rest, whilst wearing a blindfold. Participants will remain fasted for a further 4 hours. After this, a standardised liquid meal supplement (energy, 230kcal; protein, 35g; carbohydrate, 19.6g; fat, 1.1g) (SCI-MX Milkshake, SCI-MX Nutrition) will be consumed. Participants will be provided with water *ad libitum*, and volume monitored (Participants will be asked to consume the same amount of water at the same time points for each respective trial).

### 5.4.5. Concomitant medication

Participants currently taking medication will not be eligible to participate within the study. Participants will be instructed to notify the research team after taking any new medications whilst enrolled within the study.

### 5.4.6. Prohibited medication and lifestyle

Participants currently taking medication will not be eligible to participate within the study. Participants will also be asked to avoid high nitrate diet, citrus fruits and juice, vigorous exercise, alcohol and caffeine 24-hours prior to arrival to Visit 2 and 3.

## 5.5. Study completion and discontinuation

### 5.5.1. Study completion and post -study follow up

The Chief Investigator will provide a follow-up of participant medical care for participants that have permanently withdrawn from the study due to medical illness or will refer them for appropriate ongoing care. If urgent attention is required, the individual will be referred to the accident and emergency (A and E) department at the Royal Glamorgan Hospital and will be treated as a medical emergency. If any non-life- threatening abnormalities are detected, the individual will be referred by the medical supervisor for an outpatient echocardiogram and 12 lead ECG for review in Dr Coulson's Clinic at the University Hospital of Wales, of which standard healthcare practice includes care of the individuals' health and wellbeing.

### 5.5.2. Discontinuation of the study

Discontinuation of the study can be decided by either the participant or the investigators. Participants will be excluded from the study under the following circumstances:

- Clinical AMS (combined total LL score (self assessment + clinical scores) of  $\geq 5$  points and ESQ-C score  $\geq 0.7$  points)
- Headache score ( $>70$ )
- Blood pressure ( $>180$  mmHg or  $<90$  mmHg systolic blood pressure and/or  $>120$  mmHg diastolic blood pressure)
- Heart Rate ( $>$  predicted maximum heart rate [ $220 - \text{age in years}$ ])
- Oxygen Saturation ( $<70\%$ )
- If researchers are unable to find a suitable vein or failing to cannulate the participant on two consecutive occasions
- If participants feel they are unable to continue the study as a result of an unrelated injury or change in personal circumstances
- Participant chooses to voluntarily withdraw from the study

### 5.5.3. Withdrawal of informed consent

Participants may voluntarily withdraw from the study at any time and for any reasons. The

## Appendix 1

definition of a withdrawal of consent is:

- The subject does not want to participate in this study any more
- The subject does not want any further visits to the study location.
- The subject does not want any further contact regarding the study.
- The subject does not allow analysis of already obtained blood samples.

Under these circumstances, the investigators must make every effort (e.g. contact the participant by telephone, email or letter) to determine the reason of withdrawing and report this information in the case report form. Participants are free to withdraw from the study at any time without having to give a reason. In this event, “no reason provided” should be noted. All experimental data collected at subsequent visits will be considered missed. If the subject has withdrawn their consent, personalised data should be discarded, but their anonymised case report form held for audit purposes for at least 30 years (as per GCP guidance). Seeking further contact of the participant is not allowed unless for a safety issue requiring communicating and follow up.

### 5.5.4. Loss of follow-up

For the participants whose status is unclear whether they are withdrawn from the study or not, occurring when the participant does not attend the study visits without stating an intention of discontinue or withdrawal from the study. In this situation the investigators must make the effort to contact the participants and document all the steps taken to contact the subjects e.g. the date and the way of contacting (telephone, email, letter). The participant will be considered as loss of follow-up when the scheduled end time of the study visit has passed. If the visits do not reschedule the participant will be considered as withdrawn and this is to be documented in the case report form accordingly. Personalised data should be discarded and the case report form stored in the trial master file for audit purposes.

## 6. Visit schedule and assessment

Subjects must be seen for all visits on the designated day. Missed or rescheduled visits doesn't mean automatic discontinuation of the subjects from the study.

**Table 1: Assessment schedule**

Visit name	Visit 1	Visit 2	Visit 3
Participant information sheet	x		
Written informed consent	x		
Inclusion/exclusion criteria	x		
COVID-19 Checks	x	x	x
Demography	x		
Medical history	x		
Smoking history	x		
Physical exam	x		

## Appendix 1

Height	X		
BMI	X		
Body fat percentage	X		
12-lead electrocardiogram	X	X	X
Blood pressure	X	X	X
Administration of 100 mg Sildenafil		X	X
Administration of Placebo		X	X
HAH Visual Analogue Score, Lake Louise Score (LLS), ESQ-Cerebral Symptoms Questionnaire	X	X	X
Blood sampling for PK		X	X
Blood sampling of other biomarkers ( <i>see Table 2</i> )		X	X
Internal carotid and vertebral artery blood flow		X	X
Renal artery blood flow		X	X
Hepatic artery blood flow		X	X
Pulmonary artery blood flow		X	X
Minute ventilation		X	X
Partial pressures of oxygen and carbon dioxide		X	X
Haemoglobin		X	X
Haematocrit		X	X

## Appendix 1

**Table 2. Other Assessments (Visit 2 and 3)**

<b>Biomarker:</b>	<b>Whole Blood Volume (mL):</b>	<b>Collection Time Points (minutes):</b>	<b>Total Whole Blood Volume (mL):</b>	<b>Medium:</b>	<b>Technique/Function:</b>
1. S100 $\beta$ , NSE	2	60, 300, 540	6	Serum (SST)	hsELISA/ structural integrity
2. NFL, gfap, Uchl-1 and tau	2	60, 300, 540	6	Serum (SST)	hsELISA/ structural integrity
3. LOOH	1	60, 80, 100, 120, 150, 180, 210, 240, 270, 300, 420, 540	13	Serum (SST)	UV spec/Lipid peroxidation
4. PK Metabolites	6	60, 80, 100, 120, 150, 180, 210, 240, 270, 300, 420, 540	84	Plasma (K-EDTA)	LCMS/sildenafil and N-desmethylsildenafil levels
5. AFR	2	60, 80, 100, 120, 150, 180, 210, 240, 270, 300, 420, 540	22	Plasma (K-EDTA)	EPR spec/free radicals
6. Plasma NO	2	60, 80, 100, 120, 150, 180, 210, 240, 270, 300, 420, 540	22	Plasma (K-EDTA)	OBC/ nitric oxide bioavailability
7. RBC NO	2	60, 80, 100, 120, 150, 180, 210, 240, 270, 300, 420, 540	No additional whole blood required.	RBC (K-EDTA)	OBC/nitric oxide bioavailability

8. DNA oxidation	1	60, 80, 100, 120, 150, 180, 210, 240, 270, 300, 420, 540	No additional whole blood required.	RBC (K-EDTA)	HPLC/oxidative mutagenesis
9. Hb & Hct	1	60, 80, 100, 120, 150, 180, 210, 240, 270, 300, 420, 540	13	Whole Blood	Haemoglobin/ Haematocrit

**Whole Blood Required Per Visit: 166 mL**

NSE, neuron-specific enolase; NFL, neurofibrillary filament light chain; tau protein; gfap, glial fibrillary acidic protein; Uchl-1, ubiquitin C-terminal hydrolase L1; LOOH, lipid hydroperoxides; PK, pharmacokinetic measurements; AFR, ascorbate free radical; NO, nitric oxide; hsELISA, high sensitivity enzyme-linked immunosorbent; UV spec, ultraviolet spectroscopy; LCMS, liquid chromatography mass spectrometry; EPR, electron paramagnetic resonance; OBC, ozone-based chemiluminescence; HPLC, high-performance liquid chromatography; Hb, haemoglobin; Hct, haematocrit; RBC, red blood cells.

### 6.1. Subjects demographics/ other baseline characteristics

Subjects demographic and baseline characteristic data that will be collected from the participants include age, race, ethnicity, height, weight, smoking history, past and current medical conditions.

### 6.2. Physical examination

A physical examination will be performed during the pre-screening visit by the medical supervisor. It will include the examination of general appearance, cardiovascular system, respiratory system, abdomen, nervous system and locomotive (musculoskeletal) system. Information of the physical examination must be reported, and relevant findings that lead to subject exclusion must be recorded in case report form (Appendix 6).

### 6.3. Cardiovascular Screening Assessment

A resting 12-lead ECG (CT8000P, SECA, Hamburg, Germany) will be obtained and reviewed by the medical supervisor prior to any subsequent visits. If any clinically significant abnormalities are detected that require urgent attention, the participant will be referred to the accident and emergency department at the Royal Glamorgan Hospital and will be treated as a medical emergency. If any non-life-threatening abnormalities are detected, the participant will be referred by the medical supervisor for an outpatient echocardiogram and 12 lead ECG for review in Dr Coulson's Clinic at the University Hospital, Llandough. Individuals with detected abnormalities will be excluded from further participation in the study

### 6.4. Stature, Mass and Body Fat Percentage

Stature will be assessed using a stadiometer (Seca, Cardiokinetics, UK) and body mass will be assessed using a weighing scale (Seca, Cardiokinetics, UK). Body fat percentage will be also assessed using bioelectrical impedance analysis (BIA; non- invasive; Tanita BC-418MA, Japan). BIA works by sending small and harmless multi- frequency electrical currents around the body to give an estimation of body fat.

### 6.5. Haemodynamic and Respiratory Assessments

At the specified time-points for Visit 2 and 3 (illustrated in **Figure 1**), Duplex ultrasound will be used to measure blood flow in the internal carotid artery and vertebral artery, renal artery, hepatic artery and pulmonary artery. Mean arterial blood pressure (MAP) and heart rate will be measured using a blood pressure sphygmomanometer and a three-lead electrocardiogram, respectively. Finally, changes in respiratory ventilation and the partial pressures of end-tidal oxygen and carbon dioxide will be measured via capnography. These measurements are described in more detail below.

**Duplex Ultrasound:** Duplex Ultrasound incorporates the same fundamental principles as TCD to measure the speed of blood flowing through the arteries, but it also allows for the measurement of vessel diameter to quantify blood flow. Diameter and blood velocity recordings of the internal carotid artery and vertebral artery will be obtained using a 10 MHz linear array probe attached to a peripheral ultrasound machine (Terason 3000, Teratech, Burlington, MA, USA). Diameter and blood velocity recordings of the renal artery, hepatic artery and pulmonary artery will be obtained using a 10 MHz curved array transducer attached to a peripheral ultrasound machine (Aloka, ProSound Alpha 10).

**Three-lead Electrocardiogram:** A three-lead electrocardiogram (SmartMedical, Moreton-in-Marsh, Gloucestershire, UK) will be used to continuously measure heart rate. Electrodes one and two will be placed mid clavicular on the left and right side with electrode three placed mid-clavicular on the bottom left rib.

## Appendix 1

**Capnography:** Respiratory ventilation and partial pressures of end-tidal oxygen and carbon dioxide will be measured breath-by-breath via capnography (ML 206, ADInstruments, UK).

### 6.6. Haematology

Venous blood samples will be procured at the Neurovascular Research Laboratory at the University of South Wales via cannulation. Haemoglobin and haematocrit will be measured during Visits 2 and 3 at the specified time-points illustrated in Table 2 above.

### 6.7. Assessment of acute mountain sickness (AMS) and high-altitude headache (HAH)

AMS and HAH will be assessed using a combination of HAH Visual Analogue Score, LLS and the ESQ-C Symptoms Questionnaire (Appendix 13) every 60 minutes during Visit 2 and 3.

### 6.8. Other assessments

#### 6.8.1. Pharmacokinetics

PK samples will be collected from both groups during Visit 2 and 3, at the time points defined in Table 2. Untreated samples Group 2 (Placebo) will not be analysed. Venous blood samples will be collected at the Neurovascular Research Laboratory at the University of South Wales via cannulation. Blood samples will then be double spun, and the collected serum/plasma/red blood cells will be immediately snap-frozen in liquid nitrogen. The samples will be temporarily stored for less than 1 week in GK002 at the University of South Wales at  $-80^{\circ}\text{C}$ , before transportation to Cardiff University. This process will enforce all procedures outlined by the Human Tissue Authority (HTA). A material transfer agreement (Appendix 16) will be signed prior to transportation. Once received at Cardiff University, all samples will be stored in locked freezer at  $-80^{\circ}\text{C}$ .

Sildenafil and its active metabolite N-desmethylsildenafil will be extracted from plasma using a solid phase extraction method HLB extraction cartridge (Waters, Milford, MA, USA) and will be identified in the plasma using a validated LC-MS-MS method with lower limit of quantification (LLOQ) of 0.5 ng/mL (EPSRC UK National Mass Spectrometry Facility). The measured concentration will be expressed in ng/mL units, and all the concentrations below LLOQ will be recorded as zero. The following PK parameters will be determined, using a non-compartmental method with Phoenix WinNonline (Version 8.1): maximum concentration ( $C_{\text{max}}$ ); time to maximum concentration ( $T_{\text{max}}$ ); absorption rate constant ( $K_a$ ); absorption half-life ( $t_{1/2a}$ ); elimination rate constant ( $K$ ); elimination half-life ( $t_{1/2}$ ); oral clearance ( $CL/F$ ); oral volume of distribution ( $V/F$ ); area under the curve from time zero to the last measurable time point ( $AUC_{0-\text{last}}$ ); area under the curve from time zero to infinity ( $AUC_{0-\infty}$ ); and fraction unbound in plasma ( $F_u$ ).

#### 6.8.2. Other biomarkers

Obtained serum, plasma and red blood cell samples will be used to measure other biomarkers to explore whether hypoxia-induced ONS, plasma volume shifts or blood-brain-barrier integrity is associated with PK changes of Sildenafil. Biomarkers 5, 6, 7, 8 and 9 will be analysed and disposed of on the day of procurement at the University of South Wales. Only Biomarkers 1, 2 and 3 (Serum – does not contain relevant material) will remain stored at the University of South Wales prior to batch analysis. Blood sample collection time points for these biomarkers and measurement methods are outlined in **Table 2**.



### 7. Safety monitoring

#### 7.1. Adverse event

An adverse event (AE) is defined as any untoward occurrence in a study participant but this should be extended to include all research scenarios, especially medical or clinical scenarios. An AE does not necessarily have to have a causal relationship with the study treatment or procedure. An AE can therefore be any unfavourable and unintended sign (including an abnormal finding), symptom or disease temporally associated or detected as part of participation in research. This includes any occurrence that is new in onset or aggravated in severity or frequency from the baseline condition, or abnormal results of diagnostic procedures, including laboratory test abnormalities. In this study, AE may occur as result of sildenafil administration or due to the effect of the hypoxic exposure or a synergistic effect between both. Adverse events will be managed and governed by the Adverse Events Policy (Appendix 14).

#### 7.2. Serious adverse events (SAE)

##### 7.2.1 Definition of SAE

A SAE is defined by the International Council for Harmonisation of Technical Requirements for Pharmaceuticals for Human Use (ICH) as any untoward occurrence that meets any of the following conditions:

- Results in the death of the participant.
- Near miss incidents.
- Is life-threatening. The term “life-threatening” refers to an event in which the participant was at risk of death at the time of the event; it does not refer to an event which hypothetically might have caused death if it were more severe.
- Requires inpatient hospitalisation or prolongation of existing hospitalisation.
- Results in persistent or significant disability / incapacity. Any event that seriously disrupts the ability of the participant to lead a normal life, in other words leads to a persistent or permanent significant change, deterioration, injury or perturbation of the participant's body functions or structure, physical activity and/or quality of life.
- Is a congenital anomaly / birth defect. Exposure to the study drug before conception (in men or women) or during pregnancy that resulted in an adverse outcome in the child.
- Other medical events. Medical events that may jeopardise the subject or may require an intervention to prevent a characteristic or consequence of a SAE. Such events are referred to as ‘important medical events’ and are also considered as ‘serious’ in accordance with the definition of a SAE.

##### 7.2.1. SAE reporting

To ensure subjects safety, any SAE regardless the causality, occurring after the subjects signed the informed consent until 48 hours after the end of Visit 3, should be reported to the sponsor within 24 hours of the knowledge of the event. All follow up information of SAE including complication, progression of the initial SAE and the recurrence should be reported by the chief investigator as follow up information to the original event within 24 hours of receiving this information. All information regarding a SAE should be recorded in the Serious Adverse Event Report (Appendix 14b) in lines with Adverse Event Policy (Appendix 14). All SAEs, including those that have not previously been reported in the

## Appendix 1

Summary of Product Characteristics (Appendix 11), will be reported to the MHRA via the chief investigator.

### **7.2.2. Reporting of study treatment errors including misuse /abuse**

Medication errors are defined as unintentional errors in any steps of medication delivery including prescribing, dispensing, administration or monitoring of medication while under control of a healthcare professional, patient or consumer. Misuse refers to a situation whereby the investigational drug is intentionally and inappropriately used not in agreement with protocol instructions. Abuse refers to the persistence and excessive use of the investigational drug leading to harmful physiological effects. Any form of medication error, misuse or abuse that occurs in the study should be noted in the case report form. Furthermore, if associated with an AE or SAE this should be documented in the AE Report (Appendix 14a) or SAE report (Appendix 14b), respectively.

## **8. Data review and database management**

### **8.1. Site monitoring**

Prior to the commencement of the study at the Neurovascular Research Laboratory at the University of South Wales, a sponsor representative from the University of South Wales will review the protocol and data capturing requirements (e.g. the case report form) to ensure the integrity and the quality of the proposed study. Throughout the study period, a sponsor representative will examine:

- The completeness of participant records
- The accuracy of data entry
- The adherence to the protocol and GCP
- The correct storage, dispensing and disposal of the medicinal drug
- The correct storage of blood samples

The CI will be available at the site of the study to assist monitoring during these visits. The CI must provide source documents for each participant including screening and enrolment logs, case report forms and any AE/SAE reports. These documents must not include any information regarding subject's identity. This information will be located in the Trial Master File located at the Neurovascular Research Laboratory, University of South Wales. The Master File will contain all documents relating to the study, including participant consent forms, personal details forms, case report forms, any adverse/serious adverse event forms and will only be accessible by the named research team.

### **8.2. Data collection**

Excluding the consent form, all data will be entered and stored electronically on password-protected computers only accessible to the research team listed in the delegation of duties log (Appendix 7). Consent forms are to be securely stored at the University of South Wales in the Trial Master File.

### **8.3. Data management**

Data will be collected and securely stored at the University of South Wales. However, it is likely that copies of the electronic data files will be transferred to personal computers/laptops that belong to members of the research team to facilitate data analysis (i.e. completion in an office rather than a laboratory). To ensure confidentiality, all files will be password-protected and thus only accessible to the research team. Paper-based files will be kept in a locked cabinet as outlined previously. The aforementioned data will only

## Appendix 1

be accessible to the research team.

### 9. Data analysis

Statistical analysis will be performed using the Statistical Package for the Social Sciences Version 24 (SPSS Inc., Illinois, United States of America). All analysis for the proposed study will be quantitative. Distribution normality will be assessed using repeated Shapiro Wilks W tests. PK parameters will be analysed using a 2-way (condition  $\times$  time-point) repeated measures analysis of variance (ANOVA) and Bonferroni corrected post-hoc paired samples t-tests where appropriate. For comparison between groups for all other data, a 3-way (drug  $\times$  condition  $\times$  time-point) repeated measures analysis of variance (ANOVA) and Bonferroni corrected post-hoc paired samples t-tests where appropriate. Pearson Product Moment Correlations will be applied to determine relationships. Results will be presented using means, medians standard deviations, point estimates, 95% confidence intervals and P-values.

#### 9.1 Subject demographics and baseline characteristics

The number of enrolled, randomised and withdrawn subjects with subsequent reasons will be collectively summarised. Demographics, baseline characteristics and medical history will be summarised overall. Descriptive statistics will be used to calculate mean, median, standard deviations, minimum and maximum for continuous variable whereas the categorical variable will be presented as percentage.

#### 9.2 Hypothesis

The null hypothesis of the comparison between hypoxia and normoxia on PK parameters of sildenafil and its metabolite N-desmethylsildenafil are described below:

H0:  $\mu_1 = \mu_2$ . The null hypothesis is that there is no difference in mean of PK parameters of sildenafil and N-desmethylsildenafil between hypoxic ( $\mu_1$ ) and normoxic group ( $\mu_2$ ).

Versus H1:  $\mu_1 \neq \mu_2$ ; whereby there is a significant difference between the mean of PK parameters of sildenafil and N-desmethylsildenafil between hypoxic ( $\mu_1$ ) and normoxic group ( $\mu_2$ ).

#### 9.3 Pharmacokinetics

PK parameters will be calculated using Phoenix WinNonline (Version 8.1) and will be listed by hypoxia or normoxia groups. Descriptive summary statistics will be presented by hypoxia and normoxia groups and individual subjects (anonymised). The summary statistics include mean, median, standard deviation, minimum and maximum values. Any concentration below the LLOQ will be treated as zero. The individual plasma concentration data will be listed by oxygen conditions: normoxia or hypoxia and blood sampling time points. The relationship between PK/PD will be explored using graphical approach; concentration vs time.

#### 9.4 Sample size calculation

Determination of sample size was calculated using Russ Lenth Software (Power calculation in Section A60), to address our primary aim. Given that there are no previous studies investigating the effect of acute hypoxia on the PK of Sildenafil, a power calculation was performed using the mean and standard deviation delta of the AUC of Sulfamethoxazole under conditions of normoxia and hypoxia (Li et al., 2009). Assuming a standard deviation of 238.3  $\mu\text{g/mL/h}$  for the variations in Sulfamethoxazole AUC between normoxic and hypoxic conditions (Li et al., 2009), a sample size of 15 per group would provide a power of 99% to detect a difference of 202.6  $\mu\text{g/mL/h}$  between conditions ( $\alpha=0.05$ ). Therefore, we plan to recruit 30 participants (15 per group). Although a high

## Appendix 1

level of participant retention is expected with this study design, in the event of withdrawals, additional participants may be recruited until group sizes are met (N=15 per group). Participants will be recruited through poster advertisement and social media.

### 10. Ethical considerations

#### 10.1 Regulatory and ethical compliance

This clinical investigational study has been designed and should be implemented, executed, and reported in accordance with ICH Harmonised Tripartite Guideline for Good Clinical Practice.

#### 10.2 Informed consent

After providing an overview of the study alongside the participant information sheet, eligible subjects will provide written informed consent (Appendix 3). Written informed consent must be obtained before conducting any assessments on participants.

#### 10.3 Protocol amendments

Any change or addition to the protocol must be approved by the sponsor, before the implementation. Any amendment that appears to act to avoid an immediate hazard to the participant can be implemented immediately provided the sponsor is subsequently notified of the protocol amendment. Any issues regarding participant safety, the CI is responsible for taking the immediate action required to protect the participant from hazard, even if this action deviates from the protocol.

#### 10.4 Confidentiality

All participant data will be securely stored and remain confidential as outlined in Section 8.2 and 8.3.

#### 10.5 Declaration of interests

There are no interests to declare.

#### 10.6 Dissemination policy

Once the study has been completed and the study report finalised, a copy of the study results will be sent to the MHRA and will be submitted for publication and/or posted in a publicly accessible database of clinical trial results.

## 11. References

Bailey, D. M., Evans, K. A., James, P. E., McEneny, J., Young, I. S., Fall, L., Ainslie, P. N. (2009). Altered free radical metabolism in acute mountain sickness: implications for dynamic cerebral autoregulation and blood-brain barrier function. *Journal of Physiology*, 587(1), 73-85. doi:10.1113/jphysiol.2008.159855.

Bailey, D. M., Roukens, R., Knauth, M., Kallenberg, K., Christ, S., Mohr, A., Bartsch, P. (2006). Free radical-mediated damage to barrier function is not associated with altered brain morphology in high-altitude headache. *Journal of Cerebral Blood Flow and Metabolism*, 26(1), 99-111.

## Appendix 1

Bailey, D. M., Stacey, B. S., & Gumbleton, M. (2018). A Systematic Review and Meta-Analysis Reveals Altered Drug Pharmacokinetics in Humans During Acute Exposure to Terrestrial High Altitude-Clinical Justification for Dose Adjustment? *High Altitude Medicine and Biology*. doi:10.1089/ham.2017.0121

Ghofrani, H. A., Reichenberger, F., Kohstall, M. G., Mrosek, E. H., Seeger, T., Olschewski, H., Grimminger, F. (2004). Sildenafil increased exercise capacity during hypoxia at low altitudes and at Mount Everest Base Camp - A randomized, double-blind, placebo-controlled crossover trial. *Annals of Internal Medicine*, 141(3), 169-177.

Hsu, A. R., Barnholt, K. E., Grundmann, N. K., Lin, J. H., McCallum, S. W., & Friedlander, A. L. (2006). Sildenafil improves cardiac output and exercise performance during acute hypoxia, but not normoxia. *J Appl Physiol* (1985), 100(6), 2031-2040. doi:10.1152/jappphysiol.00806.2005

Jetter, A., Kinzig-Schippers, M., Walchner-Bonjean, M., Hering, U., Bulitta, J., Schreiner, P., Fuhr, U. (2002). Effects of grapefruit juice on the pharmacokinetics of sildenafil. *Clin Pharmacol Ther*, 71(1), 21-29. doi:10.1067/mcp.2002.121236

Kjaergaard, J., Snyder, E. M., Hassager, C., Olson, T. P., Oh, J. K., Johnson, B. D., & Frantz, R. P. (2007). Right ventricular function with hypoxic exercise: effects of sildenafil. *Eur J Appl Physiol*, 102(1), 87-95. doi:10.1007/s00421-007-0560-2

Ricart, A., Maristany, J., Fort, N., Leal, C., Pages, T., & Viscor, G. (2005). Effects of sildenafil on the human response to acute hypoxia and exercise. *High Alt Med Biol*, 6(1), 43-49. doi:10.1089/ham.2005.6.43

Webb, D. J., Freestone, S., Allen, M. J., & Muirhead, G. J. (1999). Sildenafil citrate and blood-pressure-lowering drugs: results of drug interaction studies with an organic nitrate and a calcium antagonist. *Am J Cardiol*, 83(5A), 21C-28C.

West, J. B., Schoene, R. B. & Milledge, J. S. (2007). *High altitude medicine and physiology*. London, : Hodder Arnold.



### **Participant Information Sheet**

**Study title:** Arterial hypoxaemia and its impact on the pharmacokinetics-pharmacodynamics of sildenafil; a randomised, double-blind, placebo-controlled trial.

#### **We invite you!**

You have been invited to participate in a research project investigating the effects of low oxygen levels on the pharmacokinetics of sildenafil. The project will be conducted by Dr James Coulson (Chief Investigator), who is a Clinical Reader in Clinical Pharmacology at Cardiff University and Honorary Consultant Physician in Clinical Pharmacology, Toxicology and General (Internal) Medicine at the Cardiff & Vale University Health Board. This project will form part of a PhD thesis for Ms. Dalal Alablani, a postgraduate research student at Cardiff University. The project will be supervised by Professor Damian Bailey, Director of the Neurovascular Research Laboratory at the University of South Wales and Professor Mark Gumbleton, Head of School of Pharmacy and Pharmaceutical Sciences at Cardiff University. Please read the information sheet below to help understand why the research is being conducted and what it will require from you, should you wish to participate. Please read all of the information carefully and take time to discuss the project with others if you wish. Feel free to contact the research team if anything is unclear or if you have any further questions (contact details are provided at the end of this document). It is not compulsory to participate in this study.

#### **What is the purpose of the study?**

When you are exposed to low levels of oxygen (e.g. at high altitude or in individuals with respiratory diseases), the way oxygen is delivered to organs is altered and there are molecules in your blood that are produced called reactive oxygen species. However, it remains unknown whether these change the way in which we absorb and utilise pharmaceutical drugs. Sildenafil is a drug that relaxes blood vessels around your body and increases blood flow to particular areas of the body. We aim to establish: 1) the levels of sildenafil in the blood circulation during 9 hours of exposure to low levels of oxygen; 2) what happens to the blood flow to the brain, lungs, kidney and liver after taking sildenafil and being exposed to 9 hours of low levels of oxygen; and 3) measure the levels of reactive oxygen species and other molecules in your blood after taking sildenafil and during 9 hours of exposure to low levels of oxygen. This study will hopefully allow us to understand whether medical drugs are altered under conditions of low oxygen levels.

#### **Why have I been invited?**

You have been invited to participate in this study as you are healthy, young (18-35 years of age) male, adult, engaging in moderate aerobic exercise (e.g. running, cycling) for more than 150 minutes, for a minimum of three times per week.

### Do I have to take part?

**No**, you do not. Your participation in this study will be voluntary. If you wish to take part in the study, you will be given this information sheet to keep and asked to sign a consent form. You will always hold the right to withdraw from the study at any time, without giving a reason.

### What will happen if I take part?

An overview of the study can be seen in Figure 1. If you are interested in taking part in the study, you will be provided this information sheet and asked to contact either Mr Stacey or Ms Alablani (details provided at the end of this document) after at least one week of consideration. We will then arrange an initial visit to the Neurovascular Research Laboratory at the University of South Wales for a pre-screening assessment (Visit 1). Following successful clearance of the pre-screening visit, you will then be randomly assigned to either Group 1 or Group 2 and be required to attend the laboratory for two more visits (Visit 2 and 3). Group 1 will receive a 100 mg dose of Sildenafil (tablet) at the beginning of Visit 2 and Visit 3. Group 2 will receive a placebo (tablet) at the beginning of Visit 2 and Visit 3. You will only be told what group you have been assigned to after the study has finished. An overview of what will happen during each visit has been outlined below.

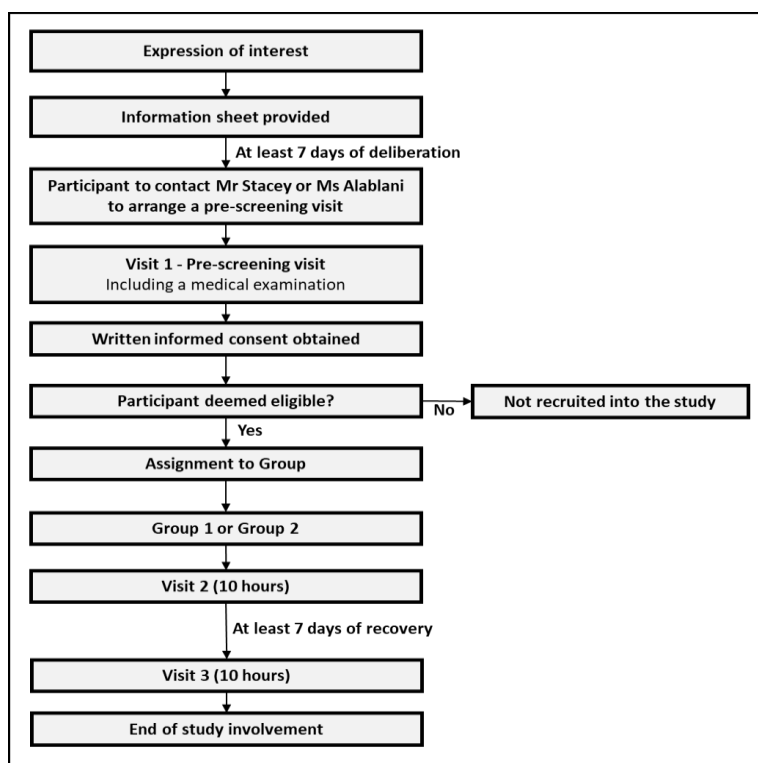


**Figure 1. Overview of study**

### **Visit 1 - Pre-screening visit (½ hour visit)**

Upon arrival to the Neurovascular Research Laboratory, a member of the research team will talk through this information sheet with you and give an overview of the protocol

## Appendix 1

below. If you are happy to proceed with the study, we will ask you to provide written informed consent. Following this, we will conduct a pre-screening assessment, which will include looking at the electrical activity of your heart (electrocardiogram) which involve attaching some wires to your chest using sticky pads (Figure 2).

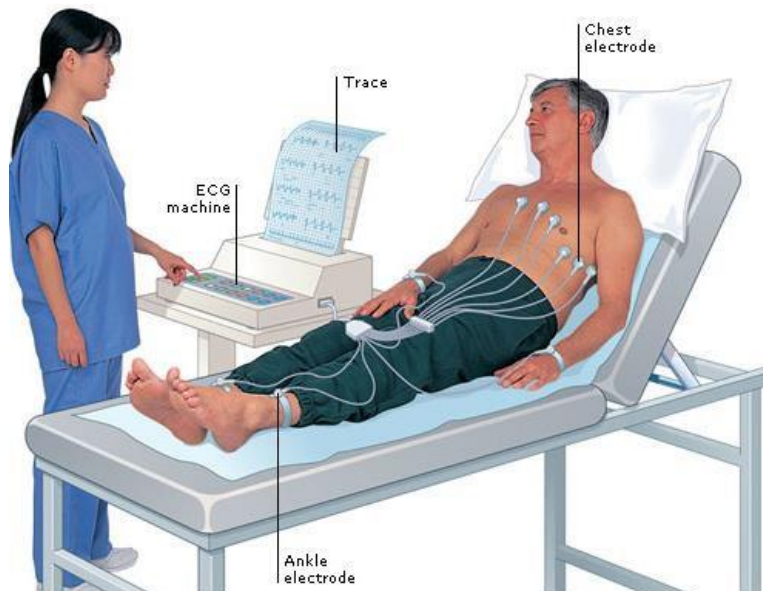


**Figure 2. A typical electrocardiogram assessment**

The medical supervisor will also ask you details about your medical history. You will be told at the end of this visit whether you are eligible to take part. If you would like to take part you will be randomly assigned to either Group 1 or Group 2. You will be asked to attend the laboratory for two more visits (Visit 2 and Visit 3) which have been detailed below. Group 1 will receive 100 mg of Sildenafil (Viagra) on both visits, whilst Group 2 will receive Placebo (lactose tablet) on both visits. You will not be told which group you have been placed in.

### **Visit 2 and 3 (10 hour visit each)**

For Visits 2 and 3, you will be required to attend both visits in the morning, having not eaten 12-hours before (overnight fast) or consumed alcohol, caffeinated beverages or partaken in intense physical activity (performing exercise at an intensity where you are breathless and unable to say a few words at a time) 24 hours prior to each visit. We also ask that you follow a low nitrite-nitrate diet, the day before these visits. This involves avoiding foods such as cured/ smoked meats, beets and leafy vegetables. These visits will be identical except, one of these visits will be under normal oxygen levels, whilst the other visit will involve exposure to low levels of oxygen (simulated high-altitude) for 9 hours in an environmental chamber. You will complete one of these

visits first, then following a minimum of 7 days recovery you will return to the laboratory to complete the other visit.

During both visits, a series of measurements will be conducted at various time points.



## Appendix 1

These have been outlined below (see “**Measurements**”). You will remain lying down or seated for the majority of the visit but you will be allowed to stand up and stretch your legs throughout the day.

### Measurements

**Body Measurements:** A measure of your height, weight and body fat percentage will be taken at the beginning of each visit.

**Blood Sampling:** We are primarily interested in whether low oxygen levels affects the amount of Sildenafil being absorbed into the body. To assess this, we require repeated blood samples over the 9 hour visit. To achieve this, a small tube (cannula) will be inserted into a vein within your lower arm in order to obtain a sample of blood. This process should only be performed once, as the plastic tube acts like a ‘tap’ that allows us to take blood without having to use a needle again. However, in the event we cannot take blood on the first attempt, we may try inserting the small tube again, on the opposite arm. We will then obtain a blood sample at time points: 1 hour (h), 1 h 20 min, 1 h 40 min, 2 h, 2.5 h, 3 h, 3.5 h, 4 h, 4.5 h, 5h, 7 h and 9h of being in the environmental chamber. The amount of blood taken in each visit will be approximately 170 mL. The blood samples obtained will be separated into serum, plasma and red blood cells. Serum samples will be stored securely at the University of South Wales until analysed and plasma/ red blood cell samples will be analysed and disposed of on the day of your visit. Plasma samples free of any cellular material (DNA) will be shipped and stored at Cardiff University for analysis. As mentioned, these blood samples will be used to measure the amount of Sildenafil being absorbed into your body. We will also use these blood samples to assess small molecules into your blood that help to give us information on the health of your blood vessels and your brain. All samples will be disposed following analysis.

We are also interested in how low oxygen levels and Sildenafil may affect blood flow and oxygen delivery to your vital organs such as the brain, lungs, liver and kidney.

**Brain Assessment:** We will assess blood flow and oxygen delivery to your brain in the blood vessels of your neck using an ultrasound machine. This will take around 5 minutes to complete each time. This will be repeated at time points: 1 h, 1 h 20 min, 1 h 40 min, 2 h, 2.5 h, 3 h, 3.5 h, 4 h, 4.5 h, 5h, 7 h and 9 h of being in the environmental chamber.

**Lung Assessment:** We will also use an ultrasound machine to measure blood flow to your lungs. This will involve placing an ultrasound probe on your chest (between your ribs) for around 5 minutes. This will be repeated at time points: 1 h, 1 h 20 min, 1 h 40 min, 2 h, 2.5 h, 3 h, 3.5 h, 4 h, 4.5 h, 5 h, 7 h and 9 h of being in the environmental chamber.

**Liver and Kidney Assessment:** We will measure blood flow to your liver and kidneys using an ultrasound machine. This will involve an ultrasound probe being placed on top of your stomach for around 5 minutes. This will be repeated at time points: 1 h, 1 h 20 min, 1 h 40 min, 2 h, 2.5 h, 3 h, 3.5 h, 4 h, 4.5 h, 5 h, 7 h and 9 h of being in the environmental chamber.

### Food/ Drink

You will be able to drink water freely throughout each visit. We will also provide you with a liquid meal (Milkshake) 5 hours after we start the experiment. Feel free to bring in food to eat after testing has finished.

### **What are the possible benefits of taking part?**

This study does not offer any immediate benefit but you will undergo a medical screening and the opportunity to experience low oxygen levels similar to that of high-altitude using an environmental chamber.

### **Am I able to take part?**

We will always try to include you into the study if you wish to participate. However, please do not volunteer if you:

- Are female
- Are younger than 18 years of age or older than 35 years of age.
- Have a known underlying medical condition
- Have a history of elevated blood pressure (> 150 mmHg systolic or > 90 mmHg diastolic) or low blood pressure (< 90 mmHg systolic or < 50 mmHg diastolic)
- Have a personal or direct familial history of cardiovascular disease including unstable angina, severe cardiac failure, stroke, or myocardial infarction
- Have a liver problem
- Have a bleeding disorder
- Have inherited eye disease or loss of vision due to non-arteritic anterior ischaemic optic neuropathy (NAION)
- Have a hereditary degenerative retinal disorder such as retinitis pigmentosa
- Have a physical deformity of the penis
- Have consumed medication in last 4 weeks, excluding paracetamol/non-steroidal anti-inflammatory medication
- Are a regular recreational drug user within the previous 10 years
- Are a smoker (past or present)
- Have previously experienced acute mountain/altitude sickness
- Have donated blood in the past 3 months
- Are known to be anaemic and/or have an iron insufficiency and/or have sickle cell anaemia
- Are known allergic reaction to Sildenafil, tradename VIAGRA®, REVATIO®
- Are lactose intolerant due to the sildenafil supplement and placebo tablet listing lactose as an active ingredient.
- Have been assessed to be unfit to participate following clinical review by the medical supervisor.
- Not willing to completed a 12-hour overnight fast, follow a low nitrite-nitrate diet, avoiding vigorous exercise, alcohol and caffeine 24-hours prior to Visit 2 and 3.
- Not willing to provide written informed consent

### **Once recruited into the study the following exclusion criteria will apply:**

- Have clinical acute mountain sickness (combined total LL score (self assessment + clinical scores) of  $\geq 5$  points and ESQ-C score  $\geq 0.7$  points)
- Have a headache score (>70)
- Have a blood pressure of >180 mmHg or <90 mmHg systolic blood pressure and/or >120 mmHg diastolic blood pressure
- Have a heart rate (> predicted maximum heart rate [220 – age in years])

## Appendix 1

- Have an oxygen saturation of <70%
- If the researchers are unable to find a suitable vein or failing to cannulate the participant on two consecutive occasions.
- If you feel you are unable to continue the study as a result of an unrelated injury or change in personal circumstances
- If you choose to voluntarily withdraw from the study

### **Expenses and payments**

You will not receive any payment for taking part in this study.

### **What are the possible disadvantages and risks of taking part?**

The most important risks to consider in this study are those listed below:

**Hypoxia (low oxygen levels):** Hypoxia may result in dizziness, headaches, nausea and/or fatigue. More severe symptoms include confusion, severe headaches, breathlessness, and/or a fast heart rate. However, you will be monitored closely throughout each visit and symptoms should ease when you are removed from the environmental chamber. It is very unlikely that this will cause any lasting damage.

**Blood Sampling:** You may experience some bruising, inflammation and discomfort from the needle insertions but the person taking your blood is fully trained in the technique and the risk of this is minimal. There is a small risk of there being an adverse event from having the cannula in your arm and you need to be aware of the possible problems and their causes. There is a risk that a small clot could form in one of the veins close to the surface of your skin. This could happen after you have left the laboratory and it could lead to a medical issue. You will know if there is a problem, because you will feel a hard lump under the skin and see some redness on the skin. If this happens:

- raise the limb to help reduce swelling
- keep active, to keep the blood circulating
- press a cold flannel over the vein to ease any pain
- rub an anti-inflammatory cream or gel on the area if the affected area is only small
- if the pain persists into the following day, call NHS 111 for further advice
- if the limb swells significantly, go straight to A&E. Do not wait for further advice because this might be something more serious.

The other risk is that of an infection being introduced into your blood stream. However, the risk of infection is lower if the cannula is in place for a shorter period of time and a swab is used to clean the skin before we introduce the cannula (please inform us of any allergies you may have before we swab the area). These risks involved with blood sampling are reduced by ensuring that the person carrying out this technique is fully trained. Although these risks are small, we need to make sure that you are fully aware that they exist before obtaining your informed written consent but also so you are aware what to do in the event these risks occur.

**Time Commitment:** Unfortunately as mentioned, Visits 2 and 3 will last approximately 10 hours each.

**Incidental Findings:** It is possible during the study that we discover you may have high or low blood pressure, or an abnormality of the heart. If this occurs we will be required to exclude you from the study. In the event of discovering a suspected clinically significant

## Appendix 1

abnormality, if urgent attention is required you will be transported and referred to the accident and emergency department (Royal Glamorgan Hospital) and treated as a medical emergency. If non-life threatening abnormalities are discovered, we will advise you to visit your general practitioner for a consultation.

***Sildenafil (Viagra) Administration (Group 1):*** It is important that you are made fully aware of any of the potential side effects associated with Sildenafil (Viagra) administration. Common side effects include: headache, nausea, facial flushing, hot flush (symptoms include a sudden feeling of heat in your upper body), indigestion, blurred vision, visual disturbance, stuffy nose and dizziness. There are also uncommon and rare side effects that have been listed in the Sildenafil Information Leaflet attached to the end of this information sheet. Please take the time to read this information and make sure to ask a member of the research team if you have any concerns or questions.

### **What if there is a problem?**

If there is a problem once you return home from the laboratory or between visits, if you believe the issue to require urgent attention, please telephone the NHS Advice line (111) and follow their advice. In this event or if you believe the problem to be non-urgent, please contact the Chief Investigator - Dr James Coulson (details provided at the end of this document). Any complaint about the way you have been dealt with during the study or any possible harm you might suffer will be addressed. If at any time during the research process you experience a problem or have a complaint, your first point of contact should be the Chief Investigator - Dr James Coulson. If you require further support, please contact Jonathan Sinfield within the University of South Wales Research Governance Office. All contact details can be found at the end of this information sheet.

### **What will happen if I don't carry on with the study?**

You are free to withdraw from the study at any time without giving a reason. There may also be an instance where you cannot/do not want to complete one component of the study. In either instance, a member of the study team will discuss with you the possibility of using any of your data that was collected while you were involved in the study for scientific purposes. Any data stored about you up to this point will not be entered into the study without your permission. If you do not want your data to be used it will be destroyed. By no means will your withdrawal affect the standard of education or care you receive in any future attendance at the University of South Wales.

### **What will happen to the results of the research study?**

Results from this study will be presented at research meetings and through peer-reviewed published scientific journals. Data presented will not be linked to any specific individual (identified by participant code) and data will typically be presented as the average of the group. It is important that you are made aware that all identifiable and sensitive data will be collected in accordance with the Data Protection Act (2018). All information will remain confidential and anonymised. Finally, this study forms the basis of a postgraduate qualification (PhD) for Ms Dalal Alablani, studying at Cardiff University. If you would like to receive a copy of the results once they have been analysed, we would be more than happy to provide you with a copy.

### **Who is organising/sponsoring the research?**

Ms Dalal Alablani's PhD at Cardiff University is bursary funded via the Prince Sattam Bin Abdulaziz University (KSA). USW will act as the study sponsor and provide indemnity and insurance cover for all staff members and participants of this study for the approved

## Appendix 1

activities taking place on USW premises.

### **Further information and contact details:**

1. General information about research: <http://research.southwales.ac.uk/>.
2. Specific information about this research project:

#### **Ms Dalal Alablani**

Research Student  
School of Pharmacy and Pharmaceutical Science  
Cardiff University  
Email: Alablanid@cardiff.ac.uk  
Phone: 07578094565

#### **Mr Benjamin Stacey**

Research Assistant  
Faculty of Life Sciences and Education  
Upper Glyntaff Campus  
University of South Wales  
UK CF37 4BD  
Email: Benjamin.stacey@southwales.ac.uk Phone:  
01443 654871

3. Additional advice regarding your participation:

#### **Professor Damian Miles Bailey (Co-Investigator)**

Research Institute of Health and Wellbeing

Lead of the Neurovascular Research Laboratory  
Faculty of Life Sciences and Education  
University of South Wales  
UK CF37 4BD  
Email: [damian.bailey@southwales.ac.uk](mailto:damian.bailey@southwales.ac.uk)  
Telephone: 01443 482296

4. Additional advice regarding your participation:

#### **Professor Mark Gumbleton (Co-investigator)**

Professor of Experimental Therapeutics and Head of School School  
of Pharmacy and Pharmaceutical Science  
Cardiff University  
Email: gumbleton@cardiff.ac.uk  
Telephone: +44 (0)29 2087 5449

5. Additional advice regarding your participation and/or medical advice/support:

#### **Dr James Coulson (Chief Investigator/Medical Supervisor)**

Clinical Reader in Clinical Pharmacology, Cardiff University; Honorary  
Consultant Physician in Clinical Pharmacology, Toxicology and General (Internal)  
Medicine, Cardiff & Vale University Health Board  
Email:

## Appendix 1

CoulsonJM@cardiff.ac.uk  
Telephone: +44 29207 46736

### 6. Research Governance Officer:

#### **Mr Jonathan Sinfield**

Research and Business Engagement  
University of South Wales  
UK CF 37 4AT  
Email: jonathan.sinfield@southwales.ac.uk  
Telephone: 01443 484518

### **Research team and affiliations:**

Professor Damian M. Bailey (University of South Wales), Professor Mark Gumbleton (Cardiff University), Dr James Coulson (Cardiff University), Ms Dalal Alablani (Cardiff University), Mr Benjamin Stacey (University of South Wales), Dr Muthanna Albaldawi (Cardiff University), Mr Angelo Iannetelli (University of South Wales), Mr Thomas Owens (University of South Wales), Mr Thomas Calverley (University of South Wales), Mr Tony Dawkins (Cardiff Metropolitan University), Dr Christopher Marley (University of South Wales), Dr Lewis Fall (University of South Wales).



**Participant Consent Form**

**Title:** Arterial hypoxaemia and its impact on the pharmacokinetics-pharmacodynamics of sildenafil; a randomised, double-blind, placebo-controlled trial

**Chief Investigator:** Dr James Coulson

**Co-investigators:** Professor Damian Bailey and Professor Mark Gumbleton

**Statement by participant (please initial each box as appropriate):**

- I have read the participant information sheet (001.F503A.02) and corresponding Sildenafil Information Leaflet for this study and I fully understand what is required of me for the study and the potential risks involved.
- My questions about the study have been answered to my satisfaction and I understand that I may ask further questions at any time.
- I understand that I will have blood taken by venepuncture through a cannula that will be in place while in the laboratory and I understand what to do if something happens after I leave the laboratory.
- I agree for my blood samples to be transferred from the laboratory for analysis elsewhere.
- I agree to provide information to the researchers under conditions of confidentiality described in the participant information sheet.
- I agree that any data collected from me in this study will be done so in accordance with the Data Protection Act (2018) and the General Data Protection Regulation (GDPR) and can be retained (up to 30 years) and used for academic publication provided I remain anonymous.
- I understand that I am free to withdraw from the study at any time. Any such withdrawal will not have any adverse impact on my studies at the University of South Wales, nor on my relationship with any academic staff (if I'm a student).
- I understand the research team will contact my General Practitioner highlighting my participant within the study.

## Appendix 1

- I consent to providing my contact details to allow the research team to contact me within the duration of the study period.
- I understand that I may be placed into the group that will consume 100 mg of Sildenafil (Viagra) on two separate occasions.

**Participant name:**

**Participant signature:**

**Assigned Participant ID:**

**Date:**

**Statement by the investigator:**

- I have explained the nature and purpose of this study to the above named participant and believe that they understand what the study involves.

**Investigator name:**

**Investigator signature:**

**Date:**



## Research Volunteers Wanted

University of  
South Wales  
Prifysgol  
De Cymru

CARDIFF  
UNIVERSITY  
PRIFYSGOL  
CAERDYDD

**We need volunteers to help understand whether being exposed to low levels of oxygen change the way the body breaks down drugs and what effect this may have on the brain, lungs, kidney, and liver.**



### WHO?

Physically active young, male adults (18 to 35 yrs.) that engage in moderate aerobic exercise (e.g., running, cycling) for more than 150 minutes, three times per week.

### WHAT?

You will be required to attend the Neurovascular Research Laboratory at the University of South Wales (Treforest) for an initial pre-screening visit to check for eligibility. You will then be required to attend two more visits (10 hours each) in which you will consume an oral dose (tablet) of Sildenafil (Viagra) or Placebo (lactose). An assessment of blood flow to your brain, lungs, liver and kidney alongside blood samples will be conducted throughout both visits. One these visits will include an exposure to simulated high-altitude (approximately 4500 meters of altitude).

### INTERESTED?

If you would like more information or would like to take part in the study, please contact the research team via:



[Benjamin.stacey@southwales.ac.uk](mailto:Benjamin.stacey@southwales.ac.uk)  
[AlablaniD@cardiff.ac.uk](mailto:AlablaniD@cardiff.ac.uk)



07951 587262



---

**Dr James  
Coulson** School  
of Medicine  
Cardiff  
University,

University Hospital,  
Llandough Penlan Road  
Cardiff  
CF64  
2XX

Dear Dr [*insert name*],

**Study title:** Arterial hypoxaemia and its impact on the pharmacokinetics-pharmacodynamics of sildenafil; a randomised, double-blind, placebo-controlled trial.

**Study number:** [*to be provided following MHRA approval*]

Your patient, [*insert name, address and date of birth*] has kindly volunteered to participate in the above study. I enclose a copy of the participant information sheet for your information.

Please could you inform me if you have any questions or concerns regarding your patient's inclusion in this study.

Thank you for your support.

Yours sincerely,

[*Signature required*]

**Dr James Coulson**

Chief Investigator

Visiting Professor, University of South Wales  
Honorary Professor of Clinical Pharmacology & Toxicology, Cardiff Metropolitan University  
Reader in Clinical Pharmacology, Cardiff University Honorary Consultant Physician, Clinical Pharmacologist and Toxicologist, Cardiff & Vale University Health Board

## Appendix 1

### Case Report Form

**Study Title:** Arterial hypoxaemia and its impact on the pharmacokinetics- pharmacodynamics of sildenafil; a randomised, double-blind, placebo-controlled trial.

#### **Pre Screening Visit (Visit 1)**

**Study Number:**

**Sponsor:**

**Site Location:**

**Date:**

**Subject ID:**

**Medical Supervisor Name:**

**Medical Supervisor Signature:**

### Demographics

**Date of Birth:**

**Ethnicity:** White

**Stature (m):**

Black

**Mass (kg):**

Mixed

**Body Fat (%):**

Asian

Other:

## Appendix 1

### Pre Screening Visit (Visit 1)

#### COVID-19

Previously contracted COVID-19? If yes, please provide a date.

Experienced COVID-19 related symptoms in the past 14 days?

Tympanic Temperature:

#### Clinical Details

Systolic blood pressure (mmHg):

Diastolic blood pressure (mmHg):

Heart rate (bpm):

Oxygen Saturation (%)

Cardiovascular System	Normal	Abnormal
Respiratory System	Normal	Abnormal
Gastrointestinal System	Normal	Abnormal
Neurovascular System	Normal	Abnormal
Locomotive System	Normal	Abnormal
Electrocardiogram	Normal	Abnormal

**Appendix 1**

**Pre-Screening Visit (Visit 1)**

**Does the participant have any history of medical disease?**

**Yes**

**No**

If **Yes**, please provided more information below:

[Redacted area]

**Does the participant meet the inclusion and exclusion criteria?**

**Yes**

**No**

If **No**, please give a reason why below:

[Redacted area]

**Has the participant provided written informed consent?**

**Yes**

**No**

If **No**, please give a reason why below:

[Redacted area]

**Will the participant be recruited into the study?**

**Yes**

**No**

**Please indicate which group the participant has been assigned to:**

**Group 1**

**Group**

**2**

**Medical Supervisor:**

**Signature:**

Appendix 1

**Case Report Form – Group 1 - Visit 2**

<b>Study Number:</b>	<input type="text"/>	<b>Sponsor:</b>	<input type="text"/>	<b>Medical Supervisor:</b>	<input type="text"/>	<b>Subject ID:</b>	<input type="text"/>
	<input type="text"/>	<b>Date:</b>	<input type="text"/>	<b>Medical Supervisor Signature:</b>	<input type="text"/>	<b>Condition:</b>	<input type="text"/>

**COVID-19**

**Previously contracted COVID-19? If yes, please provide a date.**

**Experienced COVID-19 related symptoms in the past 14 days?**

**Tympanic Temperature:**

**Case Report Form – Group 1 - Visit 2**

Please confirm that the Sildenafil tablet has been administered and provide the time of administration:

Yes

No

Time of administration:

Medical Parameters	Time of chamber exposure (min)									
	0	60	120	180	240	300	360	420	480	540
SBP (mmHg)										
DBP (mmHg)										
HR (bpm)										
SpO <sub>2</sub> (%)										
VAS (mm)										
HAH (score)										
ESQ-C (score)										

Medical Supervisor:

Medical Supervisor Signature:

Appendix 1

**Case Report Form - Group 1 - Visit 2**

Pharmacokinetic Parameters												
	Time of chamber exposure (min)											
	60	80	100	120	150	180	210	240	270	300	420	540
$C_{max}$												
$T_{max}$												
$K_a$												
$t_{1/2 a}$												
$CL/F$												
$t_{1/2}$												
$K$												
$V/F$												
$AUC_{0-t \text{ last}}$												
$AUC_{0-t \infty}$												
$F_u$												



**Case Report Form - Group 1 - Visit 2**

Metabolic Parameters												
	Time of chamber exposure (min)											
	60	80	100	120	150	180	210	240	270	300	420	540
Hb (g.dL <sup>-1</sup> )												
Hct (%)												
AFR (AU)												
Plasma NO (nM)												
RBC NO (nM)												
LOOH												
DNA OX												
S100 $\beta$		ND	ND	ND	ND	ND	ND	ND	ND		ND	
NSE		ND	ND	ND	ND	ND	ND	ND	ND		ND	
NFL		ND	ND	ND	ND	ND	ND	ND	ND		ND	
Gfap		ND	ND	ND	ND	ND	ND	ND	ND		ND	
Uhcl-1		ND	ND	ND	ND	ND	ND	ND	ND		ND	
Tau		ND	ND	ND	ND	ND	ND	ND	ND		ND	

Appendix 1

**Case Report Form - Group 1 - Visit 2**

Haemodynamic-Respiratory Parameters												
	Time of chamber exposure (min)											
	60	80	100	120	150	180	210	240	270	300	420	540
CCA <sub>Q</sub> (mL.min <sup>-1</sup> )												
ICA <sub>Q</sub> (mL.min <sup>-1</sup> )												
VA <sub>Q</sub> (mL.min <sup>-1</sup> )												
PA <sub>Q</sub> (mL.min <sup>-1</sup> )												
RA <sub>Q</sub> (mL.min <sup>-1</sup> )												
HA <sub>Q</sub> (mL.min <sup>-1</sup> )												
VE (L.min <sup>-1</sup> )												
PETO <sub>2</sub> (mmHg)												
PETCO <sub>2</sub> (mmHg)												

**Case Report Form – Group 1 - Visit 3**

<b>Study Number:</b>	<input type="text"/>	<b>Sponsor:</b>	<input type="text"/>	<b>Medical Supervisor:</b>	<input type="text"/>	<b>Subject ID:</b>	<input type="text"/>
<b>Site Location:</b>	<input type="text"/>	<b>Date:</b>	<input type="text"/>	<b>Medical Supervisor Signature:</b>	<input type="text"/>	<b>Condition:</b>	<input type="text"/>

**COVID-19**

**Previously contracted COVID-19? If yes, please provide a date.**

**Experienced COVID-19 related symptoms in the past 14 days?**

**Tympanic Temperature:**

**Case Report Form - Group 1 - Visit 3**

Please confirm that the Sildenafil tablet has been administered and provide the time of administration:

Yes  No

Time of administration:

**Medical Parameters**

	Time of chamber exposure (min)									
	0	60	120	180	240	300	360	420	480	540
SBP (mmHg)										
DBP (mmHg)										
HR (bpm)										
SpO <sub>2</sub> (%)										
VAS (mm)										
HAH (score)										
ESQ-C (score)										

Medical Supervisor:

Medical Supervisor Signature:

Appendix 1

**Case Report Form - Group 1 - Visit 3**

Pharmacokinetic Parameters												
	Time of chamber exposure (min)											
	60	80	100	120	150	180	210	240	270	300	420	540
$C_{max}$												
$T_{max}$												
$K_a$												
$t_{1/2 a}$												
CL/F												
$t_{1/2}$												
K												
V/F												
AUC <sub>0-t last</sub>												
AUC <sub>0-t<sup>∞</sup></sub>												
$F_u$												

**Case Report Form - Group 1 - Visit 3**

Metabolic Parameters												
	Time of chamber exposure (min)											
	60	80	100	120	150	180	210	240	270	300	420	540
Hb (g.dL <sup>-1</sup> )												
Hct (%)												
AFR (AU)												
Plasma NO (nM)												
RBC NO (nM)												
LOOH												
DNA OX												
S100 $\beta$		ND	ND	ND	ND	ND	ND	ND	ND		ND	
NSE		ND	ND	ND	ND	ND	ND	ND	ND		ND	
NFL		ND	ND	ND	ND	ND	ND	ND	ND		ND	
Gfap		ND	ND	ND	ND	ND	ND	ND	ND		ND	
Uhc1-1		ND	ND	ND	ND	ND	ND	ND	ND		ND	
Tau		ND	ND	ND	ND	ND	ND	ND	ND		ND	

Appendix 1

**Case Report Form - Group 1 - Visit 3**

Haemodynamic-Respiratory Parameters												
	Time of chamber exposure (min)											
	60	80	100	120	150	180	210	240	270	300	420	540
CCA <sub>Q</sub> (mL.min <sup>-1</sup> )												
ICA <sub>Q</sub> (mL.min <sup>-1</sup> )												
VA <sub>Q</sub> (mL.min <sup>-1</sup> )												
PA <sub>Q</sub> (mL.min <sup>-1</sup> )												
RA <sub>Q</sub> (mL.min <sup>-1</sup> )												
HA <sub>Q</sub> (mL.min <sup>-1</sup> )												
VE (L.min <sup>-1</sup> )												
PET <sub>O</sub> <sub>2</sub> (mmHg)												
PET <sub>CO</sub> <sub>2</sub> (mmHg)												

**Case Report Form – Group 2 - Visit 2**

<b>Study Number:</b>		<b>Sponsor:</b>		<b>Medical Supervisor:</b>		<b>Subject ID:</b>	
<b>Site Location:</b>		<b>Date:</b>		<b>Medical Supervisor Signature:</b>		<b>Condition:</b>	

**COVID-19**

**Previously contracted COVID-19? If yes, please provide a date.**

**Experienced COVID-19 related symptoms in the past 14 days?**

**Tympanic Temperature:**



**Case Report Form - Group 2 – Visit 2**

Please confirm that the placebo tablet has been administered and provide the time of administration:

Yes  No

Time of administration:

**Medical Parameters**

	Time of chamber exposure (min)									
	0	60	120	180	240	300	360	420	480	540
SBP (mmHg)										
DBP (mmHg)										
HR (bpm)										
SpO <sub>2</sub> (%)										
VAS (mm)										
HAH (score)										
ESQ-C (score)										

Medical Supervisor:

Medical Supervisor Signature:

**Case Report Form - Group 2 - Visit 2**

Metabolic Parameters												
	Time of chamber exposure (min)											
	60	80	100	120	150	180	210	240	270	300	420	540
Hb (g.dL <sup>-1</sup> )												
Hct (%)												
AFR (AU)												
Plasma NO (nM)												
RBC NO (nM)												
LOOH												
DNA OX												
S100 $\beta$		ND	ND	ND	ND	ND	ND	ND	ND		ND	
NSE		ND	ND	ND	ND	ND	ND	ND	ND		ND	
NFL		ND	ND	ND	ND	ND	ND	ND	ND		ND	
Gfap		ND	ND	ND	ND	ND	ND	ND	ND		ND	
Uhcl-1		ND	ND	ND	ND	ND	ND	ND	ND		ND	
Tau		ND	ND	ND	ND	ND	ND	ND	ND		ND	

**Case Report Form - Group 2 - Visit 2**

Haemodynamic-Respiratory Parameters												
	Time of chamber exposure (min)											
	60	80	100	120	150	180	210	240	270	300	420	540
CCA <sub>Q</sub> (mL.min <sup>-1</sup> )												
ICA <sub>Q</sub> (mL.min <sup>-1</sup> )												
VA <sub>Q</sub> (mL.min <sup>-1</sup> )												
PA <sub>Q</sub> (mL.min <sup>-1</sup> )												
RA <sub>Q</sub> (mL.min <sup>-1</sup> )												
HA <sub>Q</sub> (mL.min <sup>-1</sup> )												
VE (L.min <sup>-1</sup> )												
PETO <sub>2</sub> (mmHg)												
PETCO <sub>2</sub> (mmHg)												

Appendix 1

**Case Report Form – Group 2 - Visit 3**

<b>Study Number:</b>		<b>Sponsor:</b>		<b>Medical Supervisor:</b>		<b>Subject ID:</b>	
<b>Site Location:</b>		<b>Date:</b>		<b>Medical Supervisor Signature:</b>		<b>Condition:</b>	

**COVID-19**

**Previously contracted COVID-19? If yes, please provide a date.**

**Experienced COVID-19 related symptoms in the past 14 days?**

**Tympanic Temperature:**

**Case Report Form - Group 2 – Visit 3**

Please confirm that the placebo tablet has been administered and provide the time of administration:

Yes  No

Time of administration:

**Medical Parameters**

	Time of chamber exposure (min)									
	0	60	120	180	240	300	360	420	480	540
SBP (mmHg)										
DBP (mmHg)										
HR (bpm)										
SpO <sub>2</sub> (%)										
VAS (mm)										
HAH (score)										
ESQ-C (score)										

Medical Supervisor:

Medical Supervisor Signature:

Appendix 1

**Case Report Form - Group 2 - Visit 3**

Metabolic Parameters												
	Time of chamber exposure (min)											
	60	80	100	120	150	180	210	240	270	300	420	540
Hb (g.dL <sup>-1</sup> )												
Hct (%)												
AFR (AU)												
Plasma NO (nM)												
RBC NO (nM)												
LOOH												
DNA OX												
S100β		ND	ND	ND	ND	ND	ND	ND	ND		ND	
NSE		ND	ND	ND	ND	ND	ND	ND	ND		ND	
NFL		ND	ND	ND	ND	ND	ND	ND	ND		ND	
Gfap		ND	ND	ND	ND	ND	ND	ND	ND		ND	
Uhcl-1		ND	ND	ND	ND	ND	ND	ND	ND		ND	
Tau		ND	ND	ND	ND	ND	ND	ND	ND		ND	

**Case Report Form - Group 2 - Visit 3**

Haemodynamic-Respiratory Parameters												
	Time of chamber exposure (min)											
	60	80	100	120	150	180	210	240	270	300	420	540
CCA <sub>Q</sub> (mL.min <sup>-1</sup> )												
ICA <sub>Q</sub> (mL.min <sup>-1</sup> )												
VA <sub>Q</sub> (mL.min <sup>-1</sup> )												
PA <sub>Q</sub> (mL.min <sup>-1</sup> )												
RA <sub>Q</sub> (mL.min <sup>-1</sup> )												
HA <sub>Q</sub> (mL.min <sup>-1</sup> )												
VE (L.min <sup>-1</sup> )												
PETO <sub>2</sub> (mmHg)												
PETCO <sub>2</sub> (mmHg)												

## Appendix 1

### Study Discharge/Withdrawal

The Study Discharge/Withdrawal section should be completed if a participant has withdrawn from the study early or on the participant's final visit. Clinical details must be completed before withdrawal/discharge.

<b>Study Number:</b>	TBC	<b>Sponsor:</b>	University of South Wales
<b>Site Location:</b>	University of South Wales	<b>Date:</b>	
<b>Subject ID:</b>			
<b>Medical Supervisor:</b>		<b>Medical Supervisor Signature:</b>	

Is the participant being withdrawn early from the study? Yes  No

If yes, please provide a reason for withdrawal below:

### Clinical Details

Systolic blood pressure (mmHg):

Diastolic blood pressure (mmHg):

Heart rate (bpm):

Cardiovascular System Normal  Abnormal

Respiratory System Normal  Abnormal

Gastrointestinal System Normal  Abnormal

Neurovascular System Normal  Abnormal

Locomotive System Normal  Abnormal

Electrocardiogram Normal  Abnormal

I confirm the participant is safe to be discharged from the study

Medical Supervisor:

Medical Supervisor Signature:



**Signature Sheet and Delegation of Duties Log**

**Study title:** Arterial hypoxaemia and its impact on the pharmacokinetics-pharmacodynamics of sildenafil; a randomised, double-blind, placebo-controlled trial.

**Legend**

Use this legend to complete the “General Duties” column. For each individual listed in the “Name” column, enter the letter(s) (eg, a c, e) from the legend below that correspond to their protocol-related duties in the “General Duties” column.

a. Taking consent	i. Cannulation	q. Respiratory analysis
b. Participant recruitment	j. Blood Procurement	r. Headache Assessments
c. Pre-screening examination	k. Blood processing	s. Oxygen Saturation Assessment
d. Manual brachial blood pressure	l. Blood storage	t. Data analysis
e. Supplement (Drug/ Placebo) administration	m. Electrocardiography	u. Data interpretation
f. Supplement blinding procedures	n. Duplex Ultrasonography	v. Data custodian
g. First aid	o. Participant follow-up procedures	
h. Automated external defibrillator	p. Maintenance of hypoxic environment	

The Chief Investigator (CI) should sign below when the project is completed.

I have reviewed the information on this log and have found it to be accurate. All delegated duties were performed with my authorisation.

Signature of CI \_\_\_\_\_ Date: \_\_\_\_\_



## Appendix 1

### Personal Details Form

This form should be used by the research team to store the personal details of a participant. These details will only be used to contact participants to arrange experimental visits, to follow-up with participants after an experimental visit and to contact the participant's general practitioner. This document must be completed for all participants consented into the study and must remain in the locked cabinet in **GK002**.

**Study title:** Arterial hypoxaemia and its impact on the pharmacokinetics-pharmacodynamics of sildenafil; a randomised, double-blind, placebo-controlled trial.

**Subject ID:**

**Date:**

**Name:**

**Date of Birth:**

**Email Address:**

**Telephone Number:**

**Home Address:**

**General Practitioner Details:**

## **Appendix 1**

### **1. NAME OF THE MEDICINAL PRODUCT**

Sildenafil Teva 25 mg film-coated tablets  
Sildenafil Teva 50 mg film-coated tablets  
Sildenafil Teva 100 mg film-coated tablets

### **2. QUALITATIVE AND QUANTITATIVE COMPOSITION**

#### Sildenafil Teva 25 mg film-coated tablets

Each tablet contains sildenafil citrate equivalent to 25 mg of sildenafil.

#### Sildenafil Teva 50 mg film-coated tablets

Each tablet contains sildenafil citrate equivalent to 50 mg of sildenafil.

#### Sildenafil Teva 100 mg film-coated tablets

Each tablet contains sildenafil citrate equivalent to 100 mg of sildenafil. For the full list of excipients, see section 6.1.

### **3. PHARMACEUTICAL FORM**

Film-coated tablet.

#### Sildenafil Teva 25 mg film-coated tablets

White, oval-shaped film-coated tablets, engraved with 'S 25' on one side, and plain on the other side.

#### Sildenafil Teva 50 mg film-coated tablets

White, oval-shaped film-coated tablets, engraved with 'S 50' on one side, and plain on the other side.

#### Sildenafil Teva 100 mg film-coated tablets

White, oval-shaped film-coated tablets, engraved with 'S 100' on one side, and plain on the other side.

### **4. CLINICAL PARTICULARS**

#### **4.1 Therapeutic indications**

## Appendix 1

Sildenafil Teva is indicated in adult men with erectile dysfunction, which is the inability to achieve or maintain a penile erection sufficient for satisfactory sexual performance.

In order for Sildenafil Teva to be effective, sexual stimulation is required.

### 4.2 Posology and method of administration

#### Posology

##### *Use in adults*

The recommended dose is 50 mg taken as needed approximately one hour before sexual activity. Based on efficacy and tolerability, the dose may be increased to 100 mg or decreased to 25 mg. The maximum recommended dose is 100 mg. The maximum recommended dosing frequency is once per day. If Sildenafil Teva is taken with food, the onset of activity may be delayed compared to the fasted state (see section 6.2).

##### Special populations

##### *Elderly*

Dosage adjustments are not required in elderly patients ( $\geq 65$  years old).

##### *Renal impairment*

The dosing recommendations described in ‘Use in adults’ apply to patients with mild to moderate renal impairment (creatinine clearance = 30 - 80 mL/min).

Since sildenafil clearance is reduced in patients with severe renal impairment (creatinine clearance

<30 mL/min) a 25 mg dose should be considered. Based on efficacy and tolerability, the dose may be increased step-wise to 50 mg up to 100 mg as necessary.

##### *Hepatic impairment*

Since sildenafil clearance is reduced in patients with hepatic impairment (e.g. cirrhosis) a 25 mg dose should be considered. Based on efficacy and tolerability, the dose may be increased step-wise to

50 mg up to 100 mg as necessary.

##### *Paediatric population*

Sildenafil Teva is not indicated for individuals below 18 years of age.

##### *Use in patients taking other medicinal products*

## Appendix 1

With the exception of ritonavir for which co-administration with sildenafil is not advised (see section 4.4) a starting dose of 25 mg should be considered in patients receiving concomitant treatment with CYP3A4 inhibitors (see section 4.5).

In order to minimise the potential of developing postural hypotension in patients receiving alpha-blocker treatment, patients should be stabilised on alpha-blocker therapy prior to initiating sildenafil treatment. In addition, initiation of sildenafil at a dose of 25 mg should be considered (see sections 4.4 and 4.5).

### Method of administration

For oral use.

### **4.3 Contraindications**

Hypersensitivity to the active substance or to any of the excipients listed in section

6.1. Consistent with its known effects on the nitric oxide/cyclic guanosine monophosphate (cGMP)

pathway (see section 5.1), sildenafil was shown to potentiate the hypotensive effects of nitrates, and its

co-administration with nitric oxide donors (such as amyl nitrite) or nitrates in any form is therefore contraindicated.

The co-administration of PDE5 inhibitors, including sildenafil, with guanylate cyclase stimulators, such as riociguat, is contraindicated as it may potentially lead to symptomatic hypotension (see section 4.5).

Agents for the treatment of erectile dysfunction, including sildenafil, should not be used in men for whom sexual activity is inadvisable (e.g. patients with severe cardiovascular disorders such as unstable angina or severe cardiac failure).

Sildenafil Teva is contraindicated in patients who have loss of vision in one eye because of non-arteritic anterior ischaemic optic neuropathy (NAION), regardless of whether this episode was in connection or not with previous PDE5 inhibitor exposure (see section 4.4).

The safety of sildenafil has not been studied in the following sub-groups of patients and its use is therefore contraindicated: severe hepatic impairment, hypotension (blood pressure <90/50 mmHg), recent history of stroke or myocardial infarction and known hereditary degenerative retinal disorders

## Appendix 1

such as *retinitis pigmentosa* (a minority of these patients have genetic disorders of retinal phosphodiesterases).

### 4.4 Special warnings and precautions for use

A medical history and physical examination should be undertaken to diagnose erectile dysfunction and determine potential underlying causes, before pharmacological treatment is considered.

#### Cardiovascular risk factors

Prior to initiating any treatment for erectile dysfunction, physicians should consider the cardiovascular status of their patients, since there is a degree of cardiac risk associated with sexual activity. Sildenafil has vasodilator properties, resulting in mild and transient decreases in blood pressure (see section 5.1). Prior to prescribing sildenafil, physicians should carefully consider whether their patients with certain underlying conditions could be adversely affected by such vasodilatory effects, especially in combination with sexual activity. Patients with increased susceptibility to vasodilators include those with left ventricular outflow obstruction (e.g., aortic stenosis, hypertrophic obstructive cardiomyopathy), or those with the rare syndrome of multiple system atrophy manifesting as severely impaired autonomic control of blood pressure.

Sildenafil Teva potentiates the hypotensive effect of nitrates (see section 4.3).

Serious cardiovascular events, including myocardial infarction, unstable angina, sudden cardiac death, ventricular arrhythmia, cerebrovascular haemorrhage, transient ischaemic attack, hypertension and hypotension have been reported post-marketing in temporal association with the use of sildenafil.

Most, but not all, of these patients had pre-existing cardiovascular risk factors. Many events were reported to occur during or shortly after sexual intercourse and a few were reported to occur shortly after the use of sildenafil without sexual activity. It is not possible to determine whether these events are related directly to these factors or to other factors.

#### Priapism

Agents for the treatment of erectile dysfunction, including sildenafil, should be used with caution in patients with anatomical deformation of the penis (such as angulation,

## Appendix 1

cavernosal fibrosis or Peyronie's disease), or in patients who have conditions which may predispose them to priapism (such as sickle cell anaemia, multiple myeloma or leukaemia).

Prolonged erections and priapism have been reported with sildenafil in post-marketing experience. In the event of an erection that persists longer than 4 hours, the patient should seek immediate medical assistance. If priapism is not treated immediately, penile tissue damage and permanent loss of potency could result.

### Concomitant use with other PDE5 inhibitors or other treatments for erectile dysfunction

The safety and efficacy of combinations of sildenafil with other PDE5 Inhibitors, or other pulmonary arterial hypertension (PAH) treatments containing sildenafil, or other treatments for erectile dysfunction have not been studied. Therefore the use of such combinations is not recommended.

### Effects on vision

Cases of visual defects have been reported spontaneously in connection with the intake of sildenafil and other PDE5 inhibitors (see section 4.8). Cases of non-arteritic anterior ischaemic optic neuropathy, a rare condition, have been reported spontaneously and in an observational study in connection with the intake of sildenafil and other PDE5 inhibitors (see section 4.8). Patients should be advised that in the event of any sudden visual defect, they should stop taking Sildenafil Teva and consult a physician immediately (see section 4.3).

### Concomitant use with ritonavir

Co-administration of sildenafil with ritonavir is not advised (see section 4.5).

### Concomitant use with alpha-blockers

Caution is advised when sildenafil is administered to patients taking an alpha-blocker, as the co-administration may lead to symptomatic hypotension in a few susceptible individuals (see section 4.5). This is most likely to occur within 4 hours post sildenafil dosing. In order to minimise the potential for developing postural hypotension, patients should be hemodynamically stable on alpha-blocker therapy prior to initiating sildenafil treatment. Initiation of sildenafil at a dose of 25 mg should be considered (see section 4.2). In addition, physicians should advise patients what to do in the event of postural hypotensive symptoms.



## Appendix 1

### Effect on bleeding

Studies with human platelets indicate that sildenafil potentiates the antiaggregatory effect of sodium nitroprusside *in vitro*. There is no safety information on the administration of sildenafil to patients with bleeding disorders or active peptic ulceration. Therefore sildenafil should be administered to these patients only after careful benefit-risk assessment.

### Women

Sildenafil Teva is not indicated for use by women.

## **4.5 Interaction with other medicinal products and other forms of interaction**

### Effects of other medicinal products on sildenafil

#### *In vitro studies*

Sildenafil metabolism is principally mediated by the cytochrome P450 (CYP) isoforms 3A4 (major route) and 2C9 (minor route). Therefore, inhibitors of these isoenzymes may reduce sildenafil clearance and inducers of these isoenzymes may increase sildenafil clearance.

#### *In vivo studies*

Population pharmacokinetic analysis of clinical trial data indicated a reduction in sildenafil clearance when co-administered with CYP3A4 inhibitors (such as ketoconazole, erythromycin, cimetidine).

Although no increased incidence of adverse events was observed in these patients, when sildenafil is administered concomitantly with CYP3A4 inhibitors, a starting dose of 25 mg should be considered.

Co-administration of the HIV protease inhibitor ritonavir, which is a highly potent P450 inhibitor, at steady state (500 mg twice daily) with sildenafil (100 mg single dose) resulted in a 300 % (4-fold) increase in sildenafil  $C_{max}$  and a 1,000 % (11-fold) increase in sildenafil plasma AUC. At 24 hours, the plasma levels of sildenafil were still approximately 200 ng/mL, compared to approximately 5 ng/mL when sildenafil was administered alone. This is consistent with ritonavir's marked effects on a broad range of P450 substrates. Sildenafil had no effect on ritonavir pharmacokinetics. Based on these pharmacokinetic results co-administration of sildenafil with ritonavir is not advised (see section 4.4) and in any event

## Appendix 1

the maximum dose of sildenafil should under no circumstances exceed 25 mg within 48 hours.

Co-administration of the HIV protease inhibitor saquinavir, a CYP3A4 inhibitor, at steady state (1200 mg three times a day) with sildenafil (100 mg single dose) resulted in a 140 % increase in sildenafil  $C_{max}$  and a 210 % increase in sildenafil AUC. Sildenafil had no effect on saquinavir pharmacokinetics (see section 4.2). Stronger CYP3A4 inhibitors such as ketoconazole and itraconazole would be expected to have greater effects.

When a single 100 mg dose of sildenafil was administered with erythromycin, a moderate CYP3A4 inhibitor, at steady state (500 mg twice daily for 5 days), there was a 182 % increase in sildenafil systemic exposure (AUC). In normal healthy male volunteers, there was no evidence of an effect of azithromycin (500 mg daily for 3 days) on the AUC,  $C_{max}$ ,  $t_{max}$ , elimination rate constant, or subsequent half-life of sildenafil or its principal circulating metabolite. Cimetidine (800 mg), a cytochrome P450 inhibitor and non-specific CYP3A4 inhibitor, caused a 56 % increase in plasma sildenafil concentrations when co-administered with sildenafil (50 mg) to healthy volunteers.

Grapefruit juice is a weak inhibitor of CYP3A4 gut wall metabolism and may give rise to modest increases in plasma levels of sildenafil.

Single doses of antacid (magnesium hydroxide/aluminium hydroxide) did not affect the bioavailability of sildenafil.

Although specific interaction studies were not conducted for all medicinal products, population pharmacokinetic analysis showed no effect of concomitant treatment on sildenafil pharmacokinetics when grouped as CYP2C9 inhibitors (such as tolbutamide, warfarin, phenytoin), CYP2D6 inhibitors (such as selective serotonin reuptake inhibitors, tricyclic antidepressants), thiazide and related diuretics, loop and potassium sparing diuretics, angiotensin converting enzyme inhibitors, calcium channel blockers, beta-adrenoreceptor antagonists or inducers of CYP450 metabolism (such as rifampicin, barbiturates). In a study of healthy male volunteers, co-administration of the endothelin antagonist, bosentan, (an inducer of CYP3A4 [moderate], CYP2C9 and possibly of CYP2C19) at steady state (125 mg twice a day) with sildenafil at steady state (80 mg three times a day) resulted in 62.6% and 55.4% decrease in sildenafil AUC and  $C_{max}$ , respectively.

## Appendix 1

Therefore, concomitant administration of strong CYP3A4 inducers, such as rifampin, is expected to cause greater decreases in plasma concentrations of sildenafil.

Nicorandil is a hybrid of potassium channel activator and nitrate. Due to the nitrate component it has the potential to result in a serious interaction with sildenafil.

### *Effects of sildenafil on other medicinal*

#### *products In vitro studies:*

Sildenafil is a weak inhibitor of the cytochrome P450 isoforms 1A2, 2C9, 2C19, 2D6, 2E1 and 3A4

(IC<sub>50</sub> > 150 µM). Given sildenafil peak plasma concentrations of approximately 1 µM after recommended doses, it is unlikely that Sildenafil Teva will alter the clearance of substrates of these isoenzymes.

There are no data on the interaction of sildenafil and non-specific phosphodiesterase inhibitors such as theophylline or dipyridamole.

#### *In vivo studies:*

Consistent with its known effects on the nitric oxide/cGMP pathway (see section 5.1), sildenafil was shown to potentiate the hypotensive effects of nitrates, and its co-administration with nitric oxide donors or nitrates in any form is therefore contraindicated (see section 4.3).

Riociguat: Preclinical studies showed additive systemic blood pressure lowering effect when PDE5 inhibitors were combined with riociguat. In clinical studies, riociguat has been shown to augment the hypotensive effects of PDE5 inhibitors. There was no evidence of favourable clinical effect of the combination in the population studied. Concomitant use of riociguat with PDE5 inhibitors, including sildenafil, is contraindicated (see section 4.3).

Concomitant administration of sildenafil to patients taking alpha-blocker therapy may lead to symptomatic hypotension in a few susceptible individuals. This is most likely to occur within 4 hours post sildenafil dosing (see sections 4.2 and 4.4). In three specific drug-drug interaction studies, the alpha-blocker doxazosin (4 mg and 8 mg) and sildenafil (25 mg, 50 mg, or 100 mg) were administered simultaneously to patients with benign prostatic hyperplasia (BPH) stabilised on doxazosin therapy.

In these study populations, mean additional reductions of supine blood pressure of 7/7 mmHg,

## Appendix 1

9/5 mmHg, and 8/4 mmHg, and mean additional reductions of standing blood pressure of 6/6 mmHg, 11/4 mmHg, and 4/5 mmHg, respectively, were observed. When sildenafil and doxazosin were administered simultaneously to patients stabilised on doxazosin therapy, there were infrequent reports of patients who experienced symptomatic postural hypotension. These reports included dizziness and light-headedness, but not syncope.

No significant interactions were shown when sildenafil (50 mg) was co-administered with tolbutamide (250 mg) or warfarin (40 mg), both of which are metabolised by CYP2C9.

Sildenafil (50 mg) did not potentiate the increase in bleeding time caused by acetyl salicylic acid (150 mg).

Sildenafil (50 mg) did not potentiate the hypotensive effects of alcohol in healthy volunteers with mean maximum blood alcohol levels of 80 mg/dl.

Pooling of the following classes of antihypertensive medication: diuretics, beta-blockers, ACE inhibitors, angiotensin II antagonists, antihypertensive medicinal products (vasodilator and centrally-acting), adrenergic neurone blockers, calcium channel blockers and alpha-adrenoceptor blockers, showed no difference in the side effect profile in patients taking sildenafil compared to placebo treatment. In a specific interaction study, where sildenafil (100 mg) was co-administered with amlodipine in hypertensive patients, there was an additional reduction on supine systolic blood pressure of 8 mmHg. The corresponding additional reduction in supine diastolic blood pressure was 7 mmHg. These additional blood pressure reductions were of a similar magnitude to those seen when sildenafil was administered alone to healthy volunteers (see section 5.1).

Sildenafil (100 mg) did not affect the steady state pharmacokinetics of the HIV protease inhibitors, saquinavir and ritonavir, both of which are CYP3A4 substrates.

In healthy male volunteers, sildenafil at steady state (80 mg t.i.d.) resulted in a 49.8% increase in bosentan AUC and a 42% increase in bosentan  $C_{max}$  (125 mg b.i.d.).

### 4.6 Fertility, pregnancy and lactation

Sildenafil Teva is not indicated for use by women.

There are no adequate and well-controlled studies in pregnant or breast-feeding women.

No relevant adverse effects were found in reproduction studies in rats and rabbits following oral administration of sildenafil.

## Appendix 1

There was no effect on sperm motility or morphology after single 100 mg oral doses of sildenafil in healthy volunteers (see section 5.1).

### 4.7 Effects on ability to drive and use machines

No studies on the effects on the ability to drive and use machines have been performed.

As dizziness and altered vision were reported in clinical trials with sildenafil, patients should be aware of how they react to Sildenafil Teva, before driving or operating machinery.

### 4.8 Undesirable effects

#### Summary of the safety profile

The safety profile of sildenafil is based on 9,570 patients in 74 double-blind placebo-controlled clinical studies. The most commonly reported adverse reactions in clinical studies among sildenafil treated patients were headache, flushing, dyspepsia, nasal congestion, dizziness, nausea, hot flush, visual disturbance, cyanopsia and. vision blurred.

Adverse reactions from post-marketing surveillance has been gathered covering an estimated period >10 years. Because not all adverse reactions are reported to the Marketing Authorisation Holder and included in the safety database, the frequencies of these reactions cannot be reliably determined.

#### Tabulated list of adverse reactions

In the table below all medically important adverse reactions, which occurred in clinical trials at an incidence greater than placebo are listed by system organ class and frequency (very common ( $\geq 1/10$ ), common ( $\geq 1/100$  to  $< 1/10$ ), uncommon ( $\geq 1/1,000$  to  $< 1/100$ ), rare ( $\geq 1/10,000$  to  $< 1/1,000$ ). Within each frequency grouping, undesirable effects are presented in order of decreasing seriousness.

**Table 1: Medically important adverse reactions reported at an incidence greater than placebo in controlled clinical studies and medically important adverse reactions reported through post- marketing surveillance**

## Appendix 1

<b>System Organ Class</b>	<b>Very common (□ 1/10)</b>	<b>Common (□ 1/100 and &lt;1/10)</b>	<b>Uncommon (□ 1/1,000 and &lt;1/100)</b>	<b>Rare (□ 1/10,000 and &lt;1/1,000)</b>
<b>Infections and infestations</b>			Rhinitis	
<b>Immune system disorders</b>			Hypersensitivity	
<b>Nervous system disorders</b>	Headache	Dizziness	Somnolence, Hypoesthesia	Cerebrovascular accident, Transient ischaemic attack, Seizure,* Seizure recurrence,* Syncope
<b>Eye disorders</b>		Visual colour distortions**, Visual disturbance, Vision blurred	Lacrimation disorders***, Eye pain, Photophobia, Photopsia, Ocular hyperaemia, Visual brightness, Conjunctivitis	Non-arteritic anterior ischaemic optic neuropathy (NAION), * Retinal vascular occlusion,* Retinal haemorrhage, Arteriosclerotic retinopathy, Retinal disorder, Glaucoma, Visual field defect, Diplopia, Visual acuity reduced, Myopia, Asthenopia, Vitreous floaters, Iris disorder, Mydriasis, Halo vision, Eye oedema, Eye swelling, Eye disorder, Conjunctival hyperaemia, Eye irritation, Abnormal sensation in eye,

## Appendix 1

				Eyelid oedema, Scleral discoloration
<b>Ear and labyrinth disorders</b>			Vertigo, Tinnitus	Deafness
<b>Cardiac disorders</b>			Tachycardia, Palpitations	Sudden cardiac death,* Myocardial infarction, Ventricular arrhythmia,* Atrial fibrillation, Unstable angina
<b>Vascular disorders</b>		Flushing, Hot flush	Hypertension, Hypotension	
<b>Respiratory, thoracic and mediastinal disorders</b>		Nasal congestion	Epistaxis, Sinus congestion	Throat tightness, Nasal oedema, Nasal dryness
<b>Gastrointestin al disorders</b>		Nausea, Dyspepsia	Gastro oesophageal reflux disease, Vomiting, Abdominal pain upper, Dry mouth	Hypoaesthesia oral
<b>Skin and subcutaneous tissue disorders</b>			Rash	Stevens-Johnson Syndrome (SJS),* Toxic Epidermal Necrolysis (TEN)*
<b>Musculoskelet al and connective tissue disorders</b>			Myalgia, Pain in extremity	

## Appendix 1

<b>Renal and urinary disorders</b>			Haematuria	
<b>Reproductive system and breast disorders</b>				Penile haemorrhage, Priapism,* Haemospermia, Erection increased
<b>General disorders and administration site conditions</b>			Chest pain, Fatigue, Feeling hot	Irritability
<b>Investigations</b>			Heart rate increased	

\*Reported during post-marketing surveillance only

\*\*Visual colour distortions: Chloropsia, Chromatopsia, Cyanopsia, Erythroptosis and Xanthopsia

\*\*\*Lacrimation disorders: Dry eye, Lacrimal disorder and Lacrimation increased

### Reporting of suspected adverse reactions

Reporting suspected adverse reactions after authorisation of the medicinal product is important. It allows continued monitoring of the benefit/risk balance of the medicinal product. Healthcare professionals are asked to report any suspected adverse reactions via the Yellow Card Scheme at: [www.mhra.gov.uk/yellowcard](http://www.mhra.gov.uk/yellowcard) or search for MHRA Yellow Card in the Google Play or Apple App Store.

### **4.9 Overdose**

In single dose volunteer studies of doses up to 800 mg, adverse reactions were similar to those seen at lower doses, but the incidence rates and severities were increased. Doses of 200 mg did not result in increased efficacy but the incidence of adverse reactions (headache, flushing, dizziness, dyspepsia, nasal congestion, altered vision) was increased.

In cases of overdose, standard supportive measures should be adopted as required. Renal dialysis is not expected to accelerate clearance as sildenafil is highly bound to plasma proteins and not eliminated in the urine.



## Appendix 1

### 5. PHARMACOLOGICAL PROPERTIES

#### 5.1 Pharmacodynamic properties

Pharmacotherapeutic group: Urologicals; Drugs used in erectile dysfunction. ATC Code:

G04BE03. Mechanism of action

Sildenafil is an oral therapy for erectile dysfunction. In the natural setting, i.e. with sexual stimulation, it restores impaired erectile function by increasing blood flow to the penis.

The physiological mechanism responsible for erection of the penis involves the release of nitric oxide (NO) in the corpus cavernosum during sexual stimulation. Nitric oxide then activates the enzyme guanylate cyclase, which results in increased levels of cyclic guanosine monophosphate (cGMP), producing smooth muscle relaxation in the corpus cavernosum and allowing inflow of blood.

Sildenafil is a potent and selective inhibitor of cGMP specific phosphodiesterase type 5 (PDE5) in the corpus cavernosum, where PDE5 is responsible for degradation of cGMP. Sildenafil has a peripheral site of action on erections. Sildenafil has no direct relaxant effect on isolated human corpus cavernosum but potently enhances the relaxant effect of NO on this tissue. When the NO/cGMP pathway is activated, as occurs with sexual stimulation, inhibition of PDE5 by sildenafil results in increased corpus cavernosum levels of cGMP. Therefore sexual stimulation is required in order for sildenafil to produce its intended beneficial pharmacological effects.

#### Pharmacodynamic effects

Studies *in vitro* have shown that sildenafil is selective for PDE5, which is involved in the erection process. Its effect is more potent on PDE5 than on other known phosphodiesterases. There is a 10-fold selectivity over PDE6 which is involved in the phototransduction pathway in the retina. At maximum recommended doses, there is an 80-fold selectivity over PDE1, and over 700-fold over PDE2, 3, 4, 7, 8, 9, 10 and 11. In particular, sildenafil has greater than 4,000-fold selectivity for PDE5 over PDE3, the cAMP-specific phosphodiesterase isoform involved in the control of cardiac contractility.

#### Clinical efficacy and safety

Two clinical studies were specifically designed to assess the time window after dosing during which sildenafil could produce an erection in response to sexual stimulation. In a

## Appendix 1

penile plethysmography (RigiScan) study of fasted patients, the median time to onset for those who obtained erections of 60 % rigidity (sufficient for sexual intercourse) was 25 minutes (range 12-37 minutes) on sildenafil. In a separate RigiScan study, sildenafil was still able to produce an erection in response to sexual stimulation 4-5 hours post-dose.

Sildenafil causes mild and transient decreases in blood pressure which, in the majority of cases, do not translate into clinical effects. The mean maximum decreases in supine systolic blood pressure following 100 mg oral dosing of sildenafil was 8.4 mmHg. The corresponding change in supine diastolic blood pressure was 5.5 mmHg. These decreases in blood pressure are consistent with the vasodilatory effects of sildenafil, probably due to increased cGMP levels in vascular smooth muscle. Single oral doses of sildenafil up to 100 mg in healthy volunteers produced no clinically relevant effects on ECG.

In a study of the hemodynamic effects of a single oral 100 mg dose of sildenafil in 14 patients with severe coronary artery disease (CAD) (>70 % stenosis of at least one coronary artery), the mean resting systolic and diastolic blood pressures decreased by 7 % and 6 % respectively compared to baseline. Mean pulmonary systolic blood pressure decreased by 9 %. Sildenafil showed no effect on cardiac output, and did not impair blood flow through the stenosed coronary arteries.

A double-blind, placebo-controlled exercise stress trial evaluated 144 patients with erectile dysfunction and chronic stable angina who regularly received anti-anginal medicinal products (except nitrates). The results demonstrated no clinically relevant differences between sildenafil and placebo in time to limiting angina.

Mild and transient differences in colour discrimination (blue/green) were detected in some subjects using the Farnsworth-Munsell 100 hue test at 1 hour following a 100 mg dose, with no effects evident after 2 hours post-dose. The postulated mechanism for this change in colour discrimination is related to inhibition of PDE6, which is involved in the phototransduction cascade of the retina. Sildenafil has no effect on visual acuity or contrast sensitivity. In a small size placebo-controlled study of patients with documented early age-related macular degeneration (n=9), sildenafil (single dose, 100 mg) demonstrated no significant changes in the visual tests conducted (visual acuity, Amsler grid, colour discrimination simulated traffic light, Humphrey perimeter and photostress).

There was no effect on sperm motility or morphology after single 100 mg oral doses of sildenafil in healthy volunteers (see section 4.6).

## Appendix 1

### *Further information on clinical trials*

In clinical trials sildenafil was administered to more than 8000 patients aged 19-87. The following patient groups were represented: elderly (19.9 %), patients with hypertension (30.9 %), diabetes mellitus (20.3 %), ischaemic heart disease (5.8 %), hyperlipidaemia (19.8 %), spinal cord injury (0.6 %), depression (5.2 %), transurethral resection of the prostate (3.7 %), radical prostatectomy (3.3 %). The following groups were not well represented or excluded from clinical trials: patients with pelvic surgery, patients post-radiotherapy, patients with severe renal or hepatic impairment and patients with certain cardiovascular conditions (see section 4.3).

In fixed dose studies, the proportions of patients reporting that treatment improved their erections were 62 % (25 mg), 74 % (50 mg) and 82 % (100 mg) compared to 25 % on placebo. In controlled clinical trials, the discontinuation rate due to sildenafil was low and similar to placebo.

Across all trials, the proportion of patients reporting improvement on sildenafil were as follows: psychogenic erectile dysfunction (84 %), mixed erectile dysfunction (77 %), organic erectile dysfunction (68 %), elderly (67 %), diabetes mellitus (59 %), ischaemic heart disease (69 %), hypertension (68 %), TURP (61 %), radical prostatectomy (43 %), spinal cord injury (83 %), depression (75 %). The safety and efficacy of sildenafil was maintained in long-term studies.

### Paediatric population

The European Medicines Agency has waived the obligation to submit the results of studies with Sildenafil Teva in all subsets of the paediatric population for the treatment of erectile dysfunction. See 4.2 for information on paediatric use.

## **5.2 Pharmacokinetic properties**

### Absorption

Sildenafil is rapidly absorbed. Maximum observed plasma concentrations are reached within 30 to 120 minutes (median 60 minutes) of oral dosing in the fasted state. The mean absolute oral bioavailability is 41 % (range 25-63 %). After oral dosing of sildenafil AUC and  $C_{\max}$  increase in proportion with dose over the recommended dose range (25-100 mg).

When sildenafil is taken with food, the rate of absorption is reduced with a mean delay in  $t_{\max}$  of 60 minutes and a mean reduction in  $C_{\max}$  of 29 %.

## Appendix 1

### Distribution

The mean steady state volume of distribution ( $V_d$ ) for sildenafil is 105 l, indicating distribution into the tissues. After a single oral dose of 100 mg, the mean maximum total plasma concentration of sildenafil is approximately 440 ng/mL (CV 40 %). Since sildenafil (and its major circulating N-desmethyl metabolite) is 96 % bound to plasma proteins, this results in the mean maximum free plasma concentration for sildenafil of 18 ng/mL (38 nM). Protein binding is independent of total drug concentrations.

In healthy volunteers receiving sildenafil (100 mg single dose), less than 0.0002 % (average 188 ng) of the administered dose was present in ejaculate 90 minutes after dosing.

### Biotransformation

Sildenafil is cleared predominantly by the CYP3A4 (major route) and CYP2C9 (minor route) hepatic microsomal isoenzymes. The major circulating metabolite results from N-demethylation of sildenafil. This metabolite has a phosphodiesterase selectivity profile similar to sildenafil and an *in vitro* potency for PDE5 approximately 50 % that of the parent drug. Plasma concentrations of this metabolite are approximately 40 % of those seen for sildenafil. The N-desmethyl metabolite is further metabolised, with a terminal half-life of approximately 4 h.

### Elimination

The total body clearance of sildenafil is 41 L/h with a resultant terminal phase half-life of 3-5 h. After either oral or intravenous administration, sildenafil is excreted as metabolites predominantly in the faeces (approximately 80 % of administered oral dose) and to a lesser extent in the urine (approximately 13 % of administered oral dose).

### Pharmacokinetics in special patient groups

#### *Elderly*

Healthy elderly volunteers (65 years or over) had a reduced clearance of sildenafil, resulting in approximately 90 % higher plasma concentrations of sildenafil and the active N-desmethyl metabolite compared to those seen in healthy younger volunteers (18-45 years). Due to age-differences in plasma protein binding, the corresponding increase in free sildenafil plasma concentration was approximately 40 %.

## Appendix 1

### *Renal insufficiency*

In volunteers with mild to moderate renal impairment (creatinine clearance = 30-80 mL/min), the pharmacokinetics of sildenafil were not altered after receiving a 50 mg single oral dose. The mean AUC and  $C_{max}$  of the N-desmethyl metabolite increased up to 126 % and up to 73 % respectively, compared to age-matched volunteers with no renal impairment. However, due to high inter-subject variability, these differences were not statistically significant. In volunteers with severe renal impairment (creatinine clearance <30 mL/min), sildenafil clearance was reduced, resulting in mean increases in AUC and  $C_{max}$  of 100 % and 88 % respectively compared to age-matched volunteers with no renal impairment. In addition, N-desmethyl metabolite AUC and  $C_{max}$  values were significantly increased by 200 % and 79 % respectively.

### *Hepatic insufficiency*

In volunteers with mild to moderate hepatic cirrhosis (Child-Pugh A and B) sildenafil clearance was reduced, resulting in increases in AUC (84 %) and  $C_{max}$  (47 %) compared to age-matched volunteers with no hepatic impairment. The pharmacokinetics of sildenafil in patients with severely impaired hepatic function have not been studied.

## **5.3 Preclinical safety data**

Non-clinical data revealed no special hazard for humans based on conventional studies of safety pharmacology, repeated dose toxicity, genotoxicity, carcinogenic potential, and toxicity to reproduction and development.

## **6. PHARMACEUTICAL PARTICULARS**

### **6.1 List of excipients**

Tablet core Microcrystalline cellulose  
Calcium hydrogen phosphate anhydrous  
Croscarmellose sodium

Magnesium stearate

#### Film-coat

Poly(vinyl  
alcohol)

## Appendix 1

Titanium dioxide  
(E171) Macrogol  
3350

Talc

### 6.2 Incompatibilities

Not applicable.

### 6.3 Shelf life

3 years.

### 6.4 Special precautions for storage

This medicinal product does not require any special temperature storage conditions. Store in the original package, in order to protect from moisture.

### 6.5 Nature and contents of container

Sildenafil Teva 25 mg film-coated tablets

PVC/Aluminium blisters in cartons of 2, 4, 8 or 12 tablets.

10 x 1 tablet in PVC/Aluminium perforated unit dose blisters.

Sildenafil Teva 50 mg film-coated tablets

PVC/Aluminium blisters in cartons of 2, 4, 8, 12 or 24 tablets. 10 x 1 tablet in PVC/Aluminium perforated unit dose blisters.

Sildenafil Teva 100 mg film-coated tablets

PVC/Aluminium blisters in cartons of 2, 4, 8, 12 or 24 tablets. 10 x 1 tablet in PVC/Aluminium perforated unit dose blisters.

Not all pack sizes may be marketed.

### 6.6 Special precautions for disposal and other handling

No special requirements.

## Appendix 1

### 7. MARKETING AUTHORISATION HOLDER

Teva

B.V.

Swens

weg 5

2031GA HaarlemThe Netherlands

### 8. MARKETING AUTHORISATION NUMBER(S)

Sildenafil Teva 25 mg film-coated

tablets EU/1/09/584/002

EU/1/09/58

4/003

EU/1/09/58

4/004

EU/1/09/58

4/005

EU/1/09/58

4/006

Sildenafil Teva 50 mg film-coated

tablets EU/1/09/584/008

EU/1/09/58

4/009

EU/1/09/58

4/010

EU/1/09/58

4/011

EU/1/09/58

4/012

EU/1/09/58

4/019

## Appendix 1

Sildenafil Teva 100 mg film-coated  
tablets EU/1/09/584/014

EU/1/09/58

4/015

EU/1/09/58

4/016

EU/1/09/58

4/017

EU/1/09/58

4/018

EU/1/09/584/020

### **9. DATE OF FIRST AUTHORISATION/RENEWAL OF THE AUTHORISATION**

Date of first authorisation: 30 November

2009 Date of latest renewal: 09

September 2014

### **10. DATE OF REVISION OF THE TEXT**

08/2019

Detailed information on this product is available on the website of the European Medicines Agency <http://www.ema.europa.eu>



## Appendix 1

### PREVIOUS STUDIES USING SILDENAFIL UNDER CONDITIONS OF HYPOXIA

Study	Subjects (N)	Hypoxia Stimulus % (altitude)	Sildenafil Dose (mg)	Exercise Type	Adverse Effects
Ghofrani et al., 2004	14	10 %	50 mg	Incremental cycling	<ul style="list-style-type: none"> <li>No serious short term adverse events</li> <li>Sildenafil: 2 aggravated symptoms who already had headaches during 2 day stay at altitude</li> </ul>
Faoro et al., 2007	16	10 %	50 mg	Incremental cycling	<ul style="list-style-type: none"> <li>“No noticeable side effect of sildenafil intake”.</li> </ul>
Ricart et al., 2005	14	11 %	100 mg	Cycling @ 50%VO <sub>2</sub> max	<ul style="list-style-type: none"> <li>Hypoxia: n = 1 headache</li> <li>Hypoxia + Sildenafil: n = 2 headache</li> <li>“no erectile response”</li> </ul>
Hsu et al., 2006	10	~13 % (3874m)	50 or 100 mg	Cycling for 30 min @ 55% work capacity followed by a 6 km time trial	<ul style="list-style-type: none"> <li>“a few subjects in this investigation reported that sildenafil exacerbated headaches”</li> <li>1 withdrawal from study</li> <li>Several reported feeling worse in the treatment trial</li> </ul>
Kjaergaard et al., 2007	14	12.5 %	100 mg	Incremental cycling to exhaustion	<ul style="list-style-type: none"> <li>Mild-moderate headaches (At rest in normoxia [N=1]; at rest in hypoxia + sildenafil [N=3]; during exercise in hypoxia [N=3]; during exercise in hypoxia + sildenafil [N=6]).</li> </ul>
Richalet et al., 2005	12	~12 % (4250 m)	3 x 40 mg p/day	Incremental cycling to exhaustion	<ul style="list-style-type: none"> <li>No significant adverse effects reported</li> <li>Probable increase in headache incidence in Sildenafil treated participants.</li> </ul>

# Appendix 1

Prof. Damian Miles Bailey

## ESQ-Cerebral Symptoms Questionnaire:

Subject ID: \_\_\_\_\_

Date: \_\_\_\_\_

Exposure time: \_\_\_\_\_

Condition: \_\_\_\_\_

**Instructions: Please circle the number of each item to correspond to HOW YOU FEEL AT THIS PRESENT MOMENT. PLEASE ANSWER EVERY ITEM. If you do not have the specific symptom, please circle 0 (ie. NOT AT ALL)**

	N O T  A T  A L L	S L I G H T	S O M E W H A T	M O D E R A T E	Q U I T E  A B I T	E X T R E M E
1. I feel lightheaded:	0	1	2	3	4	5
2. I have a headache:	0	1	2	3	4	5
3. I feel dizzy:	0	1	2	3	4	5
4. I feel faint:	0	1	2	3	4	5
5. My vision is dim:	0	1	2	3	4	5
6. My coordination is off:	0	1	2	3	4	5
7. I feel weak:	0	1	2	3	4	5
8. I feel sick to my stomach (nauseous):	0	1	2	3	4	5
9. I've lost my appetite:	0	1	2	3	4	5
10. I feel sick:	0	1	2	3	4	5
11. I feel hungover:	0	1	2	3	4	5

## Appendix 1

Prof. Damian Miles Bailey

### Lake Louise AMS scoring system (2018):

Subject ID: \_\_\_\_\_

Date: \_\_\_\_\_

**Instructions: Please circle the number of each item to correspond to HOW YOU FEEL AT THIS PRESENT MOMENT. PLEASE ANSWER EVERY ITEM. If you do not have the specific symptom, please circle 0.**

#### Self-assessment score:

- |                               |   |
|-------------------------------|---|
| 1. Headache:                  | [0] None at all<br>[1] Mild headache<br>[2] Moderate headache<br>[3] Severe headache, incapacitating                            |
| 2. Gastrointestinal symptoms: | [0] Good appetite<br>[1] Poor appetite/nausea<br>[2] Moderate nausea/vomiting<br>[3] Severe, incapacitating nausea and vomiting |
| 3. Fatigue and/or weakness    | [0] Not tired or weak<br>[1] Mild fatigue/weakness<br>[2] Moderate fatigue/weakness<br>[3] Severe fatigue/weakness              |
| 4. Dizziness/light-headedness | [0] None<br>[1] Mild<br>[2] Moderate<br>[3] Severe, incapacitating  |

#### AMS Clinical Functional score:

- |   |  |
|---|--|
| 1. Overall, if you had AMS symptoms, how did they affect your activities? | [0] Not at all<br>[1] Symptoms present, but did not force any change in activity or itinerary<br>[2] My symptoms forced me to stop the ascent or to go down on my own power<br>[3] Had to be evacuated to a lower altitude |
|---|--|

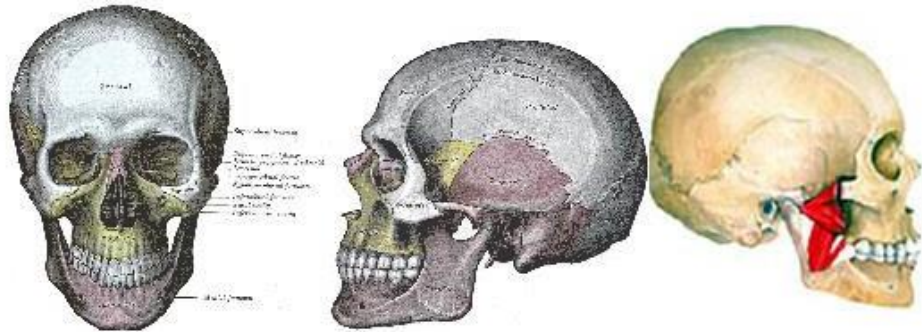
# Appendix 1

Prof. Damian Miles Bailey

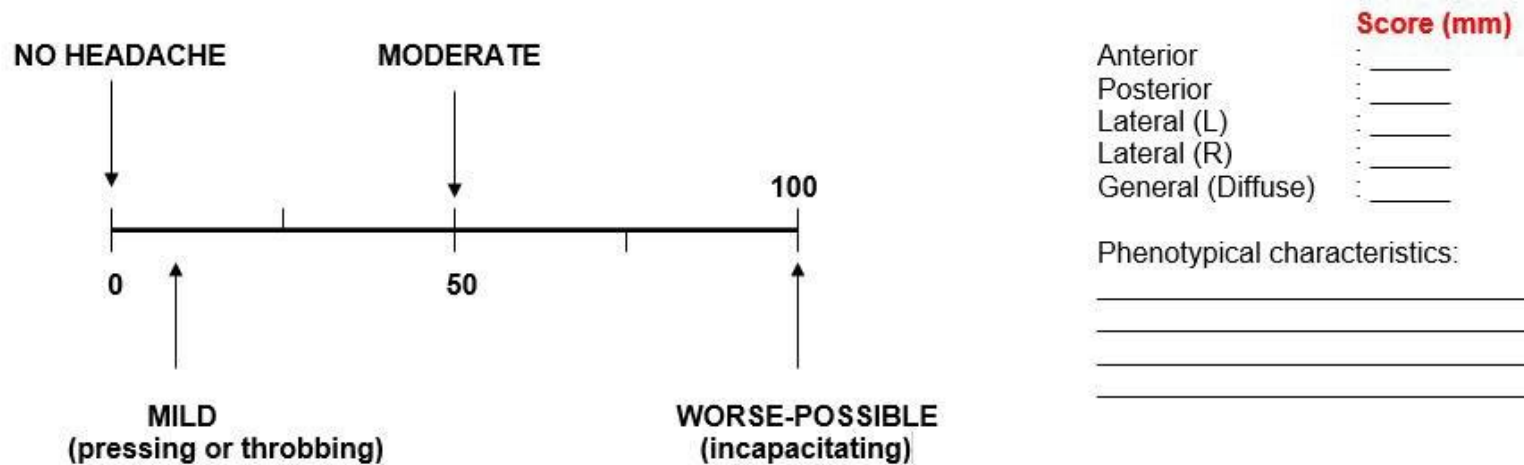
## High Altitude Headache

Name: \_\_\_\_\_

Date: \_\_\_\_\_



Please indicate on the line below how severe your headache is at the PRESENT MOMENT IN TIME:





## Neurovascular Research Laboratory

---

ADM502.02

### Policy and Process for Reporting Adverse Events

---

This SOP covers the policy and process for reporting undesirable, unexpected or untoward events (Adverse Events) that may be encountered during a research project.

#### APPROVALS:

**Prepared by:** Benjamin Stacey

Research Assistant  
University of South  
Wales

Signature \_\_\_\_\_

Date \_\_\_\_\_

**Approved by:** Damian Bailey

Professor  
University of South Wales

Signature \_\_\_\_\_

Date \_\_\_\_\_

## Appendix 1

# Policy and Process for Reporting Adverse Events

Any research project can encounter undesirable, unexpected or untoward events. These events need to be assessed, acted upon, and reported by the research team. The following policy and procedure will assist in such scenarios.

## What are adverse events?

Adverse events are any untoward event, they may be unexpected or anticipated, and can be separated into two sub categories; Adverse Events (AE) and Serious Adverse Events (SAE). All research can encounter Adverse Events, while a SAE are more likely to occur in medical or clinical research (including the administration of drugs).

It is important to understand that this policy applies to research, and events that may transpire during the conduct of research. The University has a separate policy for the reporting of accidents and incidents that occur as a result of broader day to day activities at the USW known as the '*Accidents – Incident Reporting and Management Procedure*'.

## Who does this apply to?

The policy and process for reporting adverse events applies to all members of the research team involved in the project being conducted at the Neurovascular research Laboratory, University of South Wales.

## Policy

All members of the Neurovascular Research Laboratory are required to report any suspected or actual event that meets the definition of an AE or a SAE during the research project.

It is the responsibility of all individuals to report events promptly, using the approved reporting procedure, and providing detailed and accurate information of the circumstances.

Where emergency situations are part of the AE/SAE, appropriate remedial action should be taken before completion of the AE/ SAE Report.

## Appendix 1

### Definitions

**Adverse Events (AE)** - AEs are defined as any untoward occurrence in a study participant but this should be extended to include all research scenarios, especially medical or clinical scenarios. An AE does not necessarily have to have

a causal relationship with the study treatment or procedure. An AE can therefore be any unfavourable and unintended sign (including an abnormal finding), symptom or disease temporally associated or detected as part of participation in research. This includes any occurrence that is new in onset or aggravated in severity or frequency from the baseline condition, or abnormal results of diagnostic procedures, including laboratory test abnormalities.

For research that is not clinical in nature, adverse events may still present themselves and should still be managed in line with this policy, i.e. they are recorded, reported and managed.

**Adverse Event Associated with the Use of the Drug** - An AE is considered to be associated with the use of the drug if the attribution is possible, probable, or very likely by the definitions listed below:

- **Not related:** An AE that is not related to the use of the drug.
- **Doubtful:** An AE for which an alternative explanation is more likely, e.g., concomitant drug(s), concomitant disease(s), or the relationship in time suggests that a causal relationship is unlikely.
- **Possible:** An AE that might be due to the use of the drug and for which an alternative explanation, e.g., concomitant drug(s), concomitant disease(s), is inconclusive. The relationship in time is reasonable and therefore, the causal relationship cannot be excluded.
- **Probable:** An AE that might be due to the use of the drug. The relationship in time is suggestive (e.g. confirmed by drug withdrawal). An alternative explanation is less likely, e.g. concomitant drug(s), concomitant disease(s).
- **Very likely:** An AE that is listed as a possible adverse reaction and cannot be reasonably explained by an alternative explanation, e.g., concomitant drug(s), concomitant disease(s). The relationship in time is very suggestive (e.g., the AE occurs shortly after drug administration or close to the time of maximum concentration [T<sub>max</sub>]).

**Serious Adverse Event (SAE)** - A SAE is defined by the International Council for Harmonisation of Technical Requirements for Pharmaceuticals for Human Use (ICH) as any untoward occurrence that meets any of the following conditions:

- Results in the death of the participant.
- Near miss incidents.
- Is life-threatening. The term “life-threatening” refers to an event in which the participant was at risk of death at the time of the event; it does not refer to an event which hypothetically might have caused death if it were more severe.

## Appendix 1

- Requires inpatient hospitalisation or prolongation of existing hospitalisation.

Results in persistent or significant disability / incapacity. Any event that seriously disrupts the ability of the participant to lead a normal life, in other words leads to a persistent or permanent significant change, deterioration, injury or perturbation of the participant's body functions or structure, physical activity and/or quality of life.

- Is a congenital anomaly / birth defect. Exposure to the study drug before conception (in men or women) or during pregnancy that resulted in an adverse outcome in the child.
- Other medical events. Medical events that may jeopardise the subject or may require an intervention to prevent a characteristic or consequence of a SAE. Such events are referred to as 'important medical events' and are also considered as 'serious' in accordance with the definition of a SAE.

## Process

The majority of research conducted within the Neurovascular Research Laboratory does not include the administration of new or novel drugs or medicines. Therefore, it is anticipated that if they do occur, most adverse events will be non-serious adverse events.

Regardless of the type of event that has occurred the research team must notify the PI immediately, if they are not already aware.

The event must be categorised into either an **Adverse Event (AE)** or **Serious Adverse Event (SAE)** in accordance with the definitions above. Processes for both type of event are included below.

### **Reporting Adverse Events**

Members of the research team must notify the PI as soon as an AE occurs or is suspected to have occurred. The team must act appropriately to address the event.

The PI must ensure that the Adverse Event Report (F502A) is completed at the earliest opportunity and that it includes; when the event occurred, the details of the AE, any potential study relation, action taken and resolution / closure of the AE.

The PI must ensure that the AE report is stored in the Trial Master File and that it is updated in a timely manner, when required.

If AEs have occurred during the study, the PI must ensure that the AE reporting template is completed and sent to the Research Governance Manager, who will then liaise with all relevant University departments and committees.

If an AE occurs and is considered to be related to the use of the study drug, the PI should inform the MHRA.



## Appendix 1

### Reporting Serious Adverse Events (SAE)

When a SAE occurs, the person(s) involved should be provided with first aid if required, and where necessary, taken to hospital. If the seriousness warrants, the Emergency Services must be called. If a fatal incident occurs, the ambulance and police service must be called immediately and the area left undisturbed as far as possible until they have arrived.

Members of the research team must notify the PI as soon as a SAE occurs or is suspected.

The PI must next contact the Research Governance Manager and a member of the University Health and Safety team to allow the incident to be reported in accordance with the '*Reporting of Injuries and Dangerous Occurrences Regulations (RIDDOR)*'.

The PI must ensure that the Serious Adverse Event Report (F502B) is completed at the earliest opportunity and that it includes when the event occurred, the details of the SAE, any potential study relation, action taken and resolution / closure of the SAE.

The PI must ensure that the SAE reporting template is sent to the Research Governance Manager as soon as possible, who will then liaise with all relevant University departments in accordance with Section 5.4 and 5.6 of the University's '*Reporting and Managing Incidents*' procedure (OHSS 02.01 01/18).

**For studies using a drug** - Any SAE related to the study drug should be reported to the MHRA. If the SAE has not previously been reported in the Summary of Product Characteristics for the drug and the PI believe it is related to the drug, the PI should report the Suspected Unexpected Serious Adverse Reactions (SUSARs) to the MHRA via the electronic SUSAR (eSUSAR) reporting form.

### Studies Sponsored by the University of South Wales

The PI must ensure that the entire research team (listed investigators) are familiar with the *Policy and Process for Reporting Adverse Events*.

The PI must ensure that all relevant individuals in the host organisation are notified immediately of any Serious AEs within the time frames stipulated in the host's policy.

The PI must notify the USW Research Governance Manager of any SAEs that are suspected or identified as soon as feasibly possible, who will then notify the relevant University departments.

## Appendix 1

### Revisions

Revision No.	Effective Date	Description of Change
1	24.11.20	Change to definitions and procedure.

## ADVERSE EVENT REPORT

<b>Study title:</b>			
<b>Study ID:</b>			
<b>Principal Investigator:</b>			
<b>Date of adverse event actual or suspected:</b>			
<b>Reported by:</b>		<b>Date:</b>	
<b>Reported to:</b>		<b>Date</b>	
<b>Nature of event:</b>			
<b>Is this a Serious Adverse Event?</b>	YES / NO (delete as appropriate) If YES, please complete the <b>Serious Adverse Event Report (F502B.02)</b>		
<b>Summary of Corrective and preventive action</b>			
<b>Has this event been dealt with?</b>	YES / NO (delete as appropriate)		
<b>Does this event require any further action?</b>	YES / NO (delete as appropriate)		
<b>If YES, please state:</b>			
<b>Document created by</b>			
<b>Signature</b>		<b>Dated</b>	
<b>Countersigned (Principal Investigator)</b>			
<b>Signature</b>		<b>Dated</b>	

## Appendix 1

### SERIOUS ADVERSE EVENT REPORT

A serious adverse event is any medical occurrence that results in death, is life-threatening, requires or prolongs hospitalisation, causes persistent or significant disability, results in congenital abnormalities or represents potentially serious harm to research patients and others.

*Note: Any Serious Adverse Event considered to be related to the study drug should be reported directly to the MHRA.*

<b>Participant ID:</b>	
<b>Study title:</b>	
<b>Site name:</b>	
<b>Please provide a description of the serious adverse event:</b>	
<b>Date of onset:</b>	
<b>Has the event been resolved?</b>	YES / NO (delete as appropriate)
<b>Describe how the event was addressed:</b>	
<b>Date resolved:</b>	
<b>Which serious category did the event match? (please tick)</b>	Resulted in death
	Life Threatening
	Hospitalisation, or prolongation of existing hospitalisation
	Persistent or significant disability /incapacity
	Other important medical condition
	Unrelated
	Unlikely to be related

## Appendix 1

<b>Was the event related to study participation?</b> (please tick)	Possibly related
	Probably related
	Definitely related
<b>Was the event expected?</b> (please tick)	Expected
	Not Expected
<b>Date this form was completed:</b>	
<b>Signature of person responsible for notification:</b>	
<b>Name of person responsible for notification:</b>	
<b>Position:</b>	

## Appendix 1

### Substance Storage, Withdraw and Disposal Log (GK002)

This log tracks the storage, withdrawal, and disposal of tablets within the locked cabinet held in GK002.

#### 1. Item stored

(To be completed for each packet stored. The item manufacturer, serial number, quantity of tablets per packet, expiry date, date of disposal and the person that disposed of the item must be provided)

Item	Manufacturer	Serial Number	Quantity	Expiry Date	Disposal Date	Disposed by

## Appendix 1

### 2. Items withdrawn

(To be completed for each item withdrawal. The name of the item, serial number, the number of tablets withdrawn, the date of withdrawal, the researcher conducting the withdrawal and researcher's signature, must be provided)

<b>Item:</b>		<b>Serial Number:</b>		<b>Quantity:</b>		<b>Date:</b>	
<b>Researcher Name:</b>				<b>Signature:</b>			

<b>Item:</b>		<b>Serial Number:</b>		<b>Quantity:</b>		<b>Date:</b>	
<b>Researcher Name</b>				<b>Signature:</b>			

<b>Item:</b>		<b>Serial Number:</b>		<b>Quantity:</b>		<b>Date:</b>	
<b>Researcher Name</b>				<b>Signature:</b>			

<b>Item:</b>		<b>Serial Number:</b>		<b>Quantity:</b>		<b>Date:</b>	
<b>Researcher Name</b>				<b>Signature:</b>			

# Appendix 1

Incoming Material Transfer Agreement Information Sheet			
<b>1</b>	<b>Cardiff University PI</b>		<b>School</b>
<b>2</b>	<b>Name of contact at school if not PI</b>		
<b>3</b>	<b>Please provide the details of the university, organisation, institution or body providing the material and the name of the key contact at the same.</b>		
	Name		
	Address		
	Telephone	Email	
<b>4</b>	<b>Please provide a description of the material to be received.</b>		
	<i>Note: Please include relevant quantities where known.</i>		
<b>5</b>	<b>About the material</b>		
a.	Is the material of human origin?	Yes	
		Yes - DNA	
		Yes - divided outside the human body or been rendered acellular	
		No	
b.	Is the material to be used in humans (in the research)?	Yes	
		No	
c.	Is the material readily available from another source?	Yes	
		No	
d.	Is the material available commercially?	Yes	
		No	
		If yes, please indicate the cost:	
<b>6</b>	<b>Finance</b>		
a.	Is Cardiff University required to pay the provider for the supply of the material? (If Yes, an approved CAP form is required)	Yes	
		No	
b.	If not, is Cardiff University required to pay associated preparation and transport costs?	Yes	
		No	
<b>7</b>	<b>Employees</b>		
a.	Will any non-Cardiff University employee be involved in using the material? (eg students, honorary staff, visiting fellows, third party collaborators)	Yes	
		No	
b.	If yes, please specify		
<b>8</b>	<b>Dementia Research Institute ("DRI")</b>		
a.	Is the project funded by the DRI?	Yes	
		No	
b.	Does the project use facilities or equipment funded by the DRI?	Yes	
		No	
<b>9</b>	<b>Third party funding</b>		
a.	Are you using material in a project funded by a 3 <sup>rd</sup> party (e.g. EPSRC, Wellcome Trust, Pharmaceutical co. etc.)?	Yes	
		No	
	If yes, please specify:		
b.	If Yes, please indicate the RIS a/c code:		
c.	If Yes, please identify the funder:		
<b>10</b>	<b>Timeframe and usage</b>		



## Appendix 1

a.	Please state the date the samples have been or will be received by Cardiff University.	
<p>Note: it is important that the agreement is effective from the date that the samples are first received, if they are already in Cardiff University's possession. If the samples are to be received on or by a specific date, please state this otherwise we shall endeavour to progress this as quickly as possible.</p>		
b.	Please state how you will be using the material:  If <i>Other</i> , please specify:	Testing capacity only
		Developing/modifying material
		Other
c.	Details of the requirements for storage of the material (eg temperature):	
d.	Will the material be used and/or destroyed in the course of the research?	Yes
		No
e.	What are the arrangements for return/disposal of the material post-completion of the research?	
f.	Has there been, or will there be, any personally identifiable data (eg. medical history) also provided? Please provide details:	Yes
		No
g.	Was the donor of the material living or deceased?	Living
		Deceased
		N/A
h.	Please provide a description of the project to be undertaken by Cardiff University using the materials	

### 11 Publication, results and data

a.	Please confirm the level of review and approval with which you are happy.	Provider to approve CU's Publications (ie consent is required)
		Provider to review Cardiff University's Publications
		Provider to be given copies of all Cardiff University Publications
b.	By whom do you need the results/data to be owned?	Cardiff University
		The Provider
		The Funder
c.	Is the Principal investigator happy to notify the provider of the results/data, if stipulated in the MTA?	Yes
		No

Please note that to ensure with the Human Tissue Act, the Principal Investigator will need to obtain the following from the organisation or institution transferring the material:

- a copy of the ethical approval letter (or other form of appropriate documentation) to be able to evidence satisfactorily that the samples have been sourced consistently with the legal and ethical requirements as applicable in England and Wales; and
- a copy of the donor consent form (template) to evidence that the samples have been collected, transferred and used in accordance with the donor consent; or
- evidence to support the consent exemption (if applicable).





### 12 Any other relevant information (including associated risks) in relation to the material being provided of which the Contracts Team should be aware.

--

Please return this form to [contracts@cardiff.ac.uk](mailto:contracts@cardiff.ac.uk) when complete.

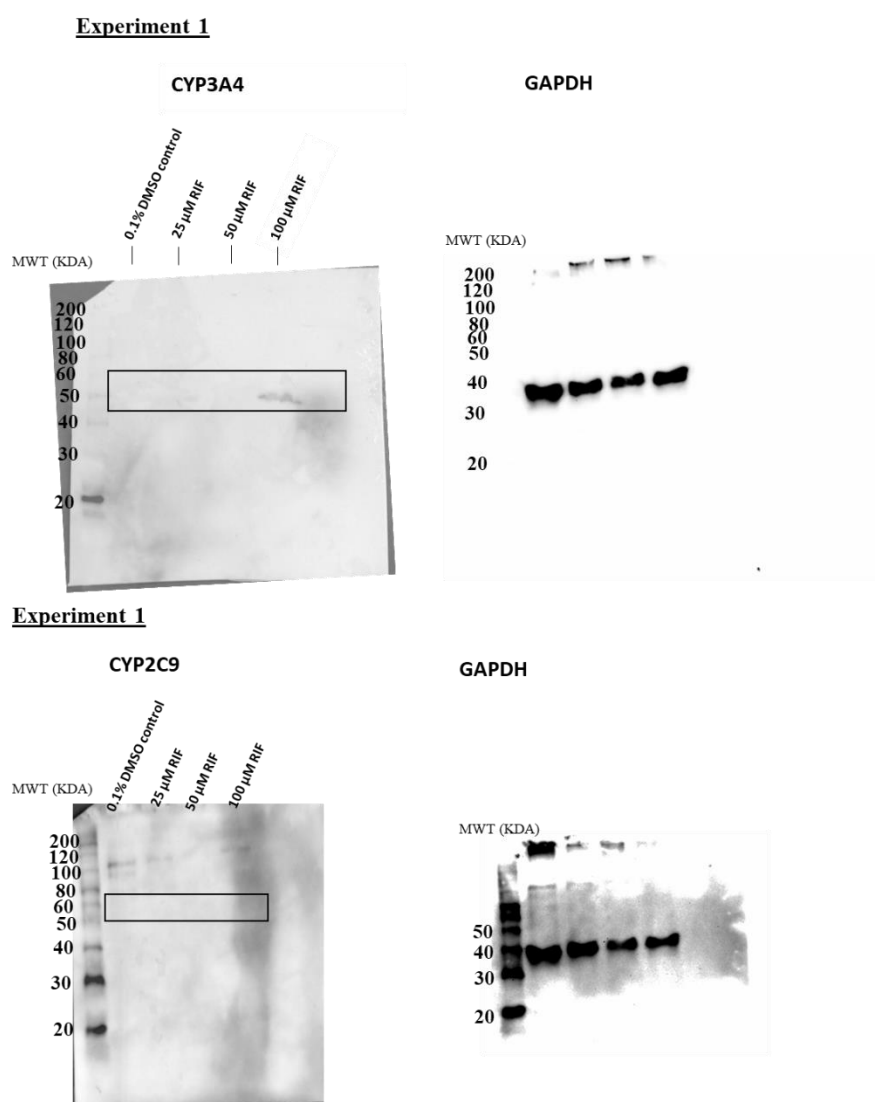
## Appendix 1

### Good clinical practice (GCP) training certificate

 <p>Ymchwil Iechyd a Gofal Cymru Health and Care Research Wales</p>	 <p>Ariennir gan Lywodraeth Cymru Funded by Welsh Government</p>
 <p><b>NIHR CRN Workforce Development</b> <i>Enabling learning and development in the Clinical Research Network</i></p>	 <p><b>National Institute for Health Research</b></p>
<h2>Certificate of Attendance</h2> <p><b>Dalal Alablani</b> attended</p> <p><b>Introduction to Good Clinical Practice (GCP):</b> A practical guide to ethical and scientific quality standards in clinical research</p> <p>on 29<sup>th</sup> October 2019</p> <p>Sessions include:</p> <ol style="list-style-type: none"><li>1. The Value of Clinical Research and the role of NIHR CRN &amp; Health and Care Research Wales</li><li>2. Introduction to research and the GCP standards</li><li>3. Preparing to deliver your study</li><li>4. Identifying and recruiting participants: Eligibility &amp; Informed Consent</li><li>5. Data collection and ongoing study delivery</li><li>6. Safety reporting and Study closure</li></ol> <p>Including EU Directives, Medicines for Human Use (Clinical Trials) Regulations and the UK Policy Framework for Health and Social Care Research, as applied to the conduct of Clinical Trials and other studies conducted in the NHS</p> <p><b>This course is accredited by the CPD Certification Service (6.5 Hours) and the Royal College of Physicians (6 CPD points) CPD Code: 125261</b></p>	

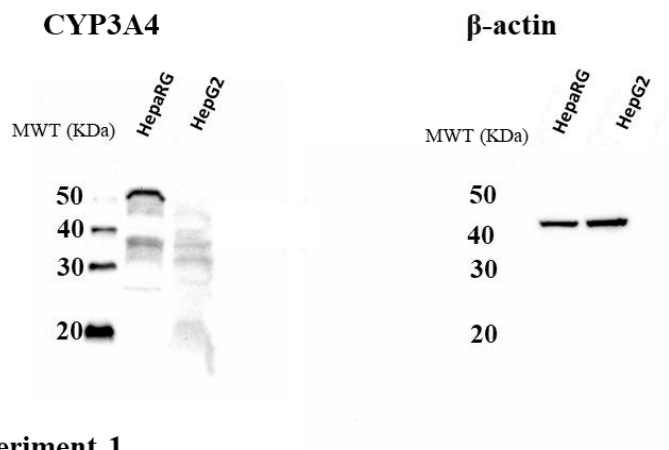
## Appendix 2- Western blot experiment data

- This section shows the entire membranes for the all-western blot experiments conducted in this thesis.

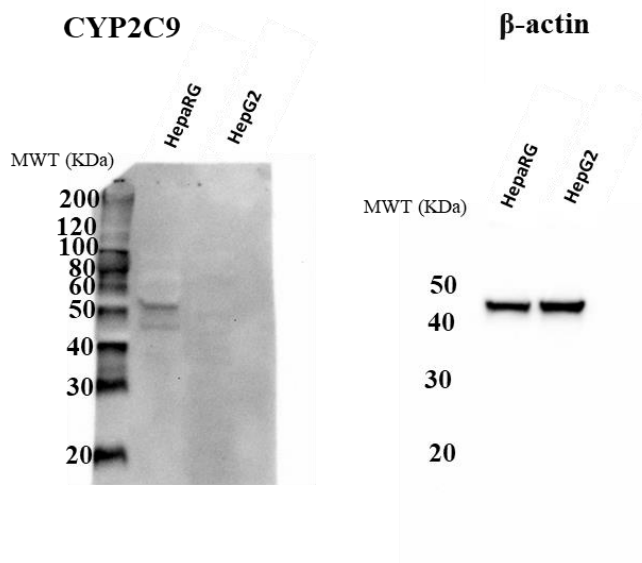


Supplementary figure 2.1 Induction of CYP3A4 and CYP2C9 protein in HepG2 after 48 h treatment with CYP450 inducer rifampicin (RIF) at 0 to 100  $\mu$ M concentrations. Supplementary Fig. 2.1A and Supplementary Fig 2.1B a scan of western blot membrane for CYP3A4 and CYP2C9, respectively involving cell lysates of 50  $\mu$ g of extracted protein loaded and separated by SDS-PAGE, electrotransferred to nitrocellulose membrane, and immunoblotted with anti-CYP3A4 (50 kDa) and anti-CYP2C9 (55 kDa) antibodies. GAPDH (37 kDa) was used as an internal control for protein loading.

**Experiment 1**

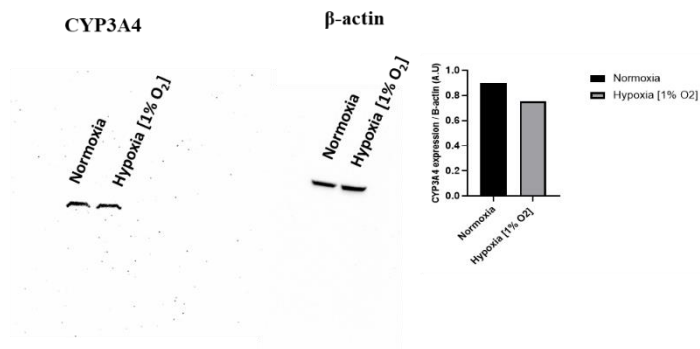


**Experiment 1**

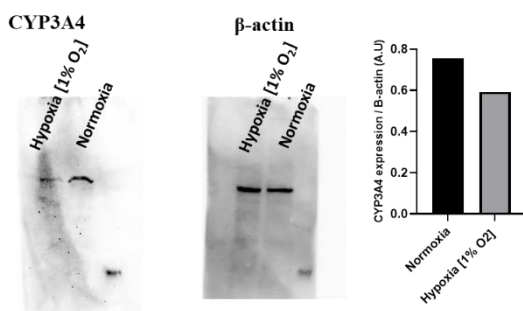


**Supplementary figure 2.2 Comparison between HepG2 and HepaRG CYP3A4 and CYP2C9 protein expression. Supplementary fig 4.9A and fig 4.9B represent the western blot analysis of CYP3A4 (50 KDa) and CYP2C9 (55 KDa).  $\beta$ -actin (42 kDa) was used as an internal control for protein loading.**

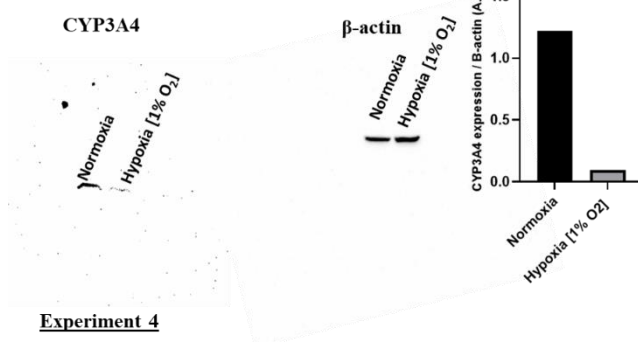
**Experiment 1**



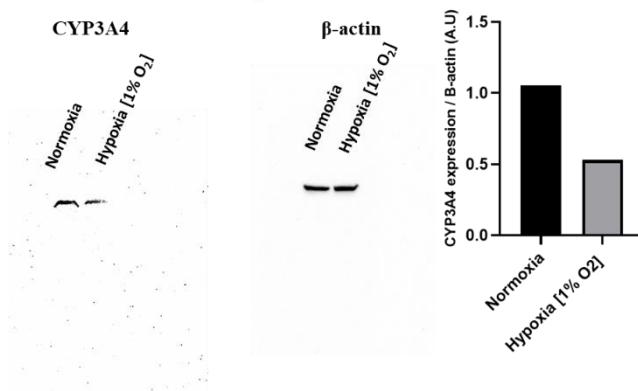
**Experiment 2**



**Experiment 3**

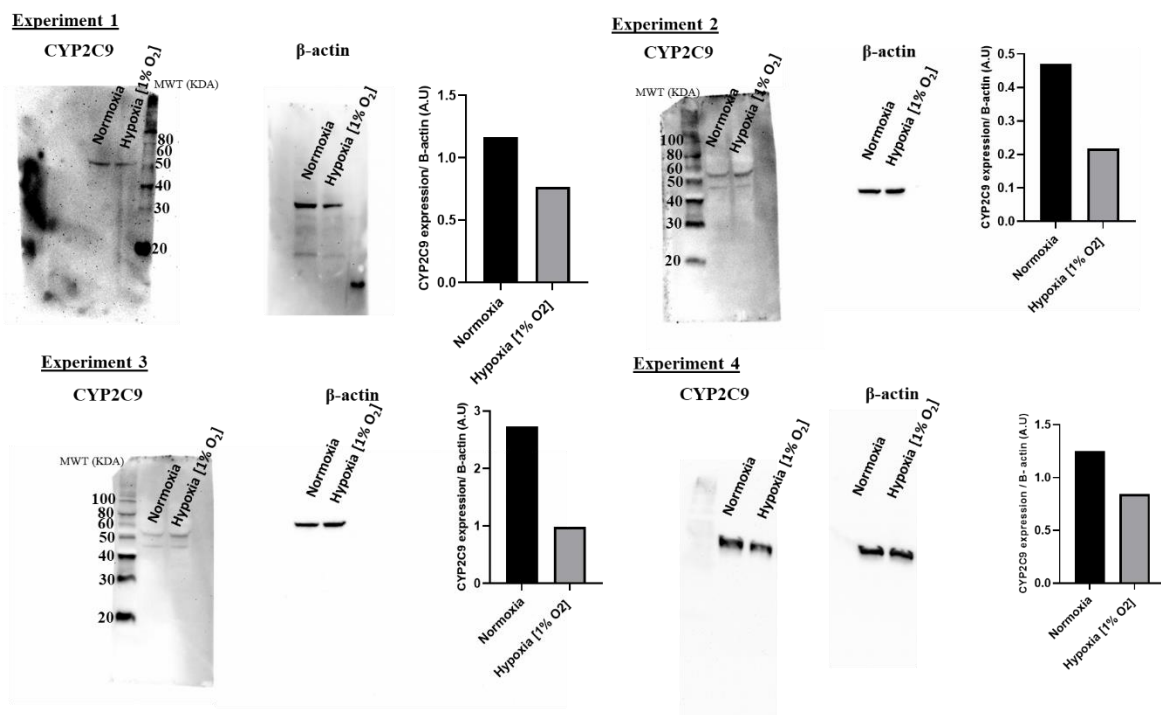


**Experiment 4**



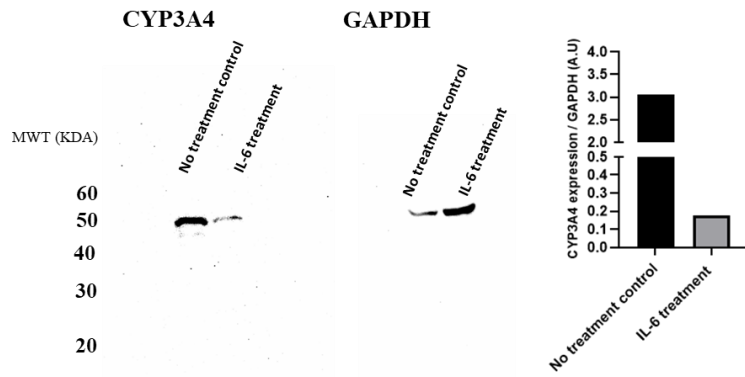
**Supplementary figure 2.3 Effect of hypoxia (1% O<sub>2</sub>) on CYP3A4 activity in 2D monolayer HepaRG. Western blot analysis of CYP3A4 (50 KDa) and the corresponding densitometry normalised to  $\beta$ -actin (42 kDa).**

## Appendix 2

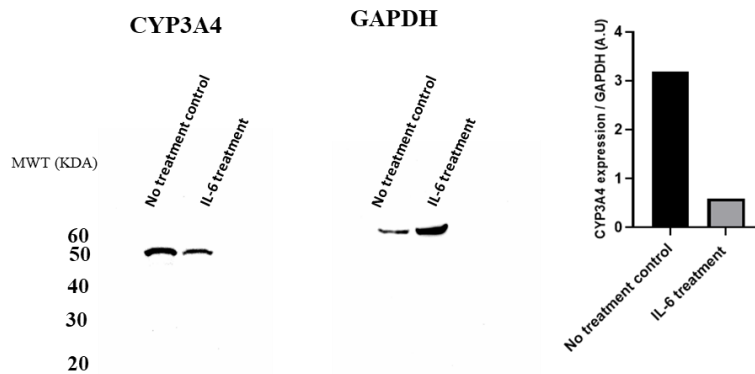


**Supplementary figure 2.4 Effect of hypoxia (1% O<sub>2</sub>) on CYP2C9 activity in 2D monolayer HepaRG. Western blot analysis of CYP2C9 (55 kDa) and the corresponding densitometry normalised to β-actin (42 kDa).**

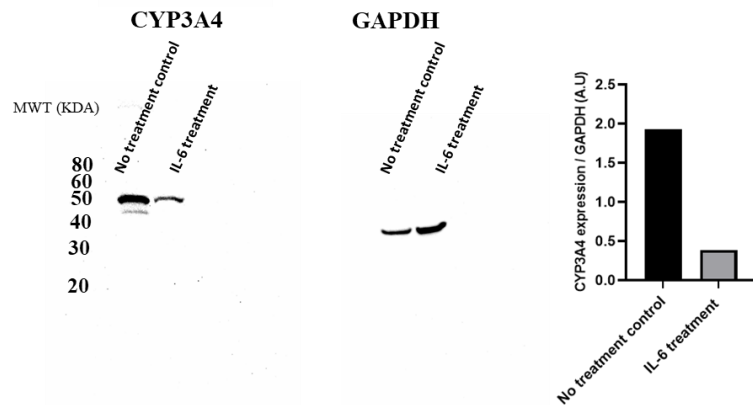
**Experiment 1**



**Experiment 2**

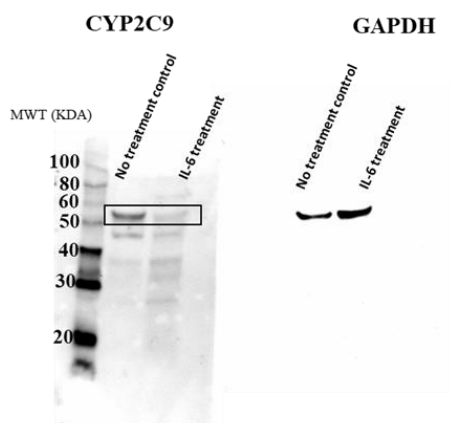


**Experiment 3**

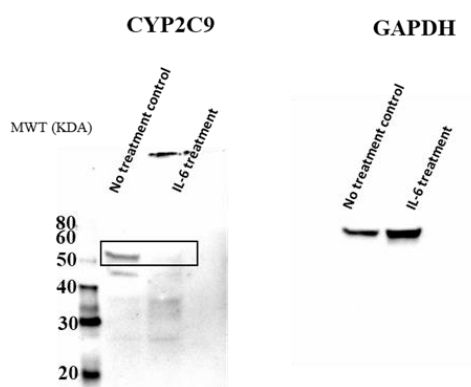


Supplementary figure 2.5 The effect of IL-6 treatment on CYP3A4 and CYP2C9 protein expression in HepaRG cells. HepaRG cells were differentiated following the standard protocol. After differentiation cells were treated with 10 ng/mL of IL-6 for 72 h under standard conditions. Original scan of Western blot membrane shows protein levels of CYP3A4 (50 kDa) in 3 different experiments. GAPDH (37 kDa) was used as internal control.

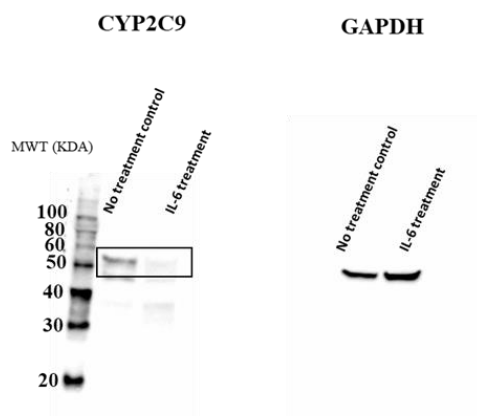
**Experiment 1**



**Experiment 2**



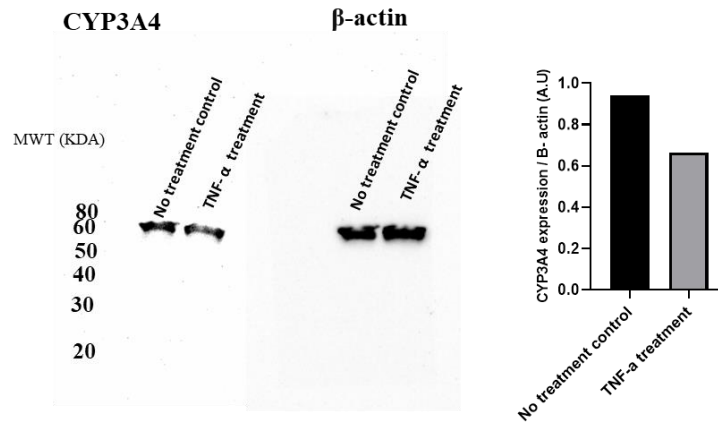
**Experiment 3**



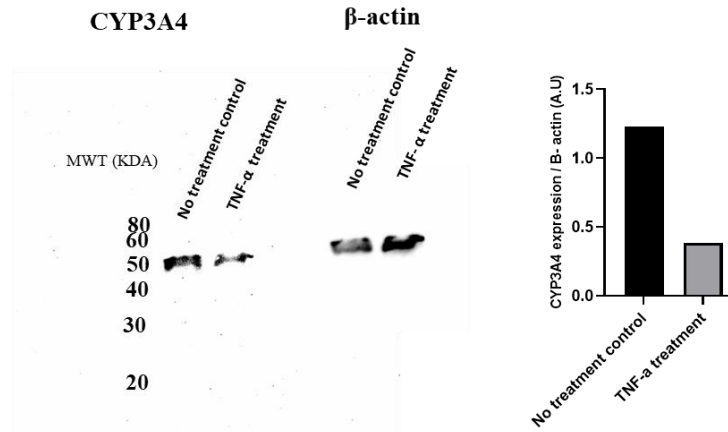
**Supplementary figure 2.6** The effect of IL-6 treatment on CYP3A4 and CYP2C9 protein expression in HepaRG cells. HepaRG cells were differentiated following the standard protocol. After differentiation cells were treated with 10 ng/mL of IL-6 for 72 h under standard conditions. Original scan of Western blot membrane shows protein levels of CYP2C9 (55 kDa) in 3 different experiments. GAPDH (37 kDa) was used as internal control.



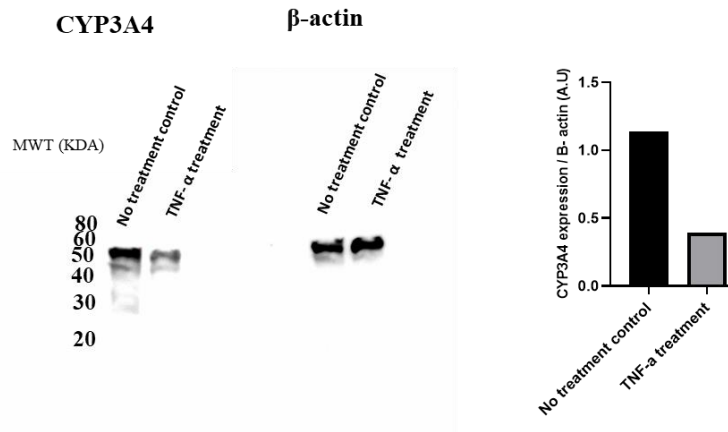
**Experiment 1**



**Experiment 2**

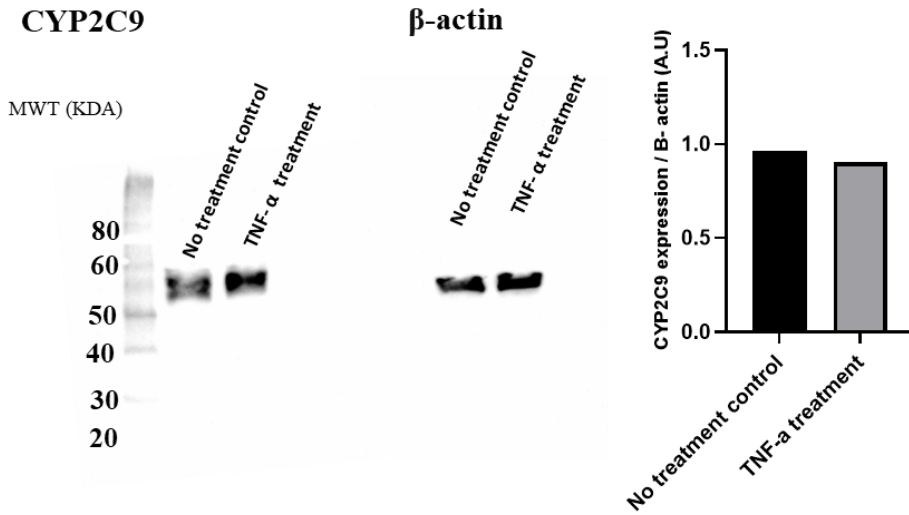


**Experiment 3**

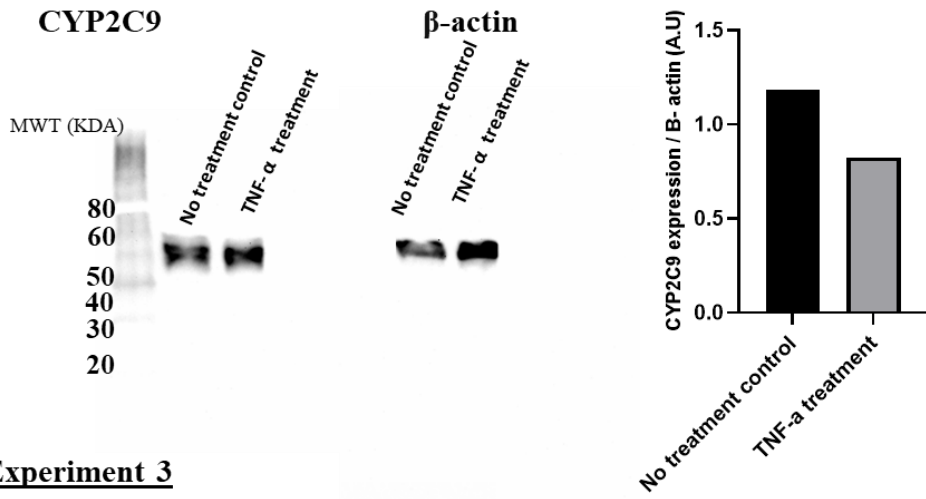


**Supplementary figure 2.7** The effect of TNF- $\alpha$  treatment on CYP3A4 protein expression in HepaRG cells. HepaRG cells were differentiated following the standard protocol. After differentiation cells were treated with 10 ng/mL of TNF- $\alpha$  for 24 h under standard conditions. Original scan of Western blot membrane shows protein levels of CYP3A4 (50 KDa) in 3 different experiments.  $\beta$ -Actin (42 KDa) was used as internal control

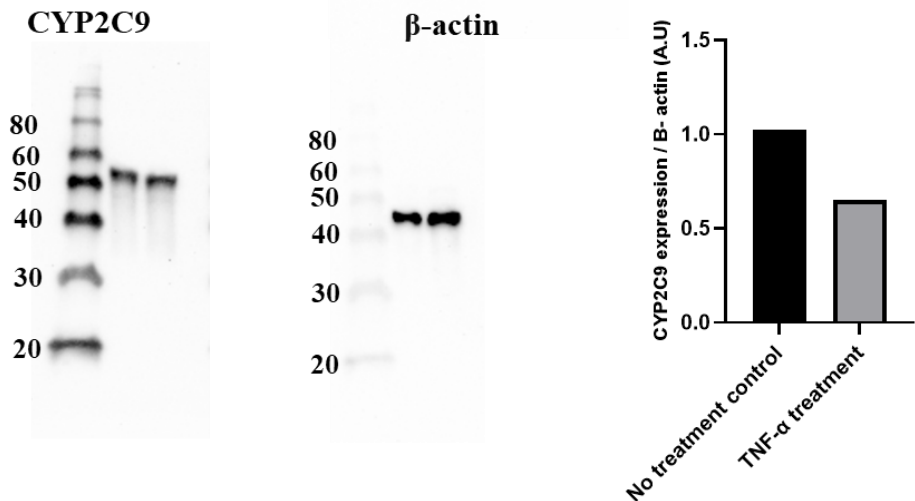
**Experiment 1**



**Experiment 2**

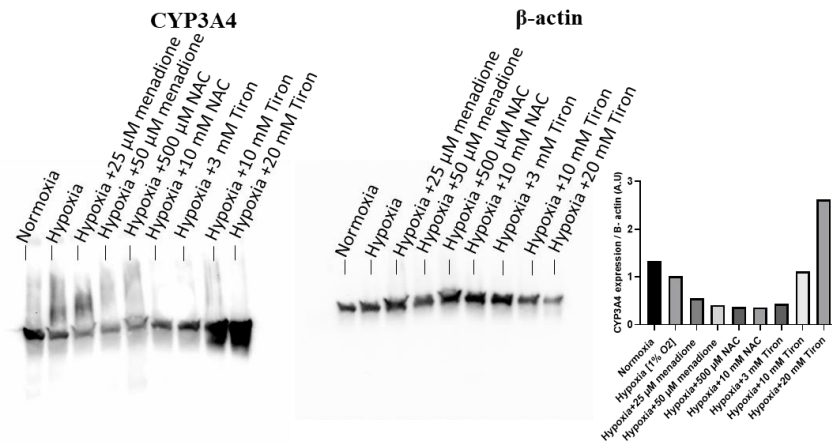


**Experiment 3**

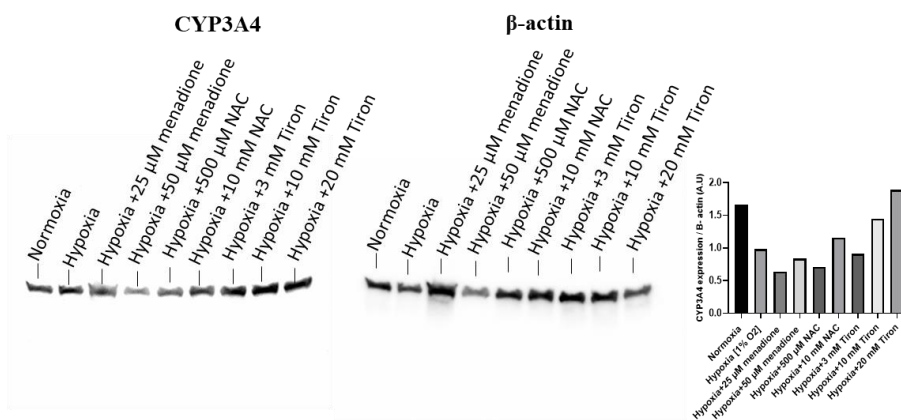


Supplementary figure 2.8 The effect of TNF- $\alpha$  treatment on CYP2C9 protein expression in HepaRG cells. HepaRG cells were differentiated following the standard protocol. After differentiation cells were treated with 10 ng/mL of TNF- $\alpha$  for 24 h under standard conditions. Original scan of Western blot membrane shows protein levels of CYP2C9 (55 KDa) in 3 different experiments.  $\beta$ -Actin (42 KDa) was used as internal control

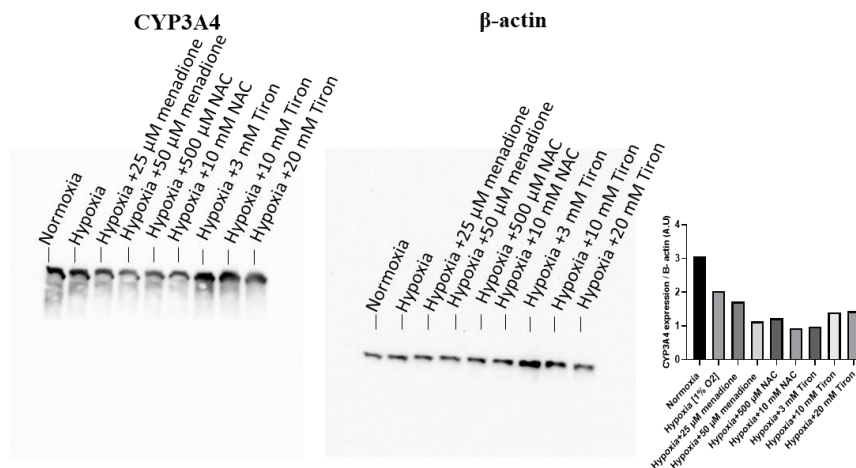
**Experiment 1**



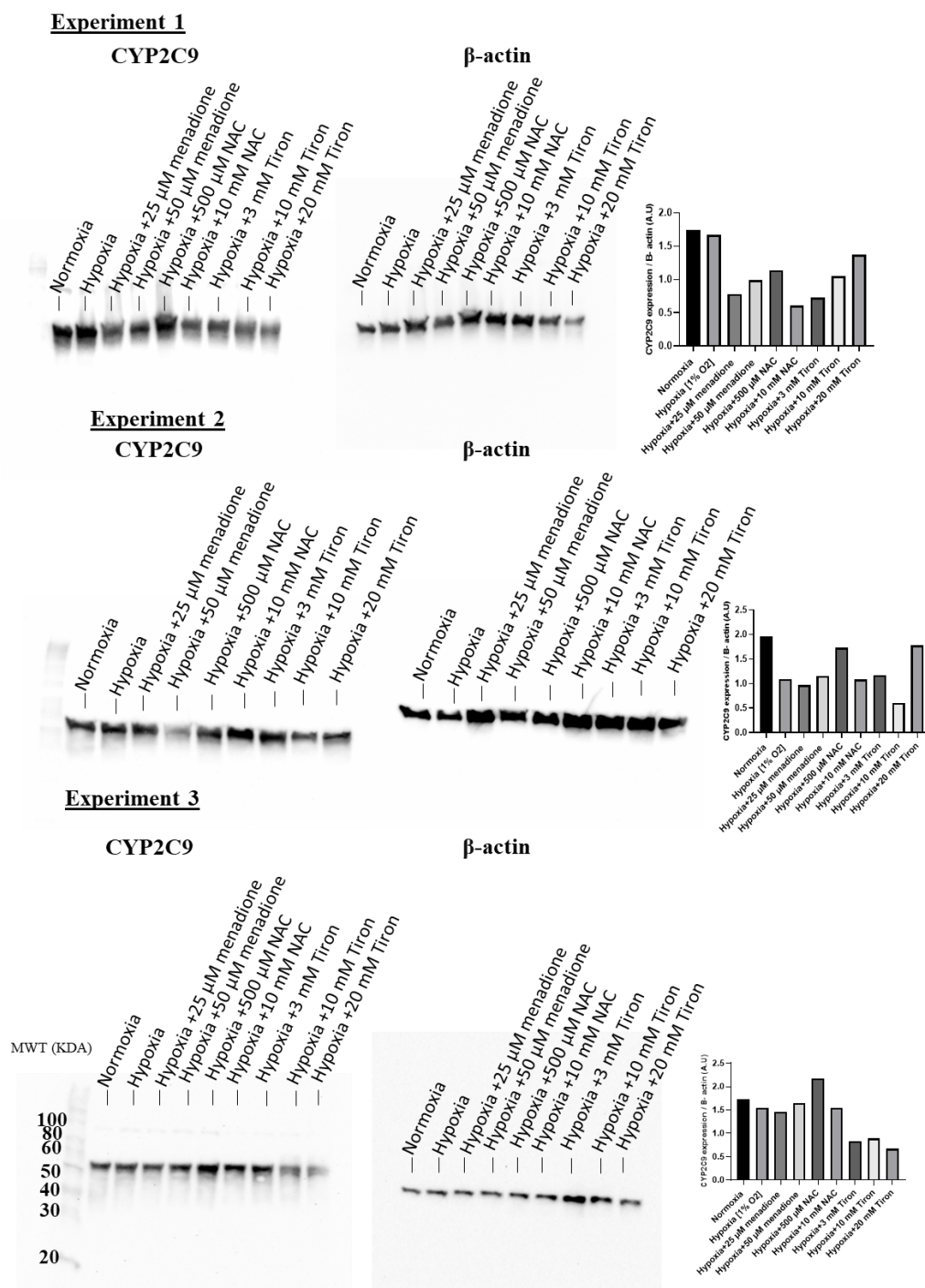
**Experiment 2**



**Experiment 3**

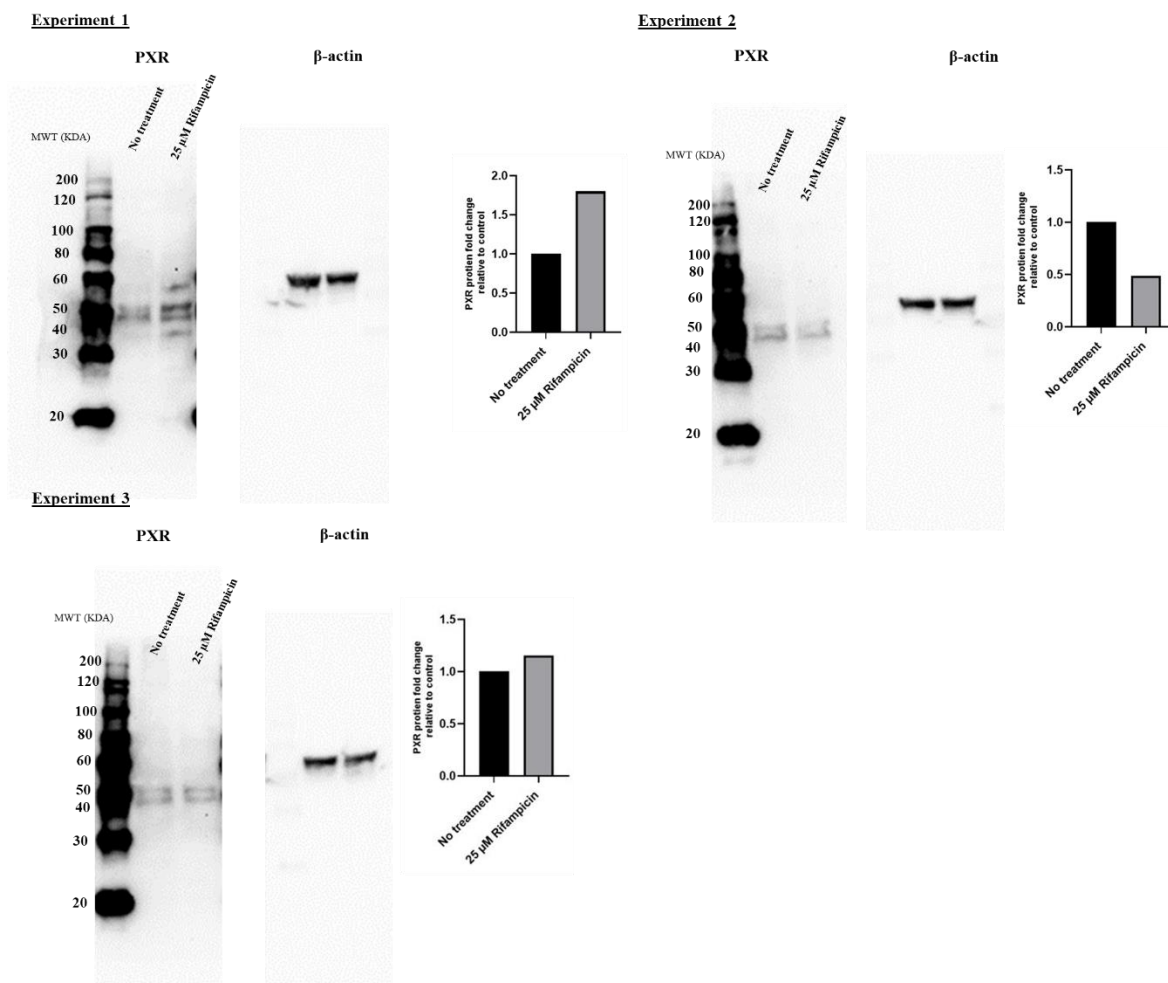


Supplementary figure 2.9 The effect of ROS induction and suppression on CYP3A4 in HepaRG cells. HepaRG cells were differentiated following the standard protocol. After differentiation cells were treated with ROS induced Menadione (25 and 50  $\mu$ M) and immediately exposed to hypoxic conditions (1% O<sub>2</sub>) for 24 h. Alternatively, cells were pre-treated for 4 h in normoxia with ROS scavenger NAC (500  $\mu$ M, 3 or 10 mM) or with Tiron (3, 10 or 20 mM). Following pre-treatment, cells were exposed to hypoxia (1% O<sub>2</sub>) for an additional 24 hours. Original scan of Western blot membrane shows protein levels of CYP3A4 (50 kDa) in 3 different experiments and its corresponding densitometry.  $\beta$ -Actin (42 kDa) was used as internal control.



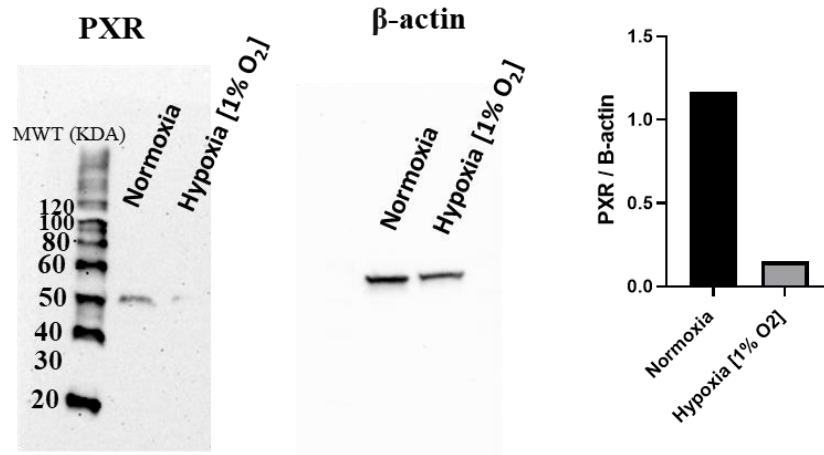
**Supplementary figure 2.10** The effect of ROS induction and suppression on CYP2C9 in HepaRG cells. HepaRG cells were differentiated following the standard protocol. After differentiation cells were treated with ROS induced Menadione (25 and 50  $\mu$ M) and immediately exposed to hypoxic conditions (1% O<sub>2</sub>) for 24 h. Alternatively, cells were pre-treated for 4 h in normoxia with ROS scavenger NAC (500  $\mu$ M, 3 or 10 mM) or with Tiron (3, 10 or 20 mM). Following pre-treatment, cells were exposed to hypoxia (1% O<sub>2</sub>) for an additional 24 hours. Original scan of Western blot membrane shows protein levels of CYP2C9 (55 kDa) in 3 different experiments and its corresponding densitometry.  $\beta$ -Actin (42 kDa) was used as internal control.

## Appendix 2

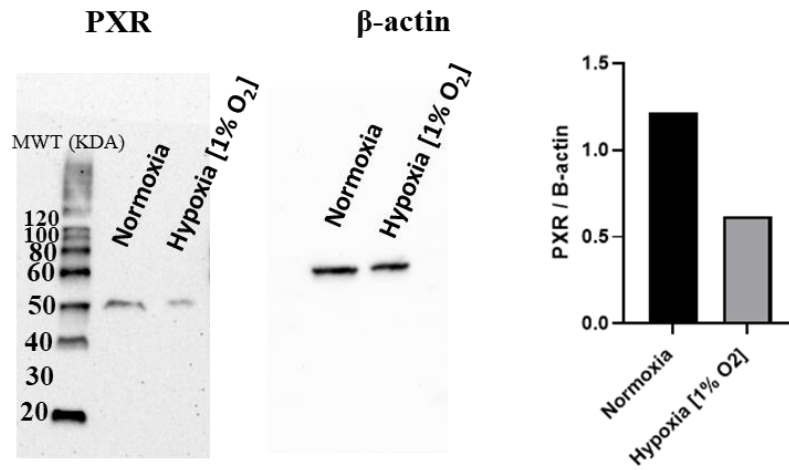


**Supplementary figure 2.11** The effect of the PXR ligand rifampicin on PXR in HepaRG cells. HepaRG cells were differentiated following the standard protocol. After differentiation cells were treated with 25 μM of rifampicin for 48 h. Untreated cells were used as control. Original scan of Western blot membrane shows protein levels of PXR (50 kDa). β-Actin (42 kDa) was used as internal control.

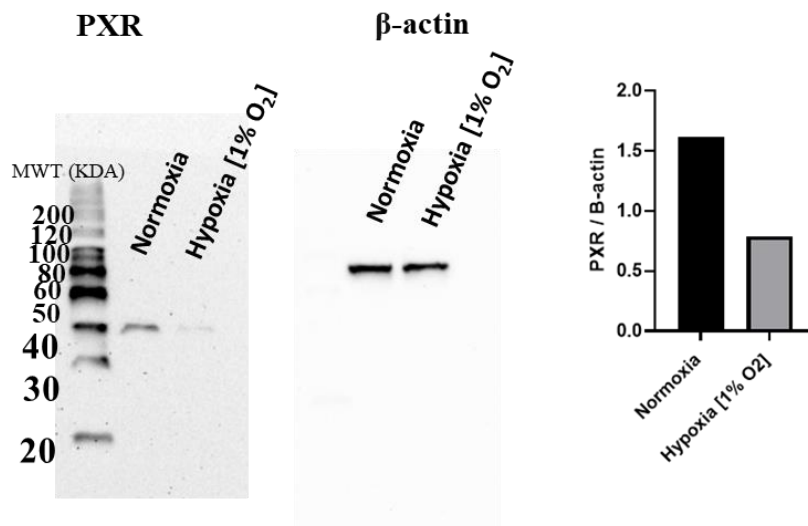
**Experiment 1**



**Experiment 2**



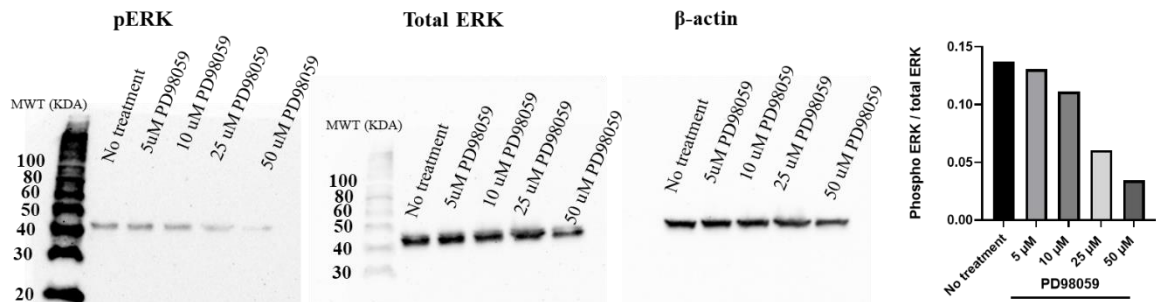
**Experiment 3**



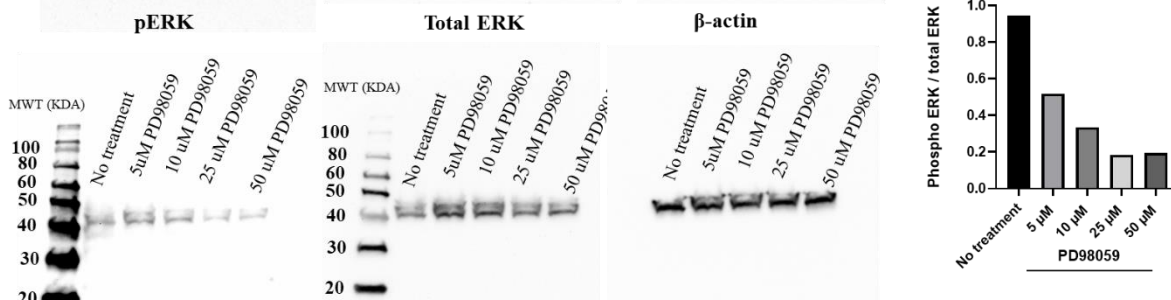
Supplementary figure 2.12 Impact of Hypoxia upon gene and protein expression of PXR. HepaRG cells were differentiated following the standard protocol. After differentiation cells were exposed to hypoxia (1% O<sub>2</sub>) for 24 h. Cells cultured under standard conditions (21% O<sub>2</sub>) were used as a control. Original scan of Western blot membrane shows protein levels of PXR (50 KDa) and its corresponding densitometry.  $\beta$ -Actin (42 KDa) was used as internal control.

## Appendix 2

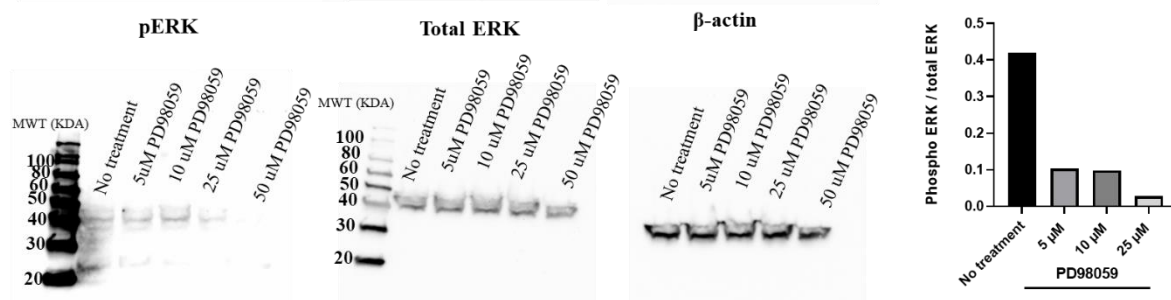
### Experiment 1



### Experiment 2



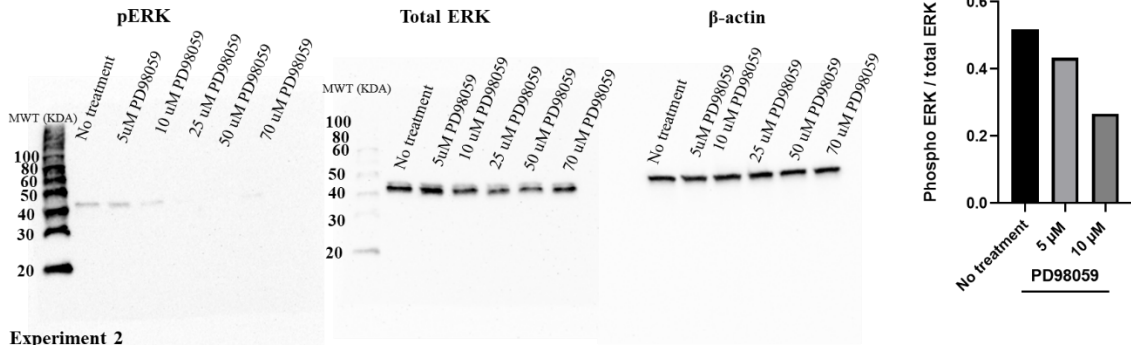
### Experiment 3



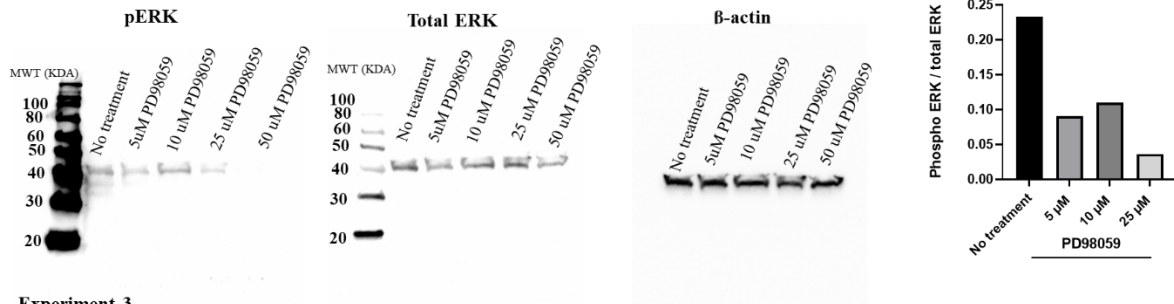
**Supplementary figure 2.13 Effect of PD98059 treatment upon ERK1/2 in HepaRG cells.** HepaRG cells were differentiated following the standard protocol. After differentiation cells were exposed to 5, 10, 25, or 50  $\mu$ M of PD98059 under normoxia for 25 h. Original scan of Western blot membrane shows protein levels of pERK1/2 (42/44 KDa), total ERK1/2 (42/44 KDa), and internal control  $\beta$ -Actin (42 KDa) of cells cultured under normoxia and under hypoxia and corresponding pERK1/2 densitometry quantification .

## Appendix 2

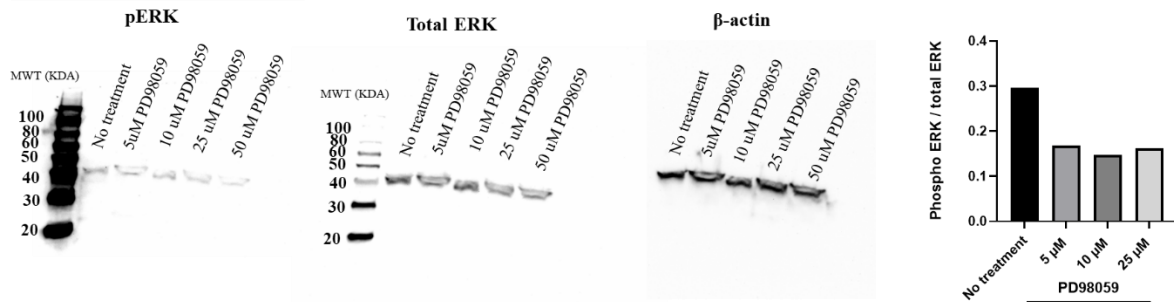
### Experiment 1



### Experiment 2



### Experiment 3

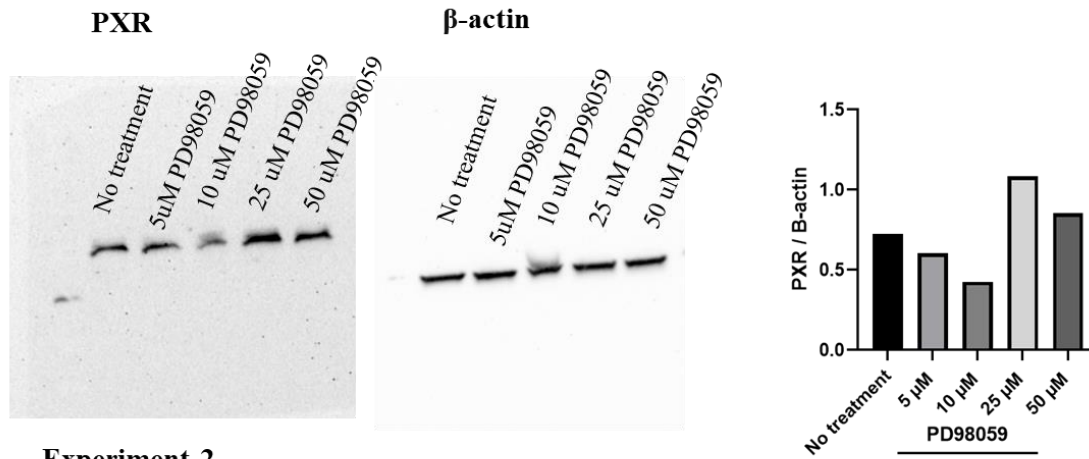


**Supplementary figure 2.14 Effect of PD98059 treatment upon ERK1/2 in HepaRG cells.** HepaRG cells were differentiated following the standard protocol. After differentiation cells were pre-exposed to 5, 10, 25, or 50  $\mu$ M of PD98059 under normoxia for 1 h. After the initial incubation, cells were transferred to the hypoxia chamber (1% O<sub>2</sub>) for additional 24 h. Original scan of Western blot membrane shows protein levels of pERK1/2 (42/44 KDa), total ERK1/2 (42/44 KDa), and internal control  $\beta$ -Actin (42 KDa) of cells cultured under normoxia and under hypoxia and corresponding pERK1/2 densitometry quantification .

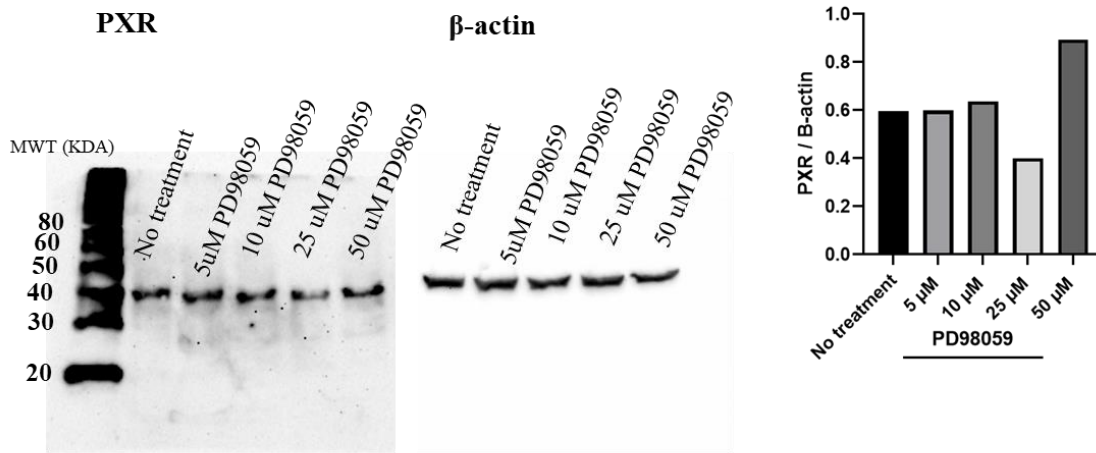


Appendix 2

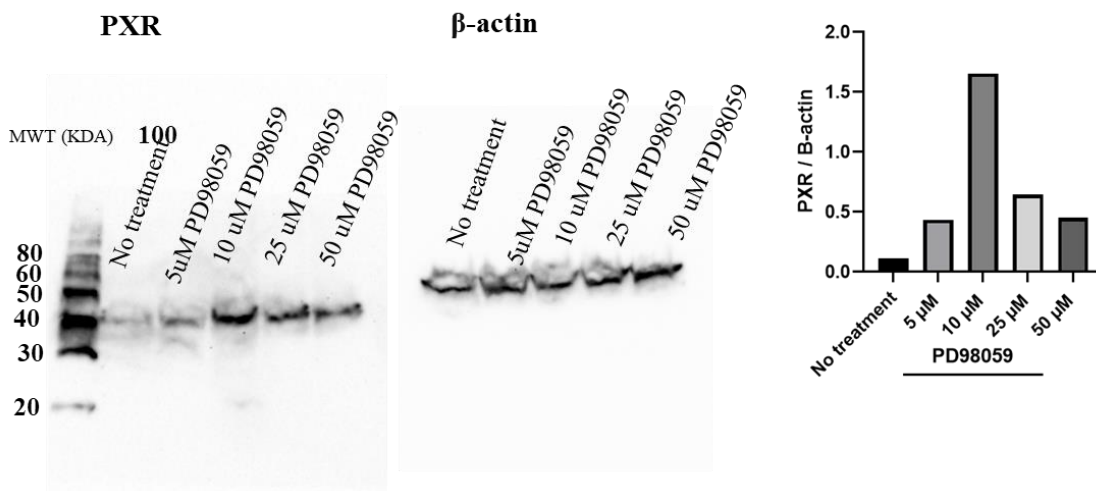
**Experiment 1**



**Experiment 2**



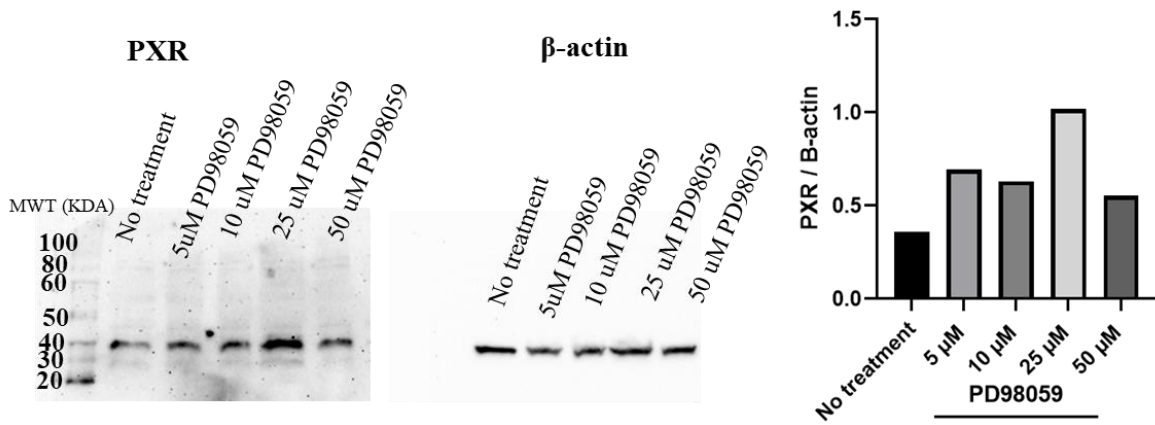
**Experiment 3**



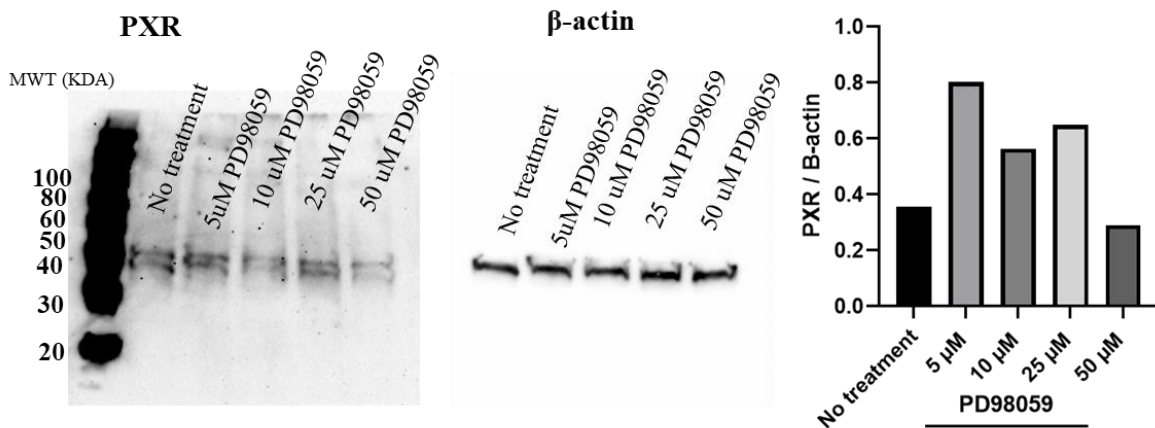
Supplementary figure 2.15 Effect of PD98059 treatment upon PXR in HepaRG cells. HepaRG cells were differentiated following the standard protocol. After differentiation cells were exposed to 5, 10, 25, or 50 μM of PD98059 under normoxia for 25 h. Original scan of Western blot membrane shows protein levels of PXR (50 KDa) and internal control β-Actin (42 KDa) and corresponding densitometry quantification.

## Appendix 2

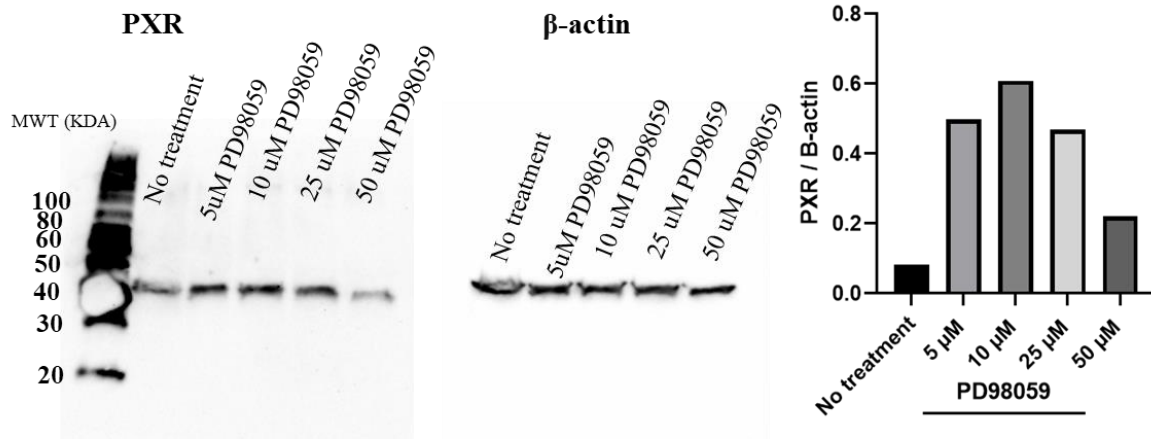
### Experiment 1



### Experiment 2



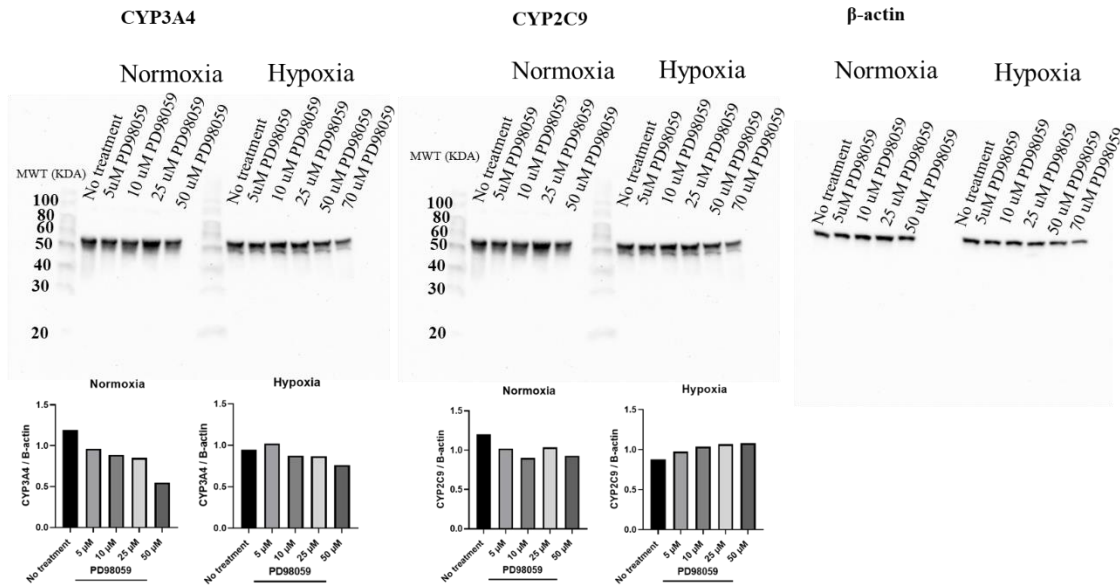
### Experiment 3



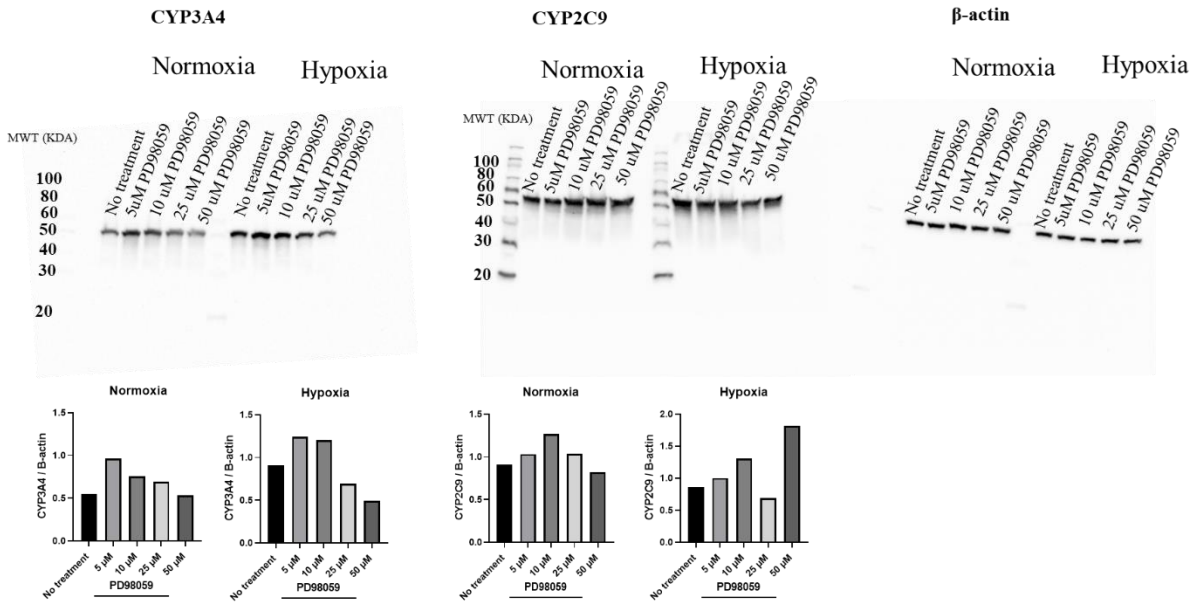
Supplementary figure 2.16 Effect of PD98059 treatment upon PXR in HepaRG cells. HepaRG cells were differentiated following the standard protocol. After differentiation cells were pre-exposed to 5, 10, 25, or 50  $\mu$ M of PD98059 under normoxia for 1 h. After the initial incubation, cells were transferred to the hypoxia chamber (1%  $O_2$ ) for additional 24 h. Original scan of Western blot membrane shows protein levels of PXR (50 KDa) and internal control  $\beta$ -Actin (42 KDa) and corresponding densitometry quantification.

# Appendix 2

## Experiment 1

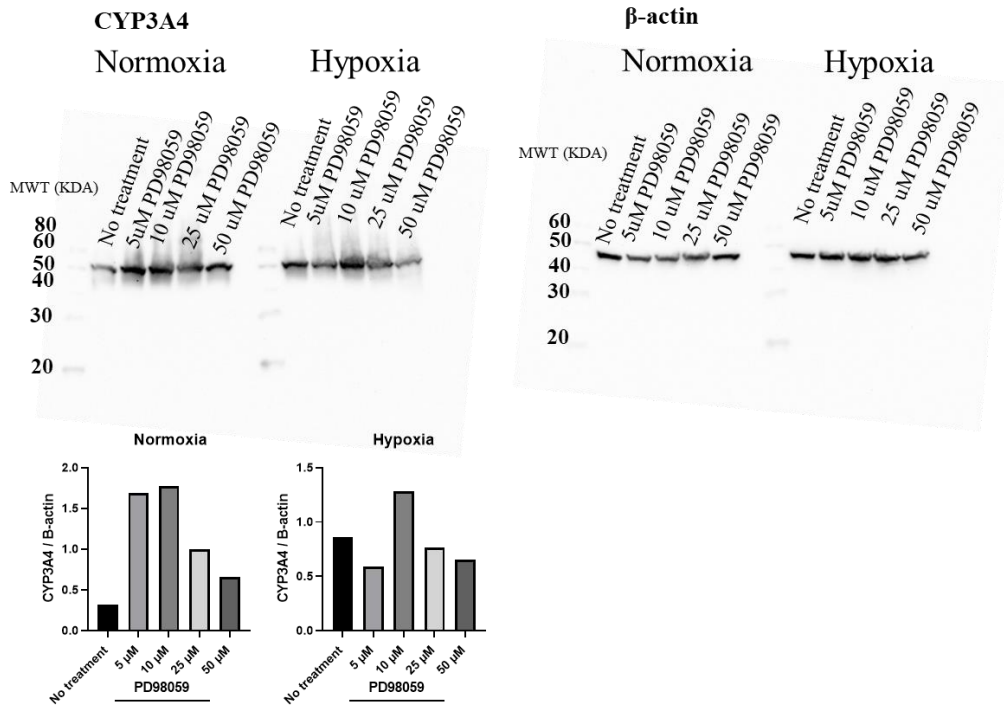


## Experiment 2

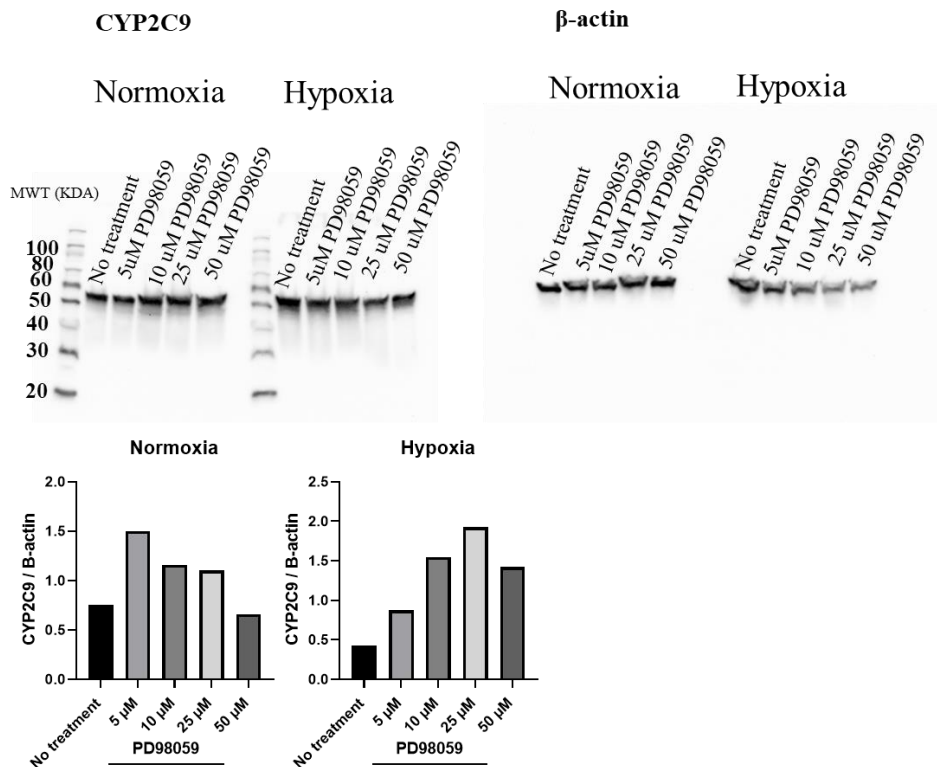


## Appendix 2

### Experiment 3

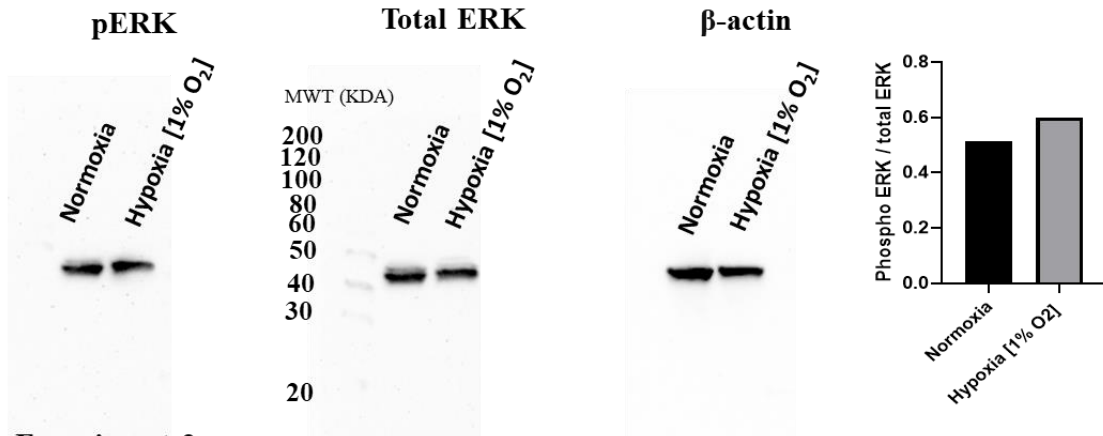


### Experiment 3

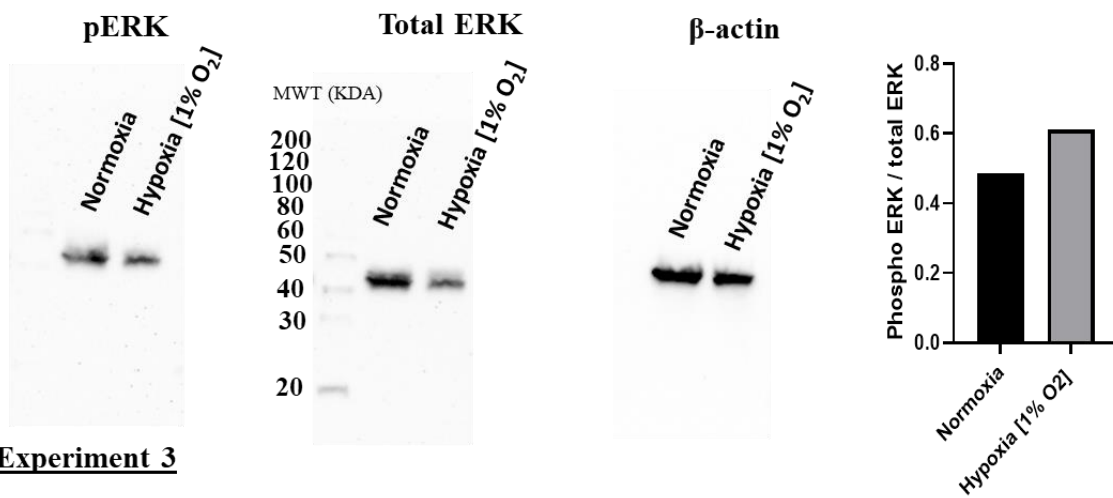


Supplementary figure 2.17 The effect of ERK1/2 inhibition by PD98059 upon CYP3A4 and CYP2C9 protein expression. HepaRG cells were differentiated following the standard protocol. After differentiation cells were pre-exposed to 5, 10, 25, or 50  $\mu\text{M}$  of PD98059 under normoxia. After the initial incubation, cells were kept in normoxia (21%  $\text{O}_2$ ) or transferred to the hypoxia chamber (1%  $\text{O}_2$ ) for additional 24 h. Original scan of Western blot membrane shows protein levels of CYP3A4 (50 kDa) and CYP2C9 (55 kDa) under normoxia or hypoxia.  $\beta$ -Actin (42 kDa) was used as internal control. Bars represents densitometry quantification of CYP3A4 and CYP2C9.

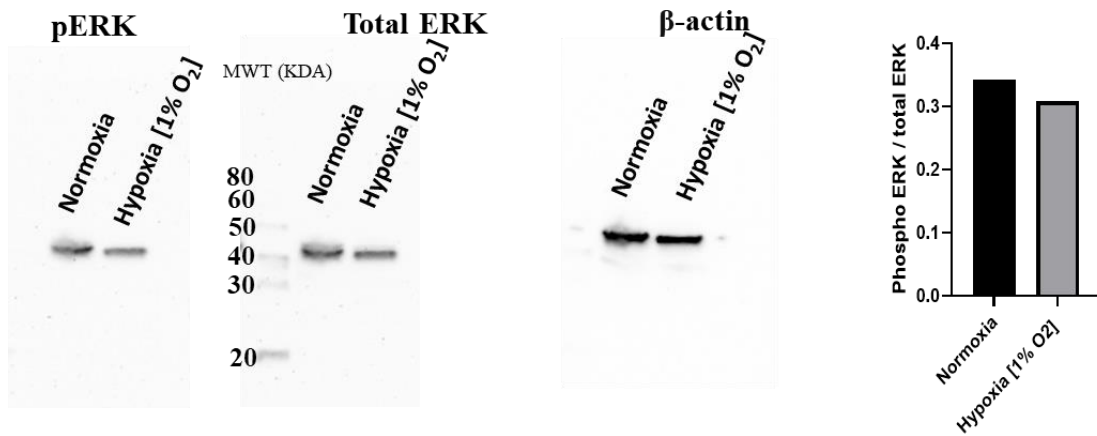
**Experiment 1**



**Experiment 2**



**Experiment 3**



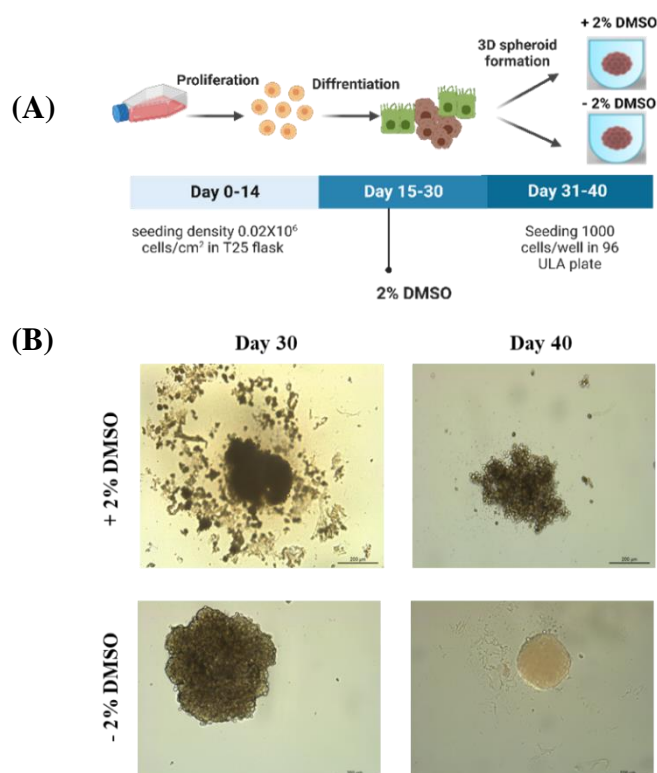
Supplementary figure 2.18 Effect of hypoxia upon ERK1/2 protein expression in HepaRG cells. HepaRG cells were differentiated following the standard protocol. After differentiation cells were exposed to hypoxia (1% O<sub>2</sub>) for 24 h. Cell cultured under normoxia were used as a control. Original scan of Western blot membrane shows protein levels of pERK1/2 (42/44 kDa), total ERK1/2 (42/44 kDa), and internal control  $\beta$ -Actin (42 kDa).

## Appendix 3

### Appendix 3.1- optimisation of the 3D spheroid HepaRG model

This section provides data from **Chapter 4**, focusing on the optimisation of the 3D spheroid HepaRG model. The experimental procedure involved the proliferation of HepaRG cells in growth media for two weeks, followed by supplementation with 2% DMSO for an additional two weeks to induce differentiation into hepatocytes and biliary-like cells. On day 30 of the culture, the cells were detached and seeded at a density of 1000 cells per well in an ultra-low attachment plate, allowing them to form 3D spheroids. Subsequently, the spheroids were cultured for 10 days using either growth media alone or growth media supplemented with 2% DMSO.

Notably, the results presented in **Supplementary Figure 3.1.1** demonstrate that the addition of DMSO induced cell death and the presence of debris within the spheroids. Conversely, spheroids cultured without DMSO did not exhibit such cellular changes.



**Supplementary Figure 3.1.1 (Supplementary Fig. 3.1.1A)** provides a schematic representation of the growth process of HepaRG cells. After reaching day 30 of culture and undergoing cell differentiation, the cells were trypsinized and seeded into ultra-low attachment plates at a density of 1000 cells per well. Two different conditions were used for the 10-day culture period: media supplemented with 2% DMSO and media without supplementation (**Supplementary Fig. 3.1.1B**). The formation of spheroids was monitored over the course of 10 days following seeding, using light microscopy. By day 40 of culture, the HepaRG cells cultured in the medium without 2% DMSO exhibited a compact and spherical shape. In contrast, spheroids cultured with the medium containing 2% DMSO showed signs of cell death and the presence of debris. The scale bars in the figure represent a length of 200 μm.

### **Appendix 3.2 -Effect of ROS manipulation on CYP3A4/2C9 in HepaRG under normoxia**

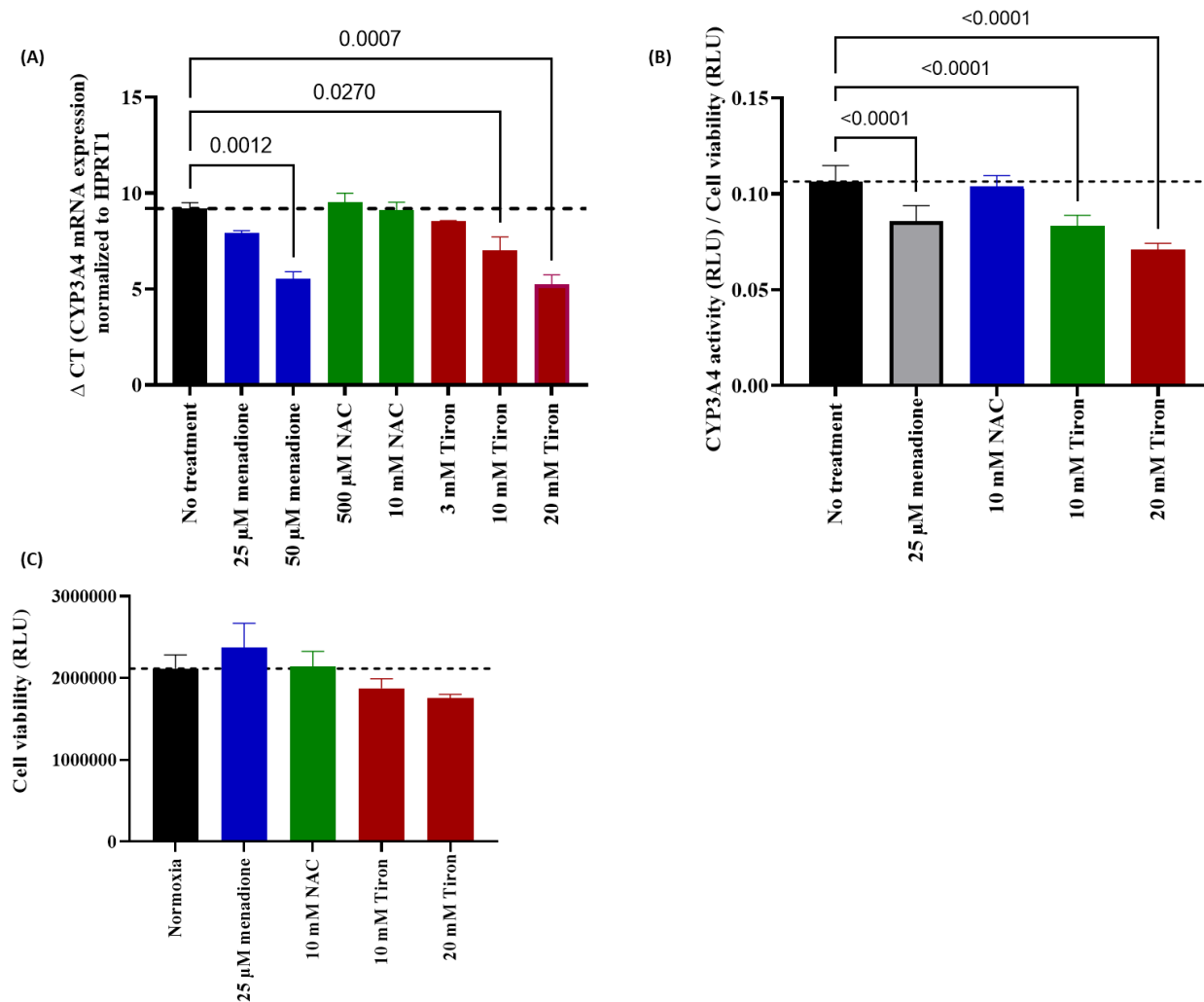
This section presents the data from **Chapter 6**, specifically focusing on the effects of inducing and suppressing reactive oxygen species (ROS) under **normoxic conditions** (21% O<sub>2</sub>) on the mRNA expression and functional activity of CYP3A4/2C9.

Here the impact of ROS manipulation on CYP3A4 and CYP2C9 was examined. HepaRG cells were cultured under normoxia (21% O<sub>2</sub>) and treated with either the ROS inducer menadione or the antioxidants N-acetyl cysteine (NAC), a global ROS scavenger, or Tiron which specifically scavenges superoxide and hydroxyl radicals.

As depicted in **Supplementary Figure 3.2.1A**, treatment with 50 µM menadione for 24 h resulted in a significant 40% reduction in CYP3A4 mRNA expression compared to the untreated control under normoxia.

Under normoxic conditions, there was no noticeable change in CYP3A4 mRNA levels in HepaRG cells treated with either 500 µM or 10 mM NAC for 28 h. However, in the Tiron-treated groups (3, 10, or 20 mM), which specifically scavenge superoxide and hydroxyl radicals, a dose-dependent decrease in CYP3A4 expression was observed. Specifically, CYP3A4 expression was downregulated by 24% in the 10 mM Tiron-treated group and by 43% in the 20 mM Tiron-treated group compared to the untreated control.

The functional activity of CYP3A4 (RLU) normalised to cell viability (RLU) in HepaRG cells, as shown in **Supplementary Figure 3.2.1B**, was significantly affected by treatment with 25 µM menadione for 24 h, resulting in a 24% decrease in CYP3A4 activity. However, treatment with 10 mM NAC for 48 h showed no significant effect on CYP3A4 activity, consistent with the mRNA expression data. In contrast, Tiron treatment for 48 h led to a considerable concentration-dependent decrease in CYP3A4 activity. Specifically, CYP3A4 activity was reduced by 20% in the 10 mM Tiron-treated group and by 30% in the 20 mM Tiron-treated group compared to the untreated control. Displayed in **Supplementary Figure 3.2.1C** are the results regarding viability, which showed no statistically significant distinctions among the treatments when compared with the untreated normoxia control. Nevertheless, there is a tendency, especially for 10 mM and 20 mM Tiron, to demonstrate slightly diminished values when contrasted with the normoxia control.



**Supplementary Figure 3.2.1 The impact of reactive oxygen species (ROS) induction and suppression on CYP3A4 in HepaRG cells.** HepaRG cells were differentiated following the standard protocol, and subsequently treated with ROS-inducing agent Menadione (at concentrations of 25 and 50  $\mu$ M) for 24 h, or with ROS scavengers NAC (at concentrations of 500  $\mu$ M, 3 mM, and 10 mM) or Tiron (at concentrations of 3 mM, 10 mM, and 20 mM) for 28 h, under normoxic conditions (21%  $O_2$ ). In **Supplementary Figure 3.2.1A**, the mRNA expression of CYP3A4, normalised to the housekeeping gene HPRT1, was measured using quantitative reverse transcription PCR (qRT-PCR). The bars represent the mean  $\pm$  standard error of the mean (SEM). The experiment was conducted independently three times, with each experiment consisting of at least three replicates. Statistical analysis was performed using one way ANOVA. **Supplementary Figure 3.2.1B** presents the functional activity of CYP3A4, measured using the P450-Glo™ assay. The activity was assessed 24 h after treatment with Menadione, and 48 h after treatment with NAC or Tiron. **Supplementary Figure 3.2.1C** is the cell viability measured by CellTiter Glo assay this data used for CYP3A4 functional activity normalization. Bars represent mean  $\pm$  SEM. N=3 independent experiments with at least six replicates each experiment. Statistical analysis involved a One-way ANOVA and subsequent Bonferroni test for assessing CYP3A4 activity in the graph, while the Kruskal-Wallis test followed by the Dunn test were applied to the cell viability figure.

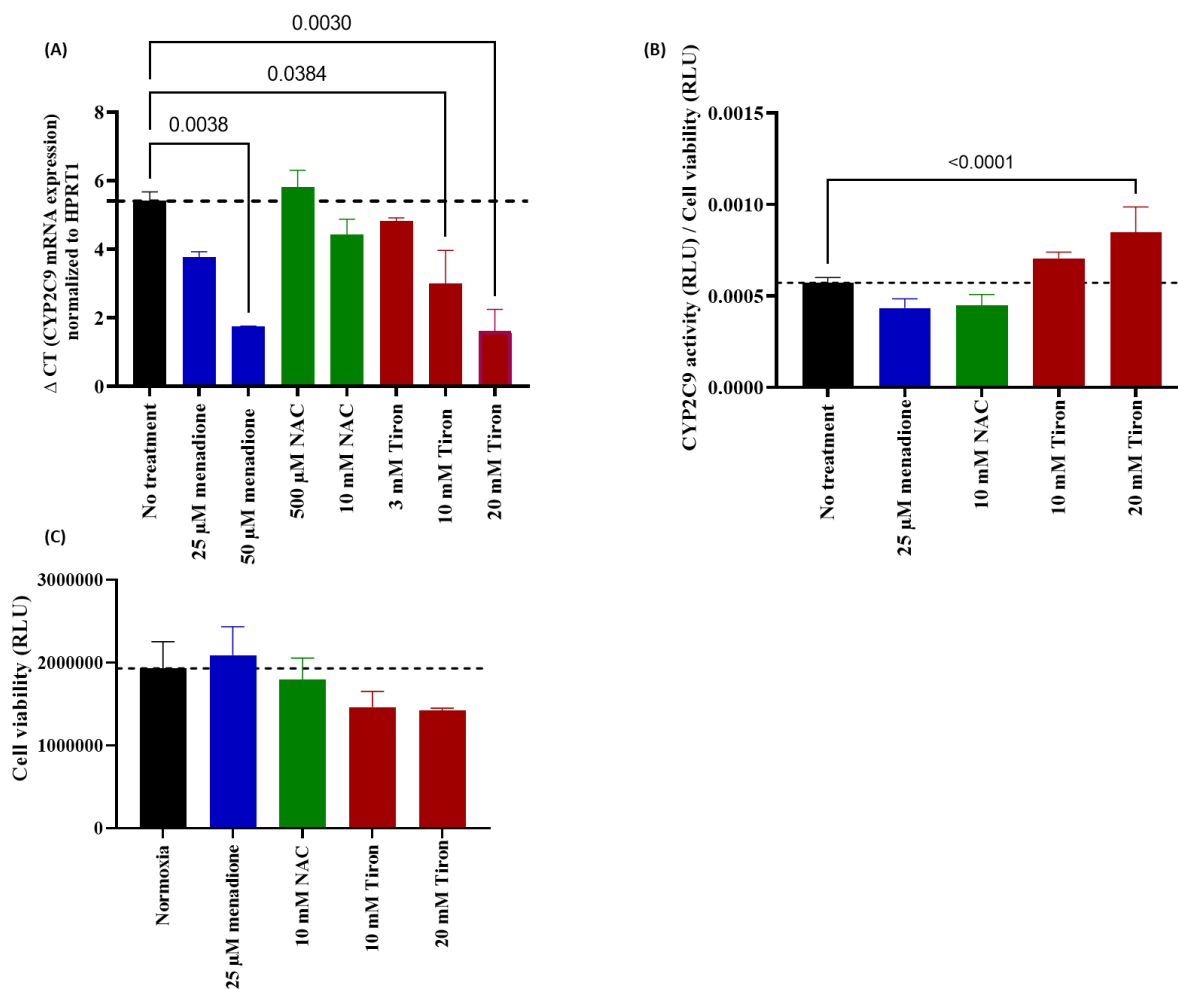


In **Supplementary Figure 3.2.2A**, the mRNA expression of CYP2C9 in HepaRG cells treated with 50  $\mu$ M menadione for 24 h showed a substantial reduction of 68% compared to the untreated control.

Under normoxic conditions, there was no significant change in CYP2C9 mRNA levels in HepaRG cells treated with either 500  $\mu$ M or 10 mM NAC for 28 h. However, treatment with Tiron (3, 10, or 20 mM) for 28 h, which specifically targets superoxide and hydroxyl radicals, resulted in a dose-dependent decrease in CYP2C9 expression. Specifically, CYP2C9 expression was downregulated by 45% in the 10 mM Tiron-treated group and by 70% in the 20 mM Tiron-treated group compared to the untreated control.

**Supplementary Figure 3.2.2B** illustrates the corresponding functional activity of CYP2C9 (RLU) normalised to cell viability (RLU) in HepaRG cells. Treatment with 25  $\mu$ M menadione for 24 h resulted in a slight decline in CYP2C9 activity, approximately 20% lower than the untreated control; however, this change was not statistically significant. In contrast to the qPCR data, Tiron treatment increased CYP2C9 activity in a concentration-dependent manner. Specifically, CYP2C9 activity increased by 40% in the 10 mM Tiron-treated group and by 60% in the 20 mM Tiron-treated group compared to the untreated control. However, treatment with 10 mM NAC did not demonstrate any positive impact on CYP2C9 activity. Presented in **Supplementary Figure 3.2.2C** are the viability outcomes, which indicated no statistically significant differences among the treatments when compared to the untreated normoxia control. However, there is a trend, particularly noticeable for 10 mM NAC and 10 mM and 20 mM Tiron, to exhibit slightly lower values when compared with the normoxia control.

## Appendix 3



**Supplementary Figure 3.2.2 The influence of reactive oxygen species (ROS) induction and suppression on CYP2C9 in HepaRG cells.** HepaRG cells were differentiated according to the standard protocol and subsequently treated with ROS-inducing agent Menadione (at concentrations of 25 and 50  $\mu$ M) for 24 h, or with ROS scavengers NAC (at concentrations of 500  $\mu$ M, 3 mM, and 10 mM) or Tiron (at concentrations of 3 mM, 10 mM, and 20 mM) for 28 h under normoxic conditions (21%  $O_2$ ). In **Supplementary Figure 3.2.2A**, the mRNA expression of CYP2C9, normalised to the housekeeping gene HPTR1, was quantified using quantitative reverse transcription PCR (qRT-PCR). The bars represent the mean  $\pm$  standard error of the mean (SEM). The experiment was independently performed three times, with each experiment consisting of at least three replicates. Statistical analysis was conducted using one way ANOVA. **Supplementary Figure 3.2.2B** illustrates the functional activity of CYP2C9, measured using the P450-Glo™ assay. The activity was assessed 24 h after treatment with Menadione and 48 h after treatment with NAC or Tiron. **Supplementary Figure 3.2.2C** is the cell viability measured by CellTiter Glo assay this data used for CYP2C9 functional activity normalization. The bars represent the mean  $\pm$  SEM. The experiment was independently conducted three times, with each experiment consisting of at least six replicates. Statistical analysis was performed using a one-way ANOVA test.

## Appendix 4- Search strategy, data extraction tables, and quality appraisal of systematic review and meta-analysis study


This section shows data related to Chapter 3 the systematic review and meta-analysis study, including search strategy, data extraction table and quality appraisal.

### Appendix 4.1: search strategy


#### MEDLINE (Ovid)

1/05/2023, 11:10 Ovid: Search Form

TRY THE NEW OVID INTERFACE v



[My Account](#) | [Ask a Cardiff University Librarian](#) | [Support & Training](#) | [Help](#) | [Feedback](#) | [Logged in as dsh1@bham.ac.uk](#)



---

[Search](#) | [Journals](#) | [Books](#) | [Multimedia](#) | [My Workspace](#) | [VisualDX](#) | [EBP Tools](#)

What's New

[Basic Search](#) | [Find Citation](#) | [Search Tools](#) | [Search Fields](#) | [Advanced Search](#)

Multi-Field Search

1 Resource selected | [List](#) | [Change](#)

**Ovid MEDLINE(R) ALL 1946 to May 30, 2023**

**Keyword** |  Author |  Title |  Journal

Enter keyword or phrase  
(\* or \$ for truncation)

Expand Term Finder +

Include Multimedia  
 Map Term to Subject Heading

**Limits** (close)

English Language  
 Review Articles  
 Humans  
 Latest Update

Publication Year: - - -

[Additional Limits](#) | [Edit Limits](#)

**▼ Search History (60)** [View Saved](#)

<input type="checkbox"/>	# ▲	Searches	Results	Type	Actions	Annotations
<input type="checkbox"/>	1	maximum plasma concentration.tw	3470	Advanced	<a href="#">Display Results</a>   <a href="#">More</a>	Contract
<input type="checkbox"/>	2	plasma half life.tw	3572	Advanced	<a href="#">Display Results</a>   <a href="#">More</a>	
<input type="checkbox"/>	3	plasma clearance.tw	5973	Advanced	<a href="#">Display Results</a>   <a href="#">More</a>	
<input type="checkbox"/>	4	drug blood level.tw	49	Advanced	<a href="#">Display Results</a>   <a href="#">More</a>	
<input type="checkbox"/>	5	drug half life.tw	235	Advanced	<a href="#">Display Results</a>   <a href="#">More</a>	
<input type="checkbox"/>	6	drug clearance.tw	1809	Advanced	<a href="#">Display Results</a>   <a href="#">More</a>	
<input type="checkbox"/>	7	drug distribution.tw	3671	Advanced	<a href="#">Display Results</a>   <a href="#">More</a>	
<input type="checkbox"/>	8	oral absorption.tw	3763	Advanced	<a href="#">Display Results</a>   <a href="#">More</a>	
<input type="checkbox"/>	9	drug absorption.tw	4612	Advanced	<a href="#">Display Results</a>   <a href="#">More</a>	
<input type="checkbox"/>	10	absorption half life.tw	413	Advanced	<a href="#">Display Results</a>   <a href="#">More</a>	
<input type="checkbox"/>	11	Biological Availability	44298	Advanced	<a href="#">Display Results</a>   <a href="#">More</a>	
<input type="checkbox"/>	12	bioavailability.tw	82673	Advanced	<a href="#">Display Results</a>   <a href="#">More</a>	
<input type="checkbox"/>	13	Pharmacokinetics	9157	Advanced	<a href="#">Display Results</a>   <a href="#">More</a>	
<input type="checkbox"/>	14	pharmacokinetics.tw	107979	Advanced	<a href="#">Display Results</a>   <a href="#">More</a>	
<input type="checkbox"/>	15	drug disposition.tw	2990	Advanced	<a href="#">Display Results</a>   <a href="#">More</a>	
<input type="checkbox"/>	16	Drug Elimination Routes	80	Advanced	<a href="#">Display Results</a>   <a href="#">More</a>	
<input type="checkbox"/>	17	drug excretion.tw	302	Advanced	<a href="#">Display Results</a>   <a href="#">More</a>	
<input type="checkbox"/>	18	drug clearance.tw	1809	Advanced	<a href="#">Display Results</a>   <a href="#">More</a>	
<input type="checkbox"/>	19	blood oxygen tension.tw	202	Advanced	<a href="#">Display Results</a>   <a href="#">More</a>	
<input type="checkbox"/>	20	blood oxygen level.tw	4607	Advanced	<a href="#">Display Results</a>   <a href="#">More</a>	
<input type="checkbox"/>	21	Oxygen Consumption	107699	Advanced	<a href="#">Display Results</a>   <a href="#">More</a>	

# Appendix 4

11/05/2023, 11:10

Ovid: Search Form

<input type="checkbox"/>	22	oxygen consumption.tw	43012	Advanced	<a href="#">Display Results</a>	<a href="#">More</a>	<input type="checkbox"/>
<input type="checkbox"/>	23	Oxygen Saturation/	623	Advanced	<a href="#">Display Results</a>	<a href="#">More</a>	<input type="checkbox"/>
<input type="checkbox"/>	24	oxygen saturation.tw	32355	Advanced	<a href="#">Display Results</a>	<a href="#">More</a>	<input type="checkbox"/>
<input type="checkbox"/>	25	Oxygen Inhalation Therapy/	15936	Advanced	<a href="#">Display Results</a>	<a href="#">More</a>	<input type="checkbox"/>
<input type="checkbox"/>	26	oxygen therapy.tw	13743	Advanced	<a href="#">Display Results</a>	<a href="#">More</a>	<input type="checkbox"/>
<input type="checkbox"/>	27	Altitude Sickness/	4289	Advanced	<a href="#">Display Results</a>	<a href="#">More</a>	<input type="checkbox"/>
<input type="checkbox"/>	28	Blood Gas Analysis/	22638	Advanced	<a href="#">Display Results</a>	<a href="#">More</a>	<input type="checkbox"/>
<input type="checkbox"/>	29	partial pressure oxygen.tw	48	Advanced	<a href="#">Display Results</a>	<a href="#">More</a>	<input type="checkbox"/>
<input type="checkbox"/>	30	oxygen deficiency.tw	1331	Advanced	<a href="#">Display Results</a>	<a href="#">More</a>	<input type="checkbox"/>
<input type="checkbox"/>	31	Pulmonary Disease, Chronic Obstructive/	49742	Advanced	<a href="#">Display Results</a>	<a href="#">More</a>	<input type="checkbox"/>
<input type="checkbox"/>	32	Chronic pulmonary disease.tw	1887	Advanced	<a href="#">Display Results</a>	<a href="#">More</a>	<input type="checkbox"/>
<input type="checkbox"/>	33	plasma protein binding.tw	3482	Advanced	<a href="#">Display Results</a>	<a href="#">More</a>	<input type="checkbox"/>
<input type="checkbox"/>	34	drug metabol*.tw	20541	Advanced	<a href="#">Display Results</a>	<a href="#">More</a>	<input type="checkbox"/>
<input type="checkbox"/>	35	Blood Chemical Analysis/	26676	Advanced	<a href="#">Display Results</a>	<a href="#">More</a>	<input type="checkbox"/>
<input type="checkbox"/>	36	high altitude.tw	13951	Advanced	<a href="#">Display Results</a>	<a href="#">More</a>	<input type="checkbox"/>
<input type="checkbox"/>	37	asthma.tw	165296	Advanced	<a href="#">Display Results</a>	<a href="#">More</a>	<input type="checkbox"/>
<input type="checkbox"/>	38	pneumonia.tw	146415	Advanced	<a href="#">Display Results</a>	<a href="#">More</a>	<input type="checkbox"/>
<input type="checkbox"/>	39	pulmonary edema.tw	16288	Advanced	<a href="#">Display Results</a>	<a href="#">More</a>	<input type="checkbox"/>
<input type="checkbox"/>	40	pulmonary embolism.tw	39009	Advanced	<a href="#">Display Results</a>	<a href="#">More</a>	<input type="checkbox"/>
<input type="checkbox"/>	41	pulmonary hypertension.tw	41719	Advanced	<a href="#">Display Results</a>	<a href="#">More</a>	<input type="checkbox"/>
<input type="checkbox"/>	42	pulmonary fibrosis.tw	23015	Advanced	<a href="#">Display Results</a>	<a href="#">More</a>	<input type="checkbox"/>
<input type="checkbox"/>	43	granulomatous lung diseases.tw	78	Advanced	<a href="#">Display Results</a>	<a href="#">More</a>	<input type="checkbox"/>
<input type="checkbox"/>	44	emphysema.tw	25714	Advanced	<a href="#">Display Results</a>	<a href="#">More</a>	<input type="checkbox"/>
<input type="checkbox"/>	45	bronchitis.tw	23244	Advanced	<a href="#">Display Results</a>	<a href="#">More</a>	<input type="checkbox"/>
<input type="checkbox"/>	46	Bronchitis/	20796	Advanced	<a href="#">Display Results</a>	<a href="#">More</a>	<input type="checkbox"/>
<input type="checkbox"/>	47	Chronic Obstructive Lung Disease.tw	4481	Advanced	<a href="#">Display Results</a>	<a href="#">More</a>	<input type="checkbox"/>
<input type="checkbox"/>	48	Respiratory Tract Diseases/	23219	Advanced	<a href="#">Display Results</a>	<a href="#">More</a>	<input type="checkbox"/>
<input type="checkbox"/>	49	chronic respiratory tract disease.tw	48	Advanced	<a href="#">Display Results</a>	<a href="#">More</a>	<input type="checkbox"/>
<input type="checkbox"/>	50	Lung Diseases/	71796	Advanced	<a href="#">Display Results</a>	<a href="#">More</a>	<input type="checkbox"/>
<input type="checkbox"/>	51	lung disease.tw	49467	Advanced	<a href="#">Display Results</a>	<a href="#">More</a>	<input type="checkbox"/>
<input type="checkbox"/>	52	drug metabolite/	0	Advanced	<a href="#">Save</a>	<a href="#">More</a>	<input type="checkbox"/>
<input type="checkbox"/>	53	(hypoxemia or hypoxaemia).tw	22124	Advanced	<a href="#">Display Results</a>	<a href="#">More</a>	<input type="checkbox"/>
<input type="checkbox"/>	54	hypoxia.tw	132743	Advanced	<a href="#">Display Results</a>	<a href="#">More</a>	<input type="checkbox"/>
<input type="checkbox"/>	55	hypoxia/	72956	Advanced	<a href="#">Display Results</a>	<a href="#">More</a>	<input type="checkbox"/>
<input type="checkbox"/>	56	27 or 30 or 31 or 32 or 36 or 37 or 38 or 39 or 40 or 41 or 42 or 43 or 44 or 45 or 46 or 47 or 48 or 49 or 50 or 51 or 53 or 54 or 55	781345	Advanced	<a href="#">Display Results</a>	<a href="#">More</a>	<input type="checkbox"/>
<input type="checkbox"/>	57	1 or 2 or 3 or 4 or 5 or 6 or 7 or 8 or 9 or 10 or 11 or 12 or 13 or 14 or 15 or 16 or 17 or 18 or 33 or 34 or 52	231678	Advanced	<a href="#">Display Results</a>	<a href="#">More</a>	<input type="checkbox"/>
<input type="checkbox"/>	58	19 or 20 or 21 or 22 or 23 or 24 or 25 or 26 or 28 or 29 or 35	226926	Advanced	<a href="#">Display Results</a>	<a href="#">More</a>	<input type="checkbox"/>

# Appendix 4

11/05/2023, 11:10

Ovid: Search Form

<input type="checkbox"/>	59 56 and 57 and 58	124	Advanced	<a href="#">Display Results</a>   <a href="#">More</a>	
<input type="checkbox"/>	60 Limit 59 to english language	119	Advanced	<a href="#">Display Results</a>   <a href="#">More</a>	

Save Remove

Combine with: AND

OR

Save All Edit Create RSS Create Auto-Alert [View Saved](#)

Email All Search History Copy Search History Link Copy Search History Details

# Appendix 4

## EMBASE (Ovid)

11/05/2023, 11:07

Ovid: Search Form

TRY THE NEW OVID INTERFACE



Ovid®

My Account [Ask a Cardiff University Librarian](#) [Support & Training](#) [Help](#) [Feedback](#) [Logged in as ddd1 abcd1234](#)  
[Logout](#)

[Search](#) [Journals](#) [Books](#) [Multimedia](#) [My Workspace](#) [VisualDX](#) [EBP Tools](#)

What's New

Search History saved as "final EMBASE search 11-5-2023"

[Basic Search](#) | [Find Citation](#) | [Search Tools](#) | [Search Fields](#) | **[Advanced Search](#)**  
[Multi-Field Search](#)

1 Resource selected [Hide](#) | [Change](#)

**Embase Classic+Embase** 1947 to 2023 Week 18

**Keyword**  Author  Title  Journal

Enter keyword or phrase  
 (" or \$ for truncation)

[Search](#)

Include Multimedia  
 Map Term to Subject Heading

**Limits** (close)

Latest Update  
 Human  
 English Language

Publication Year  -

[Additional Limits](#) [Edit Limits](#)

**Search History** (50) [View Saved](#)

#	Searches	Results	Type	Actions	Annotations
<input type="checkbox"/>	1 maximum plasma concentration,tw.	4567	Advanced	<a href="#">Display Results</a>   <a href="#">More</a>	<input type="checkbox"/> Contract
<input type="checkbox"/>	2 plasma half-life,tw.	4855	Advanced	<a href="#">Display Results</a>   <a href="#">More</a>	<input type="checkbox"/>
<input type="checkbox"/>	3 plasma clearance,tw.	7447	Advanced	<a href="#">Display Results</a>   <a href="#">More</a>	<input type="checkbox"/>
<input type="checkbox"/>	4 drug blood level,tw.	87	Advanced	<a href="#">Display Results</a>   <a href="#">More</a>	<input type="checkbox"/>
<input type="checkbox"/>	5 drug half-life,tw.	344	Advanced	<a href="#">Display Results</a>   <a href="#">More</a>	<input type="checkbox"/>
<input type="checkbox"/>	6 drug clearance,tw.	2668	Advanced	<a href="#">Display Results</a>   <a href="#">More</a>	<input type="checkbox"/>
<input type="checkbox"/>	7 drug distribution,tw.	5079	Advanced	<a href="#">Display Results</a>   <a href="#">More</a>	<input type="checkbox"/>
<input type="checkbox"/>	8 oral absorption,tw.	5022	Advanced	<a href="#">Display Results</a>   <a href="#">More</a>	<input type="checkbox"/>
<input type="checkbox"/>	9 drug absorption,tw.	6320	Advanced	<a href="#">Display Results</a>   <a href="#">More</a>	<input type="checkbox"/>
<input type="checkbox"/>	10 absorption half-life,tw.	486	Advanced	<a href="#">Display Results</a>   <a href="#">More</a>	<input type="checkbox"/>
<input type="checkbox"/>	11 Biological Availability!	57632	Advanced	<a href="#">Display Results</a>   <a href="#">More</a>	<input type="checkbox"/>
<input type="checkbox"/>	12 bioavailability,tw.	110786	Advanced	<a href="#">Display Results</a>   <a href="#">More</a>	<input type="checkbox"/>
<input type="checkbox"/>	13 Pharmacokinetics!	274903	Advanced	<a href="#">Display Results</a>   <a href="#">More</a>	<input type="checkbox"/>
<input type="checkbox"/>	14 pharmacokinetics,tw.	154411	Advanced	<a href="#">Display Results</a>   <a href="#">More</a>	<input type="checkbox"/>
<input type="checkbox"/>	15 drug disposition,tw.	4140	Advanced	<a href="#">Display Results</a>   <a href="#">More</a>	<input type="checkbox"/>
<input type="checkbox"/>	16 Drug Elimination Routes!	48321	Advanced	<a href="#">Display Results</a>   <a href="#">More</a>	<input type="checkbox"/>
<input type="checkbox"/>	17 drug excretion,tw.	446	Advanced	<a href="#">Display Results</a>   <a href="#">More</a>	<input type="checkbox"/>
<input type="checkbox"/>	18 drug clearance,tw.	2668	Advanced	<a href="#">Display Results</a>   <a href="#">More</a>	<input type="checkbox"/>
<input type="checkbox"/>	19 blood oxygen tension,tw.	319	Advanced	<a href="#">Display Results</a>   <a href="#">More</a>	<input type="checkbox"/>
<input type="checkbox"/>	20 blood oxygen level,tw.	6136	Advanced	<a href="#">Display Results</a>   <a href="#">More</a>	<input type="checkbox"/>
<input type="checkbox"/>	21 Oxygen Consumption!	127769	Advanced	<a href="#">Display Results</a>   <a href="#">More</a>	<input type="checkbox"/>

# Appendix 4

11/05/2023, 11:07

Ovid: Search Form

<input type="checkbox"/>	22	oxygen consumption.tw	60380	Advanced	<a href="#">Display Results</a>   <a href="#">More</a>	
<input type="checkbox"/>	23	Oxygen Saturation/	78896	Advanced	<a href="#">Display Results</a>   <a href="#">More</a>	
<input type="checkbox"/>	24	oxygen saturation.tw	51768	Advanced	<a href="#">Display Results</a>   <a href="#">More</a>	
<input type="checkbox"/>	25	Oxygen Inhalation Therapy/	45024	Advanced	<a href="#">Display Results</a>   <a href="#">More</a>	
<input type="checkbox"/>	26	oxygen therapy.tw	21023	Advanced	<a href="#">Display Results</a>   <a href="#">More</a>	
<input type="checkbox"/>	27	Altitude Sickness/	4194	Advanced	<a href="#">Display Results</a>   <a href="#">More</a>	
<input type="checkbox"/>	28	Blood Gas Analysis/	27065	Advanced	<a href="#">Display Results</a>   <a href="#">More</a>	
<input type="checkbox"/>	29	partial pressure oxygen.tw	59	Advanced	<a href="#">Display Results</a>   <a href="#">More</a>	
<input type="checkbox"/>	30	oxygen deficiency.tw	1873	Advanced	<a href="#">Display Results</a>   <a href="#">More</a>	
<input type="checkbox"/>	31	Pulmonary Disease, Chronic Obstructive/	86708	Advanced	<a href="#">Display Results</a>   <a href="#">More</a>	
<input type="checkbox"/>	32	Chronic pulmonary disease.tw	3696	Advanced	<a href="#">Display Results</a>   <a href="#">More</a>	
<input type="checkbox"/>	33	plasma protein binding.tw	4585	Advanced	<a href="#">Display Results</a>   <a href="#">More</a>	
<input type="checkbox"/>	34	drug metabol*.tw	26361	Advanced	<a href="#">Display Results</a>   <a href="#">More</a>	
<input type="checkbox"/>	35	Blood Chemical Analysis/	11569	Advanced	<a href="#">Display Results</a>   <a href="#">More</a>	
<input type="checkbox"/>	36	high altitude.tw	18003	Advanced	<a href="#">Display Results</a>   <a href="#">More</a>	
<input type="checkbox"/>	37	asthma.tw	260272	Advanced	<a href="#">Display Results</a>   <a href="#">More</a>	
<input type="checkbox"/>	38	pneumonia.tw	233627	Advanced	<a href="#">Display Results</a>   <a href="#">More</a>	
<input type="checkbox"/>	39	pulmonary edema.tw	25507	Advanced	<a href="#">Display Results</a>   <a href="#">More</a>	
<input type="checkbox"/>	40	pulmonary embolism.tw	86709	Advanced	<a href="#">Display Results</a>   <a href="#">More</a>	
<input type="checkbox"/>	41	pulmonary hypertension.tw	72871	Advanced	<a href="#">Display Results</a>   <a href="#">More</a>	
<input type="checkbox"/>	42	pulmonary fibrosis.tw	39001	Advanced	<a href="#">Display Results</a>   <a href="#">More</a>	
<input type="checkbox"/>	43	granulomatous lung diseases.tw	127	Advanced	<a href="#">Display Results</a>   <a href="#">More</a>	
<input type="checkbox"/>	44	emphysema.tw	42737	Advanced	<a href="#">Display Results</a>   <a href="#">More</a>	
<input type="checkbox"/>	45	bronchitis.tw	37071	Advanced	<a href="#">Display Results</a>   <a href="#">More</a>	
<input type="checkbox"/>	46	Bronchitis/	38270	Advanced	<a href="#">Display Results</a>   <a href="#">More</a>	
<input type="checkbox"/>	47	Chronic Obstructive Lung Disease.tw	6878	Advanced	<a href="#">Display Results</a>   <a href="#">More</a>	
<input type="checkbox"/>	48	Respiratory Tract Diseases/	45642	Advanced	<a href="#">Display Results</a>   <a href="#">More</a>	
<input type="checkbox"/>	49	chronic respiratory tract disease.tw	62	Advanced	<a href="#">Display Results</a>   <a href="#">More</a>	
<input type="checkbox"/>	50	Lung Diseases/	47987	Advanced	<a href="#">Display Results</a>   <a href="#">More</a>	
<input type="checkbox"/>	51	lung disease.tw	87674	Advanced	<a href="#">Display Results</a>   <a href="#">More</a>	
<input type="checkbox"/>	52	drug metabolite/	43214	Advanced	<a href="#">Display Results</a>   <a href="#">More</a>	
<input type="checkbox"/>	53	(hypoxemia or hypoxaemia).tw	35167	Advanced	<a href="#">Display Results</a>   <a href="#">More</a>	
<input type="checkbox"/>	54	hypoxia.tw	191841	Advanced	<a href="#">Display Results</a>   <a href="#">More</a>	
<input type="checkbox"/>	55	hypoxia/	139663	Advanced	<a href="#">Display Results</a>   <a href="#">More</a>	
<input type="checkbox"/>	56	27 or 30 or 31 or 32 or 36 or 37 or 38 or 39 or 40 or 41 or 42 or 43 or 44 or 45 or 46 or 47 or 48 or 49 or 50 or 51 or 53 or 54 or 55	1179346	Advanced	<a href="#">Display Results</a>   <a href="#">More</a>	
<input type="checkbox"/>	57	1 or 2 or 3 or 4 or 5 or 6 or 7 or 8 or 9 or 10 or 11 or 12 or 13 or 14 or 15 or 16 or 17 or 18 or 33 or 34 or 52	574415	Advanced	<a href="#">Display Results</a>   <a href="#">More</a>	
<input type="checkbox"/>	58	19 or 20 or 21 or 22 or 23 or 24 or 25 or 26 or 28 or 29 or 35	325427	Advanced	<a href="#">Display Results</a>   <a href="#">More</a>	

# Appendix 4

11/05/2023, 11:07 Ovid: Search Form

<input type="checkbox"/>	59 56 and 57 and 58	416	Advanced	<a href="#">Display Results</a> <a href="#">More</a>	<input type="checkbox"/>
<input type="checkbox"/>	60 Limit 59 to english language	402	Advanced	<a href="#">Display Results</a> <a href="#">More</a>	<input type="checkbox"/>

Save Remove

Combine with: **AND**

OR

---

[Save All](#) [Edit](#) [Create RSS](#) [Create Auto-Alert](#) [View Saved](#)

---

[Email All Search History](#) [Copy Search History Link](#) [Copy Search History Details](#)

To search Open Access content on Ovid, go to [Basic Search](#).

## Web of Science

The screenshot shows the Web of Science interface with the following elements:

- Header:** Clarivate logo, English language dropdown, and Products menu.
- Search Bar:** Contains the search query: "maximum plasma concentration" OR "plasma half life" OR "plasma clearance" OR "drug blood level" OR "drug half life" OR "drug clearance" OR "drug distribution" OR "oral absorption" OR "drug absorption" OR "absorption half life" OR "Biological Availability" OR "Bioavailability" OR "Pharmacokinetics" OR "drug disposition" OR "Drug Elimination Routes" OR "drug excretion" OR "drug clearance" OR "plasma protein binding" OR "drug metabolite" (Topic AND) hypoxemia OR hypoxaemia OR hypoxia OR oxygen deficiency OR "altitude-Sickness" OR "high altitude" OR "Chronic pulmonary disease" OR "chronic respiratory tract disease" OR "lung disease" OR "Chronic Obstructive Lung Disease" OR "asthma" OR "pneumonia" OR "pulmonary edema" OR "pulmonary embolism" OR "pulmonary hypertension" OR "pulmonary fibrosis" OR "granulomatous lung diseases" OR "emphysema" OR "bronchitis" (Topic AND) "blood oxygen tension" OR "blood oxygen levels" OR "oxygen consumption" OR "Oxygen Saturation" OR "oxygen therapy" OR "Oxygen Inhalation Therapy" OR "Blood Gas Analysis" OR "partial pressure oxygen" OR "oxygen therapy" OR "Blood Chemical Analysis" (Topic and English Language).
- Results:** 135 results from Web of Science. The first result is "Pathophysiology and treatment of pulmonary hypertension in sickle cell disease" by Gordeuk, VB, Castro, OL, and Machado, BE, published in *BLOOD* in February 2016, volume 127, pages 820-828. It has 87 citations and 88 references. The second result is "Adverse events with continuous doxapram infusion against late postoperative hypoxaemia" by Rosenberg, J, Kristensen, PS, L, and Overgaard, H, published in *EUROPEAN JOURNAL OF CLINICAL PHARMACOLOGY* in May 1996, volume 50, pages 191-194. It has 3 citations and 16 references.
- Refinement Tools:** Includes a search box for results, a filter by marked list, quick filters (Highly Cited Papers, Hot Papers, Review Article, Early Access, Open Access, Enriched Cited References), and citation topics (Anesthesiology).



# Appendix 4

## Scopus

The new, enhanced version of the search results page is available. [Try the new version](#)

680 document results

(TITLE-ABS-KEY ("maximum plasma concentration" OR "plasma half life" OR "plasma clearance" OR "drug blood level" OR "drug half life" OR "drug clearance" OR "drug distribution" OR "oral absorption" OR "drug absorption" OR "absorption half-life" OR "Biological Availability" OR "bioavailability" OR "Pharmacokinetics" OR "drug disposition" OR "Drug Elimination Routes" OR "drug excretion" OR "drug clearance" OR "plasma protein binding" OR "drug metabolism") AND TITLE-ABS-KEY (hypoxemia OR hypoxaemia OR hypoxia OR oxygen AND deficiency OR "Altitude Sickness" OR "high altitude" OR "Chronic pulmonary disease" OR "chronic respiratory tract disease" OR "lung disease" OR "Chronic Obstructive Lung Disease" OR "asthma" OR "pneumonia" OR "pulmonary edema" OR "pulmonary embolism" OR "pulmonary hypertension" OR "pulmonary fibrosis" OR "granulomatous lung diseases" OR "emphysema" OR "bronchitis") AND TITLE-ABS-KEY ("blood oxygen tension" OR "blood oxygen level" OR "oxygen consumption" OR "Oxygen Saturation" OR "oxygen therapy" OR "Oxygen Inhalation Therapy" OR "Blood Gas Analysis" OR "partial pressure oxygen" OR "oxygen therapy" OR "Blood Chemical Analysis")) AND (LIMIT-TO (LANGUAGE, "English"))

Search within results...

Refine results

Limit to Exclude

Open Access

- All Open Access (252) >
- Gold (80) >
- Hybrid Gold (25) >
- Bronze (82) >

Documents Secondary documents Patents

Analyze search results Show all abstracts Sort on: Date (newest)

Document title Authors Year Source Cited by

1	AV-101, a novel inhaled dry-powder formulation of imatinib, in healthy adult participants: a phase 1 single and multiple ascending dose study Open Access	Gillies, H., Niven, R., Dale, B.T., (-), McLaughlin, V.V., Kankam, M.	2023	ERJ Open Research 9(2),00433-2022	0
---	--	---	------	-----------------------------------	---

## Appendix 4.2 PK data extraction

Study / drug / rout	Condition	T1/2 (h) Mean ± SD
(Cumming et al., 1976) Antipyrine oral /IV	Hypoxia	18.4 ± 3.48
	Normoxia	8.38 ± 0.96

Study / drug / rout	Condition	t 1/2 (h) Mean ± SD	CL (l/hr) Mean ± SD	CL/F (mL.min.kg) Mean ± SD	Vd (l) Mean ± SD	Vd (l/kg) Mean ± SD
(Agnihotri et al., 1978) Antipyrine /oral	Hypoxia	8 ± 1.7	2.96 ± 0.90	0.84 ± 0.29	33 ± 5	0.54 ± 0.08
	Normoxia	8.1 ± 1.9	2.92 ± 0.60	0.83 ± 0.22	33 ± 6	0.55 ± 0.08

Study / drug / rout	Condition	*Fast t 1/2 (hr) Mean ± SD	Slow t 1/2 (h) Mean ± SD	Ka (h-1) Mean ± SD	F Mean ± SD	Fast metabolic CL (ml/min/kg) Mean ± SD	Slow metabolic CL (ml/min/kg) Mean ± SD	renal CL (ml/min/kg) Mean ± SD	Vd (l/kg) Mean ± SD	Tmax (hr) Mean ± SD	Cmax (mg/L) Mean ± SD
(Souich et al., 1983) Sulfamethazine /oral	Hypoxia	2.3 ± 0.86	7.21 ± 0.62	2.1719 ± 2.058	0.78 ± 0.11	2.22 ± 1.43	0.25 ± 0.06	0.14 ± 0.07	0.33 ± 0.13	1.86 ± 0.91	26.67 ± 12.91
	Normoxia	2.35 ± 1.06	6.4 ± 0.85	1.4438 ± 0.8757	0.89 ± 0.05	1.09 ± 0.36	0.24 ± 0.09	0.11 ± 0.03	0.2 ± 0.05	2.02 ± 0.92	28.31 ± 10.57

\* Fast t1/2 data used in meta-analysis.

Study / drug / rout	Condition	t 1/2 (h) Mean ± SD	Ke (h-1) Mean ± SD	F Mean ± SD	CL (L/kg/h) Mean ± SD	Vd ss (l/kg) Mean ± SD
(Cusack et al., 1986) Theophylline/ IV	Hypoxia	6.8 ± 0.6	0.108 ± 0.101	0.81 ± 0.04	0.05 ± 0.004	0.429 ± 0.024
	Normoxia	7.6 ± 0.8	0.101 ± 0.011	0.87 ± 0.07	0.048 ± 0.005	0.45 ± 0.021

## Appendix 4

Study / drug / rout	Condition	Apparent systemic clearance (ml/min/kg) Mean ± SD	metabolic clearance (ml/min/kg) Mean ± SD	Renal CL (ml/min/kg) Mean ± SD	t 1/2 (h) Mean ± SD	Vd (l/kg) Mean ± SD	AUC 0-t (µg.min/ml) Mean ± SD
(du Souich et al., 1989) Theophylline /IV	Hypoxia	1.03 ± 0.11	0.90 ± 0.10	0.13 ± 0.01	5.90 ± 0.59	0.48 ± 0.03	2709 ± 410
	Normoxia	1.14 ± 0.17	1.00 ± 0.15	0.13 ± 0.02	5.81 ± 0.75	0.48 ± 0.03	2607 ± 347

	Condition	t 1/2 (min)	F Mean ± SD	CL (ml/min) Mean ± SD	Renal CL (ml/min) Mean ± SD	Non renal Cl (ml/min) Mean ± SD	Fraction unchanged in urine Mean ± SD	Vd (ml/kg) Mean ± SD	Tmax (min) Mean ± SD	Cmax (mg/L) Mean ± SD
(Rowett et al., 1996) Frusemide IV	Hypoxia	90 ± 35		76.9 ± 38.8	31 ± 9	38 ± 6	0.45 ± 0.07	121 ± 44		
	Normoxia	87 ± 36		62.4 ± 21.6	29 ± 10	32 ± 19	0.49 ± 0.13	109 ± 40		
Frusemide/ oral	Hypoxia	87 ± 31	0.62 ± 0.20						96 ± 44	2.1 ± 0.6
	Normoxia	118 ± 47	0.56 ± 0.10						97 ± 38	1.9 ± 0.4

	Condition	t 1/2 (h)	F Mean ± SD	CL/F (ml/min/Kg) Mean ± SD	Tmax (hr) Mean ± SD	Cmax (mg/L) Mean ± SD
(Rowett et al., 1996) Paracetamole / oral	Hypoxia	2.0 ± 0.5	1 ± 2.9	5.8 ± 2.9	0.8 ± 0.4	10.8 ± 6.9
	Normoxia	2.1 ± 0.4	----	5.4 ± 2.3	0.8 ± 0.7	9.6 ± 5

Paracetamol data doses not included in meta analysis study.

Study / drug / rout	Condition	t 1/2α (h) Mean ± SD	t 1/2β (h) Mean ± SD	Vd (L) Mean ± SD	Cmax (ng/mL) Mean ± SD	AUC 0-t (ng/mL)h-1 Mean ± SD
(streit et al., 2005) Verapamil / IV	Hypoxia	0.08 ± 0.04	1.79 ± 0.58	207 ± 112	74.4 ± 47.3	55.9 ± 11.5
	Normoxia	0.14 ± 0.15	2.00 ± 0.98	192 ± 94	72.1 ± 25.1	58.7 ± 10.5

Study / drug / rout	Condition	t 1/2 (h) Mean ± SD	CL (ml/kg/h) Mean ± SD	Vd (ml/kg) Mean ± SD	Tmax (hr) Mean ± SD	Cmax (µg/mL) Mean ± SD	AUC 0-t (µg/mL)h-1 Mean ± SD
(streit et al., 2005) Theophylline / IV	Hypoxia	9.39 ± 1.40	33.2 ± 7.53	438 ± 46.3	0.15 ± 0.41	18.2 ± 4.16	119 ± 17.9
	Normoxia	9.29 ± 1.77	32.7 ± 4.62	428 ± 17.3	0.34 ± 0.08	20.7 ± 5.66	121 ± 7.78

Study / drug / rout	Condition	Ka (h-1) Mean ± SD	Ke/ (h-1) Mean ± SD	t 1/2 (h) Mean ± SD	t 1/2 abs (h) Mean ± SD	CL (L/kg/h) Mean ± SD	Vd (l/kg) Mean ± SD	Tmax (hr) Mean ± SD	Cmax (µg/mL) Mean ± SD	AUC 0-t (µg/mL)h-1 Mean ± SD	MRT (h) Mean ± SD
(Li et al., 2009) Sulfamethoxazole / oral	*Acute Hypoxia	2.5 ± 6.09	0.067 ± 0.006	10.37 ± 0.88	0.87 ± 0.54	0.83 ± 0.13	12.35 ± 1.82	1.7 ± 1.1	91.70 ± 15.30	1416.3 ± 202.6	13.15 ± 0.67
	Chronic Hypoxia	3.13 ± 1.86	0.063 ± 0.009	11.15 ± 1.53	0.43 ± 0.58	0.92 ± 0.22	14.65 ± 3.43	1.6 ± 1.1	98.72 ± 15.69	1298.5 ± 256	13 ± 1.01
	Normoxia	2.61 ± 2.28	0.076 ± 0.010	9.30 ± 1.11	0.66 ± 0.16	1.01 ± 0.22	13.27 ± 1.73	1.4 ± 0.3	94.42 ± 15.26	1202.5 ± 238.3	12.06 ± 0.94

\* Acute hypoxia data were used in meta analysis.

Study / drug / rout	Condition	t 1/2 (h) Mean ± SD	CL (L/kg/h) Mean ± SD	Vd (l/kg) Mean ± SD	Tmax (hr) Mean ± SD	Cmax (µg/mL) Mean ± SD	AUC 0-t (µg/mL)h-1 Mean ± SD	*AUMC (µg·ml-1-h2) Mean ± SD	MRT (h) Mean ± SD
(Zhang et al., 2016) Lidocaine hydrochloride / IM	Chronic Hypoxia (Han group)	2.44 ± 0.52	1.30 ± 0.27	4.49 ± 0.90	0.53 ± 0.12	2.74 ± 0.57	7.08 ± 1.32	17.85 ± 4.37	2.50 ± 0.25
	Chronic Hypoxia (Tibetan group)	2.44 ± 0.69	1.24 ± 0.34	4.31 ± 1.48	0.56 ± 0.17	2.78 ± 0.54	7.43 ± 1.86	17.94 ± 6.29	2.37 ± 0.31
	Normoxia	1.88 ± 0.32	1.40 ± 0.29	3.82 ± 1.01	0.50 ± 0.11	2.83 ± 0.41	6.75 ± 1.23	14.90 ± 5.23	2.21 ± 0.20

\* AUMC is the area under the first moment curve or the curve of concentration\*time versus time

Study/drug/ rout	Condition	Ke/ (h-1) Mean ± SD	t 1/2 (h) Mean ± SD	CL (mg/ng/ml)/hr Mean ± SD	Vd (mg/ng/ml) Mean ± SD	Tmax (hr) Mean ± SD	Cmax (ng/mL) Mean ± SD	AUC0-∞ (ng/mL) h-1 Mean ± SD	AUC0-t (ng/mL) h-1 Mean ± SD	MRT (h)
(Thomas et al., 2018) Alprazolam / oral	Hypoxia	0.06977 ± 0.02	9.99 ± 1.62	0.00563 ± 0.01	0.08207 ± 0.02	1.94 ± 0.17	20.04 ± 1.27	181.87 ± 27.67	143.91 ± 17.34	14.14 ± 1.94
	Normoxia	0.0575 ± 0.01	13.09 ± 1.41	0.00405 ± 0.01	0.07239 ± 0.02	1.97 ± 0.12	21.26 ± 1.40	255.47 ± 47.62	186.40 ± 27.19	17.80 ± 2.95

Appendix 4

**Appendix 4.3: Quality appraisal of included studies**

<b>(Authors, year)</b>	<b>(Cumming et al.,1976)</b>	<b>(Agnihotri et al., 1978)</b>	<b>(Souich et al., 1983)</b>	<b>(Cusack et al., 1986)</b>	<b>(du Souich et al., 1989)</b>	<b>(Rowett et al., 1996)</b>
<b>Study design</b>	Non randomise control trial	Cross over non randomise control trial	Non randomise control trial	cross-over RCT	Experimental study Before and after study without control	cross-over RCT
<b>Does the study address a clearly focused question/ hypothesis?</b>	YES	YES	YES	YES	YES	YES
<b>Was the population randomised? If YES, were appropriate methods used?</b>	NO	NO	NO	Cannot tell	Cannot tell	YES
<b>(Was allocation to intervention or comparator groups concealed?</b>	Cannot tell	NO	NO	Cannot tell	Cannot tell	NO
<b>Were the participants, investigators and people assessing the outcome ‘blinded’?</b>	Cannot tell	NO	Cannot tell	NO	NO	Cannot tell
<b>Were interventions (and comparisons) well described and appropriate?</b>	YES	YES	YES	YES	YES	YES
<b>Was ethical approval sought and received?</b>	Cannot tell	Cannot tell	Cannot tell	YES	Cannot tell	YES
<b>Was a trial protocol published?</b>	Cannot tell	Cannot tell	Cannot tell	Cannot tell	Cannot tell	Cannot tell
<b>Were the groups similar at the start of the trial?</b>	YES	YES	Cannot tell	YES	YES	YES

Appendix 4

<b>Was the sample size sufficient?</b>	Cannot tell	Cannot tell	YES	YES	Cannot tell	Cannot tell
<b>Were participants properly accounted for?</b>	Cannot tell	YES	Cannot tell	YES	YES	Cannot tell
<b>Are the statistical methods well described?</b>	NO	YES	Cannot tell	YES	YES	YES
<b>Were all important outcomes assessed, and reliably measured?</b>	YES	YES	YES	YES	YES	YES
<b>Is any sponsorship/conflict of interest reported?</b>	NO	NO	YES	NO	NO	NO
<b>Did the authors identify any limitations?</b>	NO	YES	NO	NO	NO	YES
<b>Are the conclusions the same in the abstract and the full text?</b>	YES	YES	YES	YES	YES	YES

Appendix 4

(Authors, year)	(Streit et al, 2005)	(Li et al, 2009)	(Zhang et al, 2016)	(Thomas et al, 2018)
<b>Study design</b>	Randomized, cross-over study	Open-Label, Controlled, Prospective Study	Non-randomised control trial	prospective interventional population pharmacokinetic study
<b>Does the study address a clearly focused question/hypothesis?</b>	YES	YES	YES	YES
<b>Was the population randomised? If YES, were appropriate methods used?</b>	YES	NO	NO	NO
<b>(Was allocation to intervention or comparator groups concealed?)</b>	Cannot tell	NO	NO	NO
<b>Were the participants, investigators and people assessing the outcome 'blinded'?</b>	YES	NO	NO	NO
<b>Were interventions (and comparisons) well described and appropriate?</b>	YES	YES	YES	YES
<b>Was ethical approval sought and received?</b>	YES	YES	YES	YES
<b>Was a trial protocol published?</b>	Cannot tell	Cannot tell	Cannot tell	Cannot tell
<b>Were the groups similar at the start of the trial?</b>	YES	YES	YES	YES
<b>Was the sample size sufficient?</b>	YES	YES	YES	YES

Appendix 4

<b>Were participants properly accounted for?</b>	YES	Cannot tell	YES	YES
<b>Are the statistical methods well described?</b>	YES	YES	YES	YES
<b>Were all important outcomes assessed, and reliably measured?</b>	YES	YES	YES	YES
<b>Is any sponsorship/conflict of interest reported?</b>	NO	NO	YES	NO
<b>Did the authors identify any limitations?</b>	YES	YES	YES	YES
<b>Are the conclusions the same in the abstract and the full text?</b>	YES	YES	YES	YES

